CHEMOSENSITIZING EFFECT OF NATURAL PRODUCTS AGAINST CANCERS: APPLICATIONS IN ENHANCING CHEMOTHERAPY AND IMMUNOTHERAPY

EDITED BY: Nand K. Roy, Devesh Tewari and Maria Teresa Esposito
PUBLISHED IN: Frontiers in Pharmacology and Frontiers in Oncology

frontiers Research Topics

ISSN 1664-8714
ISBN 978-2-83250-192-4
DOI 10.3389/978-2-83250-192-4

About Frontiers

Frontiers is more than just an open-access publisher of scholarly articles: it is a pioneering approach to the world of academia, radically improving the way scholarly research is managed. The grand vision of Frontiers is a world where all people have an equal opportunity to seek, share and generate knowledge. Frontiers provides immediate and permanent online open access to all its publications, but this alone is not enough to realize our grand goals.

Frontiers Journal Series

The Frontiers Journal Series is a multi-tier and interdisciplinary set of open-access, online journals, promising a paradigm shift from the current review, selection and dissemination processes in academic publishing. All Frontiers journals are driven by researchers for researchers; therefore, they constitute a service to the scholarly community. At the same time, the Frontiers Journal Series operates on a revolutionary invention, the tiered publishing system, initially addressing specific communities of scholars, and gradually climbing up to broader public understanding, thus serving the interests of the lay society, too.

Dedication to Quality

Each Frontiers article is a landmark of the highest quality, thanks to genuinely collaborative interactions between authors and review editors, who include some of the world's best academicians. Research must be certified by peers before entering a stream of knowledge that may eventually reach the public - and shape society; therefore, Frontiers only applies the most rigorous and unbiased reviews.
Frontiers revolutionizes research publishing by freely delivering the most outstanding research, evaluated with no bias from both the academic and social point of view. By applying the most advanced information technologies, Frontiers is catapulting scholarly publishing into a new generation.

What are Frontiers Research Topics?

Frontiers Research Topics are very popular trademarks of the Frontiers Journals Series: they are collections of at least ten articles, all centered on a particular subject. With their unique mix of varied contributions from Original Research to Review Articles, Frontiers Research Topics unify the most influential researchers, the latest key findings and historical advances in a hot research area! Find out more on how to host your own Frontiers Research Topic or contribute to one as an author by contacting the Frontiers Editorial Office: frontiersin.org/about/contact

CHEMOSENSITIZING EFFECT OF NATURAL PRODUCTS AGAINST CANCERS: APPLICATIONS IN ENHANCING CHEMOTHERAPY AND IMMUNOTHERAPY

Topic Editors:
Nand K. Roy, La Jolla Institute for Immunology (LJI), United States
Devesh Tewari, Delhi Pharmaceutical Sciences and Research University, India
Maria Teresa Esposito, University of Roehampton London, United Kingdom

Citation: Roy, N. K., Tewari, D., Esposito, M. T., eds. (2022). Chemosensitizing Effect of Natural Products Against Cancers: Applications in Enhancing Chemotherapy and Immunotherapy. Lausanne: Frontiers Media SA.
doi: 10.3389/978-2-83250-192-4

Table of Contents

frontiers | Frontiers in Pharmacology

TYPE Editorial
PUBLISHED 30 August 2022
DOI 10.3389/fphar.2022.988226

OPEN ACCESS

EDITED AND REVIEWED BY
Olivier Feron,
Université catholique de Louvain, Belgium

*CORRESPONDENCE
Nand K. Roy,
roy.nandkishor.iitg@gmail.com
Devesh Tewari,
dtewari3@gmail.com
Maria Teresa Esposito,
Maria.Esposito@roehampton.ac.uk

†PRESENT ADDRESS
Nand K. Roy,
La Jolla Institute for Immunology, San Diego, CA, United States

SPECIALTY SECTION
This article was submitted to Pharmacology of Anti-Cancer Drugs, a section of the journal Frontiers in Pharmacology

RECEIVED 07 July 2022
ACCEPTED 22 July 2022
PUBLISHED 30 August 2022

CITATION
Roy NK, Tewari D and Esposito MT (2022), Editorial: Chemosensitizing effect of natural products against cancers: Applications in enhancing chemotherapy and immunotherapy. *Front. Pharmacol.* 13:988226. doi: 10.3389/fphar.2022.988226

Editorial: Chemosensitizing effect of natural products against cancers: Applications in enhancing chemotherapy and immunotherapy

Nand K. Roy[1,2*†], Devesh Tewari[3*] and Maria Teresa Esposito[4*]

[1]Case Western Reserve University, Cleveland, OH, United States, [2]La Jolla Institute for Immunology, San Diego, CA, United States, [3]Department of Pharmacognosy and Phytochemistry, School of Pharmaceutical Sciences, Delhi Pharmaceutical Sciences and Research University, New Delhi, India, [4]School of Life and Health Science University of Roehampton, Roehampton, United Kingdom

KEYWORDS

natural products, cancer, chemosensitization, chemotherapy, immunotherapy

Editorial on the Research Topic
Chemosensitizing effect of natural products against cancers: Applications in enhancing chemotherapy and immunotherapy

Cancer is a complex phenomenon that encompasses over 200 different diseases that are the consequence of accumulation of genetic alterations (Roy et al., 2017). Despite the progress in the development of novel treatments for cancer, it still remains one of the prominent causes of death globally. Among the main reasons for the increasing rate of mortality is the emergence of chemoresistant or immunotolerant cancer cells that don't respond to chemotherapy or immunotherapy modalities respectively (Maeda and Khatami 2018). The adverse events and toxicities associated with the available therapeutics can also pose a risk to patients. These challenges can be overcome by the utilization of natural products and their derivatives in the therapeutic regimen and it is well evident that many of the chemotherapeutic agents, currently used in the clinical setting, such as taxol, vincristine, irinotecan, etoposide, and paclitaxel etc. are derived from natural sources. Moreover, several researches have shown that the co-administration of natural products along with chemotherapeutic agents can increase their efficacy and even reverses chemoresistance. Therefore, this Research Topic was floated to attract researches and studies related to the potential of natural products in the chemosensitization of cancer cells to enhance the effect of chemotherapy and immunotherapy.

Interestingly, the single treatment of natural product such as tetramethylpyrazine (TMP) isolated from *Ligusticum chuanxiong* Hort is shown to be effective against different cancers at preclinical stages (Yang et al.). Another example of a such paradigm was discussed by Li et al., where they have reported the anticancer potential

of gracillin, a steroidal saponin compound found in different medicinal plants such as *Rhizoma paridis*, *Pairs polyphylla*, *Dioscorea villosa*, *Acontum carmichaeli*, *Solanum incanum*, and *Solanum xanthocarpum* against non-small cell lung cancer (NSCLC) cells. Their research indicated that gracillin possesses anti-NSCLC activity through promoting autophagy of cancer that was regulated via the mTOR signaling pathway. Similarly, Chen et al. showed that α-hederin, a monodesmosidic triterpenoid saponin extracted from *Fructus akebiae* enhanced apoptosis while inhibiting the proliferation of hepatocellular carcinoma (HCC) cells through the alteration of Hippo/YAP protein signaling pathway. It was observed that the treatment of α-hederin treatment led to the increased level of proteins and genes associated with the Hippo signaling pathway. Moreover, their treatment also caused decreased nuclear YAP levels that consequently inhibited the proliferation while increasing the apoptosis of HCC cells.

Many researches over the past decades have suggested that the cancer cells develop resistance to the drugs and that can this can be circumvented by the combination of multiple drugs, acting on redundant signaling nodes. Such an effective combination approach has been studied in a case report of BRAFV600E-mutant colorectal cancer (CRC) (Cho et al.). A triple-regimen of vemurafenib that targets BRAFV600E, a topoisomerase I inhibitor (irinotecan), and cetuximab (an EGF-Receptor inhibitor, EGFRi) resulted in a complete response to the therapy. EGFRi can initiate many side effects and natural products in the therapeutic regimen can alleviate these challenges (Sui et al., 2020). In line with this, a randomized controlled study led by Liu et al. has shown that Honeysuckle, a natural product obtained from *Lonicera japonica* Thunb was effective in reducing acneiform rash incidences and severities induced by EGFRi such as cetuximab, erlotinib, gefitinib, and icotinib in colorectal and lung cancer patients. Moreover, the inclusion of natural bioactive components can also help in reversing the EGFRi resistance in cancer cells. Another study by Wu et al. highlighted the effect of Bruceine H, a derivative of *Brucea javanica* (L.), in overcoming resistance to receptor tyrosine kinase (RTK)-EGFRi in non small cell lung cancer (NSCLC) models. The authors have shown that the combination of Brucein H in the therapy increased the gefinitib response by suppressing Notch3, EGFR activation and β-catenin expression. Remarkably, the combination of Brucein H and gefinitib also induced Foxo3a, whose expression correlates with better response to EGFR inhibitors and better overall survival in NSLCC patients. Similar to this study, the comparative proteomic analysis by Cai et al. demonstrated the chemosensitizing effect of cryptotanshinone (CTS), a bioactive component of *Salvia miltiorrhiza* against gefitinib-resistant EGFR-mutant lung cancer cells. Lately, three proteins namely, catalase (CAT), heme oxygenase 1 (HMOX1), and stearoyl-CoA desaturase (SCD) identified through a proteomic analysis were validated as the important target of CTS and suggested to be a potential therapeutic target in lung cancers.

It is now well established that the cancer cells become resistant to certain kinds of therapy through the alterations of various signaling pathway (Mansoori et al., 2017). In accordance with this, Zheng et al. pointed out that the knockdown of Aldo-keto reductase 1C3 (AKR1C3) can sensitize the sorafenib-resistant hepatocellular carcinoma (HCC) cells through the inhibition of AKT kinase protein phosphorylation. Interestingly, the past literatures have indicated the importance of AKT kinase involvement in different types of cancers, and through *in silico* analysis it was also shown that it can potentially be targeted by natural products (Roy et al., 2020). In addition to targeting the Akt pathway by natural products, an interesting review by Fakhri et al. concluded that targeting the TLR/NF-κB/NLRP pathway with different kinds of bioactive phytocompounds such as phenolic compounds, alkaloids, terpenes/terpenoids, and sulfur compounds has the potential to overcome chemoresistance thereby can improve the outcome for chemotherapy and immunotherapy. Likewise, Dev et al.have discussed the role of curcumin, a polyphenol extracted from *Curcuma longa* as a RTK inhibitor. Curcumin possessed antitumorigenic effects on cancer cells through enhanced apoptosis and reduced cellular proliferation to reduced angiogenesis. These effects are mediated by inhibition of several signaling pathways including MAPK, PI3K/Akt, JAK/STAT, and NF-κB, which are often activated in response to treatment with single RTK inhibitors. An intriguing study by Yang et al. inferred that lumiflavin, a flavin analogue can diminish the cisplatin resistance of ovarian cancer stem-like cells (CSCs). Mechanistically, it was suggested that it induces its sensitization effect through the induction of inducing phenotypic differentiation of CSCs and it was due to the change in the notch signaling pathway and stem cell pathway.

Apart from natural resources derived by plants, recent years have witnessed a plethora of research that has emphasized the application of compounds derived by other natural sources or natural product-inspired synthesized molecule in cancer therapy (Newman and Cragg 2020). One such molecule is thymopentin (TP5), an immunomodulatory pentapeptide (49 amino acids) derived from the active fragment of a natural hormone called thymosin. Yu et al. have shown that TP5 can directly inhibit the stemness of colon cancer cells HCT116 as evident by reduced surface molecular markers associated with stemness such as CD133, CD44, and CD24 in addition to stemness-related genes like ALDH1, SOX2, Oct-4, and Nanog. These stemness-related changes thereby caused altered Wnt/β-catenin signaling that resulted in enhanced oxaliplatin (OXA) cytotoxicity against HCT116 cells. Also, Ragone et al.highlight the effectiveness of combination therapy of gemcitabine (Gem) and AdipoRon (AdipoR) in combating pancreatic ductal adenocarcinoma (PDAC) resistance to Gem. AdipoR is known to be the first synthetic orally active adiponectin receptor agonist suggested having an antitumorigenic

effect against different types of cancers including PDAC. They have proposed that their combination halts the cell cycle progression in cancer cells effectively and p44/42 MAPK pathway involvement in the improved treatment outcomes.

Overall, the present Research Topic received a range of remarkable original and review articles that can improve the understanding of the chemosensitizing properties of natural products. Moreover, natural products other than plant sources such as biomolecules, toxins, venoms, ligands etc. obtained/inspired from microorganisms and animal sources also open new avenues for exploration to unravel nature's treasure for drug discovery. However, the lack of articles in context to immunotherapy and clinical trials highlights the ample opportunity available in this area to fill the void in our understanding. Recent research by Messaoudene et al., 2022 have indicated the great potential of natural product in improving cancer immunotherapy and more research should be warranted in this field. Nevertheless, this Research Topic will be a great help to the scientific community to understand the relevance of natural products in cancer therapy and explore future possibilities and development in the area.

Author contributions

All authors have contributed significantly in editing the manuscripts.

Conflict of interest

The authors declare that the research was conducted in the absence of any commercial or financial relationships that could be construed as a potential conflict of interest.

Publisher's note

References

Maeda, H., and Khatami, M. (2018). Analyses of repeated failures in cancer therapy for solid tumors: Poor tumor-selective drug delivery, low therapeutic efficacy and unsustainable costs. *Clin. Transl. Med.* 7 (1), 11–20. doi:10.1186/s40169-018-0185-6

Mansoori, B., Mohammadi, A., Davudian, S., Shirjang, S., and Baradaran, B. (2017). The different mechanisms of cancer drug resistance: A brief review. *Adv. Pharm. Bull.* 7 (3), 339–348. doi:10.15171/apb.2017.041

Messaoudene, M., Pidgeon, R., Richard, C., Ponce, M., Diop, K., Benlaifaoui, M., et al. (2022). *A natural polyphenol exerts antitumor activity and circumvents anti–PD-1 resistance through effects on the gut microbiota*. *Cancer Discov.* 12 (4), 070–1087. doi:10.1158/2159-8290.CD-21-0808

Newman, D. J., and Cragg, G. M. (2020). Natural products as sources of new drugs over the nearly four decades from 01/1981 to 09/2019. *J. Nat. Prod.* 83 (3), 770–803. doi:10.1021/acs.jnatprod.9b01285

Roy, N. K., Bordoloi, D., Monisha, J., Anip, A., Padmavathi, G., and Kunnumakkara, A. B. (2017). Cancer-An overview and molecular alterations in cancer. *Fusion Genes Cancer* 2017, 1–15. doi:10.1142/9789813200944_0001

Roy, N. K., Monisha, J., Singh, A. K., Padmavathi, G., and Kunnumakkara, A. B. (2020). Isoform-specific role of Akt kinase in cancer and its selective targeting by potential anticancer natural agents. *Nat. Prod. J.* 10 (3), 322–332. doi:10.2174/2210315509666190314145257

Sui, X., Zhang, M., Han, X., Zhang, R., Chen, L., Liu, Y., et al. (2020). Combination of traditional Chinese medicine and epidermal growth factor receptor tyrosine kinase inhibitors in the treatment of non-small cell lung cancer: A systematic review and meta-analysis. *Medicine* 2020 (32), e20683. doi:10.1097/MD.0000000000020683

frontiers in Pharmacology

REVIEW
published: 15 November 2021
doi: 10.3389/fphar.2021.772510

Receptor Tyrosine Kinases and Their Signaling Pathways as Therapeutic Targets of Curcumin in Cancer

*Sareshma Sudhesh Dev, Syafiq Asnawi Zainal Abidin, Reyhaneh Farghadani, Iekhsan Othman and Rakesh Naidu**

Jeffrey Cheah School of Medicine and Health Sciences, Monash University Malaysia, Jalan Lagoon Selatan, Bandar Sunway, Malaysia

Receptor tyrosine kinases (RTKs) are transmembrane cell-surface proteins that act as signal transducers. They regulate essential cellular processes like proliferation, apoptosis, differentiation and metabolism. RTK alteration occurs in a broad spectrum of cancers, emphasising its crucial role in cancer progression and as a suitable therapeutic target. The use of small molecule RTK inhibitors however, has been crippled by the emergence of resistance, highlighting the need for a pleiotropic anti-cancer agent that can replace or be used in combination with existing pharmacological agents to enhance treatment efficacy. Curcumin is an attractive therapeutic agent mainly due to its potent anti-cancer effects, extensive range of targets and minimal toxicity. Out of the numerous documented targets of curcumin, RTKs appear to be one of the main nodes of curcumin-mediated inhibition. Many studies have found that curcumin influences RTK activation and their downstream signaling pathways resulting in increased apoptosis, decreased proliferation and decreased migration in cancer both *in vitro* and *in vivo*. This review focused on how curcumin exhibits anti-cancer effects through inhibition of RTKs and downstream signaling pathways like the MAPK, PI3K/Akt, JAK/STAT, and NF-κB pathways. Combination studies of curcumin and RTK inhibitors were also analysed with emphasis on their common molecular targets.

Keywords: curcumin, receptor tyrosine kinase, signaling pathway, polyphenol, combination therapy, tyrosine kinase inhibitor

OPEN ACCESS

Edited by:
Maria Teresa Esposito, University of Roehampton London, United Kingdom

Reviewed by:
Bharat B. Aggarwal, University of Texas MD Anderson Cancer Center, United States
Antonio Giordano, Sbarro Health Research Organization (SHRO), United States

****Correspondence:***
Rakesh Naidu
kdrakeshna@hotmail.com

Specialty section:
This article was submitted to Pharmacology of Anti-Cancer Drugs, a section of the journal Frontiers in Pharmacology

Received: *08 September 2021*
Accepted: *01 November 2021*
Published: *15 November 2021*

Citation:
Sudhesh Dev S, Zainal Abidin SA, Farghadani R, Othman I and Naidu R (2021) Receptor Tyrosine Kinases and Their Signaling Pathways as Therapeutic Targets of Curcumin in Cancer. Front. Pharmacol. 12:772510. doi: 10.3389/fphar.2021.772510

1 INTRODUCTION

In 2020, The International Agency for Research Cancer (IARC) GLOBOCAN reported approximately 19.3 million new cases of cancer and 10 million deaths globally with data from 185 countries/territories. Lung, breast, and prostate cancers were the most commonly diagnosed cancers, while lung, liver, and stomach cancers were the most common causes of cancer death (Ferlay et al., 2021). Most cancer patients undergo combination treatments, for example, surgery combined with chemotherapy or radiotherapy. Chemotherapy alone can also consist of a combination or cocktail of drugs depending on the type and stage of cancer. Common chemotherapeutic drugs can be biochemically classified into alkylating agents (e.g. cisplatin, carboplatin, and etc.), anti-metabolites (e.g. gemcitabine, 5-fluorouracil), anti-tumour antibiotics (e.g. doxorubicin, epirubicin), topoisomerase inhibitors (e.g. etoposide) and tubulin-binding drugs (e.g. vinorelbine, paclitaxel, and doclitaxel) (Dickens and Ahmed, 2018). On the other hand, targeted therapy involves strategies that specifically target characteristic features in cells or proteins that enable cancer.

Receptor tyrosine kinases (RTKs) are a group of membrane-bound receptors that play an important role in the normal function of cells. They act as signal transducers that mediate cell-to-cell communication by phosphorylating tyrosine residues on key intracellular substrate proteins. Essentially, they lie at the centre of complex interconnecting signaling pathways and are actively involved in the maintenance of cellular homeostasis through regulation of cell proliferation, differentiation, metabolism, migration, and etc. (Wheeler and Yarden, 2015). Alteration or abnormal activation of RTKs have been recurrently observed and recognised as a contributing factor in the progression of various cancers (Weigand et al., 2005; Huang et al., 2011; Wang et al., 2011; Ha et al., 2013; Gallant et al., 2015). These observations led to the development of tyrosine kinase inhibitors (TKIs), which is a well-known targeted therapy. A commonly used TKI is the epidermal growth factor receptor (EGFR) tyrosine kinase inhibitors (TKIs) against non-small cell lung cancer (NSCLC). These small molecule inhibitors inhibit the tyrosine kinase domain of EGFR (Chan and Hughes, 2014). First- (gefitinib, erlotinib), second- (afatinib, dacomitinib), and third- (osimertinib) generation EGFR TKIs have been developed with slightly different mechanisms aimed at specific activating mutations (Lin et al., 2014). Other examples of TKIs and their targets include sorafenib (VEGFR kinase, RAF, PDGFR), crizotinib (ALK kinase), sunitinib (VEGF, PDGFR), imatinib (PDGFR, ABL kinase), carfilzomib (proteasome), ribociclib (CDK4, CDK6), and others. Despite their perceived efficacy, the use of TKIs are eventually met with the rise of resistance. Tumours either show a lack of response from the beginning of treatment or they slowly develop resistance after exposure to the drug (Simasi et al., 2014). RTKs mediate the emergence of TKI resistance through their oncogenic alterations such as mutations, overexpression, abnormal fusions and autocrine activation loops (Kobayashi et al., 2005; Cepero et al., 2010; Terai et al., 2013; Enrico et al., 2020). This poses a challenge to the clinical use of TKIs against cancer. Hence, recently, many researchers have begun studying the anti-cancer effects of naturally-derived compounds, mainly from the plant species. The idea behind this effort is to find an effective adjuvant that can be administered in combination with existing anti-cancer drugs, thus eliminating the common issue of toxicity associated with combination drug treatments.

Curcumin is a hydrophobic polyphenol extracted from the herb *Curcuma longa* or commonly known as turmeric. It was first introduced in 1910, but it has recently gained attention due to its potent therapeutic properties (Miłobędzka et al., 1910; Boroumand et al., 2018). Curcumin is a diferuloylmethane and its IUPAC name is (1E, 6E)-1,7-bis(4-hydroxy-3-methoxyphenyl)-1,6-heptadiene-3,5-dione (Giordano and Tommonaro, 2019). Various studies have shown that curcumin has anti-inflammatory (Farhood et al., 2019), anti-proliferative (Teiten et al., 2011), anti-oxidant (Boroumand et al., 2018), anti-microbial (Adamczak et al., 2020), anti-metastatic (Deng et al., 2016), and anti-angiogenic (Shakeri et al., 2019) properties. These properties altogether make curcumin a powerful anti-cancer agent. In India, where turmeric has been widely used as a cooking spice and medication for thousands of years, cancer rates are much lower compared to western countries. The lowest rates of cancer in India include esophagus, colorectal, liver, pancreas, lung, breast, uterine, ovary, prostate, bladder, kidney, renal, and brain cancers as well as non-Hodgkin lymphoma, and leukemia (Hutchins-Wolfbrandt and Mistry, 2011). There is however, a lack of hard evidence proving that turmeric consumption is solely or at least majorly responsible for the reduced cancer rates. Hutchins-Wolfbrandt and Mistry (2011) describe a few studies that have looked into daily turmeric consumption in India and Nepal, however, these studies did not examine how this affected the overall prevalence of cancer. Despite the lack of proven correlations, the availability and rapid expansion of curcumin-related research especially in the last decade, points towards its viability as an anti-cancer agent. Some of the main molecular targets of curcumin include transcription factors, growth factors, inflammatory cytokines, apoptotic proteins, protein kinases, receptors, cell survival proteins, microRNAs, tumour suppressor genes and oncogenes among others (Rahmani et al., 2014; Giordano and Tommonaro, 2019). In cancer, two of the most crucial roles of curcumin involves its ability to inhibit cellular proliferation and induce apoptosis. These features of curcumin target the root cause of cancer which is abnormal cell growth and apoptotic evasion. Several molecular targets of curcumin involving these two hallmarks of cancer are inhibition of growth factors and kinases (TGF-α, EGF, VEGF, FGF, FAK, JAK, MAPKs, mTOR, and etc.) and induction of apoptotic-related proteins (Bax, Bim, Bcl-2, Bcl-XL, and etc.) (Zhou et al., 2011). An essential component regulating these processes are RTKs and curcumin has been found to target RTKs like EGFR, VEGFR, FGFR, PDGFR, and others. Curcumin mainly downregulates RTK expression, inhibits RTK activation, decreases RTK ligands and also inhibits RTK downstream signaling pathways. More recently, several studies have also reported that curcumin enhances the effects of TKIs when administered in combination and in some cases, overcoming resistance altogether. The effects of curcumin are not only mediated through RTKs and involves many other components/molecular targets as mentioned before, however, RTKs seem to be at the core of these processes. Therefore, this current review discussed the role of receptor tyrosine kinases namely epidermal growth factor receptor (EGFR), vascular endothelial growth factor receptor (VEGFR), fibroblast growth factor receptor (FGFR), platelet-derived growth factor receptor (PDGFR), insulin-like growth factor 1 receptor (IGF-1R), and hepatocyte growth factor receptor (HGFR) in cancer and how curcumin targets these RTK signaling pathways including the mitogen-activated protein kinase (MAPK), the phosphatidylinositol 3-kinases (PI3K)/Akt, the Janus Kinase/Signal Transducer and Activator of Transcription (JAK/STAT) and NF-κB pathways. These RTKs were selected because they are well documented targets of curcumin in cancer. Additionally, drug combination studies involving curcumin and tyrosine

TABLE 1 | Classification of RTKs according to family.

Class	Family	Members
I	EGFR	EGFR, ERBB2, ERBB3, ERBB4
II	Insulin R	INSR IGFR
III	PDGFR	PDGFRα, PDGFRβ, M-CSFR, KIT, FLT3L
IV	VEGFR	VEGFR1, VEGFR2, VEGFR3
V	FGFR	FGFR1, FGFR2, FGFR3, FGFR4
VI	CCK	CCK4
VII	NGFR	TRKA, TRKB, TRKC
VIII	HGFR	MET, RON
IX	EPHR	EPHA1–6, EPHB1–6
X	AXL	AXL, MER, TYRO3
XI	TIE	TIE, TEK
XII	RYK	RYK
XIII	DDR	DDR1, DDR2
XIV	RET	RET
XV	ROS	ROS
XVI	LTK	LTK, ALK
XVII	ROR	ROR1, ROR2
XVIII	MUSK	MUSK
XIX	LMR	AATYK1, AATYK2, AATYK3
XX	Undetermined	RTK106

EGFR: epidermal growth factor receptor; InsR: insulin receptor; PDGFR: platelet-derived growth factor receptor; VEGFR: vascular endothelial growth factor receptor; FGFR: fibroblast growth factor receptor; CCK: colon carcinoma kinase; NGFR, nerve growth factor receptor; HGFR: hepatocyte growth factor receptor; EphR: ephrin receptor; Axl: from the Greek word anex-elekto, or uncontrolled, a Tyro3 protein tyrosine kinase; TIE: tyrosine kinase receptor in endothelial cells; RYK: receptor related to tyrosine kinases; DDR: discoidin domain receptor; Ret: rearranged during transfection; ROS: RPTK, expressed in some epithelial cell types; LTK: leukocyte tyrosine kinase; ROR: receptor orphan; MuSK: muscle-specific kinase; LMR: Lemur. Adopted from (Ségaliny et al., 2015).

kinase inhibitors were also reviewed with a particular focus on RTK inhibitors namely those targeting EGFR, VEGFR, and PDGFR.

2 RECEPTOR TYROSINE KINASE ACTIVATION

2.1 Receptor Tyrosine Kinase Activation in Normal Cells

Tyrosine kinases can be further divided into receptor tyrosine kinases (RTKs) and non-receptor tyrosine kinases (NRTKs). Of all the 90 known tyrosine kinases, 58 are RTKs from 20 subfamilies (**Table 1**) while 32 are NRTKs from 10 subfamilies. All RTKs have a similar basic structure consisting of an amino terminal extracellular domain containing a ligand binding site, a single transmembrane α-helix, an intracellular tyrosine kinase domain, a tyrosine rich carboxy-(C) terminal and juxtamembrane regions (Lemmon and Schlessinger, 2010; Wheeler and Yarden, 2015).

RTK activation occurs through the binding of a ligand to the receptor, which then induces receptor dimerization. There are four general modes that have been proposed. These include 1) ligand-mediated dimerization, 2) ligand-mediated dimerization with receptor contacts, 3) ligand-mediated dimerization with receptors contacts and accessory molecules and lastly 4) receptor-mediated dimerization (Lemmon and Schlessinger, 2010). Once ligand-induced dimerization occurs, it activates the intracellular tyrosine kinase domain (TKD) through the transmembrane (TM) domain. The RTK TM dimer interface is very specific and contains essential structural information regarding the positioning of the catalytic domains. Interestingly, studies have found that switching the TM domains between different receptors can still result in constitutive activation as long as the catalytic domains are properly oriented (Cheatham et al., 1993; Petti et al., 1998; Li and Hristova, 2006).

Before TKDs are activated, each TKD is *cis*-autoinhibited by a specific group of intra-molecular interactions unique to each receptor. RTK activation occurs when this *cis*-autoinhibition is released after ligand binding and dimerization (Lemmon and Schlessinger, 2010). RTKs can be *cis*-autoinhibited by their activation loop, juxtamembrane region and C-terminal sequences (Mohammadi et al., 1996; Niu et al., 2002; Till et al., 2002). Transphosphorylation of tyrosine residues in each of these structures are required for activation. Certain TKDs can also be activated allosterically by their partners within a stable dimer. Autophosphorylation of RTKs occurs in several phases, with more tyrosine residues in the cytoplasmic region being autophosphorylated in a precise order (Lemmon and Schlessinger, 2010). The phosphorylated tyrosines or phosphotyrosines then become binding sites that recruit and assemble signaling molecules possessing the Src homology-2 (SH2) and phosphotyrosine-binding (PTB) domains. These specific molecules either bind directly to phosphotyrosine residues, or are indirectly recruited by binding to docking proteins phosphorylated by RTKs (Schlessinger, 2000). Some of these docking proteins include IRS1 (insulin receptor substrate-1), FRS2 and Gab1 (Grb-associated binder). These proteins further activate multiple downstream signaling pathways, with some of the main ones being the MAPK, PI3K, JAK/STAT, and PKC pathways (Lemmon and Schlessinger, 2010; Du and Lovly, 2018). These pathways regulate key processes such as survival, proliferation, differentiation, metabolism and cell-cycle control (Lemmon and Schlessinger, 2010). A more detailed account of these pathways will be included in the following sections.

2.2 Receptor Tyrosine Kinase Activation in Cancer Cells

The abnormal activation of RTKs is a multifaceted process involving not just the RTKs themselves but also partner molecules and their surrounding environments. Their association with diverse groups of cellular components further complicates the mechanics of oncogenic RTK activation. Four main mechanisms leading to aberrant activation have been proposed (**Figure 1**), which are 1) RTK overexpression, 2) gain-of-function mutations, 3) chromosomal translocations, and 4) autocrine activation. In addition to these basic mechanisms, oncogenic RTK activation can also be influenced by kinase domain duplications, microRNAs, tumour microenvironment changes, negative RTK signaling regulators,

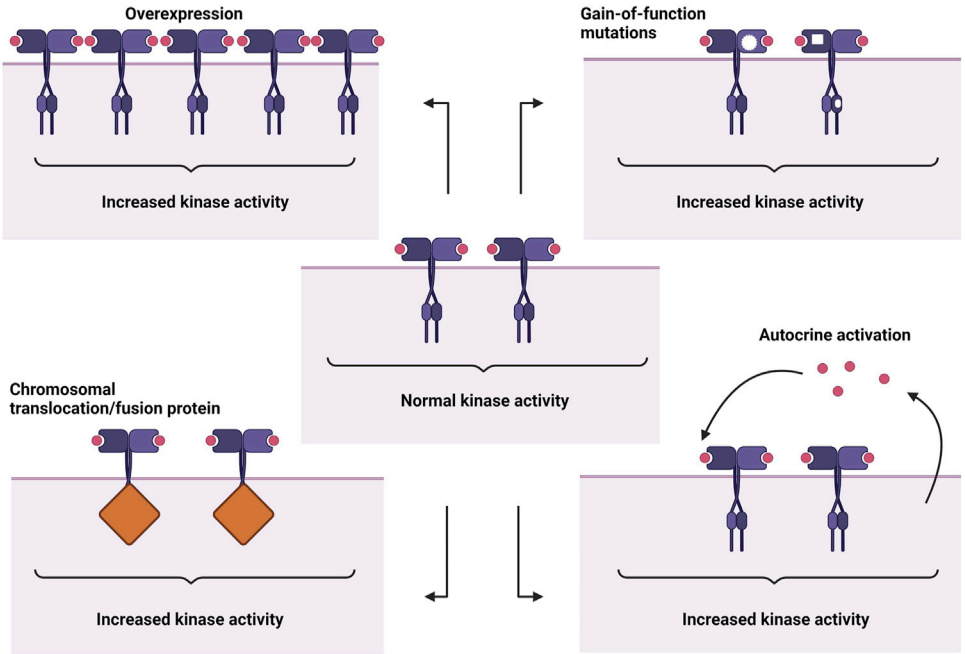

FIGURE 1 | Abnormal RTK activation mechanisms. From top left: overexpression, gain-of-function mutations, autocrine activation, chromosomal translocation/fusion protein. Created with BioRender.com.

protein tyrosine phosphatases, altered endocytic/trafficking genes and also spatial deregulation of RTKs (Casaletto and McClatchey, 2012; Du and Lovly, 2018).

2.2.1 Epidermal Growth Factor Receptor

EGFR is an extensively studied RTK especially in lung cancer and aptly encapsulates the range of RTK oncogenic alterations. The best well-studied alterations are the EGFR activating mutations that occur in NSCLC. These mutations mainly occur in exons 18, 19, 20, and 21 of the TKD gene (Shigematsu and Gazdar, 2006). Approximately 90% of all EGFR activating mutations involve exon 19 deletions and the L858R point mutation. These mutations allow EGFR activation in the absence of ligand binding and shift the equilibrium between active and inactive states of the TK, enhancing kinase activity (Gazdar, 2009). Mutations also occur in the extracellular domain (ECD) of EGFR in lung (Yu et al., 2017), brain (Idbaih et al., 2009), and colon cancers (Arena et al., 2015). Some of these mutations were found to cause ligand-independent EGFR activation, EGFR amplification and disruption of anti-EGFR mAb binding.

EGFR amplification which commonly occurs due to mutation also occurs in breast (Shao et al., 2011; Park et al., 2014), lung (Morinaga et al., 2008), ovarian (Lassus et al., 2006), and prostate (Schlomm et al., 2007) cancers. The overexpression of EGFR leads to increased surface abundance which stimulates receptor dimerization and subsequent kinase activation (Casaletto and McClatchey, 2012). RTK surface abundance is also influenced by processes involving endocytic machinery and trafficking, whereby alterations of genes/proteins involved in RTK endocytosis can enhanced RTK activation (Bremm et al., 2008; Casaletto and McClatchey, 2012). EGFR gene fusions also occur in lung cancer and the most common fusion is EGFR-RAD51, which is a fusion between the EGFR TKD and RAD51, a DNA damage response protein (Konduri et al., 2016). EGFR-RAD51 can activate MAPK and PI3K/Akt pathways and promote cytokine-independent cell proliferation and colony formation, which are hallmarks of tumour cells (Konduri et al., 2016). Other EGFR fusions in NSCLC include fusions with purine-rich element binding protein B (PURB), septin 14 gene (SEPTIN14) and a recently discovered fusion partner, kinesin family member 5B (KIF5B) (Konduri et al., 2016; Zhu et al., 2019; Xu and Shao, 2020). EGFR can be abnormally activated through kinase domain duplications (KDDs) as well. EGFR-KDDs arise from in-frame tandem duplications of EGFR exons 18–25. Activation of EGFR-KDD occurs through the formation of ligand-independent intra-molecular dimers, which in turn amplifies signaling via ligand-dependent inter-molecular dimers (Du et al., 2021). EGFR-KDD has mostly been studied in lung cancer with regard to clinical outcomes (Wang et al., 2019; Chen et al., 2020). However the first case of EGFR-KDD was reported in a patient with esophageal squamous cell carcinoma, suggesting that it may be linked to hyper-progressive disease (Wang et al., 2020). Several studies also found that EGFR can be activated in an autocrine manner. Autocrine signaling occurs when both the target cell and secreting cell are the same cell. Autocrine signaling has been demonstrated to maintain cancer stem cells and also activate EGFR in tumour cells (Wu et al., 2007; Kim et al., 2012).

2.2.2 Vascular Endothelial Growth Factor Receptor

There are three types of VEGFRs namely VEGFR1, VEGFR2, and VEGFR3 whereas there are five structurally related VEGF ligands including VEGFA, VEGFB, VEGFC, VEGFD, and placenta growth factor (PIGF) (Rapisarda and Melillo, 2012). There are also co-receptors involved in ligand binding called neuropilins (NRPs). Normal activation of VEGFRs generally lead to biological processes like angiogenesis, lymphangiogenesis, migration of endothelial cells, fatty acid uptake, etc. (Rapisarda and Melillo, 2012). VEGFRs and their ligands have been found to be expressed in lung (Tanno et al., 2004; Seto et al., 2006), breast (Filho et al., 2005; Zhao D. et al., 2015), colorectal (Lesslie et al., 2006), prostate (Chen et al., 2004), gastric (Yonemura et al., 2001) cancers. Overexpression is the most common mechanism of abnormal activation in VEGFRs. VEGFR1, and VEGF expressions were found to be elevated in pancreatic cancer cells leading to the activation of the MAPK pathway, which promoted cancer cell growth (Itakura et al., 2000). Meanwhile, an examination of 156 human gastric cancer specimens detected high expressions of VEGFR2, which correlated with poor overall survival (OS) (Lian et al., 2019). Using cDNA construct-transfected cells, they also found that VEGFR2 overexpression accelerated cell proliferation and increased cell invasive properties. VEGFR2 overexpression was also found in ovarian cancer cells (Spannuth et al., 2009), and it was linked to lower E-cadherin expression in breast cancer cells (Yan et al., 2015), suggesting its role in epithelial-mesenchymal transition. However, contradictory results were shown in a human carcinoid cell line whereby downregulation of VEGFR2 correlated to lower E-cadherin expression, suggesting the alternate roles of VEGFR2 in different cancers (Silva et al., 2011). The expression of VEGFR1, VEGFR2, and VEGFR3 has also been demonstrated to vary between the different stages of cervical (Van Trappen et al., 2003), prostate (Grivas et al., 2016) and ovarian (Klasa-Mazurkiewicz et al., 2011) cancers, with VEGFR3 being commonly overexpressed in the later stages. Autocrine activation of VEGFR occurs when VEGF ligands produced by the cancer cells proceed to activate the VEGFRs present on the same cancer cells. This autocrine feed-forward loop has been commonly demonstrated between VEGF:VEGFR2 (Jackson et al., 2002; Chatterjee et al., 2013; Song et al., 2019) and VEGFC:VEGFR3 (Kodama et al., 2008; Matsuura et al., 2009; Chen et al., 2010). Autocrine VEGF signaling also modulates treatment efficacy towards small molecule inhibitors in liver and gastric cancer, whereby higher expressions of VEGFR1/2 within the autocrine loop resulted in higher drug-induced inhibition of cell proliferation and delayed tumour growth (Peng et al., 2014; Lin et al., 2017).

2.2.3 Fibroblast Growth Factor Receptor

There are seven types of FGFRs encoded by four different genes, which are FGFR1, FGFR2, FGFR3, and FGFR4. All of them have two different isoforms produced by alternative splicing except for FGFR4. On the other hand, over twenty FGFs can be grouped into seven families (Porta et al., 2017). FGFR signaling plays an important role during embryonic development and adult life. In cancers containing genetically altered FGFRs, the most frequent alteration can be found in FGFR1 (49%), followed by FGFR3 (23%), FGFR2 (19%), and lastly FGFR4 (7%) (Liu et al., 2021). The most common alteration is the amplification of FGFR genes and based on meta-analysis data, it mainly occurred in lung, breast, and gastric cancers (Chang et al., 2014). FGFR1 amplification was present in approximately 15–18% of lung squamous cell carcinoma patients as shown by three separate studies examining cases from 2000 to 2013 (Heist et al., 2012; Craddock et al., 2013; Monaco et al., 2015). FGFR1-amplified lung and breast cancer cells were shown to have enhanced activation of MAPK and PI3K signaling pathways, increased ligand-dependent signaling, and increased expression of stem cell markers (Turner et al., 2010; Ji et al., 2016). In gastric cancers, FGFR2 amplification was linked to poor progression free survival and overall survival (Matsumoto et al., 2012; Su et al., 2014; Hur et al., 2020), however it was also associated with high sensitivity towards FGFR inhibitors, suggesting the benefits of patient stratification based on FGFR amplification status (Xie et al., 2013; Pearson et al., 2016). Besides FGFR amplification, a comprehensive list of approximately 200 point mutations have also been found in FGFRs (Gallo et al., 2015). Mutations present in all four FGFR receptors were found in breast, colon, brain, lung and head and neck squamous cell carcinomas (Gallo et al., 2015). Acquired resistance to targeted therapies has also been linked to FGFR polymorphisms and gatekeeper mutations like V561M, leading to constitutive activation of FGFR1 (Cowell et al., 2017; Ryan et al., 2019; Mao et al., 2020). FGFR2 and FGFR3 are commonly involved in the formation of oncogenic gene fusions (Porta et al., 2017). The first gene fusion discovered was between FGFR3 and the transforming acidic coiled-coil containing protein (TACC3) forming FGFR3-TACC3 in glioblastoma (Singh et al., 2012; Parker et al., 2013). FGFR3-TACC3 fusions have been observed in lung (Capelletti et al., 2014; Wang et al., 2014), cervical (Carneiro et al., 2015), bladder (Nassar et al., 2018), and nasopharyngeal (Yuan et al., 2014) cancers and usually lead to increased cell proliferation, *in vitro* transforming abilities, and activation of MAPK and ERK signaling (Nelson et al., 2016). FGFR gene fusions usually involve partners possessing dimerization domains that allow ligand-independent receptor dimerization resulting in constitutive activation (Parker et al., 2014). Other FGFR gene fusions include BAG4-FGFR1, FGFR2-BICC1, FGFR2-CASP7, FGFR2-AFF3, and FGFR3–BAIAP2L1 (Wu et al., 2013).

2.2.4 Platelet-Derived Growth Factor Receptor

There are two platelet-derived growth factors which are PDGFRα and PDGFRβ, also known as PDGFRA and PDGFRB. These two receptors are activated by five PDGFs which include PDGF-AA, PDGF-AB, PDGF-BB, PDGF-CC, and PDGF-DD (Fredriksson et al., 2004). Based on The Cancer Genome Atlas (TCGA) data, gene alterations in the PDGF family of ligands and receptors most commonly occur in lung cancer, colon cancer, and glioblastoma (Farooqi and Siddik, 2015). PDGFRB mutations in cancer have not been studied widely however, PDGFRA mutations are frequently observed in gastrointestinal stromal tumours (GISTs), especially in exon 18 (Heinrich et al., 2003; Daniels

et al., 2011; Joensuu et al., 2015). PDGFRA and KIT mutations are associated with site and origin of tumours (Penzel et al., 2005), while gain-of-function mutation, V536E, led to increased phosphorylation of ERK and STAT5, causing constitutive receptor activation (Velghe et al., 2014). These mutations can occur on the regulatory domains (extracellular domain and juxtamembrane domain) or the enzymatic domain (tyrosine kinase domain (TKD)), which can lead to ligand-independent receptor dimerization or even kinase activation without receptor dimerization altogether (Lasota and Miettinen, 2006). Overexpression of PDGFRA mRNA has been recently observed in oral squamous cell carcinoma with links to metastasis and reduced patient survival (Ong et al., 2017; Ong et al., 2018). In lung cancer, ovarian cancer and medulloblastomas, PDGFR overexpression was associated with shorter overall survival, co-amplification with other RTKs and potential prognostic value (Lassus et al., 2004; Blom et al., 2010; Tsao et al., 2011).

PDGFR gene fusions are widely observed in hematological malignancies like acute myeloid leukemia, lymphoblastic leukemia and other myeloproliferative neoplasms (MPNs). PDGFRA fuses with five other intracellular proteins and one RTK, whereas PDGFRB fusions occur with twenty-nine other intracellular proteins (Appiah-Kubi et al., 2017). FIP1L1-PDGFRA is the most recurrent PDGFRA fusion gene that was first observed in patients with hypereosinophilic syndrome (Cools et al., 2003). Kinase activation of FIP1L1-PDGFRA is mediated by the disruption of the juxtamembrane domain of PDGFRA (Stover et al., 2006). Other gene fusion partners of PDGFRA include the breakpoint cluster region (BCR) (Yigit et al., 2015), KIF5B (Score et al., 2006), the CDK5 regulatory subunit associated protein 2 (CDK5RAP2) (Walz et al., 2006) and the ETS variant transcription factor 6 (ETV6) (Yoshida et al., 2015). As for PDGFRB, approximately 70 fusions have been identified with most fusion partners normally containing an oligomerization motif that mediates dimerization, causing continuous kinase domain activation in myeloid neoplasms (Campregher et al., 2017; Sheng et al., 2017; Xu et al., 2020). Autocrine PDGFR signaling plays an essential role in cancer progression in ovarian (Matei et al., 2006), breast (Jechlinger et al., 2006), thyroid (Adewuyi et al., 2018), and brain (Lokker et al., 2002) cancers. Both PDGFR and its ligands expressed in these tumours leads to an autocrine loop that fuels activation of downstream PI3K/Akt, MAPK and STAT pathways, in addition to the maintenance of EMT and enhanced metastasis (Jechlinger et al., 2006; Matei et al., 2006; Adewuyi et al., 2018).

2.2.5 Insulin Receptor

The insulin receptor (IR) family consists of IGF-1R, IRA, IRB, IGF-1R/IR (hybrid), and IGF-2R. This review will focus on IGF-1R and IGF-2R, which are more frequently studied. IGF-1R is activated by ligands IGF-1 and IGF-2, while IGF-2R is a non-signaling receptor that mainly functions to clear IGF2 from the cell surface (Chen and Sharon, 2013). IGF-1R is overexpressed in a variety of cancers including colon (Shiratsuchi et al., 2011), pancreatic (Hakam et al., 2003), prostate (Aleksic et al., 2017), lung (Gong et al., 2009; Badzio et al., 2010), and breast (Jones et al., 2007) cancers. High levels of total IGF-1R were associated with higher tumour grade while higher levels of cytoplasmic IGF-1R were linked to a greater risk of post-radiotherapy recurrence in prostate cancer patients (Aleksic et al., 2017). Meanwhile, overexpression of IGF-1R in transgenic mice induces mammary tumour formation through activation of Akt, Erk1/Erk2, and STAT3 (Jones et al., 2007). Moreover, overexpression of IGF-1R also decreases tumour latency time, increases the proliferative genetic signature and enhances migration potential in mammary tumours in addition to protecting cells against stresses of the tumour microenvironment and apoptosis (Resnicoff et al., 1995; Valentinis and Baserga, 1996; Peretz et al., 2002; Ter Braak et al., 2017). IGF-2R has been found to be mutated in 60% of lung squamous cell carcinomas, while levels of IGF-2R appears to be much higher in the malignant stages of endometrial carcinomas (Kong et al., 2000; Pavelić et al., 2007). The existence of an autocrine loop was also found between IL-6 and IGF-1R whereby IL-6 induced expression of itself, forming a positive feedback loop further activating IL-6R, IGF-1R, IGF-1, and IGF-2 in NSCLC (Zheng et al., 2019). In acute myeloid leukemia, autocrine production of IGF-1 was shown to be responsible for the constitutive activation of IGF-1R and PI3K/Akt (Chapuis et al., 2010). Meanwhile, tumour cells have been proposed to secrete IGF-2 which binds to IGF-1R, increasing the rate of cellular proliferation through autocrine/paracrine signaling (Rasmussen and Cullen, 1998; Pavelić et al., 2003).

2.2.6 Hepatocyte Growth Factor Receptor/C-Met

The hepatocyte growth factor receptor (HGFR), also known as MET or c-Met, is encoded by the MET gene, and its ligand is the hepatocyte growth factor (HGF) (Kumar et al., 2018). There is another Met-related RTK called Ron which binds to HGF-like protein/macrophage stimulating-protein (HGFL) (Wagh et al., 2008); however, this review will only focus on c-Met. C-Met has been found to be overexpressed in breast (Zhao et al., 2017), lung (Gumustekin et al., 2012; Awad et al., 2016), ovarian (Sawada et al., 2007), colon (Lee et al., 2018), cervical (Baykal et al., 2003), renal (Miyata et al., 2003), and blood (Jücker et al., 1994) cancers. Overexpression of HGF/c-Met was observed in NSCLC which led to subsequent lymph node invasion mediated by RhoA overexpression (Gumustekin et al., 2012). Mutations were also detected in the TKD of c-Met in this study; however, results suggested that it did not significantly impact RTK activation in NSCLC. In contrast, a more recent study reported MET exon 14 mutations that occurred predominantly in older patients with lung adenocarcinomas. Patients with advanced-stage NSCLC having these mutations also had concurrent MET gene amplification (Awad et al., 2016). A meta-analysis showed that c-Met overexpression correlated to distant metastasis, large tumour size and high histologic grade in breast cancer (Zhao et al., 2017). MET gene fusions have been primarily identified in lung cancer such as the HLA-DRB1-MET (Davies et al., 2017; Blanc-Durand et al., 2020), KIF5B-MET (Gow et al., 2018), MET-UBE2H (Zhu et al., 2018a), and MET-ATXN7L1 (Zhu et al., 2018b). The first case of HLA-DRB1-MET fusion was reported, however further studies are required to elucidate the specific

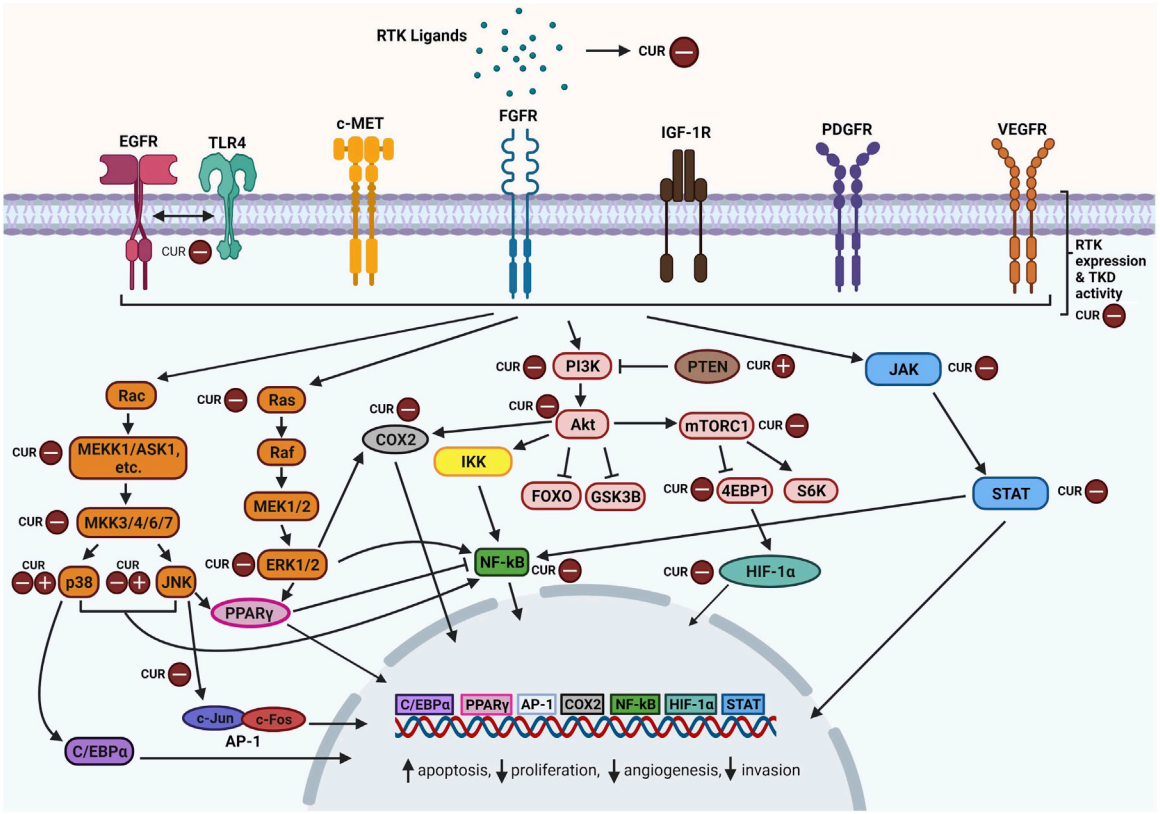

FIGURE 2 | Overview of curcumin-inhibition of RTKs and downstream MAPK, PI3K/Akt, JAK/STAT, and NF-κB pathway components. Abbreviations: RTK: Receptor tyrosine kinase; CUR: Curcumin, EGFR: Epidermal growth factor receptor, TLR4: Toll-like receptor 4, c-MET: Mesenchymal epithelial transition factor/ Hepatocyte growth factor receptor; FGFR: Fibroblast growth factor receptor; IGF-1R: The insulin-like growth factor 1 receptor; PDGFR: Platelet-derived growth factor receptor; VEGFR: Vascular endothelial growth factor receptor; TKD: Tyrosine kinase domain; Rac: Ras-related C3 botulinum toxin substrate; ASK1: Apoptosis signal-regulating kinase 1; C/EBPα: CCAAT/enhancer-binding protein alpha; JNK: c-Jun N-terminal kinases; AP-1: Activator protein 1; Ras: Rat sarcoma virus protein; Raf: Rapidly accelerated fibrosarcoma protein; MEK: Mitogen-activated protein kinase kinase; ERK: Extracellular signal-regulated kinase; PPARγ: Peroxisome proliferator-activated receptor γ; COX2: Cyclooxygenase-2; PI3K: Phosphoinositide 3-kinase; PTEN: Phosphatase and tensin homolog; Akt: Ak strain transforming; IKK: Inhibitor of nuclear factor kappa B kinase; NF-κB: nuclear factor kappa-light-chain-enhancer of activated B cells; FOXO: Forkhead box transcription factors; GSK3B: Glycogen synthase kinase 3 beta; Mtorc1: Mechanistic target of rapamycin complex 1; 4EBP1: Eukaryotic translation initiation factor 4E (eIF4E)-binding protein 1; S6K: Ribosomal protein S6 kinase; HIF-α: Hypoxia-inducible factor alpha; JAK: Janus kinase; STAT: Signal transducer and activator of transcription. Created with BioRender.com.

mechanisms of the fusion gene (Davies et al., 2017). Meanwhile, it was also proposed that the MET-UBE2H fusion protein could be a novel resistance mechanism against EGFR-TKI treatment (Zhu et al., 2018a). MET fusions that occur at exon 15 and contain the 3' MET kinase domain are thought to become activated due to constitutive dimerization of MET (Blanc-Durand et al., 2020).

Autocrine activation of HGF/c-Met signaling has also been described as a novel strategy leading to resistance against multi-kinase inhibitors in heptatocellular carcinoma (Firtina Karagonlar et al., 2016). Resistant cells were shown to have upregulated levels of HGF and activation of c-Met which when inhibited, resulted in lower migration and invasion capabilities (Firtina Karagonlar et al., 2016). Other studies examining hepatocellular carcinoma also found autocrine systems involving the Scatter factor (SF) and HGF/c-Met in metastasis as well as angiogenesis involving VEGF (Xie et al., 2001; Horiguchi et al., 2002). Autocrine activation of the MET receptor was also observed in colorectal cancer and acute myeloid leukemia involving components like β-catenin and co-activation of FGFR1 (Rasola et al., 2007; Kentsis et al., 2012).

3 RECEPTOR TYROSINE KINASE SIGNALING PATHWAYS TARGETED BY CURCUMIN IN CANCER

Activation of RTKs leads to a ripple effect whereby multiple signaling cascades are triggered to produce different outcomes. Curcumin has been found to modulate the expression of RTKs, their ligands and components particularly within their downstream MAPK, PI3K/Akt, JAK/STAT, and NF-κB pathways (**Figure 2**). Curcumin-mediated mechanisms mainly involve inhibition of specific components and in some cases, upregulation as well. Favourable outcomes have been observed in cancer cells following curcumin treatment including enhanced apoptosis, reduced cellular proliferation, reduced angiogenesis

and reduced migration. Curcumin appears to act as a tyrosine kinase inhibitor as reviewed by Golonko et al. (2019) and Farghadani and Naidu (2021), similar to the mechanism of TKI drugs but with more pronounced effects. In this section, we take a closer look at how curcumin modulates these signaling pathways.

3.1 Effects of Curcumin on Receptor Tyrosine Kinase Signaling Pathways in Cancer

3.1.1 Mitogen-Activated Protein Kinase

The mitogen-activated protein kinase (MAPK) pathway is one of the main pathways involved in the regulation of cellular proliferation, differentiation, development, apoptosis, and transformation. Three MAPK families have been well characterised which include extracellular signal-regulated kinase (ERK), Jun kinase (JNK) and p38 kinase. MAP kinases are activated in a cascade fashion following stimulation by growth factors, cytokines, stress and ceramides among others. A MAP kinase cascade is normally a series of activations involving a MAPK kinase kinase (MAPKKK), a MAPK kinase (MAPKK), and a MAP kinase (MAPK) (Zhang and Liu, 2002). The Raf-MEK-ERK is one of the well characterised MAPK signaling pathways. The multistep process that occurs after RTK activation starts with recruitment of adaptor proteins (Grb2, Sos, etc.) followed by activation of c-Raf (MAPKKK), MEK1/2 (MAPKK) and finally ERK1/2 (MAPK). ERK then translocates to the nucleus and phosphorylates transcription factors like the ternary complex factor (TCF) Elk-1, c-Myc, serum response factor accessory protein Sap-1a, Ets1, Tal, and others (Zhang and Liu, 2002). The JNK proteins also known as stress-activated protein kinases (SAPKs) are primarily activated by stress conditions like DNA damage, UV irradiation, and inflammation (Katz et al., 2007). Growth factors like EGF, PDGF, and FGF are less efficient stimulants (Kyriakis and Avruch, 2001). JNKs are directly phosphorylated by MKK4 and MKK7 (MAPKKs) while these MAPKKs are dually phosphorylated by MAPKKKs which include the MEKK family, the mixed-lineage kinase family, the apoptosis signal-regulating kinase family, TAK1 and TPL2 (Davis, 2000). Upon activation, JNKs can activate a range of proteins including the activator protein-1 (AP-1) which is formed through the dimerization of Jun (c-Jun, JunB, and JunD) and Fos (c-Fos, FosB, Fra-1, and Fra-2) proteins. Lastly, the p38 kinase has four isoforms, α, β, γ, and δ (Canovas and Nebreda, 2021). They can be phosphorylated by the MAPKKs, MKK3, MKK4, and MKK6. Prior to this, these MAPKKs are phosphorylated by MAPKKKs such as ASK1, DLK, MEKK3, MEKK4, TAK1, and etc. Overall, growth factors mainly activate the ERK1/2 cascade, partially activate JNK, and rarely activate p38 (Katz et al., 2007). Hence, this review will mainly focus on the ERK pathway.

In cancer, constitutive activation of ERK signaling is normally caused by RTK overexpression and activating mutations in RTKs or components like Ras or B-Raf (Dhillon et al., 2007). Activating mutations in K-Ras and N-Ras have been observed in many cancers and commonly lead to inefficient GTP hydrolysis, leaving Ras in a constantly active, GTP-bound state (Dhillon et al., 2007; Prior et al., 2020). There are three isoforms of Raf namely, Raf-1/C-Raf, B-Raf, and A-Raf which are direct effectors of Ras. B-Raf gene mutations are present most commonly in melanoma (40–70%) and to a lesser extent in thyroid, colorectal and ovarian cancers (Rahman et al., 2013). The missense mutation, V600E, is the most common B-Raf mutation (~90% of cancers) that results in constitutive activation of the MEK-ERK pathway without external stimuli, causing uncontrolled cellular proliferation (Cantwell-Dorris et al., 2011). C-Raf and A-Raf mutations are quite rare and it was found that C-Raf had a low basal kinase activity, which may explain its weak oncogenic effect (Emuss et al., 2005). MEK1/2 mutations are rare as well and they are mainly influenced by upstream mutations in Ras/Raf. Lastly, mutations in ERK were found to confer resistance to ERK and Raf/MEK inhibitors by disrupting drug binding and maintaining levels of ERK activity in B-raf mutant melanoma cells (Goetz et al., 2014). Oncogenic activation of JNK1 and JNK2 have been found in liver (Chang et al., 2009), pancreatic (Tian et al., 2021), bladder (Pan et al., 2016), and gastric (Mishra et al., 2010) cancers. The JNK pathway also promotes cancer cell survival via autophagy involving Bcl-2, tumour immune evasion, compensatory cell proliferation, and interaction with other signaling components such as NF-κB, p38, and JunD (Wu Q. et al., 2019). As for p38, it also acts as a tumour suppressor and inhibition of p38 mediates Ras-induced transformation (Dhillon et al., 2007). Tumour sizes have been found to be inversely correlated to p38 activity in hepatocellular carcinoma (Iyoda et al., 2003). Oncogenic MAPK signaling activated by RTKs are found in various cancers (Wu et al., 2006; Wang et al., 2012; Tang et al., 2017; Jiang et al., 2020).

In lung cancer cells, two separate studies examined the effects of curcumin on RTKs and their pathway components (Lev-Ari et al., 2006; Lev-Ari et al., 2014). Both studies found that curcumin downregulated expressions of COX-2 and *p*-ERK1/2 in a dose-dependent manner, however only one study observed downregulation of EGFR (Lev-Ari et al., 2006). EGFR signaling has been shown to induce transcription of COX-2 likely through the activation of MEK/ERK pathway, which explains the simultaneous downregulation of these components by curcumin resulting in decreased survival and enhanced apoptotic effects (Huh et al., 2003; Chi et al., 2016). Curcumin also showed dose-dependent inhibition of MyD88, TLR4, and EGFR in lung cancer cell lines (Zhang et al., 2019). Studies have found that TLR4 requires EGFR to signal and activation of TLR4 has also been linked to the MAPK pathway (Qian et al., 2008; De et al., 2015). It is possible that curcumin indirectly modulates the MAPK pathway by synergistic targeting of EGFR and TLR4. In addition, this study also found that curcumin lowered the expression levels of c-Jun and c-Fos proteins which make up AP-1, a major target of JNK. This led to decreases in other cell cycle proteins like cyclin A1, cyclin B1, cyclin D1, and etc. suggesting curcumin's role in regulating cell cycle transitions via MAPK signaling activated by RTKs (Zhang et al., 2019). Another study found that curcumin inhibited VEGF and a wide range of downstream MAPK-related components including c-Jun-p, Ras, Grb2, MEKK3, and MKK7, however, levels of

JNK and ERK seemed to be upregulated (S. S. Lin et al., 2009). JNK 1 and 2 have been observed to have opposing functions (Yin and Yang) in cellular environments (Wu Q. et al., 2019). Studies have found that JNK1 mediates cell survival while JNK2 contributes to apoptosis however, the opposite has also been observed (Arbour et al., 2002; Liu et al., 2004). Hence, through inhibition of VEGF, curcumin may have indirectly upregulated the pro-apoptotic JNK protein levels since JNK is not a direct target of curcumin (Chen and Tan, 1998; S. S.; Lin et al., 2009). Lastly, the effects of curcumin was examined in an *in vivo* cancer model involving transgenic mice expressing VEGF-A (Tung et al., 2011). Curcumin significantly downregulated levels of VEGF protein and also mRNA levels of *vegf, vegfr2 (kdr), nrp-1, egfr,* and *erk2*. *Nrp-1* is the co-receptor of *vegfr2* and it was suggested that curcumin-induced downregulation of its downstream pathways, resulted in reduced VEGF expression. This was also evidenced by downregulation of *erk2*, reaffirming that the MAPK pathway plays a role in curcumin-mediated RTK inhibition (Tung et al., 2011).

In colon cancer, curcumin downregulated the EGFR gene expression by suppressing the early growth response-1 (*egr-1*) gene and the transactivation activity of Egr-1, a transcription factor that binds to the *egfr* promoter (Chen et al., 2006). Suppression of *egr-1* gene by curcumin was via disruption of ERK signaling which led to a decrease in Elk-1 phosphorylation (Chen et al., 2006). Besides, curcumin also suppresses EGFR expression by activating PPARγ in colon carcinoma cell lines (Chen and Xu, 2005). PPARγ can be inactivated through phosphorylation by ERK and/or JNK. It was found that curcumin-induced inhibition of MAPK activity led to increased activation of PPARγ and subsequent EGFR gene downregulation (Chen and Xu, 2005). Meanwhile, treatment of colon cancer cells with curcumin or dasatinib induced significant reduction of *p*-EGFR while combination treatment led to much greater reduction of both *p*-EGFR and *p*-IGF-1R (Nautiyal et al., 2011). Accordingly, downstream *p*-ERK1/2 levels were also reduced by a larger magnitude after combination treatment which may have resulted in the reduction of COX-2 levels that was observed as well. In colon cancer cells, after 3 h of exposure to high concentration of curcumin (100 μmol/L), a cDNA microarray analysis showed that levels of MAPK-related genes like MAP3K10 and MAP4K2 and also VEGF and FGFR1 were upregulated (Van Erk et al., 2004). Several other MAPK genes like MAP2K2 and MAPK8 were downregulated after exposure to low concentrations of curcumin (30 μmol/L) for 3 h. The high concentration of curcumin used in this study was found to decrease the cell number and result in floating cells hence, the several unexpected gene expression changes observed could be toxic-related effects of curcumin (Van Erk et al., 2004).

In breast cancer cell lines that overexpress HER-2 (BT-474 and SK-BR-3-h), curcumin downregulated the HER-2 oncoprotein and also the phosphorylation of MAPK in a dose-and time-dependent manner (Lai et al., 2012). Meanwhile, in triple negative breast cancer (TNBC) cells curcumin did not alter the expression of EGFR and ERK1/2 however, it significantly reduced the levels of phosphorylated EGFR and ERK1/2, showing that it specifically inhibits activation of EGFR and its downstream signaling molecules to reduce cell proliferation (Sun et al., 2012). Curcumin was also found to reduce EGFR activation and EGF-induced phosphorylation of ERK1/2 as well as JNK activity in breast cancer cells however, there was a lack of inhibition of p38 (Squires et al., 2003). This provides evidence that curcumin inhibition occurs via RTK signaling pathways since RTKs mainly activate ERK and JNK (partially) and p38 to a much lesser extent.

Using pancreatic cancer cells, it was shown that curcumin reduced hyperglycemia-driven EGF-induced metastatic abilities (Li W. et al., 2019). Under high-glucose conditions (diabetes), which is a risk factor for pancreatic cancer, curcumin suppressed EGF levels and activation of EGFR and ERK, resulting in reduced invasive ability and inhibition of metastatic-related factors (Li W. et al., 2019). Expression of COX-2, EGFR and *p*-ERK1/2 was also suppressed by curcumin in pancreatic adenocarcinoma cells similar to what was observed in lung adenocarcinoma cells (Lev-Ari et al., 2006). Furthermore, curcumin treatment for 24 h was found to decrease the expression of VEGFR1 and VEGFR2 in HUVECs (Fu et al., 2015). Human umbilical vein endothelial cells (HUVECs) are commonly used to understand tumour angiogenesis due to their major role in vascular homeostasis. Phosphorylation of ERK was also reduced reflecting the ability of curcumin to inhibit growth and migration of endothelial cells via blocking VEGFRs and downstream MAPK signaling pathway. Curcumin also reduced COX-2 expression in VEGF-activated human intestinal microvascular endothelial cells (HIMECs) via inhibition of phosphorylation of MAPK pathway components like p44/42 MAPK, p38 MAPK, and JNK (Binion et al., 2008). In oral cancer, curcumin upregulates the expression of insulin-like growth factor binding protein-5 (IGFBP-5) by increasing the nuclear expression of CCAAT/enhancer-binding protein α (C/EBPα), which is a transcriptional regulator of IGFBP-5 (Chang et al., 2010). This upregulation of IGFBP-5 mediated by activation of p38 by curcumin allowed it to bind to IGF, limiting the activation of IGF-1R and suppressing oral carcinogenesis. Meanwhile, a combination of curcumin and cetuximab decreased levels of phosphorylated EGFR, ERK, JNK, and surprisingly p38 in cisplatin-resistant oral cancer cells which contrasts the curcumin-mediated p38 activation observed by Chang et al. (2010). Accordingly, it has been found that curcumin differentially activates/inhibits p38 in different cancers (Watson et al., 2010; Wang et al., 2013; Tung et al., 2016); however, further research is required to elucidate how RTKs fit in this process. Curcumin treatment also abrogated HGF-induced epithelial-mesenchymal transition (EMT) in oral squamous cell carcinoma and prostate cancer cells by reducing levels of phosphorylated c-Met (HGFR) and inhibiting ERK activation (Hu et al., 2016; Ohnishi et al., 2020). Furthermore, levels of *p*-ERK, VEGF, and HIF-α were reduced by curcumin in liver cancer cells the same way they were reduced in IGF-1R-knockout liver cancer cells, suggesting that curcumin suppresses tumour progression in an IGF-1R-dependent manner involving the MAPK pathway (Chen et al., 2018). Curcumin also stimulated the expression of PPARγ by interrupting EGF and PDGF

signaling in rat hepatic stellate cells (Zhou et al., 2007). This interruption involves repressing phosphorylation of PDGFR-β and EGFR and also reducing *p*-ERK and *p*-JNK. This is the second study observing the effects of curcumin on RTKs through PPARγ activation mediated by MAPK-inhibition.

3.1.2 Phosphoinositide 3-Kinase/Akt/Mechanistic Target of Rapamycin

The phosphoinositide 3-kinase (PI3K)–Akt pathway is an ubiquitous signaling network that regulates growth, metabolism, biosynthesis of macromolecules and cellular homeostasis. It is mainly activated by growth factors, insulin, and cytokines. There are three classes of PI3K enzymes, however only class I PI3Ks are involved in cancer (Zhao and Vogt, 2008). Class I PI3Ks have four different isoforms (p110α, β, γ, and δ) which are encoded by *PIK3CA, PIK3CB, PIK3CG,* and *PIK3CD* (Fruman et al., 2017). Under normal physiological conditions, PI3K activation at the plasma membrane is followed by phosphorylation of phosphatidylinositol 4, 5-bisphosphate (PtdIns(4,5)P2) (PIP_2) to produce phosphatidylinositol 3,4,5-trisphosphate (PtdIns(3,4,5)P3) (PIP_3) which acts as a second messenger (Hoxhaj and Manning, 2020). PIP_3 then acts as a docking site and recruits proteins processing the pleckstrin homology (PH) domain such as the serine-threonine kinase, Akt. There are three isoforms of Akt (Akt1, Akt2, and Akt3) and once bound to PIP_3, it is phosphorylated by phosphoinositide-dependent protein kinase 1 (PDPK1/PDK1) and mechanistic target of rapamycin (mTOR) complex 2 (mTORC2), increasing its activity (Fruman et al., 2017). Activated Akt phosphorylates many downstream substrates namely three critical proteins which are tuberous sclerosis complex 2 (TSC2), glycogen synthase kinase 3 (GSK3) and the forkhead box O (FOXO) transcription factors (TFs). Phosphorylation of TSC2 leads to activation of mTORC1 while phosphorylation of GSK3 leads to proteasomal degradation of several TFs like MYC, SREBP, nuclear factor erythroid 2-related factor 2 (NRF2), and HIF1α (Hoxhaj and Manning, 2020).

In cancer, there are four common genetic events that drive cancer progression which include 1) *PIK3CA* activating mutations, 2) PTEN loss-of-function mutations and deletions, 3) gain-of-function mutations in Akt-encoding genes, and lastly 4) amplification of RTKs that activate PI3K signaling (Hoxhaj and Manning, 2020). The PI3K pathway also plays a role in the control of glucose metabolism whereby constitutive activation of Akt promotes aerobic glycolysis and increased glucose uptake through GLUTs in cancer cells (Elstrom et al., 2004; Wieman et al., 2007). It also drives anabolic metabolism in excessively proliferating cells via promoting *de novo* lipid, nucleotide, and protein synthesis (Faridi et al., 2003; Porstmann et al., 2005; Saha et al., 2014). Moreover, the PI3K-Akt pathway has been found to trigger ROS-producing processes as well however more research in needed to elucidate the exact downstream pathways involved in ROS production in cancer cells (Chen et al., 2003; Hoxhaj and Manning, 2020). Activation of RTKs and downstream PI3K signaling have been implicated in acceleration of tumour growth, malignant transformation, and resistance in different cancers (Zhang et al., 2007; Jung et al., 2015; Starska et al., 2018).

In lung cancer, curcumin has been shown to downregulate EGFR expression by inducing expression of an E1-like ubiquitin-activating enzyme, UBE1L, which represses EGFR protein expression and promotes EGFR internalization (Jiang et al., 2014). Curcumin also reduced Akt phosphorylation and repressed the EGFR/Akt pathway through UBE1L induction. Levels of PI3Kwere also reduced in lung cancer cells following curcumin treatment, which is likely one of the pathways that resulted in the reduced VEGF expression that was also observed (S.-S. Lin et al., 2009). Furthermore, curcumin pre-treatment of lung cancer cells decreased the HGF-induced phosphorylation of c-Met and downstream PI3K signaling components like Akt, mTOR, and S6, leading to EMT inhibition (Jiao et al., 2016).

In colon cancer, curcumin combined with 5-fluorouracil (5-FU) and oxaliplatin (FOLFOX) were found to induce higher levels of apoptosis by reducing both the expression and activation of EGFR, IGF-1R, HER-2, and HER-3 by a greater magnitude then either agent alone (Patel et al., 2008). An analysis of downstream signaling components also found downregulation of expression and activation of Akt and COX-2 after curcumin and FOLFOX combination treatment. COX-2 activation and expression has been linked to Akt phosphorylation in several cancers, hence curcumin may mediate COX-2 activation by targeting RTKs and the downstream PI3K/Akt pathway (St-Germain et al., 2004; Glynn et al., 2010). Similar results were also achieved when curcumin was used to treat FOLFOX-surviving colon cancer cells, highlighting the importance of EGFR/IGF-1R/Akt signaling inhibition by curcumin in chemo-resistant cells (Patel et al., 2010). A combination of curcumin and dasatinib also resulted in the downregulation of the EGFR/IGF-1R/Akt axis, further providing evidence that this may be one of the primary mechanisms of inhibition by curcumin either alone or in synergistic combination with other anti-cancer agents (Nautiyal et al., 2011a). Gene expression analyses carried out on colon cancer cells lines found upregulation of many genes including VEGF, FGFR1, and Akt after exposure to high concentration of curcumin which contrasts the usual downregulation, however it could be toxic-related effects of the fairly high concentration of curcumin used as stated before (Van Erk et al., 2004).

In breast cancer, it was found that curcumin combined with herceptin (trastuzumab) was effective against herceptin-resistant breast cancer cells, likely mediated by the decreased levels of HER-2 oncoprotein and phosphorylated Akt (Lai et al., 2012). In another study, curcumin also inhibited the basal phosphorylation of Akt/PKB in breast cancer cells but not directly, suggesting that it could be due to the decrease in EGF-induced EGFR activation that was observed (Squires et al., 2003). The study by Borah at et al. (2020) aimed to inhibit the Hh/Gli-EGFR signaling pathway in breast cancer by co-delivering curcumin and a Hh/Gli small molecule antagonist GANT61 via polymeric nanoparticles. Based on immunofluorescence studies, they found that the GANT61-curcumin PLGA NPs managed to decrease EGFR protein expression and also PI3K expression, which may contribute to the inhibitory migration potential of breast adenocarcinoma cells.

In liver cancer, curcumin decreased VEGF, PI3K, and Akt expression, with one study suggesting that this effect is mediated via curcumin-inhibition of IGF-1R to suppress angiogenesis (Chen et al., 2018; Pan et al., 2018). Curcumin also reduced the phosphorylated PI3K/Akt levels by inhibiting tyrosine phosphorylation of PDGFRβ and EGFR, which led to activation of PPARγ and subsequent induction of apoptosis (Zhou et al., 2007). It was found that a combination of curcumin and metformin significantly reduced PI3K, *p*-Akt, and *p*-mTOR while also significantly increasing expression of PTEN, which is a negative regulator of the PI3K pathway (Zhang et al., 2018). Combination treatments for curcumin and β-phenylethyl isothiocyanate (PEITC) as well as curcumin and docetaxel were found to decrease EGFR expression and activation, PI3K expression, and *p*-Akt which led to enhanced apoptosis and reduced cell proliferation in prostate cancer cells (Kim et al., 2005; Banerjee et al., 2017). Furthermore, in hyperglycemic-pancreatic and oral cancer cells, curcumin was found to reduce cell proliferation by inhibiting the EGF/EGFR/Akt pathway (Zhen et al., 2014; Li W. et al., 2019). Besides, curcumin also decreased gene expression of EGFR and expression of PI3K (p110α), Akt, and mTOR in tongue and hypopharynx squamous cell carcinoma (SCC), highlighting the therapeutic potential of curcumin-mediated RTK inhibition in preventing head and neck cancer progression (Borges et al., 2020). Meanwhile, another study chemically induced skin carcinogenesis in transgenic mice overexpressing IGF-1 and found that a curcumin diet significantly reduced tumour multiplicity, tumour size, and cell proliferation (Kim et al., 2014). The underlying mechanism leading to these effects was curcumin-mediated inhibition of IGF-1R, insulin receptor substrate-1 (IRS-1), Akt, S6K, and eukaryotic translation initiation factor 4E-binding protein 1 (4EBP1) phosphorylation in a dose-dependent manner (Kim et al., 2014). Lastly, curcumin downregulated phosphorylation of PI3K-p85, Akt, mTOR, and further downstream effectors 4EBP1 and S6K in bladder cancer. Interestingly, IGF-1 knockdown did not alter the inhibitory effects of curcumin, suggesting that curcumin mainly acts through the IGF-2/IGF-1R pathway and downstream PI3K signaling in bladder cancer (Tian et al., 2017).

3.1.3 Janus Kinase/Signal Transducers and Activators of Transcription

The Janus kinase (JAK)–signal transducer of activators of transcription (STAT) pathway is one of the pathways involved in RTK signal transduction and it can be activated by diverse cytokines, interferons and other related components. It allows direct communication from membrane-to-nucleus through the interaction between four Janus kinases (JAKs)—JAK1, JAK2, JAK3, and TYK2, and seven signal transducers and activators of transcription (STATs)—STAT1, STAT2, STAT3, STAT4, STAT5a, STAT5b, and STAT6 (O'Shea et al., 2015). Once a ligand binds to the receptor, receptor-associated JAKs are activated and they proceed to cross-phosphorylate each other and also the intracellular tail of their receptors. This creates a docking sites for the recruitment of cytoplasmic STATs. STATs are then activated via JAK-phosphorylation and they translocate to the nucleus to regulate gene expression by binding DNA (O'Shea et al., 2015). Many RTKs engage with the JAK/STAT pathway to promote proliferation and differentiation (Boccaccio et al., 1998; Andl et al., 2004; Masamune et al., 2005).

In cancer, constitutive JAK/STAT activation normally occurs through increased expression of ligands and activating mutations of receptors, JAKs, or STAT themselves (O'Shea et al., 2015). JAK mutations have been found widely in leukemia and many solid tumours that contribute to cancer cell migration, proliferation, and invasion (Walters et al., 2006; Jeong et al., 2008; Stelloo et al., 2016; Xu et al., 2017). STAT3 and STAT5 are also commonly mutated a variety of cancers. Mechanisms leading to their constitutive activation include lack of negative regulation, somatic mutations causing hyperactivation, overstimulation, positive feedback loops and crosstalk with other signaling pathways leading to resistance, poor prognosis, tumour progression, and worse overall survival (Zhang and Lai, 2014; Halim et al., 2020). However, studies have shown that both STAT3 and STAT5 have tumour suppressor roles, reflecting their paradoxical nature (Igelmann et al., 2019). RTKs have also been shown to promote cancer progression and tumour immunosuppression via JAK/STAT pathways (Su et al., 2018; Li P. et al., 2019; Song et al., 2020).

Curcumin was found to inhibit expression of phosphorylated STAT3, JAK1 JAK2, and JAK3 in SCLC cells (Yang et al., 2012). Levels of VEGF were also downregulated after curcumin treatment however this study focused on IL-6-dependent STAT3 activation, hence it is not certain if curcumin mediated inhibition via the RTK signaling pathway. In laryngeal squamous cell carcinoma, curcumin inhibited the expression of JAK2 and phosphorylation of STAT3, which is JAK2-dependent (Hu et al., 2014). Curcumin also inhibited VEGF mRNA and protein expression via the downregulation of this JAK2/STAT3 pathway which likely reduced VEGF-induced activation of VEGFR. However, there is only a handful of studies linking the effects of curcumin to RTKs and the JAK/STAT pathway as most studies only examine how curcumin inhibits JAK/STAT directly or via other signaling pathways.

The available literature on curcumin and JAK/STAT in cancer mainly look at how curcumin inhibits phosphorylation of various JAKs and namely STAT3 and STAT5. In blood cancers, a number of studies found that curcumin downregulated phosphorylation of JAK2, JAK3, TYK2, STAT3, STAT5a, and STAT5b (Rajasingh et al., 2006; Park et al., 2008; Petiti et al., 2019). Meanwhile, it was found that curcumin did not affect the phosphorylation of STAT proteins in chronic leukemia cells but only decreased their nuclear expression (Blasius et al., 2006). Curcumin also reduces migration, proliferation, and invasion directly by modulating levels of phosphorylated JAKs and STATs or indirectly by regulating protein inhibitors of activated STAT-3 (PIAS-3), suppressors of cytokine signaling (SOCS3), and miRNAs involved in JAK/STAT activity in a range of cancers including eye, ovarian, and endometrial cancers (Saydmohammed et al., 2010; Li Y. et al., 2018). Inhibition of the JAK/STAT pathway by curcumin in esophageal cancer cells also increased cell adhesion which is normally reduced in cancer

(Zheng et al., 2018). Combination treatment of curcumin and cisplatin managed to inhibit phosphorylation of JAK and STAT3 in ovarian and papillary thyroid cancer cells leading to enhanced proliferation and reduced stemness of potential cancer stem cells (Khan AQ. et al., 2020; Sandhiutami et al., 2021). In osteosarcoma cells, curcumin inhibited the *p*-JAK2/p-STAT3 pathway which was involved in lung metastasis whereas in lung cancer, curcumin suppressed activation of p-STAT3 both *in vitro* and *in vivo* (Alexandrow et al., 2012; Sun et al., 2019). Several studies also examined the potency of curcumin analogues, FLLL31 and FLLL32, which were designed to specifically bind to JAK2 and STAT3 SH2 domains (Lin et al., 2010b). Both analogues were found to effectively suppress *p*-JAK2 and p-STAT3 and also key apoptotic proteins (Lin et al., 2010a; Lin et al., 2010b; Abuzeid et al., 2011). FLLL32 however showed very little inhibition of RTKs like EGFR, HER2 and Met (Lin et al., 2010b). Another curcumin analogue, L48H37, also decreased the phosphorylation of JAK1, JAK2, JAK3, and STAT3 in osteosarcoma cells (Lu et al., 2020). Gene expression profiling and recent RNA sequencing technology also identified both upregulation and downregulation of JAK/STAT signaling pathway components, with some of these studies also documenting changes in RTK gene expression (Van Erk et al., 2004; Teiten et al., 2009; Zhao W. et al., 2015). Further studies are needed to clarify the link between curcumin, RTKs and the JAK/STAT pathway.

3.1.4 Nuclear Factor Kappa B

The nuclear factor kappa B (NF-κB) consists of a group of transcription factors (TFs) that are responsible for many biological processes like inflammation, cell proliferation, immunity and apoptosis (Zinatizadeh et al., 2021). This family of TFs include five proteins which are RelA, RelB, c-Rel, p100, and p150. These proteins possess the rel homology domain (RHD) that assists in dimerization, binding to DNA and interaction with specific inhibitors (Zinatizadeh et al., 2021). Inhibitors of NF4EBP-κB are from the IκB inhibitor family comprising of IκBα, IκBβ, and IκBε. The association between NF-κB and IκBs form dimers that are retained in the cytoplasm in an inactive state (Dolcet et al., 2005). The phosphorylation of IκBs by IκB-kinases (IKKs) leads to IκB degradation and NF-κB liberation. NF-κB then enters the nucleus and regulates the transcription of a wide array of genes that code for growth factors, cytokines, cell adhesion molecules, pro- and anti-apoptotic proteins (Luo et al., 2005). NF-κB activation can be caused by a variety of signaling pathways including activation of Ras/MAPK, PI3K/Akt, and JAK/STAT which are commonly mediated by RTKs (Dolcet et al., 2005; Zhang et al., 2021).

In cancer, NF-κB activation can lead to apoptosis resistance through the expression of inhibitors of apoptosis (IAPs), members of anti-apoptotic Bcl-2 family and also proteins that disrupt the death receptor apoptotic pathway (Wang et al., 1998; Catz and Johnson, 2001; Kreuz et al., 2001). NF-κB activity also enhances cell cycle progression by inducing expression of key cell cycle proteins like cyclin D1 and invasion-related proteins like matrix metalloproteinases (MMPs) as well as VEGF and COX-2 that are important in tumour growth (Dolcet et al., 2005; Li et al., 2011; Li et al., 2016). Constitutive NF-κB activation has been observed in 66% of colorectal cancer cell lines whereas activating NF-κB mutations commonly occur in hematopoietic tumours (Hassanzadeh, 2011; Xia et al., 2014). Generally, mutations in upstream signaling molecules like MAPK proteins or RTKs themselves lead to constitutive activation of NF-κB in solid tumours (Tilborghs et al., 2017). Similar to many other proteins, NF-κB can act as a tumour promoter or tumour suppressor under different circumstances. As a tumour growth promoter, NF-κB has been found to induce expression of oncogenic microRNAs, promote expression of immune checkpoint proteins like PD-L1 and also act in sync with STAT3 and AP-1 to induce tumour-associated inflammation (Galardi et al., 2011; Asgarova et al., 2018; Ji et al., 2019). Meanwhile, loss or inhibition of NF-κB has been found to increase immortalization of cells and invasion, reflecting its tumour suppressive functions (Vandermark et al., 2012; O'Reilly et al., 2018). Deregulation of RTK/NF-κB signaling has been observed in various cancers (Matušan-Ilijaš et al., 2013; Spirina et al., 2017; Lai et al., 2018).

Curcumin in combination with herceptin decreased levels of NF-κB in a dose-dependent manner in HER-2-overexpressed breast cancer cells, overcoming herceptin resistance (Lai et al., 2012). Curcumin also suppressed osteopontin (OPN)-induced VEGF expression (Chakraborty et al., 2008). OPN is one of the main markers of breast cancer progression. Further analysis found that curcumin inhibited NF-κB activation which led to suppression of OPN-induced VEGF (Chakraborty et al., 2008). This suggests that curcumin may inhibit the VEGF/VEGFR signaling via NF-κB inhibition. In lung cancer, *in vivo* mice studies also showed that curcumin regulated tumour angiogenesis by decreasing VEGF expression through NF-κB inhibition (Li X. et al., 2018). Two separate studies examined combinations of curcumin with dasatinib and EGF-Receptor Related Protein (ERRP) in colon cancer. Both studies found that curcumin inhibited EGFR, IGF-1R, and NF-κB activity and this effect was more pronounced with combination treatments (Reddy et al., 2006; Nautiyal et al., 2011a). Moreover, curcumin analogues, EF31, and UBS109, were found to induce downregulation of VEGF, HIF-α, and COX-2 as well as inhibit IKKs, NF-κB translocation and NF-κB DNA binding based on *in vitro* and *in vivo* cancer studies (Olivera et al., 2012; Nagaraju et al., 2015; Rajitha et al., 2017). However, there is still a lack of studies looking into how curcumin modulates NF-κB via RTK signaling pathways or vice versa.

Similar to the JAK/STAT pathway, a range of studies have examined the direct effect of curcumin on NF-κB signaling. Curcumin was found to inhibit both NF-κB and Wnt signaling in cervical cancer while it also inhibited AP-1, NF-κB, and HPV E6 proteins in HPV-positive oral carcinoma, abolishing HPV transcription (Mishra et al., 2015; Ghasemi et al., 2019). Meanwhile, a phase I/II study on patients with multiple myeloma found that orally administered curcumin had no serious adverse effects and also reduced constitutive NF-κB activation (Vadhan-Raj et al., 2007). Furthermore, curcumin and its analogues have also been combined with cytotoxic drugs like cisplatin and doxorubicin and they were found to downregulate the drug-induced increase of NF-κB in liver and breast cancer

(Notarbartolo et al., 2005; Meiyanto et al., 2014). Other curcumin combinations involving tolfenamic acid and Chinese goldthread also inhibited cell proliferation via disruption of NF-κB translocation into the nucleus and NF-κB transcriptional activity respectively (Zhao et al., 2014; Basha et al., 2016).

4 CURCUMIN-RECEPTOR TYROSINE KINASE INHIBITOR COMBINATION

Tyrosine kinase inhibitors (TKIs) are a form of targeted therapy that interfere with the activity of oncogenic tyrosine kinases (TKs). Some of their inhibitory mechanism include competing with ATP for binding sites on the catalytic domain of TKs and decreasing phosphorylation of TKs which lead to inhibition of tumour cell repair, induction of apoptosis, and blockage of G1 phase cell division (Jiao et al., 2018). These small molecule inhibitors are orally active, safe, and effective in tumour inhibition (Arora and Scholar, 2005). As of 2019, the Food and Drug Administration (FDA) has approved 48 protein kinase inhibitors of which 25 target receptor tyrosine kinases (Roskoski, 2019). RTKIs can either be single-targeted or multi-targeted. Single-targeted RTKIs include common ones like gefitinib, erlotinib, and lapatinib that inhibit EGFR and axitinib and lenvatinib that target VEGFR while multi-tyrosine kinase inhibitors include imatinib, sorafenib, sunitinib, pazopanib, and regorafenib which target a mix of RTKs and non-RTKs (Jiao et al., 2018). Certain aspects need to be taken into account when deciding whether to use multiple single kinase inhibitors or a single multi-kinase inhibitor and these include aspects involving efficacy, pharmacokinetics, tumour microenvironment, and resistance (Broekman et al., 2011).

As with the use of most drugs, RTKI use is often followed by the rise of resistance. Mechanisms of resistance against RTKIs include mutations, gene amplification, and RTK overexpression, overexpression of downstream kinases, increased expression of drug efflux pumps, and gene fusion, most of which were mentioned in the section regarding oncogenic RTKs (Broekman et al., 2011; Jiao et al., 2018). RTKI resistance can be either primary (intrinsic) or secondary (acquired) whereby primary resistance is when there is a lack of tumour response to treatment while secondary resistance involves exposure to the RTKI and subsequent selection of resistant tumour cells (Pottier et al., 2020). As a result, combination treatments are becoming the preferred regimen to treat cancers. Many studies are examining the combination RTKIs with chemotherapy drugs, immunotherapy, and radiotherapy (Goldberg et al., 2013; Liang et al., 2018; Khan M. et al., 2020). This in turn presents a new challenge of finding a positive balance between the toxicities caused by increased drug administration and survival benefits. Curcumin is being explored as viable solution to overcome this challenge and can possibly serve as a substitute for certain drugs in combination treatments. A compelling reason for the use of curcumin in drug combinations is that its low toxicity allows doses of up to 12 000 mg a day which are well tolerated in humans (Basnet and Skalko-Basnet, 2011). The combination of curcumin and anti-cancer drugs like RTKIs, can remove a large portion of toxicity induced when two conventional drugs are combined, and indeed studies have found curcumin to reduce chemotherapy- and radiotherapy-induced side effects (Mansouri et al., 2020). Findings from a range of curcumin-RTKI combination studies are summarized in **Table 2** and will be further reviewed in the following sections.

4.1 Curcumin and Single-Targeted RTKIs

Curcumin has been studied in combination with a few single-targeted RTKIs mainly EGFR TKIs like gefitinib, erlotinib and lapatinib. In a gefitinib-resistant lung cancer cell line (H1975), a combination of 15 μM of curcumin and 1 μM of gefitinib was found to have the same antiproliferative effect as 20 μM of gefitinib (Lee et al., 2011). In addition to EGFR, c-Met and Akt reduction, this study also found that combination treatment significantly lowered tumour growth on xenograft mice models and more importantly, 60 mg/kg of gefitinib combined with 1 g/kg of curcumin showed comparable results to 120 mg/kg of gefitinib. Side effects of gefitinib like villi damage and gastrointestinal effects were also attenuated by curcumin (Lee et al., 2011). Several other curcumin and gefitinib combination studies also found that curcumin promotes the inhibitory activity of gefitinib through downregulation of EGFR, MAPK, and PI3K signaling pathways (Lee et al., 2007; Xin et al., 2017; Chen et al., 2019). It was further found that curcumin and gefitinib also suppressed Sp1-and HDAC-induced EGFR transcription which led to induction of autophagy (Chen et al., 2019). In human oral cancer SAS cells, curcuminoids (curcumin, demethoxycurcumin or bisdemethoxycurcumin) combined with gefitinib induced certain apoptotic and autophagic proteins and overall led to higher levels of cell death compared to each agent alone (Hsiao et al., 2018). Meanwhile, further *in vivo* analysis showed that gefitinib combined with curcumin and demethoxycurcumin greatly decreased tumour volume in mice. Curcumin and gefitinib-loaded nanoparticles (NPs) have also been tested in oral cancer SAS cells (Lai et al., 2019). These γ-PGA-Gef/Cur NPs induced cell death through caspase and mitochondria-dependent pathways and low doses of Gef/Cur loaded NPs significantly decreased tumour weight as well. Meanwhile, several curcumin, and erlotinib combination studies were also found to strongly inhibit tumour growth and decrease tumour weight in xenograft mice models (Li et al., 2013; Yamauchi et al., 2014). Co-administration of curcumin and erlotinib was found to reduce cell viability of lung cancer cells via ikappaB elevation (Yamauchi et al., 2014). Additionally, it was also found that a relatively lower dose of curcumin also sensitized erlotinib-resistant NSCLC cells to erlotinib's cytotoxic effects, reduced expressions of EGFR and also inhibited NF-κB activation (Li et al., 2013). A few studies also employed the use of nano-based delivery systems to combine curcumin and erlotinib. A combination of curcumin and erlotinib-loaded Methoxypoly (ethylene glycol) Poly (caprolactone) (Mpeg-pcl) was found to increase PDK4 gene and decrease αvβ3 integrin expression in colorectal cancer cells (Javadi et al., 2018). These components are involved in erlotinib-resistance, and the addition of curcumin to erlotinib treatment seems to influence associated drug resistance signaling pathways. An erlotinib and curcumin conjugated

TABLE 2 | Summary of curcumin-RTKI combination studies.

Treatment	Cancer	Molecular targets/Pathways		Ref
		In vitro	*In vivo*	
Curcumin + gefitinib	Lung	↓ EGFR	↓ EGFR Akt, c-MET, cyclin D1 and PCNA, ↑ caspase-8, -9, PARP, p38 activation	Lee et al. (2011)
		↓ EGFR/p-EGFR, Akt/p-Akt protein, ↓ mRNA and protein levels of AXL, HLJ1 and MMP, ↑ G-actin/F-actin ratio	—	Lee et al. (2007)
		↓ p38, ERK1/2 and Akt phosphorylation	—	Xin et al. (2017)
		↓ EGFR activity via inhibiting binding of HDAC1 to Sp1, ↓ EGFR, c-MET, Her-2, AXL and IGF-1R	↓ Sp1, HDAC1, EGFR, survivin and ↑ LC3, Beclin 1 and cleaved caspase-3	Chen et al. (2019)
	Oral	↓ MMP, ↑ caspase-3 and -7, AIF	↑ caspase-6, -7, Beclin 1, Bcl-2 and *p*-EGFR	Hsiao et al. (2018)
		Beclin 1, ATG5, LC3, p62/SQSTM, ULK1, VPS34		
		↑ PARP, cytochrome C, p53, caspase-9 and -3, ↓ XIAP	—	Lai et al. (2019)
Curcumin + erlotinib	Lung	↓ EGFR, *p*-EGFR, survivin, p-p65 (NF-κB), ↑ cleavage of caspase-3, -9 and cytochrome c release	—	Li et al. (2013)
		↑ ikappaB	↑ ikappaB, ↑ NF-κB	Yamauchi et al. (2014)
	Pancreatic	↑ PDK4, ↓ $\alpha_V\beta_3$ integrin	—	Javadi et al. (2018)
Curcumin + lapatinib	Breast	↑ E-cadherin, ↓ Snail, vimentin, N-cadherin, CD44, ALDH1, ABCG2, SOX2	—	Liu et al. (2015)
		↓ p-Her2, *p*-Akt, total Her2	—	Saxena et al. (2020)
Curcumin + sorafenib	Liver	↓ MMP	—	Cao et al. (2015)
		↓ cyclin D1	—	Hosseini et al. (2019)
		↑ TIMP-1, ↓ MMP-9, p65, *p*-ERK1/2, CD133	↑ TIMP-1, ↓ MMP-9, p65, *p*-ERK1/2, CD133	Hu et al. (2015)
		↓ MMP, p27, cyclin A2, cyclin B, cyclin D1, p-Rb, Bcl-xL, ↑ Bax, cleaved caspase-3 and -9	—	Bahman et al. (2018)
		—	↓ ALT, MDA, vimentin, IL-1β, NF-κB, *p*-JAK1/2, p-STAT3, HIF-α, LDH, TG, FASN, lactate, D-fructose, D-glucose, hexadecanoic acid,CPT1A, *p*-Akt, ↑ $CD4^+$ T cells, NK cells, E-cadherin, IL-4, HDL-C, apoA1, p53	Man et al. (2020)
	Thyroid	↓ *p*-ERK, *p*-Akt	—	Zhang et al. (2016)
	Renal	↓ Rb	—	Debata et al. (2013)
Curcumin + sunitinib	Renal	↓ p-Rb, cyclin D1	—	Debata et al. (2013)
Curcumin + regorafenib	Colorectal	↑ cleaved caspase-3 and LC3-II	—	Su and Wu, (2017)
		↑ cleaved PARP, ↓ *p*-MEK, *p*-ERK	—	Wu et al. (2019a)

Abbreviations: PCNA: Proliferating cell nuclear antigen; PARP: Poly (ADP-1144 ribose) polymerase; MMP: Matrix metalloproteinase; HDAC1: Histone deacetylase 1; LC3: Microtubule-associated protein 1A/1B-light chain 3; AIF: Apoptosis inducing factor; ATG5: Autophagy related 5; SQSTM: Sequestosome; ULK1: Unc-51 like autophagy activating kinase; VPS34: Vacuolar protein sorting 34; Bcl-2: B-cell lymphoma 2; XIAP: X-linked inhibitor of apoptosis protein; PDK4: Pyruvate dehydrogenase (acetyl-transferring) kinase isozyme 4; ALDH1: Aldehyde dehydrogenase 1; ABCG2: ATP-binding cassette super-family G member 2; SOX2: SRY (sex determining region Y)-box 2; TIMP1: Tissue inhibitor of metalloproteinase 1; Rb: Retinoblastoma protein; Bcl-xL: B-cell lymphoma extra large; Bax: Bcl-2-associated X protein; ALT: Alanine aminotransferase; MDA: Malondialdehyde; IL-1β: Interleukin 1 beta; HIF-α: Hypoxia-inducible factor 1-alpha; LDH: Lactate dehydrogenase; TG: Triglyceride; FASN: Fatty acid synthase; CPT1A: Carnitine palmitoyltransferase 1A; NK: Natural killer cells; IL-4: Interleukin 4; HDL-C: High density lipoprotein cholesterol; apoAI: Apolipoprotein A I.

carrier-free nanoassembly (EPC) was also developed and found to have better tumour-penetrating and anti-migratory properties in addition to the absence of systemic toxicity (Cheng et al., 2020). Lastly, combinations of curcumin and lapatinib were also found to increase lapatinib-induced inhibition of the Her2-Akt pathway, reverse lapatinib resistance and decrease metastatic potential in breast cancer cells (Liu et al., 2015; Saxena et al., 2020). Currently, only one phase I clinical trial has been conducted investigating the combination treatment of curcumin and EGFR-TKIs (gefitinib and erlotinib) (Esfahani et al., 2019). An enhanced bioavailable curcumin formulation was administered together with gefitinib or erlotinib. Overall, no evidence of toxicity was observed and adverse effects, if any, were pre-existing due to TKI therapy. Curcumin was found to improve the quality of life and appeared to be a safe adjuvant to TKI therapy.

4.2 Curcumin and Multi-Targeted RTKIs

Recently, there has been an increase in the number of studies investigating the *in vitro* combinatorial effects of curcumin and

multi-kinase inhibitors, namely sorafenib, sunitinib, and regorafenib. Sorafenib is an orally administered pyridine multi-kinase inhibitor (MKI) that inhibits RTKs like VEGFR, PDGFR, RET, and MAPK signaling components like Raf-1, Braf, Braf mutants, and c-Kit (Wilhelm et al., 2004; Di Gion et al., 2011). As of now, combination treatment of sorafenib and curcumin has mostly been studied in hepatocellular carcinoma (HCC), with most of them involving nanoparticle (NP)-based delivery. These delivery systems include directed self-assembly NPs, pH-sensitive lactosylated NPs, polymeric nanoparticle formulations of curcumin and nanomicelles (Cao et al., 2015; Hu et al., 2015; Hosseini et al., 2019; Bian and Guo, 2020). All these studies found that an NP-based combination of curcumin and sorafenib showed higher cytotoxicity and induced higher apoptosis in HCC than either one alone. Some of them also demonstrated enhanced anti-angiogenic effects (Cao et al., 2015), improved *in vivo* tissue distribution (Cao et al., 2015; Bian and Guo, 2020), good tolerance (Bian and Guo, 2020), and downregulation of biomarkers/genes involved in cancer progression (Hu et al., 2015). Free drug combination treatments of curcumin and sorafenib also showed promising results like increased apoptosis, disruption of cell cycle progression, and protection of liver function from sorafenib-induced effects (Bahman et al., 2018; Man et al., 2020). This combination also remarkably increased the proportion of $CD4^+$ T cells and natural killer cells and inhibited sorafenib-induced EMT via downregulation of JAK/STAT and NF-κB pathway proteins (Man et al., 2020). MAPK and PI3K pathway components were also reduced by curcumin and sorafenib in thyroid cancer cells, decreasing migration and invasion (Zhang et al., 2016).

Sunitinib is a pyrole multi-kinase inhibitor that mainly inhibits VEGFR and PDGFR, and it is also a first-generation MKI like sorafenib (Mendel et al., 2003; Di Gion et al., 2011). There are only a few studies that have examined curcumin-sunitinib combinations. Combinations of curcumin with erlotinib, sorafenib, and sunitinib were studied in breast cancer cells and it was found that curcumin combined with sunitinib exhibited the highest reduction of cell viability (Chen et al., 2016). This combination was brought forward into *in vivo* analysis, and the efficacy of combination treatment was higher than mono-therapy; however, no statistical significance was achieved. In addition, bovine serum albumin (BSA)-encapsulated curcumin and sunitinib was found to be more effective than this free drug combination (Chen et al., 2016). These findings inspired an additional study whereby curcumin and sunitinib were co-loaded into BSA-supermagnetic iron oxide nanoparticles (SPIOs) (Chen et al., 2017). This formulation showed the highest amount of tumour inhibition and simultaneously the least amount of toxicity while also efficiently delivering the drugs to the tumour site based on *in vitro* and *in vivo* breast cancer models. In renal cancer cells, curcumin combined with sunitinib decreased the IC50 of sunitinib by four-fold; however, this effect was not observed with sorafenib (Debata et al., 2013). This suggests that the therapeutic dose of sunitinib can be reduced when combined with suitable concentrations of curcumin.

Regorafenib is one of the newer orally active MKIs mainly targeting VEGFR and PDGFR (Strumberg and Schultheis, 2012). As such, only two studies have investigated the combination treatment of curcumin and regorafenib in colorectal cancer cells (Su and Wu, 2017; Wu CS. et al., 2019). Curcumin appeared to act like a MEK inhibitor and most likely targets other genes as well, producing a synthetic lethal effect in KRAS-mutant colorectal cancer cells (Wu CS. et al., 2019). The combination of curcumin and regorafenib only showed additive/synergistic effects in KRAS-mutant and not KRAS-wildtype cells, suggesting their possible use in the treatment KRAS-mutant colorectal cancer. Imatinib and dasatinib are first- and second-generation pyrimidine TKIs respectively, and are mainly known to be non-RTKIs,; however, both also target PDGFR (Natoli et al., 2010). Several studies have combined curcumin with both imatinib and dasatinib. Most of the studies found that curcumin enhanced the anti-leukemia effects of imatinib by downregulation of the Bcr/Abl gene (Bae et al., 2005; Gong et al., 2012; Guo et al., 2015). Nanostructured lipid carriers of curcumin and imatinib were also found to have superior effects than imatinib alone (Setareh and Jaleh, 2018; Varshosaz et al., 2021).

Furthermore, a case report stated that curcumin and imatinib successfully treated a patient having c-KIT-positive adenoid cystic carcinoma for the first time, whereby complete anatomic and metabolic response was observed after 24 months (Demiray et al., 2016). On the other hand, curcumin and dasatinib combination treatments have also shown reduced metastatic potential, regression of mice intestinal adenomas and decreased cancer stem cell populations in colon cancer cells (Nautiyal et al., 2011a; Nautiyal et al., 2011b). However, none of the studies combining curcumin and imatinib/dasatinib recorded modulations of PDGFR despite it being a known target of these two drugs. Most of these studies reported changes in downstream signaling pathway components which could possibly be due to upstream regulation of its known target, PDGFR.

5 CONCLUSION

Curcumin possesses many of the features required to be an ideal anti-cancer therapeutic agent, especially with its enigmatic ability to singularly target a legion of signaling molecules. Further studies revealed that curcumin targets RTKs and their downstream signaling pathways such as MAPK, PI3K/Akt, JAK/STAT, and NF-κB pathways which are involved in essential cellular processes like proliferation, apoptosis, cell cycle progression, and migration. Curcumin-mediated modulation of RTK expression or activation leads to positive outcomes like reduced proliferation, increased apoptosis, and decreased migration. .In many cases, the specific mechanism of action depends on the cellular environment and type of cancer.

Multiple studies have shown that curcumin can overcome resistance and enhance the apoptotic effects of existing TKI drugs. There are still many unanswered questions regarding how curcumin targets RTKs, especially whether or not direct

binding occurs. Additional studies are also required to elucidate the effects of curcumin on RTKs along with changes in the JAK/STAT and NF-κB pathways. Many existing studies examine how curcumin targets RTKs or how curcumin targets specific pathways, however, an extensive analysis would require investigating all three components simultaneously (curcumin, RTKs, and signaling pathways) to obtainclearer understanding. In addition, it would be interesting to see how non-RTKs fit into this whole process since they make up many of the essential intracellular components. One of the main limitations of curcumin is its poor bioavailability in cellular environments. Various analogues of curcumin are being developed with superior bioavailability and improved anti-cancer properties. The use of nano-delivery systems is also gaining attention, especially in the delivery of curcumin and chemotherapy drugs. .There is a need for more *in vivo* and overall toxicity studies involving curcumin and its analogues. Combination treatments of curcumin and TKIs also need to be further studied to build a more substantial basis of evidence to ease curcumin progression into clinical trials. In conclusion, among the many mechanisms employed by curcumin, inhibition of receptor tyrosine kinases appears to be a significant element. It would be crucial to explore the implications for TKI therapy and whether the integration of curcumin and TKIs can improve treatment efficacy.

AUTHOR CONTRIBUTIONS

Conceptualization, SSD and RN investigation, SSD and RN; writing—original draft preparation, SSD; writing—review and editing, SSD, RN, SA, RF, and IO All authors have read and agreed to the published version of the manuscript.

ACKNOWLEDGMENTS

The authors would like to thank Jeffrey Cheah School of Medicine and Health Sciences, Monash University, Malaysia, for providing the research facilities and support to conduct this study.

REFERENCES

Abuzeid, W. M., Davis, S., Tang, A. L., Saunders, L., Brenner, J. C., Lin, J., et al. (2011). Sensitization of Head and Neck Cancer to Cisplatin through the Use of a Novel Curcumin Analog. *Arch. Otolaryngol. Head Neck Surg.* 137, 499–507. doi:10.1001/archoto.2011.63

Adamczak, A., Ożarowski, M., and Karpiński, T. M. (2020). Curcumin, a Natural Antimicrobial Agent with Strain-specific Activity. *Pharmaceuticals (Basel)* 13, 153. doi:10.3390/ph13070153

Adewuyi, E. E., Deschenes, J., Lopez-Campistrous, A., Kattar, M. M., Ghosh, S., and McMullen, T. P. W. (2018). Autocrine Activation of Platelet-Derived Growth Factor Receptor α in Metastatic Papillary Thyroid Cancer. *Hum. Pathol.* 75, 146–153. doi:10.1016/j.humpath.2018.01.025

Aleksic, T., Verrill, C., Bryant, R. J., Han, C., Worrall, A. R., Brureau, L., et al. (2017). IGF-1R Associates with Adverse Outcomes after Radical Radiotherapy for Prostate Cancer. *Br. J. Cancer* 117, 1600–1606. doi:10.1038/bjc.2017.337

Alexandrow, M. G., Song, L. J., Altiok, S., Gray, J., Haura, E. B., and Kumar, N. B. (2012). Curcumin: a Novel Stat3 Pathway Inhibitor for Chemoprevention of Lung Cancer. *Eur. J. Cancer Prev.* 21, 407–412. doi:10.1097/CEJ.0b013e32834ef194

Andl, C. D., Mizushima, T., Oyama, K., Bowser, M., Nakagawa, H., and Rustgi, A. K. (2004). EGFR-induced Cell Migration Is Mediated Predominantly by the JAK-STAT Pathway in Primary Esophageal Keratinocytes. *Am. J. Physiol. Gastrointest. Liver Physiol.* 287, G1227–G1237. doi:10.1152/ajpgi.00253.2004

Appiah-Kubi, K., Lan, T., Wang, Y., Qian, H., Wu, M., Yao, X., et al. (2017). Platelet-derived Growth Factor Receptors (PDGFRs) Fusion Genes Involvement in Hematological Malignancies. *Crit. Rev. Oncol. Hematol.* 109, 20–34. doi:10.1016/j.critrevonc.2016.11.008

Arbour, N., Naniche, D., Homann, D., Davis, R. J., Flavell, R. A., and Oldstone, M. B. (2002). c-Jun NH(2)-terminal Kinase (JNK)1 and JNK2 Signaling Pathways Have Divergent Roles in CD8(+) T Cell-Mediated Antiviral Immunity. *J. Exp. Med.* 195, 801–810. doi:10.1084/jem.20011481

Arena, S., Bellosillo, B., Siravegna, G., Martínez, A., Cañadas, I., Lazzari, L., et al. (2015). Emergence of Multiple EGFR Extracellular Mutations during Cetuximab Treatment in Colorectal Cancer. *Clin. Cancer Res.* 21, 2157–2166. doi:10.1158/1078-0432.Ccr-14-2821

Arora, A., and Scholar, E. M. (2005). Role of Tyrosine Kinase Inhibitors in Cancer Therapy. *J. Pharmacol. Exp. Ther.* 315, 971–979. doi:10.1124/jpet.105.084145

Asgarova, A., Asgarov, K., Godet, Y., Peixoto, P., Nadaradjane, A., Boyer-Guittaut, M., et al. (2018). PD-L1 Expression Is Regulated by Both DNA Methylation and NF-kB during EMT Signaling in Non-small Cell Lung Carcinoma. *Oncoimmunology* 7, e1423170. doi:10.1080/2162402x.2017.1423170

Awad, M. M., Oxnard, G. R., Jackman, D. M., Savukoski, D. O., Hall, D., Shivdasani, P., et al. (2016). MET Exon 14 Mutations in Non-small-cell Lung Cancer Are Associated with Advanced Age and Stage-dependent MET Genomic Amplification and C-Met Overexpression. *J. Clin. Oncol.* 34, 721–730. doi:10.1200/jco.2015.63.4600

Badzio, A., Wynes, M. W., Dziadziuszko, R., Merrick, D. T., Pardo, M., Rzyman, W., et al. (2010). Increased Insulin-like Growth Factor 1 Receptor Protein Expression and Gene Copy Number in Small Cell Lung Cancer. *J. Thorac. Oncol.* 5, 1905–1911. doi:10.1097/JTO.0b013e3181f38f57

Bae, E. K., Kim, Y.-J., Lee, J.-S., Park, S., Kim, B. K., Yoon, S.-S., et al. (2005). Effect of the Combination of Imatinib Mesylate (Glivec) and Curcumin in Chronic Myeloid Leukemia Cell Line. *Cancer Res.* 65, 1208.

Bahman, A. A., Abaza, M. S. I., Khoushiash, S. I., and Al-Attiyah, R. J. (2018). Sequence-dependent E-ffect of S-orafenib in C-ombination with N-atural P-henolic C-ompounds on H-epatic C-ancer C-ells and the P-ossible M-echanism of A-ction. *Int. J. Mol. Med.* 42, 1695–1715. doi:10.3892/ijmm.2018.3725

Banerjee, S., Singh, S. K., Chowdhury, I., Lillard, J. W., Jr., and Singh, R. (2017). Combinatorial Effect of Curcumin with Docetaxel Modulates Apoptotic and Cell Survival Molecules in Prostate Cancer. *Front. Biosci. (Elite Ed.* 9, 235–245. doi:10.2741/e798

Basha, R., Connelly, S. F., Sankpal, U. T., Nagaraju, G. P., Patel, H., Vishwanatha, J. K., et al. (2016). Small Molecule Tolfenamic Acid and Dietary Spice Curcumin Treatment Enhances Antiproliferative Effect in Pancreatic Cancer Cells via Suppressing Sp1, Disrupting NF-kB Translocation to Nucleus and Cell Cycle Phase Distribution. *J. Nutr. Biochem.* 31, 77–87. doi:10.1016/j.jnutbio.2016.01.003

Basnet, P., and Skalko-Basnet, N. (2011). Curcumin: an Anti-inflammatory Molecule from a Curry Spice on the Path to Cancer Treatment. *Molecules* 16, 4567–4598. doi:10.3390/molecules16064567

Baykal, C., Ayhan, A., Al, A., Yüce, K., and Ayhan, A. (2003). Overexpression of the C-Met/HGF Receptor and its Prognostic Significance in Uterine Cervix Carcinomas. *Gynecol. Oncol.* 88, 123–129. doi:10.1016/S0090-8258(02)00073-2

Bian, Y., and Guo, D. (2020). Targeted Therapy for Hepatocellular Carcinoma: Co-delivery of Sorafenib and Curcumin Using Lactosylated pH-Responsive Nanoparticles. *Drug Des. Devel Ther.* 14, 647–659. doi:10.2147/DDDT.S238955

Binion, D. G., Otterson, M. F., and Rafiee, P. (2008). Curcumin Inhibits VEGF-Mediated Angiogenesis in Human Intestinal Microvascular Endothelial Cells

through COX-2 and MAPK Inhibition. *Gut* 57, 1509–1517. doi:10.1136/gut.2008.152496

Blanc-Durand, F., Alameddine, R., Iafrate, A. J., Tran-Thanh, D., Lo, Y. C., Blais, N., et al. (2020). Tepotinib Efficacy in a Patient with Non-small Cell Lung Cancer with Brain Metastasis Harboring an HLA-DRB1-MET Gene Fusion. *Oncologist* 25, 916–920. doi:10.1634/theoncologist.2020-0502

Blasius, R., Reuter, S., Henry, E., Dicato, M., and Diederich, M. (2006). Curcumin Regulates Signal Transducer and Activator of Transcription (STAT) Expression in K562 Cells. *Biochem. Pharmacol.* 72, 1547–1554. doi:10.1016/j.bcp.2006.07.029

Blom, T., Roselli, A., Häyry, V., Tynninen, O., Wartiovaara, K., Korja, M., et al. (2010). Amplification and Overexpression of KIT, PDGFRA, and VEGFR2 in Medulloblastomas and Primitive Neuroectodermal Tumors. *J. Neurooncol.* 97, 217–224. doi:10.1007/s11060-009-0014-2

Boccaccio, C., Andò, M., Tamagnone, L., Bardelli, A., Michieli, P., Battistini, C., et al. (1998). Induction of Epithelial Tubules by Growth Factor HGF Depends on the STAT Pathway. *Nature* 391, 285–288. doi:10.1038/34657

Borah, A., Pillai, S. C., Rochani, A. K., Palaninathan, V., Nakajima, Y., Maekawa, T., et al. (2020). GANT61 and Curcumin-Loaded PLGA Nanoparticles for GLI1 and PI3K/Akt-Mediated Inhibition in Breast Adenocarcinoma. *Nanotechnology* 31, 185102. doi:10.1088/1361-6528/ab6d20

Borges, G. A., Elias, S. T., Amorim, B., de Lima, C. L., Coletta, R. D., Castilho, R. M., et al. (2020). Curcumin Downregulates the PI3K-AKT-mTOR Pathway and Inhibits Growth and Progression in Head and Neck Cancer Cells. *Phytother Res.* 34, 3311–3324. doi:10.1002/ptr.6780

Boroumand, N., Samarghandian, S., and Hashemy, S. I. (2018). Immunomodulatory, Anti-inflammatory, and Antioxidant Effects of Curcumin. *J. Herbmed Pharmacol.* 7, 211–219. doi:10.15171/jhp.2018.33

Bremm, A., Walch, A., Fuchs, M., Mages, J., Duyster, J., Keller, G., et al. (2008). Enhanced Activation of Epidermal Growth Factor Receptor Caused by Tumor-Derived E-Cadherin Mutations. *Cancer Res.* 68, 707–714. doi:10.1158/0008-5472.Can-07-1588

Broekman, F., Giovannetti, E., and Peters, G. J. (2011). Tyrosine Kinase Inhibitors: Multi-Targeted or Single-Targeted? *World J. Clin. Oncol.* 2, 80–93. doi:10.5306/wjco.v2.i2.80

Campregher, P. V., Halley, N. D. S., Vieira, G. A., Fernandes, J. F., Velloso, E. D. R. P., Ali, S., et al. (2017). Identification of a Novel Fusion TBL1XR1-PDGFRB in a Patient with Acute Myeloid Leukemia Harboring the DEK-Nup214 Fusion and Clinical Response to Dasatinib. *Leuk. Lymphoma* 58, 2969–2972. doi:10.1080/10428194.2017.1318437

Canovas, B., and Nebreda, A. R. (2021). Diversity and Versatility of P38 Kinase Signalling in Health and Disease. *Nat. Rev. Mol. Cel Biol* 22, 346–366. doi:10.1038/s41580-020-00322-w

Cantwell-Dorris, E. R., O'Leary, J. J., and Sheils, O. M. (2011). BRAFV600E: Implications for Carcinogenesis and Molecular Therapy. *Mol. Cancer Ther.* 10, 385–394. doi:10.1158/1535-7163.Mct-10-0799

Cao, H., Wang, Y., He, X., Zhang, Z., Yin, Q., Chen, Y., et al. (2015). Codelivery of Sorafenib and Curcumin by Directed Self-Assembled Nanoparticles Enhances Therapeutic Effect on Hepatocellular Carcinoma. *Mol. Pharm.* 12, 922–931. doi:10.1021/mp500755j

Capelletti, M., Dodge, M. E., Ercan, D., Hammerman, P. S., Park, S. I., Kim, J., et al. (2014). Identification of Recurrent FGFR3-TACC3 Fusion Oncogenes from Lung Adenocarcinoma. *Clin. Cancer Res.* 20, 6551–6558. doi:10.1158/1078-0432.Ccr-14-1337

Carneiro, B. A., Elvin, J. A., Kamath, S. D., Ali, S. M., Paintal, A. S., Restrepo, A., et al. (2015). FGFR3-TACC3: A Novel Gene Fusion in Cervical Cancer. *Gynecol. Oncol. Rep.* 13, 53–56. doi:10.1016/j.gore.2015.06.005

Casaletto, J. B., and McClatchey, A. I. (2012). Spatial Regulation of Receptor Tyrosine Kinases in Development and Cancer. *Nat. Rev. Cancer* 12, 387–400. doi:10.1038/nrc3277

Catz, S. D., and Johnson, J. L. (2001). Transcriptional Regulation of Bcl-2 by Nuclear Factor Kappa B and its Significance in Prostate Cancer. *Oncogene* 20, 7342–7351. doi:10.1038/sj.onc.1204926

Cepero, V., Sierra, J. R., Corso, S., Ghiso, E., Casorzo, L., Perera, T., et al. (2010). MET and KRAS Gene Amplification Mediates Acquired Resistance to MET Tyrosine Kinase Inhibitors. *Cancer Res.* 70, 7580–7590. doi:10.1158/0008-5472.Can-10-0436

Chakraborty, G., Jain, S., Kale, S., Raja, R., Kumar, S., Mishra, R., et al. (2008). Curcumin Suppresses Breast Tumor Angiogenesis by Abrogating Osteopontin-Induced VEGF Expression. *Mol. Med. Rep.* 1, 641–646. doi:10.3892/mmr_00000005

Chan, B. A., and Hughes, B. G. (2014). Targeted Therapy for Non-small Cell Lung Cancer: Current Standards and the Promise of the Future. *Transl Lung Cancer Res.* 4, 36–54. doi:10.3978/j.issn.2218-6751.2014.05.01

Chang, J., Liu, X., Wang, S., Zhang, Z., Wu, Z., Zhang, X., et al. (2014). Prognostic Value of FGFR Gene Amplification in Patients with Different Types of Cancer: a Systematic Review and Meta-Analysis. *PLoS One* 9, e105524. doi:10.1371/journal.pone.0105524

Chang, K. W., Hung, P. S., Lin, I. Y., Hou, C. P., Chen, L. K., Tsai, Y. M., et al. (2010). Curcumin Upregulates Insulin-like Growth Factor Binding Protein-5 (IGFBP-5) and C/EBPalpha during Oral Cancer Suppression. *Int. J. Cancer* 127, 9–20. doi:10.1002/ijc.25220

Chang, Q., Chen, J., Beezhold, K. J., Castranova, V., Shi, X., and Chen, F. (2009). JNK1 Activation Predicts the Prognostic Outcome of the Human Hepatocellular Carcinoma. *Mol. Cancer* 8, 64. doi:10.1186/1476-4598-8-64

Chapuis, N., Tamburini, J., Cornillet-Lefebvre, P., Gillot, L., Bardet, V., Willems, L., et al. (2010). Autocrine IGF-1/IGF-1R Signaling Is Responsible for Constitutive PI3K/Akt Activation in Acute Myeloid Leukemia: Therapeutic Value of Neutralizing Anti-IGF-1r Antibody. *Haematologica* 95, 415–423. doi:10.3324/haematol.2009.010785

Chatterjee, S., Heukamp, L. C., Siobal, M., Schöttle, J., Wieczorek, C., Peifer, M., et al. (2013). Tumor VEGF:VEGFR2 Autocrine Feed-Forward Loop Triggers Angiogenesis in Lung Cancer. *J. Clin. Invest.* 123, 1732–1740. doi:10.1172/jci65385

Cheatham, B., Shoelson, S. E., Yamada, K., Goncalves, E., and Kahn, C. R. (1993). Substitution of the erbB-2 Oncoprotein Transmembrane Domain Activates the Insulin Receptor and Modulates the Action of Insulin and Insulin-Receptor Substrate 1. *Proc. Natl. Acad. Sci. U S A.* 90, 7336–7340. doi:10.1073/pnas.90.15.7336

Chen, A., and Xu, J. (2005). Activation of PPAR{gamma} by Curcumin Inhibits Moser Cell Growth and Mediates Suppression of Gene Expression of Cyclin D1 and EGFR. *Am. J. Physiol. Gastrointest. Liver Physiol.* 288, G447–G456. doi:10.1152/ajpgi.00209.2004

Chen, A., Xu, J., and Johnson, A. C. (2006). Curcumin Inhibits Human colon Cancer Cell Growth by Suppressing Gene Expression of Epidermal Growth Factor Receptor through Reducing the Activity of the Transcription Factor Egr-1. *Oncogene* 25, 278–287. doi:10.1038/sj.onc.1209019

Chen, D., Li, X. L., Wu, B., Zheng, X. B., Wang, W. X., Chen, H. F., et al. (2020). A Novel Oncogenic Driver in a Lung Adenocarcinoma Patient Harboring an EGFR-KDD and Response to Afatinib. *Front. Oncol.* 10, 867. doi:10.3389/fonc.2020.00867

Chen, H. X., and Sharon, E. (2013). IGF-1R as an Anti-cancer Target-Ttrials and Tribulations. *Chin. J. Cancer* 32, 242–252. doi:10.5732/cjc.012.10263

Chen, J., De, S., Brainard, J., and Byzova, T. V. (2004). Metastatic Properties of Prostate Cancer Cells Are Controlled by VEGF. *Cell Commun Adhes* 11, 1–11. doi:10.1080/15419060490471739

Chen, P., Huang, H. P., Wang, Y., Jin, J., Long, W. G., Chen, K., et al. (2019). Curcumin Overcome Primary Gefitinib Resistance in Non-small-cell Lung Cancer Cells through Inducing Autophagy-Related Cell Death. *J. Exp. Clin. Cancer Res.* 38, 254. doi:10.1186/s13046-019-1234-8

Chen, Q., Powell, D. W., Rane, M. J., Singh, S., Butt, W., Klein, J. B., et al. (2003). Akt Phosphorylates P47phox and Mediates Respiratory Burst Activity in Human Neutrophils. *J. Immunol.* 170, 5302–5308. doi:10.4049/jimmunol.170.10.5302

Chen, S., Liang, Q., Liu, E., Yu, Z., Sun, L., Ye, J., et al. (2017). Curcumin/sunitinib Co-loaded BSA-Stabilized SPIOs for Synergistic Combination Therapy for Breast Cancer. *J. Mater. Chem. B* 5, 4060–4072. doi:10.1039/C7TB00040E

Chen, S., Liang, Q., Xie, S., Liu, E., Yu, Z., Sun, L., et al. (2016). Curcumin Based Combination Therapy for Anti-breast Cancer: from *In Vitro* Drug Screening to *In Vivo* Efficacy Evaluation. *Front. Chem. Sci. Eng.* 10, 383–388. doi:10.1007/s11705-016-1574-2

Chen, Y., Jiang, L., She, F., Tang, N., Wang, X., Li, X., et al. (2010). Vascular Endothelial Growth Factor-C Promotes the Growth and Invasion of Gallbladder Cancer via an Autocrine Mechanism. *Mol. Cel Biochem* 345, 77–89. doi:10.1007/s11010-010-0562-y

Chen, Y., Zhong, W., Chen, B., Yang, C., Zhou, S., and Liu, J. (2018). Effect of Curcumin on Vascular Endothelial Growth Factor in Hypoxic HepG2 Cells via the Insulin-like Growth Factor 1 Receptor Signaling Pathway. *Exp. Ther. Med.* 15, 2922–2928. doi:10.3892/etm.2018.5783

Chen, Y. R., and Tan, T. H. (1998). Inhibition of the C-Jun N-Terminal Kinase (JNK) Signaling Pathway by Curcumin. *Oncogene* 17, 173–178. doi:10.1038/sj.onc.1201941

Cheng, C., Sui, B., Wang, M., Hu, X., Shi, S., and Xu, P. (2020). Carrier-Free Nanoassembly of Curcumin-Erlotinib Conjugate for Cancer Targeted Therapy. *Adv. Healthc. Mater.* 9, e2001128. doi:10.1002/adhm.202001128

Chi, F., Wu, R., Jin, X., Jiang, M., and Zhu, X. (2016). HER2 Induces Cell Proliferation and Invasion of Non-small-cell Lung Cancer by Upregulating COX-2 Expression via MEK/ERK Signaling Pathway. *Onco Targets Ther.* 9, 2709–2716. doi:10.2147/OTT.S96197

Cools, J., DeAngelo, D. J., Gotlib, J., Stover, E. H., Legare, R. D., Cortes, J., et al. (2003). A Tyrosine Kinase Created by Fusion of the PDGFRA and FIP1L1 Genes as a Therapeutic Target of Imatinib in Idiopathic Hypereosinophilic Syndrome. *N. Engl. J. Med.* 348, 1201–1214. doi:10.1056/NEJMoa025217

Cowell, J. K., Qin, H., Hu, T., Wu, Q., Bhole, A., and Ren, M. (2017). Mutation in the FGFR1 Tyrosine Kinase Domain or Inactivation of PTEN Is Associated with Acquired Resistance to FGFR Inhibitors in FGFR1-Driven Leukemia/lymphomas. *Int. J. Cancer* 141, 1822–1829. doi:10.1002/ijc.30848

Craddock, K. J., Ludkovski, O., Sykes, J., Shepherd, F. A., and Tsao, M. S. (2013). Prognostic Value of Fibroblast Growth Factor Receptor 1 Gene Locus Amplification in Resected Lung Squamous Cell Carcinoma. *J. Thorac. Oncol.* 8, 1371–1377. doi:10.1097/JTO.0b013e3182a46fe9

Daniels, M., Lurkin, I., Pauli, R., Erbstösser, E., Hildebrandt, U., Hellwig, K., et al. (2011). Spectrum of KIT/PDGFRA/BRAF Mutations and Phosphatidylinositol-3-Kinase Pathway Gene Alterations in Gastrointestinal Stromal Tumors (GIST). *Cancer Lett.* 312, 43–54. doi:10.1016/j.canlet.2011.07.029

Davies, K. D., Ng, T. L., Estrada-Bernal, A., Le, A. T., Ennever, P. R., Camidge, D. R., et al. (2017). Dramatic Response to Crizotinib in a Patient with Lung Cancer Positive for anHLA-DRB1-METGene Fusion. *JCO Precision Oncol.* 2017, 1–6. doi:10.1200/po.17.00117

Davis, R. J. (2000). Signal Transduction by the JNK Group of MAP Kinases. *Cell* 103, 239–252. doi:10.1016/s0092-8674(00)00116-1

De, S., Zhou, H., DeSantis, D., Croniger, C. M., Li, X., and Stark, G. R. (2015). Erlotinib Protects against LPS-Induced Endotoxicity Because TLR4 Needs EGFR to Signal. *Proc. Natl. Acad. Sci. U S A.* 112, 9680–9685. doi:10.1073/pnas.1511794112

Debata, P. R., Begum, S., Mata, A., Genzer, O., Kleiner, M. J., Banerjee, P., et al. (2013). Curcumin Potentiates the Ability of Sunitinib to Eliminate the VHL-Lacking Renal Cancer Cells 786-O: Rapid Inhibition of Rb Phosphorylation as a Preamble to Cyclin D1 Inhibition. *Anticancer Agents Med. Chem.* 13, 1508–1513. doi:10.2174/18715206113139990093

Demiray, M., Sahinbas, H., Atahan, S., Demiray, H., Selcuk, D., Yildirim, I., et al. (2016). Successful Treatment of C-Kit-Positive Metastatic Adenoid Cystic Carcinoma (ACC) with a Combination of Curcumin Plus Imatinib: A Case Report. *Complement. Ther. Med.* 27, 108–113. doi:10.1016/j.ctim.2016.06.009

Deng, Y. I., Verron, E., and Rohanizadeh, R. (2016). Molecular Mechanisms of Anti-metastatic Activity of Curcumin. *Anticancer Res.* 36, 5639–5647. doi:10.21873/anticanres.11147

Dhillon, A. S., Hagan, S., Rath, O., and Kolch, W. (2007). MAP Kinase Signalling Pathways in Cancer. *Oncogene* 26, 3279–3290. doi:10.1038/sj.onc.1210421

Di Gion, P., Kanefendt, F., Lindauer, A., Scheffler, M., Doroshyenko, O., Fuhr, U., et al. (2011). Clinical Pharmacokinetics of Tyrosine Kinase Inhibitors: Focus on Pyrimidines, Pyridines and Pyrroles. *Clin. Pharmacokinet.* 50, 551–603. doi:10.2165/11593320-000000000-00000

Dickens, E., and Ahmed, S. (2018). Principles of Cancer Treatment by Chemotherapy. *Surgery (Oxford)* 36, 134–138. doi:10.1016/j.mpsur.2017.12.002

Dolcet, X., Llobet, D., Pallares, J., and Matias-Guiu, X. (2005). NF-kB in Development and Progression of Human Cancer. *Virchows Arch.* 446, 475–482. doi:10.1007/s00428-005-1264-9

Du, Z., Brown, B. P., Kim, S., Ferguson, D., Pavlick, D. C., Jayakumaran, G., et al. (2021). Structure-function Analysis of Oncogenic EGFR Kinase Domain Duplication Reveals Insights into Activation and a Potential Approach for Therapeutic Targeting. *Nat. Commun.* 12, 1382. doi:10.1038/s41467-021-21613-6

Du, Z., and Lovly, C. M. (2018). Mechanisms of Receptor Tyrosine Kinase Activation in Cancer. *Mol. Cancer* 17, 58. doi:10.1186/s12943-018-0782-4

Elstrom, R. L., Bauer, D. E., Buzzai, M., Karnauskas, R., Harris, M. H., Plas, D. R., et al. (2004). Akt Stimulates Aerobic Glycolysis in Cancer Cells. *Cancer Res.* 64, 3892–3899. doi:10.1158/0008-5472.Can-03-2904

Emuss, V., Garnett, M., Mason, C., and Marais, R. (2005). Mutations of C-RAF Are Rare in Human Cancer Because C-RAF Has a Low Basal Kinase Activity Compared with B-RAF. *Cancer Res.* 65, 9719–9726. doi:10.1158/0008-5472.Can-05-1683

Enrico, D., Lacroix, L., Chen, J., Rouleau, E., Scoazec, J. Y., Loriot, Y., et al. (2020). Oncogenic Fusions May Be Frequently Present at Resistance of EGFR Tyrosine Kinase Inhibitors in Patients with NSCLC: A Brief Report. *JTO Clin. Res. Rep.* 1, 100023. doi:10.1016/j.jtocrr.2020.100023

Esfahani, K., Boodaghians, L., Kasymjanova, G., Agulnik, J. S., Pepe, C., Sakr, L., et al. (2019). A Phase I Open Prospective Cohort Trial of Curcumin Plus Tyrosine Kinase Inhibitors for EGFR-Mutant Advanced Non-small Cell Lung Cancer. *Jco* 37, e20611. doi:10.1200/JCO.2019.37.15_suppl.e20611

Farghadani, R., and Naidu, R. (2021). Curcumin: Modulator of Key Molecular Signaling Pathways in Hormone-independent Breast Cancer. *Cancers (Basel)* 13, 3427. doi:10.3390/cancers13143427

Farhood, B., Mortezaee, K., Goradel, N. H., Khanlarkhani, N., Salehi, E., Nashtaei, M. S., et al. (2019). Curcumin as an Anti-inflammatory Agent: Implications to Radiotherapy and Chemotherapy. *J. Cel Physiol* 234, 5728–5740. doi:10.1002/jcp.27442

Faridi, J., Fawcett, J., Wang, L., and Roth, R. A. (2003). Akt Promotes Increased Mammalian Cell Size by Stimulating Protein Synthesis and Inhibiting Protein Degradation. *Am. J. Physiol. Endocrinol. Metab.* 285, E964–E972. doi:10.1152/ajpendo.00239.2003

Farooqi, A. A., and Siddik, Z. H. (2015). Platelet-derived Growth Factor (PDGF) Signalling in Cancer: Rapidly Emerging Signalling Landscape. *Cell Biochem Funct* 33, 257–265. doi:10.1002/cbf.3120

Ferlay, J., Colombet, M., Soerjomataram, I., Parkin, D. M., Piñeros, M., Znaor, A., et al. (2021). Cancer Statistics for the Year 2020: An Overview. *Int. J. Cancer* 149, 778–789. doi:10.1002/ijc.33588

Firtina Karagonlar, Z., Koc, D., Iscan, E., Erdal, E., and Atabey, N. (2016). Elevated Hepatocyte Growth Factor Expression as an Autocrine C-Met Activation Mechanism in Acquired Resistance to Sorafenib in Hepatocellular Carcinoma Cells. *Cancer Sci.* 107, 407–416. doi:10.1111/cas.12891

Fredriksson, L., Li, H., and Eriksson, U. (2004). The PDGF Family: Four Gene Products Form Five Dimeric Isoforms. *Cytokine Growth Factor. Rev.* 15, 197–204. doi:10.1016/j.cytogfr.2004.03.007

Fruman, D. A., Chiu, H., Hopkins, B. D., Bagrodia, S., Cantley, L. C., and Abraham, R. T. (2017). The PI3K Pathway in Human Disease. *Cell* 170, 605–635. doi:10.1016/j.cell.2017.07.029

Fu, Z., Chen, X., Guan, S., Yan, Y., Lin, H., and Hua, Z. C. (2015). Curcumin Inhibits Angiogenesis and Improves Defective Hematopoiesis Induced by Tumor-Derived VEGF in Tumor Model through Modulating VEGF-VEGFR2 Signaling Pathway. *Oncotarget* 6, 19469–19482. doi:10.18632/oncotarget.3625

Galardi, S., Mercatelli, N., Farace, M. G., and Ciafrè, S. A. (2011). NF-kB and C-Jun Induce the Expression of the Oncogenic miR-221 and miR-222 in Prostate Carcinoma and Glioblastoma Cells. *Nucleic Acids Res.* 39, 3892–3902. doi:10.1093/nar/gkr006

Gallant, J. N., Sheehan, J. H., Shaver, T. M., Bailey, M., Lipson, D., Chandramohan, R., et al. (2015). EGFR Kinase Domain Duplication (EGFR-KDD) Is a Novel Oncogenic Driver in Lung Cancer that Is Clinically Responsive to Afatinib. *Cancer Discov.* 5, 1155–1163. doi:10.1158/2159-8290.Cd-15-0654

Gallo, L. H., Nelson, K. N., Meyer, A. N., and Donoghue, D. J. (2015). Functions of Fibroblast Growth Factor Receptors in Cancer Defined by Novel Translocations and Mutations. *Cytokine Growth Factor. Rev.* 26, 425–449. doi:10.1016/j.cytogfr.2015.03.003

Gazdar, A. F. (2009). Activating and Resistance Mutations of EGFR in Non-small-cell Lung Cancer: Role in Clinical Response to EGFR Tyrosine Kinase Inhibitors. *Oncogene* 28 (Suppl. 1), S24–S31. doi:10.1038/onc.2009.198

Ghasemi, F., Shafiee, M., Banikazemi, Z., Pourhanifeh, M. H., Khanbabaei, H., Shamshirian, A., et al. (2019). Curcumin Inhibits NF-kB and Wnt/β-Catenin Pathways in Cervical Cancer Cells. *Pathol. Res. Pract.* 215, 152556. doi:10.1016/j.prp.2019.152556

Giordano, A., and Tommonaro, G. (2019). Curcumin and Cancer. *Nutrients* 11, 2376. doi:10.3390/nu11102376

Glynn, S. A., Prueitt, R. L., Ridnour, L. A., Boersma, B. J., Dorsey, T. M., Wink, D. A., et al. (2010). COX-2 Activation Is Associated with Akt Phosphorylation and Poor Survival in ER-Negative, HER2-Positive Breast Cancer. *BMC Cancer* 10, 626. doi:10.1186/1471-2407-10-626

Goetz, E. M., Ghandi, M., Treacy, D. J., Wagle, N., and Garraway, L. A. (2014). ERK Mutations Confer Resistance to Mitogen-Activated Protein Kinase Pathway Inhibitors. *Cancer Res.* 74, 7079–7089. doi:10.1158/0008-5472.Can-14-2073

Goldberg, S. B., Oxnard, G. R., Digumarthy, S., Muzikansky, A., Jackman, D. M., Lennes, I. T., et al. (2013). Chemotherapy with Erlotinib or Chemotherapy Alone in Advanced Non-small Cell Lung Cancer with Acquired Resistance to EGFR Tyrosine Kinase Inhibitors. *Oncologist* 18, 1214–1220. doi:10.1634/theoncologist.2013-0168

Golonko, A., Lewandowska, H., Świsłocka, R., Jasińska, U. T., Priebe, W., and Lewandowski, W. (2019). Curcumin as Tyrosine Kinase Inhibitor in Cancer Treatment. *Eur. J. Med. Chem.* 181, 111512. doi:10.1016/j.ejmech.2019.07.015

Gong, Y., Yao, E., Shen, R., Goel, A., Arcila, M., Teruya-Feldstein, J., et al. (2009). High Expression Levels of Total IGF-1R and Sensitivity of NSCLC Cells *In Vitro* to an Anti-IGF-1r Antibody (R1507). *PLoS One* 4, e7273. doi:10.1371/journal.pone.0007273

Gong, Y., Guo, Y., and Niu, T. (2012). Curcumin Potentiates Antitumor Activity of Imatinib via Inhibition of the AKT/mTOR Signaling Pathway and Down-Regulation of Bcr-Abl Gene in Philadelphia Chromosome-Positive Acute Lymphoblastic Leukemia. *Blood* 120, 3559. doi:10.1182/blood.V120.21.3559.3559

Gow, C. H., Liu, Y. N., Li, H. Y., Hsieh, M. S., Chang, S. H., Luo, S. C., et al. (2018). Oncogenic Function of a KIF5B-MET Fusion Variant in Non-small Cell Lung Cancer. *Neoplasia* 20, 838–847. doi:10.1016/j.neo.2018.06.007

Grivas, N., Goussia, A., Stefanou, D., and Giannakis, D. (2016). Microvascular Density and Immunohistochemical Expression of VEGF, VEGFR-1 and VEGFR-2 in Benign Prostatic Hyperplasia, High-Grade Prostate Intraepithelial Neoplasia and Prostate Cancer. *Cent. Eur. J Urol* 69, 63–71. doi:10.5173/ceju.2016.726

Gumustekin, M., Kargi, A., Bulut, G., Gozukizil, A., Ulukus, C., Oztop, I., et al. (2012). HGF/c-Met Overexpressions, but Not Met Mutation, Correlates with Progression of Non-small Cell Lung Cancer. *Pathol. Oncol. Res.* 18, 209–218. doi:10.1007/s12253-011-9430-7

Guo, Y., Li, Y., Shan, Q., He, G., Lin, J., and Gong, Y. (2015). Curcumin Potentiates the Anti-leukemia Effects of Imatinib by Downregulation of the AKT/mTOR Pathway and BCR/ABL Gene Expression in Ph+ Acute Lymphoblastic Leukemia. *Int. J. Biochem. Cel Biol* 65, 1–11. doi:10.1016/j.biocel.2015.05.003

Ha, S. Y., Lee, J., Kang, S. Y., Do, I. G., Ahn, S., Park, J. O., et al. (2013). MET Overexpression Assessed by New Interpretation Method Predicts Gene Amplification and Poor Survival in Advanced Gastric Carcinomas. *Mod. Pathol.* 26, 1632–1641. doi:10.1038/modpathol.2013.108

Hakam, A., Fang, Q., Karl, R., and Coppola, D. (2003). Coexpression of IGF-1R and C-Src Proteins in Human Pancreatic Ductal Adenocarcinoma. *Dig. Dis. Sci.* 48, 1972–1978. doi:10.1023/a:1026122421369

Halim, C. E., Deng, S., Ong, M. S., and Yap, C. T. (2020). Involvement of STAT5 in Oncogenesis. *Biomedicines* 8, 316. doi:10.3390/biomedicines8090316

Hassanzadeh, P. (2011). Colorectal Cancer and NF-Kb Signaling Pathway. *Gastroenterol. Hepatol. Bed Bench* 4, 127–132.

Heinrich, M. C., Corless, C. L., Duensing, A., McGreevey, L., Chen, C. J., Joseph, N., et al. (2003). PDGFRA Activating Mutations in Gastrointestinal Stromal Tumors. *Science* 299, 708–710. doi:10.1126/science.1079666

Heist, R. S., Mino-Kenudson, M., Sequist, L. V., Tammireddy, S., Morrissey, L., Christiani, D. C., et al. (2012). FGFR1 Amplification in Squamous Cell Carcinoma of the Lung. *J. Thorac. Oncol.* 7, 1775–1780. doi:10.1097/JTO.0b013e31826aed28

Horiguchi, N., Takayama, H., Toyoda, M., Otsuka, T., Fukusato, T., Merlino, G., et al. (2002). Hepatocyte Growth Factor Promotes Hepatocarcinogenesis through C-Met Autocrine Activation and Enhanced Angiogenesis in Transgenic Mice Treated with Diethylnitrosamine. *Oncogene* 21, 1791–1799. doi:10.1038/sj.onc.1205248

Hosseini, S., Chamani, J., Sinichi, M., Bonakdar, A. M., Azad, Z., Ahangari, N., et al. (2019). The Effect of Nanomicelle Curcumin, Sorafenib, and Combination of the Two on the Cyclin D1 Gene Expression of the Hepatocellular Carcinoma Cell Line (HUH7). *Iran J. Basic Med. Sci.* 22, 1198–1202. doi:10.22038/ijbms.2019.35808.8530

Hoxhaj, G., and Manning, B. D. (2020). The PI3K-AKT Network at the Interface of Oncogenic Signalling and Cancer Metabolism. *Nat. Rev. Cancer* 20, 74–88. doi:10.1038/s41568-019-0216-7

Hsiao, Y.-T., Kuo, C.-L., Lin, J.-J., Huang, W.-W., Peng, S.-F., Chueh, F.-S., et al. (2018). Curcuminoids Combined with Gefitinib Mediated Apoptosis and Autophagy of Human Oral Cancer SAS Cellsin Vitroand Reduced Tumor of SAS Cell Xenograft Micein Vivo. *Environ. Toxicol.* 33, 821–832. doi:10.1002/tox.22568

Hu, A., Huang, J. J., Jin, X. J., Li, J. P., Tang, Y. J., Huang, X. F., et al. (2014). Curcumin Suppresses Invasiveness and Vasculogenic Mimicry of Squamous Cell Carcinoma of the Larynx through the Inhibition of JAK-2/STAT-3 Signaling Pathway. *Am. J. Cancer Res.* 5, 278–288.

Hu, B., Sun, D., Sun, C., Sun, Y. F., Sun, H. X., Zhu, Q. F., et al. (2015). A Polymeric Nanoparticle Formulation of Curcumin in Combination with Sorafenib Synergistically Inhibits Tumor Growth and Metastasis in an Orthotopic Model of Human Hepatocellular Carcinoma. *Biochem. Biophys. Res. Commun.* 468, 525–532. doi:10.1016/j.bbrc.2015.10.031

Hu, H. J., Lin, X. L., Liu, M. H., Fan, X. J., and Zou, W. W. (2016). Curcumin Mediates Reversion of HGF-Induced Epithelial-Mesenchymal Transition via Inhibition of C-Met Expression in DU145 Cells. *Oncol. Lett.* 11, 1499–1505. doi:10.3892/ol.2015.4063

Huang, Q., Snyder, D. S., Chu, P., Gaal, K. K., Chang, K. L., and Weiss, L. M. (2011). PDGFRA Rearrangement Leading to Hyper-Eosinophilia, T-Lymphoblastic Lymphoma, Myeloproliferative Neoplasm and Precursor B-Cell Acute Lymphoblastic Leukemia. *Leukemia* 25, 371–375. doi:10.1038/leu.2010.272

Huh, Y. H., Kim, S. H., Kim, S. J., and Chun, J. S. (2003). Differentiation Status-dependent Regulation of Cyclooxygenase-2 Expression and Prostaglandin E2 Production by Epidermal Growth Factor via Mitogen-Activated Protein Kinase in Articular Chondrocytes. *J. Biol. Chem.* 278, 9691–9697. doi:10.1074/jbc.M211360200

Hur, J. Y., Chao, J., Kim, K., Kim, S. T., Kim, K. M., Klempner, S. J., et al. (2020). High-level FGFR2 Amplification Is Associated with Poor Prognosis and Lower Response to Chemotherapy in Gastric Cancers. *Pathol. Res. Pract.* 216, 152878. doi:10.1016/j.prp.2020.152878

Hutchins-Wolfbrandt, A., and Mistry, A. M. (2011). Dietary Turmeric Potentially Reduces the Risk of Cancer. *Asian Pac. J. Cancer Prev.* 12, 3169–3173.

Idbaih, A., Aimard, J., Boisselier, B., Marie, Y., Paris, S., Crinière, E., et al. (2009). Epidermal Growth Factor Receptor Extracellular Domain Mutations in Primary Glioblastoma. *Neuropathol. Appl. Neurobiol.* 35, 208–213. doi:10.1111/j.1365-2990.2008.00977.x

Igelmann, S., Neubauer, H. A., and Ferbeyre, G. (2019). STAT3 and STAT5 Activation in Solid Cancers. *Cancers (Basel)* 11, 1428. doi:10.3390/cancers11101428

Itakura, J., Ishiwata, T., Shen, B., Kornmann, M., and Korc, M. (2000). Concomitant Over-expression of Vascular Endothelial Growth Factor and its Receptors in Pancreatic Cancer. *Int. J. Cancer* 85, 27–34. doi:10.1002/(sici)1097-0215(20000101)85:1<27:aid-ijc5>3.0.co;2-8

Iyoda, K., Sasaki, Y., Horimoto, M., Toyama, T., Yakushijin, T., Sakakibara, M., et al. (2003). Involvement of the P38 Mitogen-Activated Protein Kinase cascade in Hepatocellular Carcinoma. *Cancer* 97, 3017–3026. doi:10.1002/cncr.11425

Jackson, M. W., Roberts, J. S., Heckford, S. E., Ricciardelli, C., Stahl, J., Choong, C., et al. (2002). A Potential Autocrine Role for Vascular Endothelial Growth Factor in Prostate Cancer. *Cancer Res.* 62, 854–859.

Javadi, S., Rostamizadeh, K., Hejazi, J., Parsa, M., and Fathi, M. (2018). Curcumin Mediated Down-Regulation of αV β3 Integrin and Up-Regulation of Pyruvate Dehydrogenase Kinase 4 (PDK4) in Erlotinib Resistant SW480 colon Cancer Cells. *Phytother Res.* 32, 355–364. doi:10.1002/ptr.5984

Jechlinger, M., Sommer, A., Moriggl, R., Seither, P., Kraut, N., Capodiecci, P., et al. (2006). Autocrine PDGFR Signaling Promotes Mammary Cancer Metastasis. *J. Clin. Invest.* 116, 1561–1570. doi:10.1172/jci24652

Jeong, E. G., Kim, M. S., Nam, H. K., Min, C. K., Lee, S., Chung, Y. J., et al. (2008). Somatic Mutations of JAK1 and JAK3 in Acute Leukemias and Solid Cancers. *Clin. Cancer Res.* 14, 3716–3721. doi:10.1158/1078-0432.Ccr-07-4839

Ji, W., Yu, Y., Li, Z., Wang, G., Li, F., Xia, W., et al. (2016). FGFR1 Promotes the Stem Cell-like Phenotype of FGFR1-Amplified Non-small Cell Lung Cancer

Cells through the Hedgehog Pathway. *Oncotarget* 7, 15118–15134. doi:10.18632/oncotarget.7701

Ji, Z., He, L., Regev, A., and Struhl, K. (2019). Inflammatory Regulatory Network Mediated by the Joint Action of NF-kB, STAT3, and AP-1 Factors Is Involved in many Human Cancers. *Proc. Natl. Acad. Sci. U S A.* 116, 9453–9462. doi:10.1073/pnas.1821068116

Jiang, A. P., Zhou, D. H., Meng, X. L., Zhang, A. P., Zhang, C., Li, X. T., et al. (2014). Down-regulation of Epidermal Growth Factor Receptor by Curcumin-Induced UBE1L in Human Bronchial Epithelial Cells. *J. Nutr. Biochem.* 25, 241–249. doi:10.1016/j.jnutbio.2013.11.001

Jiang, W., Wang, X., Zhang, C., Xue, L., and Yang, L. (2020). Expression and Clinical Significance of MAPK and EGFR in Triple-Negative Breast Cancer. *Oncol. Lett.* 19, 1842–1848. doi:10.3892/ol.2020.11274

Jiao, D., Wang, J., Lu, W., Tang, X., Chen, J., Mou, H., et al. (2016). Curcumin Inhibited HGF-Induced EMT and Angiogenesis through Regulating C-Met Dependent PI3K/Akt/mTOR Signaling Pathways in Lung Cancer. *Mol. Ther. Oncolytics* 3, 16018. doi:10.1038/mto.2016.18

Jiao, Q., Bi, L., Ren, Y., Song, S., Wang, Q., and Wang, Y. S. (2018). Advances in Studies of Tyrosine Kinase Inhibitors and Their Acquired Resistance. *Mol. Cancer* 17, 36. doi:10.1186/s12943-018-0801-5

Joensuu, H., Rutkowski, P., Nishida, T., Steigen, S. E., Brabec, P., Plank, L., et al. (2015). KIT and PDGFRA Mutations and the Risk of GI Stromal Tumor Recurrence. *J. Clin. Oncol.* 33, 634–642. doi:10.1200/JCO.2014.57.4970

Jones, R. A., Campbell, C. I., Gunther, E. J., Chodosh, L. A., Petrik, J. J., Khokha, R., et al. (2007). Transgenic Overexpression of IGF-IR Disrupts Mammary Ductal Morphogenesis and Induces Tumor Formation. *Oncogene* 26, 1636–1644. doi:10.1038/sj.onc.1209955

Jücker, M., Günther, A., Gradl, G., Fonatsch, C., Krueger, G., Diehl, V., et al. (1994). The Met/hepatocyte Growth Factor Receptor (HGFR) Gene Is Overexpressed in Some Cases of Human Leukemia and Lymphoma. *Leuk. Res.* 18, 7–16. doi:10.1016/0145-2126(94)90003-5

Jung, K. A., Choi, B. H., and Kwak, M. K. (2015). The C-Met/pi3k Signaling Is Associated with Cancer Resistance to Doxorubicin and Photodynamic Therapy by Elevating BCRP/ABCG2 Expression. *Mol. Pharmacol.* 87, 465–476. doi:10.1124/mol.114.096065

Katz, M., Amit, I., and Yarden, Y. (2007). Regulation of MAPKs by Growth Factors and Receptor Tyrosine Kinases. *Biochim. Biophys. Acta* 1773, 1161–1176. doi:10.1016/j.bbamcr.2007.01.002

Kentsis, A., Reed, C., Rice, K. L., Sanda, T., Rodig, S. J., Tholouli, E., et al. (2012). Autocrine Activation of the MET Receptor Tyrosine Kinase in Acute Myeloid Leukemia. *Nat. Med.* 18, 1118–1122. doi:10.1038/nm.2819

Khan, A. Q., Ahmed, E. I., Elareer, N., Fathima, H., Prabhu, K. S., Siveen, K. S., et al. (2020a). Curcumin-Mediated Apoptotic Cell Death in Papillary Thyroid Cancer and Cancer Stem-like Cells through Targeting of the JAK/STAT3 Signaling Pathway. *Int. J. Mol. Sci.* 21, 438. doi:10.3390/ijms21020438

Khan, M., Zhao, Z., Arooj, S., and Liao, G. (2020b). Impact of Tyrosine Kinase Inhibitors (TKIs) Combined with Radiation Therapy for the Management of Brain Metastases from Renal Cell Carcinoma. *Front. Oncol.* 10, 1246. doi:10.3389/fonc.2020.01246

Kim, H., Park, J., Tak, K.-H., Bu, S. Y., and Kim, E. (2014). Chemopreventive Effects of Curcumin on Chemically Induced Mouse Skin Carcinogenesis in BK5.Insulin-like Growth Factor-1 Transgenic Mice. In Vitro *Cell.Dev.Biol.-Animal* 50, 883–892. doi:10.1007/s11626-014-9791-9

Kim, J., Jung, J., Lee, S. J., Lee, J. S., and Park, M. J. (2012). Cancer Stem-like Cells Persist in Established Cell Lines through Autocrine Activation of EGFR Signaling. *Oncol. Lett.* 3, 607–612. doi:10.3892/ol.2011.531

Kim, J. H., Xu, C., Keum, Y. S., Reddy, B., Conney, A., and Kong, A. N. (2005). Inhibition of EGFR Signaling in Human Prostate Cancer PC-3 Cells by Combination Treatment with Beta-Phenylethyl Isothiocyanate and Curcumin. *Carcinogenesis* 27, 475–482. doi:10.1093/carcin/bgi272

Klasa-Mazurkiewicz, D., Jarząb, M., Milczek, T., Lipińska, B., and Emerich, J. (2011). Clinical Significance of VEGFR-2 and VEGFR-3 Expression in Ovarian Cancer Patients. *Pol. J. Pathol.* 62, 31–40.

Kobayashi, S., Boggon, T. J., Dayaram, T., Jänne, P. A., Kocher, O., Meyerson, M., et al. (2005). EGFR Mutation and Resistance of Non-small-cell Lung Cancer to Gefitinib. *N. Engl. J. Med.* 352, 786–792. doi:10.1056/NEJMoa044238

Kodama, M., Kitadai, Y., Tanaka, M., Kuwai, T., Tanaka, S., Oue, N., et al. (2008). Vascular Endothelial Growth Factor C Stimulates Progression of Human Gastric Cancer via Both Autocrine and Paracrine Mechanisms. *Clin. Cancer Res.* 14, 7205–7214. doi:10.1158/1078-0432.CCR-08-0818

Konduri, K., Gallant, J. N., Chae, Y. K., Giles, F. J., Gitlitz, B. J., Gowen, K., et al. (2016). EGFR Fusions as Novel Therapeutic Targets in Lung Cancer. *Cancer Discov.* 6, 601–611. doi:10.1158/2159-8290.CD-16-0075

Kong, F. M., Anscher, M. S., Washington, M. K., Killian, J. K., and Jirtle, R. L. (2000). M6P/IGF2R Is Mutated in Squamous Cell Carcinoma of the Lung. *Oncogene* 19, 1572–1578. doi:10.1038/sj.onc.1203437

Kreuz, S., Siegmund, D., Scheurich, P., and Wajant, H. (2001). NF-kappaB Inducers Upregulate cFLIP, a Cycloheximide-Sensitive Inhibitor of Death Receptor Signaling. *Mol. Cel Biol* 21, 3964–3973. doi:10.1128/MCB.21.12.3964-3973.2001

Kumar, R., Jain, A. G., Rashid, M. U., Ali, S., Khetpal, N., Hussain, I., et al. (2018). "HGFR and FGR2: Their Roles in Progression and Metastasis of Esophageal Cancer," in *Role of Tyrosine Kinases in Gastrointestinal Malignancies*. Editor G. P. Nagaraju (Singapore: Springer Singapore), 1–14. doi:10.1007/978-981-13-1486-5_1

Kyriakis, J. M., and Avruch, J. (2001). Mammalian Mitogen-Activated Protein Kinase Signal Transduction Pathways Activated by Stress and Inflammation. *Physiol. Rev.* 81, 807–869. doi:10.1152/physrev.2001.81.2.807

Lai, H.-W., Chien, S.-Y., Kuo, S.-J., Tseng, L.-M., Lin, H.-Y., Chi, C.-W., et al. (2012). The Potential Utility of Curcumin in the Treatment of HER-2-Overexpressed Breast Cancer: AnIn VitroandIn VivoComparison Study with Herceptin. *Evidence-Based Complement. Altern. Med.* 2012, 1–12. doi:10.1155/2012/486568

Lai, K. C., Chueh, F. S., Hsiao, Y. T., Cheng, Z. Y., Lien, J. C., Liu, K. C., et al. (2019). Gefitinib and Curcumin-Loaded Nanoparticles Enhance Cell Apoptosis in Human Oral Cancer SAS Cells *In Vitro* and Inhibit SAS Cell Xenografted Tumor *In Vivo*. *Toxicol. Appl. Pharmacol.* 382, 114734. doi:10.1016/j.taap.2019.114734

Lai, S. W., Bamodu, O. A., Tsai, W. C., Chang, Y. M., Lee, W. H., Yeh, C. T., et al. (2018). The Therapeutic Targeting of the FGFR1/Src/NF-Kb Signaling axis Inhibits Pancreatic Ductal Adenocarcinoma Stemness and Oncogenicity. *Clin. Exp. Metastasis* 35, 663–677. doi:10.1007/s10585-018-9919-5

Lasota, J., and Miettinen, M. (2006). KIT and PDGFRA Mutations in Gastrointestinal Stromal Tumors (GISTs). *Semin. Diagn. Pathol.* 23, 91–102. doi:10.1053/j.semdp.2006.08.006

Lassus, H., Sihto, H., Leminen, A., Joensuu, H., Isola, J., Nupponen, N. N., et al. (2006). Gene Amplification, Mutation, and Protein Expression of EGFR and Mutations of ERBB2 in Serous Ovarian Carcinoma. *J. Mol. Med. (Berl)* 84, 671–681. doi:10.1007/s00109-006-0054-4

Lassus, H., Sihto, H., Leminen, A., Nordling, S., Joensuu, H., Nupponen, N. N., et al. (2004). Genetic Alterations and Protein Expression of KIT and PDGFRA in Serous Ovarian Carcinoma. *Br. J. Cancer* 91, 2048–2055. doi:10.1038/sj.bjc.6602252

Lee, J.-Y., Yu, S.-L., Huang, J.-Y., Chen, W.-J., Chen, J. J. W., Yang, P.-C., et al. (2007). Synergistic Antitumor Activity of Epidermal Growth Factor Receptor Tyrosine Kinase Inhibitor Gefitinib and Curcumin in Non-small-cell Lung Cancer. *Cancer Res.* 67, 4783.

Lee, J. Y., Lee, Y. M., Chang, G. C., Yu, S. L., Hsieh, W. Y., Chen, J. J., et al. (2011). Curcumin Induces EGFR Degradation in Lung Adenocarcinoma and Modulates P38 Activation in Intestine: the Versatile Adjuvant for Gefitinib Therapy. *PLoS One* 6, e23756. doi:10.1371/journal.pone.0023756

Lee, S. J., Lee, J., Park, S. H., Park, J. O., Lim, H. Y., Kang, W. K., et al. (2018). c-MET Overexpression in Colorectal Cancer: A Poor Prognostic Factor for Survival. *Clin. Colorectal Cancer* 17, 165–169. doi:10.1016/j.clcc.2018.02.013

Lemmon, M. A., and Schlessinger, J. (2010). Cell Signaling by Receptor Tyrosine Kinases. *Cell* 141, 1117–1134. doi:10.1016/j.cell.2010.06.011

Lesslie, D. P., Summy, J. M., Parikh, N. U., Fan, F., Trevino, J. G., Sawyer, T. K., et al. (2006). Vascular Endothelial Growth Factor Receptor-1 Mediates Migration of Human Colorectal Carcinoma Cells by Activation of Src Family Kinases. *Br. J. Cancer* 94, 1710–1717. doi:10.1038/sj.bjc.6603143

Lev-Ari, S., Starr, A., Katzburg, S., Berkovich, L., Rimmon, A., Ben-Yosef, R., et al. (2014). Curcumin Induces Apoptosis and Inhibits Growth of Orthotopic Human Non-small Cell Lung Cancer Xenografts. *J. Nutr. Biochem.* 25, 843–850. doi:10.1016/j.jnutbio.2014.03.014

Lev-Ari, S., Starr, A., Vexler, A., Karaush, V., Loew, V., Greif, J., et al. (2006). Inhibition of Pancreatic and Lung Adenocarcinoma Cell Survival by Curcumin

Is Associated with Increased Apoptosis, Down-Regulation of COX-2 and EGFR and Inhibition of Erk1/2 Activity. *Anticancer Res.* 26, 4423–4430.

Li, E., and Hristova, K. (2006). Role of Receptor Tyrosine Kinase Transmembrane Domains in Cell Signaling and Human Pathologies. *Biochemistry* 45, 6241–6251. doi:10.1021/bi060609y

Li, J., Lau, G. K., Chen, L., Dong, S. S., Lan, H. Y., Huang, X. R., et al. (2011). Interleukin 17A Promotes Hepatocellular Carcinoma Metastasis via NF-kB Induced Matrix Metalloproteinases 2 and 9 Expression. *PLoS One* 6, e21816. doi:10.1371/journal.pone.0021816

Li, P., Huang, T., Zou, Q., Liu, D., Wang, Y., Tan, X., et al. (2019a). FGFR2 Promotes Expression of PD-L1 in Colorectal Cancer via the JAK/STAT3 Signaling Pathway. *J. Immunol.* 202, 3065–3075. doi:10.4049/jimmunol.1801199

Li, S., Liu, Z., Zhu, F., Fan, X., Wu, X., Zhao, H., et al. (2013). Curcumin Lowers Erlotinib Resistance in Non-small Cell Lung Carcinoma Cells with Mutated EGF Receptor. *Oncol. Res.* 21, 137–144. doi:10.3727/096504013x13832473330032

Li, S., Zhou, Y., Zheng, X., Wu, X., Liang, Y., Wang, S., et al. (2016). Sphk1 Promotes Breast Epithelial Cell Proliferation via NF-Kb-P65-Mediated Cyclin D1 Expression. *Oncotarget* 7, 80579–80585. doi:10.18632/oncotarget.13013

Li, W., Wang, Z., Xiao, X., Han, L., Wu, Z., Ma, Q., et al. (2019b). Curcumin Attenuates Hyperglycemia-Driven EGF-Induced Invasive and Migratory Abilities of Pancreatic Cancer via Suppression of the ERK and AKT Pathways. *Oncol. Rep.* 41, 650–658. doi:10.3892/or.2018.6833

Li, X., Ma, S., Yang, P., Sun, B., Zhang, Y., Sun, Y., et al. (2018a). Anticancer Effects of Curcumin on Nude Mice Bearing Lung Cancer A549 Cell Subsets SP and NSP Cells. *Oncol. Lett.* 16, 6756–6762. doi:10.3892/ol.2018.9488

Li, Y., Sun, W., Han, N., Zou, Y., and Yin, D. (2018b). Curcumin Inhibits Proliferation, Migration, Invasion and Promotes Apoptosis of Retinoblastoma Cell Lines through Modulation of miR-99a and JAK/STAT Pathway. *BMC Cancer* 18, 1230. doi:10.1186/s12885-018-5130-y

Lian, L., Li, X. L., Xu, M. D., Li, X. M., Wu, M. Y., Zhang, Y., et al. (2019). VEGFR2 Promotes Tumorigenesis and Metastasis in a Pro-angiogenic-independent Way in Gastric Cancer. *BMC Cancer* 19, 183. doi:10.1186/s12885-019-5322-0

Liang, H., Liu, X., and Wang, M. (2018). Immunotherapy Combined with Epidermal Growth Factor Receptor-Tyrosine Kinase Inhibitors in Non-small-cell Lung Cancer Treatment. *Onco Targets Ther.* 11, 6189–6196. doi:10.2147/OTT.S178497

Lin, L., Deangelis, S., Foust, E., Fuchs, J., Li, C., Li, P. K., et al. (2010a). A Novel Small Molecule Inhibits STAT3 Phosphorylation and DNA Binding Activity and Exhibits Potent Growth Suppressive Activity in Human Cancer Cells. *Mol. Cancer* 9, 217. doi:10.1186/1476-4598-9-217

Lin, L., Hutzen, B., Zuo, M., Ball, S., Deangelis, S., Foust, E., et al. (2010b). Novel STAT3 Phosphorylation Inhibitors Exhibit Potent Growth-Suppressive Activity in Pancreatic and Breast Cancer Cells. *Cancer Res.* 70, 2445–2454. doi:10.1158/0008-5472.CAN-09-2468

Lin, S. S., Lai, K. C., Hsu, S. C., Yang, J. S., Kuo, C. L., Lin, J. P., et al. (2009). Curcumin Inhibits the Migration and Invasion of Human A549 Lung Cancer Cells through the Inhibition of Matrix Metalloproteinase-2 and -9 and Vascular Endothelial Growth Factor (VEGF). *Cancer Lett.* 285, 127–133. doi:10.1016/j.canlet.2009.04.037

Lin, Y., Wang, X., and Jin, H. (2014). EGFR-TKI Resistance in NSCLC Patients: Mechanisms and Strategies. *Am. J. Cancer Res.* 4, 411–435.

Lin, Y., Zhai, E., Liao, B., Xu, L., Zhang, X., Peng, S., et al. (2017). Autocrine VEGF Signaling Promotes Cell Proliferation through a PLC-dependent Pathway and Modulates Apatinib Treatment Efficacy in Gastric Cancer. *Oncotarget* 8, 11990–12002. doi:10.18632/oncotarget.14467

Liu, G., Chen, T., Ding, Z., Wang, Y., Wei, Y., and Wei, X. (2021). Inhibition of FGF-FGFR and VEGF-VEGFR Signalling in Cancer Treatment. *Cell Prolif* 54, e13009. doi:10.1111/cpr.13009

Liu, J., Minemoto, Y., and Lin, A. (2004). c-Jun N-Terminal Protein Kinase 1 (JNK1), but Not JNK2, Is Essential for Tumor Necrosis Factor Alpha-Induced C-Jun Kinase Activation and Apoptosis. *Mol. Cel Biol* 24, 10844–10856. doi:10.1128/MCB.24.24.10844-10856.2004

Liu, J., Chen, X., Mao, Y., and Shen, K. (2015). Effect of Curcumin on Lapatinib Sensitivity and Lapatinib Resistance Associated EMT and Stem-like Phenotype in HER2 Positive Breast Cancer. *Jco* 33, e11594. doi:10.1200/jco.2015.33.15_suppl.e11594

Lokker, N. A., Sullivan, C. M., Hollenbach, S. J., Israel, M. A., and Giese, N. A. (2002). Platelet-derived Growth Factor (PDGF) Autocrine Signaling Regulates Survival and Mitogenic Pathways in Glioblastoma Cells: Evidence that the Novel PDGF-C and PDGF-D Ligands May Play a Role in the Development of Brain Tumors. *Cancer Res.* 62, 3729–3735.

Longatto Filho, A., Martins, A., Costa, S. M., and Schmitt, F. C. (2005). VEGFR-3 Expression in Breast Cancer Tissue Is Not Restricted to Lymphatic Vessels. *Pathol. Res. Pract.* 201, 93–99. doi:10.1016/j.prp.2004.11.008

Lu, K. H., Wu, H. H., Lin, R. C., Lin, Y. C., Lu, P. W., Yang, S. F., et al. (2020). Curcumin Analogue L48H37 Suppresses Human Osteosarcoma U2OS and MG-63 Cells' Migration and Invasion in Culture by Inhibition of uPA via the JAK/STAT Signaling Pathway. *Molecules* 26, 30. doi:10.3390/molecules26010030

Luo, J. L., Kamata, H., and Karin, M. (2005). IKK/NF-kappaB Signaling: Balancing Life and Death-Aa New Approach to Cancer Therapy. *J. Clin. Invest.* 115, 2625–2632. doi:10.1172/JCI26322

Man, S., Yao, J., Lv, P., Liu, Y., Yang, L., and Ma, L. (2020). Curcumin-enhanced Antitumor Effects of Sorafenib via Regulating the Metabolism and Tumor Microenvironment. *Food Funct.* 11, 6422–6432. doi:10.1039/c9fo01901d

Mansouri, K., Rasoulpoor, S., Daneshkhah, A., Abolfathi, S., Salari, N., Mohammadi, M., et al. (2020). Clinical Effects of Curcumin in Enhancing Cancer Therapy: A Systematic Review. *BMC Cancer* 20, 791. doi:10.1186/s12885-020-07256-8

Mao, P., Cohen, O., Kowalski, K. J., Kusiel, J. G., Buendia-Buendia, J. E., Cuoco, M. S., et al. (2020). Acquired FGFR and FGF Alterations Confer Resistance to Estrogen Receptor (ER) Targeted Therapy in ER+ Metastatic Breast Cancer. *Clin. Cancer Res.* 26, 5974–5989. doi:10.1158/1078-0432.Ccr-19-3958

Masamune, A., Satoh, M., Kikuta, K., Suzuki, N., and Shimosegawa, T. (2005). Activation of JAK-STAT Pathway Is Required for Platelet-Derived Growth Factor-Induced Proliferation of Pancreatic Stellate Cells. *World J. Gastroenterol.* 11, 3385–3391. doi:10.3748/wjg.v11.i22.3385

Matei, D., Emerson, R. E., Lai, Y. C., Baldridge, L. A., Rao, J., Yiannoutsos, C., et al. (2006). Autocrine Activation of PDGFRalpha Promotes the Progression of Ovarian Cancer. *Oncogene* 25, 2060–2069. doi:10.1038/sj.onc.1209232

Matsumoto, K., Arao, T., Hamaguchi, T., Shimada, Y., Kato, K., Oda, I., et al. (2012). FGFR2 Gene Amplification and Clinicopathological Features in Gastric Cancer. *Br. J. Cancer* 106, 727–732. doi:10.1038/bjc.2011.603

Matsuura, M., Onimaru, M., Yonemitsu, Y., Suzuki, H., Nakano, T., Ishibashi, H., et al. (2009). Autocrine Loop between Vascular Endothelial Growth Factor (VEGF)-C and VEGF Receptor-3 Positively Regulates Tumor-Associated Lymphangiogenesis in Oral Squamoid Cancer Cells. *Am. J. Pathol.* 175, 1709–1721. doi:10.2353/ajpath.2009.081139

Matušan-Ilijaš, K., Damante, G., Fabbro, D., Đorđević, G., Hadžisejdić, I., Grahovac, M., et al. (2013). EGFR Expression Is Linked to Osteopontin and Nf-Kb Signaling in clear Cell Renal Cell Carcinoma. *Clin. Transl Oncol.* 15, 65–71. doi:10.1007/s12094-012-0889-9

Meiyanto, E., Putri, D. D., Susidarti, R. A., Murwanti, R., SardjimanFitriasari, A., Fitriasari, A., et al. (2014). Curcumin and its Analogues (PGV-0 and PGV-1) Enhance Sensitivity of Resistant MCF-7 Cells to Doxorubicin through Inhibition of HER2 and NF-kB Activation. *Asian Pac. J. Cancer Prev.* 15, 179–184. doi:10.7314/apjcp.2014.15.1.179

Mendel, D. B., Laird, A. D., Xin, X., Louie, S. G., Christensen, J. G., Li, G., et al. (2003). *In Vivo* antitumor Activity of SU11248, a Novel Tyrosine Kinase Inhibitor Targeting Vascular Endothelial Growth Factor and Platelet-Derived Growth Factor Receptors: Determination of a Pharmacokinetic/pharmacodynamic Relationship. *Clin. Cancer Res.* 9, 327–337.

Miłobędzka, J., Kostanecki, S. V., and Lampe, V. (1910). Zur Kenntnis des Curcumins. *Ber. Dtsch. Chem. Ges.* 43, 2163–2170. doi:10.1002/cber.191004302168

Mishra, A., Kumar, R., Tyagi, A., Kohaar, I., Hedau, S., Bharti, A. C., et al. (2015). Curcumin Modulates Cellular AP-1, NF-kB, and HPV16 E6 Proteins in Oral Cancer. *Ecancermedicalscience* 9, 525. doi:10.3332/ecancer.2015.525

Mishra, P., Senthivinayagam, S., Rangasamy, V., Sondarva, G., and Rana, B. (2010). Mixed Lineage Kinase-3/JNK1 Axis Promotes Migration of Human Gastric Cancer Cells Following Gastrin Stimulation. *Mol. Endocrinol.* 24, 598–607. doi:10.1210/me.2009-0387

Miyata, Y., Ashida, S., Nakamura, T., Mochizuki, Y., Koga, S., Kanetake, H., et al. (2003). Overexpression of Hepatocyte Growth Factor Receptor in Renal

Carcinoma Cells Indirectly Stimulates Tumor Growth *In Vivo*. *Biochem. Biophys. Res. Commun.* 302, 892–897. doi:10.1016/S0006-291X(03)00281-X

Mohammadi, M., Schlessinger, J., and Hubbard, S. R. (1996). Structure of the FGF Receptor Tyrosine Kinase Domain Reveals a Novel Autoinhibitory Mechanism. *Cell* 86, 577–587. doi:10.1016/s0092-8674(00)80131-2

Monaco, S. E., Rodriguez, E. F., Mahaffey, A. L., and Dacic, S. (2015). FGFR1 Amplification in Squamous Cell Carcinoma of the Lung with Correlation of Primary and Metastatic Tumor Status. *Am. J. Clin. Pathol.* 145, 55–61. doi:10.1093/ajcp/aqv013

Morinaga, R., Okamoto, I., Fujita, Y., Arao, T., Sekijima, M., Nishio, K., et al. (2008). Association of Epidermal Growth Factor Receptor (EGFR) Gene Mutations with EGFR Amplification in Advanced Non-small Cell Lung Cancer. *Cancer Sci.* 99, 2455–2460. doi:10.1111/j.1349-7006.2008.00962.x

Nagaraju, G. P., Zhu, S., Ko, J. E., Ashritha, N., Kandimalla, R., Snyder, J. P., et al. (2015). Antiangiogenic Effects of a Novel Synthetic Curcumin Analogue in Pancreatic Cancer. *Cancer Lett.* 357, 557–565. doi:10.1016/j.canlet.2014.12.007

Nassar, A. H., Lundgren, K., Pomerantz, M., Van Allen, E., Harshman, L., Choudhury, A. D., et al. (2018). Enrichment of FGFR3-TACC3 Fusions in Patients with Bladder Cancer Who Are Young, Asian, or Have Never Smoked. *JCO Precision Oncol.* 2, 1–11. doi:10.1200/po.18.00013

Natoli, C., Perrucci, B., Perrotti, F., Falchi, L., and Iacobelli, S. (2010). Tyrosine Kinase Inhibitors. *Curr. Cancer Drug Targets* 10, 462–483. doi:10.2174/156800910791517208

Nautiyal, J., Banerjee, S., Kanwar, S. S., Yu, Y., Patel, B. B., Sarkar, F. H., et al. (2011a). Curcumin Enhances Dasatinib-Induced Inhibition of Growth and Transformation of colon Cancer Cells. *Int. J. Cancer* 128, 951–961. doi:10.1002/ijc.25410

Nautiyal, J., Kanwar, S. S., Yu, Y., and Majumdar, A. P. (2011b). Combination of Dasatinib and Curcumin Eliminates Chemo-Resistant colon Cancer Cells. *J. Mol. Signal.* 6, 7. doi:10.1186/1750-2187-6-7

Nelson, K. N., Meyer, A. N., Siari, A., Campos, A. R., Motamedchaboki, K., and Donoghue, D. J. (2016). Oncogenic Gene Fusion FGFR3-TACC3 Is Regulated by Tyrosine Phosphorylation. *Mol. Cancer Res.* 14, 458–469. doi:10.1158/1541-7786.Mcr-15-0497

Niu, X. L., Peters, K. G., and Kontos, C. D. (2002). Deletion of the Carboxyl Terminus of Tie2 Enhances Kinase Activity, Signaling, and Function. Evidence for an Autoinhibitory Mechanism. *J. Biol. Chem.* 277, 31768–31773. doi:10.1074/jbc.M203995200

Notarbartolo, M., Poma, P., Perri, D., Dusonchet, L., Cervello, M., and D'Alessandro, N. (2005). Antitumor Effects of Curcumin, Alone or in Combination with Cisplatin or Doxorubicin, on Human Hepatic Cancer Cells. Analysis of Their Possible Relationship to Changes in NF-kB Activation Levels and in IAP Gene Expression. *Cancer Lett.* 224, 53–65. doi:10.1016/j.canlet.2004.10.051

O'Reilly, L. A., Putoczki, T. L., Mielke, L. A., Low, J. T., Lin, A., Preaudet, A., et al. (2018). Loss of NF-Kb1 Causes Gastric Cancer with Aberrant Inflammation and Expression of Immune Checkpoint Regulators in a STAT-1-dependent Manner. *Immunity* 48, 570–e8. e578. doi:10.1016/j.immuni.2018.03.003

O'Shea, J. J., Schwartz, D. M., Villarino, A. V., Gadina, M., McInnes, I. B., and Laurence, A. (2015). The JAK-STAT Pathway: Impact on Human Disease and Therapeutic Intervention. *Annu. Rev. Med.* 66, 311–328. doi:10.1146/annurev-med-051113-024537

Ohnishi, Y., Sakamoto, T., Zhengguang, L., Yasui, H., Hamada, H., Kubo, H., et al. (2020). Curcumin Inhibits Epithelial-Mesenchymal Transition in Oral Cancer Cells via C-Met Blockade. *Oncol. Lett.* 19, 4177–4182. doi:10.3892/ol.2020.11523

Olivera, A., Moore, T. W., Hu, F., Brown, A. P., Sun, A., Liotta, D. C., et al. (2012). Inhibition of the NF-Kb Signaling Pathway by the Curcumin Analog, 3,5-Bis(2-Pyridinylmethylidene)-4-Piperidone (EF31): Anti-inflammatory and Anti-cancer Properties. *Int. Immunopharmacol* 12, 368–377. doi:10.1016/j.intimp.2011.12.009

Ong, H. S., Gokavarapu, S., Tian, Z., Li, J., Xu, Q., Cao, W., et al. (2017). PDGFRA mRNA Is Overexpressed in Oral Cancer Patients as Compared to normal Subjects with a Significant Trend of Overexpression Among Tobacco Users. *J. Oral Pathol. Med.* 46, 591–597. doi:10.1111/jop.12571

Ong, H. S., Gokavarapu, S., Tian, Z., Li, J., Xu, Q., Zhang, C. P., et al. (2018). PDGFRA mRNA Overexpression Is Associated with Regional Metastasis and Reduced Survival in Oral Squamous Cell Carcinoma. *J. Oral Pathol. Med.* 47, 652–659. doi:10.1111/jop.12713

Pan, C. W., Liu, H., Zhao, Y., Qian, C., Wang, L., and Qi, J. (2016). JNK2 Downregulation Promotes Tumorigenesis and Chemoresistance by Decreasing P53 Stability in Bladder Cancer. *Oncotarget* 7, 35119–35131. doi:10.18632/oncotarget.9046

Pan, Z., Zhuang, J., Ji, C., Cai, Z., Liao, W., and Huang, Z. (2018). Curcumin Inhibits Hepatocellular Carcinoma Growth by Targeting VEGF Expression. *Oncol. Lett.* 15, 4821–4826. doi:10.3892/ol.2018.7988

Park, H. S., Jang, M. H., Kim, E. J., Kim, H. J., Lee, H. J., Kim, Y. J., et al. (2014). High EGFR Gene Copy Number Predicts Poor Outcome in Triple-Negative Breast Cancer. *Mod. Pathol.* 27, 1212–1222. doi:10.1038/modpathol.2013.251

Park, J., Ayyappan, V., Bae, E. K., Lee, C., Kim, B. S., Kim, B. K., et al. (2008). Curcumin in Combination with Bortezomib Synergistically Induced Apoptosis in Human Multiple Myeloma U266 Cells. *Mol. Oncol.* 2, 317–326. doi:10.1016/j.molonc.2008.09.006

Parker, B. C., Annala, M. J., Cogdell, D. E., Granberg, K. J., Sun, Y., Ji, P., et al. (2013). The Tumorigenic FGFR3-TACC3 Gene Fusion Escapes miR-99a Regulation in Glioblastoma. *J. Clin. Invest.* 123, 855–865. doi:10.1172/jci67144

Parker, B. C., Engels, M., Annala, M., and Zhang, W. (2014). Emergence of FGFR Family Gene Fusions as Therapeutic Targets in a Wide Spectrum of Solid Tumours. *J. Pathol.* 232, 4–15. doi:10.1002/path.4297

Patel, B. B., Gupta, D., Elliott, A. A., Sengupta, V., Yu, Y., and Majumdar, A. P. (2010). Curcumin Targets FOLFOX-Surviving colon Cancer Cells via Inhibition of EGFRs and IGF-1R. *Anticancer Res.* 30, 319–325.

Patel, B. B., Sengupta, R., Qazi, S., Vachhani, H., Yu, Y., Rishi, A. K., et al. (2008). Curcumin Enhances the Effects of 5-fluorouracil and Oxaliplatin in Mediating Growth Inhibition of colon Cancer Cells by Modulating EGFR and IGF-1R. *Int. J. Cancer* 122, 267–273. doi:10.1002/ijc.23097

Pavelić, J., Radaković, B., and Pavelić, K. (2007). Insulin-like Growth Factor 2 and its Receptors (IGF 1R and IGF 2R/mannose 6-phosphate) in Endometrial Adenocarcinoma. *Gynecol. Oncol.* 105, 727–735. doi:10.1016/j.ygyno.2007.02.012

Pavelić, K., Kolak, T., Kapitanović, S., Radosević, S., Spaventi, S., Kruslin, B., et al. (2003). Gastric Cancer: the Role of Insulin-like Growth Factor 2 (IGF 2) and its Receptors (IGF 1R and M6-P/IGF 2R). *J. Pathol.* 201, 430–438. doi:10.1002/path.1465

Pearson, A., Smyth, E., Babina, I. S., Herrera-Abreu, M. T., Tarazona, N., Peckitt, C., et al. (2016). High-Level Clonal FGFR Amplification and Response to FGFR Inhibition in a Translational Clinical Trial. *Cancer Discov.* 6, 838–851. doi:10.1158/2159-8290.Cd-15-1246

Peng, S., Wang, Y., Peng, H., Chen, D., Shen, S., Peng, B., et al. (2014). Autocrine Vascular Endothelial Growth Factor Signaling Promotes Cell Proliferation and Modulates Sorafenib Treatment Efficacy in Hepatocellular Carcinoma. *Hepatology* 60, 1264–1277. doi:10.1002/hep.27236

Penzel, R., Aulmann, S., Moock, M., Schwarzbach, M., Rieker, R. J., and Mechtersheimer, G. (2005). The Location of KIT and PDGFRA Gene Mutations in Gastrointestinal Stromal Tumours Is Site and Phenotype Associated. *J. Clin. Pathol.* 58, 634–639. doi:10.1136/jcp.2004.021766

Peretz, S., Kim, C., Rockwell, S., Baserga, R., and Glazer, P. M. (2002). IGF1 Receptor Expression Protects against Microenvironmental Stress Found in the Solid Tumor. *Radiat. Res.* 158, 174–180. doi:10.1667/0033-7587(2002)158[0174:irepam]2.0.co;2

Petiti, J., Rosso, V., Lo Iacono, M., Panuzzo, C., Calabrese, C., Signorino, E., et al. (2019). Curcumin Induces Apoptosis in JAK2-Mutated Cells by the Inhibition of JAK2/STAT and mTORC1 Pathways. *J. Cel Mol Med* 23, 4349–4357. doi:10.1111/jcmm.14326

Petti, L. M., Irusta, P. M., and DiMaio, D. (1998). Oncogenic Activation of the PDGF Beta Receptor by the Transmembrane Domain of P185neu*. *Oncogene* 16, 843–851. doi:10.1038/sj.onc.1201590

Porstmann, T., Griffiths, B., Chung, Y. L., Delpuech, O., Griffiths, J. R., Downward, J., et al. (2005). PKB/Akt Induces Transcription of Enzymes Involved in Cholesterol and Fatty Acid Biosynthesis via Activation of SREBP. *Oncogene* 24, 6465–6481. doi:10.1038/sj.onc.1208802

Porta, R., Borea, R., Coelho, A., Khan, S., Araújo, A., Reclusa, P., et al. (2017). FGFR a Promising Druggable Target in Cancer: Molecular Biology and New Drugs. *Crit. Rev. Oncol. Hematol.* 113, 256–267. doi:10.1016/j.critrevonc.2017.02.018

Pottier, C., Fresnais, M., Gilon, M., Jérusalem, G., Longuespée, R., and Sounni, N. E. (2020). Tyrosine Kinase Inhibitors in Cancer: Breakthrough and Challenges of Targeted Therapy. *Cancers (Basel)* 12. doi:10.3390/cancers12030731

Prior, I. A., Hood, F. E., and Hartley, J. L. (2020). The Frequency of Ras Mutations in Cancer. *Cancer Res.* 80, 2969–2974. doi:10.1158/0008-5472.Can-19-3682

Qian, Y., Deng, J., Geng, L., Xie, H., Jiang, G., Zhou, L., et al. (2008). TLR4 Signaling Induces B7-H1 Expression through MAPK Pathways in Bladder Cancer Cells. *Cancer Invest.* 26, 816–821. doi:10.1080/07357900801941852

Rahman, M. A., Salajegheh, A., Smith, R. A., and Lam, A. K. (2013). B-raf Mutation: A Key Player in Molecular Biology of Cancer. *Exp. Mol. Pathol.* 95, 336–342. doi:10.1016/j.yexmp.2013.10.005

Rahmani, A. H., Al Zohairy, M. A., Aly, S. M., and Khan, M. A. (2014). Curcumin: a Potential Candidate in Prevention of Cancer via Modulation of Molecular Pathways. *Biomed. Res. Int.* 2014, 761608. doi:10.1155/2014/761608

Rajasingh, J., Raikwar, H. P., Muthian, G., Johnson, C., and Bright, J. J. (2006). Curcumin Induces Growth-Arrest and Apoptosis in Association with the Inhibition of Constitutively Active JAK-STAT Pathway in T Cell Leukemia. *Biochem. Biophys. Res. Commun.* 340, 359–368. doi:10.1016/j.bbrc.2005.12.014

Rajitha, B., Nagaraju, G. P., Shaib, W. L., Alese, O. B., Snyder, J. P., Shoji, M., et al. (2017). Novel Synthetic Curcumin Analogs as Potent Antiangiogenic Agents in Colorectal Cancer. *Mol. Carcinog* 56, 288–299. doi:10.1002/mc.22492

Rapisarda, A., and Melillo, G. (2012). Role of the VEGF/VEGFR axis in Cancer Biology and Therapy. *Adv. Cancer Res.* 114, 237–267. doi:10.1016/B978-0-12-386503-8.00006-5

Rasmussen, A. A., and Cullen, K. J. (1998). Paracrine/autocrine Regulation of Breast Cancer by the Insulin-like Growth Factors. *Breast Cancer Res. Treat.* 47, 219–233. doi:10.1023/a:1005903000777

Rasola, A., Fassetta, M., De Bacco, F., D'Alessandro, L., Gramaglia, D., Di Renzo, M. F., et al. (2007). A Positive Feedback Loop between Hepatocyte Growth Factor Receptor and Beta-Catenin Sustains Colorectal Cancer Cell Invasive Growth. *Oncogene* 26, 1078–1087. doi:10.1038/sj.onc.1209859

Reddy, S., Rishi, A. K., Xu, H., Levi, E., Sarkar, F. H., and Majumdar, A. P. (2006). Mechanisms of Curcumin- and EGF-Receptor Related Protein (ERRP)-dependent Growth Inhibition of colon Cancer Cells. *Nutr. Cancer* 55, 185–194. doi:10.1207/s15327914nc5502_10

Resnicoff, M., Abraham, D., Yutanawiboonchai, W., Rotman, H. L., Kajstura, J., Rubin, R., et al. (1995). The Insulin-like Growth Factor I Receptor Protects Tumor Cells from Apoptosis *In Vivo*. *Cancer Res.* 55, 2463–2469.

Roskoski, R. (2019). Properties of FDA-Approved Small Molecule Protein Kinase Inhibitors. *Pharmacol. Res.* 144, 19–50. doi:10.1016/j.phrs.2019.03.006

Ryan, M. R., Sohl, C. D., Luo, B., and Anderson, K. S. (2019). The FGFR1 V561M Gatekeeper Mutation Drives AZD4547 Resistance through STAT3 Activation and EMT. *Mol. Cancer Res.* 17, 532–543. doi:10.1158/1541-7786.Mcr-18-0429

Saha, A., Connelly, S., Jiang, J., Zhuang, S., Amador, D. T., Phan, T., et al. (2014). Akt Phosphorylation and Regulation of Transketolase Is a Nodal point for Amino Acid Control of Purine Synthesis. *Mol. Cel* 55, 264–276. doi:10.1016/j.molcel.2014.05.028

Sandhiutami, N. M. D., Arozal, W., Louisa, M., Rahmat, D., and Wuyung, P. E. (2020). Curcumin Nanoparticle Enhances the Anticancer Effect of Cisplatin by Inhibiting PI3K/AKT and JAK/STAT3 Pathway in Rat Ovarian Carcinoma Induced by DMBA. *Front. Pharmacol.* 11, 603235. doi:10.3389/fphar.2020.603235

Sawada, K., Radjabi, A. R., Shinomiya, N., Kistner, E., Kenny, H., Becker, A. R., et al. (2007). c-Met Overexpression Is a Prognostic Factor in Ovarian Cancer and an Effective Target for Inhibition of Peritoneal Dissemination and Invasion. *Cancer Res.* 67, 1670–1679. doi:10.1158/0008-5472.Can-06-1147

Saxena, A. R., Ilic, Z., Sripada, V., and Crawford, D. R. (2020). Lower Concentrations of Curcumin Inhibit Her2-Akt Pathway Components in Human Breast Cancer Cells, and Other Dietary Botanicals Potentiate This and Lapatinib Inhibition. *Nutr. Res.* 78, 93–104. doi:10.1016/j.nutres.2020.05.007

Saydmohammed, M., Joseph, D., and Syed, V. (2010). Curcumin Suppresses Constitutive Activation of STAT-3 by Up-Regulating Protein Inhibitor of Activated STAT-3 (PIAS-3) in Ovarian and Endometrial Cancer Cells. *J. Cel Biochem* 110, 447–456. doi:10.1002/jcb.22558

Schlessinger, J. (2000). Cell Signaling by Receptor Tyrosine Kinases. *Cell* 103, 211–225. doi:10.1016/s0092-8674(00)00114-8

Schlomm, T., Kirstein, P., Iwers, L., Daniel, B., Steuber, T., Walz, J., et al. (2007). Clinical Significance of Epidermal Growth Factor Receptor Protein Overexpression and Gene Copy Number Gains in Prostate Cancer. *Clin. Cancer Res.* 13, 6579–6584. doi:10.1158/1078-0432.Ccr-07-1257

Score, J., Curtis, C., Waghorn, K., Stalder, M., Jotterand, M., Grand, F. H., et al. (2006). Identification of a Novel Imatinib Responsive KIF5B-PDGFRA Fusion Gene Following Screening for PDGFRA Overexpression in Patients with Hypereosinophilia. *Leukemia* 20, 827–832. doi:10.1038/sj.leu.2404154

Ségaliny, A. I., Tellez-Gabriel, M., Heymann, M. F., and Heymann, D. (2015). Receptor Tyrosine Kinases: Characterisation, Mechanism of Action and Therapeutic Interests for Bone Cancers. *J. Bone Oncol.* 4, 1–12. doi:10.1016/j.jbo.2015.01.001

Setareh, J., and Jaleh, V. (2018). Co-delivery of Curcumin and Imatinib by Nanostructured Lipid Carriers in the Treatment of Lymphoma. *Int. Pharm. Acta* 1, 37–38. doi:10.22037/ipa.v1i1.19945

Seto, T., Higashiyama, M., Funai, H., Imamura, F., Uematsu, K., Seki, N., et al. (2006). Prognostic Value of Expression of Vascular Endothelial Growth Factor and its Flt-1 and KDR Receptors in Stage I Non-small-cell Lung Cancer. *Lung Cancer* 53, 91–96. doi:10.1016/j.lungcan.2006.02.009

Shakeri, A., Ward, N., Panahi, Y., and Sahebkar, A. (2019). Anti-angiogenic Activity of Curcumin in Cancer Therapy: a Narrative Review. *Curr. Vasc. Pharmacol.* 17, 262–269. doi:10.2174/1570161116666180209113014

Shao, M. M., Zhang, F., Meng, G., Wang, X. X., Xu, H., Yu, X. W., et al. (2011). Epidermal Growth Factor Receptor Gene Amplification and Protein Overexpression in Basal-like Carcinoma of the Breast. *Histopathology* 59, 264–273. doi:10.1111/j.1365-2559.2011.03921.x

Sheng, G., Zeng, Z., Pan, J., Kou, L., Wang, Q., Yao, H., et al. (2017). Multiple MYO18A-PDGFRB Fusion Transcripts in a Myeloproliferative Neoplasm Patient with T(5;17)(q32;q11). *Mol. Cytogenet.* 10, 4. doi:10.1186/s13039-017-0306-8

Shigematsu, H., and Gazdar, A. F. (2006). Somatic Mutations of Epidermal Growth Factor Receptor Signaling Pathway in Lung Cancers. *Int. J. Cancer* 118, 257–262. doi:10.1002/ijc.21496

Shiratsuchi, I., Akagi, Y., Kawahara, A., Kinugasa, T., Romeo, K., Yoshida, T., et al. (2011). Expression of IGF-1 and IGF-1R and Their Relation to Clinicopathological Factors in Colorectal Cancer. *Anticancer Res.* 31, 2541–2545.

Silva, S. R., Bowen, K. A., Rychahou, P. G., Jackson, L. N., Weiss, H. L., Lee, E. Y., et al. (2011). VEGFR-2 Expression in Carcinoid Cancer Cells and its Role in Tumor Growth and Metastasis. *Int. J. Cancer* 128, 1045–1056. doi:10.1002/ijc.25441

Simasi, J., Schubert, A., Oelkrug, C., Gillissen, A., and Nieber, K. (2014). Primary and Secondary Resistance to Tyrosine Kinase Inhibitors in Lung Cancer. *Anticancer Res.* 34, 2841–2850.

Singh, D., Chan, J. M., Zoppoli, P., Niola, F., Sullivan, R., Castano, A., et al. (2012). Transforming Fusions of FGFR and TACC Genes in Human Glioblastoma. *Science* 337, 1231–1235. doi:10.1126/science.1220834

Song, F., Chen, Q., Rao, W., Zhang, R., Wang, Y., Ge, H., et al. (2019). OVA66 Promotes Tumour Angiogenesis and Progression through Enhancing Autocrine VEGF-VEGFR2 Signalling. *EBioMedicine* 41, 156–166. doi:10.1016/j.ebiom.2019.02.051

Song, X., Liu, Z., and Yu, Z. (2020). EGFR Promotes the Development of Triple Negative Breast Cancer through JAK/STAT3 Signaling. *Cancer Manag. Res.* 12, 703–717. doi:10.2147/CMAR.S225376

Spannuth, W. A., Nick, A. M., Jennings, N. B., Armaiz-Pena, G. N., Mangala, L. S., Danes, C. G., et al. (2009). Functional Significance of VEGFR-2 on Ovarian Cancer Cells. *Int. J. Cancer* 124, 1045–1053. doi:10.1002/ijc.24028

Spirina, L. V., Usynin, Y. A., Yurmazov, Z. A., Slonimskaya, E. M., Kolegova, E. S., and Kondakova, I. V. (2017). Transcription Factors NF-kB, HIF-1, HIF-2, Growth Factor VEGF, VEGFR2 and Carboanhydrase IX mRNA and Protein Level in the Development of Kidney Cancer Metastasis. *Mol. Biol. (Mosk)* 51, 372–377. doi:10.7868/s0026898417020197

Squires, M. S., Hudson, E. A., Howells, L., Sale, S., Houghton, C. E., Jones, J. L., et al. (2003). Relevance of Mitogen Activated Protein Kinase (MAPK) and Phosphotidylinositol-3-Kinase/protein Kinase B (PI3K/PKB) Pathways to Induction of Apoptosis by Curcumin in Breast Cells. *Biochem. Pharmacol.* 65, 361–376. doi:10.1016/S0006-2952(02)01517-4

St-Germain, M. E., Gagnon, V., Mathieu, I., Parent, S., and Asselin, E. (2004). Akt Regulates COX-2 mRNA and Protein Expression in Mutated-PTEN Human Endometrial Cancer Cells. *Int. J. Oncol.* 24, 1311–1324. doi:10.3892/ijo.24.5.1311

Starska, K., Forma, E., Lewy-Trenda, I., Stasikowska-Kanicka, O., Skóra, M., and Bryś, M. (2018). Fibroblast Growth Factor Receptor 1 and 3 Expression Is Associated with Regulatory PI3K/AKT Kinase Activity, as Well as Invasion and Prognosis, in Human Laryngeal Cancer. *Cel Oncol (Dordr)* 41, 253–268. doi:10.1007/s13402-017-0367-z

Stelloo, E., Versluis, M. A., Nijman, H. W., de Bruyn, M., Plat, A., Osse, E. M., et al. (2016). Microsatellite Instability Derived JAK1 Frameshift Mutations Are Associated with Tumor Immune Evasion in Endometrioid Endometrial Cancer. *Oncotarget* 7, 39885–39893. doi:10.18632/oncotarget.9414

Stover, E. H., Chen, J., Folens, C., Lee, B. H., Mentens, N., Marynen, P., et al. (2006). Activation of FIP1L1-PDGFRalpha Requires Disruption of the Juxtamembrane Domain of PDGFRalpha and Is FIP1L1-independent. *Proc. Natl. Acad. Sci. U S A.* 103, 8078–8083. doi:10.1073/pnas.0601192103

Strumberg, D., and Schultheis, B. (2012). Regorafenib for Cancer. *Expert Opin. Investig. Drugs* 21, 879–889. doi:10.1517/13543784.2012.684752

Su, C., Wang, W., and Wang, C. (2018). IGF-1-induced MMP-11 Expression Promotes the Proliferation and Invasion of Gastric Cancer Cells through the JAK1/STAT3 Signaling Pathway. *Oncol. Lett.* 15, 7000–7006. doi:10.3892/ol.2018.8234

Su, C. L., and Wu, C. S. (2017). Synthetic Lethality of K-Ras Mutant Human Colorectal Cancer Cells by Phytochemical Curcumin and FDA-Approved Targeted Drug Regorafenib. *FASEB J.* 31, 630–646.

Su, X., Zhan, P., Gavine, P. R., Morgan, S., Womack, C., Ni, X., et al. (2014). FGFR2 Amplification Has Prognostic Significance in Gastric Cancer: Results from a Large International Multicentre Study. *Br. J. Cancer* 110, 967–975. doi:10.1038/bjc.2013.802

Sun, X. D., Liu, X. E., and Huang, D. S. (2012). Curcumin Induces Apoptosis of Triple-Negative Breast Cancer Cells by Inhibition of EGFR Expression. *Mol. Med. Rep.* 6, 1267–1270. doi:10.3892/mmr.2012.1103

Sun, Y., Liu, L., Wang, Y., He, A., Hu, H., Zhang, J., et al. (2019). Curcumin Inhibits the Proliferation and Invasion of MG-63 Cells through Inactivation of the P-JAK2/p-STAT3 Pathway. *Onco Targets Ther.* 12, 2011–2021. doi:10.2147/OTT.S172909

Tang, L., Yang, J., Chen, J., Yu, J., Zhou, Q., Lu, X., et al. (2017). IGF-1R Promotes the Expression of Cyclin D1 Protein and Accelerates the G1/S Transition by Activating Ras/Raf/MEK/ERK Signaling Pathway. *Int. J. Clin. Exp. Pathol.* 10, 11652–11658.

Tanno, S., Ohsaki, Y., Nakanishi, K., Toyoshima, E., and Kikuchi, K. (2004). Human Small Cell Lung Cancer Cells Express Functional VEGF Receptors, VEGFR-2 and VEGFR-3. *Lung Cancer* 46, 11–19. doi:10.1016/j.lungcan.2004.03.006

Teiten, M. H., Eifes, S., Reuter, S., Duvoix, A., Dicato, M., and Diederich, M. (2009). Gene Expression Profiling Related to Anti-inflammatory Properties of Curcumin in K562 Leukemia Cells. *Ann. N. Y Acad. Sci.* 1171, 391–398. doi:10.1111/j.1749-6632.2009.04890.x

Teiten, M. H., Gaascht, F., Cronauer, M., Henry, E., Dicato, M., and Diederich, M. (2011). Anti-proliferative Potential of Curcumin in Androgen-dependent Prostate Cancer Cells Occurs through Modulation of the Wingless Signaling Pathway. *Int. J. Oncol.* 38, 603–611. doi:10.3892/ijo.2011.905

Ter Braak, B., Siezen, C. L., Lee, J. S., Rao, P., Voorhoeve, C., Ruppin, E., et al. (2017). Insulin-like Growth Factor 1 Receptor Activation Promotes Mammary Gland Tumor Development by Increasing Glycolysis and Promoting Biomass Production. *Breast Cancer Res.* 19, 14. doi:10.1186/s13058-017-0802-0

Terai, H., Soejima, K., Yasuda, H., Nakayama, S., Hamamoto, J., Arai, D., et al. (2013). Activation of the FGF2-FGFR1 Autocrine Pathway: a Novel Mechanism of Acquired Resistance to Gefitinib in NSCLC. *Mol. Cancer Res.* 11, 759–767. doi:10.1158/1541-7786.Mcr-12-0652

Tian, B., Zhao, Y., Liang, T., Ye, X., Li, Z., Yan, D., et al. (2017). Curcumin Inhibits Urothelial Tumor Development by Suppressing IGF2 and IGF2-Mediated PI3K/AKT/mTOR Signaling Pathway. *J. Drug Target.* 25, 626–636. doi:10.1080/1061186x.2017.1306535

Tian, X., Traub, B., Shi, J., Huber, N., Schreiner, S., Chen, G., et al. (2021). c-Jun N-Terminal Kinase 2 Suppresses Pancreatic Cancer Growth and Invasion and Is Opposed by C-Jun N-Terminal Kinase 1. *Cancer Gene Ther.* 1–14. doi:10.1038/s41417-020-00290-5

Tilborghs, S., Corthouts, J., Verhoeven, Y., Arias, D., Rolfo, C., Trinh, X. B., et al. (2017). The Role of Nuclear Factor-Kappa B Signaling in Human Cervical Cancer. *Crit. Rev. Oncol. Hematol.* 120, 141–150. doi:10.1016/j.critrevonc.2017.11.001

Till, J. H., Becerra, M., Watty, A., Lu, Y., Ma, Y., Neubert, T. A., et al. (2002). Crystal Structure of the MuSK Tyrosine Kinase: Insights into Receptor Autoregulation. *Structure* 10, 1187–1196. doi:10.1016/s0969-2126(02)00814-6

Tsao, A. S., Wei, W., Kuhn, E., Spencer, L., Solis, L. M., Suraokar, M., et al. (2011). Immunohistochemical Overexpression of Platelet-Derived Growth Factor Receptor-Beta (PDGFR-β) Is Associated with PDGFRB Gene Copy Number Gain in Sarcomatoid Non-small-cell Lung Cancer. *Clin. Lung Cancer* 12, 369–374. doi:10.1016/j.cllc.2011.02.002

Tung, C. L., Jian, Y. J., Chen, J. C., Wang, T. J., Chen, W. C., Zheng, H. Y., et al. (2016). Curcumin Downregulates P38 MAPK-dependent X-ray Repair Cross-Complement Group 1 (XRCC1) Expression to Enhance Cisplatin-Induced Cytotoxicity in Human Lung Cancer Cells. *Naunyn Schmiedebergs Arch. Pharmacol.* 389, 657–666. doi:10.1007/s00210-016-1235-5

Tung, Y. T., Chen, H. L., Lai, C. W., Shen, C. J., Lai, Y. W., and Chen, C. M. (2011). Curcumin Reduces Pulmonary Tumorigenesis in Vascular Endothelial Growth Factor (VEGF)-overexpressing Transgenic Mice. *Mol. Nutr. Food Res.* 55, 1036–1043. doi:10.1002/mnfr.201000654

Turner, N., Pearson, A., Sharpe, R., Lambros, M., Geyer, F., Lopez-Garcia, M. A., et al. (2010). FGFR1 Amplification Drives Endocrine Therapy Resistance and Is a Therapeutic Target in Breast Cancer. *Cancer Res.* 70, 2085–2094. doi:10.1158/0008-5472.CAN-09-3746

Vadhan-Raj, S., Weber, D. M., Wang, M., Giralt, S. A., Thomas, S. K., Alexanian, R., et al. (2007). Curcumin Downregulates NF-kB and Related Genes in Patients with Multiple Myeloma: Results of a Phase I/II Study. *Blood* 110, 1177. doi:10.1182/blood.V110.11.1177.1177

Valentinis, B., and Baserga, R. (1996). The IGF-I Receptor Protects Tumor Cells from Apoptosis Induced by High Concentrations of Serum. *Biochem. Biophys. Res. Commun.* 224, 362–368. doi:10.1006/bbrc.1996.1034

Van Erk, M. J., Teuling, E., Staal, Y. C., Huybers, S., Van Bladeren, P. J., Aarts, J. M., et al. (2004). Time- and Dose-dependent Effects of Curcumin on Gene Expression in Human colon Cancer Cells. *J. Carcinog* 3, 8. doi:10.1186/1477-3163-3-8

Van Trappen, P. O., Steele, D., Lowe, D. G., Baithun, S., Beasley, N., Thiele, W., et al. (2003). Expression of Vascular Endothelial Growth Factor (VEGF)-C and VEGF-D, and Their Receptor VEGFR-3, during Different Stages of Cervical Carcinogenesis. *J. Pathol.* 201, 544–554. doi:10.1002/path.1467

Vandermark, E. R., Deluca, K. A., Gardner, C. R., Marker, D. F., Schreiner, C. N., Strickland, D. A., et al. (2012). Human Papillomavirus Type 16 E6 and E 7 Proteins Alter NF-kB in Cultured Cervical Epithelial Cells and Inhibition of NF-kB Promotes Cell Growth and Immortalization. *Virology* 425, 53–60. doi:10.1016/j.virol.2011.12.023

Varshosaz, J., Jandaghian, S., Mirian, M., and Sajjadi, S. E. (2021). Co-delivery of Rituximab Targeted Curcumin and Imatinib Nanostructured Lipid Carriers in Non-hodgkin Lymphoma Cells. *J. Liposome Res.* 31, 64–78. doi:10.1080/08982104.2020.1720718

Velghe, A. I., Van Cauwenberghe, S., Polyansky, A. A., Chand, D., Montano-Almendras, C. P., Charni, S., et al. (2014). PDGFRA Alterations in Cancer: Characterization of a Gain-Of-Function V536E Transmembrane Mutant as Well as Loss-Of-Function and Passenger Mutations. *Oncogene* 33, 2568–2576. doi:10.1038/onc.2013.218

Wagh, P. K., Peace, B. E., and Waltz, S. E. (2008). Met-related Receptor Tyrosine Kinase Ron in Tumor Growth and Metastasis. *Adv. Cancer Res.* 100, 1–33. doi:10.1016/S0065-230X(08)00001-8

Walters, D. K., Mercher, T., Gu, T. L., O'Hare, T., Tyner, J. W., Loriaux, M., et al. (2006). Activating Alleles of JAK3 in Acute Megakaryoblastic Leukemia. *Cancer Cell* 10, 65–75. doi:10.1016/j.ccr.2006.06.002

Walz, C., Curtis, C., Schnittger, S., Schultheis, B., Metzgeroth, G., Schoch, C., et al. (2006). Transient Response to Imatinib in a Chronic Eosinophilic Leukemia Associated with Ins(9;4)(q33;q12q25) and a CDK5RAP2-PDGFRA Fusion Gene. *Genes Chromosomes Cancer* 45, 950–956. doi:10.1002/gcc.20359

Wang, C. Y., Mayo, M. W., Korneluk, R. G., Goeddel, D. V., and Baldwin, A. S., Jr. (1998). NF-kappaB Antiapoptosis: Induction of TRAF1 and TRAF2 and

C-IAP1 and C-IAP2 to Suppress Caspase-8 Activation. *Science* 281, 1680–1683. doi:10.1126/science.281.5383.1680

Wang, J., Gui, Z., Deng, L., Sun, M., Guo, R., Zhang, W., et al. (2012). c-Met Upregulates Aquaporin 3 Expression in Human Gastric Carcinoma Cells via the ERK Signalling Pathway. *Cancer Lett.* 319, 109–117. doi:10.1016/j.canlet.2011.12.040

Wang, J., Li, X., Xue, X., Ou, Q., Wu, X., Liang, Y., et al. (2019). Clinical Outcomes of EGFR Kinase Domain Duplication to Targeted Therapies in NSCLC. *Int. J. Cancer* 144, 2677–2682. doi:10.1002/ijc.31895

Wang, R., Wang, L., Li, Y., Hu, H., Shen, L., Shen, X., et al. (2014). FGFR1/3 Tyrosine Kinase Fusions Define a Unique Molecular Subtype of Non-small Cell Lung Cancer. *Clin. Cancer Res.* 20, 4107–4114. doi:10.1158/1078-0432.Ccr-14-0284

Wang, W., Wu, M., Liu, M., Yan, Z., Wang, G., Mao, D., et al. (2020). Hyperprogression to Camrelizumab in a Patient with Esophageal Squamous Cell Carcinoma Harboring EGFR Kinase Domain Duplication. *J. Immunother. Cancer* 8, e000793. doi:10.1136/jitc-2020-000793

Wang, W. Z., Li, L., Liu, M. Y., Jin, X. B., Mao, J. W., Pu, Q. H., et al. (2013). Curcumin Induces FasL-Related Apoptosis through P38 Activation in Human Hepatocellular Carcinoma Huh7 Cells. *Life Sci.* 92, 352–358. doi:10.1016/j.lfs.2013.01.013

Wang, Z., Longo, P. A., Tarrant, M. K., Kim, K., Head, S., Leahy, D. J., et al. (2011). Mechanistic Insights into the Activation of Oncogenic Forms of EGF Receptor. *Nat. Struct. Mol. Biol.* 18, 1388–1393. doi:10.1038/nsmb.2168

Watson, J. L., Greenshields, A., Hill, R., Hilchie, A., Lee, P. W., Giacomantonio, C. A., et al. (2010). Curcumin-induced Apoptosis in Ovarian Carcinoma Cells Is P53-independent and Involves P38 Mitogen-Activated Protein Kinase Activation and Downregulation of Bcl-2 and Survivin Expression and Akt Signaling. *Mol. Carcinog* 49, 13–24. doi:10.1002/mc.20571

Weigand, M., Hantel, P., Kreienberg, R., and Waltenberger, J. (2005). Autocrine Vascular Endothelial Growth Factor Signalling in Breast Cancer. Evidence from Cell Lines and Primary Breast Cancer Cultures *In Vitro*. *Angiogenesis* 8, 197–204. doi:10.1007/s10456-005-9010-0

Wheeler, D. L., and Yarden, Y. (2015). *Receptor Tyrosine Kinases: Family and Subfamilies*. New York, United States: Springer.

Wieman, H. L., Wofford, J. A., and Rathmell, J. C. (2007). Cytokine Stimulation Promotes Glucose Uptake via Phosphatidylinositol-3 kinase/Akt Regulation of Glut1 Activity and Trafficking. *Mol. Biol. Cel* 18, 1437–1446. doi:10.1091/mbc.e06-07-0593

Wilhelm, S. M., Carter, C., Tang, L., Wilkie, D., McNabola, A., Rong, H., et al. (2004). BAY 43-9006 Exhibits Broad Spectrum Oral Antitumor Activity and Targets the RAF/MEK/ERK Pathway and Receptor Tyrosine Kinases Involved in Tumor Progression and Angiogenesis. *Cancer Res.* 64, 7099–7109. doi:10.1158/0008-5472.Can-04-1443

Wu, C. S., Wu, S. Y., Chen, H. C., Chu, C. A., Tang, H. H., Liu, H. S., et al. (2019a). Curcumin Functions as a MEK Inhibitor to Induce a Synthetic Lethal Effect on KRAS Mutant Colorectal Cancer Cells Receiving Targeted Drug Regorafenib. *J. Nutr. Biochem.* 74, 108227. doi:10.1016/j.jnutbio.2019.108227

Wu, Q., Wu, W., Fu, B., Shi, L., Wang, X., and Kuca, K. (2019b). JNK Signaling in Cancer Cell Survival. *Med. Res. Rev.* 39, 2082–2104. doi:10.1002/med.21574

Wu, W., O'Reilly, M. S., Langley, R. R., Tsan, R. Z., Baker, C. H., Bekele, N., et al. (2007). Expression of Epidermal Growth Factor (EGF)/transforming Growth Factor-Alpha by Human Lung Cancer Cells Determines Their Response to EGF Receptor Tyrosine Kinase Inhibition in the Lungs of Mice. *Mol. Cancer Ther.* 6, 2652–2663. doi:10.1158/1535-7163.Mct-06-0759

Wu, Y., Hooper, A. T., Zhong, Z., Witte, L., Bohlen, P., Rafii, S., et al. (2006). The Vascular Endothelial Growth Factor Receptor (VEGFR-1) Supports Growth and Survival of Human Breast Carcinoma. *Int. J. Cancer* 119, 1519–1529. doi:10.1002/ijc.21865

Wu, Y. M., Su, F., Kalyana-Sundaram, S., Khazanov, N., Ateeq, B., Cao, X., et al. (2013). Identification of Targetable FGFR Gene Fusions in Diverse Cancers. *Cancer Discov.* 3, 636–647. doi:10.1158/2159-8290.Cd-13-0050

Xia, Y., Shen, S., and Verma, I. M. (2014). NF-κB, an Active Player in Human Cancers. *Cancer Immunol. Res.* 2, 823–830. doi:10.1158/2326-6066.Cir-14-0112

Xie, L., Su, X., Zhang, L., Yin, X., Tang, L., Zhang, X., et al. (2013). FGFR2 Gene Amplification in Gastric Cancer Predicts Sensitivity to the Selective FGFR Inhibitor AZD4547. *Clin. Cancer Res.* 19, 2572–2583. doi:10.1158/1078-0432.Ccr-12-3898

Xie, Q., Liu, K. D., Hu, M. Y., and Zhou, K. (2001). SF/HGF-c-Met Autocrine and Paracrine Promote Metastasis of Hepatocellular Carcinoma. *World J. Gastroenterol.* 7, 816–820. doi:10.3748/wjg.v7.i6.816

Xin, J., Jue, W., Huifen, S., Ran, R., Kai, X., Xiangming, T., et al. (2017). Curcumin Co-treatment Ameliorates Resistance to Gefitinib in Drug-Resistant NCI-H1975 Lung Cancer Cells. *J. Traditional Chin. Med.* 37, 355–360. doi:10.1016/S0254-6272(17)30071-7

Xu, H., and Shao, C. (2020). KIF5B-EGFR Fusion: A Novel EGFR Mutation in Lung Adenocarcinoma. *Onco Targets Ther.* 13, 8317–8321. doi:10.2147/OTT.S263994

Xu, X., Lu, Q., Wang, Z., Cai, P., Zeng, Z., Zhang, L., et al. (2021). Identification of a Novel CSNK2A1-PDGFRB Fusion Gene in a Patient with Myeloid Neoplasm with Eosinophilia. *Cancer Res. Treat.* 53, 889–892. doi:10.4143/crt.2020.1272

Xu, Y., Jin, J., Xu, J., Shao, Y. W., and Fan, Y. (2017). JAK2 Variations and Functions in Lung Adenocarcinoma. *Tumour Biol.* 39, 1010428317711140. doi:10.1177/1010428317711140

Yamauchi, Y., Izumi, Y., Yamamoto, J., and Nomori, H. (2014). Coadministration of Erlotinib and Curcumin Augmentatively Reduces Cell Viability in Lung Cancer Cells. *Phytother Res.* 28, 728–735. doi:10.1002/ptr.5056

Yan, J. D., Liu, Y., Zhang, Z. Y., Liu, G. Y., Xu, J. H., Liu, L. Y., et al. (2015). Expression and Prognostic Significance of VEGFR-2 in Breast Cancer. *Pathol. Res. Pract.* 211, 539–543. doi:10.1016/j.prp.2015.04.003

Yang, C. L., Liu, Y. Y., Ma, Y. G., Xue, Y. X., Liu, D. G., Ren, Y., et al. (2012). Curcumin Blocks Small Cell Lung Cancer Cells Migration, Invasion, Angiogenesis, Cell Cycle and Neoplasia through Janus Kinase-STAT3 Signalling Pathway. *PLoS One* 7, e37960. doi:10.1371/journal.pone.0037960

Yigit, N., Wu, W. W., Subramaniyam, S., Mathew, S., and Geyer, J. T. (2015). BCR-PDGFRA Fusion in a T Lymphoblastic Leukemia/lymphoma. *Cancer Genet.* 208, 404–407. doi:10.1016/j.cancergen.2015.04.007

Yonemura, Y., Fushida, S., Bando, E., Kinoshita, K., Miwa, K., Endo, Y., et al. (2001). Lymphangiogenesis and the Vascular Endothelial Growth Factor Receptor (VEGFR)-3 in Gastric Cancer. *Eur. J. Cancer* 37, 918–923. doi:10.1016/S0959-8049(01)00015-6

Yoshida, M., Tamagawa, N., Nakao, T., Kanashima, H., Ueda, H., Murakami, A., et al. (2015). Imatinib Non-responsive Chronic Eosinophilic Leukemia with ETV6-PDGFRA Fusion Gene. *Leuk. Lymphoma* 56, 768–769. doi:10.3109/10428194.2014.938330

Yu, S., Zhang, Y., Pan, Y., Cheng, C., Sun, Y., and Chen, H. (2017). The Non-small Cell Lung Cancer EGFR Extracellular Domain Mutation, M277E, Is Oncogenic and Drug-Sensitive. *Onco Targets Ther.* 10, 4507–4515. doi:10.2147/OTT.S131999

Yuan, L., Liu, Z. H., Lin, Z. R., Xu, L. H., Zhong, Q., and Zeng, M. S. (2014). Recurrent FGFR3-TACC3 Fusion Gene in Nasopharyngeal Carcinoma. *Cancer Biol. Ther.* 15, 1613–1621. doi:10.4161/15384047.2014.961874

Zhang, H., Bajraszewski, N., Wu, E., Wang, H., Moseman, A. P., Dabora, S. L., et al. (2007). PDGFRs Are Critical for PI3K/Akt Activation and Negatively Regulated by mTOR. *J. Clin. Invest.* 117, 730–738. doi:10.1172/jci28984

Zhang, H. F., and Lai, R. (2014). STAT3 in Cancer-Friend or Foe? *Cancers (Basel)* 6, 1408–1440. doi:10.3390/cancers6031408

Zhang, H. H., Zhang, Y., Cheng, Y. N., Gong, F. L., Cao, Z. Q., Yu, L. G., et al. (2018). Metformin Incombination with Curcumin Inhibits the Growth, Metastasis, and Angiogenesis of Hepatocellular Carcinoma *In Vitro* and *In Vivo*. *Mol. Carcinog* 57, 44–56. doi:10.1002/mc.22718

Zhang, J., Yu, J., Xie, R., Chen, W., and Lv, Y. (2016). Combinatorial Anticancer Effects of Curcumin and Sorafenib towards Thyroid Cancer Cells via PI3K/Akt and ERK Pathways. *Nat. Prod. Res.* 30, 1858–1861. doi:10.1080/14786419.2015.1074229

Zhang, L., Tao, X., Fu, Q., Ge, C., Li, R., Li, Z., et al. (2019). Curcumin Inhibits Cell Proliferation and Migration in NSCLC through a Synergistic Effect on the TLR4/MyD88 and EGFR Pathways. *Oncol. Rep.* 42, 1843–1855. doi:10.3892/or.2019.7278

Zhang, W., and Liu, H. T. (2002). MAPK Signal Pathways in the Regulation of Cell Proliferation in Mammalian Cells. *Cell Res* 12, 9–18. doi:10.1038/sj.cr.7290105

Zhang, X., Hu, B., Sun, Y. F., Huang, X. W., Cheng, J. W., Huang, A., et al. (2021). Arsenic Trioxide Induces Differentiation of Cancer Stem Cells in Hepatocellular Carcinoma through Inhibition of LIF/JAK1/STAT3 and NF-kB Signaling Pathways Synergistically. *Clin. Transl Med.* 11, e335. doi:10.1002/ctm2.335

Zhao, D., Pan, C., Sun, J., Gilbert, C., Drews-Elger, K., Azzam, D. J., et al. (2015a). VEGF Drives Cancer-Initiating Stem Cells through VEGFR-2/Stat3 Signaling to Upregulate Myc and Sox2. *Oncogene* 34, 3107–3119. doi:10.1038/onc.2014.257

Zhao, L., and Vogt, P. K. (2008). Class I PI3K in Oncogenic Cellular Transformation. *Oncogene* 27, 5486–5496. doi:10.1038/onc.2008.244

Zhao, W., Wang, Y., Wang, Y., Gao, N., Han, Z., and Yu, H. (2015b). Potential Anti-cancer Effect of Curcumin in Human Lung Squamous Cell Carcinoma. *Thorac. Cancer* 6, 508–516. doi:10.1111/1759-7714.12222

Zhao, X., Qu, J., Hui, Y., Zhang, H., Sun, Y., Liu, X., et al. (2017). Clinicopathological and Prognostic Significance of C-Met Overexpression in Breast Cancer. *Oncotarget* 8, 56758–56767. doi:10.18632/oncotarget.18142

Zhao, Y., Collier, J. J., Huang, E.-C., and Whelan, J. (2014). Turmeric and Chinese Goldthread Synergistically Inhibit Prostate Cancer Cell Proliferation and NF-kB Signaling. *Ffhd* 4, 312–339. doi:10.31989/ffhd.v4i7.1

Zhen, L., Fan, D., Yi, X., Cao, X., Chen, D., and Wang, L. (2014). Curcumin Inhibits Oral Squamous Cell Carcinoma Proliferation and Invasion via EGFR Signaling Pathways. *Int. J. Clin. Exp. Pathol.* 7, 6438–6446.

Zheng, B. Z., Liu, T. D., Chen, G., Zhang, J. X., and Kang, X. (2018). The Effect of Curcumin on Cell Adhesion of Human Esophageal Cancer Cell. *Eur. Rev. Med. Pharmacol. Sci.* 22, 551–560. doi:10.26355/eurrev_201801_14209

Zheng, X., Lu, G., Yao, Y., and Gu, W. (2019). An Autocrine IL-6/IGF-1R Loop Mediates EMT and Promotes Tumor Growth in Non-small Cell Lung Cancer. *Int. J. Biol. Sci.* 15, 1882–1891. doi:10.7150/ijbs.31999

Zhou, H., Beevers, C. S., and Huang, S. (2011). The Targets of Curcumin. *Curr. Drug Targets* 12, 332–347. doi:10.2174/138945011794815356

Zhou, Y., Zheng, S., Lin, J., Zhang, Q. J., and Chen, A. (2007). The Interruption of the PDGF and EGF Signaling Pathways by Curcumin Stimulates Gene Expression of PPARgamma in Rat Activated Hepatic Stellate Cell *In Vitro*. *Lab. Invest.* 87, 488–498. doi:10.1038/labinvest.3700532

Zhu, Y. C., Wang, W. X., Li, X. L., Xu, C. W., Chen, G., Zhuang, W., et al. (2019). Identification of a Novel Icotinib-Sensitive EGFR-SEPTIN14 Fusion Variant in Lung Adenocarcinoma by Next-Generation Sequencing. *J. Thorac. Oncol.* 14, e181–e183. doi:10.1016/j.jtho.2019.03.031

Zhu, Y. C., Wang, W. X., Song, Z. B., Zhang, Q. X., Xu, C. W., Chen, G., et al. (2018a). MET-UBE2H Fusion as a Novel Mechanism of Acquired EGFR Resistance in Lung Adenocarcinoma. *J. Thorac. Oncol.* 13, e202–e204. doi:10.1016/j.jtho.2018.05.009

Zhu, Y. C., Wang, W. X., Xu, C. W., Zhang, Q. X., Du, K. Q., Chen, G., et al. (2018b). Identification of a Novel Crizotinib-Sensitive MET-Atxn7l1 Gene Fusion Variant in Lung Adenocarcinoma by Next Generation Sequencing. *Ann. Oncol.* 29, 2392–2393. doi:10.1093/annonc/mdy455

Zinatizadeh, M. R., Schock, B., Chalbatani, G. M., Zarandi, P. K., Jalali, S. A., and Miri, S. R. (2021). The Nuclear Factor Kappa B (NF-kB) Signaling in Cancer Development and Immune Diseases. *Genes Dis.* 8, 287–297. doi:10.1016/j.gendis.2020.06.005

Conflict of Interest: The authors declare that the research was conducted in the absence of any commercial or financial relationships that could be construed as a potential conflict of interest.

Publisher's Note: All claims expressed in this article are solely those of the authors and do not necessarily represent those of their affiliated organizations, or those of the publisher, the editors and the reviewers. Any product that may be evaluated in this article, or claim that may be made by its manufacturer, is not guaranteed or endorsed by the publisher.

frontiers in Pharmacology

REVIEW
published: 16 December 2021
doi: 10.3389/fphar.2021.764331

Tetramethylpyrazine: A Review of Its Antitumor Potential and Mechanisms

*Shaojie Yang[1], Shuodong Wu[1], Wanlin Dai[2], Liwei Pang[1], Yaofeng Xie[3], Tengqi Ren[1], Xiaolin Zhang[1], Shiyuan Bi[1], Yuting Zheng[1], Jingnan Wang[1], Yang Sun[1], Zhuyuan Zheng[1] and Jing Kong[1]**

[1]Biliary Surgery (2nd General) Unit, Department of General Surgery, Shengjing Hospital of China Medical University, Shenyang, China, [2]Innovation Institute of China Medical University, Shenyang, China, [3]Department of Cardiology, Shengjing Hospital of China Medical University, Shenyang, China

Cancer remains a major public health threat. The mitigation of the associated morbidity and mortality remains a major research focus. *From a molecular biological perspective*, cancer is defined as uncontrolled cell division and abnormal cell growth caused by various gene mutations. Therefore, there remains an urgent need to develop safe and effective antitumor drugs. The antitumor effect of plant extracts, which are characterized by relatively low toxicity and adverse effect, has attracted significant attention. For example, increasing attention has been paid to the antitumor effects of tetramethylpyrazine (TMP), the active component of the Chinese medicine Chuanqiong, which can affect tumor cell proliferation, apoptosis, invasion, metastasis, and angiogenesis, as well as reverse chemotherapeutic resistance in neoplasms, thereby triggering antitumor effects. Moreover, TMP can be used in combination with chemotherapeutic agents to enhance their effects and reduce the side effect associated with chemotherapy. Herein, we review the antitumor effects of TMP to provide a theoretical basis and foundation for the further exploration of its underlying antitumor mechanisms and promoting its clinical application.

Keywords: tetramethylpyrazine, ligustrazine, antitumor, apoptosis, metastasis, angiogenesis, chemotherapy, multidrug resistant

OPEN ACCESS

Edited by:
Nand K. Roy,
Case Western Reserve University, United States

Reviewed by:
Mukerrem Betul Yerer Aycan, Erciyes University, Turkey
Xiaonan Gao, Shandong Normal University, China
Asieh Heirani-Tabasi, Tehran University of Medical Sciences, Iran

****Correspondence:***
Jing Kong
kongjing1998@163.com

Specialty section:
This article was submitted to Pharmacology of Anti-Cancer Drugs, a section of the journal Frontiers in Pharmacology

Received: *25 August 2021*
Accepted: *18 November 2021*
Published: *16 December 2021*

Citation:
Yang S, Wu S, Dai W, Pang L, Xie Y, Ren T, Zhang X, Bi S, Zheng Y, Wang J, Sun Y, Zheng Z and Kong J (2021) Tetramethylpyrazine: A Review of Its Antitumor Potential and Mechanisms. Front. Pharmacol. 12:764331. doi: 10.3389/fphar.2021.764331

1 INTRODUCTION

Cancer remains a global public health threat caused by numerous factors, including aging, smoking (Bach, 2009; Thun et al., 2013), unhealthy dietary habits (Xiao et al., 2011), environmental pollution (Raaschou-Nielsen et al., 2013), lack of activity, and obesity (Wang et al., 2012; Islami et al., 2017). According to the global disease burden statistics published by the Washington University, cancer-related deaths account for approximately 15% of all deaths (Global Burden of Disease, Mortality and Causes of Death Collaborators, 2015). The Global Cancer Observatory 2020 database reported an estimated 19,292,789 cancer cases and 9,958,133 cancer-related deaths in 2020. Female breast cancer has surpassed lung cancer as the most common cancer, with an estimated 2,261,419 new cases, accounting for 11.7% of all cancer cases, followed by lung (11.4%), colorectal (10.0%), prostate (7.3%), and gastric cancers (5.6%). Lung cancer remained the leading cause of death due to cancer, with an estimated 1,796,144 deaths in 2020, accounting for 18.0% of all cancer-related deaths, followed by colorectal cancer (9.4%), liver cancer (8.3%), gastric cancer (7.7%), and female breast cancer (6.9%). The incidence of cancer and its associated mortality present significant variations according to region and sex (Sung et al., 2021). Compared with the 2020 estimates, new cases and

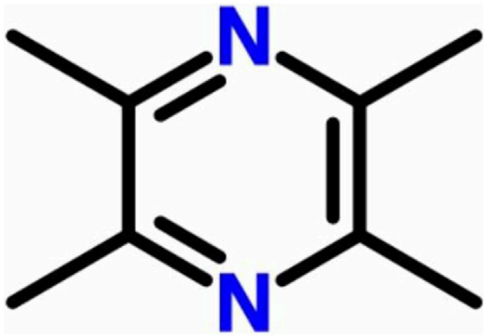

FIGURE 1 | Chemical structure of tetramethylpyrazine.

deaths in 2040 are expected to increase by 49% and 62%, respectively. In the next 20 years, the burden of cancer will continue to increase (Cao et al., 2021).

The Chinese medicine Chuanqiong is the dry rhizome of the plant *Ligusticum chuanxiong* Hort, which belongs to the family *Apiaceae*. It has a pungent flavor with a unique aroma and is beneficial for the liver, gallbladder, and pericardium meridian. Chuanqiong has a high medicinal value with respect to activating blood circulation to dissipate blood stasis. The main components of Chuanqiong include alkaloids, phenols, and volatile oil (Wen et al., 2021). Among them, the main alkaloid component is tetramethylpyrazine (TMP) (**Figure 1**), also known as ligustrazine (chemical name: 2,3,5,6-tetramethylpyrazine; pyrazine; molecular formula: $C_8H_{12}N_2$). TMP is an effective monomer obtained from the alkaloid of Chuanqiong and is also the main active substance in Chuanqiong. Previous studies have shown that TMP can exert antithrombosis, antiplatelet agglutination, antioxidation, and anti-ischemia reperfusion injury effects, improve microcirculation (Zou et al., 2018; Li et al., 2019; Zhou et al., 2020), and is widely used in various traumatic conditions and surgical treatments (Li et al., 2006; Yan et al., 2019). Additionally, TMP is used in the treatment of renal dysfunction (Sun et al., 2020), coronary heart disease (Wang et al., 2017), diabetes (Jiao et al., 2019), and cerebral infarction (Xu et al., 2017). At present, studies on the pharmacological role and clinical applications of TMP are very broad, and researchers are continuing to gain a deeper understanding of its characteristics.

In this review, we summarize the antitumor properties and potential mechanisms underlying the role of TMP in various tumors based on *in vitro* and *in vivo* studies. In addition to affecting the malignant biological behavior of tumor cells, TMP has protective effects on corresponding nontumor normal tissues. TMP can also be combined with chemotherapeutic agents to strengthen the damaging effects on tumors and can reduce the poisonous adverse effects caused by chemotherapeutic drugs, such as cardiac toxicity (Yang et al., 2019) and kidney toxicity (Michel and Menze, 2019). We compile these scientific pieces of evidence in this review to promote future research into the clinical application of TMP and further explore the potential treatment targets of TMP. We searched for almost all published papers related to the treatment of tumors with TMP in PubMed (https://pubmed.ncbi.nlm.nih.gov/) and summarized all the reports in this review. There is a large amount of research on TMP published in databases in Asia. Since these articles were not published in English, data provided in them remain unknown to researchers in other parts of the world.

2 OVERVIEW OF TETRAMETHYLPYRAZINE

TMP has traditional significance in the treatment of ischemic cerebrovascular disease (Li et al., 2015) and in a wide range of other clinical applications. TMP, in combination with other drugs, is used widely in clinical practice. In recent years, studies have shown that TMP has various effects, including blood glucose and lipid regulation, hepatic protection, and mitigates inflammation and vascular endothelial cell injury (Guo et al., 2016), and has enormous potential for future clinical application. TMP is also widely used in basic clinical treatment, and researchers have very broadly studied various aspects of it, such as its sedative and analgesic effects (Liang et al., 2005; Gao et al., 2008), antithrombotic effects (Cai et al., 2014), protection against ischemia reperfusion injury (Qian et al., 2014; Zhang et al., 2014; Zhang et al., 2018), and effects on blood vessels (Shan Au et al., 2003; Xu et al., 2014).

3 ANTITUMOR MECHANISM UNDERLYING THE EFFECTS OF TETRAMETHYLPYRAZINE IN MULTIPLE ORGANS

TMP has shown antitumor effects on various tumor types (**Figure 2**), including brain glioma (Cai et al., 2014), breast (Fan et al., 2021), prostate (Zhou et al., 2020), and lung cancers (Huang et al., 2018). Tumor growth can be reversed by applying different concentrations of TMP to tumor cells. Researchers have developed *in vitro* strategies for assessing the dosage, efficacy, and potential molecular mechanisms underlying the effects of TMP in different tumor cells (Fu et al., 2008; Huang et al., 2018; Zhou et al., 2020). TMP exhibits various antitumor effect on different tumor cells. TMP regulates various molecular signal pathways to alter the malignant biological behavior of tumor cells, including proliferation (Fu et al., 2008), cell cycle regulation (Yu et al., 2012), apoptosis (Cheng et al., 2007), invasion (Xu et al., 2018), metastasis (Fu et al., 2008), and angiogenesis (Jia et al., 2016). TMP also exhibits antiproliferative and antiangiogenic potential in a variety of *in vivo* models including a xenograft mouse model (Yu et al., 2012) and other experimental animal models (Fu et al., 2008). Overall, TMP has shown promising potential as an antitumor drug. In this review, we elaborate on the resistance of tumors to TMP according to body systems and the significant protection of organs around the tumor.

3.1 Brain and nervous system

Glioma is the most common tumor of the central nervous system that originates in glial cells. Over the past 30 years, the incidence of glioma has increased at a rate of 1%–2% per year (Chen et al.,

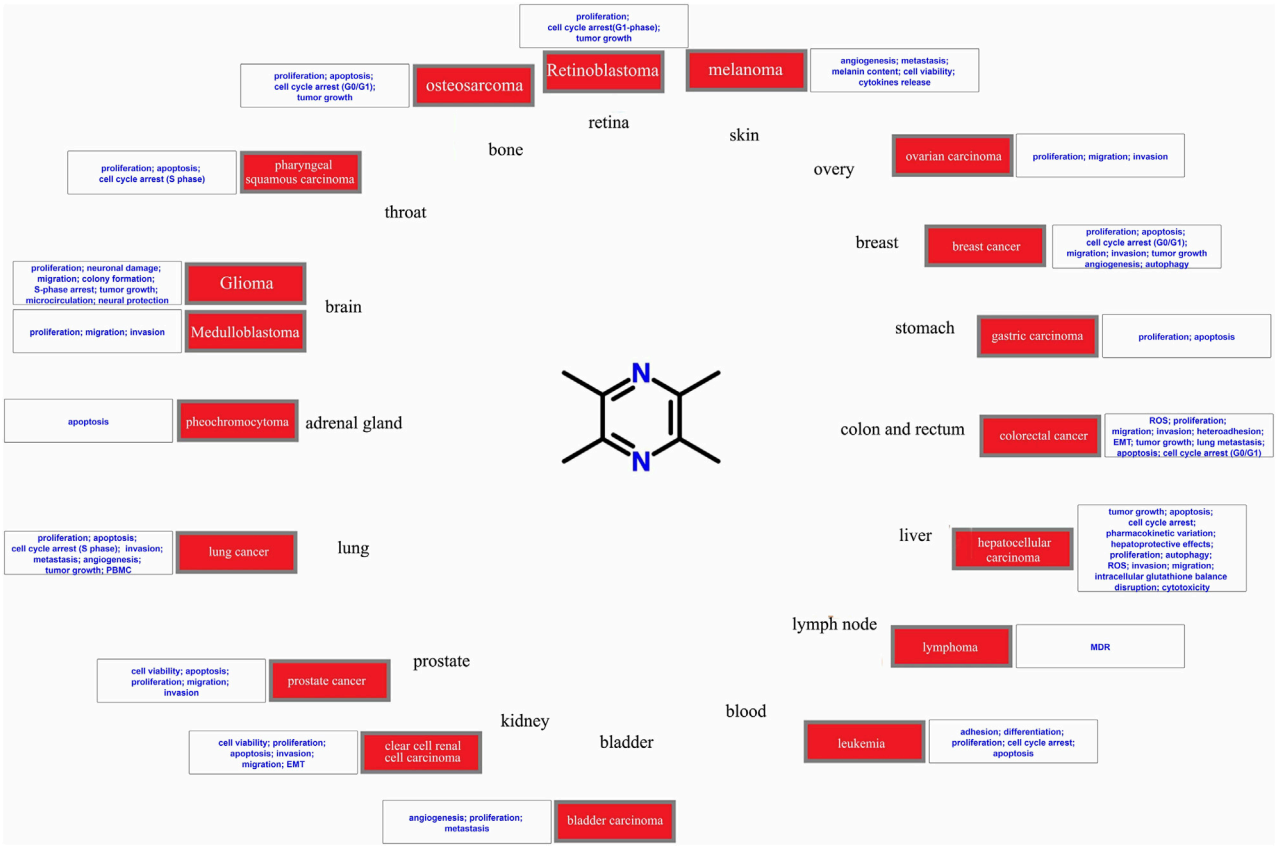

FIGURE 2 | Diseases involved in the current study of the antitumor potential of tetramethylpyrazine.

2020). At present, treatment modalities available for glioma include surgery, chemotherapy, and radiotherapy; gene therapy and immunotherapy have also been actively studied. However, the overall efficacy is not ideal (Eslahi et al., 2021). Fu et al. (2008) investigated the possible therapeutic efficacy of TMP against a rat glioma cell line (C6) and gliomas transplanted into rat brains. The authors found that TMP can suppress glioma activity, including growth, and protect neurons against glioma-induced excitotoxicity. C-X-C chemokine receptor type 4 (CXCR4), initially discovered for its involvement in human immunodeficiency virus entry and leukocyte trafficking, is overexpressed in more than 23 human cancers. Zhuang et al. have reported that TMP could downregulate CXCR4 in C6 cells, and further inhibit cell migration, proliferation, and colony formation, and induce S phase arrest more effectively than AMD3100 (a CXCR4 antagonist). The *in vivo* experiments in rats implanted with C6 cells showed results analogous to those found *in vitro* (Yu et al., 2012). In subsequent studies, TMP was found to effectively promote cerebral neurocyte survival by inhibiting hydrogen peroxide (H_2O_2)-induced increase in the intracellular concentration of Ca^{2+} and glutamate release. Upon using a glioma–neuronal coculturing system, TMP was more effective in these functions compared with AMD3100 (Chen et al., 2013). In 2014, Zhuang et al. studied the presence of high levels of invasion caused by neovascularization of gliomas using a venous endothelial cell line (ECV304) and a rat model. TMP inhibited neovascularization, fibrosis, and thrombosis under pathological conditions, contributing to the downregulation of CXCR4 through the SDF-1/CXCR4 axis (Cai et al., 2014).

There is a relative paucity of research on other tumors of the nervous system. The classic PI3K/AKT pathway remains to be fully investigated, and TMP has been found to affect the downstream functional protein, resulting in a change in tumor biological behavior. In a medulloblastoma cell line (Daoy), TMP inhibited the PI3K/AKT and mTOR signaling pathways by upregulating miR-211 to affect the proliferative, migratory, and invasive abilities of Daoy cells with the increase in the expression of caspase-3, caspase-9, and Bax, and a decrease in the expression of Bcl-2, MMP-2, MMP-9, and Vim (Xu et al., 2018). TMP blocked H_2O_2-induced apoptosis by regulating the expression of the members of the Bcl-2 family, suppressing cytochrome c release, and activating the caspase cascade in the rat pheochromocytoma-derived cell line PC12 (Cheng et al., 2007).

In contrast to the negative impact on tumor tissue, TMP plays a protective role in brain damage via a mechanism mainly related to the antioxidation or antiapoptotic pathways. *In vivo* and *in vitro* experimental studies have shown that TMP can improve cobalt chloride-induced oxidative stress and brain

TABLE 1 | Clinical application of tetramethylpyrazine (TMP) in cancer therapy.

S. no	Research target	Treatment	Research indicator	Effect
1	38 patients with lung cancer	80 mg of TMP added to 5% GS for intravenous infusion	Activation, adhesion, gathering and release of platelet; plasma VII C, vWF, Fg	Positive
2	56 patients with NHL	5 mg/kg a day intravenous TMP infusions	MDR and overexpression of P-glycoprotein (P-gp)	Positive

nerve injury, via a mechanism involving the increased expressions of nuclear factor erythroid 2-related factor 2 (NRF2) and glutamyl cystine ligase to promote the synthesis of glutathione (GSH) and reduce the levels of reactive oxygen species (ROS). Meanwhile, TMP inhibited the expressions of hypoxia-inducible factor 1α (HIF-1α) and nicotinamide adenine dinucleotide phosphate oxidase 2 (NOX2), to inhibit ROS production mediated by HIF-1α and NOX2. Through these two antioxidant pathways, TMP blocks apoptosis, restores mitochondrial function, and protects the brain cells (Guan et al., 2015). TMP may stimulate neuronal differentiation of human neuroblastoma SH-SY5Y cells by enhancing the recruitment of Ac-H3 and Ac-H4 to the topoisomerase II β gene promoter region to regulate neuronal development (Yan et al., 2014). TMP can also activate the mitogen-activated protein kinase (MAPK) signaling pathway by promoting the phosphorylation of extracellular signal-regulated kinase (ERK) 1/2 and reducing the phosphorylation of P38, thereby promoting brain neural stem cell proliferation and differentiation into neuronal cells under hypoxic conditions (Tian et al., 2010). TMP has a therapeutic effect on neurological diseases. TMP effectively reversed scopolamine-induced memory impairment in rats by improving postsynaptic protein synthesis and restoring the signal conduction of cyclophosphate/protein kinase A/the cAMP response element-binding protein (CREB) pathway (Wu et al., 2013). In cultured microglial cells stimulated with Aβ25-35, TMP repressed the inflammatory response in the presence of interferon (IFN)-γ and blocked ROS generation and phosphorylation of Akt to alleviate the inflammatory progression of Alzheimer's disease (Kim et al., 2014).

3.2 Respiratory system

Lung cancer has the highest incidence and mortality rate worldwide. Among its subtypes, nonsmall cell lung cancer (NSCLC) is the main histological type and accounts for 85% of all cases. Most patients are already in the middle and late stages of the disease when diagnosed (Herbst et al., 2018). In recent years, precision treatment modalities for lung cancer, such as targeted therapy, antiangiogenic treatment, and immunotherapy, have been rapidly developed. However, the survival period of lung cancer is still unsatisfactory (Hirsch et al., 2017). A study on the lung cancer cell lines A549 and 95D conducted by Huang et al. (2018) showed that TMP decreased cell viability in a dose- and time-dependent manner and suppressed the carcinogenesis of lung cancer cells by arresting the cell cycle at the S phase and inducing mitochondria-dependent apoptosis by regulating caspase-3 and Bax/Bcl-2. Cyclooxygenase (COX)-2 plays an important role in tumorigenesis and is a critical factor for the invasion and metastasis of lung cancer. Zheng et al. (2012) found that TMP exhibited the same dose- and time-dependent inhibitory effect on the proliferation of the lung cancer cell line A549 by suppressing cell cycle progression, which resulted in the inhibition of invasion *in vitro* and suppression of metastatic growth in an *in vivo* metastatic nude mouse model by targeting COX-2.

Hematogenous metastasis is often diagnosed in early-stage lung cancer, particularly, small cell lung cancer. Tumor growth and metastasis of lung cancer depend on the formation of a neovasculature. Antiangiogenic treatment has gradually attracted significant attention (Yi et al., 2019). Research on the pulmonary vascular cell model (microvascular endothelial cell line: HMEC-1) showed that TMP could suppress angiogenesis and tumor growth in lung cancer by blocking the BMP/Smad/Id-1 signaling pathway in a dose- and time-dependent manner. In addition, the administration of TMP inhibited the tumor growth of A549 xenografts in nude mice, with reduced expression of CD31, phosphorylated Smad1/5/8, and Id-1 (Jia et al., 2016). Lung cancer patients predominantly express type 2 cytokines. After investigating peripheral blood mononuclear cells obtained from lung cancer patients, Wei et al. (2002, 2004) reported that TMP could reverse the predominant type 2 status. This predominant expression of Th2 type cytokines may be related to a lower expression of T-bet or a higher expression of GATA3, with which TMP interferes.

The interaction of platelets in the blood and with TMP can also affect lung cancer progression. TMP, as a blood-activating agent, could increase the adhesion of the lung cancer cell lines PGCL3 and PAa to fibronectin but inhibit the invasion of PGCL3 cells in a Boyden chamber (Zhang et al., 1999). In a comparison of advanced cases of lung carcinoma and matched control subjects, TMP has been shown to have an antimetastatic effect on lung carcinoma as it inhibited the adhesion and aggregatory functions of blood platelets and the activity of coagulation factors (Chen et al., 1997).

3.3 Urinary system

Prostate cancer is a common malignant tumor among men, often treated with antiandrogen therapy. Most patients will be nondependent on androgen after 18–24 months of treatment (Cornford et al., 2021).

In prostate cancer cells, TMP treatment reduces viability and increases the rate of apoptosis in a dose-dependent manner. During the expression of long noncoding RNA, DPP10-AS1 is upregulated and becomes associated with CREB-binding protein to induce H3K27ac enrichment at the promoter region of the forkhead box M1 (*FOXM1*) gene (Zhou et al., 2020). Hormone-refractory

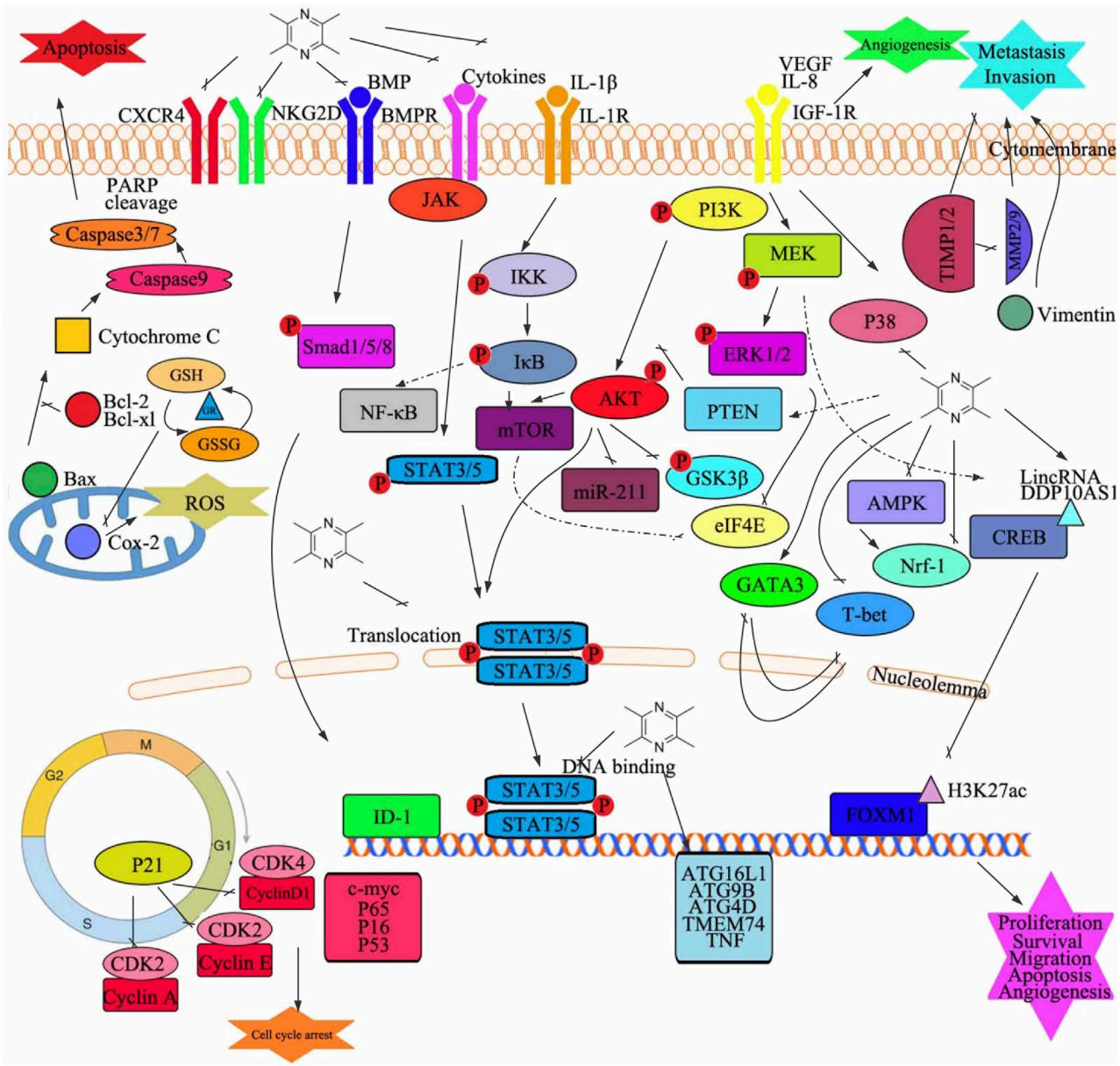

FIGURE 3 | Graphical summary of the antitumor mechanisms underlying the role of tetramethylpyrazine. Tetramethylpyrazine acts on multiple signaling pathways in cancer cells to modulate several changes in phenotype such as cell proliferation, apoptosis, cell cycle arrest, migration, invasion, and angiogenesis. GSH, glutathione; GR, glutathione reductase; Bax, Bcl2-associated X protein; GSSG, oxidized glutathione; Cox-2, cytochrome c oxidase subunit II; ROS, reactive oxygen species; P, phosphorylation; NF-κB, nuclear factor kappa B; STAT, signal transducer and activator of transcription; CXCR4, C-X-C motif chemokine receptor 4; NKG2D, killer cell lectin-like receptor K1; BMP, bone morphogenetic protein; BMPR, bone morphogenetic protein receptor; JAK, Janus kinase; IL, interleukin; PARP, poly(ADP-ribose) polymerase; VEGF, vascular endothelial growth factor; IGF-1R, insulin-like growth factor 1 receptor; IKK, I-kappaB kinase; mTOR, mechanistic target of rapamycin kinase; miR, microRNA; PI3K, phosphatidylinositol 3-kinase; ERK, extracellular signal-regulated kinase; MEK, mitogen-activated protein kinase; PTEN, phosphatase and tensin; AKT, protein kinase B; GSK3β, glycogen synthase kinase 3 beta; eIF4E, eukaryotic translation initiation factor 4E; GATA3, GATA-binding protein 3; T-bet, T-box transcription factor 21; Nrf-1, nuclear respiratory factor 1; CREB, DNA-binding transcriptional regulator CreB; AMPK, protein kinase AMP-activated catalytic subunit alpha 1; MMP, matrix metalloproteinase; TIMP, tissue inhibitors of metalloproteinase; ID-1, inhibitor of DNA binding 1; FOXM1, forkhead box M1; ATG4D, autophagy-related 4D cysteine peptidase; TMEM74, transmembrane protein 74; TNF, tumor necrosis factor; c-myc, transcriptional regulator Myc-like; CDK, cyclin-dependent kinases; ATG16L1, autophagy-related 16 like 1; ATG9B, autophagy-related 9B

prostate cancer (HRPC) is the final progression stage of prostate cancer and the most difficult to treat. Most patients have concomitant bone metastasis or pelvic lymph node metastasis when the diagnosis is confirmed. Whole-body chemotherapy or palliation is the main treatment modality for HRPC; however, the clinical efficacy is not ideal (Heber et al., 2019). In the HRPC cell line PC-3, TMP reduces cell proliferation and promotes apoptosis by modulating the availability of eIF4E mainly through the mTOR and

TABLE 2 | Antitumor effect of tetramethylpyrazine against the tumor models of multiple organs.

S. no	Research target	Molecular target	Mode of action	Reference
Brain and nervous system				
1	Glioma cell line (C6) and gliomas transplanted into rat brains	Glutamate-induced increase in intracellular calcium	Proliferation, neuronal damage, and migration	Fu et al. (2008)
2	Glioma cell line (C6) and rats implanted with C6 cells	CXCR4	Migration, proliferation, colony formation, and S-phase arrest; tumor growth and microcirculation	Yu et al. (2012)
3	Glioma cell line (C6) and cerebral neurocytes	CXCR4	Inhibition and neural protection	Chen et al. (2013)
4	Umbilical vein endothelial cell line (ECV304), corneal neovascularization, and pulmonary fibrosis in rat model	SDF-1/CXCR4 axis	Neovascularization, fibrosis, and thrombosis	Cai et al. (2014)
5	Medulloblastoma cell line (Daoy)	MiR-211, PI3K/AKT, and mTOR pathways	Proliferation, migration, and invasion	Xu et al. (2018)
6	Rat pheochromocytoma-derived cell line (PC12)	Bcl-2, Bax, cytochrome c, and caspase-3	Apoptosis	Cheng et al. (2007)
Respiratory system				
7	Lung cancer cell line (A549, 95D)	Caspase-3 and Bax/Bcl-2	Proliferation, apoptosis, cell cycle arrest (S phase)	Huang et al. (2018)
8	Lung cancer cell line (A549) and metastatic nude mouse model	COX-2 and MMP-2/TIMP-2	Proliferation, cell cycle arrest, invasion, and metastasis	Zheng et al. (2012)
9	Lung cancer cell line (A549), microvascular endothelial cell line (HMEC-1), A549 xenograft in nude mice	BMP/Smad/Id-1 pathway	Proliferation, migration, angiogenesis, and tumor growth	Jia et al. (2016)
10	Lung cancer patients and PBMCs	Th2 type cytokines, T-bet/GATA3	PBMC	Wei et al., 2002 and 2004
11	Lung cancer cell line (PGCL3 and PAa)	No mention	Adhesion and invasion	Zhang et al. (1999)
12	Advanced cases of lung carcinoma	PAdT, PagT, VIII:C, dWF, and Fg	Metastasis	Chen et al. (1997)
Urinary system				
13	Prostate cancer cells (PCa cells)	DPP10-AS1/CBP/FOXM1 signaling pathway	Cell viability and apoptosis	Zhou et al. (2020)
14	Hormone-refractory prostate cancer cell line (PC-3)	EIF4E, mTOR, and MEK/ERK signaling pathways	Proliferation and apoptosis	Han et al. (2015)
15	Prostate cancer cell line (PC-3)	FOXM1	Proliferation, migration, and invasion	Zhou et al. (2017)
16	Renal cell carcinoma cell line (ccRCC)	NKG2D pathway, NKG2DLs, MICA/B, E-cadherin, vimentin, and fibronectin	Cell viability, proliferation, apoptosis, invasion, migration, and EMT	Luan et al. (2016)
17	Bladder carcinoma cells (T24)	Glutathione metabolism and glycerophospholipid metabolism	Angiogenesis, proliferation, and metastasis	Cui et al., 2019 and 2020
Blood and immune system				
18	T-cell leukemia cell line (SKW-3)	ICAM-1 and LFA-1	Adhesion	Zhao et al. (2000)
19	Leukemia cell line (HL-60)	C-myc, p27, CDK2, and cyclinE1	Differentiation, proliferation, and cell cycle arrest	Wu et al. (2011)
20	Acute lymphoblastic leukemia cell line (Jurkat and SUP-B15)	GSK-3β, NF-κB, and c-myc	Proliferation, apoptosis, and cell cycle arrest	Wang et al. (2015)
21	Leukemia cell line (U937)	Bcl-2, caspase-3	Proliferation, apoptosis, and cell cycle arrest	Wang et al. (2015)
22	Non-Hodgkin's lymphoma (NHL) patients	P-glycoprotein (P-gp)	MDR	Yang and Jiang, (2010)
Digestive system				
23	Rats with DEN-induced HCC	Mitochondrial apoptotic pathway; Akt and ERK pathway	Tumor growth, apoptosis, and cell cycle arrest(G2/M)	Cao et al. (2015)
24	Mice with hepatic precancerous lesions	Serum marker enzymes, bile canaliculi hyperplasia	Pharmacokinetic variation and hepatoprotective effects	Feng et al. (2014)
25	HCC cell line (HepG2)	P53, Bcl-2/Bax protein ratio, cytochrome c, and caspase	Proliferation, mitochondrial apoptosis, cell cycle arrest (G0/G1 phase)	Bi et al. (2016)
26	HCC cell line (HepG2) and xenograft tumor models	Caspase-3 and PARP	Proliferation, autophagy, apoptosis, and ROS	Cao et al. (2015)

(Continued on following page)

TABLE 2 | (*Continued*) Antitumor effect of tetramethylpyrazine against the tumor models of multiple organs.

S. no	Research target	Molecular target	Mode of action	Reference
27	HCC cell line (HepG2)	IL-1R1/IκB/IKK/NF-κB signaling pathway	Invasion and migration	Wang et al. (2020)
28	HCC cell line (HepG2)	GSH/GSSG	Intracellular glutathione balance disruption and cytotoxicity	Ishida et al. (2012)
29	Gastric cancer cell line (SGC7901)	ROS, AMPK, cytochrome c, caspase-9, caspase-3, and mitochondrial membrane potential	Apoptosis	Yi et al. (2013)
30	Gastric cancer cell line (SGC-7901)	NF-xBp65, cyclinD1, and p16	Proliferation and apoptosis	Ji et al. (2014)
31	Colorectal cancer cell lines (SW480 and CT26)	P53-dependent mitochondrial pathway	Apoptosis, cell cycle arrest (G0/G1)	Bian et al. (2021)
32	Colorectal cancer cell line (HCT-116) and tumor-bearing mice	EMT(TGF-β1) and Wnt/β-catenin pathway (p-Akt, p-GSK-3β)	ROS, proliferation, migration, invasion, heteroadhesion, EMT, tumor growth, and lung metastasis *in vivo*	Zou et al. (2018)
Reproductive system				
33	Breast cancer cell line (MDA-MB-231) and xenograft tumors in nude mice	No mention	Proliferation, apoptosis, and cell cycle arrest (G0/G1)	Pan et al. (2015)
34	Breast cancer cell line (MDA-MB-231)	Akt and caspase-3	Proliferation, apoptosis, migration, and invasion	Shen et al. (2018)
35	Human breast cancer cell lines (MCF-7, MDA-MB-231), murine mammary carcinoma cell line (4T1), and 4T1 tumor-bearing mouse model	STAT3	Proliferation, migration, and tumor growth	Fan et al. (2021)
36	Triple-negative breast cancer cell line (MDA-MB-231)	Heparanase	Angiogenesis and autophagy	Li et al. (2021)
37	Ovarian cancer (OC) cell line (SK-OV-3 and OVCAR-3)	MiR-211	Proliferation, migration, and invasion	Zhang et al. (2021)
38	Ovarian carcinoma cell line (SKOV3)	IL-8 and ERK1/2, p38, and AP-1 pathways	Invasion and migration	Yin et al. (2011)
Other organs				
39	Melanoma cell line (B16F10) spontaneous metastasis model	CD34 and VEGF	Angiogenesis and metastasis	Chen et al. (2009)
40	UVA-induced melanoma/keratinocyte coculture system	TRP1, MITF, MAPK, TNFα, IL-1β, IL-8, and GM-CSF	Melanin content, cell viability, and cytokines release	Yeom et al. (2014)
41	Retinoblastoma cell line (WERI-Rb1), WERI-Rb1 cells injected into the eyes of athymic nude mice	Nrf-1 and CXCR4	Proliferation, cell cycle arrest(G1-phase), and tumor growth	Wu et al., 2017 and 2019
42	Osteosarcoma cell line (MG-63, SAOS-2, and U2OS), xenograft tumor mouse model	NF-κB, p65, BCL-2, and cyclin D1	Proliferation, apoptosis, cell cycle arrest (G0/G1), tumor growth	Wang et al. (2013)
43	Pharyngeal squamous cell line (FADU), HeLa, Hep G2, MCF-7, and A549	Depolarization of mitochondrial membrane potential	Proliferation, apoptosis, cell cycle arrest (S phase)	Wang et al. (2019)
Adriamycin				
44	HCC cell line (HepG2/ADM)	P-gp170 and MDR1	MDR	Mei et al. (2004)
45	HCC cell line (BEL-7402/ADM)	P-glycoprotein, MDR1, MRP2, MRP3, and MRP5	MDR	Wang et al. (2010)
46	Breast cancer cell line (MCF-7/ADR)	No mention	MDR	Zhou et al. (2007)
47	Breast cancer cell line (MCF-7/dox)	P-glycoprotein (P-gp)	MDR	Zhang et al. (2012)
48	Breast cancer cell line (MCF-7/A) and tumor xenografts *in vivo*	GSH, GSTπ, and JNK	Proliferation, ADR resistance, MDR	Zhang et al. (2014)
49	Breast cancer cell line (MCF-7/A)	EGFR/PI3K/Akt pathway	ADR resistance, apoptosis	Chen et al. (2014)
50	Human myelogenous leukemia cell line (K562/A02)	GSTπ	MDR	Song et al. (2011)
51	Breast cancer tissue samples and breast cancer cell lines (MCF-7 and T47D)	JAK2/STAT3 pathway	Epirubicin resistance	Liu et al. (2020)
Cisplatin				
52	Lewis lung cancer mice (nonsmall cell lung cancer)	VEGF, KLF4, and ADAMTS1	Tumor growth and angiogenesis	Tang et al. (2017)
53	Lung cancer cell line (A549, SPC-A-1, and LTEP-G-2) and implanted human lung cancer in mice	TrxR/Trx system, NF-κB, AKT, and ERK signaling pathways	MDR, ROS, apoptosis, tumor growth	Ai et al. (2016)

(Continued on following page)

TABLE 2 | (*Continued*) Antitumor effect of tetramethylpyrazine against the tumor models of multiple organs.

S. no	Research target	Molecular target	Mode of action	Reference
54	Bladder cancer cell line (Pumc-91/ADM and T24/DDP)	MRP1, GST, BCL-2, and TOPO-II	MDR and cell cycle arrest	Wang et al. (2016)
Paclitaxel				
55	Lung cancer cell line (A549)	VEGF, MMP2, TGF-β1, and E-cadherin	Metastasis	Xie et al. (2019)
56	Ovarian cancer cell line (A2780 and SKOV3) and A2780-heterografted BALB/c nude mice	ERK1/2 and Akt pathways	Angiogenesis, apoptosis, proliferation, and migration	Zou et al. (2019)
T-OA				
57	S180 mice (sarcoma)	NF-κB/p65 and COX-2	Pharmacokinetic evaluation and antitumor activity	Wang et al. (2013)
58	HCC cell line (Bel-7402)	NF-κB/p65 and COX-2	Apoptosis	Zhang et al. (2015)
59	HCC cell line (HepG2) and HT-29, HeLa, and BGC-823	No mention	Cytotoxicity, apoptosis, and nephrotoxicity	Chu et al. (2014)
DT-010				
60	Breast cell line (MCF-7)	GRP78	Dox-induced toxicity, apoptosis	Wang et al. (2016)
61	Breast cancer cell line (MCF-7/ADR)	P53, P-glycoprotein, and mitochondrial complex II	Proliferation, apoptosis, glycolysis, mitochondrial function, and metabolic process	Zhou et al. (2019)
62	Breast cancer cell line (MCF-7 and MDA-MB-231)	Mitochondrial complex II	Proliferation, cell cycle arrest, ROS generation, and mitochondrial dysfunction	Wang et al. (2016)
CSTMP				
63	Lung cancer cell line (A549)	IRE1α-TRAF2-ASK1 complex, ER stress, and JNK activation	Proliferation, cell cycle arrest, mitochondria-dependent apoptosis	Zhang et al. (2016)
64	Myeloma cell line (RPMI8226)	CHOP, GRP78, GRP94, cleaved caspase-12, PERK-eIF2α, IRE1α, and ATF6	Apoptosis, ER stress, and mitochondrial dysfunction	Sun et al. (2016)

MEK/ERK signaling pathways to inhibit cap-dependent translation (Han et al., 2015). In addition, Zhou et al. (2017) reported that TMP inhibited PC-3 cell proliferation, migration, and invasion by downregulating *FOXM1* through treatment with TMP and a pcDNA–FOXM1 plasmid.

Clear cell renal cell carcinoma (ccRCC) is the commonest type of kidney cancer. The associated mortality rate is as high as 47%, making it a significant threat to patients (Jonasch et al., 2021). The antitumor efficacy of TMP was investigated in the human ccRCC cell line and found to inhibit ccRCC cell viability, proliferation, apoptosis, invasion, and migration by inhibiting the NKG2D-related signaling pathway to further suppress epithelial–mesenchymal transition (EMT) progression. The binding of NKG2D to its ligands activates natural killer (NK) cells to increase NK cell-mediated cytotoxicity against cancer cells with a high expression of major histocompatibility complex class I chain-related molecules A and B (Luan et al., 2016). BA-12, a TMP–betulinic acid derivative, exhibits potent antitumor activities by blocking angiogenesis to inhibit the growth and metastasis of bladder carcinoma cells (T24); this involves interfering with GSH metabolism and activating glycerophospholipid metabolism (Cui et al., 2019; Cui et al., 2020).

TMP plays a renoprotective role by protecting kidney tissues and cells against apoptosis, has an antioxidant function to ameliorate kidney injury and kidney tissue fibrosis. Yang et al. (2011) found that TMP can improve the pathological conditions of rats with diabetic nephropathy induced by streptozocin by decreasing the expression of vascular endothelial growth factor (VEGF). Another study reported that TMP plays a protective role against kidney injury among rats. Its mechanism may involve the inhibition of the P38 MAPK expression and the transcriptional factor forkhead box O1 which blocks the signal transduction pathway mediated by these two proteins, thus playing an antiapoptotic role. In addition, TMP plays a protective role against human renal proximal tubule injury induced by sodium arsenate, via a mechanism involving the inhibition of ROS production, increasing the level of GSH, and increasing cytochrome C oxidase activity to improve mitochondrial dysfunction (Gong et al., 2015). TMP also induces tubulointerstitial fibrosis and resists ureteric obstruction via multiple pathways. Possible mechanisms involved in this change include the transdifferentiation of renal tubular mesenchymal cells and exerting antioxidant effects. This process downregulates the expression of TGF43L protein and connective tissue growth factor, and upregulates hepatocyte growth factor and BMP-7 (Yuan et al., 2012).

3.4 Blood and immune system

Acute leukemia is the commonest malignant tumor among children and adolescents, mainly treated with chemotherapy. Treatment failure and recurrence caused by reduced chemotherapy sensitivity and drug resistance are major challenges faced during leukemia treatment (Cartel et al., 2021). Lymphocyte function-associated antigen-1 (LFA-1) is expressed on the surfaces of the T-cell leukemia cell line

SKW-3. Red blood cells coupled with intercellular adhesion molecule-1 (ICAM-1) are carriers for LFA-1 and ICAM-1, which mediate the adhesion properties of cells (Zhao et al., 2000). Small doses of TMP induce the nonterminal differentiation and proliferation of the leukemia cell line HL-60 in a dose- and time-dependent manner, in addition to synergistically blocking the cell cycle progression of HL-60 cells in the G0/G1 phase (Wu et al., 2011). In acute lymphoblastic leukemia cell lines Jurkat and SUP-B15, TMP induces apoptosis and causes cell cycle arrest at the G0/G1 phase by downregulating GSK-3β, which further prevents the induced translocation of NF-κB and c-myc from the cytoplasm to the nucleus (Wang et al., 2015). In the leukemia cell line U937, TMP inhibits cellular proliferation and induces apoptosis, via a mechanism possibly associated with its impact on the cell cycle distribution, regulation of Bcl-2 expression, and finally via caspase-3 activation (Wang et al., 2015).

Research has shown that TMP also plays an effective role in the treatment of lymphoma. Among 60 patients, TMP was found to act as a salvage agent in combination with chemotherapy and could increase the response rate, prolong the progression-free survival with manageable toxicity, and correlate with p-glycoprotein (P-gp) expression in relapsed or refractory non-Hodgkin's lymphoma (NHL) (Yang et al., 2010).

3.5 Digestive system

Hepatocellular carcinoma (HCC) is one of the most common malignant tumors. The latest data show that the incidence of HCC is the sixth highest, with the third highest mortality rate (Yeung et al., 2022) among all malignant tumors. More than 80% of the HCC patients are already in an advanced stage at diagnosis or lose the opportunity for surgery. Even among patients who have undergone radical surgery, the 2-year recurrence rate remains at up to 50% (Shiffman, 2018). This high recurrence rate may be related to the resistance to single-agent chemotherapy or combined chemotherapy (Perboni et al., 2010). TMP could significantly inhibit tumor development in rats with diethylnitrosamine-induced HCC by inducing apoptosis and cell cycle arrest at the G2/M phase through the mitochondrial apoptotic pathway (Cao et al., 2015). Upon detecting pharmacokinetic variations of TMP phosphate after oral administration in mice with hepatic precancerous lesions, TMP was partly effective in protecting the liver from carcinogenesis initiated by diethylnitrosamine; hepatic insufficiency could alter its pharmacokinetics (Feng et al., 2014).

TMP significantly inhibited HCC cell line (HepG2) proliferation, and induced cell cycle arrest at the G0/G1 checkpoint and caspase-dependent mitochondrial apoptosis *in vitro* (Bi et al., 2016). TMP induced ROS generation and the inhibition of ROS reduced the antitumor function to regulate autophagy and proliferation by cleaving caspase-3 and PARP in HepG2 cells and xenograft tumor models (Cao et al., 2015). As a major active component of TOGA, a novel conjugate, TMP could prevent the invasion and migration of HepG2 cells induced by tumor-associated macrophages or IL-1β through the IL-1R1/IκB/IKK/NF-κB signaling pathway with the decreased expression of the EMT-related proteins Snail and Vimentin (Wang et al., 2020). As a model compound, 3-hydro-2,2,5,6-TMP (DHP-3) exerted cytotoxic activity by disrupting the intracellular GSH balance in HepG2 cells in a concentration range of 10 μM–1 mM and significantly so at the highest concentration (Ishida et al., 2012). TMP could alleviate the hepatotoxicity resulting from cyclophosphamide treatment as evidenced by improvement in the structure and function of the liver, and inhibition of oxidative stress and inflammation with accompanying pyroptosis, which was positively correlated with the inhibition of the Txnip/Trx/NF-κB pathway (Ma et al., 2021).

TMP also has an inhibitory effect against gastrointestinal tumors. The induction of apoptosis by TMP in the gastric carcinoma cell line SGC7901 is associated with the activation of the ROS/AMPK (AMP-activated protein kinase) pathway, and AMPK activation induces apoptosis through the mitochondrial apoptotic pathway (Yi et al., 2013). TMP also exhibits significant antiproliferative and proapoptotic properties, regulated by NF-κB, p65, cyclinD1, and p16 in SGC-7901 cells (Ji et al., 2014). TMP could induce colorectal cancer cell line (SW480 and CT26) apoptosis via a p53-dependent mitochondrial pathway and cell cycle arrest at the G0/G1 phase; TMP-induced apoptosis and cell cycle arrest were markedly reversed by pifithrin-α (a p53 inhibitor) (Bian et al., 2021). TMP possesses a water-soluble pyrazine skeleton and can inhibit the proliferation and metastasis of cancer cells. Zou et al. (2018) synthesized a compound by replacing the trimethoxyphenyl group of piperlongumine 1 with a TMP moiety. In the colorectal cancer cell line HCT-116, this compound increased ROS levels, and inhibited proliferation, migration, invasion, and heteroadhesion to a greater extent than piperlongumine 1 through EMT induced by TGF-β1 and Wnt/β-catenin activation by inhibiting Akt and GSK-3β phosphorylation, in addition to suppressing tumor growth and lung metastasis *in vivo* to prolong the survival of tumor-bearing mice (Zou et al., 2018).

3.6 Reproductive system

Breast cancer is one of the most common malignant tumors worldwide and its associated mortality rate is the second highest among all malignant tumors (Siegel et al., 2020).

Based on the expression of estrogen receptor (ER), progesterone receptor (PR), human epidermal growth factor receptor-2 (HER2), and Ki-67, breast cancer can be divided into the following types: the luminal (luminal or hormone receptor positive) A, luminal B, Her-2 overexpression, and basal-like (substrate) types (Viale et al., 2019). The molecular profiles of breast cancer are closely related to their pathological features and clinical prognosis (Tran and Bedard, 2011). Endocrine treatments, such as tamoxifen administration and chemotherapy often cause drug resistance, which leads to a relatively poor prognosis (Viedma-Rodríguez et al., 2014). In the breast cancer cell line MDA-MB-231, TMP inhibited cell survival, and induced apoptosis and cell cycle arrest at the G0/G1 phase. The *in vivo* findings among xenograft tumors established in nude mice were consistent with those found *in vitro* (Pan et al., 2015). TMP significantly inhibited the viability, migration, and invasion rates, and increased the apoptosis of cells in a dose-dependent manner, as in MDA-MB-231 cells, by inhibiting the

activity of Akt and increasing the activity of caspase-3 (Shen et al., 2018). Signal transducer and activator of transcription 3 (STAT3) is overexpressed and hyperactivated in tumors. Statmp-151, a TMP derivative, could also act as a novel small molecule Stat3 inhibitor against breast cancer by influencing the mitochondrial membrane potential and ROS generation (Fan et al., 2021).

ER/PR-positive patients account for approximately 70% of all breast cancer patients; triple-negative breast cancer accounts for 19%, and the Her-2 overexpression type accounts for the remainder (Viale et al., 2019). ER positivity is often considered a good prognostic factor. Due to the lack of corresponding treatment targets, triple-negative breast cancer is considered to have the worst prognosis among patients with breast cancer. TMP, as a component of SANT, a novel Chinese herbal monomer combination, decreased tumor growth and angiogenesis *in vivo* and *in vitro* by modulating autophagy in heparinase-overexpressed triple-negative breast cancer. During this process, the expression levels of the *ATG16L1*, *ATG9B*, and *ATG4D* genes increased and those of the *TMEM74* and *TNF* genes decreased. Additionally, the protein levels of HB-EGF, thrombospondin-2, amphiregulin, leptin, IGFBP-9, EGF, coagulation factor III, and MMP-9 (pro and active forms) in the tumor decreased, whereas those of serpin E1 and platelet factor 4 increased (Li et al., 2021).

Chemotherapy is an important strategy for treating breast cancer; however, the occurrence of drug resistance during chemotherapy often leads to failure of breast cancer treatment (Holohan et al., 2013). Drug resistance has become one of the main obstacles to breast cancer treatment. Consensus regarding the use of TMP to relieve tumor resistance has been reached.

Due to a lack of an effective early detection method, typical clinical symptoms are the most important reasons for delaying ovarian cancer diagnosis. Approximately 70% of the patients with ovarian cancer are diagnosed at an advanced stage (Snijders et al., 2017). The high mortality rate of ovarian cancer is attributed to the characteristics of its distant metastasis (Li et al., 2005). TMP can reduce the viability, proliferation, migration, and invasion ability of the human ovarian carcinoma cell lines SK-OV-3 and OVCAR-3 by regulating miR-211, and the EMT is also involved in this process (Zhang et al., 2021). TMP also inhibits the invasion and migration of SK-OV-3 cells by decreasing the expression of IL-8 through the ERK1/2, p38, and AP-1 signaling pathways, and IL-8 expression was significantly inhibited after coincubation with PD98059 (an ERK inhibitor) and SB203580 (a p38 inhibitor) (Yin et al., 2011).

3.7 Other organs

Malignant melanoma has a high invasiveness and is associated with a high mortality rate. Early-stage melanoma can be surgically resected, and the 5-year survival rate can reach 95%. However, advanced, or unresectable melanoma constitutes a major challenge in the treatment of melanoma (Ubellacker et al., 2020). In the melanoma cell line B16F10 spontaneous metastasis model, TMP inhibited tumor metastasis through its antiangiogenic activity by decreasing the expression of CD34 and VEGF in the primary tumor tissue and reducing the number of metastase nodi on the lung surface (Chen et al., 2009). TMP was also studied in an ultraviolet A-induced melanoma/keratinocyte coculture system, in which it regulates melanogenesis by enhancing inflammation and decreasing the levels of melanogenic factors (TRP1, MITF, and MAPK) (Yeom et al., 2014).

Retinoblastoma is the most common ocular tumor among children and causes extensive damage. Wu et al. (2017) reported interesting findings on the treatment of retinoblastoma with TMP. In the retinoblastoma cell line WERI-Rb1, TMP significantly downregulated the expression of CXCR4 in a time-dependent manner by reducing the expression of the transcription factor nuclear respiratory factor-1 (Nrf-1). Moreover, it inhibited cell proliferation as an effective CXCR4 antagonist (such as AMD3100) and induced G1-phase arrest in cells seeded at high-density. In addition, TMP protected normal retinal neurocytes from H_2O_2-induced damage by downregulating CXCR4 (Wu et al., 2017; Wu et al., 2019).

In osteosarcoma cell lines (MG-63, SAOS-2, and U2OS), TMP inhibited cell proliferation and induced apoptosis and G0/G1 arrest in a dose-dependent manner by upregulating the expressions of cytosolic NF-κB and p65, while downregulating the nuclear expressions of NF-κB, p65, Bcl-2, and cyclin D1. In addition, TMP exerted an antitumor effect against osteosarcoma in a xenograft tumor mouse model and exhibited a low level of toxicity (Wang et al., 2013). Wang et al. (2019). Synthesized TMP dimers and seven TMP tetramers were linked by alkane diamine, most of which showed better cytotoxicity than the TMP monomer. The TMP dimer 8e linked with decane-1,10-diamine exhibited the highest cytotoxicity in the pharyngeal squamous carcinoma cell line FADU and induced the apoptosis of FaDu cells by depolarizing the mitochondrial membrane potential and S phase cell cycle arrest.

4 EFFECTS AND REVERSE FUNCTION OF MULTIDRUG RESISTANCE TO CHEMOTHERAPEUTIC AGENTS

Tumor multidrug resistance (MDR) is a major obstacle to cancer chemotherapy. MDR involves the imbalance of multiple mechanisms, including the decrease in concentration of intracellular drugs, changes in drug target molecules, metabolic detoxification, and DNA damage repair function (Tinoush et al., 2020). The need to overcome MDR in tumor cells and improve the efficacy of antitumor drugs remains a key challenge that must be addressed. Recent studies suggest that TMP may reverse tumor MDR, although the mechanism for this remains elusive.

Chemotherapy significantly impacts the physique of the patient, which reduces their tolerance of chemotherapy and overall quality of life. Therefore, it is necessary to continue to explore new treatment options to allow patients undergoing chemotherapy to obtain more benefits. TMP treatment of patients with advanced tumors can reduce toxicity and enhance the efficacy of chemotherapy. For patients with poor general conditions and a strong willingness to use traditional Chinese medicine, a combination of traditional Chinese medicine

and chemotherapy may be an option. The amphiphilic paclitaxel-ss-TMP conjugate that readily self-assembles into stable nanoparticles in aqueous solution belongs to a redox-responsive carrier-free nanosystem with intrinsic amphiphilicity, which exhibits higher cytotoxicity by being associated with a greater apoptosis rate and cell cycle arrest than monotherapy or combination therapy with free drugs. In addition, this treatment also shows tumor-specific accumulation and excellent antitumor activity in A2780 xenograft mice (Zou et al., 2021).

4.1 Adriamycin

Adriamycin, also known as doxorubicin, is an antitumor antibiotic that inhibits the synthesis of RNA and DNA. This drug nonspecifically targets the cell cycle and has a damaging effect on tumor cells in various phases of the growth cycle. Therefore, it exhibits a wide range of biochemical effects on the body and has a strong cytotoxic effect (Li et al., 2021; Riaz and Hussain, 2021). The effectiveness of Adriamycin in the treatment of cancer has been limited by the development of drug resistance. TMP showed a potentiating effect on the cytotoxicity of Adriamycin *in vitro* and partly reversed adriamycin resistance in the resistant mouse cell line EAC (Hu et al., 1993). TMP can reverse MDR of the HCC cell line HepG2/ADM by enhancing the density of adriamycin in the cell and increasing its cytotoxicity. In this process, the transcriptional activity of MDR1 and the expression of P-gp170 decreases (Mei et al., 2004). TMP also reverses MDR in the HCC cell line BEL-7402/ADM (Wang et al., 2010). Zhou (2007) showed that the average initial adriamycin efflux rate in the breast cancer cell line MCF-7/ADR was higher than that in MCF-7. After treatment with TMP, the drug efflux rate of the MCF-7/ADR cells was reduced to approximately half of that in cells without inhibitors. In the breast cancer cell line MCF-7/Dox, TMP increased the intracellular concentration of adriamycin and inhibited the P-gp-mediated efflux of doxorubicin in a dose-dependent manner, which was induced by inhibiting the ATPase activity of P-gp (Zhang et al., 2012). DLJ14, a TMP piperazine derivative, could serve as a promising chemo-sensitization candidate for the reversal of MDR in the breast cancer cell line (MCF-7/A). It increases the intracellular accumulation of adriamycin by inhibiting the GSH level and the GSH peroxidase and GSH S-transferase (GST) activity (Zhang et al., 2014). Combination treatment with DLJ14 and adriamycin could inhibit the growth of adriamycin-resistant MCF-7/A cells by inhibiting the EGFR/PI3K/Akt survival pathway and inducing apoptosis via the mitochondrial-apoptosis pathway (Chen et al., 2014). Overexpression of GSTπ is one of the mechanisms that contributes to MDR. DLJ14 may trigger the reversal of MDR in adriamycin-resistant human myelogenous leukemia (K562/A02) cells by modulating the expression of GSTπ and GST-related enzymes (Song et al., 2011). The cardiotoxicity and endotheliotoxicity of adriamycin limit its clinical application in cancer treatment. TMP protects the vascular endothelium against adriamycin-induced injury by upregulating 14-3-3γ expression, promoting the translocation of Bcl-2 into the mitochondria, closing mPTP, maintaining MMP, inhibiting the RIRR mechanism, suppressing oxidative stress, improving mitochondrial function, and alleviating adriamycin-induced endotheliotoxicity (Yang et al., 2019). Epirubicin is an isomer of adriamycin. TMP reverted epirubicin resistance by inhibiting the JAK2/STAT3 pathway and decreasing fibrinogen gamma chain (FGG) expression in breast cancer; the elimination of cancer stem cells has also been observed during this process (Liu et al., 2020).

4.2 Cisplatin

Cisplatin inhibits DNA function and cell mitosis (Hamano et al., 2021). Cisplatin has a wide antitumor spectrum and is used in the treatment of head and neck squamous cell carcinoma, ovarian cancer, embryonic cancer, lung cancer, and thyroid cancer (Fang et al., 2021; Prayuenyong et al., 2021). In Lewis lung cancer mice, TMP with cisplatin exhibited additional or synergistic effects with respect to inhibiting tumor growth effectively; the mechanism involved reducing the expression of the angiogenesis-promoting factor VEGF and increasing the expression of the angiogenesis inhibitors KLF4 and ADAMTS1 (Tang et al., 2017). Ai et al. (2016)-designed TMP–curcumin hybrids (10a–u). Compound 10d inhibited the proliferation of the drug-sensitive lung cancer cell lines A549, SPC-A-1, and LTEP-G-2, and drug-resistant A549/DDP cells, by suppressing the TrxR/Trx system and promoting intracellular ROS accumulation and cancer cell apoptosis. Compound 10d also inhibited the growth of implanted human drug-resistant lung cancer in mice. TMP enhances the cytotoxic effect of antitumor agents on the bladder cancer cell lines Pumc-91/ADM and T24/DDP in response to adriamycin, which results in cell cycle arrest in the G1/S phase due to the decrease in the levels of MRP1, GST, and Bcl-2 and increase in the levels of topoisomerase-II (Wang et al., 2016). Cisplatin is one of the most effective broad-spectrum cancer chemotherapy drugs that exhibits serious adverse effects, such as acute renal injury. A study on cisplatin-treated rats showed that TMP might be a potential candidate for neoadjuvant chemotherapy due to its antioxidant, antiinflammatory, and antiapoptotic effects, in addition to its effect on Nrf2, the HMGB1/TLR4/NF-κB signaling pathway, and PPAR-γ expression (Michel and Menze, 2019).

4.3 Paclitaxel

Paclitaxel, a natural secondary metabolite obtained from the bark of *Taxus chinensis* var. *mairei* via cell culture exhibits a good antitumor effect, particularly against ovarian (Lau et al., 2020), cervical (Kitagawa et al., 2015), and breast cancers (Untch et al., 2016). For the treatment of NSCLC, dequalinium-modified paclitaxel plus TMP micelles destroyed vasculogenic mimicry channels and inhibit tumor metastasis (Xie et al., 2019). In the ovarian cancer cell lines A2780 and SKOV3, TMP in combination with paclitaxel suppressed angiogenesis by inhibiting the ERK1/2 and Akt pathways and promoted the apoptosis of tumor cells to enhance the antitumor effects of paclitaxel compared with treatment alone. In A2780 xenograft mouse models, TMP augmented the antitumor effects of paclitaxel by influencing

cell proliferation and angiogenesis as well as decreasing paclitaxel toxicity (Zou et al., 2019).

5 DERIVATIVES AND COMPOUNDS OF TETRAMETHYLPYRAZINE

Many active monomers used in traditional Chinese medicine and their derivatives or analogs can be used to overcome the low bioavailability of traditional Chinese medicines. They can ameliorate the clinical symptoms and prevent tumor recurrence. In addition, traditional Chinese medicine compounds can strengthen the antitumor effects (compared with single Chinese medicine monomers) (Luan et al., 2020). Below, we summarize the characteristics of three TMP derivatives and compounds [T-OA, DT-010, and (E)-2-(2-chlorostyryl)-3,5,6-trimethylpyrazine (CSTMP)] and expound their role in tumor treatment.

5.1 T-OA

T-OA, an antitumor TMP derivative with the chemical name 3βhydroxyolea-12-en-28-oic acid-3,5,6-trimethylpyrazin-2-methylester, has been shown to have effective anticancer activity (Fu et al., 2017). It exerts its antitumor activity and pharmacokinetic characteristics by preventing the expression of the nuclear transcription factor NF-κB/p65 and COX-2 in S180 mice (sarcoma) (Wang et al., 2013). Compared with cisplatin, T-OA is more toxic to the HCC cell line Bel-7402 than to three other cancer cell lines (HeLa, HT-29, and BGC-823), and plays a role in apoptosis by preventing the expression of NF-κB/p65 and COX-2 in Bel-7402 cells (Zhang et al., 2015). Although the poor solubility of T-OA results in low oral bioavailability, T-OA liposomes could significantly promote its intestinal lymphatic transport and enhance its oral bioavailability (Li et al., 2020). T-OA(6a), as a T-OA derivative designed by Chu et al. (2014), induced apoptosis in the HCC cell line HepG2 via nuclear fragmentation and exhibited lower nephrotoxicity. Additionally, T-OA(6a) exhibited good levels of cytotoxicity and possessed better hydrophilicity than T-OA in the cancer cell lines HepG2, HT-29, HeLa, and BGC-823 (Chu et al., 2014).

5.2 DT-010

DT-010, a novel synthetic compound of Danshensu and TMP, has been found to possess a cardioprotective effect with respect to myocardial ischemia/reperfusion injury in clinical studies (Xie et al., 2021). In the breast cell line MCF-7, DT-010 was more potent than TMP, Danshensu, or a combination of the two with respect to potentiating doxorubicin-induced toxicity; cotreatment with DT-010 and doxorubicin increased the level of apoptosis relative to doxorubicin alone. DT-010 and doxorubicin exhibit a synergistic antitumor effect in breast cancer by downregulating the glycolytic pathway and GRP78. DT-010 also protects against doxorubicin-induced cardiotoxicity (Wang et al., 2016), restores doxorubicin-induced apoptosis, and significantly inhibits growth when combined with doxorubicin. DT-010 overcomes doxorubicin resistance through a dual action by simultaneously inhibiting P-gp-mediated drug efflux and influencing the metabolic process (Zhou et al., 2019). DT-010 potently inhibits cell proliferation by inducing cytotoxicity and promoting cell cycle arrest in the breast cancer cell lines MCF-7 and MDA-MB-231; this effect is attributed to the suppression of the mitochondrial function. Further studies have shown that DT-010 suppresses succinate-induced mitochondrial respiration and impairs mitochondrial complex II enzyme activity to trigger ROS generation and mitochondrial dysfunction (Wang et al., 2016). Tang et al. (2018) suggested DT-010 as a potential therapeutic agent for effectively combating the cardiotoxicity of doxorubicin. DT-010 prevents doxorubicin-induced morphological changes and directly inhibits the generation of ROS. As cardiotoxicity is multifactorial, DT-010 could also inhibit the induction of autophagosome formation by regulating the upstream Akt/AMPK/mTOR signaling pathway (Tang et al., 2018).

5.3 CSTMP

CSTMP, a TMP analog, was designed and synthesized based on the pharmacophores of TMP and resveratrol (Ding et al., 2016). In the lung cancer cell line A549, CSTMP inhibited cell proliferation and induced cell cycle arrest and apoptosis through IRE1α-TRAF2-ASK1 complex-mediated ER stress, JNK activation, and mitochondrial dysfunction. The process could also be reversed by treatment with IRE1α siRNA (Zhang et al., 2016). CSTMP showed significant cytotoxic effects in the human myeloma cell line RPMI8226 by promoting caspase- and mitochondria-dependent apoptosis with increasing expressions of endoplasmic reticulum stress-related proteins (CHOP, GRP78, GRP94, and cleaved caspase-12) and activation of multiple ER stress transducers (PERK-eIF2α, IRE1α, and ATF6) (Sun et al., 2016).

Certain synthesized derivatives or compounds exhibit superior anticancer effects and fewer adverse effects than the available chemotherapeutic drugs or TMP monomers. These advantages are attributed to their relatively improved biosafety and lower toxicity, and successfully targeting proliferation, apoptosis, invasion, angiogenesis, cell cycle, and mitochondrial membrane potential. Synthetic TMP–betulin derivatives (TBs) have been proposed, with most demonstrating a better antitumor activity than betulin in HeLa, HepG2, BGC-823, and HT-29 cell lines. Among them, compound TB-01 showed the best antitumor effect and the lowest toxicity on normal cells, and demonstrated better cytotoxicity than cisplatin toward cancer cells. In addition, TB-01 induced early apoptosis in HepG2 cells and blocked the cell cycle at the G1 phase (Guo et al., 2020). Xu et al. (2015) designed novel TMP–triterpene derivatives, among which compound 4a exhibited better cytotoxic activity against Bel-7402, HT-29, MCF-7, HeLa, and HepG2 than cisplatin by depolarizing the mitochondrial membrane potential and increasing the intracellular free Ca^{2+} concentration (Xu et al., 2015). Dipeptide derivatives of TBA (a TMP compound) and amino acid were also designed by Xu et al. (2017), of which BA-25 exhibited the highest cytotoxic activity in tumor cell lines (HepG2, HT-29, HeLa, BCG-823, and A549) compared with cisplatin. BA-25 induced apoptosis associated with loss of mitochondrial membrane potential and increased intracellular free Ca^{2+} concentration (Xu et al., 2017). Wang et al. (2012) applied the "combination principle" in drug discovery and used several effective antitumor ingredients of Shi Quan Da Bu Wan as starting materials to synthesize TMP derivatives, which showed antiproliferative activities against

HCT-8, Bel-7402, BGC-823, A-549, and A2780 human cancer cell lines and suppressed normal angiogenesis (Wang et al., 2012).

6 CLINICAL TRIALS IN TUMOR TREATMENT

To overcome the clinical applications of TMP in tumor treatment, clinical trials remain essential. Most of the aforementioned treatment modalities of tumors involving TMP remain on the cellular and animal stage. Data obtained from human experiments remain limited (**Table 1**). Yang et al. (2010) administered intravenous TMP infusions to 56 patients with NHL in conjunction with chemotherapy with an application dose of 5 mg/kg and a maximum dose of 400 mg/day. Chen et al. (1997) combined 80 mg of TMP and 5% GS for intravenous infusion to affect platelet function and the coagulation state in 38 patients with lung cancer at a rate of 60–70 drops/min. These two studies suggest the potential use of TMP as an antitumor agent. Research on the antitumor effects of TMP requires the cooperation of various research organizations, which will promote the development of TMP-related drugs, improve its safety and treatment outcomes.

7 CONCLUSION AND FUTURE PERSPECTIVES

Several preclinical and clinical studies have independently verified that TMP exhibits chemical prevention and treatment potential for various cancers. Therefore, based on the above results, we can suggest factors that have led to the antitumor activity of TMP (**Figure 3** and **Table 2**). However, there remains a need for sufficient evidence to continue to study the exact antitumor mechanism underlying the role of TMP and promote its clinical application in the treatment of cancer. Therefore, future research should focus on elucidating the precise anticancer mechanism underlying the role of TMP. Studies should continue to investigate MDR and TMP from various aspects and targets, to explain their mechanisms, as well as to evaluate the safety and effectiveness of TMP to facilitate its clinical application.

AUTHOR CONTRIBUTIONS

SY, SW, and JK designed the study and revised the manuscript. WD, LP, YX, TR, XZ, SB, YZ, JW, YS, and ZZ performed the literature search. SY drafted the manuscript. All authors contributed to the article and approved the submitted version.

FUNDING

The present study was supported by the Shenyang Science and Technology Innovation Talent Support Program for Youth and Midlife (grant no. RC200121) and The 345 Talent Project Program of China Medical University Shengjing Hospital (grant no. 2019-40A).

REFERENCES

Ai, Y., Zhu, B., Ren, C., Kang, F., Li, J., Huang, Z., et al. (2016). Discovery of New Monocarbonyl Ligustrazine-Curcumin Hybrids for Intervention of Drug-Sensitive and Drug-Resistant Lung Cancer. *J. Med. Chem.* 59, 1747–1760. doi:10.1021/acs.jmedchem.5b01203

Bach, P. B. (2009). Smoking as a Factor in Causing Lung Cancer. *JAMA* 301, 539–541. doi:10.1001/jama.2009.57

Bi, L., Yan, X., Chen, W., Gao, J., Qian, L., and Qiu, S. (2016). Antihepatocellular Carcinoma Potential of Tetramethylpyrazine Induces Cell Cycle Modulation and Mitochondrial-dependent Apoptosis: Regulation of P53 Signaling Pathway in Hepg2 Cells *In Vitro*. *Integr. Cancer Ther.* 15, 226–236. doi:10.1177/1534735416637424

Bian, Y., Yang, L., Sheng, W., Li, Z., Xu, Y., Li, W., et al. (2021). Ligustrazine Induces the Colorectal Cancer Cells Apoptosis via P53-dependent Mitochondrial Pathway and Cell Cycle Arrest at the G0/g1 Phase. *Ann. Palliat. Med.* 10, 1578–1588. doi:10.21037/apm-20-288

Cai, X., Chen, Z., Pan, X., Xia, L., Chen, P., Yang, Y., et al. (2014). Inhibition of Angiogenesis, Fibrosis and Thrombosis by Tetramethylpyrazine: Mechanisms Contributing to the Sdf-1/cxcr4 axis. *PloS one* 9, e88176. doi:10.1371/journal.pone.0088176

Cao, J., Miao, Q., Miao, S., Bi, L., Zhang, S., Yang, Q., et al. (2015). Tetramethylpyrazine (Tmp) Exerts Antitumor Effects by Inducing Apoptosis and Autophagy in Hepatocellular Carcinoma. *Int. Immunopharmacol* 26, 212–220. doi:10.1016/j.intimp.2015.03.028

Cao, J., Miao, Q., Zhang, J., Miao, S., Bi, L., Zhang, S., et al. (2015). Inhibitory Effect of Tetramethylpyrazine on Hepatocellular Carcinoma: Possible Role of Apoptosis and Cell Cycle Arrest. *J. Biol. Regul. Homeost Agents* 29, 297–306.

Cao, W., Chen, H. D., Yu, Y. W., Li, N., and Chen, W. Q. (2021). Changing Profiles of Cancer burden Worldwide and in china: A Secondary Analysis of the Global Cancer Statistics 2020. *Chin. Med. J. (Engl)* 134, 783–791. doi:10.1097/CM9.0000000000001474

Cartel, M., Mouchel, P. L., Gotanègre, M., David, L., Bertoli, S., Mansat-De Mas, V., et al. (2021). Inhibition of Ubiquitin-specific Protease 7 Sensitizes Acute Myeloid Leukemia to Chemotherapy. *Leukemia* 35, 417–432. doi:10.1038/s41375-020-0878-x

Chen, J., Wang, W., Wang, H., Liu, X., and Guo, X. (2014). Combination Treatment of Ligustrazine Piperazine Derivate Dlj14 and Adriamycin Inhibits Progression of Resistant Breast Cancer through Inhibition of the Egfr/pi3k/akt Survival Pathway and Induction of Apoptosis. *Drug Discov. Ther.* 8, 33–41. doi:10.5582/ddt.8.33

Chen, L., Lu, Y., Wu, J. M., Xu, B., Zhang, L. J., Gao, M., et al. (2009). Ligustrazine Inhibits B16f10 Melanoma Metastasis and Suppresses Angiogenesis Induced by Vascular Endothelial Growth Factor. *Biochem. Biophys. Res. Commun.* 386, 374–379. doi:10.1016/j.bbrc.2009.06.042

Chen, L. H., Pan, C., Diplas, B. H., Xu, C., Hansen, L. J., Wu, Y., et al. (2020). The Integrated Genomic and Epigenomic Landscape of Brainstem Glioma. *Nat. Commun.* 11, 3077. doi:10.1038/s41467-020-16682-y

Chen, S. X., Wang, L. X., and Xing, L. L. (1997). Effects of Tetramethylpyrazine on Platelet Functions of Advanced Cases of Lung Carcinoma. *Zhongguo Zhong Xi Yi Jie He Za Zhi* 17, 531–533.

Chen, Z., Pan, X., Georgakilas, A. G., Chen, P., Hu, H., Yang, Y., et al. (2013). Tetramethylpyrazine (Tmp) Protects Cerebral Neurocytes and Inhibits Glioma by Down Regulating Chemokine Receptor Cxcr4 Expression. *Cancer Lett.* 336, 281–289. doi:10.1016/j.canlet.2013.03.015

Cheng, X. R., Zhang, L., Hu, J. J., Sun, L., and Du, G. H. (2007). Neuroprotective Effects of Tetramethylpyrazine on Hydrogen Peroxide-Induced Apoptosis in Pc12 Cells. *Cell Biol Int* 31, 438–443. doi:10.1016/j.cellbi.2006.10.001

Chu, F., Xu, X., Li, G., Gu, S., Xu, K., Gong, Y., et al. (2014). Amino Acid Derivatives of Ligustrazine-Oleanolic Acid as New Cytotoxic Agents. *Molecules* 19, 18215–18231. doi:10.3390/molecules191118215

Collaborators, G. M. a. C. o. D. (2015). Global, Regional, and National Age-Sex Specific All-Cause and Cause-specific Mortality for 240 Causes of Death, 1990-2013: A Systematic Analysis for the Global burden of Disease Study 2013. *Lancet (London, England)* 385, 117–171. doi:10.1016/S0140-6736(14)61682-2

Cornford, P., van den Bergh, R. C. N., Briers, E., Van den Broeck, T., Cumberbatch, M. G., De Santis, M., et al. (2021). Eau-eanm-estro-esur-siog Guidelines on Prostate Cancer. Part Ii-2020 Update: Treatment of Relapsing and Metastatic Prostate Cancer. *Eur. Urol.* 79, 263–282. doi:10.1016/j.eururo.2020.09.046

Cui, H., Guo, W., Zhang, B., Li, G., Li, T., Yuan, Y., et al. (20202019). Correction: Cui, H., et al. BA-12 Inhibits Angiogenesis via Glutathione Metabolism Activation. Int. J. Mol. Sci. 2019, 20, 4062. *Int. J. Mol. Sci.* 21, 4062. doi:10.3390/ijms21186814

Cui, H., Guo, W., Zhang, B., Li, G., Li, T., Yuan, Y., et al. (2019). Ba-12 Inhibits Angiogenesis via Glutathione Metabolism Activation. *Ijms* 20, 4062. doi:10.3390/ijms20164062

Ding, Y., Liao, W., He, X., Xiang, W., and Lu, Q. (2016). CSTMP Exerts Anti-inflammatory Effects on LPS-Induced Human Renal Proximal Tubular Epithelial Cells by Inhibiting TLR4-Mediated NF-Kb Pathways. *Inflammation* 39, 849–859. doi:10.1007/s10753-016-0315-5

Eslahi, M., Dana, P. M., Asemi, Z., Hallajzadeh, J., Mansournia, M. A., and Yousefi, B. (2021). The Effects of Chitosan-Based Materials on Glioma: Recent Advances in its Applications for Diagnosis and Treatment. *Int. J. Biol. Macromol* 168, 124–129. doi:10.1016/j.ijbiomac.2020.11.180

Fan, C., Wang, Y., Huang, H., Li, W., Ma, J., Yao, D., et al. (2021). The Tetramethylpyrazine Derivative Statmp-151: A Novel Small Molecule Stat3 Inhibitor with Promising Activity against Breast Cancer. *Front. Pharmacol.* 12, 651976. doi:10.3389/fphar.2021.651976

Fang, C.-Y., Lou, D.-Y., Zhou, L.-Q., Wang, J.-C., Yang, B., He, Q.-J., et al. (2021). Natural Products: Potential Treatments for Cisplatin-Induced Nephrotoxicity. *Acta Pharmacol. Sin.* doi:10.1038/s41401-021-00620-9

Feng, L., Mao, W., Zhang, J., Liu, X., Jiao, Y., Zhao, X., et al. (2014). Pharmacokinetic Variations of Tetramethylpyrazine Phosphate after Oral Administration in Hepatic Precancerous Mice and its Hepatoprotective Effects. *Drug Dev. Ind. Pharm.* 40, 1–8. doi:10.3109/03639045.2012.756513

Fu, J., Dong, X. X., Zeng, Z. P., Yin, X. B., Li, F. W., and Ni, J. (2017). Preparation and Physicochemical Characterization of T-Oa Plga Microspheres. *Chin. J. Nat. Med.* 15, 912–916. doi:10.1016/S1875-5364(18)30007-4

Fu, Y. S., Lin, Y. Y., Chou, S. C., Tsai, T. H., Kao, L. S., Hsu, S. Y., et al. (2008). Tetramethylpyrazine Inhibits Activities of Glioma Cells and Glutamate Neuro-Excitotoxicity: Potential Therapeutic Application for Treatment of Gliomas. *Neuro Oncol.* 10, 139–152. doi:10.1215/15228517-2007-051

Gao, Y., Xu, C., Liang, S., Zhang, A., Mu, S., Wang, Y., et al. (2008). Effect of Tetramethylpyrazine on Primary Afferent Transmission Mediated by P2x3 Receptor in Neuropathic Pain States. *Brain Res. Bull.* 77, 27–32. doi:10.1016/j.brainresbull.2008.02.026

Gong, X., Ivanov, V. N., Davidson, M. M., and Hei, T. K. (2015). Tetramethylpyrazine (Tmp) Protects against Sodium Arsenite-Induced Nephrotoxicity by Suppressing Ros Production, Mitochondrial Dysfunction, Pro-inflammatory Signaling Pathways and Programed Cell Death. *Arch. Toxicol.* 89, 1057–1070. doi:10.1007/s00204-014-1302-y

Guan, D., Su, Y., Li, Y., Wu, C., Meng, Y., Peng, X., et al. (2015). Tetramethylpyrazine Inhibits CoCl2 -induced Neurotoxicity through Enhancement of Nrf2/GCLc/GSH and Suppression of HIF1α/NOX2/ROS Pathways. *J. Neurochem.* 134, 551–565. doi:10.1111/jnc.13161

Guo, M., Liu, Y., and Shi, D. (2016). Cardiovascular Actions and Therapeutic Potential of Tetramethylpyrazine (Active Component Isolated from Rhizoma Chuanxiong): Roles and Mechanisms. *Biomed. Res. Int.* 2016, 2430329. doi:10.1155/2016/2430329

Guo, W. B., Zhang, H., Yan, W. Q., Liu, Y. M., Zhou, F., Cai, D. S., et al. (2020). Design, Synthesis, and Biological Evaluation of Ligustrazine - Betulin Amino-Acid/dipeptide Derivatives as Anti-tumor Agents. *Eur. J. Med. Chem.* 185, 111839. doi:10.1016/j.ejmech.2019.111839

Hamano, H., Ikeda, Y., Goda, M., Fukushima, K., Kishi, S., Chuma, M., et al. (2021). Diphenhydramine May Be a Preventive Medicine against Cisplatin-Induced Kidney Toxicity. *Kidney Int.* 99, 885–899. doi:10.1016/j.kint.2020.10.041

Han, J., Song, J., Li, X., Zhu, M., Guo, W., Xing, W., et al. (2015). Ligustrazine Suppresses the Growth of Hrpc Cells through the Inhibition of Cap- Dependent Translation via Both the Mtor and the Mek/erk Pathways. *Anticancer Agents Med. Chem.* 15, 764–772. doi:10.2174/1871520615666150305112120

Heber, S., Sallaberger-Lehner, M., Hausharter, M., Volf, I., Ocenasek, H., Gabriel, H., et al. (2019). Exercise-based Cardiac Rehabilitation Is Associated with a Normalization of the Heart Rate Performance Curve Deflection. *Scand. J. Med. Sci. Sports* 29, 1364–1374. doi:10.1111/sms.13462

Herbst, R. S., Morgensztern, D., and Boshoff, C. (2018). The Biology and Management of Non-small Cell Lung Cancer. *Nature* 553, 446–454. doi:10.1038/nature25183

Hirsch, F. R., Scagliotti, G. V., Mulshine, J. L., Kwon, R., Curran, W. J., Wu, Y. L., et al. (2017). Lung Cancer: Current Therapies and New Targeted Treatments. *Lancet* 389, 299–311. doi:10.1016/S0140-6736(16)30958-8

Holohan, C., Van Schaeybroeck, S., Longley, D. B., and Johnston, P. G. (2013). Cancer Drug Resistance: An Evolving Paradigm. *Nat. Rev. Cancer* 13, 714–726. doi:10.1038/nrc3599

Hu, Y. P., Lin, J., Wang, Q. D., Yie, Q. X., and Zhang, T. M. (1993). Reversal of Adriamycin Resistance by Verapamil and Ligustrazini in Mouse Ehrlich Ascites Cancer. *Yao Xue Xue Bao* 28, 75–78.

Huang, H. H., Liu, F. B., Ruan, Z., Zheng, J., Su, Y. J., and Wang, J. (2018). Tetramethylpyrazine (Tmpz) Triggers S-phase Arrest and Mitochondria-dependent Apoptosis in Lung Cancer Cells. *Neoplasma* 65, 367–375. doi:10.4149/neo_2018_170112N26

Ishida, T., Takechi, S., and Yamaguchi, T. (2012). Possible Involvement of Glutathione Balance Disruption in Dihydropyrazine-Induced Cytotoxicity on Human Hepatoma Hepg2 Cells. *J. Toxicol. Sci.* 37, 1065–1069. doi:10.2131/jts.37.1065

Islami, F., Chen, W., Yu, X. Q., Lortet-Tieulent, J., Zheng, R., Flanders, W. D., et al. (2017). Cancer Deaths and Cases Attributable to Lifestyle Factors and Infections in china, 2013. *Ann. Oncol.* 28, 2567–2574. doi:10.1093/annonc/mdx342

Ji, A. J., Liu, S. L., Ju, W. Z., and Huang, X. E. (2014). Anti-proliferation Effects and Molecular Mechanisms of Action of Tetramethypyrazine on Human Sgc-7901 Gastric Carcinoma Cells. *Asian Pac. J. Cancer Prev.* 15, 3581–3586. doi:10.7314/apjcp.2014.15.8.3581

Jia, Y., Wang, Z., Zang, A., Jiao, S., Chen, S., and Fu, Y. (2016). Tetramethylpyrazine Inhibits Tumor Growth of Lung Cancer through Disrupting Angiogenesis via Bmp/smad/id-1 Signaling. *Int. J. Oncol.* 48, 2079–2086. doi:10.3892/ijo.2016.3443

Jiao, Y., Zhang, S., Zhang, J., and Du, J. (2019). Tetramethylpyrazine Attenuates Placental Oxidative Stress, Inflammatory Responses and Endoplasmic Reticulum Stress in a Mouse Model of Gestational Diabetes Mellitus. *Arch. Pharm. Res.* 42, 1092–1100. doi:10.1007/s12272-019-01197-y

Jonasch, E., Walker, C. L., and Rathmell, W. K. (2021). Clear Cell Renal Cell Carcinoma Ontogeny and Mechanisms of Lethality. *Nat. Rev. Nephrol.* 17, 245–261. doi:10.1038/s41581-020-00359-2

Kim, M., Kim, S. O., Lee, M., Lee, J. H., Jung, W. S., Moon, S. K., et al. (2014). Tetramethylpyrazine, a Natural Alkaloid, Attenuates Pro-inflammatory Mediators Induced by Amyloid β and Interferon-γ in Rat Brain Microglia. *Eur. J. Pharmacol.* 740, 504–511. doi:10.1016/j.ejphar.2014.06.037

Kitagawa, R., Katsumata, N., Shibata, T., Kamura, T., Kasamatsu, T., Nakanishi, T., et al. (2015). Paclitaxel Plus Carboplatin versus Paclitaxel Plus Cisplatin in Metastatic or Recurrent Cervical Cancer: The Open-Label Randomized Phase Iii Trial Jcog0505. *J. Clin. Oncol.* 33, 2129–2135. doi:10.1200/JCO.2014.58.4391

Lau, T. S., Chan, L. K. Y., Man, G. C. W., Wong, C. H., Lee, J. H. S., Yim, S. F., et al. (2020). Paclitaxel Induces Immunogenic Cell Death in Ovarian Cancer via Tlr4/ikk2/snare-dependent Exocytosis. *Cancer Immunol. Res.* 8, 1099–1111. doi:10.1158/2326-6066.CIR-19-0616

Li, H., Yang, X., Shi, W., Ma, Z., Feng, G. K., Yin, Y. L., et al. (2015). Protective Effects of Tetramethylpyrazine on Cerebrovascular Regulations in Rats with Chronic Alcoholic Encephalopathy. *Biomed. Environ. Sci.* 28, 691–695. doi:10.3967/bes2015.098

Li, L. L., Zhang, Z. R., Gong, T., He, L. L., and Deng, L. (2006). Simultaneous Determination of Gastrodin and Ligustrazine Hydrochloride in Dog Plasma by

Gradient High-Performance Liquid Chromatography. *J. Pharm. Biomed. Anal.* 41, 1083–1087. doi:10.1016/j.jpba.2006.02.023

Li, Q. W., Zhang, G. L., Hao, C. X., Ma, Y. F., Sun, X., Zhang, Y., et al. (2021). Sant, a Novel Chinese Herbal Monomer Combination, Decreasing Tumor Growth and Angiogenesis via Modulating Autophagy in Heparanase Overexpressed Triple-Negative Breast Cancer. *J. Ethnopharmacol* 266, 113430. doi:10.1016/j.jep.2020.113430

Li, S., Jin, S., Wang, X., Song, N., Wang, P., Chen, F., et al. (2020). Intestinal Lymphatic Transport Study of Antitumor lead Compound T-Oa with Liposomes. *Pak J. Pharm. Sci.* 33, 631–640.

Li, W., Luo, L., Shi, W., Yin, Y., and Gao, S. (2021). Ursolic Acid Reduces Adriamycin Resistance of Human Ovarian Cancer Cells through Promoting the Hur Translocation from Cytoplasm to Nucleus. *Environ. Toxicol.* 36, 267–275. doi:10.1002/tox.23032

Li, Y., Dong, X., Yin, Y., Su, Y., Xu, Q., Zhang, Y., et al. (2005). Bj-tsa-9, a Novel Human Tumor-specific Gene, Has Potential as a Biomarker of Lung Cancer. *Neoplasia* 7, 1073–1080. doi:10.1593/neo.05406

Li, Z., Yulei, J., Yaqing, J., Jinmin, Z., Xinyong, L., Jing, G., et al. (2019). Protective Effects of Tetramethylpyrazine Analogue Z-11 on Cerebral Ischemia Reperfusion Injury. *Eur. J. Pharmacol.* 844, 156–164. doi:10.1016/j.ejphar.2018.11.031

Liang, S. D., Xu, C. S., Zhou, T., Liu, H. Q., Gao, Y., and Li, G. L. (2005). Tetramethylpyrazine Inhibits Atp-Activated Currents in Rat Dorsal Root Ganglion Neurons. *Brain Res.* 1040, 92–97. doi:10.1016/j.brainres.2005.01.076

Liu, Y. L., Yan, Z. X., Xia, Y., Xie, X. Y., Zhou, K., Xu, L. L., et al. (2020). Ligustrazine Reverts Anthracycline Chemotherapy Resistance of Human Breast Cancer by Inhibiting Jak2/stat3 Signaling and Decreasing Fibrinogen Gamma Chain (Fgg) Expression. *Am. J. Cancer Res.* 10, 939–952.

Luan, X., Zhang, L. J., Li, X. Q., Rahman, K., Zhang, H., Chen, H. Z., et al. (2020). Compound-based Chinese Medicine Formula: From Discovery to Compatibility Mechanism. *J. Ethnopharmacol* 254, 112687. doi:10.1016/j.jep.2020.112687

Luan, Y., Liu, J., Liu, X., Xue, X., Kong, F., Sun, C., et al. (2016). Tetramethypyrazine Inhibits Renal Cell Carcinoma Cells through Inhibition of Nkg2d Signaling Pathways. *Int. J. Oncol.* 49, 1704–1712. doi:10.3892/ijo.2016.3670

Ma, X., Ruan, Q., Ji, X., Yang, J., and Peng, H. (2021). Ligustrazine Alleviates Cyclophosphamide-Induced Hepatotoxicity via the Inhibition of Txnip/Trx/NF-Kb Pathway. *Life Sci.* 274, 119331. doi:10.1016/j.lfs.2021.119331

Mei, Y., Shi, Y. J., Zuo, G. Q., Gong, J. P., Liu, C. A., Li, X. H., et al. (2004). Study on Ligustrazine in Reversing Multidrug Resistance of Hepg2/adm Cell *In Vitro*. *Zhongguo Zhong Yao Za Zhi* 29, 970–973.

Michel, H. E., and Menze, E. T. (2019). Tetramethylpyrazine Guards against Cisplatin-Induced Nephrotoxicity in Rats through Inhibiting HMGB1/TLR4/NF-Kb and Activating Nrf2 and PPAR-γ Signaling Pathways. *Eur. J. Pharmacol.* 857, 172422. doi:10.1016/j.ejphar.2019.172422

Miller, K. D., Fidler-Benaoudia, M., Keegan, T. H., Hipp, H. S., Jemal, A., and Siegel, R. L. (2020). Cancer Statistics for Adolescents and Young Adults, 2020. *CA Cancer J. Clin.* 70, 443–459. doi:10.3322/caac.2159010.3322/caac.21637

Pan, J., Shang, J. F., Jiang, G. Q., and Yang, Z. X. (2015). Ligustrazine Induces Apoptosis of Breast Cancer Cells *In Vitro* and *In Vivo*. *J. Cancer Res. Ther.* 11, 454–458. doi:10.4103/0973-1482.147378

Perboni, G., Costa, P., Fibbia, G. C., Morandini, B., Scalzini, A., Tagliani, A., et al. (2010). Sorafenib Therapy for Hepatocellular Carcinoma in an Hiv-Hcv Coinfected Patient: A Case Report. *Oncologist* 15, 142–145. doi:10.1634/theoncologist.2010-0010

Prayuenyong, P., Baguley, D. M., Kros, C. J., and Steyger, P. S. (2021). Preferential Cochleotoxicity of Cisplatin. *Front. Neurosci.* 15, 695268. doi:10.3389/fnins.2021.695268

Qian, W., Xiong, X., Fang, Z., Lu, H., and Wang, Z. (20142014). Protective Effect of Tetramethylpyrazine on Myocardial Ischemia-Reperfusion Injury. *Evid. Based Complement. Alternat Med.* 2014, 107501. doi:10.1155/2014/107501

Raaschou-Nielsen, O., Andersen, Z. J., Beelen, R., Samoli, E., Stafoggia, M., Weinmayr, G., et al. (2013). Air Pollution and Lung Cancer Incidence in 17 European Cohorts: Prospective Analyses from the European Study of Cohorts for Air Pollution Effects (Escape). *Lancet Oncol.* 14, 813–822. doi:10.1016/S1470-2045(13)70279-1

Riaz, I. B., and Hussain, S. A. (2021). Perioperative Treatment in Muscle-Invasive Bladder Cancer: Analysis of Secondary Endpoints in a Randomized Trial Comparing Gemcitabine and Cisplatin versus Dose-Dense Methotrexate, Vinblastine, Adriamycin, and Cisplatin. *Eur. Urol.* 79, 222–224. doi:10.1016/j.eururo.2020.09.018

Shan Au, A. L., Kwan, Y. W., Kwok, C. C., Zhang, R. Z., and He, G. W. (2003). Mechanisms Responsible for the *In Vitro* Relaxation of Ligustrazine on Porcine Left Anterior Descending Coronary Artery. *Eur. J. Pharmacol.* 468, 199–207. doi:10.1016/s0014-2999(03)01691-1

Shen, J., Zeng, L., Pan, L., Yuan, S., Wu, M., and Kong, X. (2018). Tetramethylpyrazine Regulates Breast Cancer Cell Viability, Migration, Invasion and Apoptosis by Affecting the Activity of Akt and Caspase-3. *Oncol. Lett.* 15, 4557–4563. doi:10.3892/ol.2018.7851

Shiffman, M. L. (2018). The Next Wave of Hepatitis C Virus: The Epidemic of Intravenous Drug Use. *Liver Int.* 38 Suppl 1 (Suppl. 1), 34–39. doi:10.1111/liv.13647

Snijders, A. M., Lee, S. Y., Hang, B., Hao, W., Bissell, M. J., and Mao, J. H. (2017). Fam83 Family Oncogenes Are Broadly Involved in Human Cancers: An Integrative Multi-Omics Approach. *Mol. Oncol.* 11, 167–179. doi:10.1002/1878-0261.12016

Song, Y. N., Guo, X. L., Zheng, B. B., Liu, X. Y., Dong, X., Yu, L. G., et al. (2011). Ligustrazine Derivate DLJ14 Reduces Multidrug Resistance of K562/A02 Cells by Modulating GSTπ Activity. *Toxicol. Vitro* 25, 937–943. doi:10.1016/j.tiv.2011.03.002

Sun, W., Li, A., Wang, Z., Sun, X., Dong, M., Qi, F., et al. (2020). Tetramethylpyrazine Alleviates Acute Kidney Injury by Inhibiting NLRP3/HIF-1α and A-poptosis. *Mol. Med. Rep.* 22, 2655–2664. doi:10.3892/mmr.2020.11378

Sun, X., Liao, W., Wang, J., Wang, P., Gao, H., Wang, M., et al. (2016). Cstmp Induces Apoptosis and Mitochondrial Dysfunction in Human Myeloma Rpmi8226 Cells via Chop-dependent Endoplasmic Reticulum Stress. *Biomed. Pharmacother.* 83, 776–784. doi:10.1016/j.biopha.2016.07.045

Sung, H., Ferlay, J., Siegel, R. L., Laversanne, M., Soerjomataram, I., Jemal, A., et al. (2021). Global Cancer Statistics 2020: Globocan Estimates of Incidence and Mortality Worldwide for 36 Cancers in 185 Countries. *CA Cancer J. Clin.* 71, 209–249. doi:10.3322/caac.21660

Tang, F., Zhou, X., Wang, L., Shan, L., Li, C., Zhou, H., et al. (2018). A Novel Compound Dt-010 Protects against Doxorubicin-Induced Cardiotoxicity in Zebrafish and H9c2 Cells by Inhibiting Reactive Oxygen Species-Mediated Apoptotic and Autophagic Pathways. *Eur. J. Pharmacol.* 820, 86–96. doi:10.1016/j.ejphar.2017.12.021

Tang, J. H., Zhang, H. M., Zhang, Z. H., and Zhang, X. L. (2017). Effect of Tetramethylpyrazine Combined with Cisplatin on Vegf, Klf4 and Adamts1 in lewis Lung Cancer Mice. *Asian Pac. J. Trop. Med.* 10, 813–818. doi:10.1016/j.apjtm.2017.08.001

Thun, M. J., Carter, B. D., Feskanich, D., Freedman, N. D., Prentice, R., Lopez, A. D., et al. (2013). 50-year Trends in Smoking-Related Mortality in the united states. *N. Engl. J. Med.* 368, 351–364. doi:10.1056/NEJMsa1211127

Tian, Y., Liu, Y., Chen, X., Zhang, H., Shi, Q., Zhang, J., et al. (2010). Tetramethylpyrazine Promotes Proliferation and Differentiation of Neural Stem Cells from Rat Brain in Hypoxic Condition via Mitogen-Activated Protein Kinases Pathway *In Vitro*. *Neurosci. Lett.* 474, 26–31. doi:10.1016/j.neulet.2010.02.066

Tinoush, B., Shirdel, I., and Wink, M. (2020). Phytochemicals: Potential lead Molecules for Mdr Reversal. *Front. Pharmacol.* 11, 832. doi:10.3389/fphar.2020.00832

Tran, B., and Bedard, P. L. (2011). Luminal-b Breast Cancer and Novel Therapeutic Targets. *Breast Cancer Res.* 13, 221. doi:10.1186/bcr2904

Ubellacker, J. M., Tasdogan, A., Ramesh, V., Shen, B., Mitchell, E. C., Martin-Sandoval, M. S., et al. (2020). Lymph Protects Metastasizing Melanoma Cells from Ferroptosis. *Nature* 585, 113–118. doi:10.1038/s41586-020-2623-z

Untch, M., Jackisch, C., Schneeweiss, A., Conrad, B., Aktas, B., Denkert, C., et al. (2016). Nab-paclitaxel versus Solvent-Based Paclitaxel in Neoadjuvant Chemotherapy for Early Breast Cancer (Geparsepto-gbg 69): A Randomised, Phase 3 Trial. *Lancet Oncol.* 17, 345–356. doi:10.1016/S1470-2045(15)00542-2

Viale, G., Hanlon Newell, A. E., Walker, E., Harlow, G., Bai, I., Russo, L., et al. (2019). Ki-67 (30-9) Scoring and Differentiation of Luminal a- and Luminal B-like Breast Cancer Subtypes. *Breast Cancer Res. Treat.* 178, 451–458. doi:10.1007/s10549-019-05402-w

Viedma-Rodríguez, R., Baiza-Gutman, L., Salamanca-Gómez, F., Diaz-Zaragoza, M., Martínez-Hernández, G., Ruiz Esparza-Garrido, R., et al. (2014). Mechanisms Associated with Resistance to Tamoxifen in Estrogen Receptor-Positive Breast Cancer (Review). *Oncol. Rep.* 32, 3–15. doi:10.3892/or.2014.3190

Wang, C., Li, Y., Yang, X., Bi, S., Zhang, Y., Han, D., et al. (2017). Tetramethylpyrazine and Astragaloside Iv Synergistically Ameliorate Left Ventricular Remodeling and Preserve Cardiac Function in a Rat Myocardial Infarction Model. *J. Cardiovasc. Pharmacol.* 69, 34–40. doi:10.1097/FJC.0000000000000437

Wang, J., Hong, G., Li, G., Wang, W., and Liu, T. (2019). Novel Homo-Bivalent and Polyvalent Compounds Based on Ligustrazine and Heterocyclic Ring as Anticancer Agents. *Molecules* 24. doi:10.3390/molecules24244505

Wang, J. B., Jiang, Y., Liang, H., Li, P., Xiao, H. J., Ji, J., et al. (2012). Attributable Causes of Cancer in china. *Ann. Oncol.* 23, 2983–2989. doi:10.1093/annonc/mds139

Wang, L., Chan, J. Y., Zhou, X., Cui, G., Yan, Z., Wang, L., et al. (2016). A Novel Agent Enhances the Chemotherapeutic Efficacy of Doxorubicin in Mcf-7 Breast Cancer Cells. *Front. Pharmacol.* 7, 249. doi:10.3389/fphar.2016.00249

Wang, L., Zhang, X., Cui, G., Chan, J. Y., Wang, L., Li, C., et al. (2016). A Novel Agent Exerts Antitumor Activity in Breast Cancer Cells by Targeting Mitochondrial Complex Ii. *Oncotarget* 7, 32054–32064. doi:10.18632/oncotarget.8410

Wang, P., She, G., Yang, Y., Li, Q., Zhang, H., Liu, J., et al. (2012). Synthesis and Biological Evaluation of New Ligustrazine Derivatives as Anti-tumor Agents. *Molecules* 17, 4972–4985. doi:10.3390/molecules17054972

Wang, P., Zhang, Y., Xu, K., Li, Q., Zhang, H., Guo, J., et al. (2013). A New Ligustrazine Derivative-Ppharmacokinetic Evaluation and Antitumor Activity by Suppression of Nf-Kappab/p65 and Cox-2 Expression in S180 Mice. *Pharmazie* 68, 782–789.

Wang, S., Lei, T., and Zhang, M. (2016). The Reversal Effect and its Mechanisms of Tetramethylpyrazine on Multidrug Resistance in Human Bladder Cancer. *PloS one* 11, e0157759. doi:10.1371/journal.pone.0157759

Wang, X., Tan, Y., Zhang, Y., Xu, Z., Xu, B., Lei, H., et al. (2020). The Novel Glycyrrhetinic Acid-Tetramethylpyrazine Conjugate Toga Induces Anti-hepatocarcinogenesis by Inhibiting the Effects of Tumor-Associated Macrophages on Tumor Cells. *Pharmacol. Res.* 161, 105233. doi:10.1016/j.phrs.2020.105233

Wang, X. B., Wang, S. S., Zhang, Q. F., Liu, M., Li, H. L., Liu, Y., et al. (2010). Inhibition of Tetramethylpyrazine on P-Gp, Mrp2, Mrp3 and Mrp5 in Multidrug Resistant Human Hepatocellular Carcinoma Cells. *Oncol. Rep.* 23, 211–215.

Wang, X. J., Xu, Y. H., Yang, G. C., Chen, H. X., and Zhang, P. (2015). Tetramethylpyrazine Inhibits the Proliferation of Acute Lymphocytic Leukemia Cell Lines via Decrease in GSK-3β. *Oncol. Rep.* 33, 2368–2374. doi:10.3892/or.2015.3860

Wang, X. J., Yang, G. C., Chen, H. X., Zhang, P., and Xu, Y. H. (2015). Study on Effect of Tetramethylpyrazine on Proliferation and Apoptosis of Leukemic U937 Cells and its Mechanism. *Zhongguo Zhong Yao Za Zhi* 40, 2186–2190.

Wang, Y., Fu, Q., and Zhao, W. (2013). Tetramethylpyrazine Inhibits Osteosarcoma Cell Proliferation via Downregulation of NF-Kb *In Vitro* and *In Vivo*. *Mol. Med. Rep.* 8, 984–988. doi:10.3892/mmr.2013.1611

Wei, H., Sun, R., Xiao, W., Feng, J., Zhen, C., Xu, X., et al. (2004). Type Two Cytokines Predominance of Human Lung Cancer and its Reverse by Traditional Chinese Medicine Ttmp. *Cell Mol Immunol* 1, 63–70.

Wei, H., Tian, Z., Xu, X., Feng, J., and Xiao, W. (2002). Expression of Transcription Factor T-Bet/gata3 in Lung Cancer Patients and its Interference by the Traditional Chinese Herbal Medicine. *Zhonghua Zhong Liu Za Zhi* 24, 34–37.

Wen, J., Li, S., Zheng, C., Wang, F., Luo, Y., Wu, L., et al. (2021). Tetramethylpyrazine Nitrone Improves Motor Dysfunction and Pathological Manifestations by Activating the PGC-1α/Nrf2/HO-1 Pathway in ALS Mice. *Neuropharmacology* 182, 108380. doi:10.1016/j.neuropharm.2020.108380

Wu, N., Xu, L., Yang, Y., Yu, N., Zhang, Z., Chen, P., et al. (2017). Tetramethylpyrazine-mediated Regulation of Cxcr4 in Retinoblastoma Is Sensitive to Cell Density. *Mol. Med. Rep.* 15, 2481–2488. doi:10.3892/mmr.2017.6293

Wu, N., Yang, Y., Yu, N., Wu, Y., Han, X., Chen, S., et al. (2019). Tetramethylpyrazine Downregulates Transcription of the CXC Receptor 4 (CXCR4) via Nuclear Respiratory Factor-1 (Nrf-1) in WERI-Rb1 R-etinoblastoma C-ells. *Oncol. Rep.* 42, 1214–1224. doi:10.3892/or.2019.7233

Wu, W., Yu, X., Luo, X. P., Yang, S. H., and Zheng, D. (2013). Tetramethylpyrazine Protects against Scopolamine-Induced Memory Impairments in Rats by Reversing the Camp/pka/creb Pathway. *Behav. Brain Res.* 253, 212–216. doi:10.1016/j.bbr.2013.07.052

Wu, Y., Xu, Y., Gu, X., Hu, Y., and Wang, C. (2011). Molecular Mechanism of Tetramethylpyrazine to Induce Human Promyelocytic Hl-60 Leukemia Cells Differentiation. *Zhongguo Zhong Yao Za Zhi* 36, 3007–3011.

Xiao, H. J., Liang, H., Wang, J. B., Huang, C. Y., Wei, W. Q., Boniol, M., et al. (2011). Attributable Causes of Cancer in china: Fruit and Vegetable. *Chin. J. Cancer Res.* 23, 171–176. doi:10.1007/s11670-011-0171-7

Xie, C., Luo, J., Hu, H., Wang, L., Yu, P., Xu, L., et al. (2021). A Novel Danshensu/tetramethypyrazine Derivative Attenuates Oxidative Stress-Induced Autophagy Injury via the Ampk-Mtor-Ulk1 Signaling Pathway in Cardiomyocytes. *Exp. Ther. Med.* 21, 118. doi:10.3892/etm.2020.9550

Xie, H. J., Zhao, J., Zhuo-Ma, D., Zhan-Dui, N., Er-Bu, A., and Tsering, T. (2019). Inhibiting Tumour Metastasis by Dqa Modified Paclitaxel Plus Ligustrazine Micelles in Treatment of Non-small-cell Lung Cancer. *Artif. Cell Nanomed Biotechnol* 47, 3465–3477. doi:10.1080/21691401.2019.1653900

Xu, B., Chu, F., Zhang, Y., Wang, X., Li, Q., Liu, W., et al. (2015). A Series of New Ligustrazine-Triterpenes Derivatives as Anti-tumor Agents: Design, Synthesis, and Biological Evaluation. *Int. J. Mol. Sci.* 16, 21035–21055. doi:10.3390/ijms160921035

Xu, B., Yan, W. Q., Xu, X., Wu, G. R., Zhang, C. Z., Han, Y. T., et al. (2017). Combination of Amino Acid/dipeptide with Ligustrazine-Betulinic Acid as Antitumor Agents. *Eur. J. Med. Chem.* 130, 26–38. doi:10.1016/j.ejmech.2017.02.036

Xu, D., Chi, G., Zhao, C., and Li, D. (2018). Ligustrazine Inhibits Growth, Migration and Invasion of Medulloblastoma Daoy Cells by Up-Regulation of Mir-211. *Cell Physiol Biochem* 49, 2012–2021. doi:10.1159/000493712

Xu, Q., Xia, P., Li, X., Wang, W., Liu, Z., and Gao, X. (2014). Tetramethylpyrazine Ameliorates High Glucose-Induced Endothelial Dysfunction by Increasing Mitochondrial Biogenesis. *PloS one* 9, e88243. doi:10.1371/journal.pone.0088243

Xu, S. H., Yin, M. S., Liu, B., Chen, M. L., He, G. W., Zhou, P. P., et al. (2017). Tetramethylpyrazine-2'-o-sodium Ferulate Attenuates Blood-Brain Barrier Disruption and Brain Oedema after Cerebral Ischemia/reperfusion. *Hum. Exp. Toxicol.* 36, 670–680. doi:10.1177/0960327116657401

Yan, S., Yue, Y. Z., Zong, Y., and Zeng, L. (2019). Tetramethylpyrazine Improves Postoperative Tissue Adhesion: A Drug Repurposing. *Chin. J. Integr. Med.* 25, 554–560. doi:10.1007/s11655-018-3021-3

Yan, Y., Zhao, J., Cao, C., Jia, Z., Zhou, N., Han, S., et al. (2014). Tetramethylpyrazine Promotes SH-Sy5y Cell Differentiation into Neurons through Epigenetic Regulation of Topoisomerase IIβ. *Neuroscience* 278, 179–193. doi:10.1016/j.neuroscience.2014.08.010

Yang, B., Li, H., Qiao, Y., Zhou, Q., Chen, S., Yin, D., et al. (2019). Tetramethylpyrazine Attenuates the Endotheliotoxicity and the Mitochondrial Dysfunction by Doxorubicin via 14-3-3γ/Bcl-2. *Oxid Med. Cel Longev* 2019, 5820415. doi:10.1155/2019/5820415

Yang, Q. H., Liang, Y., Xu, Q., Zhang, Y., Xiao, L., and Si, L. Y. (2011). Protective Effect of Tetramethylpyrazine Isolated from Ligusticum Chuanxiong on Nephropathy in Rats with Streptozotocin-Induced Diabetes. *Phytomedicine* 18, 1148–1152. doi:10.1016/j.phymed.2011.05.003

Yang, X. G., and Jiang, C. (2010). Ligustrazine as a Salvage Agent for Patients with Relapsed or Refractory Non-hodgkin's Lymphoma. *Chin. Med. J. (Engl)* 123, 3206–3211.

Yeom, G. G., Min, S., and Kim, S. Y. (2014). 2,3,5,6-tetramethylpyrazine of Ephedra Sinica Regulates Melanogenesis and Inflammation in a Uva-Induced Melanoma/keratinocytes Co-culture System. *Int. Immunopharmacol* 18, 262–269. doi:10.1016/j.intimp.2013.11.028

Yeung, S. F., Zhou, Y., Zou, W., Chan, W. L., and Ching, Y. P. (2022). TEC Kinase Stabilizes PLK4 to Promote Liver Cancer Metastasis. *Cancer Lett.* 524, 70–81. doi:10.1016/j.canlet.2021.08.038

Yi, B., Liu, D., He, M., Li, Q., Liu, T., and Shao, J. (2013). Role of the Ros/ampk Signaling Pathway in Tetramethylpyrazine-Induced Apoptosis in Gastric Cancer Cells. *Oncol. Lett.* 6, 583–589. doi:10.3892/ol.2013.1403

Yi, M., Jiao, D., Qin, S., Chu, Q., Wu, K., and Li, A. (2019). Synergistic Effect of Immune Checkpoint Blockade and Anti-angiogenesis in Cancer Treatment. *Mol. Cancer* 18, 60. doi:10.1186/s12943-019-0974-6

Yin, J., Yu, C., Yang, Z., He, J. L., Chen, W. J., Liu, H. Z., et al. (2011). Tetramethylpyrazine Inhibits Migration of Skov3 Human Ovarian Carcinoma Cells and Decreases the Expression of Interleukin-8 via the Erk1/2, P38 and Ap-1 Signaling Pathways. *Oncol. Rep.* 26, 671–679. doi:10.3892/or.2011.1334

Yu, K., Chen, Z., Pan, X., Yang, Y., Tian, S., Zhang, J., et al. (2012). Tetramethylpyrazine-mediated Suppression of C6 Gliomas Involves Inhibition of Chemokine Receptor Cxcr4 Expression. *Oncol. Rep.* 28, 955–960. doi:10.3892/or.2012.1866

Yuan, X. P., Liu, L. S., Fu, Q., and Wang, C. X. (2012). Effects of Ligustrazine on Ureteral Obstruction-Induced Renal Tubulointerstitial Fibrosis. *Phytother Res.* 26, 697–703. doi:10.1002/ptr.3630

Zhang, C., Shen, M., Teng, F., Li, P., Gao, F., Tu, J., et al. (2018). Ultrasound-enhanced Protective Effect of Tetramethylpyrazine via the Ros/hif-1a Signaling Pathway in an *In Vitro* Cerebral Ischemia/reperfusion Injury Model. *Ultrasound Med. Biol.* 44, 1786–1798. doi:10.1016/j.ultrasmedbio.2018.04.005

Zhang, C., Teng, F., Tu, J., and Zhang, D. (2014). Ultrasound-enhanced Protective Effect of Tetramethylpyrazine against Cerebral Ischemia/reperfusion Injury. *PloS one* 9, e113673. doi:10.1371/journal.pone.0113673

Zhang, C., Yan, W., Li, B., Xu, B., Gong, Y., Chu, F., et al. (2015). A New Ligustrazine Derivative-Selective Cytotoxicity by Suppression of NF-κB/p65 and COX-2 Expression on Human Hepatoma Cells. Part 3. *Int. J. Mol. Sci.* 16, 16401–16413. doi:10.3390/ijms160716401

Zhang, H., Ding, S., and Xia, L. (2021). Ligustrazine Inhibits the Proliferation and Migration of Ovarian Cancer Cells via Regulating Mir-211. *Biosci. Rep.* 41, BSR20200199. doi:10.1042/BSR20200199

Zhang, J., Liang, Y., Lin, Y., Liu, Y., You, Y., and Yin, W. (2016). IRE1α-TRAF2-ASK1 Pathway is Involved in CSTMP-Induced Apoptosis and ER Stress in Human Non-small Cell Lung Cancer A549 Cells. *Biomed. Pharmacother.* 82, 281–289. doi:10.1016/j.biopha.2016.04.050

Zhang, P., Pei, Y., and Qi, Y. (1999). Influence of Blood-Activating Drugs on Adhesion and Invasion of Cells in Lung Cancer Patients. *Zhongguo Zhong Xi Yi Jie He Za Zhi* 19, 103–105.

Zhang, P., Zheng, B. B., Wang, H. Y., Chen, J. H., Liu, X. Y., and Guo, X. L. (2014). Dlj14, a Novel Chemo-Sensitization Agent, Enhances Therapeutic Effects of Adriamycin against Mcf-7/a Cells Both *In Vitro* and *In Vivo*. *J. Pharm. Pharmacol.* 66, 398–407. doi:10.1111/jphp.12168

Zhang, Y., Liu, X., Zuo, T., Liu, Y., and Zhang, J. H. (2012). Tetramethylpyrazine Reverses Multidrug Resistance in Breast Cancer Cells through Regulating the Expression and Function of P-Glycoprotein. *Med. Oncol.* 29, 534–538. doi:10.1007/s12032-011-9950-8

Zhao, H., Zhu, C., Li, X., Dong, X., Zhuang, F., Wang, X., et al. (2000). Tetramethylpyrazine Inhibits Phytohemagglutinin-Induced Upregulation of Icam-1 and Lfa-1 Mediated Leukocyte Adhesion. *Clin. Hemorheol. Microcirc.* 23, 145–151.

Zheng, C. Y., Xiao, W., Zhu, M. X., Pan, X. J., Yang, Z. H., and Zhou, S. Y. (2012). Inhibition of Cyclooxygenase-2 by Tetramethylpyrazine and its Effects on A549 Cell Invasion and Metastasis. *Int. J. Oncol.* 40, 2029–2037. doi:10.3892/ijo.2012.1375

Zhou, C., Shen, P., and Cheng, Y. (2007). Quantitative Study of the Drug Efflux Kinetics from Sensitive and Mdr Human Breast Cancer Cells. *Biochim. Biophys. Acta* 1770, 1011–1020. doi:10.1016/j.bbagen.2007.02.011

Zhou, Q., Chen, S., Li, H., Yang, B., Chen, T., Hu, T., et al. (2020). Tetramethylpyrazine Alleviates Iron Overload Damage in Vascular Endothelium via Upregulating Ddahii Expression. *Toxicol. Vitro* 65, 104817. doi:10.1016/j.tiv.2020.104817

Zhou, X., Wang, A., Wang, L., Yin, J., Wang, L., Di, L., et al. (2019). A Danshensu-Tetramethylpyrazine Conjugate Dt-010 Overcomes Multidrug Resistance in Human Breast Cancer. *Front. Pharmacol.* 10, 722. doi:10.3389/fphar.2019.00722

Zhou, Y., Ji, Z., Yan, W., Zhou, Z., Li, H., and Xiao, Y. (2017). Tetramethylpyrazine Inhibits Prostate Cancer Progression by Downregulation of Forkhead Box M1. *Oncol. Rep.* 38, 837–842. doi:10.3892/or.2017.5768

Zhou, Y., Zhou, Z., Ji, Z., Yan, W., Li, H., and Yu, X. (2020). Tetramethylpyrazine Reduces Prostate Cancer Malignancy through Inactivation of the DPP10-AS1/CBP/FOXM1 S-ignaling P-athway. *Int. J. Oncol.* 57, 314–324. doi:10.3892/ijo.2020.5036

Zou, J., Gao, P., Hao, X., Xu, H., Zhan, P., and Liu, X. (2018). Recent Progress in the Structural Modification and Pharmacological Activities of Ligustrazine Derivatives. *Eur. J. Med. Chem.* 147, 150–162. doi:10.1016/j.ejmech.2018.01.097

Zou, L., Liu, X., Li, J., Li, W., Zhang, L., Fu, C., et al. (2021). Redox-sensitive Carrier-free Nanoparticles Self-Assembled by Disulfide-Linked Paclitaxel-Tetramethylpyrazine Conjugate for Combination Cancer Chemotherapy. *Theranostics* 11, 4171–4186. doi:10.7150/thno.42260

Zou, L., Liu, X., Li, J., Li, W., Zhang, L., Li, J., et al. (2019). Tetramethylpyrazine Enhances the Antitumor Effect of Paclitaxel by Inhibiting Angiogenesis and Inducing Apoptosis. *Front. Pharmacol.* 10, 707. doi:10.3389/fphar.2019.00707

Zou, Y., Zhao, D., Yan, C., Ji, Y., Liu, J., Xu, J., et al. (2018). Novel Ligustrazine-Based Analogs of Piperlongumine Potently Suppress Proliferation and Metastasis of Colorectal Cancer Cells *In Vitro* and *In Vivo*. *J. Med. Chem.* 61, 1821–1832. doi:10.1021/acs.jmedchem.7b01096

Conflict of Interest: The authors declare that the research was conducted in the absence of any commercial or financial relationships that could be construed as a potential conflict of interest.

Publisher's Note: All claims expressed in this article are solely those of the authors and do not necessarily represent those of their affiliated organizations, or those of the publisher, the editors, and the reviewers. Any product that may be evaluated in this article, or claim that may be made by its manufacturer, is not guaranteed or endorsed by the publisher.

frontiers in Pharmacology

CASE REPORT
published: 16 December 2021
doi: 10.3389/fphar.2021.795381

Triple-Regimen of Vemurafenib, Irinotecan, and Cetuximab for the Treatment of BRAF^{V600E}-Mutant CRC: A Case Report and Review

Su Min Cho[1], *Abdullah Esmail*[2] *and Maen Abdelrahim*[2,3,4]*

[1]Department of Medicine, Houston Methodist Hospital, Houston, TX, United States, [2]Section of GI Oncology, Department of Medical Oncology, Houston Methodist Cancer Center, Houston, TX, United States, [3]Cockrell Center of Advanced Therapeutics Phase I Program, Houston Methodist Research Institute, Houston, TX, United States, [4]Weill Cornell Medical College, New York, NY, United States

Mutation of the BRAF proto-oncogene is found in approximately 10% of colorectal cancers (CRC), with much of the mutation conferred by a V600E mutation. Unlike other CRC subtypes, BRAF-mutant CRC have had relatively limited response to conventional therapies and overall poor survival. We present the case of a 75-year-old man with severe nonischemic cardiomyopathy on a LifeVest who was found to have a transverse colonic mass with widespread hepatic metastatic disease and was subsequently found to have BRAF^{V600E}-mutant CRC (MSI High/dMMR). After a failed therapy with FOLFOX and pembrolizumab, the patient was started on a regimen of vemurafenib, irinotecan, and cetuximab (VIC) based on the SWOG 1406 trial which had shown improved progression-free survival and response rate for the treatment of BRAF^{V600E}-mutant metastatic CRC. After 40 cycles of VIC, the patient attained complete response and is in remission off chemotherapy with significant improvement. This case highlights the effectiveness of the triple-regimen of vemurafenib, irinotecan, and cetuximab as a treatment option for BRAF^{V600E}-mutant CRC, which is a treatment regimen based on the SWOG 1406 trial, and also demonstrates the synergistic role of BRAF^{V600E} inhibitors and EGFR inhibitors in the treatment of BRAF^{V600E}-mutant CRC.

Keywords: BRAF, CRC, Vemurafenib, Irinotecan, Cetuximab, Metastasis, SWOG, Immunotherapy, Chemotherapy

OPEN ACCESS

Edited by:
Devesh Tewari,
Lovely Professional University, India

Reviewed by:
Lars Petter Jordheim,
Université de Lyon, France
Caren Lee Hughes,
Mayo Clinic Florida, United States

***Correspondence:**
Maen Abdelrahim
mabdelrahim@houstonmethodist.org

Specialty section:
This article was submitted to Pharmacology of Anti-Cancer Drugs, a section of the journal Frontiers in Pharmacology

Received: *15 October 2021*
Accepted: *05 November 2021*
Published: *16 December 2021*

Citation:
Cho SM, Esmail A and Abdelrahim M (2021) Triple-Regimen of Vemurafenib, Irinotecan, and Cetuximab for the Treatment of BRAF^{V600E}-Mutant CRC: A Case Report and Review. Front. Pharmacol. 12:795381. doi: 10.3389/fphar.2021.795381

INTRODUCTION

Colorectal cancer (CRC) is one of the leading causes of death in the world. In the United States alone, it represents the third most common cancer mortality with up to 53,200 deaths in 2020 (Biller and Schrag, 2021).

Up to a third of patients initially present with stage IV metastatic disease at the time of diagnosis, requiring systemic therapy for chance of cure (Zacharakis et al., 2010). 5-Fluorouracil was the first chemotherapy which proved effective against CRC, and new therapeutic agents and regimens have since been adopted (Duschinsky et al., 1957; Heidelberger et al., 1957; Biller and Schrag, 2021).

The mitogen-activated protein kinases (MAPK) is a chain of kinases and proteins that relay extracellular signals via a biochemical cascade to influence essential intracellular processes such as growth, differentiation, migration, and apoptosis (Dhillon et al., 2007). A dysregulation of this signal cascade can therefore lead to uncontrolled growth and proliferation, leading to tumorigenesis

(Ascierto et al., 2012). BRAF is one of the protein kinases that is frequently mutated, perhaps due to fewer mutations necessary for its constitutive activation (Michaloglou et al., 2008). Mutation of the BRAF proto-oncogene is found in approximately 10% of colorectal cancers (CRC), with much of the mutation conferred by a V600E mutation (Kopetz et al., 2019). BRAF-mutant CRCs pose a special challenge for oncologists due to their relatively limited response to conventional therapies and overall poor survival (Kopetz et al., 2019).

Greater understanding of the pathogenesis of CRC has paved the way to numerous therapies, ranging from chemotherapy to targeted therapies. Currently, irinotecan combined with cetuximab is one of the regimens approved for treatment of metastatic CRC (Kopetz et al., 2017; Kopetz et al., 2021). On April 8, 2020, the Food and Drug Administration (FDA) approved encorafenib in combination with cetuximab for the treatment of patients with metastatic CRC with $BRAF^{V600E}$ mutation after a positive Phase III trial (Kopetz et al., 2019). In addition, an older randomized clinical trial called SWOG 1406 showed that the addition of vemurafenib to the irinotecan/cetuximab regimen showed improved progression-free survival and response rate for the treatment of $BRAF^{V600E}$-mutant metastatic CRC (Kopetz et al., 2017; Kopetz et al., 2021). Here we present a case highlighting the effectiveness of the triple-combination therapy of vemurafenib, irinotecan, and cetuximab in the treatment of metastatic $BRAF^{V600E}$-mutant CRC. This regimen, based on the SWOG 1406 trial, demonstrates a potential new option for treating metastatic $BRAF^{V600E}$-mutant CRC. We also explore other potential treatment options currently under study, which reveal the synergistic role of an EGFR inhibitor and a $BRAF^{V600E}$ inhibitor.

Case Presentation

We present the case of a 75-year-old man with severe nonischemic cardiomyopathy on LifeVest who initially presented on December 2017 with progressive abdominal pain for 2 months. The patient was initially suspected as having a gastric ulcer by his primary care physician and was therefore referred to a gastroenterologist for endoscopic evaluation. Upper endoscopy however was only positive for a hiatal hernia. The patient's abdominal pain continued to worsen, and he developed additional symptoms nausea, decreased appetite, fatigue, constipation. The patient visited the emergency room given the progress nature of his symptoms. CT imaging showed a circumferential narrowing of the mid-transverse colon with widespread hepatic metastatic disease. Subsequent colonoscopy showed a fungating, infiltrating, and ulcerated partially obstructing mass in the transverse colon with subsequent biopsy revealing poorly differentiated invasive adenocarcinoma on January 2018. Molecular testing was positive for BRAF-V600E mutation. Mismatch repair protein analysis was notable for loss of expression of MLH1 and PMS2. Microsatellite instability analysis was MSI-High, with instability of microsatellite markers NR-21, BAT-26, BAT-25, NR-24, and MONO-27.

The patient was started on palliative FOLFOX and was then started on bevacizumab during the third cycle of FOLFOX. This regimen was chosen due to initial concerns for GI perforation and overall poor performance status. CT chest/abdomen/pelvis was obtained every 3 months to assess therapy response. However, subsequent imaging showed progression of disease despite four cycles of FOLFOX and two cycles of bevacizumab. The treatment regimen was switched to pembrolizumab, but disease progression was still seen despite three cycles of pembrolizumab.

In May 2018 the patient was started on a triple-combination therapy consisting of vemurafenib, irinotecan, and cetuximab (VIC), which was based on the SWOG 1406 clinical trial (Kopetz et al., 2017). This decision was made based on his prior therapy failures as well as the promising results of the SWOG 1406 clinical trial (Kopetz et al., 2017). At this point in time, the regimen of encorafenib and cetuximab had not yet been FDA approved (Kopetz et al., 2019). Extensive discussion was held with the patient and family regarding therapy strategy and side-effect profile, and ultimately they agreed to the experimental therapy with continued goal of palliative therapy. The dosing and frequency was modeled after that of the SWOG 1406 clinical trial (Kopetz et al., 2017; Kopetz et al., 2021). The patient received IV cetuximab at a dose of 500 mg/m^2 (800 mg for our patient) followed by IV irinotecan at 180 mg/m2 (288 mg for our patient) on days 1 and 15, with courses repeated every 28 days (Kopetz et al., 2017; Kopetz et al., 2021). The patient also received PO vemurafenib 960 mg twice daily on days 1 through 28, with a single cycle consisting of 28 days. After five cycles of VIC therapy, the patient's metastatic lesions of the liver had significantly decreased in size. CT imaging was continually obtained every 3 months, and each additional imaging showed either stable disease or disease regression. After 40 cycles of VIC, the patient attained complete response and is in remission off chemotherapy with significant improvement in his weight, performance status, and quality of life (**Figure 1**, **Figure 2).** As of today October 2021 the patient has remained disease-free off of chemotherapy for 9 months without obvious disease recurrence, but continued surveillance CT imaging will still be performed to monitor for recurrence.

Of note, before the patient was started on VIC, the patient had been followed by a cardiologist for his nonischemic cardiomyopathy with a severely depressed LVEF 20–24%. The patient was not a candidate for an automatic implantable cardioverter defibrillator (AICD) and therefore had been on a LifeVest. Given the overall poor outlook from his metastatic disease, the patient had decided to discontinue his LifeVest for improved quality of life at the risk of a sudden cardiac death. However, after attaining complete response to VIC, the patient was able to undergo implantation of a cardiac resynchronization therapy with defibrillation (CRT-D) device with significant improvement to his functional status. The patient and his family have been very happy with the care they received in the hospital and the clinic.

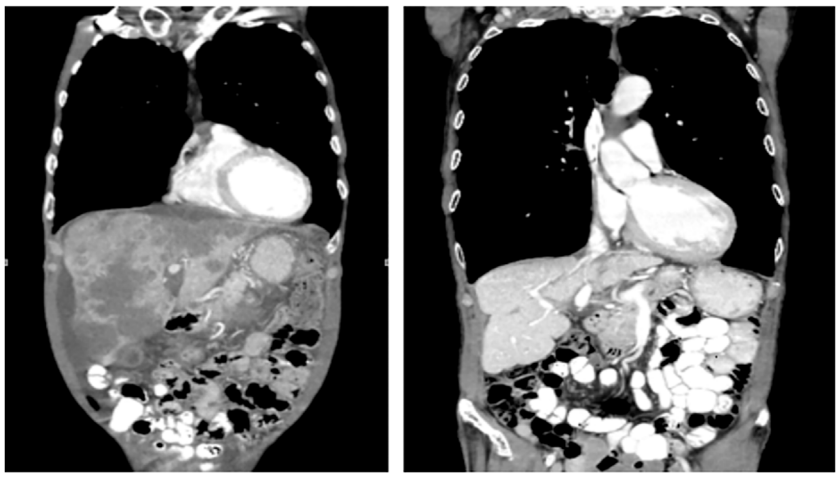

FIGURE 1 | Extensive hepatic metastasis present before initiation of VIC **(left)**. In remission after 40 cycles of VIC **(right)**.

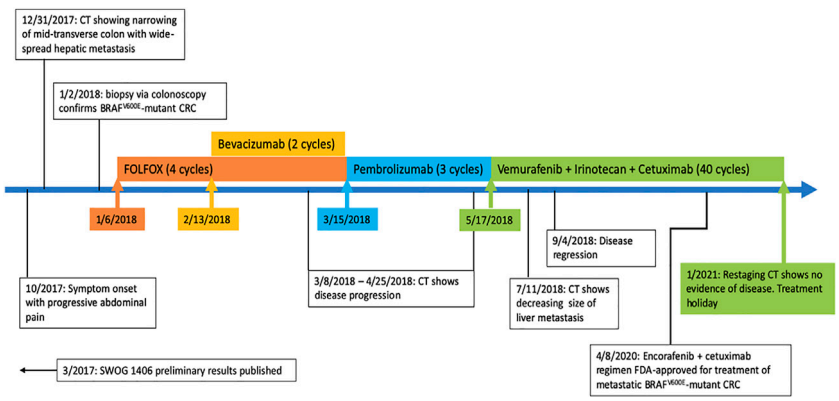

FIGURE 2 | Timeline of management of metastatic BRAF^{V600E}-mutant CRC (colorectal cancer).

DISCUSSION

Vemurafenib is a selective BRAF^{V600E}inhibitor that had been approved by the FDA in 2011 for treatment of BRAF^{V600E}-mutant metastatic melanoma, though it had limited efficacy when used as monotherapy against CRC (Korphaisarn and Kopetz, 2016). Irinotecan, a topoisomerase I inhibitor, was approved for treatment of metastatic CRC refractory to 5-FU in 1996 and is now a key drug for treatment of metastatic CRC given the survival advantage of irinotecan-based regimen (Fujita et al., 2015). Cetuximab is a monoclonal antibody against the epidermal growth factor receptor (EGFR) inhibitor. A 2004 clinical trial showed clinically-significant activity of cetuximab when given alone or in combination with irinotecan for irinotecan-refractory metastatic CRC, with greater ORR and PFS for the combination therapy as opposed to the monotherapy (Cunningham et al., 2004).

For our patient, we have chosen the triple therapy of VIC (vemurafenib + irinotecan + cetuximab) because at the time of therapy initiation (2018) the doublet regimen of encorafenib and cetuximab, based on the positive phase III trial in 2019 (8), had not yet been FDA approved. Our patient was started on VIC in 2018, and the preliminary results of the randomized phase II SWOG 1406 clinical trial published in 2017 had shown clinically-significant benefit of adding vemurafenib to the combined irinotecan/cetuximab therapy (Kopetz et al., 2017). The SWOG 1406 trial was comprised of 106 participants who had previously received 1 or 2 prior regimens except for anti-EGFR agents (Kopetz et al., 2017; Kopetz et al., 2021). Compared to the doublet irinotecan/cetuximab therapy, the triple therapy showed improved median PFS (4.4 vs 2 months) and improved response rate (17 vs 4%) (Kopetz et al., 2017; Kopetz et al., 2021). The primary conclusion of the study was that inhibition of both EGFR and BRAF combined with irinotecan was effective for the treatment of BRAF^{V600E}-mutant CRC (Kopetz et al., 2017; Kopetz et al., 2021). Our patient's PFS (36 months) has far exceeded what was shown in the study. The reason for our patient's superior clinical response is unclear, but we suspect

this was due to a distinct molecular and immunohistochemical characteristic of our patient's cancer that was more responsive to the VIC regimen. A significant challenge was the patient's cardiac comorbidity, namely his cardiomyopathy with an LVEF 20–24%. In view of this condition, the patient required close monitoring of his QTc (by EKG before each cycle) and volume status while receiving his chemotherapy. The overall poor prognosis had made him ineligible for an ICD, and in fact the patient's LifeVest was discontinued during the initial stages of chemotherapy to improve his quality of life. This is no longer the case after having achieved remission, and now the patient was able to have an CRT-D device implanted.

A major strength to this case is that this case was not directly affiliated with the SWOG clinical study. We believe this allowed for a non-biased approach to our treatment regimen and assessment of the treatment response. The limitation of this case report, on the other hand, is that this is a report regarding a single patient. However, not many publications experimenting with the VIC regimen are found in the literature aside from the primary SWOG trial. One similar finding is a 2020 case report demonstrating complete response of metastatic $BRAF^{V600E}$-mutant CRC to a regimen of fluorouracil + VIC (Wang et al., 2019). The 44 year-old patient was refractory to a regimen of capecitabine + oxaliplatin and had developed metastatic disease (Wang et al., 2019). The patient's first cycle was irinotecan + 5-FU with subsequent cycles composed of a quad-therapy of 5-FU + VIC, and after 10 total cycles the patient had attained complete recession of metastases (Wang et al., 2019). The general conclusion of this case was similar to that of our case and the SWOG trial, aside from the concomitant usage of 5-FU along with the VIC.

The BEACON CRC phase III trial showed effectiveness of the triple regimen of encorafenib + cetuximab + binimetinib compared to the control (cetuximab + irinotecan or cetuximab + FOLFIRI) for treatment-refractory metastatic CRC (Kopetz et al., 2019). There was a clinically significant increase in median overall survival of patients who had received the triple therapy (9.0 months) compared to the control group (5.4 months) (Kopetz et al., 2019). It is worth noting that the trial had also explored the efficacy of a doublet therapy (encorafenib + cetuximab) which had a median overall survival of 8.4 months (Kopetz et al., 2019). This doublet therapy of encorafenib + cetuximab is now FDA approved for treatment of metastatic $BRAF^{V600E}$-mutant CRC. Of note, encorafenib is a $BRAF^{V600E}$ inhibitor just like vemurafenib which gives further gives credence to the effectiveness of utilizing both EGFR and BRAF inhibition as in like the SWOG trial.

Currently, there is research analyzing the effectiveness of the triple regimen (encorafenib + cetuximab + binimetinib) for metastatic $BRAF^{V600E}$-mutant CRC (Grothey et al., 2020). The ANCHOR CRC trial is currently in phase II, and so far it has shown effectiveness of the afore-mentioned triple therapy as a first-line metastatic treatment, with an overall response rate of 50 and 85% of patients with decreased tumor size so far (Grothey et al., 2020). This is in contrast to the BEACON CRC trial which had enrolled patients with treatment-refractory metastatic CRC (Kopetz et al., 2019).

A recent 2018 study of 142 patients analyzed the treatment efficacy of dabrafenib + panitumumab + trametinib (D + P + T) (Corcoran et al., 2018). Dabrafenib is a $BRAF^{V600E}$ inhibitor and panitumumab is an inhibitor of EGFR, just like vemurafenib and cetuximab are, respectively (Addeo et al., 2010; Abraham and Stenger, 2014). This study also added trametinib, a MEK inhibitor which had been FDA approved for use in $BRAF^{V600E/V600K}$ mutated melanoma (Hoffner and Benchich, 2018). The median PFS for the D + P + T, D + P, and T + P arms were 4.2, 2.6, and 3.5 months respectively (Corcoran et al., 2018). The overall response rate was 21, 10, and 0% respectively (Corcoran et al., 2018). The median overall survival was 9.1 months, 13.2, and 8.2 respectively (Corcoran et al., 2018). In conclusion, the usage of the triple regimen of MEK + $BRAF^{V600E}$ + EGFR inhibitors had greater overall response rate and PFS, while the dual-regimen of $BRAF^{V600E}$ + EGFR inhibitors had the greater median overall survival.

Overall, our case highlights the effectiveness of the triple-regimen of vemurafenib, irinotecan, and cetuximab as a treatment option for $BRAF^{V600E}$-mutant CRC, a treatment regimen based on the SWOG 1406 trial. Our case demonstrates a patient with serious cardiac comorbidity who was able to tolerate the cancer regimen and attain complete response. The current treatment trend for this metastatic $BRAF^{V600E}$-mutant CRC at this time appears to revolve around the usage of both a BRAF inhibitor as well as an EGFR mutation.

DATA AVAILABILITY STATEMENT

The original contributions presented in the study are included in the article/Supplementary Material, further inquiries can be directed to the corresponding author.

AUTHOR CONTRIBUTIONS

CS and EA reviewed the literature; CS, EA and AM contributed to the design of the manuscript and manuscript drafting, and revision of the manuscript for intellectual content; CS imaged analysis and interpretation; AM was responsible for the critical revision of the manuscript for intellectual content; and all authors issued final approval for the version to be submitted.

ACKNOWLEDGMENTS

The assistance provided by Eva Zsigmond as scientific editing was greatly appreciated.

REFERENCES

Abraham, J., and Stenger, M. (2014). Dabrafenib in Advanced Melanoma with BRAF V600E Mutation. *J. Community Support. Oncol.* 12 (2), 48–49. doi:10.12788/jcso.0014

Addeo, R., Caraglia, M., Cerbone, D., Frega, N., Cimmino, G., Abbruzzese, A., et al. (2010). Panitumumab: a New Frontier of Target Therapy for the Treatment of Metastatic Colorectal Cancer. *Expert Rev. Anticancer Ther.* 10 (4), 499–505. doi:10.1586/era.10.28

Ascierto, P. A., Kirkwood, J. M., Grob, J. J., Simeone, E., Grimaldi, A. M., Maio, M., et al. (2012). The Role of BRAF V600 Mutation in Melanoma. *J. Transl Med.* 10, 85. doi:10.1186/1479-5876-10-85

Biller, L. H., and Schrag, D. (2021). Diagnosis and Treatment of Metastatic Colorectal Cancer: A Review. *JAMA* 325 (7), 669–685. doi:10.1001/jama.2021.0106

Corcoran, R. B., André, T., Atreya, C. E., Schellens, J. H. M., Yoshino, T., Bendell, J. C., et al. (2018). Combined BRAF, EGFR, and MEK Inhibition in Patients with BRAFV600E-Mutant Colorectal Cancer. *Cancer Discov.* 8 (4), 428–443. doi:10.1158/2159-8290.CD-17-1226

Cunningham, D., Humblet, Y., Siena, S., Khayat, D., Bleiberg, H., Santoro, A., et al. (2004). Cetuximab Monotherapy and Cetuximab Plus Irinotecan in Irinotecan-Refractory Metastatic Colorectal Cancer. *N. Engl. J. Med.* 351 (4), 337–345. doi:10.1056/NEJMoa033025

Dhillon, A. S., Hagan, S., Rath, O., and Kolch, W. (2007). MAP Kinase Signalling Pathways in Cancer. *Oncogene* 26 (22), 3279–3290. doi:10.1038/sj.onc.1210421

Duschinsky, R., Pleven, E., and Heidelberger, C. (1957). The Synthesis of 5-fluoropyrimidines. *J. Am. Chem. Soc.* 79, 4559–4560. doi:10.1021/ja01573a087

Fujita, K., Kubota, Y., Ishida, H., and Sasaki, Y. (2015). Irinotecan, a Key Chemotherapeutic Drug for Metastatic Colorectal Cancer. *World J. Gastroenterol.* 21 (43), 12234–12248. doi:10.3748/wjg.v21.i43.12234

Grothey, A., Tabernero, J., Taieb, J., Yaeger, R., Yoshino, T., Maiello, E., et al. (2020). LBA-5 ANCHOR CRC: a Single-Arm, Phase 2 Study of Encorafenib, Binimetinib Plus Cetuximab in Previously Untreated BRAF V600E-Mutant Metastatic Colorectal Cancer. *Ann. Oncol.* 31, S242–S243. doi:10.1016/j.annonc.2020.04.080

Heidelberger, C., Chaudhuri, N. K., Danneberg, P., Mooren, D., Griesbach, L., Duschinsky, R., et al. (1957). Fluorinated Pyrimidines, a New Class of Tumour-Inhibitory Compounds. *Nature* 179 (4561), 663–666. doi:10.1038/179663a0

Hoffner, B., and Benchich, K. (2018). Trametinib: A Targeted Therapy in Metastatic Melanoma. *J. Adv. Pract. Oncol.* 9 (7), 741–745. doi:10.6004/jadpro.2018.9.7.5

Kopetz, S., Grothey, A., Yaeger, R., Van Cutsem, E., Desai, J., Yoshino, T., et al. (2019). Encorafenib, Binimetinib, and Cetuximab in BRAF V600E-Mutated Colorectal Cancer. *N. Engl. J. Med.* 381 (17), 1632–1643. doi:10.1056/NEJMoa1908075

Kopetz, S., Guthrie, K. A., Morris, V. K., Lenz, H. J., Magliocco, A. M., Maru, D., et al. (2021). Randomized Trial of Irinotecan and Cetuximab with or without Vemurafenib in BRAF-Mutant Metastatic Colorectal Cancer (SWOG S1406). *J. Clin. Oncol.* 39 (4), 285–294. doi:10.1200/JCO.20.01994

Kopetz, S., McDonough, S. L., Morris, V. K., Lenz, H-J., Magliocco, A. M., Atreya, C. E., et al. (2017). Randomized Trial of Irinotecan and Cetuximab with or without Vemurafenib in BRAF-Mutant Metastatic Colorectal Cancer (SWOG 1406). *J. Clin. Oncol.* 35 (4), 520. doi:10.1200/jco.2017.35.4_suppl.520

Korphaisarn, K., and Kopetz, S. (2016). BRAF-directed Therapy in Metastatic Colorectal Cancer. *Cancer J.* 22 (3), 175–178. doi:10.1097/PPO.0000000000000189

Michaloglou, C., Vredeveld, L. C., Mooi, W. J., and Peeper, D. S. (2008). BRAF(E600) in Benign and Malignant Human Tumours. *Oncogene* 27 (7), 877–895. doi:10.1038/sj.onc.1210704

Wang, Z., Dai, W. P., and Zang, Y. S. (2019). Complete Response with Fluorouracil and Irinotecan with a BRAFV600E and EGFR Inhibitor in BRAF-Mutated Metastatic Colorectal Cancer: a Case Report. *Onco Targets Ther.* 12, 443–447. doi:10.2147/OTT.S180845

Zacharakis, M., Xynos, I. D., Lazaris, A., Smaro, T., Kosmas, C., Dokou, A., et al. (2010). Predictors of Survival in Stage IV Metastatic Colorectal Cancer. *Anticancer Res.* 30 (2), 653–660. doi:10.1186/s12885-017-3336-z

Conflict of Interest: The authors declare that the research was conducted in the absence of any commercial or financial relationships that could be construed as a potential conflict of interest.

frontiers in Pharmacology

ORIGINAL RESEARCH
published: 15 February 2022
doi: 10.3389/fphar.2022.779715

Thymopentin-Mediated Inhibition of Cancer Stem Cell Stemness Enhances the Cytotoxic Effect of Oxaliplatin on Colon Cancer Cells

Peng-Cheng Yu[1,2†], Di Liu[1,2†], Zeng-Xiang Han[1,3†], Fang Liang[1], Cui-Yun Hao[2], Yun-Tao Lei[2], Chang-Run Guo[2], Wen-Hui Wang[2], Xing-Hua Li[2], Xiao-Na Yang[2], Chang-Zhu Li[4], Ye Yu[2]* and Ying-Zhe Fan[1]**

[1]Interventional Cancer Institute of Chinese Integrative Medicine, Putuo Hospital, Shanghai University of Traditional Chinese Medicine, Shanghai, China, [2]School of Basic Medicine and Clinical Pharmacy, China Pharmaceutical University, Nanjing, China, [3]Three Departments of Oncology, Weifang Traditional Chinese Medicine Hospital, Weifang, China, [4]State Key Laboratory of Utilization of Woody Oil Resource, Hunan Academy of Forestry, Changsha, China

OPEN ACCESS

Edited by:
Devesh Tewari,
Lovely Professional University, India

Reviewed by:
Justine Bailleul,
University of California, Los Angeles, United States
Yulin Ren,
The Ohio State University, United States

***Correspondence:**
Chang-Zhu Li
lichangzhu2013@aliyun.com
Ye Yu
yuye@cpu.edu.cn
Ying-Zhe Fan
yingzhefan@126.com

†These authors have contributed equally to this work

Specialty section:
This article was submitted to Pharmacology of Anti-Cancer Drugs, a section of the journal Frontiers in Pharmacology

Received: 19 September 2021
Accepted: 31 January 2022
Published: 15 February 2022

Citation:
Yu P-C, Liu D, Han Z-X, Liang F, Hao C-Y, Lei Y-T, Guo C-R, Wang W-H, Li X-H, Yang X-N, Li C-Z, Yu Y and Fan Y-Z (2022) Thymopentin-Mediated Inhibition of Cancer Stem Cell Stemness Enhances the Cytotoxic Effect of Oxaliplatin on Colon Cancer Cells. Front. Pharmacol. 13:779715. doi: 10.3389/fphar.2022.779715

Thymopentin (TP5) is an immunomodulatory pentapeptide that has been widely used in malignancy patients with immunodeficiency due to radiotherapy and chemotherapy. Here, we propose that TP5 directly inhibits the stemness of colon cancer cells HCT116 and therefore enhances the cytotoxicity of oxaliplatin (OXA) in HCT116 cells. In the absence of serum, TP5 was able to induce cancer stemness reduction in cultured HCT116 cells and significantly reduced stemness-related signals, such as the expression of surface molecular markers (CD133, CD44 and CD24) and stemness-related genes (ALDH1, SOX2, Oct-4 and Nanog), and resulted in altered Wnt/β-catenin signaling. Acetylcholine receptors (AchRs) are implicated in this process. OXA is a common chemotherapeutic agent with therapeutic effects in various cancers. Although TP5 had no direct effect on the proliferation of HCT116, this pentapeptide significantly increased the sensitivity of HCT116 to OXA, where the effect of TP5 on the stemness of colon cancer cells through stimulation of AchRs may contribute to this process. Our results provide a promising strategy for increasing the sensitivity of colon cancer cells to chemotherapeutic agents by incorporating immunomodulatory peptides.

Keywords: thymopentin (TP5), colon cancer cells, oxaliplatin, AChRs, cancer stem cell (CSC)

INTRODUCTION

Colorectal cancer (CRC) is one of the common malignant tumors of the gastrointestinal system, and the current 5-year survival rate of colorectal cancer is 66% worldwide, but the 5-year survival rate of patients with advanced disease is only 13% (Miller et al., 2019). Currently, the main treatments for colorectal cancer include surgical resection, radiotherapy, and immune anti-cancer therapy (Ciombor et al., 2015). Numerous studies have shown that cancer stem cells (CSCs) are the core factor leading to postoperative recurrence, radiotherapy insensitivity, and immunotherapy resistance in tumor patients (Regan et al., 2017; Tosoni et al., 2017; Luo et al., 2018). Cancer stem cells are a very small subpopulation of tumor cells with unlimited self-renewal, multidirectional differentiation potential and high malignancy, which have been shown to be present in many types of tumors including colon cancer, and they confer tumor metastasis,

chemoresistance and sustained adaptation to the microenvironment (Kreso and Dick, 2014; Fearon and Carethers, 2015).

During tumor treatment, cancer stem cells exhibit a high degree of insensitivity to chemotherapy and radiotherapy (Zhao, 2016). It has been found that colorectal cancer stem cells are intrinsically resistant to first-line chemotherapeutic agents for rectal cancer, such as 5-fluorouracil and oxaliplatin (OXA) (Hammond et al., 2016). In addition, cancer stem cells are theoretically mostly in a quiescent state, while oncologic therapies such as radiotherapy and chemotherapy target proliferating tumor cells (Phi et al., 2018). Therefore, in many colorectal cancer patients, although good therapeutic results can be achieved at the beginning of drug administration, an avalanche of multidrug resistance soon occurs and tumors progress rapidly (Hervieu et al., 2021). The mechanism of this phenomenon may be due to the fact that chemotherapeutic drugs do not act on cancer stem cells when killing proliferating tumor cells (Van der Jeught et al., 2018). This screening pressure creates a competitive advantage for cancer stem cells, thus allowing cancer stem cells and their derivatives to become the main body of advanced tumors, exacerbating tumor resistance, progression and metastasis (Ayob and Ramasamy, 2018). On the other hand, surgical resection of tumors or radiotherapy cannot guarantee the removal of all cancer stem cells, and a very small number of cancer stem cells can become tumorigenic cells. Therefore, cancer stem cells are an important cause of drug resistance in tumor treatment and of recurrence and metastasis after treatment (Zhu et al., 2009; Lytle et al., 2019; Clara et al., 2020). Colon cancer stem cells can express specific surface markers such as CD24, CD44 and CD133, which are highly resistant to radiotherapy and chemotherapy (Du et al., 2008). ALDH1, OCT4, SOX2 and Nanog are all markers of the stemness state of cancer stem cells and are important in maintaining the nature and drug resistance of cancer stem cells (Chambers et al., 2003; Tirosh et al., 2016; Anorma et al., 2018; Bocci et al., 2019).

TP5 is a synthetic pentapeptide derived from the active fragment of thymosin (49 amino acids), which exhibits very strong immunomodulatory activity in many animal models and *in vitro* assays of human cells (Patruno et al., 2012; Zhang et al., 2019). Numerous *in vivo* studies have shown that TP5 can be effective in the treatment of various diseases such as primary and secondary immunodeficiency, autonomic immunodeficiency, and severe infections (Fabrizi et al., 2006; Csaba, 2016). The combined application of chemotherapy and immunotherapy is a very effective modality in the treatment of tumors. TP5 can be used as a good immune adjuvant in the treatment of tumors, enhancing the immune system and reducing the side effects of chemotherapy and radiotherapy (Singh et al., 1998; Bodeya et al., 2000). In addition to the immune system, TP5 can also act directly on tumor cell-related signaling pathways (Li et al., 2010). Our previous study found that the immunomodulatory peptides thymosin and TP5 could inhibit the proliferation of leukemia cells and induce their differentiation into granulocytes (Fan et al., 2006a; Fan et al., 2006b).

In the present study, we found that TP5 can directly inhibit cultured colon cancer stem cells in medium without serum, and reduce the expression of cancer stem cell markers: CD44, CD24 and CD133, and stem-cell related genes: ALDH2, SOX2, OCT4 and Nanog. Additionally, although TP5 could not inhibit the proliferation of colon cancer cells directly, this peptide could promote the anti-proliferative effect of chemotherapeutic drug OXA on colon cancer cells HCT116, and acetylcholine receptors (AchRs) are implicated in this process.

RESULTS

TP5 Inhibits the Formation of HCT116 Cancer Stem Cell Spheroids

Cancer stem cells have a very typical growth pattern in that they can be grown in suspension in serum-free medium with the addition of growth factors, eventually forming cancer stem cell spheroids with a three-dimensional structure. The ability to form spheroids is an important way to identify cancer stem cells *in vitro* (Masuda et al., 2016). Therefore, we investigated the effect of TP5 on spheroid formation of HCT116 cancer stem cells. The number of cancer stem cell spheroids was significantly less in HCT116 cells treated with TP5 than in the control group, and the spheroid formation rate was significantly decreased in a concentration-dependent manner (**Figures 1A,B**), indicating that TP5 reduced the stemness of HCT116 cancer stem cells and inhibited the self-renewal and proliferation ability of cancer stem cells.

TP5 Reduces the Expression of Cancer Stem Cell Markers in HCT116 Cells

To further verify the effect of TP5 on colon cancer stem cells, we used flow cytometry to detect the expression of cancer stem cell markers CD24, CD44 and CD133, which are surface markers that can be specifically expressed by colon cancer stem cells (Jaggupilli and Elkord, 2012; Sahlberg et al., 2014). In the concentration range of 100–800 μM, TP5 could concentration-dependently decrease the expression of CD24, CD44 and CD133 in HCT116 cells (**Figures 1C–H**). The percentage of CD24-positive cells decreased from 29.7 ± 1.9% to 26.9 ± 2.1%, 24.7 ± 2.9%, 21.5 ± 0.9% and 20.4 ± 1.2%, after 48 h of action of 100, 200, 400, and 800 μM of TP5, respectively (**Figures 1C,D**). The percentage of CD44-positive cells decreased from 48.0 ± 2.4% to 46.0 ± 2.1%, 44.2 ± 6.6%, 36.6 ± 5.8%, and 34.5 ± 4.3%, respectively (**Figures 1E,F**). The percentage of CD133 positive cells decreased from 63.4 ± 0.5% to 63.9 ± 0.5%, 63.2 ± 1.5%, 58.5 ± 1.7%, and 53.4 ± 1.0%, respectively (**Figures 1G,H**).

TP5 Inhibits LoVo Cancer Stem Cell Spheroid Formation and Reduces the Expression of Cancer Stem Cell Markers

We also investigated the effect of TP5 on cancer stem cell spheroid formation of another cell line, LoVo. The number of

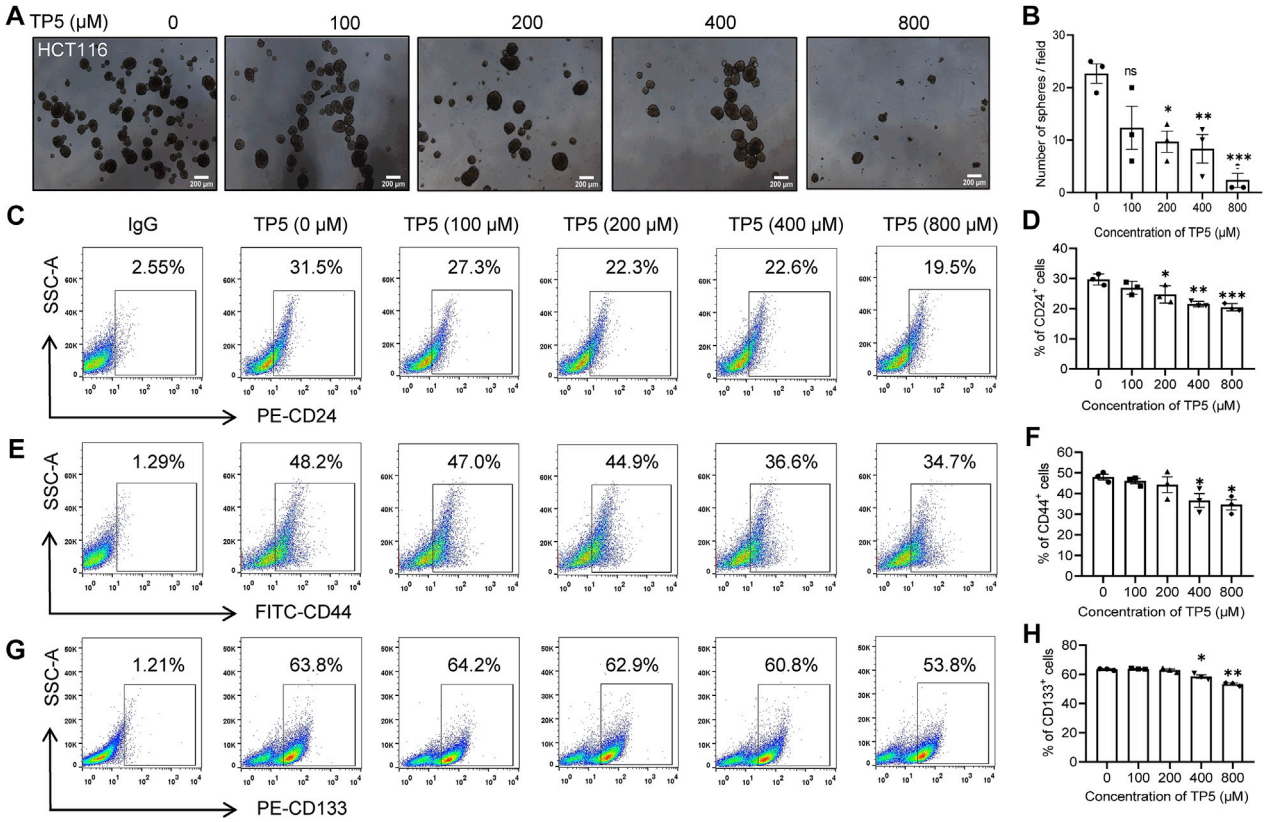

FIGURE 1 | TP5 inhibits the stemness of cancer stem cells in HCT116 cells. **(A, B)** Representative photomicrographs of sphere formation experiments **(A)** and statistical analysis of the number of spheres with diameter ≥140 μm in visual field **(B)**. HCT116 cells were incubated with different treatments of TP5 (0, 100, 200, 400, and 800 μM) and grown in serum-free medium for 6 days. Scale bar = 200 μm. **(C–H)** Flow cytometer analysis of the expression of CD24, CD44 or CD133 **(C, E, G)** and pooled data of cell surface markers CD24 **(D)**, CD44 **(F)** and CD133 **(H)** (n = 3 independent experiments). All data are expressed as mean ± SD; $^{*}p < 0.05$, $^{**}p < 0.01$ and $^{***}p < 0.001$ vs. control, one-way ANOVA with Dunnett's post-hoc test, **(A)**, [F (4, 10) = 8.265, $p = 0.0033$], **(B)**, [F (4, 10) = 11.76, $p = 0.0008$] [F (4, 10) = 5.039 $p = 0.0174$], [F (4, 10) = 34.00, $p < 0.0001$].

cancer stem cell spheroids was significantly less in LoVo cells treated with TP5 than in the control group, and the rate of spheroid formation was also significantly decreased (**Figures 2A,B**), indicating that TP5 also reduced the stemness of LoVo cancer stem cells. At a concentration of 800 μM, TP5 reduced the expression of CD24, CD44 and CD133 in HCT116 cells (**Figures 1C–H**). The percentage of CD24-positive cells decreased from 18.7 ± 1.8% to 14.0 ± 0.4% after 24 h of TP5 at 800 μM (**Figures 2C,D**). The percentage of CD44-positive cells decreased from 30.7 ± 1.3% to 23.7 ± 1.8%, respectively (**Figures 2E,F**). After 24 h of TP5 at 400 and 800 μM, the percentage of CD133 positive cells decreased from 54.8 ± 1.1% to 49.3 ± 1.2% and 47.2 ± 1.1%, respectively (**Figures 2G,H**). These results suggest that TP5 inhibition of cancer stem cells is not limited to HCT116 cells.

TP5 Reduces the Expression of Cancer Stem Cell-Related Genes in HCT116 Cells

Although TP5 inhibits both HCT116 and LoVo cancer stem cells, it has a slightly stronger ability to inhibit HCT116 stem cell formation, we therefore focused on HCT116 as an example and continued to investigate the mechanism of TP5 inhibition of cancer stem cell formation and its application.

ALDH1, OCT4, SOX2 and Nanog are all stemness markers of cancer stem cells and have important roles in maintaining the nature of cancer stem cells and drug resistance (Anorma et al., 2018). We used Real-time PCR to detect the expression of cancer stem cell-related genes ALDH1, SOX-2, OCT-4, and Nanog. The expressions of ALDH1, SOX-2, OCT-4 and Nanog were significantly decreased after 100–800 μM TP5 were applied to HCT116 cells for 48 h (**Figures 3A–D**). It is suggested that TP5 may inhibit the self-renewal and tumorigenesis of colon cancer stem cells by regulating the important stemness genes ALDH1, SOX-2, OCT-4, and Nanog. Additionally, 100–800 μM TP5 also could significantly decrease the expression of CD24, CD44 and CD133 genes in HCT116 cells (**Figures 3E–G**). We also examined ALDH enzyme activity as a marker of cancer stem cell stemness (Jiang et al., 2019). TP5 concentration-dependently inhibited ALDH activity in HCT116 cells (after 48 h of TP5 action at 100, 200, 400, and 800 μM, ALDH activity decreased to 0.94 ± 0.10, 0.70 ± 0.05, 0.69 ± 0.02 and 0.33 ± 0.02; **Figure 3H**).

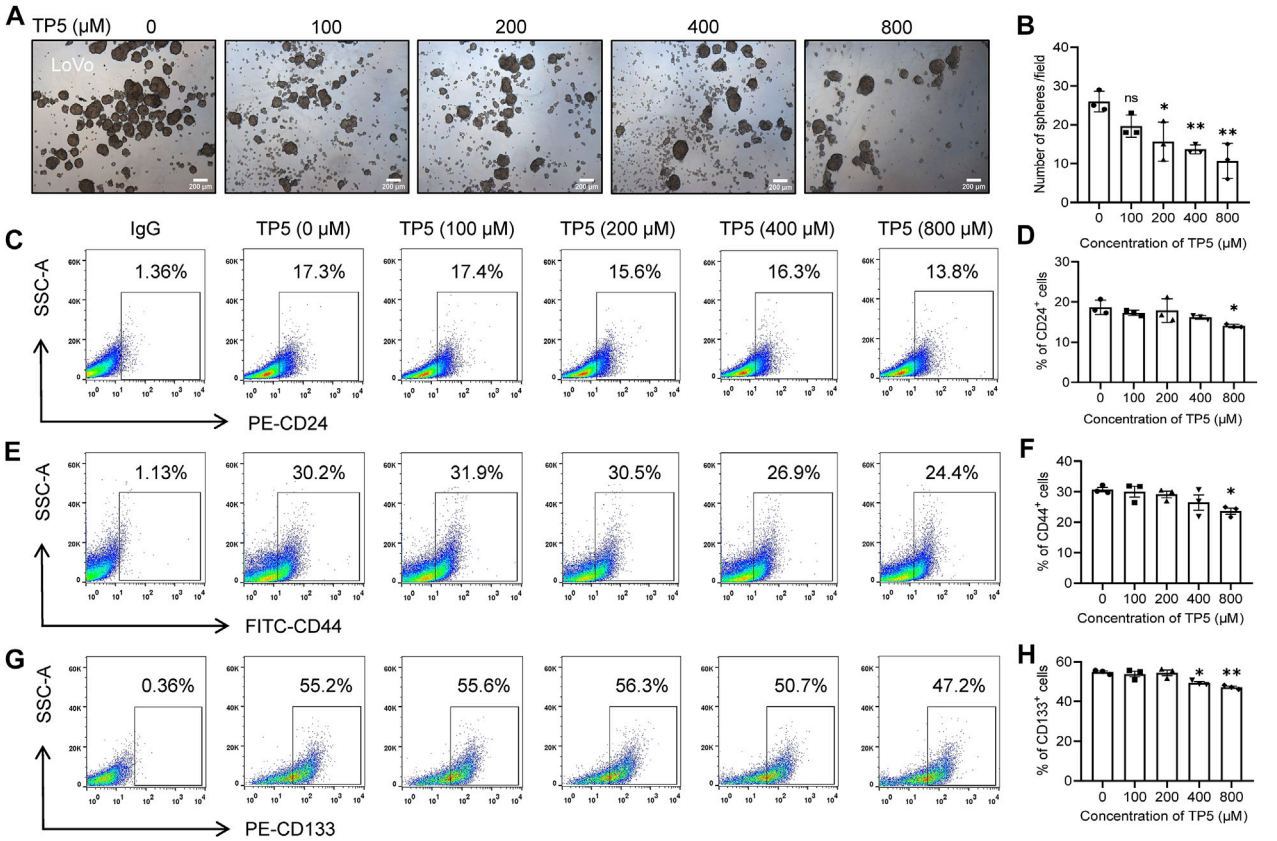

FIGURE 2 | TP5 inhibits the stemness of cancer stem cells in LoVo cells. **(A, B)** Representative photomicrographs of sphere formation experiments **(A)** and statistical analysis of the number of spheres with diameter ≥140 μm in visual field **(B)**. LoVo cells were incubated with different treatments of TP5 (0, 100, 200, 400, and 800 μM) and grown in serum-free medium for 6 days. Scale bar = 200 μm. **(C–H)** Flow cytometer analysis of the expression of CD24, CD44 or CD133 **(C, E, G)** and pooled data of cell surface markers CD24 **(D)**, CD44 **(F)** and CD133 **(H)** (n = 3 independent experiments). All data are expressed as mean ± SD; $^{*}p < 0.05$, $^{**}p < 0.01$ versus control, one-way ANOVA with Dunnett's post-hoc test, **(B)**, [F (4, 10) = 8.484, $p = 0.0030$], **(D)**, [F (4, 10) = 3.795, $p = 0.0397$], **(F)**, [F (4, 10) = 3.397 $p = 0.0531$], **(H)**, [F (4, 10) = 11.09, $p = 0.0011$].

Effect of TP5 on Wnt/β-Catenin Signaling Pathway

The Wnt signaling pathway is a key pathway for cancer stem cell development, and the sustained activation of the Wnt signaling pathway leads to the generation of cancer stem cells, which is an important factor for tumor resistance to conventional chemotherapy. Therefore, blocking the Wnt signaling pathway may be the key to removing cancer stem cells for the treatment of colon cancer (Polakis, 2007). β-catenin is a key downstream effector molecule in the Wnt signaling pathway (Liu et al., 2002). After the action of TP5 at 100–800 μM (**Figure 4**), HCT116 cells exhibited decreased PI3K (110 β) expression (100–400 μM effective), decreased AKT (P-Ser473 + Tyr474) phosphorylation levels (400–800 μM effective), and decreased WNT1 expression (200–800 μM effective); phosphorylated β-catenin (Ser33/37/Thr41) was increased (100–800 μM effective), leading to β-catenin degradation and expression decreased (800 μM effective) (the slightly different sensitivity of these indicators to TP5 may be due to some complex association of these factors), suggesting that TP5 inhibited colon cancer stem cells by affecting the wnt/β-catenin signaling pathway, which in turn inhibited colon cancer stem cells.

TP5 Reduces Intracellular Calcium Concentration in HCT116 Cells

As a universal second messenger, calcium ions (Ca^{2+}) promote the growth and metastasis of certain malignant tumor cells (Roderick and Cook, 2008; Yang et al., 2021). The self-renewal, drug resistance, and tumorigenic properties of colon cancer stem cells may function by regulating the inward flow of Ca^{2+} (Terrie et al., 2019); Ca^{2+} can promote the growth and spread of cancer stem cells. The percentage of Fluo-4 positive cells decreased from 52.0 ± 2.1% to 47.5 ± 3.0%, 43.5 ± 6.7%, 38.3 ± 2.4% and 32.5 ± 0.6% after 24 h of action of TP5 on HCT116 cells with 100, 200, 400 and 800 μM, respectively (**Figures 5A,B**), indicating that TP5 can concentration dependently

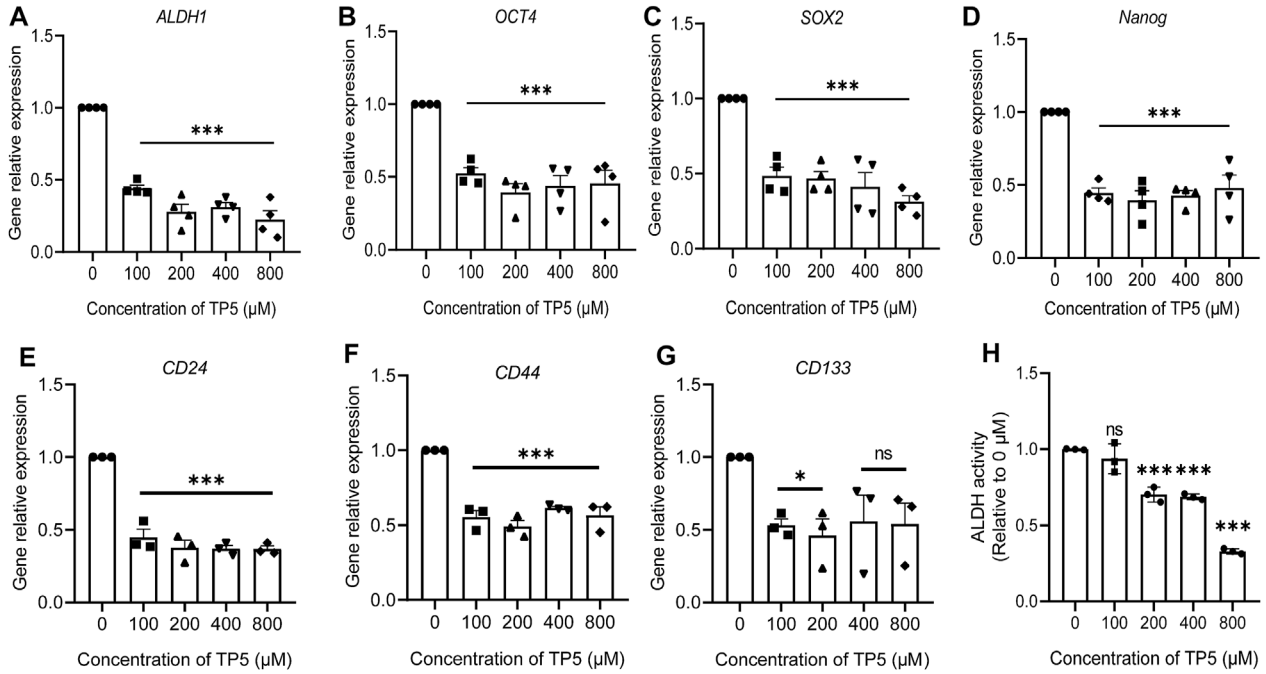

FIGURE 3 | TP5 reduced the expression of cancer stem cell-related genes in HCT116 cells. **(A–G)** RT-qPCR analysis of relative mRNA expression of CSC-associated genes ALDH1 **(A)**, SOX-2 **(B)**, Oct-4 **(C)**, Nanog **(D)**, CD24 **(E), CD44 (F**) and CD133 **(G)** in HCT116 cells. **(H)** ALDH activity before and after treatment with different concentrations of TP5 (n = 3–4 independent experiments). All data are expressed as mean ± SD; *p < 0.05 and ***p < 0.001 vs. control, one-way ANOVA with Dunnett's post hoc test, **(A)**, F (4, 15) = 63.02, p < 0.0001, **(B)**, F (4, 15) = 17.52, p < 0.0001, **(C)**, F (4, 15) = 22.74, p < 0.0001, **(D)**, F (4, 15) = 22.83, p < 0.0001, **(E)**, F (4, 10) = 3.392, p = 0.0533, **(F)**, F (4, 10) = 53.61, p < 0.0001, **(G)**, F (4, 10) = 29.41, p < 0.0001, **(H)**, (F (4, 10) = 83.55, p < 0.0001; ns, not significant.

reduce the intracellular Ca^{2+} concentration of HCT116 cells and thus inhibit the properties of cancer stem cells.

TP5 Promotes the Anti-proliferative Effect of OXA on Colon Cancer Cells

Given the possible resistance of cancer stem cells to chemotherapeutic agents (Prieto-Vila et al., 2017) and the diminished proliferation inhibition of tumor cells by chemotherapeutic agents, the direct inhibitory effect of TP5 on colon cancer stem cells suggests that the combination of TP5 with chemotherapeutic agents may enhance the therapeutic effect of these chemotherapeutic agents. Consistent with this speculation, we show that 25–100 μM of chemotherapeutic drug OXA produced inhibition on the proliferation of HCT116 in a concentration-dependent manner, while 100–800 μM TP5 significantly enhanced the anti-proliferative effect of OXA (**Figure 6A**).

To rule out the possibility that TP5 significantly enhanced the anti-proliferative effect of OXA on HCT116 because TP5 directly inhibited the proliferation of HCT116 cells, we treated HCT116 cells with TP5 for 48 h and observed its inhibitory effect on the proliferation of HCT116.100–800 μM TP5 did not cause significant visible changes in the cell viability and morphology of HCT116 cells compared with the control (**Figures 6B,D**); also, 100–800 μM TP5 did not induce apoptosis in HCT116 cells (**Figure 6C**). These results suggested that TP5 did not have a direct effect on the proliferation, morphology, and apoptosis of HCT116 cells.

To further verify whether TP5 promotes the antitumor effect of OXA by inhibiting colon cancer stem cells, we measured the expression of cancer stem cell markers CD24 and CD44 by flow cytometry after TP5 and OXA were co-administered to colon cancer HCT116 cells for 24 h. Compared with the control group, 5 μM OXA could not change the proportion of CD24-positive cells (28.6 ± 0.5% vs 27.8 ± 0.5%, p > 0.05; **Figures 7A,B**), while the proportion of CD24-positive cells decreased from 28.6 ± 0.5% to 18.3 ± 0.3% after 800 μM TP5 was administered to HCT116 cells for 24 h (p < 0.01, **Figures 7A,B**). Co-administration of TP5 (800 μM) with OXA (5 μM) further reduced the proportion of CD24-positive cells to 15.7 ± 0.4% (p < 0.01, **Figures 7A,B**). Similarly, 5 μM OXA could not change the proportion of CD44-positive cells, while the proportion of CD44-positive cells decreased from 46.6 ± 0.7% to 36.7 ± 0.7% after 24 h of 800 μM TP5 action on HCT116 cells, and the combined administration of TP5 (800 μM) with OXA (75 μM) further reduced the proportion of CD44-positive cells proportion to 33.6 ± 0.4% (p < 0.01, **Figures 7C,D**). It suggests that TP5 may inhibit colon cancer stem cells and therefore possibly sensitize the antitumor effect of OXA.

TP5 Inhibits HCT116 Cancer Stem Cells *via* Acetylcholine Receptors (nAchRs)

Our previous studies suggested that D-tubocurarine (TUB), an antagonist of nAchRs (Fan et al., 2006b), significantly

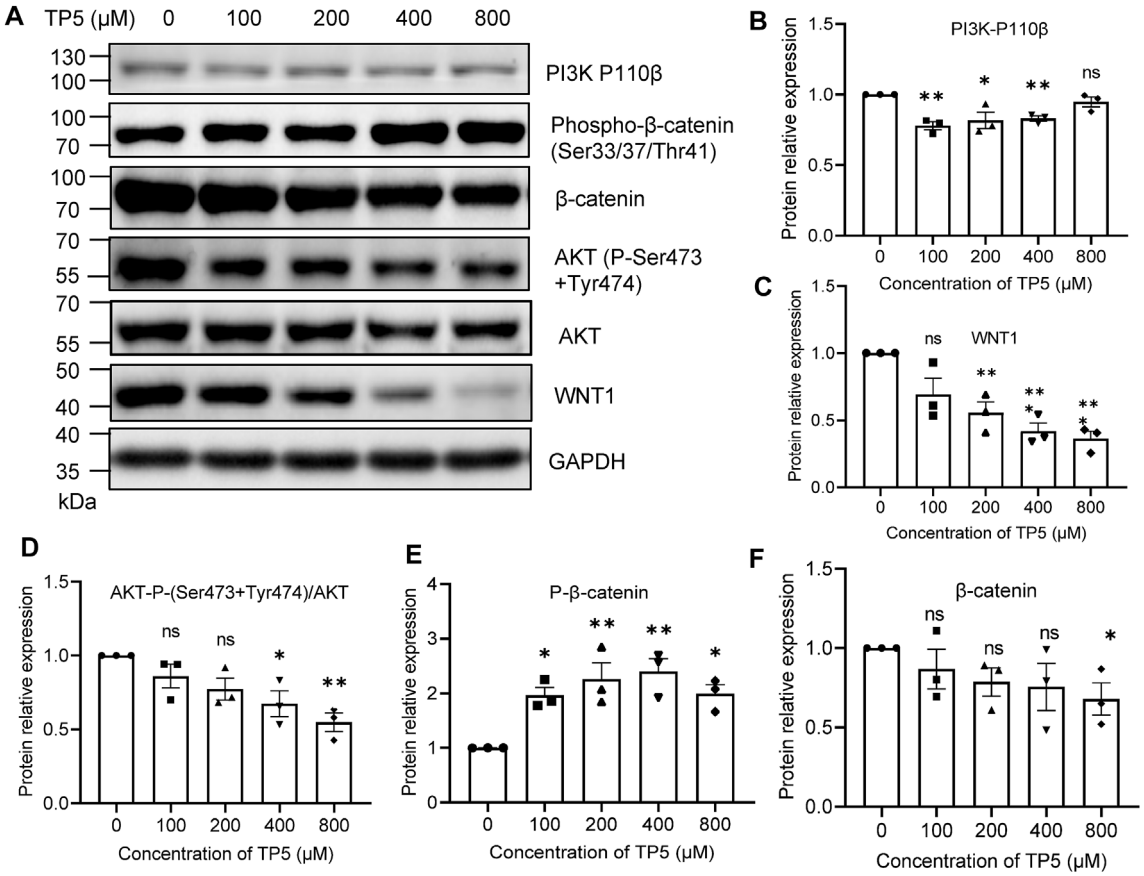

FIGURE 4 | Effect of TP5 on Wnt/β-catenin signaling pathway. **(A–F)** Typical Western blot analysis **(A)** and pooled data of protein expression levels of PI3K-P110 β **(B)**, WNT1**(C)**, P-AKT**(D)**, P-β-catenin **(E)** and β-catenin **(F)**. Histograms are expressed as induction rates in triplicate for the GAPDH control. All data are expressed as mean ± SD; $^{*}p < 0.05$, $^{**}p < 0.01$ and $^{***}p < 0.001$, one-way ANOVA with Dunnett's post hoc test, **(B)**, F (4, 10) = 7.486, $p = 0.0047$, **(C)**, F (4, 10) = 11.47, $p = 0.0009$, **(D)**, F (4, 10) = 6.387, $p = 0.0081$, **(E)**, F (4, 10) = 7.421, $p = 0.0048$, **(F)**, F (4, 10) = 1.342, $p = 0.3204$; ns, not significant.

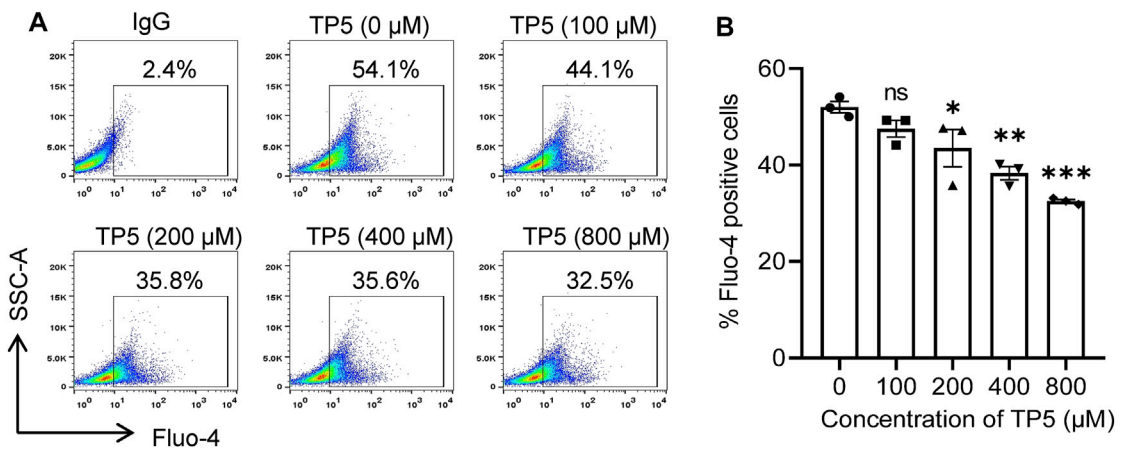

FIGURE 5 | TP5 reduces intracellular calcium concentration in HCT116 cells. **(A, B)** Representative cellular calcium decrease **(A)** and the summary of three independent experiments **(B)**. Altered intracellular calcium concentration of HCT116 cells after various concentrations of TP5 treatment. All data are expressed as mean ± SD; $^{*}p < 0.05$, $^{**}p < 0.01$ and $^{***}p < 0.001$, one-way ANOVA with Dunnett's post hoc test [F (4, 10) = 13.81, $p < 0.001$]; ns, not significant.

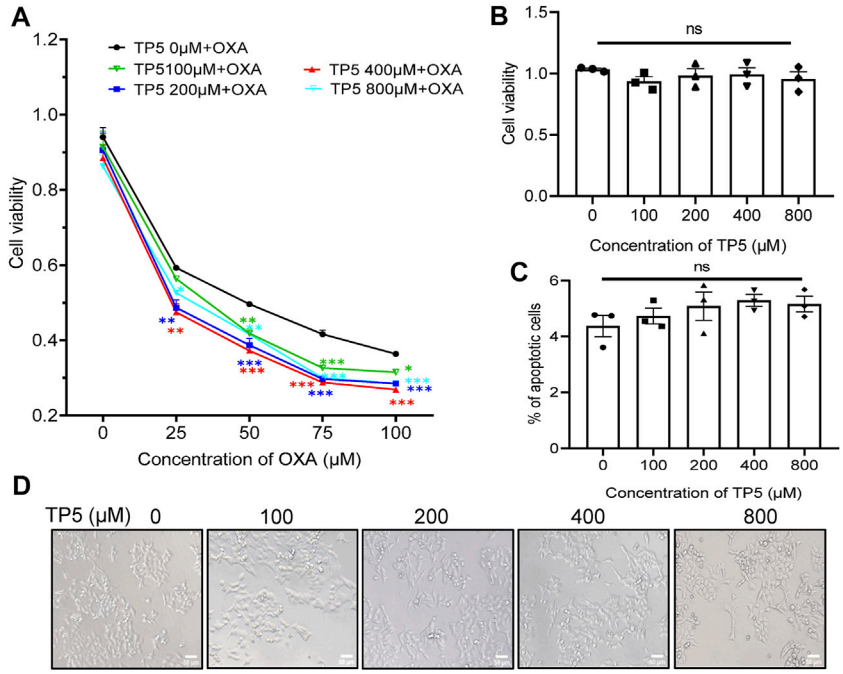

FIGURE 6 | TP5 promotes the anti-proliferative effect of OXA on colon cancer cells. **(A)** The HCT116 cell viability measured by MTT assay at different concentrations of TP5 and OXA. HCT116 cells were exposed to different concentrations of TP5 (0, 100, 200, 400, and 800 μM) and OXA (0, 25, 50, 75, and 100 μM) for 48 h. **(B)** The HCT116 cell viability measured by MTT assay after treatment with TP5 for 48 h only. **(C)** Apoptosis of HCT116 cells analyzed by Annexin V/PI staining by flow cytometry after treatment with different concentrations of TP5. **(D)** Morphological changes observed in TP5-treated HCT116 cells and untreated cells. Scale bar = 50 μm. All data are expressed as mean ± SD; $^{*}p < 0.05$, $^{**}p < 0.01$ and $^{***}p < 0.001$, two-way ANOVA with Dunnett's post hoc test **(A)**, F (4, 50) = 25.15, $p < 0.0001$, and one-way ANOVA with Dunnett's post hoc test **(B)** and **(C)**, F (4, 10) = 0.6217, $p = 0.6575$, **(C)**, F (4, 10) = 1.132, $p = 0.3952$; ns, not significant.

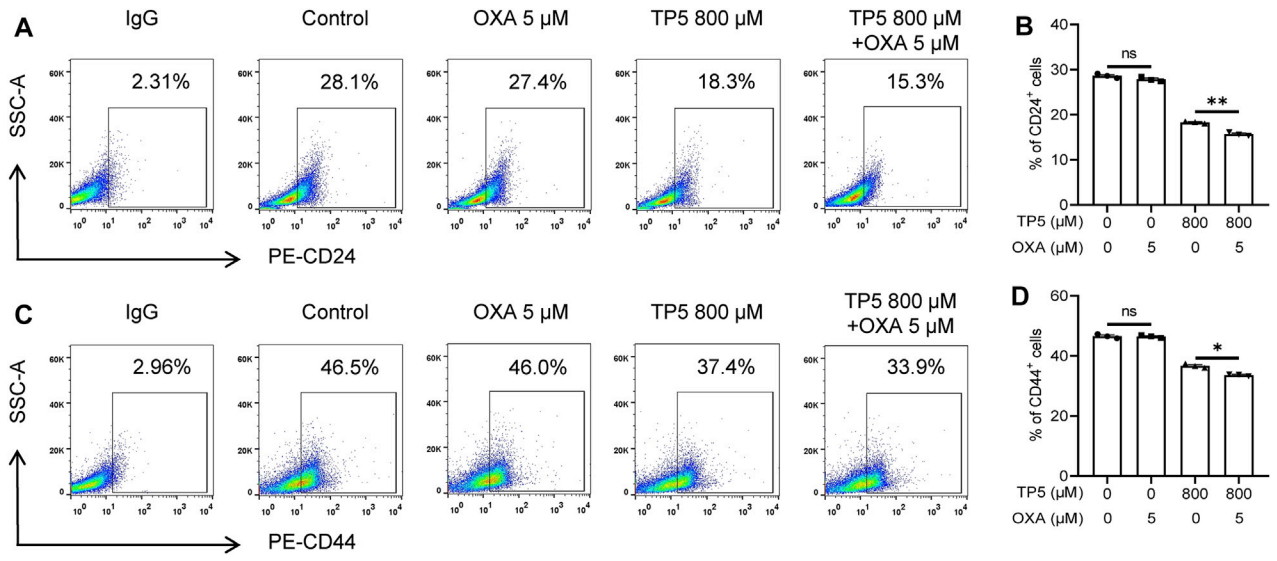

FIGURE 7 | TP5 promotes the inhibitory effect of OXA on colon cancer stem cells. **(A–D)** Flow cytometer analysis of the expression of CD24 **(A)** and CD44 **(C)** in HCT116 cells after OXA and TP5 treatments, and pooled data of cell surface markers CD24 **(B)**, CD44 **(D)** ($n = 3$ independent experiments). All data are represented as mean ± SD; $^{*}p < 0.05$ and $^{**}p < 0.01$, unpaired two-tailed Student's t-test. ns, not significant.

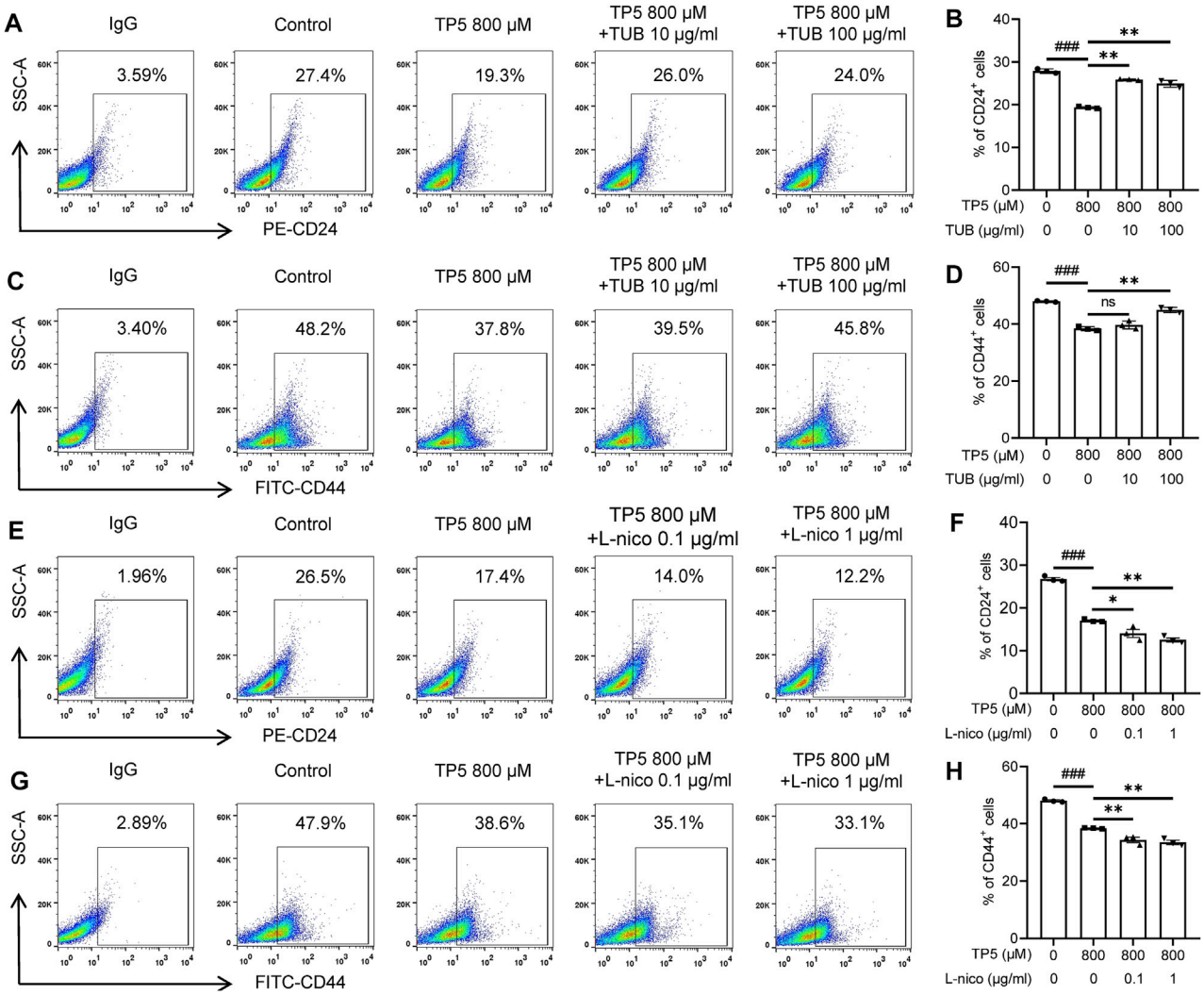

FIGURE 8 | TP5 inhibits HCT116 cancer stem cells via acetylcholine receptors (AchRs). **(A–D)** Flow cytometric analysis of CSC surface markers CD24 **(A, B)** and CD44 **(C, D)** in HCT116 cells treated with TP5-conjugated AchR inhibitor D-Tubocurarine (TUB). **(E–H)** Flow cytometric analysis of CSC surface markers CD24 **(E, F)** and CD44 **(G, H)** in HCT116 cells treated with TP5-conjugated AchR agonist L-nicotine (L-Nico). Data are represented as mean ± SD of three independent experiments; $^{*}p < 0.05$, $^{**}p < 0.01$ and $^{***}p < 0.001$, one-way ANOVA with Tukey's post hoc test, **(A)**, $F(3, 8) = 158.6$, $p < 0.0001$, **(B)**, $F(3, 8) = 71.08$, $p < 0.0001$, **(C)**, $F(3, 8) = 123.9$, $p < 0.0001$, **(D)**, $F(3, 8) = 120.8$, $p < 0.0001$; ns, not significant.

antagonized the inhibitory effect of TP5 on the proliferation of leukemic HL60 cells, whereas the inhibitor of muscarinic acetylcholine receptors (mAchRs), atropine (Atr), did not have this antagonistic effect, suggesting that the inhibitory proliferative effect of TP5 on leukemic cells may be achieved through nAchRs (Fan et al., 2006a). We further investigated whether TP5 inhibited nAchRs via acetylcholine receptors in HCT116 colon cancer stem cells by using agonists and antagonists of nAchRs. TUB (10–100 μg/ml) significantly antagonized this effect of TP5 (**Figures 8A–D**). After 24 h of TP5 action on HCT116 cells with 800 μM, the percentage of CD24-positive cells decreased from 27.9 ± 0.5% to 19.3 ± 0.3% ($p < 0.01$) and the percentage of CD44-positive cells decreased from 48.0 ± 0.3% to 38.4 ± 0.7% ($p < 0.001$); whereas the early addition of 10 μg/ml or 100 μg/ml TUB, the proportion of CD24-positive cells reversed to 25.9 ± 0.2% ($p < 0.01$, vs. 19.3 ± 0.3%) and 24.9 ± 0.8% ($p < 0.01$, vs. 19.3 ± 0.3%); the proportion of CD44-positive cells reversed to 39.7 ± 1.4% ($p > 0.05$ vs. 38.4 ± 0.7%) and 45.0 ± 0.9% ($p < 0.01$ vs. 38.4 ± 0.7%).

In contrast, the cholinergic agonist the nicotine L-Nicotine (L-Nico) further promoted the inhibitory effect of TP5 on cancer stem cells in colon cancer cells (**Figures 8E–H**). Pretreatments of L-Nico (0.1 and 1 μg/ml) further reduced the proportion of CD24-positive cells to 14.0 ± 1.7%, 12.5 ± 0.9% ($p < 0.01$, vs. 19.3 ± 0.3%), and the proportion of CD44-positive cells to 34.3 ± 1.6%, and 33.5 ± 1.2% ($p < 0.05$ vs. 38.4 ± 0.7%).

We further found that the inhibitor TUB (1–100 μg/ml) significantly blocked the TP5-promoted proliferation inhibition of HCT116 by OXA, whereas the agonist L-Nico promoted this

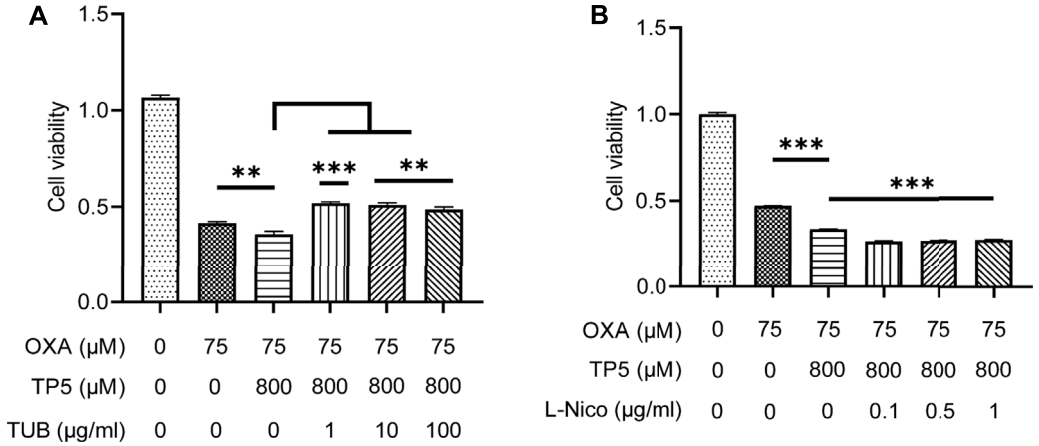

FIGURE 9 | TP5 promotes the inhibitory effect of OXA on colon cancer cell proliferation *via* AchRs. **(A, B)** HCT116 cells were tested for cell viability after treatment with TP5 and OXA, or in combination with AchR inhibitors TUB (1, 10 and 100 μg/ml) **(A)**, or with AchR agonists L-Nico (0.1, 0.5 and 1 μg/ml) **(B)** for 48 h. All data are represented as mean ± SD. $^{**}p < 0.01$, $^{***}p < 0.001$, unpaired two-tailed Student's *t*-test; ns, not significant.

effect of TP5 (**Figure 9A, B**), implying that nAchRs might be involved in TP5-mediated inhibition of HCT116 colon cancer stem cells inhibition, thereby interrupting the TP5-promoted proliferation inhibition of HCT116 by oxaliplatin. Certainly, since restoration of cell viability in the presence of TP5 is only partial, there may be other mechanisms for TP5 to act on HCT116 cells in addition to nAchRs.

DISCUSSION

According to a large number of clinical studies (Costantini et al., 2019), TP5 is indicated for immune impairment due to malignant tumors and therefore can be used frequently in tumor patients and is very safe, with very few toxic side effects, both subcutaneously and intravenously (Xiaojing et al., 2017). In the present study, we found that the immunomodulatory peptide TP5 can not only be used as a good immune adjuvant in the treatment of tumors, but also can act directly on colon cancer cells. TP5 could not inhibit the proliferation of colon cancer cells HCT116, but it could enhance the anti-proliferative effect of chemotherapeutic drug oxaliplatin on colon cancer cells HCT116.

Evidence from the following aspects suggests that TP5 can effectively influence the stemness of HCT116 cancer stem cells. *First*, the ability of sphere formation is an important method to identify cancer stem cells *in vitro* (Cao et al., 2011). After TP5 action, the number of cancer stem cell spheroids formed by HCT116 cells was significantly reduced, and the spheroid formation rate was also significantly decreased, indicating that TP5 inhibited the self-renewal and proliferation ability of cancer stem cells. *Secondly*, CD24, CD44 and CD133 are specific surface markers that can be expressed by colon cancer stem cells (Choi et al., 2009); ALDH1, OCT4, SOX2 and Nanog are all markers of stemness status of cancer stem cells, which are important for maintaining the nature and drug resistance of cancer stem cells (Liu et al., 2013). TP5 significantly decreased the expression of these important stemness genes, thus inhibiting stemness of colon cancer stem cells. *Third*, the self-renewal, drug resistance and tumorigenicity of colon cancer stem cells may function by regulating the inward flow of Ca^{2+} (Yang et al., 2020). Ca^{2+} promote the growth and proliferation of cancer stem cells. TP5 can concentration-dependently decrease the intracellular calcium ion concentration in HCT116 cells, thus inhibiting the properties of cancer stem cells. *Fourth*, the wnt/β-catenin signaling pathway is a key pathway for cancer stem cell development (Valkenburg et al., 2011). Sustained activation of the wnt signaling pathway leads to the generation of cancer stem cells, thus blocking the wnt/β-catenin signaling pathway may be the key to removing cancer stem cells for the treatment of colon cancer (Krishnamurthy and Kurzrock, 2018). TP5 can inhibit cancer stem cells by inhibiting the PI3K/Akt/wnt/β-catenin signaling pathway to inhibit cancer stem cells, thereby suppressing colon cancer stem cells.

The mechanism by which TP5 enhances the antitumor effect of the chemotherapeutic drug OXA by affecting the stemness of HCT116 cancer stem cells may be as follows. 1. Cancer stem cells have an enhanced ability to repair DNA damage, which induces resistance to chemotherapy, including resistance to DNA-damaging drugs (Yu et al., 2017). TP5 inhibits colon cancer stem cells and reduces the ability of cancer stem cells to repair DNA damage, thereby enhancing stem cell sensitivity to the DNA-damaging drug OXA. 2. Cancer stem cells, like stem cells, can be more viable through multiple mechanisms that can avoid cell death due to apoptosis and senescence (Sabisz and Skladanowski, 2009; Triana-Martinez et al., 2020). TP5 can inhibit colon cancer stem cells, thus reducing the viability of stem cells and thus enhancing the cytotoxicity of chemotherapeutic drugs on cancer stem cells. 3. TP5 and OXA target both HCT116 tumor cells and stem cells, producing a synergistic effect. TP5 acts mainly on cancer stem cells and OXA acts mainly on tumor cells. However, OXA also reduced the expression of CD24 and CD44, which are specific surface markers for colon cancer stem cells,

while TP5 mildly enabled OXA to exert an inhibitory effect on stem cell stemness. Thus, the synergistic effect between the two ultimately enhanced the antitumor effect of OXA.

Colorectal cancer is the third most common cancer and the fourth most common cause of death in the world, with approximately 700,000 deaths worldwide each year (Rawla et al., 2019). The development and metastasis of cancer is thought to be caused by cancer stem cells. Cancer stem cells are latent in the body, ready to metastasize and cause tumor recurrence in a more aggressive and drug-resistant form (Chang, 2016). Colon cancer stem cells are highly resistant to radiotherapy and chemotherapy, and most drugs can act on tumor cells but are ineffective against cancer stem cells. Therefore, inhibition of cancer stem cells is a critical and difficult point in tumor treatment (Ordonez-Moran et al., 2015; Hirata et al., 2019). TP5 can promote the antitumor effect of oxaliplatin by inhibiting colon cancer stem cells, suggesting that TP5 may become a novel drug to target cancer stem cells, thus reducing cancer recurrence rate and improving tumor treatment efficacy, and may provide a new treatment option for patients with drug-refractory colorectal cancer. Nevertheless, many questions are still unclear: here, can TP5 inhibit colon cancer stem cells, however, does TP5 have any effect on other types of cancer stem cells, and does TP5 act directly on acetylcholine receptors.

Finally, for the adjuvant treatment of TP5, the dose is mainly intramuscular or subcutaneous and may be 50 mg per day (Conant et al., 1992; Fabrizi et al., 2006; Wolf et al., 2011). One study evaluated the clinical efficacy and tolerability of high-dose intravenous TP5 in 16 patients with melanoma (Cascinelli et al., 1998). Patients received 1 g of intravenous TP5 every 2 days for 7 weeks and were then evaluated; responders received a follow-up course of 2 g of intravenous TP5 every 2 days for 5 weeks. In this study, high-dose intravenous TP5 administered three times weekly enhances immune function in patients with cutaneous and subcutaneous metastases from melanoma without associated side effects (Cascinelli N et al., 1998). Therefore, TP5 may reach relatively high concentrations at the local administration site, but the concentrations in the whole blood of patients may be lower than in our experiments. This study might not directly guide the clinical application of TP5 at this time, but offers the possibility of continuing to modify the TP5 sequence to increase its potency to act on cancer stem cells and protect against immune repair, such as through some unnatural amino acid substitutions, cyclization modifications, etc. Therefore, further research on these scientific questions may lay a solid theoretical foundation for the realization of immunomodulatory peptide TP5/TP5 analogs alone or in combination with chemotherapeutic drugs for the clinical treatment of colon cancer.

MATERIALS AND METHODS

Chemicals and Cell Culture

TP5 was purchased from ChemBest Research Laboratories Ltd. (China). Oxaliplatin (OXA), D-tufosine pentahydrate (TUB) and L-nicotine (L-Nico) were purchased from MedChemExpress (USA). HCT116 cells were cultured in RPMI-1640 medium (C11875500BT, Gibco) supplemented with 10% fetal bovine serum (10099–141, Gibco), penicillin (100 IU/ml) and streptomycin (100 μg/ml, C0222, Beyotime). LoVo cells were cultured in F-12K Nutrient Mixture (21127–022, Gibco) supplemented with 10% fetal bovine serum (10099–141, Gibco), penicillin (100 IU/ml) and streptomycin (100 μg/ml, C0222, Beyotime). Cells were incubated in a humidified incubator containing 5% CO_2 at 37°C.

Sphere Formation Test

The serum-free medium for spheroid culture consisted of DMEM/F12 (SH30023.01, HyClone) medium supplemented with 0.4% BSA (B2064-100G, Sigma), 20 ng/ml human recombinant epidermal growth factor (AF-100-15-100UG, PeproTech), 20 ng/ml human recombinant basic fibroblast growth factor (100–18 B-10UG, PeproTech), 25 μg/ml human insulin (HY-P0035, MCE), 2% B27 supplement (50×) (17504–044, Gibco), and 0.1% 2-mercaptoethanol (21985023, Gibco). Cells were plated in Corning Ultra-Low Attachment 24-well plates (3473, Costar) at a density of 5,000 viable cells/well and grown in serum-free medium. Cells were grown for 6 days and the number of spheroids was counted under the microscope (DMI3000 B, Leica) as previously described (Tominaga et al., 2019).

Flow Cytometry

HCT116 cells or LoVo cells (1.5×10^5 cells/well) were seeded in 12-well plates and exposed to different concentrations of TP5 for 24 h. The supernatant was then removed and cells were digested with 0.25% trypsin (25200-072, Gibco). After washing, cells were resuspended in 100 ul of PBS (ST476, Beyotime). For surface staining, cells were labeled with PE-CD24 (555428, BD Pharmingen), FITC-CD44 (555478, BD Pharmingen), and PE-CD133 (12-1338-41, eBiosciences) (He et al., 2021). Cell suspensions were incubated with the appropriate antibodies for 30 min at room temperature in the dark, followed by a washing step to remove unlabeled antibodies. Flow cytometry analysis was performed using BD FACS Jazz™ (BD Biosciences) and analyzed by FlowJo software.

RT—qPCR Assay

Total RNA was isolated and reverse transcribed using EZ-press RNA purification kit (B0004-plus, EZBioscience) and PrimeScript RT kit (RR047A, TaKaRa), respectively, according to the manufacturer's instructions (Wang et al., 2013), and qPCR was performed using TB Green Premix Ex Taq (RR420A. TaKaRa) for qPCR. relative changes in gene expression were determined using the 2-ΔΔCt method, and relative mRNA expression was normalized to GAPDH. Following primer sets were used for analyzing the expression of specific genes including ALDH1, forward: 5′-ACGCCAGACTTACCTGTCCTACTC-3′ and reverse: 5′- TCTTGCCACTCACTGAATCATGCC-3′; SOX-2, forward: 5′- GCTCGCAGACCTACATGAACGG-3′, and reverse: 5′-AGCTGGCCTCGGACTTGACC -3′; OCT-4, forward: 5′- GATGTGGTCCGAGTGTGGTTCTG-3′and reverse: 5′-CGAGGAGTACAGTGCAGTGAAGTG -3′; Nanog,

forward: 5′- AGCAATGGTGTGACGCAGAAGG-3′, and reverse: 5′-ACCAGGTCTGAGTGTTCCAGGAG -3′; CD24, forward: 5′- CTCCTACCCACGCAGATTTATTC-3′, and reverse: 5′-AGAGTGAGACCACGAAGAGAC-3′; CD44, forward: 5′- CTGCCGCTTTGCAGGTGTA-3′, and reverse: 5′-CATTGTGGGCAAGGTGCTATT-3′; CD133, forward: 5′- AGT CGGAAACTGGCAGATAGC-3′, and reverse: 5′-GGTAGTGTT GTACTGGGCCAAT-3′; GAPDH, forward: 5′-TTGGTATCG TGGAAGGACT-3′, and reverse: 5′-GGATGATGTTCTGGA GAGC-3′.

Aldehyde Dehydrogenase Activity Assay

ALDH activity was assessed using an ALDH activity detection kit (BC0755, Solarbio) according to the manufacturer's instructions (Jiang et al., 2019). HCT116 cells (3.5×10^5 cells/well) were seeded in 6-well plates with different treatments of TP5 (0, 100, 200, 400, and 800 μM) for 48 h at 37°C. Cells were lysed with ultrasound, centrifuged and the supernatant (100 μL/well) was transferred to UV-Star 96-well plates (655801, Greiner Bio-one) and incubated at 37°C for 10 min. ALDH activity was measured at 340 nm using a microplate reader (VarioskanTM LUX, Thermo).

Western Blot Analysis

After treatment with TP5 (100, 200, 400 and 800 μM) for 48 h, total proteins from HCT116 cells were lysed in lysis buffer (P0013, Beyotime) containing 1% cocktail (B14001, Bimake) (Li et al., 2012; Wang et al., 2017). Cell lysates were cleared by centrifugation at 12,000 rpm for 15 min at 4°C. The concentration of total protein was determined using the Enhanced BCA Protein Assay Kit (P0010, Beyotime). Protein sample buffer was added and samples were boiled at 100°C for 10 min. Briefly, 20 μg of protein was loaded into each lane and transferred to a polyvinylidene difluoride (PVDF) membrane. The membranes were incubated overnight at 4°C with primary antibody, and secondary antibodies anti-rabbit IgG HRP-conjugated (1: 3,000, 7074S, Cell Signaling Technology) and anti-mouse IgG HRP-conjugated (1: 3,000, 7076S, Cell Signaling Technology) were incubated at 25°C for incubate for 2 h. The primary antibodies used are Beta Catenin Rabbit Polyclonal Antibody (1: 1,000, 51067-2-AP, Proteintech), WNT1 Rabbit Polyclonal Antibody (1: 1,000, 27935-1-AP, Proteintech), Phospho-beta Catenin (Ser33/37/Thr41) antibody (1: 1,000, 9561, Cell Signaling Technology), AKT1 (Phospho-Ser473 + Tyr474) antibody (1: 1,000, 12669, Abcam), PI3K p110 (beta) polyclonal antibody (1: 1,000, 20584-1-AP, Proteintech), AKT1 polyclonal antibody (1: 1,000, 10176-2-AP, Proteintech), and GAPDH (1: 10,000, 60004-I-Ig, Proteintech). Phosphorylated protein bands were categorized as their total protein level, and other bands were categorized as GAPDH.

Molecular Probes Fluo-4 AM Calcium Assay

HCT116 cells were incubated in 12-well plates with different treatments of TP5 (0, 100, 200, 400, 800 μM) for 24 h at 37°C. To determine the cellular calcium concentration (He et al., 2021), the cell membrane Ca^{2+}-free concentration was assessed using the fluorescent Ca^{2+}-probe Fluo-4 AM (S1060, Beyotime). Briefly, cells were incubated in PBS at 37°C with 2 μM Fluo-4 AM for 30 min in the dark, followed by three washes with PBS. Binding buffer (500 μL) containing 1% FBS (Gibco, Australia) was added and incubated for 30 min in the dark at room temperature. The results were then evaluated by flow cytometry. The excitation wavelength was 488 nm and the emission wavelength was 520 nm. The experiment was repeated at least three times.

Cell Viability Assay

Cell viability was assessed using the MTT assay kit (C0009, Beyotime) according to the manufacturer's protocol (Foldbjerg et al., 2011). HCT116 cells were seeded in 96-well plates at a density of 15 × 103 cells/well and incubated overnight at 37°C. Next, cells were treated with TP5 and OXA and incubated for 48 h 10 μl MTT was added to each well and incubation was continued for 4 h. The absorbance was measured at 570 nm using a microplate reader (VarioskanTM LUX, Thermo). Cell viability was estimated by comparing the relative absorbance values with those of the untreated samples.

Annexin V/Propidium Iodide Staining Assay

The extent of apoptosis in treated HCT116 cells was assessed using the Annexin V-FITC/PI Apoptosis Assay Kit (556547, BD Pharmingen) according to the manufacturer's instructions (Park et al., 2017). HCT116 cells (1.5×10^5 cells/well) were seeded in 12-well plates, exposed to different concentrations of TP5 for 48 h, and stained with 5 μl of FITC-labeled Annexin V and 5 μl of PI simultaneously at room temperature, protected from light. Stained cells were analyzed using a fluorescence-activated cell sorter flow cytometer (BD FACS Jazz™, BD Biosciences). A minimum of 10,000 cells were used for each analysis, and experiments were performed in triplicate.

Statistical Analysis

Data are expressed as mean ± SD. All experiments were performed independently, at least 3 times. Statistical analyses were performed as described in each corresponding legend. Differences between two groups were assessed by unpaired two-sided Student's t-test, and differences between multiple groups were assessed by one- or two-way ANOVA and Dunnett's post hoc test. p less than 0.05 was considered statistically significant.

DATA AVAILABILITY STATEMENT

The original contributions presented in the study are included in the article/Supplementary Material, further inquiries can be directed to the corresponding authors.

AUTHOR CONTRIBUTIONS

P-CY: Methodology, Validation, Formal analysis, Investigation, Data Curation, Visualization, and Writing-Original draft. DL: Methodology, Validation, Formal analysis, Investigation, and Data Curation. Z-XH: Methodology, Validation, and Funding acquisition. FL: Investigation and Data Curation. C-YH: Methodology, Investigation and Data Curation. Y-TL: Methodology, Investigation and Data Curation. C-RG: Methodology, Investigation and Data Curation. W-HW:

Methodology, Investigation and Funding acquisition. X-HL: Investigation and Resources. X-NY: Validation and Resources. C-ZL: Methodology, Validation, Formal analysis, Investigation, Resources, Data Curation, Writing-Review and Editing, Visualization, Supervision, Project administration, and Funding acquisition. Y-ZF: Methodology, Validation, Formal analysis, Investigation, Resources, Supervision, Project administration, and Funding acquisition. YY: Conceptualization, Methodology, Validation, Formal analysis, Investigation, Resources, Data Curation, Writing-Review and Editing, Visualization, Supervision, Project administration, and Funding acquisition.

FUNDING

This study was supported with funds from the National Natural Science Foundation of China with grant numbers 81603409 (Y-ZF), 31570832 (YY) and 31971146 (YY), Natural Science Foundation of Jiangsu Province (BK20202002 to YY), Innovation and Entrepreneurship Talent Program of Jiangsu Province (YY), State Key Laboratory of Utilization of Woody Oil Resource with grant number 2019XK2002 (C-ZL), Hunan "Huxiang" High-level Talent Program (2021 to YY), and "Xing Yao" Leading Scholars of China Pharmaceutical University (2021) (YY).

REFERENCES

Anorma, C., Hedhli, J., Bearrood, T. E., Pino, N. W., Gardner, S. H., Inaba, H., et al. (2018). Surveillance of Cancer Stem Cell Plasticity Using an Isoform-Selective Fluorescent Probe for Aldehyde Dehydrogenase 1A1. *ACS Cent. Sci.* 4 (8), 1045–1055. doi:10.1021/acscentsci.8b00313

Ayob, A. Z., and Ramasamy, T. S. (2018). Cancer Stem Cells as Key Drivers of Tumour Progression. *J. Biomed. Sci.* 25 (1), 20–18. doi:10.1186/s12929-018-0426-4

Bocci, F., Gearhart-Serna, L., Boareto, M., Ribeiro, M., Ben-Jacob, E., Devi, G. R., et al. (2019). Toward Understanding Cancer Stem Cell Heterogeneity in the Tumor Microenvironment. *Proc. Natl. Acad. Sci. U S A.* 116 (1), 148–157. doi:10.1073/pnas.1815345116

Bodeya, B., Bodeya, B., jr, Siegel, S. E., and Kaiser, H. E. (2000). Review of Thymic Hormones in Cancer Diagnosis and Treatment. *Int. J. Immunopharmacol.* 22, 261–273. doi:10.1016/s0192-0561(99)00084-3

Cao, L., Zhou, Y., Zhai, B., Liao, J., Xu, W., Zhang, R., et al. (2011). Sphere-forming Cell Subpopulations with Cancer Stem Cell Properties in Human Hepatoma Cell Lines. *BMC Gastroenterol.* 11, 71. doi:10.1186/1471-230X-11-71

Cascinelli, N., Belli, F., Mascheroni, L., Lenisa, L., and Clemente, C. (1998). Evaluation of Clinical Efficacy and Tolerability of Intravenous High Dose Thymopentin in Advanced Melanoma Patients. *Melanoma Res.* 8 (1), 83–89. doi:10.1097/00008390-199802000-00014

Chambers, I., Colby, D., Robertson, M., Nichols, J., Lee, S., Tweedie, S., et al. (2003). Functional Expression Cloning of Nanog, a Pluripotency Sustaining Factor in Embryonic Stem Cells. *Cell* 113 (5), 643–655. doi:10.1016/s0092-8674(03)00392-1

Chang, J. C. (2016). Cancer Stem Cells: Role in Tumor Growth, Recurrence, Metastasis, and Treatment Resistance. *Medicine (Baltimore)* 95 (1 Suppl. 1), S20–S25. doi:10.1097/MD.0000000000004766

Choi, D., Lee, H. W., Hur, K. Y., Kim, J. J., Park, G. S., Jang, S. H., et al. (2009). Cancer Stem Cell Markers CD133 and CD24 Correlate with Invasiveness and Differentiation in Colorectal Adenocarcinoma. *World J. Gastroenterol.* 15 (18), 2258–2264. doi:10.3748/wjg.15.2258

Ciombor, K. K., Wu, C., and Goldberg, R. M. (2015). Recent Therapeutic Advances in the Treatment of Colorectal Cancer. *Annu. Rev. Med.* 66, 83–95. doi:10.1146/annurev-med-051513-102539

Clara, J. A., Monge, C., Yang, Y., and Takebe, N. (2020). Targeting Signalling Pathways and the Immune Microenvironment of Cancer Stem Cells - a Clinical Update. *Nat. Rev. Clin. Oncol.* 17 (4), 204–232. doi:10.1038/s41571-019-0293-2

Conant, M. A., Calabrese, L. H., Thompson, S. E., Poiesz, B. J., Rasheed, S., Hirsch, R. L., et al. (1992). Maintenance of CD4+ Cells by Thymopentin in Asymptomatic HIV-Infected Subjects: Results of a Double-Blind, Placebo-Controlled Study. *AIDS* 6 (11), 1335–1339. doi:10.1097/00002030-199211000-00016

Costantini, C., Bellet, M. M., Pariano, M., Renga, G., Stincardini, C., Goldstein, A. L., et al. (2019). A Reappraisal of Thymosin Alpha1 in Cancer Therapy. *Front. Oncol.* 9, 873. doi:10.3389/fonc.2019.00873

Csaba, G. (2016). The Immunoendocrine Thymus as a Pacemaker of Lifespan. *Acta Microbiol. Immunol. Hung* 63 (2), 139–158. doi:10.1556/030.63.2016.2.1

Du, L., Wang, H., He, L., Zhang, J., Ni, B., Wang, X., et al. (2008). CD44 Is of Functional Importance for Colorectal Cancer Stem Cells. *Clin. Cancer Res.* 14 (21), 6751–6760. doi:10.1158/1078-0432.CCR-08-1034

Fabrizi, F., Dixit, V., and Martin, P. (2006). Meta-analysis: the Adjuvant Role of Thymopentin on Immunological Response to Hepatitis B Virus Vaccine in End-Stage Renal Disease. *Aliment. Pharmacol. Ther.* 23 (11), 1559–1566. doi:10.1111/j.1365-2036.2006.02923.x

Fan, Y. Z., Chang, H., Yu, Y., Liu, J., and Wang, R. (2006a). Thymosin Alpha1 Suppresses Proliferation and Induces Apoptosis in Human Leukemia Cell Lines. *Peptides* 27 (9), 2165–2173. doi:10.1016/j.peptides.2006.03.012

Fan, Y. Z., Chang, H., Yu, Y., Liu, J., Zhao, L., Yang, D. J., et al. (2006b). Thymopentin (TP5), an Immunomodulatory Peptide, Suppresses Proliferation and Induces Differentiation in HL-60 Cells. *Biochim. Biophys. Acta* 1763 (10), 1059–1066. doi:10.1016/j.bbamcr.2006.07.004

Fearon, E. R., and Carethers, J. M. (2015). Molecular Subtyping of Colorectal Cancer: Time to Explore Both Intertumoral and Intratumoral Heterogeneity to Evaluate Patient Outcome. *Gastroenterology* 148 (1), 10–13. doi:10.1053/j.gastro.2014.11.024

Foldbjerg, R., Dang, D. A., and Autrup, H. (2011). Cytotoxicity and Genotoxicity of Silver Nanoparticles in the Human Lung Cancer Cell Line, A549. *Arch. Toxicol.* 85 (7), 743–750. doi:10.1007/s00204-010-0545-5

Hammond, W. A., Swaika, A., and Mody, K. (2016). Pharmacologic Resistance in Colorectal Cancer: a Review. *Ther. Adv. Med. Oncol.* 8 (1), 57–84. doi:10.1177/1758834015614530

He, X., Wan, J., Yang, X., Zhang, X., Huang, D., Li, X., et al. (2021). Bone Marrow Niche ATP Levels Determine Leukemia-Initiating Cell Activity via P2X7 in Leukemic Models. *J. Clin. Invest.* 131 (4), e140242. doi:10.1172/JCI140242

Hervieu, C., Christou, N., Battu, S., and Mathonnet, M. (2021). The Role of Cancer Stem Cells in Colorectal Cancer: From the Basics to Novel Clinical Trials. *Cancers (Basel)* 13 (5), 1092. doi:10.3390/cancers13051092

Hirata, A., Hatano, Y., Niwa, M., Hara, A., and Tomita, H. (2019). Heterogeneity of Colon Cancer Stem Cells. *Adv. Exp. Med. Biol.* 1139, 115–126. doi:10.1007/978-3-030-14366-4_7

Jaggupilli, A., and Elkord, E. (2012). Significance of CD44 and CD24 as Cancer Stem Cell Markers: an Enduring Ambiguity. *Clin. Dev. Immunol.* 2012, 708036. doi:10.1155/2012/708036

Jiang, T., Zhao, J., Yu, S., Mao, Z., Gao, C., Zhu, Y., et al. (2019). Untangling the Response of Bone Tumor Cells and Bone Forming Cells to Matrix Stiffness and Adhesion Ligand Density by Means of Hydrogels. *Biomaterials* 188, 130–143. doi:10.1016/j.biomaterials.2018.10.015

Kreso, A., and Dick, J. E. (2014). Evolution of the Cancer Stem Cell Model. *Cell Stem Cell* 14 (3), 275–291. doi:10.1016/j.stem.2014.02.006

Krishnamurthy, N., and Kurzrock, R. (2018). Targeting the Wnt/Beta-Catenin Pathway in Cancer: Update on Effectors and Inhibitors. *Cancer Treat. Rev.* 62, 50–60. doi:10.1016/j.ctrv.2017.11.002

Li, J., Liu, C. H., and Wang, F. S. (2010). Thymosin Alpha 1: Biological Activities, Applications and Genetic Engineering Production. *Peptides* 31 (11), 2151–2158. doi:10.1016/j.peptides.2010.07.026

Li, V. S., Ng, S. S., Boersema, P. J., Low, T. Y., Karthaus, W. R., Gerlach, J. P., et al. (2012). Wnt Signaling through Inhibition of β-catenin Degradation in an Intact Axin1 Complex. *Cell* 149 (6), 1245–1256. doi:10.1016/j.cell.2012.05.002

Liu, C., Li, Y., Semenov, M., Han, C., Baeg, G. H., Tan, Y., et al. (2002). Control of Beta-Catenin Phosphorylation/degradation by a Dual-Kinase Mechanism. *Cell* 108 (6), 837–847. doi:10.1016/s0092-8674(02)00685-2

Liu, A., Yu, X., and Liu, S. (2013). Pluripotency Transcription Factors and Cancer Stem Cells: Small Genes Make a Big Difference. *Chin. J. Cancer* 32 (9), 483–487. doi:10.5732/cjc.012.10282

Luo, M., Shang, L., Brooks, M. D., Jiagge, E., Zhu, Y., Buschhaus, J. M., et al. (2018). Targeting Breast Cancer Stem Cell State Equilibrium through Modulation of Redox Signaling. *Cell Metab.* 28 (1), 69–e6. doi:10.1016/j.cmet.2018.06.006

Lytle, N. K., Ferguson, L. P., Rajbhandari, N., Gilroy, K., Fox, R. G., Deshpande, A., et al. (2019). A Multiscale Map of the Stem Cell State in Pancreatic Adenocarcinoma. *Cell* 177 (3), 572–e22. doi:10.1016/j.cell.2019.03.010

Masuda, M., Uno, Y., Ohbayashi, N., Ohata, H., Mimata, A., Kukimoto-Niino, M., et al. (2016). TNIK Inhibition Abrogates Colorectal Cancer Stemness. *Nat. Commun.* 7, 12586. doi:10.1038/ncomms12586

Miller, K. D., Nogueira, L., Mariotto, A. B., Rowland, J. H., Yabroff, K. R., Alfano, C. M., et al. (2019). Cancer Treatment and Survivorship Statistics, 2019. *CA Cancer J. Clin.* 69 (1), 363–385. doi:10.3322/caac.2155110.3322/caac.21565

Ordóñez-Morán, P., Dafflon, C., Imajo, M., Nishida, E., and Huelsken, J. (2015). HOXA5 Counteracts Stem Cell Traits by Inhibiting Wnt Signaling in Colorectal Cancer. *Cancer Cell* 28 (6), 815–829. doi:10.1016/j.ccell.2015.11.001

Park, H. J., Park, J. B., Lee, S. J., and Song, M. (2017). Phellinus Linteus Grown on Germinated Brown Rice Increases Cetuximab Sensitivity of KRAS-Mutated Colon Cancer. *Int. J. Mol. Sci.* 18 (8), 1746. doi:10.3390/ijms18081746

Patruno, A., Tosco, P., Borretto, E., Franceschelli, S., Amerio, P., Pesce, M., et al. (2012). Thymopentin Down-Regulates Both Activity and Expression of iNOS in Blood Cells of Sézary Syndrome Patients. *Nitric Oxide* 27 (3), 143–149. doi:10.1016/j.niox.2012.06.002

Phi, L. T. H., Sari, I. N., Yang, Y. G., Lee, S. H., Jun, N., Kim, K. S., et al. (2018). Cancer Stem Cells (CSCs) in Drug Resistance and Their Therapeutic Implications in Cancer Treatment. *Stem Cell Int.* 2018, 5416923. doi:10.1155/2018/5416923

Polakis, P. (2007). The many Ways of Wnt in Cancer. *Curr. Opin. Genet. Dev.* 17 (1), 45–51. doi:10.1016/j.gde.2006.12.007

Prieto-Vila, M., Takahashi, R. U., Usuba, W., Kohama, I., and Ochiya, T. (2017). Drug Resistance Driven by Cancer Stem Cells and Their Niche. *Int. J. Mol. Sci.* 18 (12), 2574. doi:10.3390/ijms18122574

Rawla, P., Sunkara, T., and Barsouk, A. (2019). Epidemiology of Colorectal Cancer: Incidence, Mortality, Survival, and Risk Factors. *Prz Gastroenterol.* 14 (2), 89–103. doi:10.5114/pg.2018.81072

Regan, J. L., Schumacher, D., Staudte, S., Steffen, A., Haybaeck, J., Keilholz, U., et al. (2017). Non-Canonical Hedgehog Signaling Is a Positive Regulator of the WNT Pathway and Is Required for the Survival of Colon Cancer Stem Cells. *Cell Rep.* 21 (10), 2813–2828. doi:10.1016/j.celrep.2017.11.025

Roderick, H. L., and Cook, S. J. (2008). Ca2+ Signalling Checkpoints in Cancer: Remodelling Ca2+ for Cancer Cell Proliferation and Survival. *Nat. Rev. Cancer* 8 (5), 361–375. doi:10.1038/nrc2374

Sabisz, M., and Skladanowski, A. (2009). Cancer Stem Cells and Escape from Drug-Induced Premature Senescence in Human Lung Tumor Cells: Implications for Drug Resistance and *In Vitro* Drug Screening Models. *Cell Cycle* 8 (19), 3208–3217. doi:10.4161/cc.8.19.9758

Sahlberg, S. H., Spiegelberg, D., Glimelius, B., Stenerlöw, B., and Nestor, M. (2014). Evaluation of Cancer Stem Cell Markers CD133, CD44, CD24: Association with AKT Isoforms and Radiation Resistance in colon Cancer Cells. *PLoS One* 9 (4), e94621. doi:10.1371/journal.pone.0094621

Singh, V. K., Biswas, S., Mathur, K. B., Haq, W., Garg, S. K., and Agarwal, S. S. (1998). Thymopentin and Splenopentin as Immunomodulators. Current Status. *Immunol. Res.* 17 (3), 345–368. doi:10.1007/BF02786456

Terrié, E., Coronas, V., and Constantin, B. (2019). Role of the Calcium Toolkit in Cancer Stem Cells. *Cell Calcium* 80, 141–151. doi:10.1016/j.ceca.2019.05.001

Tirosh, I., Venteicher, A. S., Hebert, C., Escalante, L. E., Patel, A. P., Yizhak, K., et al. (2016). Single-cell RNA-Seq Supports a Developmental Hierarchy in Human Oligodendroglioma. *Nature* 539 (7628), 309–313. doi:10.1038/nature20123

Tominaga, K., Minato, H., Murayama, T., Sasahara, A., Nishimura, T., Kiyokawa, E., et al. (2019). Semaphorin Signaling via MICAL3 Induces Symmetric Cell Division to Expand Breast Cancer Stem-like Cells. *Proc. Natl. Acad. Sci. U S A.* 116 (2), 625–630. doi:10.1073/pnas.1806851116

Tosoni, D., Pambianco, S., Ekalle Soppo, B., Zecchini, S., Bertalot, G., Pruneri, G., et al. (2017). Pre-clinical Validation of a Selective Anti-cancer Stem Cell Therapy for Numb-Deficient Human Breast Cancers. *EMBO Mol. Med.* 9 (5), 655–671. doi:10.15252/emmm.201606940

Triana-Martínez, F., Loza, M. I., and Domínguez, E. (2020). Beyond Tumor Suppression: Senescence in Cancer Stemness and Tumor Dormancy. *Cells* 9 (2), 346. doi:10.3390/cells9020346

Valkenburg, K. C., Graveel, C. R., Zylstra-Diegel, C. R., Zhong, Z., and Williams, B. O. (2011). Wnt/β-catenin Signaling in Normal and Cancer Stem Cells. *Cancers (Basel)* 3 (2), 2050–2079. doi:10.3390/cancers3022050

Van der Jeught, K., Xu, H. C., Li, Y. J., Lu, X. B., and Ji, G. (2018). Drug Resistance and New Therapies in Colorectal Cancer. *World J. Gastroenterol.* 24 (34), 3834–3848. doi:10.3748/wjg.v24.i34.3834

Wang, X., Liu, Q., Hou, B., Zhang, W., Yan, M., Jia, H., et al. (2013). Concomitant Targeting of Multiple Key Transcription Factors Effectively Disrupts Cancer Stem Cells Enriched in Side Population of Human Pancreatic Cancer Cells. *PLoS One* 8 (9), e73942. doi:10.1371/journal.pone.0073942

Wang, J., Sun, L. F., Cui, W. W., Zhao, W. S., Ma, X. F., Li, B., et al. (2017). Intersubunit Physical Couplings Fostered by the Left Flipper Domain Facilitate Channel Opening of P2X4 Receptors. *J. Biol. Chem.* 292 (18), 7619–7635. doi:10.1074/jbc.M116.771121

Wolf, E., Milazzo, S., Boehm, K., Zwahlen, M., and Horneber, M. (2011). Thymic Peptides for Treatment of Cancer Patients. *Cochrane Database Syst. Rev.* 2011 (2), CD003993. doi:10.1002/14651858.CD003993.pub3

Xiaojing, C., Yanfang, L., Yanqing, G., and Fangfang, C. (2017). Thymopentin Improves Cardiac Function in Older Patients with Chronic Heart Failure. *Anatol J. Cardiol.* 17 (1), 24–30. doi:10.14744/AnatolJCardiol.2016.6692

Yang, L., Shi, P., Zhao, G., Xu, J., Peng, W., Zhang, J., et al. (2020). Targeting Cancer Stem Cell Pathways for Cancer Therapy. *Signal. Transduct Target. Ther.* 5 (1), 8. doi:10.1038/s41392-020-0110-5

Yang, T., Wang, P., Yin, X., Zhang, J., Huo, M., Gao, J., et al. (2021). The Histone Deacetylase Inhibitor PCI-24781 Impairs Calcium Influx and Inhibits Proliferation and Metastasis in Breast Cancer. *Theranostics* 11 (5), 2058–2076. doi:10.7150/thno.48314

Yu, W. K., Wang, Z., Fong, C. C., Liu, D., Yip, T. C., Au, S. K., et al. (2017). Chemoresistant Lung Cancer Stem Cells Display High DNA Repair Capability to Remove Cisplatin-Induced DNA Damage. *Br. J. Pharmacol.* 174 (4), 302–313. doi:10.1111/bph.13690

Zhang, L., Wei, X., Zhang, R., Petitte, J. N., Si, D., Li, Z., et al. (2019). Design and Development of a Novel Peptide for Treating Intestinal Inflammation. *Front. Immunol.* 10, 1841. doi:10.3389/fimmu.2019.01841

Zhao, J. (2016). Cancer Stem Cells and Chemoresistance: The Smartest Survives the Raid. *Pharmacol. Ther.* 160, 145–158. doi:10.1016/j.pharmthera.2016.02.008

Zhu, L., Gibson, P., Currle, D. S., Tong, Y., Richardson, R. J., Bayazitov, I. T., et al. (2009). Prominin 1 marks Intestinal Stem Cells that Are Susceptible to Neoplastic Transformation. *Nature* 457 (7229), 603–607. doi:10.1038/nature07589

Conflict of Interest: The authors declare that the research was conducted in the absence of any commercial or financial relationships that could be construed as a potential conflict of interest.

Publisher's Note: All claims expressed in this article are solely those of the authors and do not necessarily represent those of their affiliated organizations, or those of the publisher, the editors and the reviewers. Any product that may be evaluated in this article, or claim that may be made by its manufacturer, is not guaranteed or endorsed by the publisher.

frontiers in Pharmacology

ORIGINAL RESEARCH
published: 18 February 2022
doi: 10.3389/fphar.2022.835166

Reducing Acneiform Rash Induced by EGFR Inhibitors With Honeysuckle Therapy: A Prospective, Randomized, Controlled Study

Zhen Liu[1], Tian Tian[1], Binbin Wang[2], Demin Lu[3], Jian Ruan[1] and Jianzhen Shan[1]**

[1]Department of Medical Oncology, the First Affiliated Hospital, Zhejiang University School of Medicine, Hangzhou, China, [2]Department of Medical Oncology, Zhejiang Hospital of Traditional Chinese Medicine, Hangzhou, China, [3]Department of Medical Oncology, the Second Affiliated Hospital, Zhejiang University School of Medicine, Hangzhou, China

Background: Epidermal growth factor receptor inhibitors (EGFRIs), including cetuximab, erlotinib, gefitinib and icotinib, have been proven to be effective in treating colorectal cancer or lung cancer. However, most of patients who receive EGFRIs treatment experience cutaneous toxicities, such as acneiform or papulopustular rashes, which affects quality of life and leads to discontinuation of cancer therapies. Honeysuckle is a traditional herb historically used to treat skin rash for thousands of years in Eastern Asia and showed proven safety in human.

Methods: To investigate whether honeysuckle therapy could control EGFRIs induced acneiform rashes, a total of 139 colorectal and lung cancer patients with EGFRIs treatments were recruited in a prospective study. Patients were randomized to 3 arms (Arm A: prophylactic treatment with honeysuckle before rash occurred; Arm B: symptomatic treatment with honeysuckle when rash occurred; Arm C: conventional treatment with minocycline and a topical solution when rash occurred). The incidences, severities and recovery time of acneiform rash were observed in each arm.

Results: Honeysuckle treatment reduced incidences of EGFRIs induced acneiform rash, which were 56.5, 68.1 and 71.7% in Arm A, B and C, respectively ($p = 0.280$). Severities of rash (CTCAE grade 2 and 3) were significantly lower in prophylactic honeysuckle treatment (Arm A) compared to conventional treatment (Arm C) ($p = 0.027$), which was 10–21%, respectively. Patients with honeysuckle treatment recovered more quickly from pruritus, the median time was 22, 36 and 58 days in Arm A, B and C, respectively ($p = 0.016$).

Conclusion: Honeysuckle was effective in reducing incidences and severities of EGFRIs induced acneiform rash, especially for prophylactic treatment.

Keywords: honeysuckle, acneiform rash, EGFR inhibitors, colorectal cancer, NSCLC

Edited by:
Devesh Tewari,
Lovely Professional University, India

Reviewed by:
Weiqiang Lu,
East China Normal University, China
Gabriella Fabbrocini,
University of Naples Federico II, Italy

****Correspondence:***
Jianzhen Shan
shanjz@zju.edu.cn
Jian Ruan
software233@zju.edu.cn

Specialty section:
This article was submitted to Pharmacology of Anti-Cancer Drugs, a section of the journal Frontiers in Pharmacology

Received: *14 December 2021*
Accepted: *27 January 2022*
Published: *18 February 2022*

Citation:
Liu Z, Tian T, Wang B, Lu D, Ruan J and Shan J (2022) Reducing Acneiform Rash Induced by EGFR Inhibitors With Honeysuckle Therapy: A Prospective, Randomized, Controlled Study. Front. Pharmacol. 13:835166. doi: 10.3389/fphar.2022.835166

INTRODUCTION

Epidermal growth factor receptor (EGFR) targeted therapies, including the monoclonal antibodies (mAbs) cetuximab and panitumumab, and the EGFR tyrosine kinase inhibitors (TKIs) erlotinib, gefitinib and lapatinib have been proved to be effective in a range of tumors, such as colorectal cancer (CRC), non-small cell lung cancer (NSCLC) and breast cancer (Xu et al., 2017). Theses EGFR

inhibitors (EGFRIs) showed generally low hematological, gastrointestinal side-effects and hair loss compared with cytotoxic agents. However, the cutaneous toxicities, presented by itching, redness, swelling or pain, are more common during EGFRIs treatment, which occurs in 65–90% of patients (Fabbrocini et al., 2015).

Both classes of EGFRIs may induce cutaneous adverse events. The skin toxicities affect both patient quality of life (QoL) and treatment compliance. The severe adverse effects can also predispose the skin to bacterial, fungal, or viral infections, which leads to a discontinuation of the antineoplastic therapy (Braden and Anadkat, 2016).

The most common cutaneous side effect is acneiform rash (follicular papulopustular), which eruptions on the face, scalp, chest, and upper back. It is a dose-dependent skin toxicity, and usually develops in the first 1–2 weeks, peaks at 3–4 weeks on therapy, but can often persist over several months (Fabbrocini et al., 2015). Although a large number of patients receiving EGFRIs experience acneiform, few controlled studies have been conducted to determine the best practices for its management.

Honeysuckle (*Lonicera japonica Thunb*), a classical herb that has been utilized in China, Korea, Japan and other East-Asian countries for treating skin rash and influenza for thousands of years (Shang et al., 2011; He et al., 2013). It is used in traditional medicine owing to its pharmacological properties including anti-oxidation (Leung et al., 2006), anti-inflammation (Kang et al., 2010; Chen et al., 2012), anti-cancer (Leung et al., 2008; Liao et al., 2013), as well as anti-bacteria and anti-virus (Zhou et al., 2015; Lee et al., 2017). The aqueous extract of honeysuckle (chrysanthemum tea) can relieve fever and flu-like symptoms (Shang et al., 2011). Therefore, we designed this prospective, randomized, controlled clinical trial, aimed to investigated whether honeysuckle could reduce the incidence and severity of acneiform induced by EGFRIs. The data presented herein would provide a novel, easily conducted and affordable approach to treat EGFRIs induced skin toxicities.

MATERIALS AND METHODS

Study Design and Treatments

The clinical trial was designed as a prospective, open-label, randomized, multicenter study and performed synchronously in the First Affiliated Hospital of Zhejiang University, the Second Affiliated Hospital of Zhejiang University and Zhejiang Hospital of Traditional Chinese Medicine from June 2017 to December 2020. To evaluated the efficacy of honeysuckle on EGFRIs induced acneiform, patients were randomized to 3 arms: prophylactic treatment (Arm A), symptomatic treatment (Arm B) and conventional treatment (Arm C) in a 1:1:1 ratio.

Arm A: Prophylactic treatment. Once EGFRIs therapy started, patients received the prophylactic treatment with decocted honeysuckle (10 g honeysuckle in 200 ml soup) orally twice daily. In case grade ≥1 acneiform rash occurred, external application of decocted honeysuckle was given in addition to oral treatment. For external application, 50 g honeysuckle was decocted in 1,000 ml water on soft fire for 10 min. Three or four-layer gauze was soaked in decocted honeysuckle that was cooled to 38°C. The gauze was then gently squeezed and was spread on the skin where rashes were located for 15 min, three times daily, until rashes recovered.

Arm B: Symptomatic treatment. When grade ≥1 acneiform rash occurred, patients started to be treated with decocted honeysuckle both orally twice daily and externally three times daily as described in Arm A.

Arm C: Conventional treatment. Patients in this group received only conventional treatment, that is minocycline at 100 mg per day, combined with a topical solution containing 2% clindamycin and 1% hydrocortisone, twice daily when grade ≥1 acneiform rash occurred.

The scale used for evaluating acneiform rash was the National Cancer Institute Common Terminology Criteria for Adverse Events (NCI-CTCAE) grading scale, version 4.03.

Patients

Adult patients (age ≥18 years) with pathological diagnosis of metastatic NSCLC harboring activating EGFR driver mutations (treated with erlotinib, gefitinib or icotinib) and patients of metastatic colorectal cancer (CRC) with wild-type RAS gene (treated with cetuximab) were enrolled. The Eastern Cooperative Oncology Group (ECOG) performance status had to be 0 to 3. Adequate organ functions and an estimated life expectancy of more than 12 weeks were required. Patients with short-term usage of EGFRIs (less than 3 months) and concurrent skin diseases were excluded for analyses.

Outcome Measures

The primary outcome measure was the incidences of EGFRIs-related acneiform rash among 3 arms. The secondary outcome measures included the duration from onset of grade ≥2 acneiform rashes relieved to grade 1 or 0 and the safety of honeysuckle treatment.

Patients were evaluated every 2–3 weeks, and were followed up for at least 6 months after EGFRI therapies. Adverse effects (AEs) were graded according to the NCI-CTCAE scale.

EGFRI Therapy

Patients with CRC were treated with cetuximab at an initial dose of 400 mg/m^2, then 250 mg/m^2 per week subsequently. Patients with NSCLC harboring activating EGFR driver mutations were treated with erlotinib 150 mg po QD, gefitinib 250 mg po QD or icotinib 125 mg po TID according to National Comprehensive Cancer Network (NCCN) or Chinese Society of Clinical Oncology (CSCO) guidelines.

If grade ≥3 acneiform rashes occurred, EGFRI therapies were discontinued until the rashes reduced to grade ≤1.

Statistical Analysis

Continuous data were presented as medians and ranges, whose differences were analyzed by using one-way ANOVA. Discrete data were presented as frequency or percentage, whose differences were evaluated using Fisher's exact test or Pearsons' chi-squared test. Calculation was performed by SPSS (version 21.0, IBM Corp). $p < 0.05$ was considered statistically significant.

TABLE 1 | Demographic characteristics and baseline clinical parameters of the participants.

	Arm A (n = 46)	Arm B (n = 47)	Arm C (n = 46)	*p* Value
Age, years	53.2 ± 21.1	49.5 ± 20.5	54.7 ± 19.9	0.641
Gender (male), %	58.7%	59.5%	56.5%	0.538
Disease, n				0.739
CRC	14	11	11	
NSCLC	35	34	34	
EGFRI, n				0.821
Cetuximab	14	11	11	
Erlotinib	11	10	10	
Gefitinib	12	10	10	
Icotinib	12	14	14	
ECOG PS, n				0.742
0	14	12	13	
1	20	24	23	
2	9	9	6	
3(NSCLC)	3	1	3	

Ethics

The study conformed to the principles of good clinical practice guidelines (GCP). All patients provided written informed consents. The study protocol was approved by the Ethics Committee of the Second Affiliated Hospital of Zhejiang University with protocol #2016-IIT-111.

RESULTS

Patient Characteristics

In total, 182 patients met the inclusion criteria and were recruited. 43 patients were excluding due to short-term usage of EGFRIs (less than 3 months), 139 patients were finally analyzed, with 46 or 47 patients in each arm. Demographic characteristics such as age, gender and diseases were balanced among 3 arms (**Table 1**).

Incidence of Acneiform Rash

The overall incidences of acneiform rash were 56.5, 68.1 and 71.7% in Arm A, B and C, respectively (**Table 2**). No grade 4 or 5 AEs occurred. Prophylactic treatment (Arm A) had the lowest overall incidence of acneiform rash, although no significant statistically differences were observed among 3 groups ($p = 0.280$). Particularly, CTCAE grade 2 and 3 rashes were significantly lower in prophylactic honeysuckle treatment (Arm A) compared to conventional treatment (Arm C) ($p = 0.027$), which was 10–21%, respectively. The incidences of acneiform rashes among different EGFRIs varied (**Table 3**). As shown in **Table 2**, the incidence of grade 2 and 3 in Arm A was 21.7%, much lower than Arm B (38.3%) and Arm C (45.6%), indicating that prophylactic treatment of honeysuckle could reduce grade 2 and 3 rashes in all drug groups.

Pruritus is a frequent symptom caused by acneiform rash, which usually leads to quality of life deteriorated. Patients with prophylactic treatment of honeysuckle (Arm A) experienced delayed onset of pruritus, the median time were 18, 16, and 14 days after initiation of EGFRI therapies in Arm A, B and C, respectively (**Table 4**). Patients with honeysuckle treatment also recovered more quickly, which were 22, 36 and 58 days after onset of pruritus in Arm A, B and C, respectively ($p = 0.016$).

Notably, 8 patients in Arm A, 5 patients in Arm B and 4 patients in Arm C experienced complete recovery of acneiform rashes (**Figure 1**).

TABLE 2 | Incidence of acneiform rashes in each group.

	Arm A (n = 46)	Arm B (n = 47)	Arm C (n = 46)	*p* Value
Overall incidence, n (%)	26 (56.5)	32 (68.1)	33 (71.7)	0.280
Grade, n (%)				0.151
0	21 (43.5)	14 (29.8)	13 (28.3)	
1	15 (32.6)	15 (36.2)	12 (26.1)	
2	8 (17.4)	16 (34.0)	14 (30.4)	
3	2 (4.3)	2 (4.3)	7 (15.2)	

Safety

1 patient in Arm A and 2 patients in Arm B developed CTCAE grade 1 gastrointestinal discomfort after taking decocted honeysuckle orally. No other honeysuckle relevant AEs were found. Honeysuckle also did not increase EGFRIs related AEs.

DISCUSSION

EGFRIs have been proven to be effective in various types of solid tumors. In colorectal cancer, cetuximab, an IgG1 chimeric monoclonal antibody against EGFR, was associated with a significant improvement in overall survival (OS, hazard ratio [HR] for death, 0.77; 95% confidence interval [CI], 0.64 to 0.92; $p = 0.005$) and in progression-free survival (PFS, HR, 0.68; 95% CI, 0.57 to 0.80; $p < 0.001$) (Jonker et al., 2007). In NSCLC patients, EGFR tyrosine kinase inhibitors (TKIs) erlotinib, gefitinib and icotinib prolonged PFS significantly compared with chemotherapy (Pan et al., 2014; Batson et al., 2017). However, EGFRIs induced acneiform rash occurs in 65–90% of patients (Fabbrocini et al., 2015), and persistent pruritus is debilitating and severely affects quality of life, sometimes leads to a discontinuation of cancer therapy.

Honeysuckle is a classical herb that has been widely utilized with proven safety for treating skin rash and influenza for thousands of years in Eastern Asia. The aqueous extract of honeysuckle (chrysanthemum tea) is easily prepared. Besides low toxicity and extensive accessibility, the prices of herbal medicines are usually affordable. More importantly, the therapeutic effects of honeysuckle on acneiform rash were much better than conventional treatment, as we demonstrated in this study.

Acneiform rashes usually develop in the first 1–2 weeks after EGFRI therapy. In this study, we found that prophylactic treatment with honeysuckle showed promising efficacy in reducing the incidence and severity of EGFRIs induced acneiform rash. Therefore, prophylactic treatments are crucial, and appropriate medication should be considered throughout the whole course of EGFRI therapy aiming to minimize skin toxicities.

The mechanism of honeysuckle in reducing acneiform rashes is not clear. EGFR is expressed in the basal layer of the *epidermis*, which plays a crucial role in several cell activities, such as barrier function,

TABLE 3 | Incidences and gradings of acneiform rashes with different EGFRIs treatment.

	Cetuximab (n = 36)	Erlotinib (n = 31)	Gefitinib (n = 32)	Icotinib (n = 40)	*p* Value
Overall incidence, n (%)	27 (75.0)	23 (74.2)	20 (62.5)	20 (50.0)	0.080
Grade, n (%)	17 (47.2)	16 (51.6)	24 (75.0)	34 (85.0)	0.003
0/1					
2	13 (36.1)	11 (35.5)	7 (21.9)	6 (15.0)	
3	6 (16.7)	4 (12.9)	1 (3.1)	0 (0.0)	

TABLE 4 | Incidence and grading of acneiform rash with pruritus.

	No. of cases	Onset, median (day)	From onset until resolution, median (day)
Arm A (n = 46)	10	18	22*
Arm B (n = 47)	11	16	36
Arm C (n = 46)	13	14	58

*p = *0.016 (Arm A vs Arm C).*

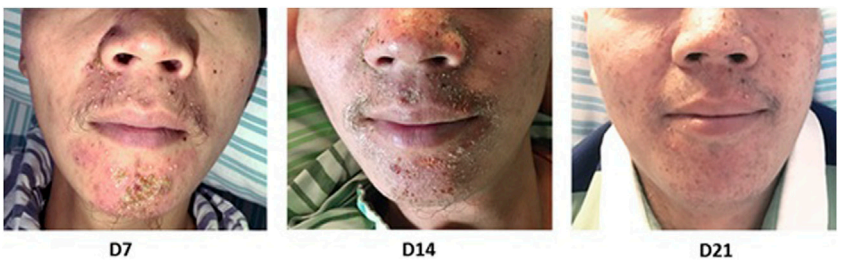

FIGURE 1 | A representative patient in Arm B who recovered from grade 2 acneiform rash by honeysuckle treatment for 3 weeks.

inflammation and innate host defense (Lichtenberger et al., 2013). Obviously, EGFRIs inhibit both EGFR overexpressed in tumor cells and the one expressed in normal cells of the *epidermis*. EGFR inhibition induces the expression of chemokines that enhance skin inflammation through leukocyte recruitment, vascular dilation, and edema (Segaert and Van Cutsem, 2005; Lacouture, 2006). Feng *et al.* reported that cynaroside was the primary flavonoid component of honeysuckle, which alleviated serum levels of inflammatory factors including IL-1β and TNF-α, and suppressed the biomarker of pro-inflammatory macrophage M1 phenotype (iNOS+) and promotes the anti-inflammatory M2 polarization (CD206+) *in vivo* (Feng et al., 2021). Liu and his colleagues demonstrated that honeysuckle derived miR2911 down-regulated TGF-β1 promoted T lymphocytes infiltration (Liu et al., 2021). Totally, it is presumed that honeysuckle may exert the protective effects of acneiform rash mainly through its active ingredients of chlorogenic acid compounds, including chlorogenic acid and isochlorogenic acid.

However, due to the limited number of patients and short follow-up time, our understanding of honeysuckle is still limited. 139 patients were randomized to 4 EGFRIs treatment groups, 30–40 patients per each group. The analysis did not report influences of honeysuckle in terms of PFS and OS of patients. The detailed molecular mechanisms of honeysuckle also need further investigation.

CONCLUSION

In summary, this prospective, randomized, controlled study suggested that honeysuckle is a promising treatment to reduce the incidences and severities of EGFRI-related acneiform rashes. Due to its low toxicity, extensive accessibility and affordable price, prophylactic treatment with honeysuckle is recommended for patients with EGFRIs therapies.

DATA AVAILABILITY STATEMENT

The original contributions presented in the study are included in the article/supplementary material, further inquiries can be directed to the corresponding author.

ETHICS STATEMENT

The studies involving human participants were reviewed and approved by the First Affiliated Hospital, Zhejiang University School of Medicine, the Second Affiliated Hospital, Zhejiang University School of Medicine and Zhejiang Hospital of Traditional Chinese Medicine. The patients/participants provided their written informed consent to participate in this study.

AUTHOR CONTRIBUTIONS

The study is conceived and designed by JS and BW and is performed by JS, BW, DL, and ZL. The data is analyzed by JS, TT, and JR. The manuscript is written by ZL, TT, and JS. All authors have read and approved the final manuscript.

FUNDING

This work is supported by grants from the National Natural Science Foundation of China (81602635), Zhejiang Provincial Natural Science Foundation (LY21H160042) and Zhejiang Medical and Health Project (2017205840, 2018274816, 2019334185).

REFERENCES

Batson, S., Mitchell, S. A., Windisch, R., Damonte, E., Munk, V. C., and Reguart, N. (2017). Tyrosine Kinase Inhibitor Combination Therapy in First-Line Treatment of Non-small-cell Lung Cancer: Systematic Review and Network Meta-Analysis. *Onco Targets Ther.* 10, 2473–2482. doi:10.2147/OTT.S134382

Braden, R. L., and Anadkat, M. J. (2016). EGFR Inhibitor-Induced Skin Reactions: Differentiating Acneiform Rash from Superimposed Bacterial Infections. *Support Care Cancer* 24 (9), 3943–3950. doi:10.1007/s00520-016-3231-1

Chen, W. C., Liou, S. S., Tzeng, T. F., Lee, S. L., and Liu, I. M. (2012). Wound Repair and Anti-inflammatory Potential of *Lonicera japonica* in Excision Wound-Induced Rats. *BMC Complement. Altern. Med.* 12, 226. doi:10.1186/1472-6882-12-226

Fabbrocini, G., Panariello, L., Caro, G., and Cacciapuoti, S. (2015). Acneiform Rash Induced by EGFR Inhibitors: Review of the Literature and New Insights. *Skin Appendage Disord.* 1 (1), 31–37. doi:10.1159/000371821

Feng, J., Liu, Z., Chen, H., Zhang, M., Ma, X., Han, Q., et al. (2021). Protective Effect of Cynaroside on Sepsis-Induced Multiple Organ Injury through Nrf2/HO-1-dependent Macrophage Polarization. *Eur. J. Pharmacol.* 911, 174522. doi:10.1016/j.ejphar.2021.174522

He, L., Xu, X., Li, Y., Li, C., Zhu, Y., Yan, H., et al. (2013). Transcriptome Analysis of Buds and Leaves Using 454 Pyrosequencing to Discover Genes Associated with the Biosynthesis of Active Ingredients in *Lonicera japonica* Thunb. *PLoS One* 8 (4), e62922. doi:10.1371/journal.pone.0062922

Jonker, D. J., O'Callaghan, C. J., Karapetis, C. S., Zalcberg, J. R., Tu, D., Au, H. J., et al. (2007). Cetuximab for the Treatment of Colorectal Cancer. *N. Engl. J. Med.* 357 (20), 2040–2048. doi:10.1056/NEJMoa071834

Kang, O. H., Choi, J. G., Lee, J. H., and Kwon, D. Y. (2010). Luteolin Isolated from the Flowers of *Lonicera japonica* Suppresses Inflammatory Mediator Release by Blocking NF-kappaB and MAPKs Activation Pathways in HMC-1 Cells. *Molecules* 15 (1), 385–398. doi:10.3390/molecules15010385

Lacouture, M. E. (2006). Mechanisms of Cutaneous Toxicities to EGFR Inhibitors. *Nat. Rev. Cancer* 6 (10), 803–812. doi:10.1038/nrc1970

Lee, Y. R., Yeh, S. F., Ruan, X. M., Zhang, H., Hsu, S. D., Huang, H. D., et al. (2017). Honeysuckle Aqueous Extract and Induced Let-7a Suppress Dengue Virus Type 2 Replication and Pathogenesis. *J. Ethnopharmacol* 198, 109–121. doi:10.1016/j.jep.2016.12.049

Leung, H. W., Hour, M. J., Chang, W. T., Wu, Y. C., Lai, M. Y., Wang, M. Y., et al. (2008). P38-associated Pathway Involvement in Apoptosis Induced by Photodynamic Therapy with *Lonicera japonica* in Human Lung Squamous Carcinoma CH27 Cells. *Food Chem. Toxicol.* 46 (11), 3389–3400. doi:10.1016/j.fct.2008.08.022

Leung, H. W., Kuo, C. L., Yang, W. H., Lin, C. H., and Lee, H. Z. (2006). Antioxidant Enzymes Activity Involvement in Luteolin-Induced Human Lung Squamous Carcinoma CH27 Cell Apoptosis. *Eur. J. Pharmacol.* 534 (1-3), 12–18. doi:10.1016/j.ejphar.2006.01.021

Liao, J. C., Chang, W. T., Lan, Y. H., Hour, M. J., and Lee, H. Z. (2013). Application of Proteomics to Identify the Target Molecules Involved in Lonicera Japonica-Induced Photokilling in Human Lung Cancer CH27 Cells. *BMC Complement. Altern. Med.* 13, 244. doi:10.1186/1472-6882-13-244

Lichtenberger, B. M., Gerber, P. A., Holcmann, M., Buhren, B. A., Amberg, N., Smolle, V., et al. (2013). Epidermal EGFR Controls Cutaneous Host Defense and Prevents Inflammation. *Sci. Transl Med.* 5 (199), 199ra111. doi:10.1126/scitranslmed.3005886

Liu, C., Xu, M., Yan, L., Wang, Y., Zhou, Z., Wang, S., et al. (2021). Honeysuckle-derived microRNA2911 Inhibits Tumor Growth by Targeting TGF-B1. *Chin. Med.* 16 (1), 49. doi:10.1186/s13020-021-00453-y

Pan, H., Liu, R., Li, S., Fang, H., Wang, Z., Huang, S., et al. (2014). Effects of Icotinib on Advanced Non-small Cell Lung Cancer with Different EGFR Phenotypes. *Cell Biochem Biophys* 70 (1), 553–558. doi:10.1007/s12013-014-9955-y

Segaert, S., and Van Cutsem, E. (2005). Clinical Signs, Pathophysiology and Management of Skin Toxicity during Therapy with Epidermal Growth Factor Receptor Inhibitors. *Ann. Oncol.* 16 (9), 1425–1433. doi:10.1093/annonc/mdi279

Shang, X., Pan, H., Li, M., Miao, X., and Ding, H. (2011). *Lonicera japonica* Thunb.: Ethnopharmacology, Phytochemistry and Pharmacology of an Important Traditional Chinese Medicine. *J. Ethnopharmacol* 138 (1), 1–21. doi:10.1016/j.jep.2011.08.016

Xu, M. J., Johnson, D. E., and Grandis, J. R. (2017). EGFR-targeted Therapies in the post-genomic Era. *Cancer Metastasis Rev.* 36 (3), 463–473. doi:10.1007/s10555-017-9687-8

Zhou, Z., Li, X., Liu, J., Dong, L., Chen, Q., Liu, J., et al. (2015). Honeysuckle-encoded Atypical microRNA2911 Directly Targets Influenza A Viruses. *Cell Res* 25 (1), 39–49. doi:10.1038/cr.2014.130

Conflict of Interest: The authors declare that the research was conducted in the absence of any commercial or financial relationships that could be construed as a potential conflict of interest.

Publisher's Note: All claims expressed in this article are solely those of the authors and do not necessarily represent those of their affiliated organizations, or those of the publisher, the editors and the reviewers. Any product that may be evaluated in this article, or claim that may be made by its manufacturer, is not guaranteed or endorsed by the publisher.

frontiers in Pharmacology

ORIGINAL RESEARCH
published: 22 February 2022
doi: 10.3389/fphar.2022.837503

Integrating Gemcitabine-Based Therapy With AdipoRon Enhances Growth Inhibition in Human PDAC Cell Lines

Angela Ragone, Alessia Salzillo, Annamaria Spina, Silvio Naviglio and Luigi Sapio*

Department of Precision Medicine, University of Campania "Luigi Vanvitelli", Naples, Italy

Pancreatic ductal adenocarcinoma (PDAC) accounts for 90% of all pancreatic cancers. Albeit its incidence does not score among the highest in cancer, PDAC prognosis is tremendously fatal. As a result of either aggressiveness or metastatic stage at diagnosis, chemotherapy constitutes the only marginally effective therapeutic approach. As gemcitabine (Gem) is still the cornerstone for PDAC management, the low response rate and the onset of resistant mechanisms claim for additional therapeutic strategies. The first synthetic orally active adiponectin receptor agonist AdipoRon (AdipoR) has recently been proposed as an anticancer agent in several tumors, including PDAC. To further address the AdipoR therapeutic potential, herein we investigated its pharmacodynamic interaction with Gem in human PDAC cell lines. Surprisingly, their simultaneous administration revealed a more effective action in contrasting PDAC cell growth and limiting clonogenic potential than single ones. Moreover, the combination AdipoR plus Gem persisted in being effective even in Gem-resistant MIA PaCa-2 cells. While a different ability in braking cell cycle progression between AdipoR and Gem supported their cooperating features in PDAC, mechanistically, PD98059-mediated p44/42 MAPK ablation hindered combination effectiveness. Taken together, our findings propose AdipoR as a suitable partner in Gem-based therapy and recognize the p44/42 MAPK pathway as potentially involved in combination outcomes.

Keywords: PDAC, AdipoRon, gemcitabine, cell cycle, P44/42 MAPK, drug resistance

OPEN ACCESS

Edited by:
Devesh Tewari,
Lovely Professional University, India

Reviewed by:
Michael VanSaun,
University of Kansas Medical Center, United States
Elisa Lozano,
University of Salamanca, Spain

****Correspondence:***
Silvio Naviglio
silvio.naviglio@unicampania.it

Specialty section:
This article was submitted to Pharmacology of Anti-Cancer Drugs, a section of the journal Frontiers in Pharmacology

Received: *16 December 2021*
Accepted: *26 January 2022*
Published: *22 February 2022*

Citation:
Ragone A, Salzillo A, Spina A, Naviglio S and Sapio L (2022) Integrating Gemcitabine-Based Therapy With AdipoRon Enhances Growth Inhibition in Human PDAC Cell Lines. Front. Pharmacol. 13:837503. doi: 10.3389/fphar.2022.837503

INTRODUCTION

According to Global Cancer Statistics 2020, pancreatic cancer (PC) ranks the seventh leading cause of cancer death worldwide, with an estimated 466,003 deaths against 495,773 new cases (Collisson et al., 2019; Sung et al., 2021). Although its incidence rate and the number of casualties do not reach the top score of cancers, PC is currently considered one of the most aggressive malignancies due to a rapidly progressive and fatal prognosis (Carioli et al., 2021).

Arising from either ductal or acinar cells of the exocrine portion, pancreatic ductal adenocarcinoma (PDAC) accounts for 90% of all pancreatic cancers, while the remainder chiefly evolves from Langerhans islets (Gao et al., 2020). While this latter subtype is typically linked to an abnormal hormone secretion even at the early stage, facilitating its detection and diagnosis, PDAC is almost a symptom-free disease until metastases, or rather when the advanced stage leaves no longer chances of recovery (Mpilla et al., 2020).

In addition to the histological characterization, molecular subtyping is essentially guiding preclinical and clinical therapeutic strategies and treatment in malignancies, including leukemia and breast and colorectal cancers (Esposito et al., 2015; Verret et al., 2020; Singh et al., 2021; Tewari et al., 2021). Collecting the existing molecular data, a similar subgroup grading has recently been made even in PDAC (Collisson et al., 2019). Albeit quite promising, this therapeutic approach has not been fully translated in clinical yet; thus, chemotherapy still remains the best option for curing PDAC patients (Qian et al., 2020). Indeed, considering the advanced and metastasized stages at diagnosis, the surgical resection rate remains very low in PDAC (Huang et al., 2019).

Two distinct chemotherapeutic regimens currently recognize the first-line approach in progressive PDAC, namely, FOLFIRINOX (folinic acid, 5-fluorouracil, irinotecan, oxaliplatin) and gemcitabine (Gem) plus nab-paclitaxel (Riedl et al., 2021). Although FOLFIRINOX provides significant results in improving both overall and median progression-free survival, its toxicity drastically restricts administration for patients with good performance status (Damm et al., 2021). Therefore, either alone or in combination, Gem remains the standard of care for advanced PDAC, as well as neoadjuvant therapy (Oba et al., 2020). Regrettably, the limited toxicity and the extensive usage of Gem usually conflict with a very low response rate and resistant mechanism acquisition (Amrutkar and Gladhaug, 2017; Fu et al., 2021).

Despite the huge efforts made to improve prevention and treatment over the years, only weak signs of progress have been obtained in PDAC, where prognosis still remains extremely poor with a less than 10% 5-year survival rate (Collisson et al., 2019). Moreover, recent perspective reports indicate a harsh increase in both incidence and mortality rates in the next two decades, making PDAC the primary cause of cancer-related death in the near future (Christenson et al., 2020). Therefore, identifying novel therapeutic approaches is absolutely mandatory in an attempt to counteract the PDAC ascent.

An increasing number of studies have provided consistent evidence supporting the potential anticancer role of AdipoRon (AdipoR) in several preclinical cancer models, including myeloma and breast, prostate, and ovarian cancers (Nigro et al., 2021). More recently, we also described how AdipoR can energetically inhibit cell proliferation in osteosarcoma cells (Sapio et al., 2020). As a synthetic orally active adiponectin receptor agonist, AdipoR exerts comparable pharmacological properties to those of its template, such as anti-obesity, antidiabetic, and anti-ischemic features (Nigro et al., 2021). Antineoplastic effects have been reported even in PDAC where, delaying cell cycle progression in the G0/G1 phase, AdipoR induces both *in vitro* and *in vivo* growth arrest (Messaggio et al., 2017; Akimoto et al., 2018). The assessment of the AdipoR-mediated mechanisms has revealed the involvement of AMPK dependent and independent pathways in PDAC. Precisely, beyond the canonical activation of AMPK and its related downstream target acetyl-CoA carboxylase (ACC), AdipoR has been described to module pathways as signal transducer and activator of transcription 3 (STAT3), protein kinase B (PKB), extracellular signal-regulated kinase 1/2 (ERK1/2), and p38 (Messaggio et al., 2017; Akimoto et al., 2018).

Taking the outlined state of art into account, the present study has been conceived to further explore the AdipoR relevance in PDAC therapy. Specifically, since no data currently provide information on the AdipoR plus Gem combination outcome, herein we addressed potential cooperating effects between these two compounds in PDAC. Using MIA PaCa-2 and PANC-1 as human PDAC cell lines, combinatory and single drug effectiveness was evaluated by multiple methodological approaches. Starting from the biological results, estimated by cell growth and colony forming assays, we characterized the cell phase distribution and initially investigated the molecular mechanisms underlying single and combination stimulations. Finally, combination and AdipoR usefulness were further explored in MIA PaCa-2 Gem-resistant cells.

MATERIALS AND METHODS

Cell Culture Maintenance and Drug Treatments

MIA PaCa-2 and PANC-1 human PDAC cell lines were purchased by the American Type Culture Collection (ATCC) and maintained at 37°C in a 5% CO_2 humidified atmosphere, using Dulbecco's Minimum Essential Medium (DMEM) (ECM0728L; Euroclone) supplemented with 10% fetal bovine serum (FBS) (ECS0180L; Euroclone) and 1% penicillin/streptomycin (ECB3001D; Euroclone) as culture medium. Typically, cells were equally seeded and kept under standard growing conditions for 24 h. The following day, AdipoR and Gem were supplemented to fresh media, either individually or in combination, and PDAC cells were incubated for times and concentrations provided in each experimental condition. Ultimately, adherent cells were trypsinized and collected with potential floating ones, before being centrifuged for 5 min at 1,500 RPM. Since AdipoRon and gemcitabine were dissolved in DMSO and H_2O, respectively, an equal solvent rate (% v/v) was used as a negative control.

Chemical Reagents and Antibodies

Chemicals: AdipoRon (#SML0998; Sigma-Aldrich), gemcitabine (#G6423, Sigma-Aldrich), trypan blue (#T8154; Sigma-Aldrich), propidium iodide (#P4864; Sigma-Aldrich), crystal violet (#C0775; Sigma-Aldrich), PD98059 (#P215; Sigma-Aldrich), dimethyl sulfoxide (DMSO) (A3672; AppliChem), and ethanol absolute anhydrous (308603; Carlo Erba). Antibodies: α-Tubulin (#3873; Cell Signaling Technology), cyclin E1 (#4129; Cell Signaling Technology), p44/42 MAPK (#9102; Cell Signaling Technology), phospho-p44/42 MAPK (#9101; Cell Signaling Technology), cyclin A1 (sc-751; Santa Cruz Biotechnology), vinculin (sc-73614; Santa Cruz Biotechnology), and $p27^{KIP1}$ (ab3203; Abcam).

Assessment of Drug-Mediated Effects on Living and Death Cells

A total number of 8×10^4 MIA PaCa-2 and 1×10^5 PANC-1 cells were moved in 6-well plates and kept in a standard growing state

for 24 h. AdipoR and Gem, either alone or in combination, were subsequently added to new media and allowed to act in PDAC cells. For each experiment, times and concentrations are indicated in the Results section and Figure legends. Usually, pelleted cells were resuspended in 1.5 ml DMEM and diluted 1:1 with trypan blue, which, crossing damaged membrane, discriminates living from dead cells. Specifically, 10 µl of both media containing cells and blue dye (0.4%, v/v) were mixed, and the relative cell content was established using a Bürker chamber, where the number of unstained (living) and stained (dead) cells was recorded. Each point has been counted at least twice in each experimental procedure.

Flow Cytometry Analysis

Cytometric analysis was performed to define the respective cell phase distribution in reaction to different stimuli. A procedure similar to that described in point 2.3 was applied to seed, treat, and collect PDAC cells. Subsequently, pelleted samples were resuspended first in 300 µl PBS (ECB4004lL; Euroclone) and then in 700 µl ice-cold absolute ethanol. Fixed cells were stored at −20°C until analysis. Before investigation, the samples were spun down for 5 min at 1,500 RPM and incubated with PI staining solution containing 15 µg/ml PI and 20 µg RNase A (R5503; Sigma-Aldrich) in PBS for 10 min at room temperature in the dark side. For each experimental condition, at least 20,000 events were acquired and analyzed by FACS-Celesta (BD Biosciences).

Colony Forming Assay

PDAC cells were seeded in 6-well plates at a density of 1.5×10^3 per well (MIA PaCa-2 and MIA PaCa-2 RES) or 2×10^3 (PANC-1) and exposed to different times and concentrations of AdipoR, Gem, and combination (see Results for more details). At the established endpoint, media was discarded, and newly formed colonies were stained with crystal violet solution (1% aqueous solution) for 10 min. The staining solution was later removed, and wells were washed several times in distillate water. Colonies have been allowed to air dry naturally and acquired by photographic equipment. Quantification analysis has been performed by determining the optical density (OD) of dissolved colony-bound crystal violet staining in 10% acetic acid at 590 nm by an Infinite 200 PRO Microplate Reader (Tecan Life Sciences).

Western Blotting

Depending on the target protein, an amount of 10–30 µg of total extracts was loaded and separated by sodium dodecyl sulfate–polyacrylamide gel electrophoresis (SDS-PAGE) for each sample. Subsequently, sample proteins were transferred onto nitrocellulose membranes (GEH10600008; Amersham) by the Mini Trans-Blot system (Bio-Rad Laboratories). After washing in tris-buffered saline (TBS) supplemented with 0.05% Tween 20 (TC287; HIMEDIA), films were blocked 1 h in 5% no-fat dry milk (A0530; AppliChem) aimed at covering potentially free spots into the nitrocellulose membrane. Incubation overnight at 4°C has been chosen for primary antibody binding. In the following days, horseradish peroxidase (HRP)-conjugated secondary antibodies, reacting against the related primary species, were applied to the membrane for 1 h at room temperature. Each incubation step was preceded and followed by three 5-min rinses in T-TBS. Finally, protein-related light signals were acquired by ChemiDoc™ (Bio-Rad Laboratories) using the enhanced luminol-based chemiluminescent substrate (E-IR-R301; Elabscience) as a detection system for HRP.

Protein Extraction and Western Blotting Sample Preparation

A number of 4.8×10^5 (MIA PaCa-2) or 6×10^5 (PANC-1) cells were plated in 100 mm plates and left free to attach for 24 h. In the next day, media was replaced with a fresh one containing AdipoR, Gem, and the combination in doses and timelines reported in the Results section, and Figure legends. At every experimental point, cells were collected and spun down at 1,500 RPM for 5 min. Pellets were later resuspended in 3–5 volumes of RIPA buffer (R0278; Sigma-Aldrich) supplemented with protease and phosphatase inhibitors cocktail (#5872; Cell Signaling Technology). After 30 min, samples were further centrifuged at 14,000 RPM for 15 min at 4°C, and the supernatant was recovered and assessed for the relative protein content by Bradford Assay (39222; SERVA). Protein samples were first mixed 1:1 with Laemmli 2× (S3401; Sigma-Aldrich) and later boiled at 95°C for 6 min.

Development of Gemcitabine-Resistant MIA PaCa-1 Cells

MIA PaCa-2 cells were chronically exposed to increasing Gem concentration over a period of 4 months. Specifically, starting from 1 nM, cells were cultured in media containing Gem until they grew steadily. A higher cumulative Gem dosage was subsequently applied, and the resistant procedure was repeated as long as a final concentration of 200 nM was reached. At each step, cells were amplified, harvested, and cryopreserved in liquid nitrogen or an ultralow-temperature freezer. The obtained MIA PaCa-2 Gem-resistant cells were finally cultured in drug-free medium for up to 2 weeks before performing the reported experiments.

Statistical Analysis

Results are indicated as average value ± SD of biological independent replicates. Significance has been defined using either Student's t-test, to compare the mean of two samples, or analysis of variance (ANOVA) followed by Turkey's test, to discriminate differences between more than two experimental groups. In both cases, values of less than 0.05 were recognized as significant. Densitometric analyses have been carried out by ImageJ (NIH, Bethesda).

RESULTS

AdipoRon Affects Cell Growth and Slows Down Cell Cycle Progression in PDAC Cells

Recently, two different studies have reported the AdipoR ability in suppressing tumor growth in PDAC (Messaggio et al., 2017;

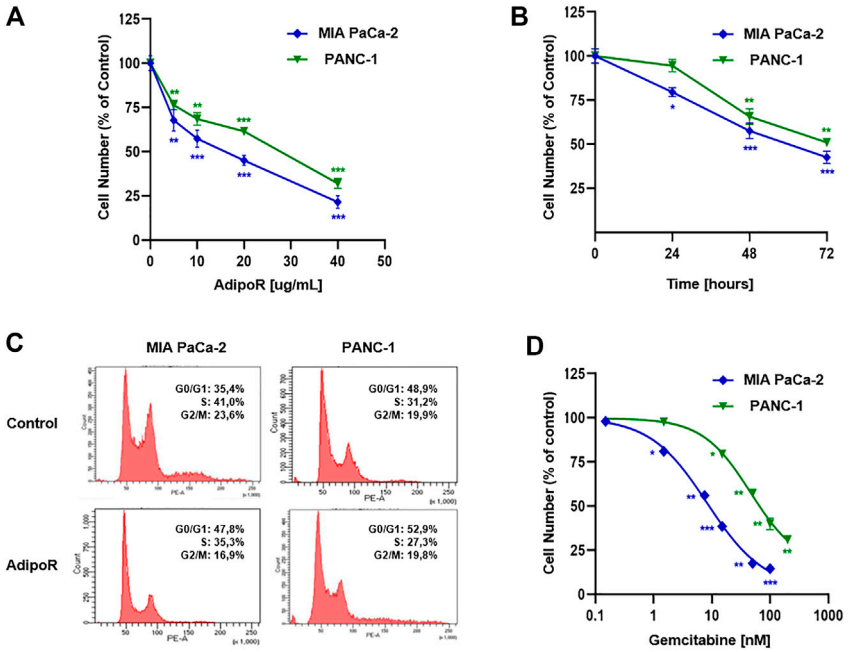

FIGURE 1 | Evaluation of single drug-mediated effects in PDAC cells. **(A)** MIA PaCa-2 and PANC-1 cells were exposed for 48 h to increasing AdipoR concentrations (10–40 μg/ml). **(B)** Cell growth curves were established in reaction to 10 μg/ml AdipoR over a period of 72 h. **(C)** Representative cell cycle profiles were obtained in MIA PaCa-2 and PANC-1 cells treated and not (control) with 10 μg/ml AdipoR for 24 h. **(D)** Dose effect induced by 48 h of Gem administration in MIA PaCa-2 and PANC-1 cells. In each experimental condition, the relative cell number was estimated in triplicate and expressed in figure as % of control. $^{*}p < 0.05$, $^{**}p < 0.01$, $^{***}p < 0.001$ by unpaired Student's t-test.

Akimoto et al., 2018). In order to extend and corroborate these findings, herein we first established the AdipoR impact in two distinct human PDAC cell lines, namely, MIA PaCa-2 and PANC-1.

In agreement with the previously published results, AdipoR exposure induced a remarkable cell growth decrease in PDAC cells, almost in a dose-dependent manner, without substantial differences between MIA PaCa-2 and PANC-1 cell types (**Figure 1A**).

Choosing 10 μg/ml as a subsequent effective working dosage, time course experiments up to 72 h showed a near time dependency in MIA PaCa-2, where a cell number decrease of 20, 42, and 57 percent was recorded at 24, 48, and 72 h, respectively (**Figure 1B**). A different trend was obtained in PANC-1, in which no considerable responsiveness to AdipoR was observed at 24 h (**Figure 1B**).

Notably, AdipoR-mediated antiproliferative properties were supported by an increase in the G0/G1 phase and a concomitant decrease of both S and G2/M phases in MIA PaCa-2 (**Figure 1C**). Precisely, the cell amount in G0/G1 moved from 35 to 48% after 24 h of treatment with 10 μg/ml AdipoR, while both S and G2/M phases diminished approximately 6%, concurrently.

Interestingly, although 10 μg/ml AdipoR was not effective in impacting PANC-1 cell growth after 24 h, changes in cell cycle distribution were detected. Similar to MIA PaCa-2, AdipoR provoked a G0/G1 intensification and an S-phase depletion in PANC-1, albeit in this latter cell model the magnitude was less sharp. Conversely, no G2/M involvement seems to occur in AdipoR-treated PANC-1 cells (**Figure 1C**). Overall, these findings further recognize AdipoR as an antiproliferative compound in PDAC and support its peculiarity in slowing down cell cycle progression.

Gemcitabine Influences Cell Growth With a Different Extent in PDAC Cells

Before exploring the consequences of the combination treatment AdipoR plus Gem in PDAC models, we preliminarily addressed the Gem-mediated cell growth impact on both employed cells.

Evaluating a wide concentration range, **Figure 1D** displays a different aptitude in reacting to Gem between MIA PaCa-2 and PANC-1. While MIA PaCa-2 showed great responsiveness to Gem already at very low concentration, the PANC-1 ability in resisting Gem was further confirmed when high dosages were applied. Exposing MIA PaCa-2 to 50 or 100 nM Gem for 48 h, for instance, nearly affected the totality of the cells, differently from PANC-1, in which the inhibition rate was roughly 40 and 60%, respectively. Taken together, these results remark an effective yet different Gem sensitivity between the examined PDAC cells.

Combination AdipoR Plus Gem Improves Single Outcomes in PDAC Cells

With the purpose of addressing potential cooperating effects in PDAC models, we subsequently combined effective concentrations of both AdipoR and Gem in a constant

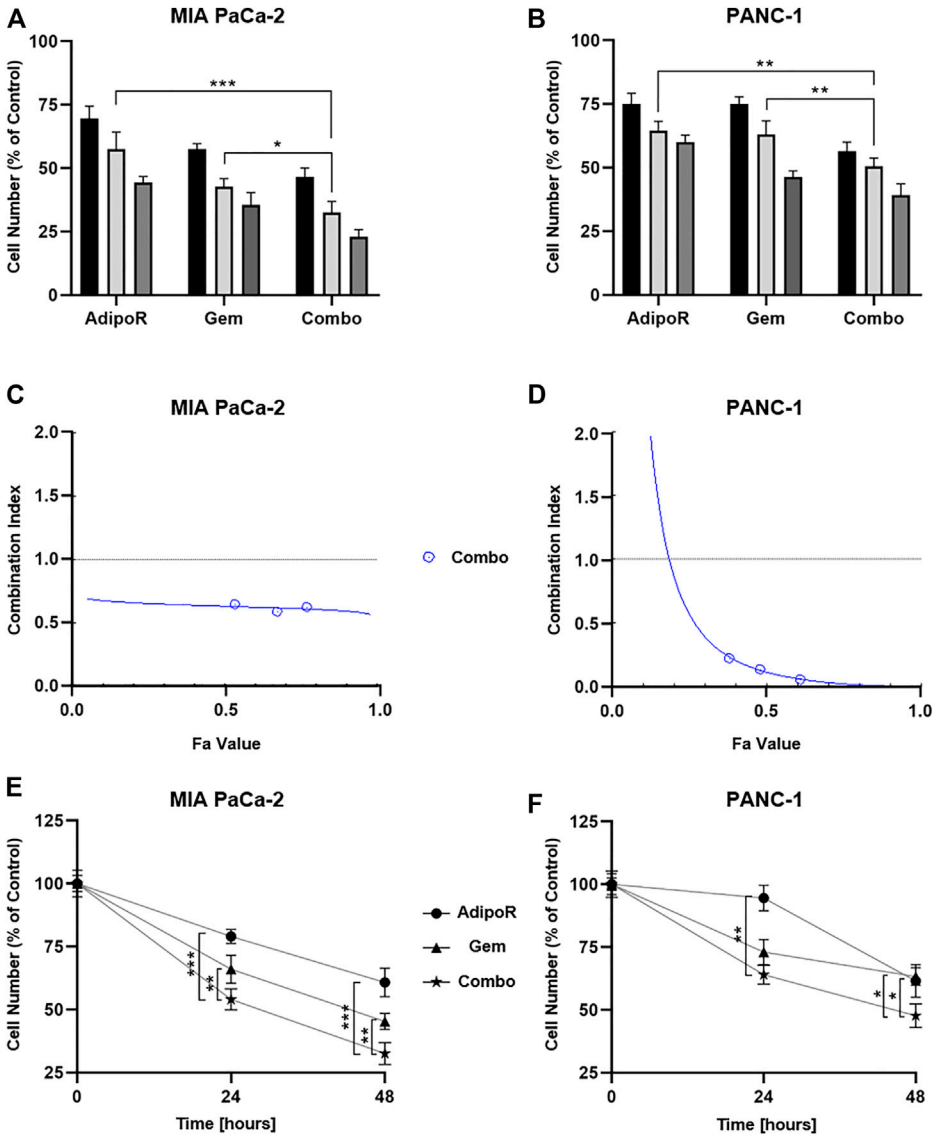

FIGURE 2 | Assessment of single and combinatory outcomes in PDAC cells. **(A)** 5 (black bar), 10 (light gray), and 20 μg/ml (gray) of AdipoR were added to MIA PaCa-2 cell medium for 48 h, either alone or in combination with 7.5 (black bar), 15 (light gray), and 30 nM (gray) Gem. Colors of the columns reflect those of single drug concentrations in combination setting. **(B)** Identical AdipoR amounts were instead mixed with 25 (black bar), 50 (light gray), and 100 nM (gray) Gem in PANC-1. Representative Fa-CI report obtained in MIA PaCa-2 **(C)** and PANC-1 **(D)**. **(E)** MIA PaCa-2 growth curves achieved after 24 and 48 h under 10 μg/ml AdipoR, 15 nM Gem, and AdipoR plus Gem, respectively. The same AdipoR concentration (10 μg/ml) and a different Gem amount (50 nM) were applied in PANC-1 time course experiments **(F)**. For each stimulation, cell number was estimated at least in triplicate and reported in figure as average ± SD in % of control. $^{*}p < 0.05$, $^{**}p < 0.01$, $^{***}p < 0.001$ by Tukey's multiple comparisons test.

dilution ratio, and the relative outcome in cell growth was later assessed.

Specifically, three different doses of both AdipoR (5, 10, and 20 μg/ml) and Gem (7.5, 15, and 30 nM) were employed in MIA PaCa-2, exhibiting a clear dose dependency (**Figure 2A**). But even more interestingly, the concomitant use of AdipoR plus Gem further counteracted MIA PaCa-2 cell proliferation, suggesting a positive interplay between these two compounds. Compared with 5 μg/ml AdipoR and 7.5 nM Gem, combination treatment improved single outcomes by nearly 33% and 20%, respectively. This tendency became even more pronounced at the highest tested doses, raising inhibition values of 47 and 34% versus AdipoR and Gem, individually (**Figure 2A**).

The different Gem responsiveness has required the use of higher concentrations in PANC-1 (25, 50, and 100 nM), while no changes in AdipoR doses were applied. In line with MIA PaCa-2 results, even in PANC-1, all three tested mixtures enhanced the anticancer effects of single treatments (**Figure 2B**). Minimal fluctuations were observed in response to the increasing combinations in PANC-1.

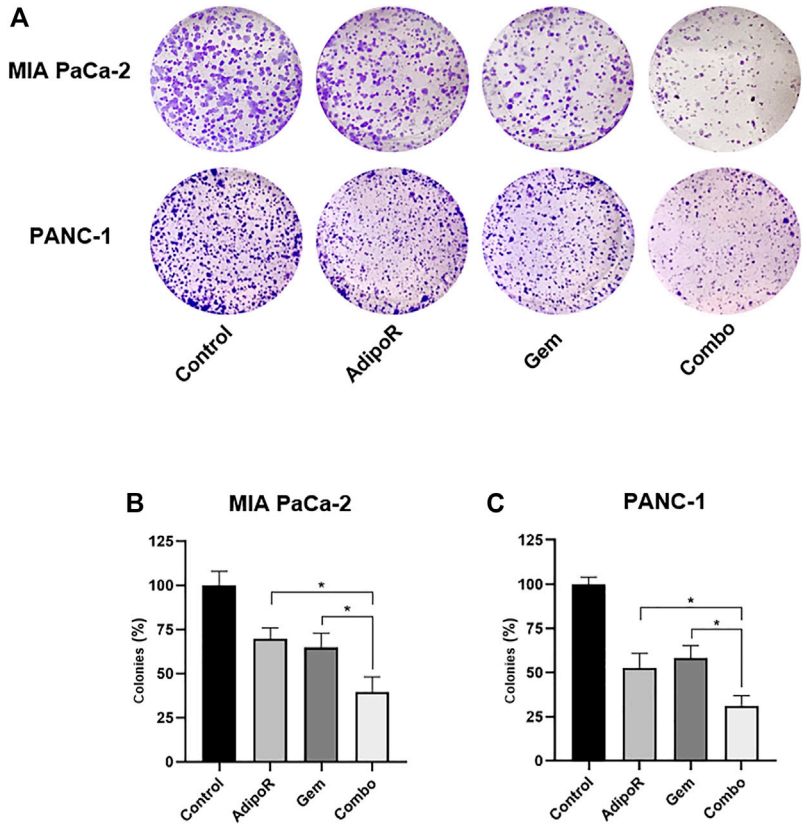

FIGURE 3 | Estimation of single and combinatory impacts on clonogenic potential in PDAC cells. MIA PaCa-2 and PANC-1 were treated and not (control) with the same AdipoR concentration (2 μg/ml) but different Gem amounts (4 vs 6 nM), both individually and in combination, for 8 and 10 days, respectively. Representative stained wells are displayed in **(A)**, while the relative quantification analysis has been reported in **(B)** (MIA PaCa-2) and **(C)** (PANC-1). Experiments were reproduced thrice and plotted on a graph as mean value ± SD in % of control. *$p < 0.05$ by Tukey's multiple comparisons test.

CompuSyn analysis was subsequently performed with the purpose of defining drug-drug interaction and the relative combination index (CI). Plotting dose-effect curves of both single and combination agents, the Chou-Talalay method discriminates among additive (CI = 1), synergism (CI < 1), and antagonism (CI > 1) effects, using the median-effect equation (Chou, 2010). The MIA PaCa-2 Fa-CI plot revealed a robust synergistic action already at very low concentrations, maintaining a constant trend even when combination affected 90% of cells (**Figure 2C**). Albeit in all tested conditions CI estimation supported a synergic action, the Fa-CI plot unveiled a different tendency in PANC-1 (**Figure 2D**).

Lately, we performed time-course experiments, using 10 μg/ml AdipoR plus 15 nM in MIA PaCa-2 or 50 nM Gem in PANC-1. Although co-administration AdipoR plus Gem improved single drug-mediated cell reduction in both PDAC models, different curves were outlined over time. Whilst a time dependency was revealed in reaction to both single and combination treatments in MIA PaCa-2 (**Figure 2E**), no clear reliance on treatment duration was observed in reaction to Gem in PANC-1. Moreover, comparing combination versus AdipoR, time exposure did not amplify the gap (**Figure 2F**).

Collectively, these data show that the combination of AdipoR plus Gem impairs MIA PaCa-2 and PANC-1 cell growth more effectively compared with single ones. In addition, as suggested by CompuSyn analysis, a potential synergism might exist between these two compounds.

Co-Administration AdipoR Plus Gem Minimizes the Clonogenic Potential in PDAC Cells

The clonogenic assay is considered a valuable *in vitro* assay for monitoring undifferentiated potential and anchorage-independent growth (Rajendran and Jain, 2018). Given that Gem and AdipoR have been proved to act as effective agents in mitigating colony formation, we successively addressed the potential impact of combination AdipoR plus Gem on this PDAC feature (Messaggio et al., 2017; Alhothali et al., 2019; Zhou et al., 2019).

Aiming at defining the consequences of long-term exposure, PDAC cells were seeded at very low density and treated with AdipoR and Gem, both individually and in combination, until newly-formed colonies became viewable. The employment of a small amount of AdipoR and Gem moderately impaired PDAC colony-forming ability, separately (**Figure 3**). Conversely, a very strong reduction in PDAC clonogenic potential was observed when the same doses of AdipoR and Gem were put together (**Figure 3A**). Quantification analysis revealed a further enhancement in colonies reduction of

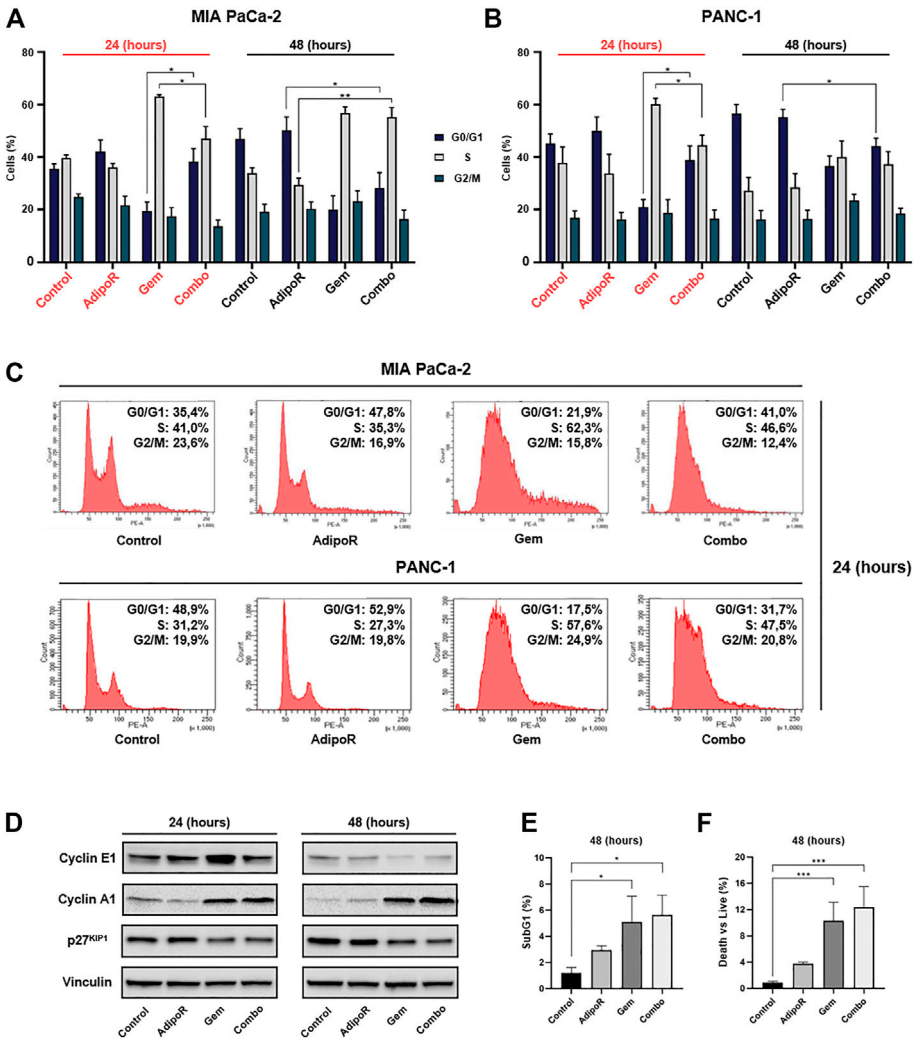

FIGURE 4 | Investigation of single and combinatory consequences on cell cycle distribution in PDAC cells. MIA PaCa-2 was exposed and not (control) to 10 μg/ml AdipoR, 15 nM Gem, and AdipoR plus Gem over a period of 24 and 48 h **(A)**. PANC-1 cells, instead, were treated and not (control) with 10 μg/ml AdipoR, 50 nM Gem, and combination for the same temporal extension **(B)**. Subsequently, the relative cell phase distribution was defined by FACSCelesta™ using PI as DNA staining. MIA PaCa-2 and PANC-1 representative histogram plots at 24 h **(C)**. **(D)** Cyclin A1, cyclin E1, and $p27^{KIP1}$ expression levels were obtained in reaction to 10 μg/ml AdipoR, 15 nM Gem, and combination in MIA PaCa-2. **(E)** Relative subG1 amount. **(F)** Trypan blue discrimination analysis. Either **(E)** or **(F)** show MIA PaCa-2 results cultured in media containing AdipoR, Gem, and AdipoR plus Gem under the same **(B)** experimental conditions. Displayed data are expressed in percentage as average value ± SD of three independent experiments. $^{*}p < 0.05$, $^{**}p < 0.01$, $^{***}p < 0.001$ by Tukey's multiple comparisons test.

nearly 40% compared to Gem alone in MIA PaCa-2, as a result of both number and size decrease (**Figure 3B**). Consistent results were also obtained in PANC-1 (**Figure 3C**).

Altogether, this evidence indicates a stronger and deeper outcome in limiting PDAC clonogenic potential made by combinatory treatment AdipoR plus Gem compared to single-agent administration.

AdipoR Plus Gem Differently Affects Cell Cycle Phases' Distribution in PDAC Cells

To figure out how the combination treatment AdipoR plus Gem affected PDAC cell growth, we successively performed cell cycle analysis intended to determine the cell phase distribution in reaction to our stimuli. Comprehensively, single and combination treatments were performed in both PDAC models for up to 48 h, and the relative DNA content was later detected by flow cytometry using propidium iodide (PI) as basepair intercalating dye.

Depending on the concentration employed, Gem has been reported to induce both S and G2 phase arrest in PDAC models (Miao et al., 2016; Montano et al., 2017; Passacantilli et al., 2018; Kumarasamy et al., 2020). In agreement with these findings, in MIA PaCa-2, we observed a remarkable S-phase accumulation in reaction to 24h Gem administration (**Figures 4A,C**). In respect of untreated cells, Gem raised S-phase from 40 to 62% at the expense of G0/G1 (−14%) and partly G2/M (−7%). A similar but more pronounced tendency was observed

at 48 h as a result of changes in both cell density and nutrients occurring in control cells, rather than a Gem-mediated action (**Figure 4A**). Quite the contrary, AdipoR intensified the G0/G1 cell amount and decreased both S and G2/M phases at 24 h, while at 48 h, the G0/G1 enrichment was only supported by S-phase reduction.

Looking at the cell phase distribution in reaction to AdipoR plus Gem, different but intermediate features were detected in comparison with single agents. In this respect, after 24 h, combination displayed a G0/G1 amount closer to AdipoR, while conversely, the simultaneous presence of both AdipoR and Gem for additional 24 h exhibited an S-phase accumulation similar to Gem (**Figures 4A,C**). A quite comparable pattern was also obtained in PANC-1, especially following 24 h of treatment (**Figures 4B,C**).

In agreement with the recorded cell phase distribution, considerable changes were also detected in cyclin A1 and E1 levels, and cyclin-dependent kinase inhibitor $p27^{KIP1}$, in reaction to both single and combined stimuli (**Figure 4D**; **Supplementary Figure S1**).

Analysis of subG1 population, which usually includes hypodiploid cells undergoing DNA fragmentation, showed a substantial increase in reaction to both Gem and combination at 48 h compared with untreated cells (**Figure 4E**). The absence of significant additive cytotoxic effects between Gem and combination was also confirmed in trypan blue exclusion assay, which revealed only minimal changes in death vs living cells in response to these two conditions (**Figure 4F**). Overall, these findings reveal a different ability in braking cell cycle progression among AdipoR, Gem, and combination.

p44/42 MAPK Is Dynamically Involved in AdipoR Plus Gem Outcomes in PDAC Cells

As the most frequent mutated gene, abnormal KRAS hyperactivation occurs recurrently in PDAC (Buscail et al., 2020). Consequently, dysregulation of the p44/42 MAPK pathway has been recognized in PDAC, assuming a possible correlation between its expression and tumor prognosis (Furukawa, 2015).

Modulation of p44/42 MAPK has also been detected in response to Gem administration in both *in vitro* and *in vivo* PDAC models, and in patients (Jin et al., 2017; Ryu et al., 2021). Correspondingly, although the AdipoR-related molecular mechanisms remain largely unknown, its antiproliferative action has been linked to p44/42 MAPK activation in PDAC (Akimoto et al., 2018). Recently, we also observed AdipoR-mediated p44/42 MAPK stimulation in osteosarcoma cell lines (Sapio et al., 2020).

Taking into account the mentioned findings and the relevance of this pleiotropic pathway in regulating the entirety of cell functions (Guo et al., 2020), we first addressed the involvement of p44/42 MAPK in reaction to our stimuli.

With this purpose, MIA PaCa-2 and PANC-1 cells were treated with AdipoR and Gem, alone and in co-administration, for up to 48 h and subsequently analyzed for p44/42 MAPK phosphorylation status.

In the absence of substantial protein amount variations, we recognized a different combination capability in modulating p44/42 MAPK phosphorylation between these two cell lines. Specifically, while in MIA PaCa-2, the concomitant administration of AdipoR with Gem resulted in p44/42 MAPK activation at 48 h (**Figure 5A**), in PANC-1, instead phospho-p44/42 MAPK upregulation was already apparent at 24 h and maintained up to 48 h (**Figure 5B**).

To further investigate the p44/42 MAPK involvement in combination-mediated effects, we subsequently tested the impact of MEK1/MEK2 inhibitor PD98059 on AdipoR plus Gem outcomes in MIA PaCa-2 cells. Bearing in mind that long-term exposure to downstream blockade of MAPK deeply impairs PDAC cell growth (Wong et al., 2016), we chose 10 μM for 24 h as effective dosage of PD98059 and time to mitigate p44/42 MAPK signaling and affect MIA PaCa-2 cell growth, marginally (**Figure 5C**; **Supplementary Figure S2A**).

Although the combination of AdipoR plus Gem improved cell growth inhibition compared with single ones, PD98059 partially counteracted combination effectiveness, reducing the inhibition rate of approximately 25% relative to p44/42 MAPK-proficient counterpart (**Figure 5D**). Comparable experiments performed in PANC-1 also revealed a PD98059-mediated capacity in hindering the combination anticancer action (**Figure 5E**), albeit MEK1/MEK2 inhibitor alone affected cell growth in a more effective manner with respect to MIA PaCa-2 (**Supplementary Figures S2B,C**).

On the whole, these findings suppose an involvement of p44/42 MAPK pathway in AdipoR plus Gem combination response.

Combination AdipoR Plus Gem Impairs Cell Growth Even in MIA PaCa-2-Resistant Cells

Although Gem displays one of the highest response rates compared to other anticancer agents in PDAC, resistance outbreak occurs already within few weeks of initiating dosing (Amrutkar and Gladhaug, 2017). As a result of Gem-induced refractivity, PDAC generally becomes more aggressive, causing a further reduction in overall survival (Quinonero et al., 2019).

To further speculate the usefulness of AdipoR-based therapy in PDAC, we first developed stable MIA PaCa-2 cell lines resistant to Gem (Gem-Res). Thereafter, MIA PaCa-2 and MIA PaCa-2 Gem-Res cells were cultured in a medium containing 10 μg/ml AdipoR and 15 nM Gem, both individually and in combination for up to 48 h. As previously described in MIA PaCa-2, combination treatment resulted in a further cell growth reduction compared to AdipoR and Gem singularly, both at 24 and 48 h (**Figures 6A,B**). Remarkably, even though Gem was ineffective in reducing the cell number in MIA PaCa-2 Gem-Res cells, AdipoR induced a 25% growth inhibition, and even more interestingly, co-administration AdipoR plus Gem affected cell proliferation by another 18% with respect to AdipoR alone at 48 h (**Figure 6B**).

Using a higher dose from the one previously employed in **Figure 3**, Gem abrogated the colony forming ability in MIA

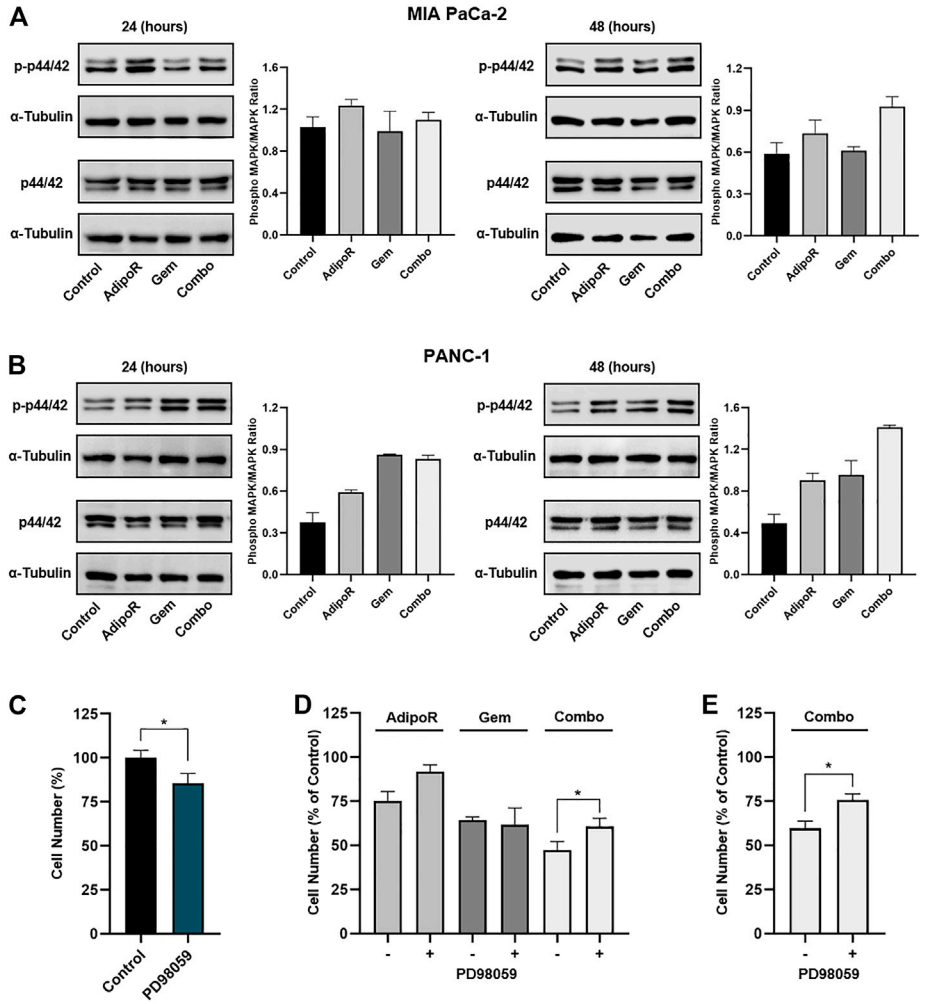

FIGURE 5 | Evaluation of p44/42 MAPK involvement in AdipoR plus Gem effects. MIA PaCa-2 **(A)** and PANC-1 **(B)** were treated and not (control) with 10 μg/ml AdipoR, 15 nM (MIA PaCa-2) or 50 nM (PANC-1) Gem, and AdipoR plus Gem over a period of 48 h. Thereafter, either single or combination consequences on p44/42 MAPK activation (phosphorylation) were estimated by Western blotting. Phospho-MAPK/MAPK ratio results from the quotient of phospho-p44/42 MAPK and its relative housekeeping on the gel divided by a quotient of p44/42 and its relative α-tubulin. **(C)** MIA PaCa-2 was exposed and not (control) to 10 μM PD98059 for 24 h, and the cell growth percentage was established. **(D)** MIA PaCa-2 single and combination treatments in MAPK-proficient and -hampered background. **(E)** Combination treatments containing 10 μg/ml AdipoR plus 50 nM Gem were carried out in PANC-1 cells with or without PD98059 inhibitor. Two hours of PD98059 pretreatment preceded and not individual and combinatory administration. Results are depicted in percentage as mean ± SD of three independent experiments. *$p < 0.05$ by Tukey's multiple comparisons or Student's t-test.

PaCa-2, while conversely, in Gem-Res cells, the same amount marginally affected the growing colony (**Figure 6C**). Interestingly, either alone or in combination with Gem, AdipoR administration reduced clonogenic potential by 45 and 55%, correspondingly (**Figure 6D**).

Despite being less pronounced than MIA PaCa-2, flow cytometry analysis showed AdipoR persistence in braking cell cycle progression even in MIA PaCa-2 Gem-Res. Like the sensitive cells, increased G0/G1 phase was observed in the resistant ones supplemented with AdipoR (**Figure 6E**). But even more interesting, reducing both S and G2/M phases, the concomitant administration of AdipoR and Gem enhanced the G0/G1 accumulation compared with AdipoR alone (**Figure 6E**). Remarkably, no substantial changes were detected between Gem-treated and untreated cells, confirming the loss of chemotherapy responsiveness by this cell line.

Taken together, these data indicate that the combination AdipoR plus Gem is effective in preventing growth and colony formation even in Gem-resistant MIA PaCa-2 cells.

DISCUSSION

The existing therapeutic options have failed to provide an appropriate response in PDAC, reinforcing the unlucky privilege of being one of the deadliest cancers worldwide (Latenstein et al., 2020). Regrettably, even immunotherapy, which has recently revolutionized the drug regimes in cancer

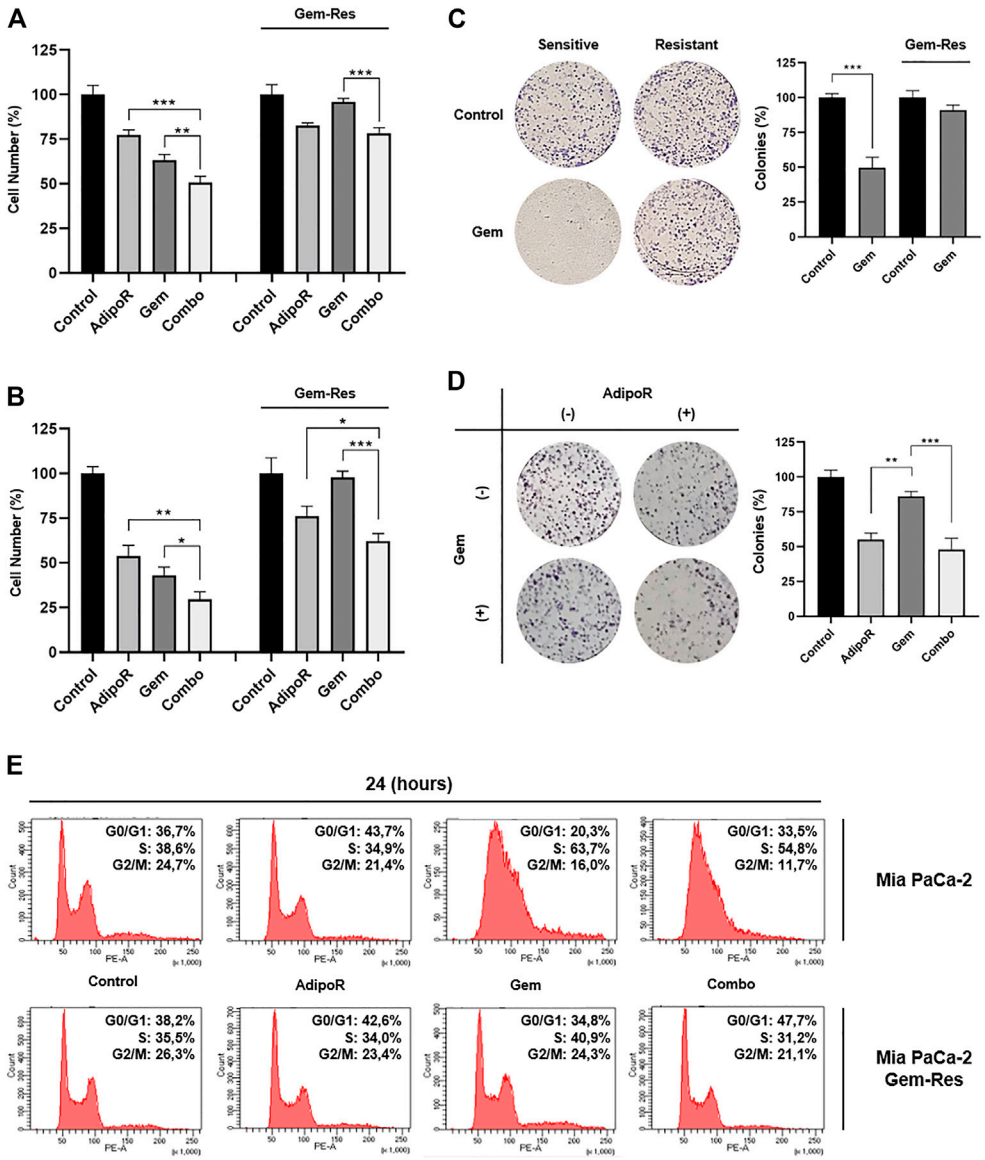

FIGURE 6 | Responsiveness of MIA PaCa-2 Gem-resistant cells to single and combinatory treatments. Either MIA PaCa-2 Gem-sensitive and -resistant cells were treated and not (control) with 10 μg/ml AdipoR, 15 nM Gem, and AdipoR plus Gem for 24 **(A)** and 48 h **(B)**; thereafter, the relative impact on cell growth was addressed. **(C)** Cell media of both MIA PaCa-2 Gem-sensitive and -resistant cells were supplemented with and without (control) 10 nM Gem for 8 days. Illustrative violet-stained wells are shown on the left side, the relative quantification on the right. **(D)** MIA PaCa-2 Gem-resistant cells undergoing AdipoR (10 μg/ml) and Gem (5 nM) individually and combinatory treatments were tested for colony-forming ability. Images and quantification assay are provided in Figure. **(E)** MIA PaCa-2 Gem-sensitive and -resistant were incubated either with single or combination drugs as indicated in **(A)**. FACSCelesta^{TM} analysis was later performed with the purpose of defining the drug-induced consequences on cell phase distribution. Reported results are indicated in percentage as median value ± SD of triplicate experiments. $^{*}p < 0.05$, $^{**}p < 0.01$, $^{***}p < 0.001$ by Tukey's multiple comparisons or Student's t-test.

treatment (Makaremi et al., 2021), has shown few successful chances in PDAC due to tumor-related stroma abundance (Panchal et al., 2021).

Therefore, besides radiation and surgical resection, chemotherapy represents the only partially effective pharmacological approach in PDAC, irrespective of tumor stage (Qian et al., 2020). Despite the clinical approval of novel chemotherapeutics and formulations, Gem still remains a cornerstone for PDAC management, and Gem-based therapy constitutes the widely used partner in combination therapy (Christenson et al., 2020). Unfortunately, the limited success rate of Gem treatment and the relative ease in developing chemoresistance warrant for more effective therapeutic approaches in PDAC.

Recently, the first synthetic adiponectin receptor agonist is emerging as a promising anticancer compound in several tumors, including myeloma and breast, prostate, and ovarian cancers (Nigro et al., 2021). Convincing evidence is

also emerging in PDAC, where AdipoR suppresses tumor growth and induces cell death, mainly through apoptosis and necroptosis induction (Messaggio et al., 2017; Akimoto et al., 2018).

With the purpose of further addressing the AdipoR candidacy in PDAC treatment, herein we investigated the potential outcome of its dynamic interaction with Gem in MIA PaCa-2 and PANC-1 cells. Albeit quite preliminary, our results reveal no shortcomings in using these two compounds together; quite to the contrary, their combination could have a greater therapeutic impact compared with single ones. Moreover, as suggested by CompuSyn analysis, potential synergistic action could exist between AdipoR and Gem. The cooperative interaction is clearly supported by cell growth and colony results, which shows a combination-mediated stronger and deeper outcome in limiting PDAC tumorigenicity. Additionally, either AdipoR or combination kept their therapeutic effectiveness even in MIA PaCa-2 cells that developed resistance to Gem administration.

Although countless other compounds have been tested over the last years, only two Gem-based combination therapies have been approved and employed in clinical for advanced PDAC treatment, namely, erlotinib and nab-Paclitaxel (Elsayed and Abdelrahim, 2021). However, while the successful rate of combination Gem plus erlotinib is strictly dependent on the EGFR status and other potential signatures (Hoyer et al., 2021), serious side effects have been reported in PDAC patients treated with Gem plus nab-paclitaxel, including neutropenia, peripheral neuropathy, and fatigue (Blomstrand et al., 2019). In addition to supporting its antineoplastic role in PDAC, our findings first recognize AdipoR as a novel potential candidate in Gem-based multidrug therapy. If subsequently confirmed by *in vivo* and trial studies, combination AdipoR plus Gem could represent an additional pharmacological choice in PDAC, especially for metastatic unresectable patients whose survival is currently under 1 year, even with an optimal chemotherapy regimen.

Mechanistically, the combination action could be explained by a different capability in slowing down cell cycle progression between AdipoR and Gem. Although in different cancer types, both Akimoto and Ramzan reported an AdipoR-mediated G0/G1 phase delay, which results in tumor growth arrest (Akimoto et al., 2018; Ramzan et al., 2019). More recently, we also observed a similar functional mechanism in the AdipoR-induced osteosarcoma stunting (Sapio et al., 2020). In agreement with the exhibiting findings, our results confirmed the ability of this compound in affecting G0/G1, as well as of Gem in blocking the S-phase (Miao et al., 2016; Montano et al., 2017; Waissi et al., 2021). Surprisingly, each compound retains its respective peculiarity even when combined. Indeed, the simultaneous administration showed intermediate features between AdipoR and Gem, wherein Gem is still arresting in S phase and AdipoR in G0/G1. Therefore, rather than inducing cytotoxic effects, our findings could suggest an experimental model in which a sum of different phase slowdown, mediated by single agents, further reduces PDAC growth.

Signaling pathway examination revealed a possible involvement of p44/42 MAPK in the responses elicited by AdipoR plus Gem in PDAC cells. In this regard, while combination stimulated p44/42 MAPK activation, PD98059-mediated p44/42 MAPK impairment partially counteracted its effectiveness. Interestingly, analog results were also observed in reaction to AdipoR, thus supposing that a proficient activation of this pathway is functional for this compound.

Different studies have reported an AdipoR-mediated p44/42 MAPK hyperphosphorylation in different pathological conditions, including in cancer (Messaggio et al., 2017; Akimoto et al., 2018). In this regard, in our previous study, we also reported how AdipoR induces a robust p44/42 MAPK activation in osteosarcoma cells (Sapio et al., 2020). In accordance with Akimoto's results (Akimoto et al., 2018), herein we demonstrated that p44/42 MAPK activation is needed to allow a proper AdipoR antitumor action and combination outcome. Even though not in cancer models, additional studies further support the functional p44/42 MAPK role in either AdipoR- or adiponectin-mediated effects (Koskinen et al., 2011; Zhang et al., 2011; Alvarez et al., 2012; Wang et al., 2020). In this respect, Wang and coworkers have recently proved that ameliorating cell viability, apoptosis, and reactive oxygen species (ROS) production, AdipoR stimulates bone regeneration in ATDC5 cells via p44/42 MAPK pathway (Wang et al., 2020). Interestingly, when p44/42 MAPK was irreversibly suppressed by PD98059, AdipoR failed to rescue impaired apoptosis and chondrogenesis of cells. Although our results recognize this pathway as potentially involved in combination effectiveness; we cannot rule out that other signaling pathways that might be involved in, especially because the PD98059-mediated action just results in an incomplete combination rescue. In this respect, as far as known, the most common multidrug resistances are related to ATP-binding cassette (ABC) transporters, which, regulating drug absorption, distribution, and excretion, play a crucial role in overcoming drug-induced cytotoxicity (Robey et al., 2018). Recently, different ABC family members have been reported to be involved in Gem resistance, expressly in PDAC (Xu et al., 2013; Lu et al., 2019; Okada et al., 2021). Interestingly, a positive correlation between adiponectin and ABCA1 levels has been observed in visceral adipose tissue (Vincent et al., 2019). Moreover, adiponectin has been described to increase both mRNA and protein levels of ABCA1 in HepG2 hepatocellular carcinoma cells (Matsuura et al., 2007). Despite no evidence currently reports AdipoR-induced ABC modulation yet, this association could explain how this receptor agonist overcomes Gem ineffectiveness in MIA PaCa-2-resistant cells. Therefore, targeting experiments aimed at defining their relative engagement will be performed shortly.

CONCLUSION

In conclusion, we first provide evidence of enhanced performances in constraining PDAC progression when

AdipoR and Gem are combined. Apart from supporting the antineoplastic feature, our results recognize an additional and newly AdipoR therapeutic usage in PDAC, potentially as a partner in Gem-based combination therapy.

Considering the current orphan status for this illness, finding out novel and more effective pharmacological strategies could help in improving both PDAC prognosis and survival. In this regard, our promising *in vitro* results may encourage the development of future supplementary studies aimed at addressing the feasibility of AdipoR plus Gem approval in clinical practice.

DATA AVAILABILITY STATEMENT

The raw data supporting the conclusion of this article will be made available by the corresponding author, without undue reservation.

AUTHOR CONTRIBUTIONS

Conceptualization: LS and SN; validation: AR; formal analysis: ASp.; investigation: AR and ASa; writing—original draft preparation: LS and AR; writing—review and editing: LS and SN; visualization: ASa; supervision: SN; and funding acquisition: LS. All authors have read and agreed to the published version of the manuscript.

FUNDING

This research was funded by V:ALERE 2020 (Vanvitelli per la Ricerca Program).

ACKNOWLEDGMENTS

We are grateful to professors Vincenzo Carafa and Lucia Altucci for sharing FACS tools.

SUPPLEMENTARY MATERIAL

The Supplementary Material for this article can be found online at: https://www.frontiersin.org/articles/10.3389/fphar.2022.837503/full#supplementary-material

Supplementary Figure 1 | Quantification analysis of the cell cycle related proteins. **(A)** Cyclin E1/Vinculin Ratio. **(B)** Cyclin A1/Vinculin Ratio. **(C)** $p27^{KIP1}$/Vinculin Ratio. ImageJ-mediated quantification analysis has been performed processing three distinct Western blotting experiments for every cell cycle related protein, and housekeeping protein (Vinculin). Median value ± SD of the relative Ratio is reported in chart. Representative Western blotting films are displayed in **Figure 4D**.

Supplementary Figure 2 | Effects of PD98059 inhibitor on p44/42 MAPK phosphorylation in PDAC cells. MIA PaCa-2 **(A)** and PANC-1 **(C)** were treated and not (control) with 10 μM PD98059 for 2 h with the purpose of assessing both phospho-p44/42 and p44/42 levels by Western Blotting. **(B)** Growth impact of 10 μM PD98059 for 24 h in PANC-1 cells, expressed in percentage of control as mean ± SD of three independent experiments. *$p < 0.05$ by unpaired Student's t-test.

REFERENCES

Akimoto, M., Maruyama, R., Kawabata, Y., Tajima, Y., and Takenaga, K. (2018). Antidiabetic Adiponectin Receptor Agonist AdipoRon Suppresses Tumour Growth of Pancreatic Cancer by Inducing RIPK1/ERK-dependent Necroptosis. *Cell Death Dis.* 9 (8), 804. doi:10.1038/s41419-018-0851-z

Alhothali, M., Mathew, M., Iyer, G., Lawrence, H. R., Yang, S., Chellappan, S., et al. (2019). Fendiline Enhances the Cytotoxic Effects of Therapeutic Agents on PDAC Cells by Inhibiting Tumor-Promoting Signaling Events: A Potential Strategy to Combat PDAC. *Int. J. Mol. Sci.* 20 (10), 1. doi:10.3390/ijms20102423

Alvarez, G., Visitación Bartolomé, M., Miana, M., Jurado-López, R., Martín, R., Zuluaga, P., et al. (2012). The Effects of Adiponectin and Leptin on Human Endothelial Cell Proliferation: a Live-Cell Study. *J. Vasc. Res.* 49 (2), 111–122. doi:10.1159/000332332

Amrutkar, M., and Gladhaug, I. P. (2017). Pancreatic Cancer Chemoresistance to Gemcitabine. *Cancers* 9 (11), 1. doi:10.3390/cancers9110157

Blomstrand, H., Scheibling, U., Bratthäll, C., Green, H., and Elander, N. O. (2019). Real World Evidence on Gemcitabine and Nab-Paclitaxel Combination Chemotherapy in Advanced Pancreatic Cancer. *BMC Cancer* 19 (1), 40. doi:10.1186/s12885-018-5244-2

Buscail, L., Bournet, B., and Cordelier, P. (2020). Role of Oncogenic KRAS in the Diagnosis, Prognosis and Treatment of Pancreatic Cancer. *Nat. Rev. Gastroenterol. Hepatol.* 17 (3), 153–168. doi:10.1038/s41575-019-0245-4

Carioli, G., Malvezzi, M., Bertuccio, P., Boffetta, P., Levi, F., La Vecchia, C., et al. (2021). European Cancer Mortality Predictions for the Year 2021 with Focus on Pancreatic and Female Lung Cancer. *Ann. Oncol.* 32 (4), 478–487. doi:10.1016/j.annonc.2021.01.006

Chou, T. C. (2010). Drug Combination Studies and Their Synergy Quantification Using the Chou-Talalay Method. *Cancer Res.* 70 (2), 440–446. doi:10.1158/0008-5472.CAN-09-1947

Christenson, E. S., Jaffee, E., and Azad, N. S. (2020). Current and Emerging Therapies for Patients with Advanced Pancreatic Ductal Adenocarcinoma: a Bright Future. *Lancet Oncol.* 21 (3), e135–e145. doi:10.1016/S1470-2045(19)30795-8

Collisson, E. A., Bailey, P., Chang, D. K., and Biankin, A. V. (2019). Molecular Subtypes of Pancreatic Cancer. *Nat. Rev. Gastroenterol. Hepatol.* 16 (4), 207–220. doi:10.1038/s41575-019-0109-y

Damm, M., Efremov, L., Birnbach, B., Terrero, G., Kleeff, J., Mikolajczyk, R., et al. (2021). Efficacy and Safety of Neoadjuvant Gemcitabine Plus Nab-Paclitaxel in Borderline Resectable and Locally Advanced Pancreatic Cancer-A Systematic Review and Meta-Analysis. *Cancers* 13 (17), 4326. doi:10.3390/cancers13174326

Elsayed, M., and Abdelrahim, M. (2021). The Latest Advancement in Pancreatic Ductal Adenocarcinoma Therapy: A Review Article for the Latest Guidelines and Novel Therapies. *Biomedicines* 9 (4), 389. doi:10.3390/biomedicines9040389

Esposito, M. T., Zhao, L., Fung, T. K., Rane, J. K., Wilson, A., Martin, N., et al. (2015). Synthetic Lethal Targeting of Oncogenic Transcription Factors in Acute Leukemia by PARP Inhibitors. *Nat. Med.* 21 (12), 1481–1490. doi:10.1038/nm.3993

Fu, Y., Ricciardiello, F., Yang, G., Qiu, J., Huang, H., Xiao, J., et al. (2021). The Role of Mitochondria in the Chemoresistance of Pancreatic Cancer Cells. *Cells* 10 (3), 497. doi:10.3390/cells10030497

Furukawa, T. (2015). Impacts of Activation of the Mitogen-Activated Protein Kinase Pathway in Pancreatic Cancer. *Front. Oncol.* 5, 23. doi:10.3389/fonc.2015.00023

Gao, H. L., Wang, W. Q., Yu, X. J., and Liu, L. (2020). Molecular Drivers and Cells of Origin in Pancreatic Ductal Adenocarcinoma and Pancreatic Neuroendocrine Carcinoma. *Exp. Hematol. Oncol.* 9, 28. doi:10.1186/s40164-020-00184-0

Guo, Y. J., Pan, W. W., Liu, S. B., Shen, Z. F., Xu, Y., and Hu, L. L. (2020). ERK/MAPK Signalling Pathway and Tumorigenesis. *Exp. Ther. Med.* 19 (3), 1997–2007. doi:10.3892/etm.2020.8454

Hoyer, K., Hablesreiter, R., Inoue, Y., Yoshida, K., Briest, F., Christen, F., et al. (2021). A Genetically Defined Signature of Responsiveness to Erlotinib in Early-Stage Pancreatic Cancer Patients: Results from the CONKO-005 Trial. *EBioMedicine* 66, 103327. doi:10.1016/j.ebiom.2021.103327

Huang, L., Jansen, L., Balavarca, Y., Molina-Montes, E., Babaei, M., van der Geest, L., et al. (2019). Resection of Pancreatic Cancer in Europe and USA: an International Large-Scale Study Highlighting Large Variations. *Gut* 68 (1), 130–139. doi:10.1136/gutjnl-2017-314828

Jin, X., Pan, Y., Wang, L., Ma, T., Zhang, L., Tang, A. H., et al. (2017). Fructose-1,6-bisphosphatase Inhibits ERK Activation and Bypasses Gemcitabine Resistance in Pancreatic Cancer by Blocking IQGAP1-MAPK Interaction. *Cancer Res.* 77 (16), 4328–4341. doi:10.1158/0008-5472.CAN-16-3143

Koskinen, A., Juslin, S., Nieminen, R., Moilanen, T., Vuolteenaho, K., and Moilanen, E. (2011). Adiponectin Associates with Markers of Cartilage Degradation in Osteoarthritis and Induces Production of Proinflammatory and Catabolic Factors through Mitogen-Activated Protein Kinase Pathways. *Arthritis Res. Ther.* 13 (6), R184. doi:10.1186/ar3512

Kumarasamy, V., Ruiz, A., Nambiar, R., Witkiewicz, A. K., and Knudsen, E. S. (2020). Chemotherapy Impacts on the Cellular Response to CDK4/6 Inhibition: Distinct Mechanisms of Interaction and Efficacy in Models of Pancreatic Cancer. *Oncogene* 39 (9), 1831–1845. doi:10.1038/s41388-019-1102-1

Latenstein, A. E. J., van der Geest, L. G. M., Bonsing, B. A., Groot Koerkamp, B., Haj Mohammad, N., de Hingh, I. H. J. T., et al. (2020). Nationwide Trends in Incidence, Treatment and Survival of Pancreatic Ductal Adenocarcinoma. *Eur. J. Cancer* 125, 83–93. doi:10.1016/j.ejca.2019.11.002

Lu, Y., Xu, D., Peng, J., Luo, Z., Chen, C., Chen, Y., et al. (2019). HNF1A Inhibition Induces the Resistance of Pancreatic Cancer Cells to Gemcitabine by Targeting ABCB1. *EBioMedicine* 44, 403–418. doi:10.1016/j.ebiom.2019.05.013

Makaremi, S., Asadzadeh, Z., Hemmat, N., Baghbanzadeh, A., Sgambato, A., Ghorbaninezhad, F., et al. (2021). Immune Checkpoint Inhibitors in Colorectal Cancer: Challenges and Future Prospects. *Biomedicines* 9 (9), 1. doi:10.3390/biomedicines9091075

Matsuura, F., Oku, H., Koseki, M., Sandoval, J. C., Yuasa-Kawase, M., Tsubakio-Yamamoto, K., et al. (2007). Adiponectin Accelerates Reverse Cholesterol Transport by Increasing High Density Lipoprotein Assembly in the Liver. *Biochem. Biophys. Res. Commun.* 358 (4), 1091–1095. doi:10.1016/j.bbrc.2007.05.040

Messaggio, F., Mendonsa, A. M., Castellanos, J., Nagathihalli, N. S., Gorden, L., Merchant, N. B., et al. (2017). Adiponectin Receptor Agonists Inhibit Leptin Induced pSTAT3 and *In Vivo* Pancreatic Tumor Growth. *Oncotarget* 8 (49), 85378–85391. doi:10.18632/oncotarget.19905

Miao, X., Koch, G., Ait-Oudhia, S., Straubinger, R. M., and Jusko, W. J. (2016). Pharmacodynamic Modeling of Cell Cycle Effects for Gemcitabine and Trabectedin Combinations in Pancreatic Cancer Cells. *Front. Pharmacol.* 7, 421. doi:10.3389/fphar.2016.00421

Montano, R., Khan, N., Hou, H., Seigne, J., Ernstoff, M. S., Lewis, L. D., et al. (2017). Cell Cycle Perturbation Induced by Gemcitabine in Human Tumor Cells in Cell Culture, Xenografts and Bladder Cancer Patients: Implications for Clinical Trial Designs Combining Gemcitabine with a Chk1 Inhibitor. *Oncotarget* 8 (40), 67754–67768. doi:10.18632/oncotarget.18834

Mpilla, G. B., Philip, P. A., El-Rayes, B., and Azmi, A. S. (2020). Pancreatic Neuroendocrine Tumors: Therapeutic Challenges and Research Limitations. *World J. Gastroenterol.* 26 (28), 4036–4054. doi:10.3748/wjg.v26.i28.4036

Nigro, E., Daniele, A., Salzillo, A., Ragone, A., Naviglio, S., and Sapio, L. (2021). AdipoRon and Other Adiponectin Receptor Agonists as Potential Candidates in Cancer Treatments. *Int. J. Mol. Sci.* 22 (11), 5569. doi:10.3390/ijms22115569

Oba, A., Ho, F., Bao, Q. R., Al-Musawi, M. H., Schulick, R. D., and Del Chiaro, M. (2020). Neoadjuvant Treatment in Pancreatic Cancer. *Front. Oncol.* 10, 245. doi:10.3389/fonc.2020.00245

Okada, Y., Takahashi, N., Takayama, T., and Goel, A. (2021). LAMC2 Promotes Cancer Progression and Gemcitabine Resistance through Modulation of EMT and ATP-Binding Cassette Transporters in Pancreatic Ductal Adenocarcinoma. *Carcinogenesis* 42 (4), 546–556. doi:10.1093/carcin/bgab011

Panchal, K., Sahoo, R. K., Gupta, U., and Chaurasiya, A. (2021). Role of Targeted Immunotherapy for Pancreatic Ductal Adenocarcinoma (PDAC) Treatment: An Overview. *Int. Immunopharmacol* 95, 107508. doi:10.1016/j.intimp.2021.107508

Passacantilli, I., Panzeri, V., Terracciano, F., Delle Fave, G., Sette, C., and Capurso, G. (2018). Co-treatment with Gemcitabine and Nab-Paclitaxel Exerts Additive Effects on Pancreatic Cancer Cell Death. *Oncol. Rep.* 39 (4), 1984–1990. doi:10.3892/or.2018.6233

Qian, Y., Gong, Y., Fan, Z., Luo, G., Huang, Q., Deng, S., et al. (2020). Molecular Alterations and Targeted Therapy in Pancreatic Ductal Adenocarcinoma. *J. Hematol. Oncol.* 13 (1), 130. doi:10.1186/s13045-020-00958-3

Quiñonero, F., Mesas, C., Doello, K., Cabeza, L., Perazzoli, G., Jimenez-Luna, C., et al. (2019). The challenge of Drug Resistance in Pancreatic Ductal Adenocarcinoma: a Current Overview. *Cancer Biol. Med.* 16 (4), 688–699. doi:10.20892/j.issn.2095-3941.2019.0252

Rajendran, V., and Jain, M. V. (2018). *In Vitro* Tumorigenic Assay: Colony Forming Assay for Cancer Stem Cells. *Methods Mol. Biol.* 1692, 89–95. doi:10.1007/978-1-4939-7401-6_8

Ramzan, A. A., Bitler, B. G., Hicks, D., Barner, K., Qamar, L., Behbakht, K., et al. (2019). Adiponectin Receptor Agonist AdipoRon Induces Apoptotic Cell Death and Suppresses Proliferation in Human Ovarian Cancer Cells. *Mol. Cell Biochem* 461 (1–2), 37–46. doi:10.1007/s11010-019-03586-9

Riedl, J. M., Posch, F., Horvath, L., Gantschnigg, A., Renneberg, F., Schwarzenbacher, E., et al. (2021). Gemcitabine/nab-Paclitaxel versus FOLFIRINOX for Palliative First-Line Treatment of Advanced Pancreatic Cancer: A Propensity Score Analysis. *Eur. J. Cancer* 151, 3–13. doi:10.1016/j.ejca.2021.03.040

Robey, R. W., Pluchino, K. M., Hall, M. D., Fojo, A. T., Bates, S. E., and Gottesman, M. M. (2018). Revisiting the Role of ABC Transporters in Multidrug-Resistant Cancer. *Nat. Rev. Cancer* 18 (7), 452–464. doi:10.1038/s41568-018-0005-8

Ryu, W. J., Han, G., Lee, S. H., and Choi, K. Y. (2021). Suppression of Wnt/β-Catenin and RAS/ERK Pathways Provides a Therapeutic Strategy for Gemcitabine-Resistant Pancreatic Cancer. *Biochem. Biophys. Res. Commun.* 549, 40–46. doi:10.1016/j.bbrc.2021.02.076

Sapio, L., Nigro, E., Ragone, A., Salzillo, A., Illiano, M., Spina, A., et al. (2020). AdipoRon Affects Cell Cycle Progression and Inhibits Proliferation in Human Osteosarcoma Cells. *J. Oncol.* 2020, 7262479. doi:10.1155/2020/7262479

Singh, M. P., Rai, S., Pandey, A., Singh, N. K., and Srivastava, S. (2021). Molecular Subtypes of Colorectal Cancer: An Emerging Therapeutic Opportunity for Personalized Medicine. *Genes Dis.* 8 (2), 133–145. doi:10.1016/j.gendis.2019.10.013

Sung, H., Ferlay, J., Siegel, R. L., Laversanne, M., Soerjomataram, I., Jemal, A., et al. (2021). Global Cancer Statistics 2020: GLOBOCAN Estimates of Incidence and Mortality Worldwide for 36 Cancers in 185 Countries. *CA Cancer J. Clin.* 71 (3), 209–249. doi:10.3322/caac.21660

Tewari, D., Bawari, S., Sharma, S., DeLiberto, L. K., and Bishayee, A. (2021). Targeting the Crosstalk between Canonical Wnt/β-Catenin and Inflammatory Signaling Cascades: A Novel Strategy for Cancer Prevention and Therapy. *Pharmacol. Ther.* 227, 107876. doi:10.1016/j.pharmthera.2021.107876

Verret, B., Sourisseau, T., Stefanovska, B., Mosele, F., Tran-Dien, A., and André, F. (2020). The Influence of Cancer Molecular Subtypes and Treatment on the Mutation Spectrum in Metastatic Breast Cancers. *Cancer Res.* 80 (15), 3062–3069. doi:10.1158/0008-5472.CAN-19-3260

Vincent, V., Thakkar, H., Aggarwal, S., Mridha, A. R., Ramakrishnan, L., and Singh, A. (2019). ATP-binding Cassette Transporter A1 (ABCA1) Expression in Adipose Tissue and its Modulation with Insulin Resistance in Obesity. *Diabetes Metab. Syndr. Obes.* 12, 275–284. doi:10.2147/DMSO.S186565

Waissi, W., Amé, J. C., Mura, C., Noël, G., and Burckel, H. (2021). Gemcitabine-Based Chemoradiotherapy Enhanced by a PARP Inhibitor in Pancreatic Cancer Cell Lines. *Int. J. Mol. Sci.* 22 (13), 1. doi:10.3390/ijms22136825

Wang, Z., Tang, J., Li, Y., Wang, Y., Guo, Y., Tu, Q., et al. (2020). AdipoRon Promotes Diabetic Fracture Repair through Endochondral Ossification-Based Bone Repair by Enhancing Survival and Differentiation of Chondrocytes. *Exp. Cell Res.* 387 (2), 111757. doi:10.1016/j.yexcr.2019.111757

Wong, M. H., Xue, A., Baxter, R. C., Pavlakis, N., and Smith, R. C. (2016). Upstream and Downstream Co-inhibition of Mitogen-Activated Protein Kinase and PI3K/Akt/mTOR Pathways in Pancreatic Ductal Adenocarcinoma. *Neoplasia* 18 (7), 425–435. doi:10.1016/j.neo.2016.06.001

Xu, M., Li, L., Liu, Z., Jiao, Z., Xu, P., Kong, X., et al. (2013). ABCB2 (TAP1) as the Downstream Target of SHH Signaling Enhances Pancreatic Ductal Adenocarcinoma Drug Resistance. *Cancer Lett.* 333 (2), 152–158. doi:10.1016/j.canlet.2013.01.002

Zhi, Z., Hongxian, W., Baogui, S., and Qiuyan, D. (2011). Vcam-1 Promoted by Leptin Could Be Offset by Adiponectin through the Activation of Ampk via Adipor1 Receptor of Vecs in 3d Vessel Model. *Heart* 97, A32. doi:10.1136/heartjnl-2011-300867.91

Zhou, C., Qian, W., Ma, J., Cheng, L., Jiang, Z., Yan, B., et al. (2019). Resveratrol Enhances the Chemotherapeutic Response and Reverses the Stemness Induced by Gemcitabine in Pancreatic Cancer Cells via Targeting SREBP1. *Cell Prolif.* 52 (1), e12514. doi:10.1111/cpr.12514

Conflict of Interest: The authors declare that the research was conducted in the absence of any commercial or financial relationships that could be construed as a potential conflict of interest.

Publisher's Note: All claims expressed in this article are solely those of the authors and do not necessarily represent those of their affiliated organizations, or those of the publisher, the editors, and the reviewers. Any product that may be evaluated in this article, or claim that may be made by its manufacturer, is not guaranteed or endorsed by the publisher.

frontiers in Oncology

SYSTEMATIC REVIEW
published: 01 March 2022
doi: 10.3389/fonc.2022.834072

Modulation of TLR/NF-κB/NLRP Signaling by Bioactive Phytocompounds: A Promising Strategy to Augment Cancer Chemotherapy and Immunotherapy

Sajad Fakhri[1], *Seyed Zachariah Moradi*[1,2], *Akram Yarmohammadi*[3], *Fatemeh Narimani*[3], *Carly E. Wallace*[4] *and Anupam Bishayee*[4*]

[1] Pharmaceutical Sciences Research Center, Health Institute, Kermanshah University of Medical Sciences, Kermanshah, Iran, [2] Medical Biology Research Center, Health Technology Institute, Kermanshah University of Medical Sciences, Kermanshah, Iran, [3] Student Research Committee, Kermanshah University of Medical Sciences, Kermanshah, Iran, [4] College of Osteopathic Medicine, Lake Erie College of Osteopathic Medicine, Bradenton, FL, United States

OPEN ACCESS

Edited by:
Nand K. Roy,
Case Western Reserve University,
United States

Reviewed by:
Elancheran Ramakrishnan,
Annamalai University, India
Bertrand Liagre,
Université de Limoges,
France

***Correspondence:**
Anupam Bishayee
abishayee@lecom.edu;
abishayee@gmail.com

Specialty section:
This article was submitted to Pharmacology of Anti-Cancer Drugs, a section of the journal Frontiers in Oncology

Received: 12 December 2021
Accepted: 26 January 2022
Published: 01 March 2022

Citation:
Fakhri S, Moradi SZ, Yarmohammadi A, Narimani F, Wallace CE and Bishayee A (2022) Modulation of TLR/NF-κB/NLRP Signaling by Bioactive Phytocompounds: A Promising Strategy to Augment Cancer Chemotherapy and Immunotherapy. Front. Oncol. 12:834072. doi: 10.3389/fonc.2022.834072

Background: Tumors often progress to a more aggressive phenotype to resist drugs. Multiple dysregulated pathways are behind this tumor behavior which is known as cancer chemoresistance. Thus, there is an emerging need to discover pivotal signaling pathways involved in the resistance to chemotherapeutic agents and cancer immunotherapy. Reports indicate the critical role of the toll-like receptor (TLR)/nuclear factor-κB (NF-κB)/Nod-like receptor pyrin domain-containing (NLRP) pathway in cancer initiation, progression, and development. Therefore, targeting TLR/NF-κB/NLRP signaling is a promising strategy to augment cancer chemotherapy and immunotherapy and to combat chemoresistance. Considering the potential of phytochemicals in the regulation of multiple dysregulated pathways during cancer initiation, promotion, and progression, such compounds could be suitable candidates against cancer chemoresistance.

Objectives: This is the first comprehensive and systematic review regarding the role of phytochemicals in the mitigation of chemoresistance by regulating the TLR/NF-κB/NLRP signaling pathway in chemotherapy and immunotherapy.

Methods: A comprehensive and systematic review was designed based on Web of Science, PubMed, Scopus, and Cochrane electronic databases. The Preferred Reporting Items for Systematic Reviews and Meta-Analyses guidelines were followed to include papers on TLR/NF-κB/NLRP and chemotherapy/immunotherapy/chemoresistance by phytochemicals.

Results: Phytochemicals are promising multi-targeting candidates against the TLR/NF-κB/NLRP signaling pathway and interconnected mediators. Employing phenolic compounds, alkaloids, terpenoids, and sulfur compounds could be a promising strategy for managing cancer chemoresistance through the modulation of the TLR/NF-

κB/NLRP signaling pathway. Novel delivery systems of phytochemicals in cancer chemotherapy/immunotherapy are also highlighted.

Conclusion: Targeting TLR/NF-κB/NLRP signaling with bioactive phytocompounds reverses chemoresistance and improves the outcome for chemotherapy and immunotherapy in both preclinical and clinical stages.

Keywords: TLR - toll-like receptor, NF-κB – nuclear factor-kappa B, NLRP, phytochemicals, chemotherapy, immunotherapy, signaling pathways, molecular pharmacology

INTRODUCTION

Chemoresistance occurs when tumors mutate in response to cancer chemotherapy, yielding a more aggressive phenotype that results in chemotherapy failure (1). This has been a major obstacle in cancer chemotherapy and immunotherapy. Despite various attempts to overcome drug resistance and restore the sensitivity of chemotherapeutic drugs, the results thus far have been unsatisfactory (2). Several pathophysiological mechanisms and multiple dysregulated pathways are responsible for chemotherapy and immunotherapy resistance. Thus, revealing the critical dysregulated pathways in cancer chemoresistance would improve clinical outcomes and prevent/manage the development of chemoresistance, therefore limiting the progression and invasion of cancer (3). Amongst the dysregulated mediators, toll-like receptor (TLR) (4), nuclear factor-κB (NF-κB), and Nod-like receptor pyrin domain-containing (NLRP) (5), as well as the associated TLR/NF-κB/NLRP pathway, have been shown to contribute to cancer chemoresistance. In recent years, researchers have been seeking novel alternative agents with multiple targets, higher efficacy, and less side effects that can combat cancer chemoresistance.

Plant secondary metabolites are multi-targeting anticancer agents that target the cancer-associated pathways, including cellular senescence (6), Hippo signaling (7), Wnt/β-catenin (8), Janus kinase (JAK)/signal transducer and activator of transcription (STAT) (9), phosphoinositide 3-kinases (PI3K)/Akt/mammalian target of rapamycin (mTOR) (10), hypoxia-inducible factor-1α (HIF-1α) (11), and activator protein 1 (AP-1) (12). Phenolic compounds, alkaloids, terpenes/terpenoids, and sulfur-containing compounds demonstrated anticancer potential by modulating tumorigenic signaling pathways (6, 13). Emerging evidence has shown the influence of chemoresistance on cancer therapy (5, 14, 15). Although phytochemicals have exhibited critical regulatory roles in the modulation of TLR, NF-κB, and NLRP in combating cancer (16–18), there is no review report on the potential of phytochemicals in targeting TLR/NF-κB/NLRP pathway and pivotally interconnected pathways during chemoresistance. Thus, there is an imperative need to discover the precise dysregulated pathways involved in chemoresistance as well as to develop new strategies and alternative therapies to combat cancer chemoresistance. This is the first systematic and comprehensive review regarding crucial chemoresistance mechanisms and the therapeutic potential of plant secondary metabolites in combating cancer chemoresistance by targeting the TLR/NF-κB pathway and interconnected mediators. The need to develop novel phytocompound delivery systems to fight cancer chemoresistance is also highlighted.

RESISTANCE MECHANISMS IN CANCER CHEMOTHERAPY

Chemoresistance is one of the critical obstacles that affects the efficacy of anticancer drugs. Several factors contribute to the development of cancer chemoresistance. The most common cause of resistance to anticancer agents is the overexpression of energy-dependent transporters that export anticancer agents from the cancer cells (1). Consequently, decreased drug accumulation is another manner of chemotherapeutic resistance, which prevents drug-induced DNA damage and cancer cell apoptosis. Reduced sensitivity to drug-associated apoptosis plays a vital role in the resistance to anticancer drugs (19). Chemotherapy failure can be contributed in part to specific genetic and epigenetic alterations in addition to host factors. Cancer cells have a variety of genetic alterations depending on the tissue and patterns of oncogene activation and tumor suppressor gene inactivation. The use of powerful anticancer agents on cancer cells with these genetic factors leads to the development of drug-resistance mechanisms and the rapid achievement of chemoresistance in various cancer types. Host elements, such as rapid metabolism, poor absorption, and drug excretion, cause low serum levels of the drugs and thus a disposition towards chemoresistance. Host factors also reduce drug delivery to the tumor site, especially in solid bulky tumors with low cell penetration and high molecular weight. Additional mechanisms of cancer cell chemoresistance include receptor loss and mutations in the drug binding site (20).

The administration of various drugs has shown promising effects on chemotherapy with high cure rates by targeting multiple mechanisms of cell entrance. However, cancer cells may develop adaptations to resist these chemotherapeutic drugs, termed multidrug resistance (MDR). MDR strategies include reduced drug accumulation within the cancer cells, decreased uptake, increased efflux, and changes in the membrane lipid properties. These MDR mechanisms limit the apoptosis in cancer cells that are typically induced by anticancer agents, reduce DNA repair mechanisms, and dysregulate the cell cycle and checkpoints in cancer cells. An alternative method to overcome MDR is the use of combination therapy (21). Multidrug resistance proteins (MRPs) decrease the efficacy of

anticancer drugs and decrease drug penetration in cancer cells. An additional therapeutic approach involves identifying MDR biomarkers before or during the treatment program (22, 23).

Reduced drug uptake and cell surface molecule mutations are other drug resistance mechanisms. Methods of drug entry into cells includes endocytosis and receptor binding followed by internalization of the drug. An example of the later strategy includes immunotoxins. Cancer cells with defective endocytosis are resistant to immunotoxins and toxins (24, 25).

Drug efflux from cancer cells is accomplished through various pumps. For example, ATP-binding cassette (ABC) transporters [e.g., P-glycoprotein (P-gp)] play an essential role in drug-related clinical resistance. P-gp levels are increased in several cancers through typical molecular mechanisms and directly correlate with chemotherapy resistance (26). Thus, P-gp expressing cells develop in tumors following *in vivo* exposure to chemotherapeutic agents. In certain cancer types, elevated P-gp resulted in clinical relapse and decreased P-gp showed therapeutic potential. Accordingly, drugs transported by P-gp have a low chemotherapy response. Therefore, P-gp inhibitors have therapeutic potential in chemotherapy. Despite the high expression of P-gp in solid tumors (e.g., colon and renal cancer), no chemoresistance was shown, implying other methods of drug resistance are at work. Recent research has demonstrated the involvement of the ABC transporter multixenobiotic resistance (MXR) and MRPs in drug resistance. These results express the need to consider treatment with nonspecific inhibitors of ABC transporters or a cocktail of specific inhibitors with the broadest spectrum effect (27).

Another mechanism of chemoresistance is reduced intracellular drug activation and improved drug inactivation by phase I and/or II enzymes in the intestine, liver, and tumor (28). Cytochrome P450s (CYPs) are critical phase I metabolism enzymes that act as an oxidation catalyzer in many anticancer drugs. Genetic mutations in CYPs have shown significant effects on the toxicity and efficacy of anticancer agents that are primarily metabolized by CYPs. Carboxylesterase, deoxycytidine, cytidine deaminase, kinase, and epoxide hydrolase are enzymes involved in the detoxification and/or activation of some anticancer drugs. Mutations in these enzymes may alter their activity and play a role in the chemoresistance process. Cancer cells can become drug-resistant by decreasing drug activation through the reduction or mutation of kinases (29). The aforementioned dysregulated mechanisms that contribute to chemoresistance lead to rapid metabolism/excretion, poor tolerance and downstream oxidative stress, apoptosis/autophagy, and inflammation. **Figure 1** summarizes the major factors involved in cancer chemoresistance.

In addition to the above mechanisms, evasion of apoptosis/autophagy/necrosis is critical to tumor resistance. In any pathological condition, programmed cell death pathways, including apoptosis, and autophagy are the cause of death through intracellular pathways. Such cell death programs may cooperatively determine the fate of malignant neoplasms. Programmed necrosis and apoptosis always contribute to cell death, however, autophagy can play either pro-death or pro-survival roles (30). The mitochondrial (intrinsic) pathway and death receptor (extrinsic) pathway are two methods of apoptosis. Initiation of both pathways ultimately proceeds through caspase-related cascades. A group of cysteine proteases plays an important role in inflammation and apoptosis by cleaving a variety of nuclear and cytoplasmic mediators. Apoptotic caspases can be either initiator or executioner caspases. These include initiator caspase-2, caspase-8, caspase-9, and caspase-10 and executioner caspase-3, caspase-6, and caspase-7. In regard to the initiator caspases, CD95 (APO-1/Fas) and tumor necrosis factor (TNF)-related apoptosis-inducing ligand (TRAIL) are members of the TNF receptor superfamily of death receptors which recruits caspase-8, forming a multimeric complex at the plasma membrane that subsequently activates caspase-3. Caspase-8 causes the release of cytochrome c by increasing the permeability of the outer mitochondrial membrane through cleavage of Bid, a BH3-only protein, and translocation to the mitochondria (31, 32). Mitochondrial apoptosis-induced channel (MAC) also increases the release of cytochrome c, which activates caspase-3 through the creation of pro-caspase-9, apoptotic protease activating factor 1 (Apaf-1), and the apoptosome. The apoptosome converts pro-caspase-9 to its active form, caspase-9, which then activates caspase-3 (31). Apaf-1 forms an oligomeric apoptosome which determines the apoptotic pathway upon binding with ATP and cytochrome c. Such apoptotic pathways are controlled by various negative and positive regulators, which play a critical role in chemoresistance (33).

The B-cell lymphoma 2 (Bcl-2) family of proteins consists of anti-apoptotic and pro-apoptotic proteins. The former includes B-cell lymphoma-extra-large (Bcl-xL), Bcl-2, and myeloid-cell leukemia 1 (Mcl-1), while the latter includes Bcl-2-associated X protein (Bax), Bcl-2 homologous antagonist/killer (Bak), and BH3. Bak and Bax enhance the formation of MAC, while Mcl-1, Bcl-2, and Bcl-xL inhibit its formation (34). Apart from the established roles of Bak and Bax in apoptosis, the ratio of pro-apoptotic/anti-apoptotic proteins is what governs apoptosis, rather than individual protein expression. In cancer cells, the upregulation of anti-apoptotic mediators allows cells to evade apoptosis. This also allows cancer cells to escape apoptosis even when exposed to chemotherapeutic drugs, which would otherwise induce apoptosis in susceptible cells (35). Thus, dysregulation of the pro-apoptotic/anti-apoptotic protein ratio is another mechanism of chemotherapy resistance due to decreased apoptosis of cancer cells.

In cancer cells, the activities of both pro- and anti-apoptotic mediators are controlled by Jun amino terminal kinase (JNK) and p38-mitogen-activated protein kinase (MAPK). The latter increases p53 and apoptosis in chemoresistant cells through the protein kinase B (Akt)/Forkhead box O3 (FoxO) pathway. Insulin-like growth factor 1 suppresses apoptosis *via* casein kinase 2 and PI3K/Akt pathways, which in turn arrests Smac/DIABLO release and suppresses caspase activity (36). In addition, p53 mutations reduce chemoresistance through modulatory roles on mitochondrial function, leading to increased chemosensitivity. The overexpression of tissue

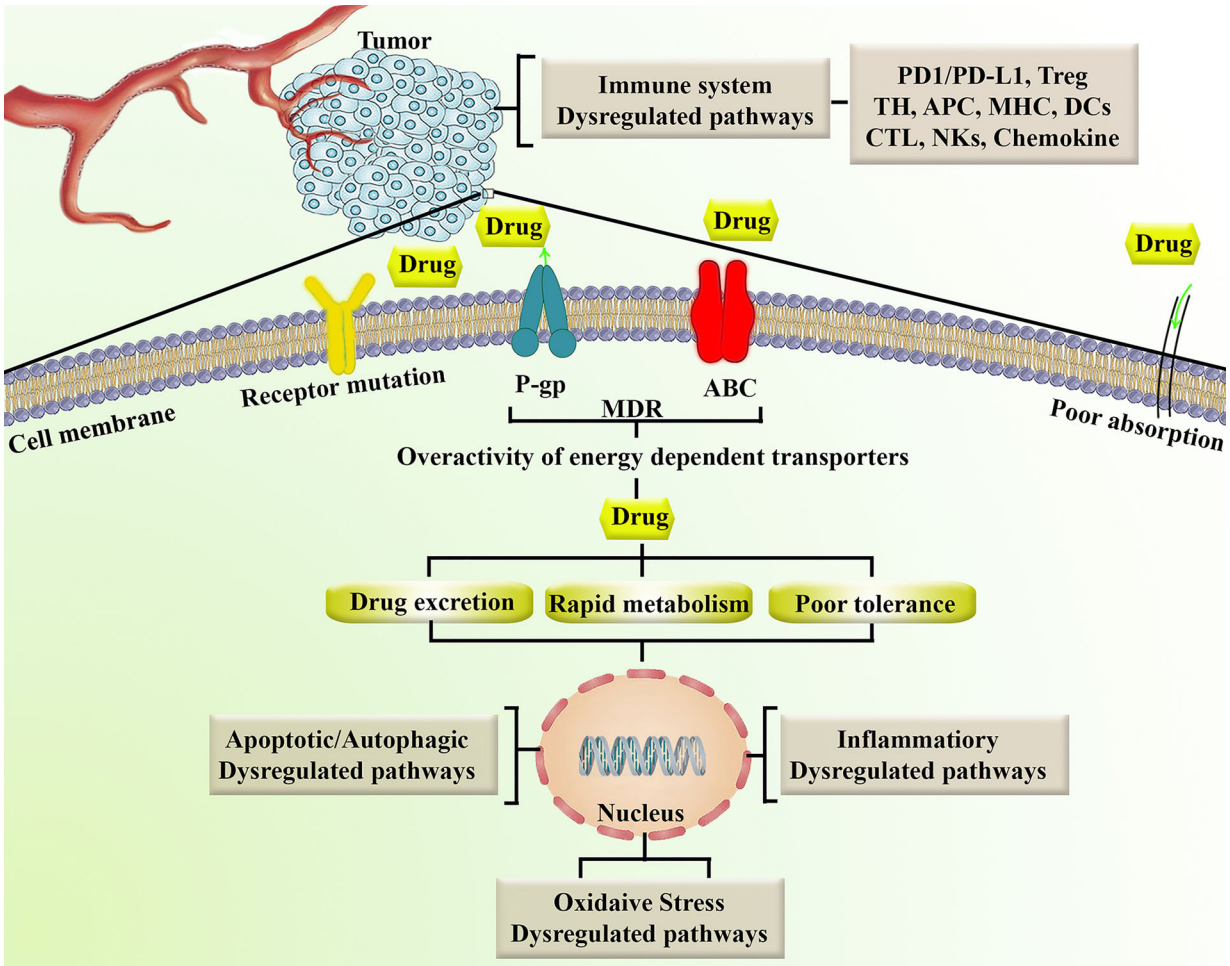

FIGURE 1 | Representation of major factors involved in chemoresistance. ABC, ATP-binding cassette; APC, antigen-presenting cell; CTL, cytotoxic T lymphocytes; DCs, Dendritic cells; MDR, multidrug resistance; MHC, major histocompatibility complex; NKs, natural killer cells; P-gp, P-glycoproyein; PD1/PD-L1, programmed cell death-1/programmed cell death-ligand 1; TH, T helper; Treg, T regulatory.

inhibitor of metalloproteinase-1 (TIMP) compromises chemotherapy response *via* NF-κB and PI3K/Akt signaling pathways (37). The actin-bundling protein, fascin, plays an important role in breast cancer chemoresistance by increasing the level of anti-apoptotic proteins and blocking the entry of the pro-apoptotic proteins caspase-3 and caspase-9 (37). Notch-1 and survivin are other signaling pathways that contribute to chemoresistance by activating targets involved in cell survival, thereby inhibiting apoptosis in tumor cells (38).

Other mechanisms of tumor resistance are related to dysregulated autophagy. Autophagy allows cells to regain ATP and vital biosynthetic factors in tumor microenvironments that are hypoxic and starved, promoting cancer cell survival. Autophagy acts as a critical modulator of intracellular hemostasis, tumor suppression, aging, cell death, and tumor chemoresistance (39). However, autophagy acts as a double-edged sword, as it also plays a role in the initiation, growth, development, and invasion of tumor cells. Accordingly, the PI3K/Akt/mTOR signaling pathway plays a crucial role in autophagy by modulating cell growth, cell survival, protein synthesis, motility, cell metabolism, cell death, and chemoresistance (39). This also downregulates the pro-apoptotic mediators Bim and Bad (40). Apoptotic mediators and autophagy are also regulated by upstream JNK and p38MAPK, thereby playing a vital role in modulating chemoresistance (41). Many anticancer drugs disrupt the balance between autophagy and apoptosis by altering the genetic/epigenetic phenotype and inhibiting PI3K/Akt/mTOR in cancer cells, thereby leading to the development of chemoresistance (41).

RESISTANCE MECHANISMS IN CANCER IMMUNOTHERAPY

Immunotherapy resistance is a primary and/or acquired resistance of tumor cells to immunotherapy (42). The inhibitors of programmed cell death-1/programmed cell death-

ligand 1 (PD-1/PD-L1) increase the release of interferon γ (IFN-γ) and upregulate the JAK/STAT signaling pathway. This activates IFN regulatory factor 8 (IRF8), causing hyperprogression (HPD) (43). HPD is a primary form of drug resistance (44) associated with mutations of epidermal growth factor receptor (EGFR) [33], murine double minute (MDM) gene (43), and chromosome 11 region 13 (43).

Attenuation of immune checkpoints potentially stimulates regulatory T cells (Tregs), creating an immunosuppressive microenvironment and modulating autoantigenicity antigen shedding or endocytic antigens to mediate immune escape (45). Such conditions trigger the polarization of immunosuppressive cells, such as M2 macrophages, antigen-presenting cells (APCs), and myelocytes, producing immunosuppressive cytokines. This also stimulates T helper type 1 (TH1) and TH17-mediated inflammatory conditions to upregulate oncogenic pathways and accelerate tumor growth and immunotherapy resistance (43, 46). Consequently, dendritic cells (DCs), B lymphocytes, monocyte-macrophages, and other APCs such as fibroblasts, endothelial cells, mesothelial cells, and epithelial cells are interconnected with tumor-specific antigen (TSA)/tumor-associated (TAA), conferring immunogenicity and T cell infiltration in tumors. Autophagy and the endoplasmic reticulum (ER) determine the tumor-associated immunogenicity of cell death (47). Dysregulation of antigen presenting signaling pathways, including mutations of the proteasome, transporters, and major histocompatibility complex (MHC), is cross-talked with T cell activity and tumor immune escape. MHC mutations are classified into structural defects, changes in the receptor-binding domain, and epigenetic changes (48). In some cancer types, tumor cells are able to escape lysis mediated by cytotoxic T lymphocytes (CTLs) and natural killer cells (NKs) through the overexpression of MHC-I. This allows tumor cells to escape the immune system (49).

The dysregulation of emerging signaling pathways in tumor cells is another mechanism of immunotherapy resistance. For instance, IFN-γ, produced by T cells and APCs, binds to related receptors to activate JAK2 (50). This leads to interaction with STAT1, which modulates downstream cascades. IFN-γ allows tumor cells to escape the immune system by increasing the expression of PD-L1 on the surface of tumor cells (51). IFN-γ also upregulates C-X-C motif chemokine ligand (CXCL)-9 and CXCL-10 chemokines and promotes antitumor immune cell effects (51). Additionally, IFN-γ exerts pro-apoptotic and antitumor properties through binding to cell surface receptors and triggering downstream mediators to suppress tumor cells (51). In patients receiving immunotherapeutic agents, tumor cells alter IFN-γ and JAK/STAT1 signaling pathways. Tumor analysis of chemoresistant patients receiving anti-cytotoxic T-lymphocyte-associated protein 4 (CTLA-4) agents had mutations in IFN-γ pathway genes, JAK1/2, and interferon regulatory factors (52). This allowed tumor cells to evade T cells, thus resisting the anti-CTLA-4 treatment. Loss of polybromo and BRG1-associated factors (PBAF) complex increased the ability of chromatin to regulate IFN-γ as well as increased production of CXCL-9/CXCL-10 to recruit T cells to tumor tissue (53). In human cancers, expression of Pbrm1 and Arid2 is correlated with the presentation of T cell cytotoxicity genes, leading to immunotherapy resistance (53).

Spranger et al. (54) demonstrated that the infiltration of T cells and recruitment of DCs into the total mesorectal excision (TME) could be suppressed by tumor-intrinsic β-catenin activation *via* decreased expression of CCL4. Because DCs prevent migration into epithelial-to-mesenchymal transition (EMT), no antigen can be presented to T cells, halting their cytotoxic effects. From another mechanistic point, upregulation of MAPK signaling damages the function and infiltration of tumor-infiltrating lymphocytes through the expression of vascular endothelial growth factor (VEGF) and cytokines such as interleukin-8 (IL-8) (55). Under these conditions, induction of Tregs ultimately leads to tumor immune evasion. Loss of tumor suppressor phosphatase and tensin homolog (PTEN) leads to activation of PI3K signaling, which is associated with increased anti-inflammatory cytokines, such as VEGF and C–C motif chemokine ligand 2 (CCL2), reduced infiltration of CD8+ T cells into tumors, and decreased IFN-γ expression, conferring resistance of PD-1 blockade therapy against tumors (56).

Tumor cells develop immunotherapy resistance by altering tumor cell metabolism through multiple metabolic changes, termed tumor metabolic reprogramming (57). One such mechanism utilizes aerobic glycolysis to create a hypoxic acidic environment which prevents normal metabolism of immune cells and impairs T cell function and infiltration (58). Furthermore, glucose consumed by tumor cells may restrict T cell metabolism, which leads to inhibition of mTOR, decreased glycolytic capacity in T cells, and production of intracellular IFN-γ (59).

TLR/NF-κB/NLRP SIGNALING PATHWAY IN CANCER INITIATION AND PROGRESSION AND CHEMORESISTANCE

TLRs are members of the type I transmembrane proteins and are conserved pattern-recognition receptors (PRRs) that are activated by various pathogen-associated molecular patterns (PAMPs). These membrane proteins are heavily expressed on the surface of several cells, including monocytes, macrophages, and DCs. The three constructional domains of TLRs' include a leucine-rich repeats (LRRs) motif, a transmembrane domain, and a cytoplasmic domain. Each of these domains have a specific function. For example, pathogen recognition is performed by the LRR motif, while signal initiation is performed by interaction of the TIR domain with the signal transduction adaptors. This receptor family is extremely important for pathogen recognition by the innate immune system (60, 61). Recently, several reports have indicated the association between cancer and TLRs. Specifically, the TLR4 signaling pathway is the most tightly linked with inflammatory response and cancer initiation and progression (16).

TLRs are involved in tumor progression, however they may display either anti- or pro-tumor metastasis and growth

features (62). Activation of TLR4 increased IL-6 and IL-8 production in breast cancer (63). In some cancers, TLR4 induced the production of nitric oxide and IL-6 (64). In prostate cancer cells, TLR4 activation enhanced the expression of transforming growth factor-β1 (TGF-β1) and VEGF, which promoted tumor progression (65). Some studies have shown poorer outcomes for breast, colon, and pancreatic cancers when TLR4 is overexpressed (63, 64). The myeloid differentiation factor 88 (MyD88) pathway of TLR4 has been shown to improve carcinogenesis. Yusef et al. (66) found that TLR4 demonstrated antitumor activity in skin cancer. The role of TLR4 should be further evaluated in various cancer types. Overall, these results suggest that the release of various inflammatory mediators, cytokines, and chemokines activates TLR4 and may participate in cancer formation.

TLRs are strong actuators of the inflammatory response, activation of which triggers the production of interferons, chemokines, cytokines, and NF-κB. The NF-κB pathway plays a crucial role in various diseases through regulation of cell proliferation, differentiation, immunity, and apoptosis (67). The NF-κB family consists of five crucial parts: p50, p52, p65/RelA, c-Rel, and RelA. NF-κB acts as a transcription factor by binding DNA, which activates gene transcription. Several genes involved in the progression and development of cancer are regulated by NF-κB, such as those involved in proliferation, apoptosis, and migration. Improper or constitutive NF-κB activation has been found in many malignant human tumors (68).

Typically, NF-κB is bound to IκB (IκB) in the cytoplasm. In times of stress, reactive oxygen species (ROS) and inflammatory stimuli degrade the IkB complex to activate NF-κB, releasing inflammatory cytokines such as tumor necrosis factor-alpha (TNF-α), IL-1, IL-6, and IL-2. This inflammatory cascade suppresses apoptosis and induces cellular invasion, proliferation, and metastasis, aiding in chemoresistance [52]. Prevailing reports have shown that activation of NF-κB by tumors assists in the development of chemotherapy resistance. NF-κB activation plays a key role in hindering the effectiveness of chemotherapeutic agents. Tumor cells exposed to chemotherapeutic drugs or radiation showed increased activation of NF-κB, which enforced the expression of MDR P-gp. Meanwhile, NF-κB suppression improved the apoptotic response to radiation therapy (69).

Members of the NLR family play an essential role in the signaling pathways of the innate immune system by activating or inhibiting inflammasomes. Damage-associated molecular patterns (DAMPs) and PAMPs activate NLRs and absent in melanoma 2 (AIM-2)-like receptors (ALRs), which bind to associated cytosolic domains to activate caspases. As a result, caspases upregulate IL-18 and IL-1β, which results in apoptosis and pyroptosis (70). On the other hand, dysregulation of NLR contributes to various autoimmune and inflammatory diseases. Thus, NLR can play a role in tumor suppression or tumor promotion in the initiation, development, and regression of cancer (71). Therefore, targeting the TLR/NF-κB/NLRP signaling pathway may facilitate improvement in the regulation of cancer initiation/progression and associated chemoresistance.

TLR/NF-κB/NLRP SIGNALING PATHWAY IN CANCER IMMUNOTHERAPY

TLRs are part of a family of recognition receptors which play a pivotal role in the host immune system (72–74). TLRs are expressed by B cells, macrophages, monocytes, NK cells, mast cells, neutrophils, and basophils. TLRs stimulate pro-inflammatory chemokines and cytokines to activate the innate and adaptive immune systems. The activation of TLR4 can induce associated adaptor proteins, including MyD88, TIR domain-containing adapter molecule 1 (TICAM1), TIR domain-containing adapter molecule 2 (TICAM2), and TIR domain-containing adaptor protein (TIRAP). Some ligands (e.g., lipopolysaccharides and toxins) bind TLRs to activate the immune response. According to Nagai et al. (75), the co-receptor myeloid differentiation factor-2 (MD-2) increased the translocation of TLR4 to form a heterotrimer of CD14/TLR4/MD-2 (76). This may lead to two distinct signaling pathways, the MyD88 pathway and the toll/IL-1R domain-containing adapter-inducing IFN-β (TRIF) pathway. Tumor necrosis factor receptor-associated factor 6 (TRAF6) activates extracellular signal-regulated kinase (ERK), MAPKs, and the p38 signaling pathway. Alternatively, TLR4 activates the MyD88-independent pathway to upregulate NF-κB and suppress IκB kinase epsilon (IKK). MyD88-dependent and MyD88-independent pathways also contribute to host defense and engage the immune response. In addition, TLRs activate IRFs, which increase the transcription of interferon-α (IFN-α) and interferon-β (IFN-β) (77). NLRP is the downstream mediator of NF-κB, which is interconnected with the inflammasomes. Inflammasomes are receptors/sensors of the innate immune system that regulate caspase-1 activation in response to host-derived proteins. Accordingly, NLRP activates apoptosis cascades which contributes to cancer chemoresistance. Overall, TLR/NF-κB/NLRP play critical roles in the development of cancer chemoresistance mediated by the attenuation of apoptosis, inflammation, oxidative stress, and autophagy. As shown in **Figure 2**, the immune system is also cross-talked with dysregulated major signaling pathways of chemoresistance.

METHODOLOGY FOR LITERATURE SEARCH ON THE EFFECT OF PHYTOCHEMICALS ON CHEMOTHERAPY AND IMMUNOTHERAPY RESISTANCE

We have performed a systematic review on vital mechanisms and the therapeutic potential of plant secondary metabolites in combating cancer chemoresistance utilizing the PRISMA guideline. Scholarly electronic databases, including Scopus, Science Direct, Cochrane, and PubMed, were used for the literature search. The search included all English language articles through October 30, 2021. The following keywords were used for the search: chemoresistance [full text] OR (cancer OR malignancy OR neoplasm OR melanoma OR leukemia OR carcinoma) [title/abstract] AND (nuclear factor kappa* OR

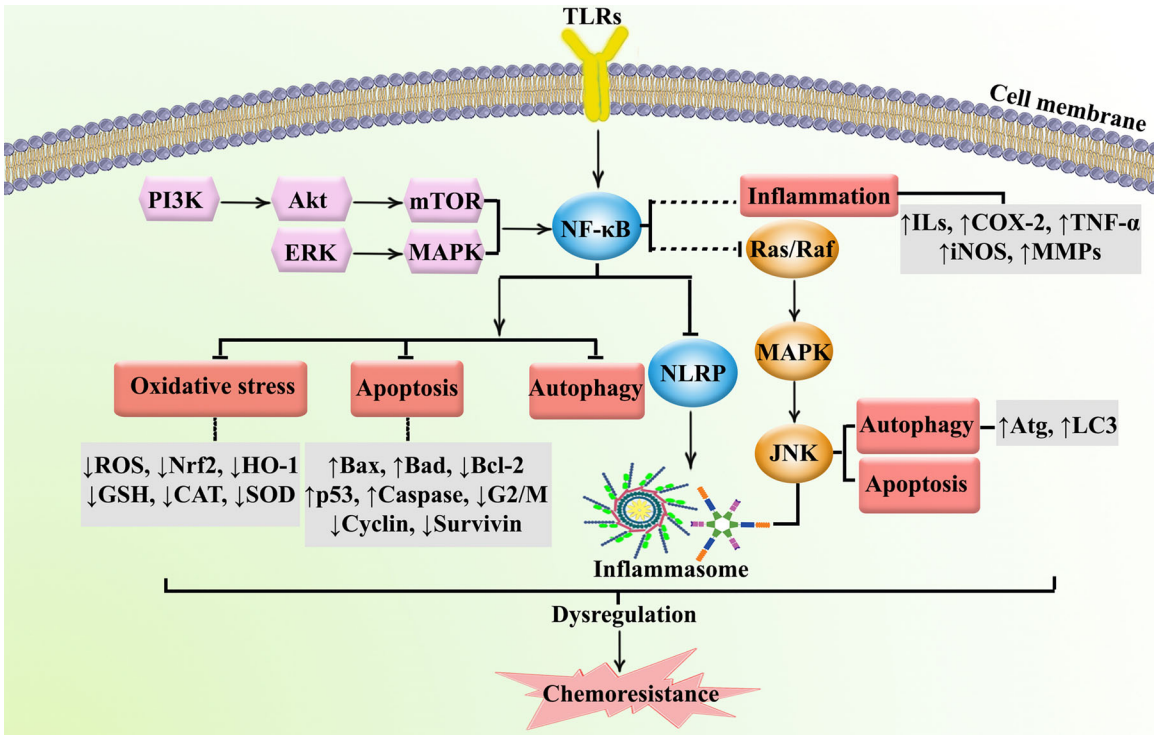

FIGURE 2 | Major dysregulated pathways in cancer chemoresistance. Atg, autophagy-related; CAT, catalase; COX-2, cyclooxygenase; ERK, extracellular-regulated kinase; GSH, glutathione; HO-1, heme oxygenase 1; ILs, interleukins; iNOS, inducible nitric oxide synthase; JNK, c-Jun N-terminal kinase; LC3, microtubule-associated protein 1A/1B-light chain 3; MAPK, mitogen-activated protein kinase; MMP, matrix-metalloproteinase; mTOR, mammalian target of rapamycin; NLRP, nod-like receptor pyrin domain-containing; Nrf-2, nuclear factor-erythroid factor 2-related factor 2; PI3K, phosphoinositide 3-kinases; ROS, reactive oxygen species; SOD, superoxide dismutase; TNF-α, tumor necrosis factor-α.

NF-κB OR toll-like* OR nod-like receptor* OR NLRP) AND (chemotherapy OR chemoresistance OR immunotherapy OR chemo-therapy OR chemo-resistance OR immune-therapy) [title/abstract] AND (herb OR plant OR natural product OR secondary metabolite OR polyphenol* OR terpen* OR alkaloid* OR flavonoid* OR glucosinolate* OR coumarin*). Two independent authors (S.F. and S.Z.M.) designed and applied the search strategy, which was finalized by the senior author (A.B.).

Of the initial 1392 articles, 205 articles were excluded due to duplicated results, 297 articles were excluded as they were review articles, 691 articles were excluded according to their title/abstract, 229 articles were excluded according to their full text information, and 4 articles were omitted since they were not in English. Ultimately, 267 articles were included in this systematic review. **Figure 3** depicts the PRISMA flowchart, which displays the literature search process and selection of relevant studies.

MULTI-TARGETING PHYTOCHEMICALS IN CANCER THERAPY

Plant secondary metabolites are potential modulators of multiple dysregulated pathways due to their various pharmacological properties, including antioxidant, anti-inflammatory, and anticancer effects (78, 79). An increasing number of pre-clinical and clinical studies have shown that chemopreventive agents may regulate the aforementioned dysregulated signaling pathways, such as TLR, NF-κB, and NLRP, thereby preventing or treating multiple cancer complications (16). Considering the critical role of TLR/NF-κB/NLRP in the progression of chemotherapy and immunotherapy resistance, discovering multi-targeting therapeutic agents could assist in combating cancer chemoresistance and immunoresistance. Several reports have addressed the potential of phytochemicals in the attenuation of TLR/NF-κB/NLRP. Therefore, phenolic compounds, alkaloids, terpenes/terpenoids, and sulfur compounds have been proposed as potential agents in the prevention and treatment of chemoresistance and immunoresistance.

PHYTOCHEMICALS AUGMENT CHEMOTHERAPY AND IMMUNOTHERAPY THROUGH TLR/NF-κB/NLRP PATHWAY

Phytochemicals may be used as alternative anticancer agents to prevent chemoresistance. This is made possible by surpassing the

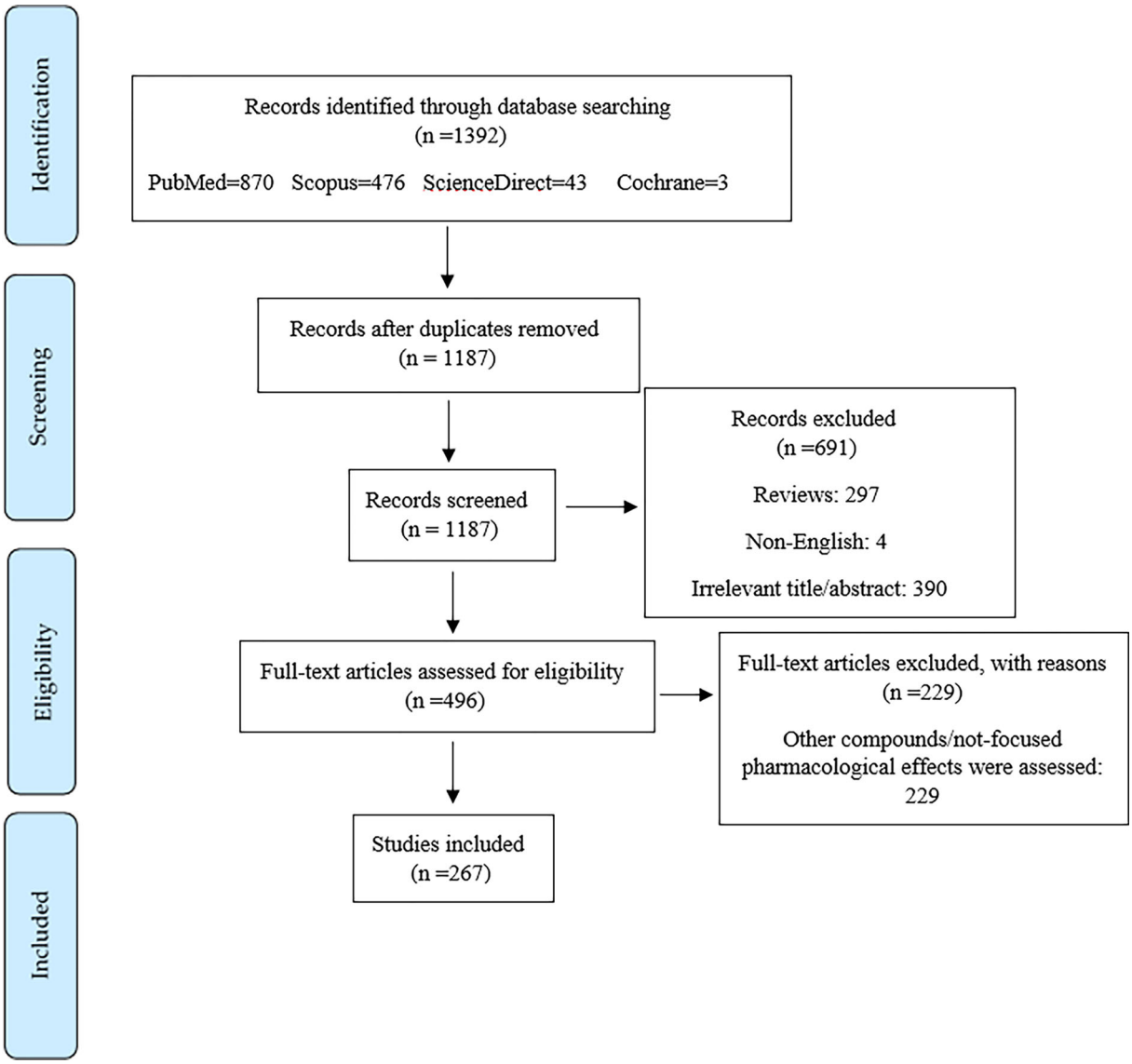

FIGURE 3 | PRISMA flowchart on the process of literature search and selection of relevant studies.

resistance barrier in multiple pathways, leading to increased effectiveness. Another benefit of utilizing phytochemicals is that they lower the dose frequency and thus the toxicity of chemotherapeutic agents. The principal mechanism of these phytochemical effects is through the inhibition or overexpression of certain proteins, enzymes, and other cancer cell metabolites.

Phenolic Compounds

Natural polyphenols are an important class of plant secondary metabolites that play an active role against different types of stress. The considerable volume of reported data proposed that diets rich in phenolic compounds could decrease the incidence of several cancers. Curcumin (**Figure 4**) is a well-known phytochemical with several important biological activities, including anticarcinogenic, neuroprotective, anti-inflammatory, and anti-SARS-CoV-2 effects (6, 13, 80–85). Curcumin suppressed the proliferation of MHCC97H liver cancer cells *in vitro* by promoting the formation of intracellular ROS, increasing apoptosis, and activating caspase-3, caspase-8, and TLR4/MyD-88 signaling (86). Furthermore, suppression of HSP70/TLR4 signaling was reported as another anticancer mechanism of curcumin in liver cancer (87). Curcumin also inhibited the growth of liver cancer *in vivo* and *in vitro via* diminished expression of inflammatory factors, such as cyclooxygenase-2 (COX-2), prostaglandin E2, IL-1β, and IL-6, as well as inhibition of the TLR4/NF-κB signaling pathway. Moreover, curcumin reduced VEGF, granulocyte-colony-stimulating factor (G-CSF),

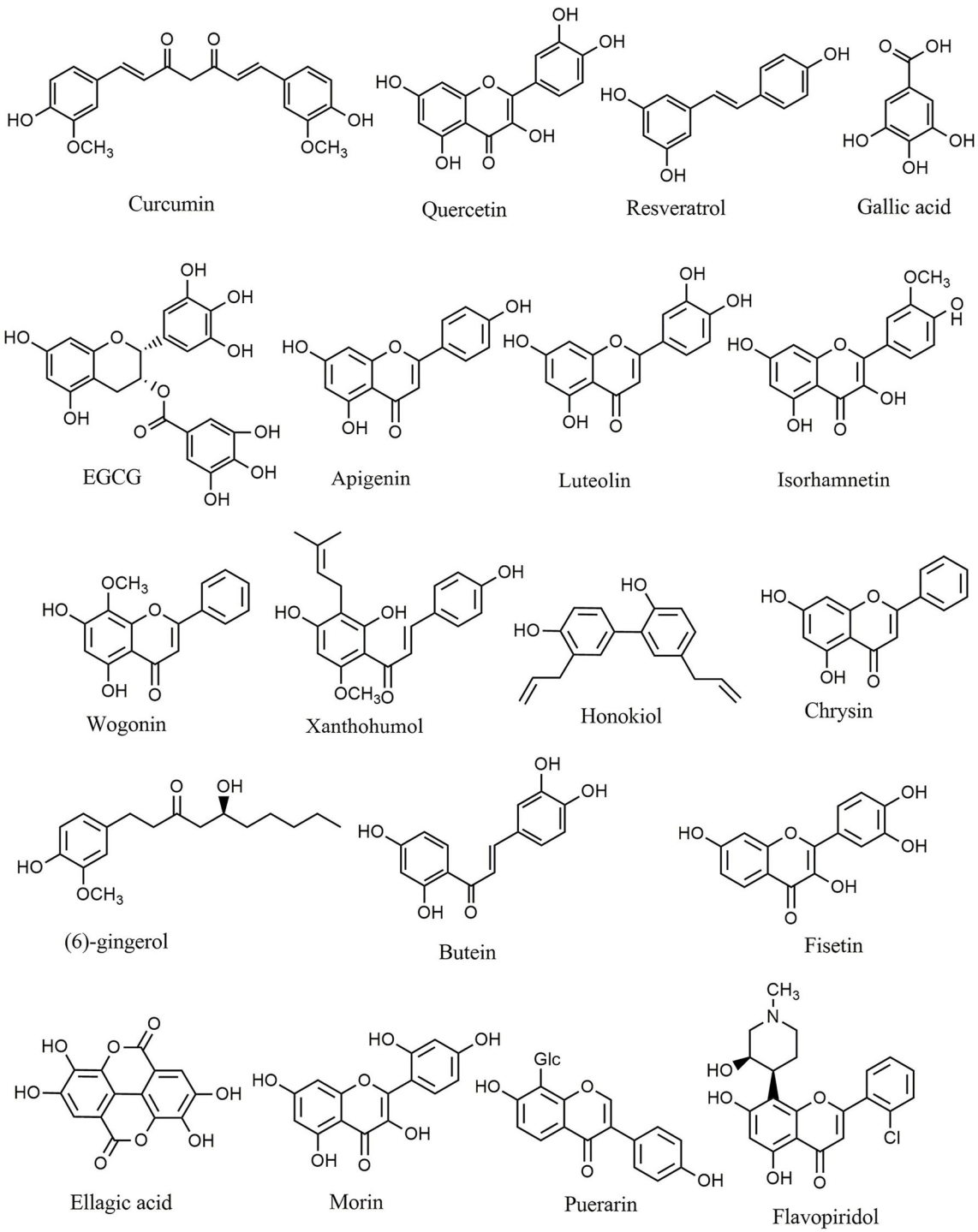

FIGURE 4 | Chemical structures of selected phenolic compounds that modulate the TLR/NF-κB/NLRP signaling in cancer.

and granulocyte–macrophage colony-stimulating factor (GM-CSF) (88). Additionally, curcumin decreased the migration and proliferation of non-small-cell lung cancer cell (NSCLC) cells *via* interfering with EGFR and TLR4/MyD88 pathways and increasing cell cycle arrest in the G2/M phase (89). Treatment with curcumin has also decreased the viability of MCF-7 and MDA-MB-231 breast cancer cells, activated TLR4/TRIF/IRF-3 signaling through the inhibition of IFN-α/β, and reduced the expression of TLR4 and IRF-3 (90). In a similar study, curcumin reduced cell proliferation, inhibited NF-κB, downregulated

cyclin D1, and modulated expression of TLR3 in head and neck squamous cell carcinomas (HNSCC) (91). Other reported antitumor mechanisms of curcumin include inhibition of NF-κB, cell cycle arrest, upregulation of E-cadherin, and modulation of Wnt/β-catenin signaling (92, 93). Deng et al. investigated the synergistic inflammatory and immunomodulatory activity of curcumin in combination with total ginsenosides for the treatment of HepG2 liver cancer cells in a BALB/c mice model. The results demonstrated that combination treatment inhibited the growth of liver cancer, reduced the expression of PD-L1, and suppressed the TLR4/NF-κB and NF-κB/matrix metalloproteinase-9 (MMP-9) signaling pathways (94). Curcumin exerts antineoplastic effects on various *in vitro* and *in vivo* cancer models, including lung (95), colorectal (96–98), bladder (99, 100), pancreatic (101, 102), and breast (103) cancers *via* interfering with the expression of TNF-α, HIF-1α, COX-2, VEGF, NF-κB, Axin2, IL-10, IL-8, and IL-6 and participating in the PI3K/Akt/mTOR/NF-κB/Wnt pathway. Additionally, curcumin promoted apoptosis, inhibited NF-κB, MMP-9, MMP-2, and MAPK, and activated sirtuin 1 (SIRT1) in HNSCC, osteoclastoma, and monocytic leukemia SHI-1 cancer cells (104–107). The known plant flavonoid quercetin is widely distributed in many vegetables, seeds, leaves, and grains and shows promising biological properties. Quercetin (**Figure 4**) and curcumin act synergistically together to promote apoptosis in K562 leukemia cells by interfering with the p53, TGF-α, and NF-κB pathways (108).

Resveratrol belongs to the stilbenoid group of polyphenols that exhibit high antioxidant and antitumor potential, which can be found in more than 70 plant species, particularly in grapes' seeds and skin. Resveratrol (**Figure 4**) and quercetin potentiated the antineoplastic activity of curcumin in myeloid, adenocarcinoma, and HNSCC cells (109–111). Resveratrol reduced dimethylbenz(a)anthracene (DMBA) induced cutaneous carcinogenesis both *in vitro* and *in vivo via* inhibition of angiogenesis. It was reported that TLR4 is a significant mediator involved in the chemoprevention achieved by resveratrol (112). Moreover, resveratrol diminished the inflammatory responses induced by lipopolysaccharide in SW480 and Caco-2 colon cancer cell lines by reducing the activation, expression, and production of inducible NO synthase (iNOS), mRNA, TLR4, and NF-κB (113). Furthermore, resveratrol suppressed the activity of COX, AMP-activated protein kinase (AMPK), PI3K/Akt/NF-κB pathway, DNA methyltransferase, and CYP1A1 in acute myeloid leukemia (AML), colon, and pancreatic cancer cells (114–116). In similar studies, resveratrol exerted substantial antineoplastic activity against multiple cancer cell lines, including melanoma (117), lung (118, 119), glioblastoma (120), head, neck (109), hepatocellular (121), colorectal (122), and breast (123) cancer cells by interfering with dicer-like 1 (DCL1)/translationally controlled tumor protein (TCTP), Akt/NF-κB, retinoblastoma protein (pRB), VEGF, AMPK, and $p21^{Waf1/Cip1}$ signaling pathways. Luteoloside (known as Cynaroside), 7-O-glucoside of luteolin, is a flavone agent that inhibited metastasis and proliferation of SNU-449, Hep3B, and mouse lung cancer cells through inhibition of caspase-1, NLRP3, and IL-1β (124).

Gallic acid is a natural antioxidant found in various fruits and tea leaves that belongs to the polyphenolic class of secondary metabolites. Various pharmacological effects of gallic acid include antioxidant, anti-inflammatory, and antineoplastic activities. There have been multiple studies which report that gallic acid (**Figure 4**) inhibited the progression of T24 and AGS gastric cancer cells *via* suppression of PI3K/Akt/NF-κB signaling and promotion of mitochondrial dysfunction (125, 126). Furthermore, quercetin inhibited the invasion and migration of Caco-2 cells *via* regulation of the TLR4/NF-κB pathway and decreasing MMP-2 and MMP-9 (127). In a similar study, inhibition of NF-κB, p53 induction, apoptosis, and cell cycle arrest were reported as the primary anticancer mechanisms of quercetin against the HeLa cervical cancer cell line (128). Additionally, quercetin showed antitumor activity against lung (A549 and H460) (129, 130), prostate (PC3 and LNCaP) (131), breast (MCF-7) (132), and oral SCC (133) cancer cells *via* induction of apoptosis and downregulation of IL-6/STAT-3 and NF-κB. The results demonstrated that combination of quercetin with chrysin suppressed the migration and invasion of nickel via downregulation of TLR4/NF-κB signaling in human lung cancer cells *in vitro* (134). Octyl gallate exerted significant efficacy against heat shock protein 90α (HSP90α) levels, eHSP90α–TLR4 ligation, M2-macrophages, and tumor growth in a pancreatic ductal adenocarcinoma mouse model (135).

Moreover, several studies have been performed to investigate the various biological effects of epigallocatechin 3-gallate (EGCG), a powerful polyphenolic isolated from green tea. EGCG showed significant anti-inflammatory, antioxidant, anticancer, and neuroprotective potential in different studies. Treatment with EGCG (**Figure 4**) downregulated the expression of NLRP1, caspase-1, and IL-1β in the melanoma cell lines HS294T and 1205Lu (136). The main antineoplastic mechanisms of EGCG includes inhibition of TNF-α and tissue factor expression (137), activation of forkhead box O3 (138), downregulation of Her-2/Neu signaling (139), decreased expression of IL-1RI (140), and modulation of MMP-2 activity (141). Furthermore, EGCG induced apoptosis and suppressed cancer cell proliferation in nasopharyngeal (142), bladder (143), hepatocellular (144), breast (145), and colon (146) cancers.

Similarly, apigenin is another polyphenolic substance with significant anticancer potential *via* modulating different signaling pathways *in vitro* and *in vivo*. Treatment with apigenin induced apoptosis, suppressed glycogen synthase kinase-3 (GSK-3)/NF-κB, and downregulated Bcl-xL, CCL2, CXCL-8, IL1A, Bcl-2, and VEGF in pancreatic (PANC-1 and BxPC-3) (147), prostate (PC-3) (148, 149), and breast (MDA-MB-231) cancer cells (150), as well as the athymic nu/nu nude (151) and TRAMP mice (152) cancer models. In addition to apigenin, luteolin (**Figure 4**) has significant anticancer properties. Luteolin interfered with the PI3K/Akt/NF-κB/Snail and MAPK pathways in the gastric adenocarcinoma cell line CRL-1739, the lung cancer cell line A549, and the AML cell line THP-1 (153–155). Additionally, luteolin 8-C-b-fucopyranoside

suppressed secretion of MMP-9, IL-8, ERK/NF-κB, and ERK/AP-1 signaling in MCF-7 cancer cells *in vitro* (156). The *in silico* evaluations also showed that luteolin and other plant-derived secondary metabolites (e.g., myricetin, quercetin, apigenin, and baicalein) displayed anticancer properties *via* the estrogen receptor-α (157).

Isorhamnetin (**Figure 4**) is another polyphenolic compound that induced apoptosis and inhibited proliferation of lung (158) and breast (159) cancer cells by interfering with IL-13, NF-κB, MAPK, and Akt signaling. Similarly, wogonin (**Figure 4**) promoted apoptosis and suppressed the invasion and proliferation of chronic lymphocytic leukemia and the liver cancer cell lines Bel7402 and HepG2 by interfering with ERK/AKT, NF-κB/Bcl–2, and EGFR signaling pathways (160, 161). Another polyphenolic structure, xanthohumol (**Figure 4**), appears to have anticancer properties *via* significantly suppressing the angiogenesis, proliferation, and production of inflammatory mediators in breast cancer xenografts (162). Xanthohumol also reduced the expression of CXCR4 and inhibited cancer cell invasion (163). Similarly, p-hydroxycinnamic acid facilitated cell cycle arrest and suppressed the growth and migration of MDA-MB-231 cells *via* downregulation of NF-κB (164). The flavonoid wogonoside demonstrated anticancer effects *in vitro* against MCF7 and MDA-MB-231 cancer cells through inhibition of migration, invasion, and TRAF-2/TRAF-4 expression (165). In similar studies, inhibiting COX-2, EGFR, NF-κB, and the ERK pathway is the main anticancer mechanism of scutellarein in A549 cells (166). Likewise, hydroxysafflor yellow A (167), rosmarinic acid (168, 169), and magnolol (170) diminished the progression of hepatocellular carcinoma *in vitro* and *in vivo* by suppressing ERK/MAPK, ERK/NF-κB, and NF-κB signaling. Lung cancer cells treated with hexamethoxy flavanone-o-[rhamnopyranosyl-(1→4)-rhamnopyranoside, a flavonoid glycoside compound isolated from *Murraya paniculata* (171), hesperetin (172), honokiol (**Figure 4**) (173, 174), and inotilone (174) had higher levels of apoptosis-related mediators and attenuated activity of EGFR, PI3K/Akt/MAPK, and STAT3/NF-κB/COX-2 signaling pathways. Investigation into the effects of eupatilin (175, 176), polysaccharide krestin (177), tilianin (178), silibinin (179–181), chrysin (**Figure 4**) (182–186), (6)-gingerol (**Figure 4**) (187), and butein (**Figure 4**) (188) against gastric, breast, ovarian, pharyngeal squamous, prostate, renal, myeloid leukemia, and T cell leukemia/lymphoma cancer cells *in vitro* and *in vivo* demonstrated that these polyphenolics exert significant effects *via* attenuation of angiogenesis, Akt, tumor growth, AP-1, NF-κB, and TLR4.

Fisetin (**Figure 4**) (189–194), gallotannin (195), astragalin (196–198), ellagic acid (**Figure 4**) (199–201), morin (**Figure 4**) (202, 203), flavopiridol (**Figure 4**) (204), puerarin (**Figure 4**) (205), icariin (206), acteoside (207), and acacetin (208, 209) are some of the other polyphenolic agents that inhibited the proliferation and invasion of breast, prostate, hepatocellular, myeloma, and colon cancer cells *via* increased apoptosis and inhibition of TNF-α, iNOS, NF-κB, COX-2, JAK/STAT3, Akt, and IL-6 mediators and signaling pathways.

In further studies, eriodictyol (210, 211), calycosin (212), cudraflavone B (213), protocatechualdehyde (214), and naringin (215) exerted significant antitumor effects against several cancers including breast (MDA-MB-231), glioblastoma (A172, CHG-5, and U87 MG), ovarian (SKOV3), and liver (HepG2) cancer cells by promoting senescence, apoptosis, and interfering with GSK-3β, TGF-β1, SMAD2/3, SLUG, vimentin, β-catenin, NF-κB, COX-2, and cyclin D1, amongst other enzymes and signaling pathways.

In summary, polyphenols play a significant role in the prevention and treatment of cancer. Curcumin, apigenin, quercetin, and resveratrol are the most important polyphenols with reported information on their mechanisms of action and clinical trials. In several reported studies, polyphenols can interfere with a variety of anticancer pathways, including TLR/NF-κB/NLRP and interconnected pathways. Consequently, polyphenols could be considered promising treatment options in conjunction with other cancer treatment strategies. **Table 1** provides the various anticancer phenolic compounds that interfere with the TLR/NF-κB/NLRP pathway to combat chemoresistance.

Terpenes and Terpenoids

Terpenes and terpenoids represent large classes of natural products isolated from multiple vegetative sources. These phytochemicals exert several therapeutic effects, including anticancer, cardioprotective, neuroprotective, and hepatoprotective activities. Each terpene/terpenoid compound is composed of several isoprenes (a five-carbon unit) that are assembled in thousands of ways. Zerumbone (**Figure 5**), an important sesquiterpene isolated from ginger, suppressed lung and colon tumors in mice *via* induction of apoptosis and inhibition of proliferation, heme oxygenase 1 (HO-1), and NF-κB expression (216). Andrographolide (**Figure 5**) is a bioactive phytochemical obtained from *Andrographis paniculata* that belongs to the diterpenoid compounds. Likewise, andrographolide showed antitumor activity against B16 melanoma cells, C57BL/6J mice (217), and RIP1-Tag2 mice (218) *via* suppression of TLR4/NF-κB signaling, thereby reducing the expression of CXCR4 and Bcl-6. Additionally, treatment with andrographolide inhibited the proliferation of SW620 colon cancer cells *in vitro via* interfering with the TLR4/NF-κB/MMP-9 signaling pathway (219).

Carnosic acid (**Figure 5**), one of the principal phenolic diterpenes isolated from rosmarinus officinalis, possesses antimicrobial, antioxidative, and anti-carcinogenic properties. Carnosic acid nanoparticles induced apoptosis in Bel7402 and MHCC97-H hepatic carcinoma cell lines *in vitro via* suppression of NF-κB, caspase-3, TLR4, MyD88, TRAF-6, interleukin 1 receptor associated kinase 1 (IRAK-1), and IRAK-4 (220). Similarly, triptolide (**Figure 5**) is an active natural phytochemical isolated from *Tripterygium wilfordii* Hook F that exhibits a wide range of pharmacological effects, including anti-diabetic, neuroprotective, anti-inflammatory, and antitumor activities. Triptolide is a well-known diterpenoid that blocks the NF-κB survival pathways and activates ERK1/2 and p38a in PC3 cancer cells (221). Additionally, triptolide decreased the expression of MMP-9, AP-1, and NF-κB signaling pathways in MCF-7 cells (222) and attenuated the angiogenesis and invasion of thyroid

TABLE 1 | Anticancer phenolic compounds interfering with the TLR/NF-κB/NLRP pathway and cross-talked mediators against chemoresistance.

Compound	Types of study	Cell line(s)/tumor model(s)	Mechanisms of action	References
Curcumin	*In vitro*	Hepatocellular carcinoma cells (MHCC97H)	↑ROS/TLR4/caspase pathway; ↓cell proliferation; ↑apoptosis; ↑ROS formation; ↑caspase-8; ↑caspase-3	(86)
	In vitro	Hepatocellular carcinoma cells (HepG2)	↓TLR4; ↓proliferation; ↓invasion; ⊥ S phase cell cycle; ↑apoptosis; ↓HSP70; ↓EHSP70	(87)
	In vitro and *in vivo*	Human liver cancer cells (HepG2, MHCC–97H, and huh–7); Xenograft model mice	↓TLR4/NF–κB; ↓VEGF; ↓COX-2; ↓PGE2; ↓IL–1β; ↓IL–6	(88)
	In vitro	Lung adenocarcinoma cells (H226, NSCLC, NCI–A549, NCI –H226)	↓TLR4/MyD88; ↓migration; ↓proliferation; ↓EGFR; ⊥G2/M phase cell cycle	(89)
	In vitro	Breast cancer cells (MDA-MB-231, MCF-7)	↑TLR4/TRIF/IRF-3; ↓IFN-α/β; ↓TLR4; ↓IRF-3	(90)
	In vitro	Head and neck squamous cell carcinomas (HNSCC)	↓NF-κB; ↓TLR3; ↓proliferation; ↓cyclin D1	(91)
	In vitro	Nasopharyngeal carcinoma cells (HK1 and HONE1)	↓NF-κB; ↑E-Cadherin	(93)
	In vitro	Human mantle cell lymphoma	↓NF-κB; ⊥G1/S phases cell cycle; ↓IKK; ↓phosphorylation of IκBα and p65	(92)
	In vitro and *in vivo*	Human liver cancer cell (HepG2); Male nude mice models of liver cancer	↓TLR4/NF-κB; ↓Tregs; ↓MMP-9; ↓PD-L1; ↓NF-κB/MMP-9	(94)
	In vitro and *in vivo*	Lung cancer cell (A549); BALB/c nude mice	↓NF-κB; ↓tumor growth; ↓Notch-1; ↓HIF-1; ↓VEGF	(95)
	In vivo	C57BL/6 male mice	↓Wnt/β–catenin; ↓Axin2; ↓tumor number; ↓Tumor size; ↓β–catenin; ↓cell proliferation	(97)
	In vivo	A/J mice model	↓NF-κB; ↓Cell proliferation; ↓PI3K/Akt/mTOR; ↓AMPK	(96)
	In vitro	Colorectal carcinoma cell (HCT–116)	↓NF-κB	(98)
	In vitro	Albino rats' model of bladder cancer	↓NF-κB; ↓Bcl-2; ↓IL-6; ↓P65	(99)
	In vitro and *in vivo*	Human bladder cancer cell (T24, UMUC3); Male nude mice	↓NF-κB p65; ↓IKKκ/NF-κB/COX-2; ↓COX-2 expression; ⊥ G2/M phase cell cycle; ↓CDK1; ↓cyclin A; ↓cyclin B; ↓cyclin D1;	(100)
	Clinical trials	Patients with advanced pancreatic cancer	↓NF-κB; ↓COX-2; ↓pSTAT 3	(102)
	In vitro	Pancreatic cancer cells (Su86.86, PL8, Panc1, BxPC3, MiaPaca2, E3LZ10.7, and Capan1, PL5)	↓NF-κB; ↑apoptosis; ↓IL-6; ↓IL-8; ↓TNF-α	(101)
	In vitro	Breast cancer cell (MCF-7)	↓NF-κB; ↓MMP; ↓AP-1; ↓PKCα; ↓MAPK	(103)
	In vitro	HNSCC cell (FaDu and Cal27)	↓NF-κB; ↑caspase-9; ↑caspase-8; ↑ATM/CHK2	(105)
	In vitro	Monocytic leukemia cell (SHI-1)	↓NF-κB; ↓Bcl-2; ↓ERK; ↑p38 MAPK; ↑JNK; ↑caspase-3; ↓MMP-2; ↓MMP-9	(106)
	In vitro and in vivo	SCID mice; Acute monocytic leukemia SHI-1 cells	↓NF-κB and ERK; ↓PCNA; ↑cleaved caspase-3; ↑p38 and JNK; ↓MMP-2 and MMP-9	(107)
	In vitro	Human osteoclastoma cell (GCT cells)	↑Apoptosis; ↓NF-κB; ↑caspase-3; ↓MMP-9; ↑JNK	(104)
Curcumin & Quercetin	*In vitro*	Chronic myeloid leukemia (CML) (K562)	↓NF-κB; ↑apoptosis; ↓IFN-c; ↓AKT1; ↓CDKN1B; ↑p21 $^{Waf1/cip1}$; ↑FasL; ↑Fas	(108)
Curcumin & Quercetin	*In vitro*	CML cell (K562/CCL-243)	↑BTG2; ↑CDKN1A; ↑FAS; ↓CDKN1B; ↓AKT1; ↓IFN-c; ↑p21 $^{Waf1/cip1}$	(111)
Curcumin & Quercetin	*In vitro*	Human melanoma cell (A375)	↓Cell proliferation; ↓Wnt/β-catenin; ↓DVL2; ↓cyclin D1; ↓COX2; ↓Axin2; ↓BCL2; ↑caspase 3/7; ↑PARP cleavage	(110)
Curcumin & Resveratrol	*In vitro* and *in vivo*	HNSCC; BALB/c mice	↓NF-κB; ↑PARP-1 cleavage; ↑Bax/Bcl-2 ratio; ↓ERK1; ↓ERK2 phosphorylation	(109)
Resveratrol	*In vivo*	Female C3H/HeN mice	↓Angiogenesis; ↓MMP-2; ↓MMP-9; ↑IL-12	(112)
	In vitro	Human colon adenocarcinoma cells (SW480, Caco-2)	↓NF-κB; ↓TLR4 expression; ↓NO; ↓iNOS;	(113)
	In vitro	Colon cancer cell (HCT-116 and SW-480)	↓NF-κB; ↓CYP1A1 activity; ↓DNA methyltransferase; ↓COX; ↓cytokine production; ↓AMPK	(116)
	In vitro	Pancreatic cancer cell (BxPC-3 and Panc-1)	↓PI3K/Akt/NF-κB; ↓cell proliferation; ↓cell migration; ↓cell invasion; ↓p-Akt; ↓p-NF-κB	(115)
	In vitro	Acute myeloid leukemia cell (OCI/AML3, OCIM2)	↓NF-κB; ↓cell proliferation; ⊥S phase cell cycle; ↑apoptosis	(114)
	In vitro	Melanoma cell line (LU1205, LU1205, 1205lu, FEMX, WM35, WM793, HHMSX, OM431, WM9, LOX)	↓NF-κB; ↓STAT3; ↓cFLIP; ↓Bcl-XL	(117)
	In vitro	Human lung carcinoma (A549, HCC-15)	↓NF-κB; ↓p-Akt; ↓Bcl-2; ↓Bcl-XL	(119)
	In vitro	Human lung carcinoma (A549)	↓NF-κB; ↓pRB; ↓p21$^{Waf1/Cip1}$; ↑Apoptosis;	(118)
	In vitro	Glioblastoma cell (T98G)	↓NF-κB; ↓MGMT	(120)

(Continued)

TABLE 1 | Continued

Compound	Types of study	Cell line(s)/tumor model(s)	Mechanisms of action	References
	In vitro and *in vivo*	BALB/c mice; HNSCC (CAL-27, SCC-15)	↓NF-κB; ↑PARP-1 cleavage; ↑Bax/Bcl-2 ratio; ↓ERK1; ↓ERK2 phosphorylation	(109)
	In vitro and *in vivo*	Hepatocellular carcinoma cells HepG2 cells; Xenograft models	↓NF-κB; ↓VEGF	(121)
	In vitro	Colorectal cancer cell (HCT116/L-OHP)	↓NF-κB; ↓cAMP; ↓MDR1; ↓NF-κB; ↓p-IκBα; ↓MDR1; ↑pAMPK	(122)
	In vitro	Human liver cancer cell (HepG2); Breast cancer cell (MDA-MB-231)	↓JNK/NF-κB; ↑DLC1 and ↓TCTP; ↓N-WASP; ↑Cdc42	(123)
Luteoloside	*In vitro and in vivo*	Mouse lung metastasis model; Hepatocellular carcinoma cell (SNU-449, Hep3B)	↓NLRP3; ↓cleavage of caspase-1; ↓IL-1β	(124)
Gallic Acid	*In vitro*	Human bladder cancer cells (T24)	↓PI3K/Akt/NF-κB; ↑apoptosis; ↑cleaved caspase-3; ↑Bax, P53; ↑cyt c; ↓Bcl-2; ↓p-PI3K; ↓pAkt; ↓p-IkBa; ↓p-IKKa; ↓p-NF-κB p65	(126)
	In vitro	Human gastric cancer cell (AGS)	↓NF-κB; ↓MMP-2/9	(125)
Quercetin	*In vitro*	Human colon adenocarcinoma cell (Caco-2)	↓TLR4/NF-κB; ↓migration; ↓Invasion; ↓MMP–2; ↓MMP –9	(127)
	In vitro	Human cervical cancer cell (HeLa)	↓NF-κB; ↑p53; ↑apoptosis; ⊥ G2/M cell cycle arrest; ↑Bcl-2; ↑cyt c; ↑Apaf-1	(128)
	In vitro	Lung cancer cell (A549)	↓NF-κB; ↓IL-6/STAT-3; ↓IL-6; ↑Apoptosis	(130)
	In vitro	Lung cancer cells (H460)	↓NF-κB; ↑apoptosis; ↑TRAILR; ↑caspase-10; ↑DFF45; ↑TNFR 1; ↑FAS; ↑DNA damage	(129)
	In vitro	Breast cancer cells (MDA-MB-231, MCF-7)	↑Apoptosis; ↓Hsp27, Hsp70 and Hsp90;	(132)
	In vitro	Oral squamous cell carcinoma (OSCC)	↓NF-κB; ↓tumor incidence; ↑apoptosis; ↓Bcl-2; ↓Bax	(133)
	In vitro	Prostate cancer cells (PC3, LNCaP)	↓NF-κB; ↓PI3K/Akt; ↓MAPK/ERK; ↑apoptosis; ⊥G1 phase cell cycle arrest; ↓P38; ↓ABCG2	(131)
Quercetin and chrysin	*In vitro*	Human lung adenocarcinoma cell (A549)	↓TLR4/NF-κB	(134)
Octyl Gallate	*In vitro* and *in vivo*	Adenocarcinoma cell (AsPC-1, Panc 02); Monocytic leukemia cell (THP-1); Male C57BL/6 mice	↓EHSP90α–TLR4 ligation; ↓HSP90α level; ↓M2-macrophages; ↓tumor growth	(135)
EGCG	*In vitro*	Human melanoma cell (1205Lu and HS294T)	↓NLRP1; ↓caspase-1; ↓IL-1β	(136)
	In vitro	Monocytic leukemia cell (THP-1)	↓TLR4; ↓NF-κB; ↓tissue factor; ↓TNF-α; ↓p-p38; ↓ERK1/2; ↓JNK	(137)
	In vitro	Breast cancer cell (NF639)	↓NF-κB; ↓colony growth; ↓Cell invasion; ↓protein kinase CK2	(138)
	In vitro	Breast cancer cell (SMF, NF639)	↓NF-κB; ↓Her-2/Neu signaling; ↓Cell growth; ↓PI3K; ↓Akt; ↓cell proliferation	(139)
	In vitro	Pancreatic adenocarcinoma cell (Colo357)	↓NF-κB; ↓IL-1RI; ↑apoptosis	(140)
	In vitro and *in vivo*	Breast cancer cell (MCF-7)	↓NF-κB; ↓MMP-2; ↓FAK; ↓MT1-MMP; ↓VEGF	(141)
	In vitro and *in vivo*	Bladder cancer cells (SW780); Xenograft mice	↓NF-κB; ↓MMP-9	(143)
	In vitro and *in vivo*	Nude mice; Hepatocellular carcinoma cells (HepG2, Huh-7, PLC/PRF/5)	↓NF-κB; ↓Bcl-2; ↓Bcl-XL	(144)
	In vitro and *in vivo*	Breast cancer cell (4T1); BALB/c mice	↓MDSCs; ↓Arg-1/iNOS/Nox2/NF-κB/STAT3	(145)
	In vitro	Human colorectal cancer cells (RKO, HT-29, HCT-116)	↑NF-κB-p65; ⊥ G2/M and G1 phases cell cycle; ↑p21; ↑p53; ↓Survivin	(146)
Apigenin	*In vitro*	Human pancreatic cancer cell (PANC-1, BxPC-3)	↑Apoptosis; ↓GSK-3/NF-κB; ⊥G2/M phase cell cycle	(147)
	In vitro	Cancer stem cells; Prostate cancer cell (PC3)	↓PI3K/Akt/NF-κB; ↑p21; ↑p27; ↑caspases-8, caspase-3; ↑TNF-α; ↑Bax; ↑cyt c; ↓MMP-2, -9; p105/p50; ↓PI3K	(149)
	In vitro	Prostate carcinoma cell (PC-3)	↓NF-κB; ↑apoptosis	(148)
	In vitro	Breast cancer cell (MDA-MB-231)	↓CCL2; ↓CXCL-8; ↓IL1A	(150)
	In vivo	Xenograft athymic nu/nu nude mice	↓Cell proliferation; ↓Her2/neu; ↓VEGF	(151)
	In vivo	TRAMP mice	↓NF-κB; ↓tumor volumes; ↓Phosphorylation IκBα; ↓IKK; ↓Bcl2; ↓Bcl-XL; ↓cyclin D1; ↓COX-2; ↓VEGF	(152)

(Continued)

TABLE 1 | Continued

Compound	Types of study	Cell line(s)/tumor model(s)	Mechanisms of action	References
Luteolin	*In vitro*	Lung adenocarcinoma cell (A549)	↓NF-κB–Snail; ↓E-cadherin; ↓PI3K/Akt/IκBa–	(153)
	In vitro	Monocytic leukemia cell (THP-1)	↓NF-κB; ↓MAPK; ↑HO-1; ↑pAkt; ↓IL-6; ↓IL-8; ↓SICAM-1; ↓MCP-1	(154)
	In vitro	Gastric cancer cell (CRL–1739)	↑NF–κB; ↑IL–8; ↑IL–10	(155)
Luteolin 8-C-b-fucopyranoside	*In vitro*	Breast cancer cell (MCF7)	↓ERK/NF-κB; ↓MMP-9; ↓IL-8; ↓ERK/AP-1	(156)
Isorhamnetin	*In vitro*	Lung adenocarcinoma cell (A549)	↓NF-κBp65; ↑apoptosis	(158)
	In vitro	Breast cancer cell (MCF7 or MDA-MB-468)	↓Cell proliferation; ↑Apoptosis; ↓Akt/mTOR; ↓MEK/ERK phosphorylation	(159)
Wogonin	*In vitro* and *in vivo*	C57BL/6 mice; Lymphocytic leukemia cell (TCL1)	↓NF-κB	(161)
	In vitro	Human hepatocellular cancer cells (Bel7402, HepG2)	↓NF–κB/Bcl–2; ↓cell proliferation; ↓cell invasion; ↑Apoptosis; ↓EGFR; ↓ERK/AKT; ↓cyclin D1	(160)
Xanthohumol	*In vitro* and *in vivo*	Breast cancer cell (MCF-7); Xenografts nude mice	↓NF-κB; ↓angiogenesis; ↓Cell proliferation	(162)
	In vitro	Breast cancer cells (MDA-MB-231, MCF-7); Colorectal cancer cells (HCT8, HCT116); Pancreatic carcinoma cell (Panc-1)	↓CXCR4; ↓cell invasion	(163)
P-hydroxycinnamic acid	*In vitro*	Breast cancer cells (MDA-MB-231)	↓NF-κB; ⊥G1 phase cell cycle; ⊥G2/M phase cell cycle	(164)
Wogonoside	*In vitro*	Breast cancer cells (MDA-MB-231)	↓NF-κB; ↓cell invasion; ↓cell migration; ↓TNF-α; ↓TRAF-2; ↓TRAF-4; ↓Twist1; ↓MMP-9; ↓MMP-2; ↓vimentin	(165)
Scutellarein	*In vitro*	Lung adenocarcinoma cell (A549)	↓NF-κB; ↓COX-2; ↓EGFR; ↓ERK	(166)
Hydroxysafflor yellow A	*In vitro* and *in vivo*	Murine hepatoma cell (H22); Male Kunming mice	↓NF-κB; ↓Angiogenesis; ↓ERK/MAPK; ↓cyclinD1; ↓c-myc; ↓c-Fos	(167)
Rosmarinic acid	*In vitro* and *in vivo*	Male Kunming mice; Hepatocellular carcinoma cell (H22)	↓Tumor growth; ↓IL-6; ↓IL-10; ↓STAT3; ↑Bax; ↑caspase-3; ↓Bcl-2	(169)
	In vitro	Human leukemia cell (U937)	↓NF-κB	(168)
Magnolol	*In vivo*	BALB/cAnN.Cg-Foxn1nu/CrlNarl mice	↓ERK/NF-κB; ↑apoptosis; ↓tumor progression; ↓ MMP-9; ↓ VEGF; ↓ XIAP; ↓cyclin D1	(170)
HMFRR	*In vitro*	Lung adenocarcinoma cell (A549, PC9)	↓STAT3/NF-κB/COX-2; ↓ EGFR/PI3K/Akt; ↓EGFR	(171)
Hesperetin	*In vivo*	Swiss albino mice	↓NF-κB; ↑TNF-α; ↓PCNA; ↓CYP1A1	(172)
Honokiol	*In vitro* and *in vivo*	Orthotopic mouse model; Prostate cancer cell (MiaPaCa, Colo-357)	↓NF-κB; ↓sonic hedgehog; ↓CXCR4	(173)
	In vitro	Lung adenocarcinoma cell (A549, H460)	↓C-FLIP; ↓cell migration	(174)
Inotilone	*In vitro* and *in vivo*	Lung adenocarcinoma cell (A549); Mouse Lewis lung carcinoma cell lines; C57BL/6 male mice	↓NF-κB; ↓PI3K/Akt/MAPK; ↓MMP-2/9; ↓IL-8; ↓NO; ↓TNF-α; ↓cell migration; ↓PI3K; ↓PAkt	(174)
Eupatilin	*In vitro*	Gastric cancer cell (MKN-1)	↓NF-κB; ↓tumor invasion; ↑Caspase-3; ↓MMPs	(175)
	In vitro	Prostate cancer cell (PC3, LNCaP)	↓PTEN and NF-κB; ↑p53; ↑p21; ↑p27; ⊥G1 phases cell cycle arrest	(176)
Polysaccharide krestin	*In vivo*	Tumor-bearing neu transgenic mice	↓Cell growth; ↑T cell; ↑NK cell	(177)
Tilianin	*In vitro*	Pharyngeal squamous carcinoma cells (FaDu)	↑TLR4/p38/JNK/NF-κB; ↑Apoptosis; ↑TLR4; ↓Bcl-2; ↓Bcl-XL; ↑Bad; ↑Bax; ↑PARP; ↑cyt c; ↑caspase-3	(178)
Silibinin	*In vitro* and *in vivo*	Prostate cancer cells (PC3, WPE-1 NA-22, RWPE-1, WPE-1 NB-14); C57Bl/6 mice	↓NF-κB; ↓MCP-1; ↓CAF; ↓AP-1	(181)
	In vitro	Prostate carcinoma cell (DU145)	↓NF-κB	(179)
	In vitro	Hepatocellular cancer cells (HepG2); Prostate cancer cells (PC-3)	↓NF-κB; ↓Phospholipase A2	(180)
Chrysin	*In vitro* and *in vivo*	Renal cell carcinoma (RCC); Wistar rats	↓NF-κB; ↓COX-2; ↓iNOS	(182)
	In vivo	Swiss albino mice	↓NF-κB; ↓PCNA, ↓COX-2	(185)
	In vitro	Lung adenocarcinoma cell (A549); Human cervical cancer cell (HeLa)	↓NF-κB; ↓Mcl-1; ↓pSTAT3; ↓TRAIL; ↑glutathione depletion; ↓STAT3	(183)
	In vivo	Wistar rats	↓NF-κB; ↓PCNA; ↓CAT; ↓GPX; ↓SOD	(184)

(Continued)

TABLE 1 | Continued

Compound	Types of study	Cell line(s)/tumor model(s)	Mechanisms of action	References
	In vitro and *in vivo*	Cervical cancer cell (HeLa); BALB/c-nu mice	↓NF-κB/Twist Axis	(186)
(6)-Gingerol	*In vitro* and *in vivo*	Myeloid leukemia cells (U937 and K562); Xenograft mice	↓NF-κB; ↑ROS	(187)
Butein	*In vitro* and *in vivo*	T cell leukemia/lymphoma (MT-4, HUT-102); Mice harboring ATLL xenograft	↓NF-κB; ⊥G1 cell cycle arrest; ↓Tumor growth; ↓AP-1; ↓Akt	(188)
Fisetin	*In vitro*	Colorectal cancer cell (HCT116, HT29)	↓Wnt/EGFR/NF-κB; ↑apoptosis; ↓COX2;	(190)
	In vitro	Prostate cancer cell (PC-3)	↓PI3K/Akt and JNK; ↓MMP-2/9; ↓MMP-2 and MMP-9	(191)
	In vitro	Laryngeal carcinoma cell (TU212)	Regulation of Akt/NF-κB/mTOR and ERK1/2	(194)
	In vitro	Pancreatic cancer cell (AsPC-1)	↓NF-κB; ↓DR3; ↓p-NF-κB/p65	(189)
	In vivo	Autochthonous Wistar rats	↓NF-κB; apoptosis induction of p53	(192)
Gallotannin	*In vitro* and *in vivo*	Colorectal cancer cell (HCT116, HT29); Xenografts in NOD/SCID mice	↓NF-κB; ↓IL-6; ↓TNFα; ↓IL-1α; ↓VEGFA	(195)
Astragalin	*In vitro* and *in vivo*	Colorectal cancer cell (HCT116); Xenograft in nude mice	↓NF-κB; ↓cell proliferation; ↓cell migration; ⊥G0/G1 phase cell cycle; ↑apoptosis; ↓Bax; ↓Bcl-2; ↓P53; ↓caspase-3,6,7,8,9	(198)
	In vitro	Lung cancer cell (A549)	↓NF-κB; ↓ERK-1/2; ↓Akt	(197)
	In vitro and *in vivo*	Stomach cancer cell (MKN45); C57/BL female mouse	↑TLR4	(196)
Ellagic acid	*In vivo*	Wistar albino rats	↓NF-κB; ↓TNF-α; ↓IL-6; ↓COX-2; ↓iNOS	(199)
	In vitro and *in vivo*	Pancreatic carcinoma (PANC-1); Xenografted mice	↓NF-κB; ⊥G1 phase cell cycle; ↓COX-2; ↑E-cadherin ↓Vimentin	(201)
Morin	*In vivo*	Wistar albino rats	↓NF-κB; ↓TNF-α; ↓IL-6; ↓COX-2; ↓PGE-2	(203)
	In vitro	Lung carcinoma cell (A549); Cervical cancer cell (HeLa)	↓NF-κB; ↓cyclin D1; ↓COX-2; ↓MMP-9	(202)
Flavopiridol	*In vitro*	Non-small cell lung carcinoma cell (A549), Colon cancer cells (HCT-116, HCT-15)	↓NF-κB	(204)
Puerarin	*In vitro*	Bladder cancer cell (T24)	↓NF-κB; ↓proliferation; ↑Apoptosis; ↑miR-16; ↓COX-2	(205)
Icariin	*In vitro*	Human myeloma cell (U266)	↓JAK/STAT3; ↓STAT3; ↓VEGF; ↓MMP-9; ↓STAT3	(206)
Acteoside	*In vitro*	Hepatocellular carcinoma cell (HepG2, HuH7)	↓NF-κB	(207)
Acacetin	*In vitro* and *in vivo*	Xenografted mice; Prostate cancer cell (DU145)	↓NF-κB/Akt; ↓XIAP; ↓COX-2	(209)
	In vitro	Prostate cancer cell (DU145)	↓NF-κB; ↓p38MAPK; ↓AP-1-binding	(208)
Eriodictyol	*In vitro*	Glioblastoma cells (A172, U87 MG)	↓Cell proliferation; ↓apoptosis; ↓EMT markers; ↓p38 MAPK/GSK-3β/ZEB1	(211)
	In vitro and *in vivo*	Glioblastoma cells (CHG-5, U87 MG); Mouse xenograft model	↓PI3K/Akt/NF-κB; ↑apoptosis	(210)
Calycosin	*In vitro*	Hepatocellular carcinoma cell (HepG2)	↓Bcl-2; ↑Bax; ↑Caspase-3; ⊥ G0/G1 phase cell cycle; ↓Akt; ↓TGF-β1; ↓SMAD2/3; ↓SLUG; ↓vimentin	(212)
Cudraflavone B	*In vitro*	OSCC	⊥sub-G1 phase cell cycle; ↑p27	(213)
Protocatechualdehyde	*In vitro*	Breast cancer cell (MCF-7, MDA-MB-231)	↓NF-κB; ↓GSK-3β; ↓β-catenin; ↓cyclin D1	(214)
Naringin	*In vitro*	Ovarian cancer cells (SKOV3/DDP)	↓NF-κB; ↓COX-2	(215)

carcinoma cells *in vitro* and *in vivo* (223–226). Ursolic acid (**Figure 5**) exerts anti-inflammatory activity *via* suppression of the TLR4-MyD88 pathway and decreased production of inflammatory factors, including IL-1β, TNF-α, and IL-6 in abelson murine leukemia macrophage (RAW 264.7) cells (227). In a similar study, ursolic acid demonstrated significant *in vitro* and *in vivo* anticancer activity against DU145 and LNCaP prostate adenocarcinoma cells, as well as a mouse model *via* diminished CXCR4/CXCL-12 signaling axis and reduced activation of NF-κB (228). Furthermore, ursolic acid induced apoptosis and inhibited growth in several *in vitro* pancreatic and colon cancer models by interfering with PI3K/Akt/NF-κB, STAT, GSK, TRAIL, and JNK pathways (229, 230). In addition to ursolic acid, heteronemin (**Figure 5**) showed significant antiproliferative effects against AML cells *via* targeting NF-κB, Ras, MAPK, AP-1, and c-myc (231). Soyasaponins, bioactive phytochemicals found in a multitude of legumes, downregulated TLR4/MyD88 signaling and decreased TNF-α, IL-6, COX-2, NO, IL-1β, and iNOS in inflammatory macrophages (232). Oleanolic acid (**Figure 5**), another triterpenoid structure, and its synthetic derivative SZC014 showed considerable antitumor effects against the hepatocellular cancer cell lines HepG2, interfering with NF-κB

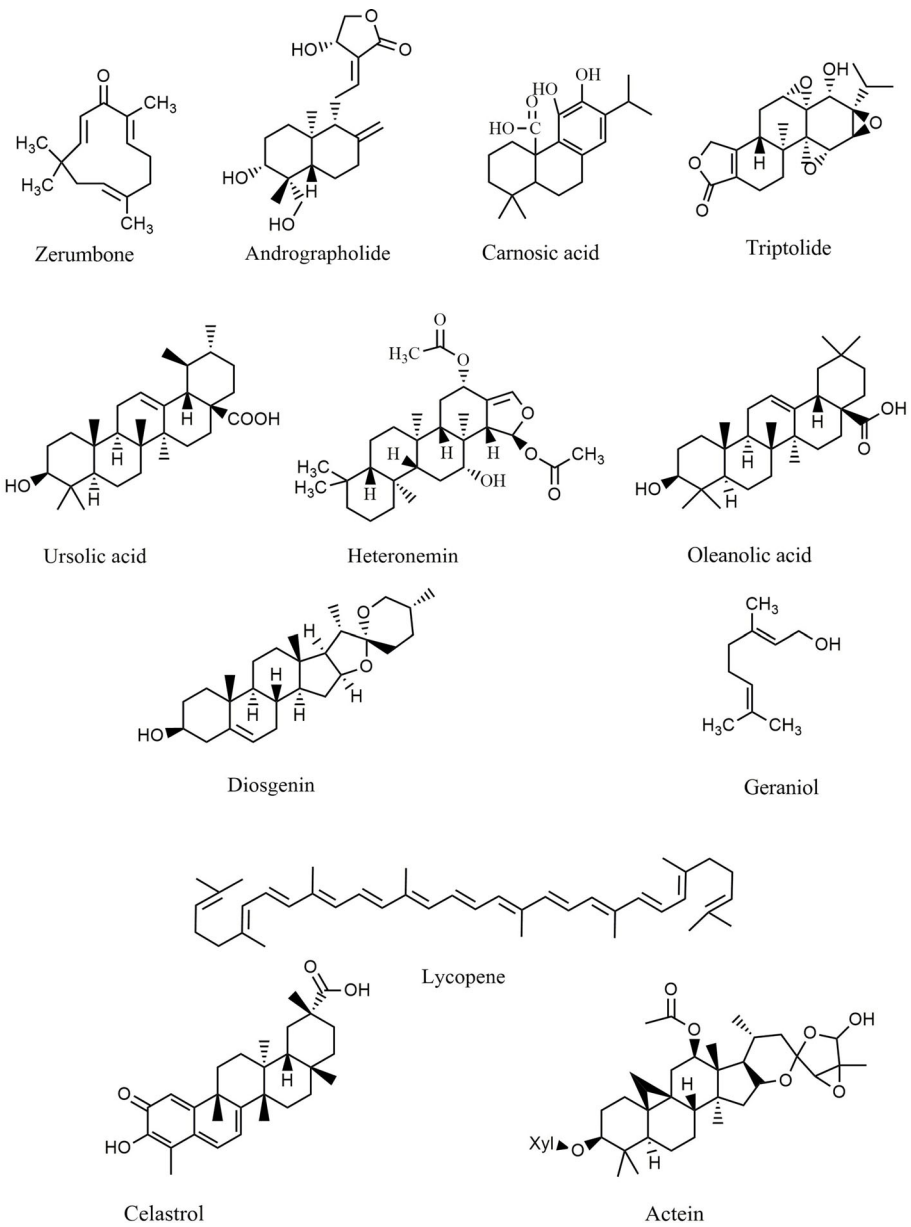

FIGURE 5 | Chemical structures of selected terpenes/terpenoids that modulate the TLR/NF-κB/NLRP signaling in cancer.

and nuclear factor-erythroid factor 2-related factor 2 (Nrf-2)/antioxidant response element (ARE) signaling (233, 234). Additionally, inhibition of IκB kinase and suppression of NF-κB signaling are the primary anticancer mechanisms of lycopene (**Figure 5**) in breast and prostate cancer cells (235).

The monoterpene geraniol (**Figure 5**) is an acyclic isoprenoid derived from essential oils. Geraniol attenuated tongue carcinogenesis *via* decreased activation of NF-κB (236). Additionally, the NF-κB and STAT3 pathways are the chemopreventive mechanisms of andrographolide *via* inhibition of inflammatory mediators (237). Moreover, treatment with celastrol (**Figure 5**) downregulated NF-κB and reduced the expression of IL-6 in prostate and breast cancer cells (238, 239). In a similar study, actein (**Figure 5**) strongly suppressed the growth of MDA-MB-453 cells by enhancing the cytoplasmic calcium and modulating the MAPK/ERK kinase (MEK) and NF-κB pathways (240).

Diosgenin (**Figure 5**), a known steroidal triterpenoid with two pentacyclic rings, is found in *Trigonella foenum graecum* (241). Progesterone, pregnenolone, cortisone, and other steroids can be synthesized from diosgenin, which comprises more than 60% of commercial synthetic steroids (242). Diosgenin has shown several biological activities, including anticancer, antidiabetic, anti-infectious, anti-inflammatory, and anticoagulant effects (242).

Diosgenin exerted significant antitumor potential *via* induction of apoptosis and suppression of inflammation. It also inhibited the invasion, metastasis, angiogenesis, and proliferation of various cancer cell lines. Accordingly, targeting inflammation-related pathways, including NF-κB and STAT3, is one of the main anticarcinogenic mechanisms of diosgenin (241, 242). Diosgenin displayed antiproliferative effects in HEp-2 and M4Beu cell lines *via* enhancing the production and release of apoptosis-inducing factors, increasing the Bax/Bcl-2 ratio, modulating caspase-3, and facilitating the activation of p53 (243). Furthermore, diosgenin induced apoptosis in the colon cancer cell lines HT-29 and HCT-116 *in vitro* by interfering with COX-2 signaling and increasing DNA fragmentation, caspase-3, and 5-lipoxygenase activity (244). Additionally, diosgenin sensitized colorectal cancer cells to apoptosis induced by TRAIL *via* activation of the p38MAPK pathway, overexpression of death receptor-5 (DR5), and downregulation of the Akt pathway (245).

Several compounds belonging to the terpenes and terpenoids classes exhibit antineoplastic properties by affecting various stages of tumor development, including suppression of the initiation and progression of tumorigenesis through promoting apoptosis, cell cycle arrest, inhibition of metastasis, angiogenesis, invasion, and downregulation of several intracellular signaling pathways, including TLR4, STAT3, NF-κB, and MMP-9. These compounds are promising therapeutic agents due to the massive progression in delineating the details of their anticancer action. **Table 2** provides the various anticancer terpenes/terpenoids that interfere with the TLR/NF-κB/NLRP pathway to counter chemoresistance.

Alkaloids

Alkaloids are another group of plant secondary metabolites that hold a substantial role in the defensive and internal immune processes of plants. Antioxidative, antimicrobial, antiprotozoal, anti-inflammatory, and anticancer activities are some of the important biological activities of alkaloids. Vinblastine and camptothecin are two important compounds belonging to the alkaloid group that have been properly developed and received the Food and Drug Administration's approval for the treatment of different cancers. Sophoridine (**Figure 6**) inhibited macrophage-mediated immunosuppression by interfering with the TLR4/IRF-3 pathway, downregulating IL-10, CD206, and arginase 1 (Arg-1), and upregulating IL-12α, IFN-β, and iNOS in RAW264.7 and MFC cell lines (246). Moreover, matrine (**Figure 6**) demonstrated anticancer activity by regulating immunity, increasing TLR8 and TLR7, and activating MyD88-dependent signaling (247). Additionally, matrine inhibited the invasion and proliferation of breast and prostate cancer cells via downregulation of VEGF/Akt, MMP-2, and MMP-9 through the NF-κB signaling pathways (248, 249). Furthermore, hypaconitine (**Figure 6**), another alkaloidal agent, inhibited the adhesion, invasion, and migration of the A549 cell line (250). In addition to hypaconitine, alpinetin showed significant anticancer properties, diminishing the transcription of HIF-1α, NF-κB, and the ROS/NF-κB/HIF-1α axis in breast cancer cells (251). In a similar study, berberine (**Figure 6**), a well-known alkaloid, inhibited the proliferation of lung cancer cells and induced apoptosis through upregulation of Bcl-2/Bax, NF-κB, COX-2, MMP-2, and Akt/ERK pathways (252–254). Likewise, berberine suppressed the NLRP3 inflammasome in MDA-MB-231 cells *in vitro* (255). Treatment with berberine inhibited MMP-2, MMP-9, NF-κB, focal adhesion kinase (FAK), urokinase-type plasminogen activator (u-PA), and IKK in SCC-4 cancer cells (256). Additionally, berberine prevented DMBA-induced breast carcinogenesis in Sprague Dawley rats (257) and inhibited the growth of MDA-MB-231 cells *via* decreased IL-6, TNF-α, and NF-κB (258). Furthermore, berberine exerted anticancer activity *via* targeting variant pathways, such as NF-κB/COX-2, p38/JNK, AP-2/telomerase reverse transcriptase (hTERT), cytochrome-c/caspase, and HIF-1α/VEGF signaling in human gastric and NSCLC cell lines (259, 260). The alkaloid anisodamine (**Figure 6**) is another anticancer compound that inhibited the growth, invasion, and proliferation of HepG2 cells and suppressed the expression and activation of IFN-γ, IL-27, NLRP3, IL-4, and TNF-α (261). In a similar study, a steroidal alkaloid, cyclopamine (**Figure 6**), induced apoptosis and suppressed the proliferation of HEL and TF1a cells *via* induction of PKC, COX-2 overexpression, PARP cleavage, and modulation of MAPK/Akt signaling (262). The main anticancer mechanisms of cepharanthine and tetrandrine (**Figure 6**) against Jurkat T leukemia cells (263) are the modulation of PI3K/Akt/mTOR signaling, induction of apoptosis, cell cycle arrest, and phosphorylation of JNK and p38. Another alkaloid structure, piperlongumine (**Figure 6**), appears to have anticancer properties *via* downregulating c-Met expression and NF-κB activity in renal, colon, lung, and prostate carcinoma cells (264–268). Harmine (269), fangchinoline (270), sinapine (271), gramine (272), cepharanthine (273), piperine (274, 275), lamellarin D (276), ipobscurine (277), chelerythrine (278), dihydrochelerythrine (279), tryptanthrin (280), and neferine (**Figure 6**) (281) are some of the other alkaloid agents that exert significant anticancer activity through modulation of VEGF, AP-1, fibroblast growth factor receptor 4 (FGFR4)/fibroblast growth factor receptor substrate 2α (FRS2α)-ERK1/2, NF-κB, Nrf-2/Kelch-like ECH-associated protein 1 (Keap-1), MMP-2, MMP-9, and STAT3.

Overall, alkaloids are phytochemicals with significant potential to suppress the *in vitro* and *in vivo* growth/invasion of various cancers. By interfering with TLR/NF-κB/NLRP, alkaloids, especially berberine, matrine, and evodiamine, diminish cancer chemoresistance and facilitate the induction of apoptosis, inflammation, oxidative stress, and autophagy in cancer cells. **Table 3** provides various anticancer alkaloids that interfere with the TLR/NF-κB/NLRP pathway against chemoresistance.

Sulfur-Containing Compounds and Miscellaneous Agents

Sulforaphane (**Figure 7**) suppressed TLR3-mediated NF-κB in PCI15A SCC cells (282). In addition, sulforaphane inhibited the expression of MMP-9, phosphorylation of IκB, and activation of NF-κB in MCF-7 cells (283). Another sulfur-containing compound, shikonin (**Figure 7**), appears to have anticancer properties *via* suppressing the migration, adhesion, viability,

TABLE 2 | Anticancer terpenes/terpenoids interfering with the TLR/NF-κB/NLRP pathway and cross-linked mediators against chemoresistance.

Compound	Types of study	Cell line(s)/tumor model(s)	Mechanisms of action	References
Zerumbone	*In vivo*	Mouse model of colorectal and lung caner	↓NF-κB; ↑Apoptosis; ↓proliferation; ↓HO-1	(216)
Andrographolide	*In vitro* and *in vivo*	Murine tumor cell (B16 melanoma); C57BL/6J mice	↓TLR4/NF-κB signaling; ↓CXCR4; ↓Bcl-6	(217)
	In vitro and *in vivo*	RIP1-Tag2 mice models; Insulinoma cell (β-TC-6)	↓TLR4/NF-κB signaling	(218)
	In vitro	Human colon cancer cell (SW620)	↓TLR4/NF–κB/MMP–9	(219)
Carnosic acid	*In vitro* and *in vivo*	Xenograft mice model; BALB/c Akt-knockout mice; Liver cancer cell (MHCC97-H and Bel7402)	↓NF-κB; ↓TLR4; ↑caspase-3; ↓MyD88; ↓TRAF-6; ↓IRAK-1; ↓IRAK-4	(220)
Triptolide	*In vitro* and *in vivo*	FEN1 E160D mice; Prostate cancer cell (PC3)	↓NF-κB; ↑ERK1/2; ↑p38	(221)
	In vitro	Breast cancer cell (MCF-7)	↓NF-κB; ↓MMP-9; ↓AP-1	(222)
	In vitro and *in vivo*	Anaplastic thyroid carcinoma cells (TA-K and 8505C); Nude mice	↓NF-κB; ↓angiogenesis; ↓cell invasion; ↓cyclin D1; ↓VEGF	(224)
	In vitro	Hepatocellular carcinoma cell (MHCC-97H)	↓NF-κB; ↓MMP-9; ↓invasion; ↓tumorigenesis	(225)
	In vitro	Gastric adenocarcinoma (AGS)	↓NF-κB signaling	(223)
	In vitro and *in vivo*	Gastric tumor cell (MGC-803 and HGC-27); Xenograft mice	↓Notch1; ↓NF-κB; ↓RBPJ, ↓IKKα, IKKβ	(226)
Ursolic acid	*In vitro*	Abelson murine leukemia macrophage (RAW 264.7)	↓TLR4-MyD88 pathway; ↓IL-1β; ↓TNF-α; ↓IL-6	(227)
	In vitro and *in vivo*	Prostate cancer cells (DU145, LNCaP); Transgenic mouse model of prostate adenocarcinoma (TRAMP mice)	↓NF-κB; ↓CXCR4; ↓CXCR4/CXCL-12 signaling	(228)
	In vitro	Colon cancer cell (SW480 and LoVo)	↑Apoptosis; ↓MMP-9; ↓COX-2; ↓p300/NF-κB signaling	(229)
	In vitro	Breast cancer cell (T47D, MCF-7, MDA-MB-231	↓NF–κB; ↓viability; ↑apoptosis; ↓cyclin–D1; ↑caspase–3	(230)
Heteronemin	*In vitro*	Acute myeloid leukemia cell (HL-60)	↓NF-κB; ↓Ras; ↓MAPK; ↓AP-1; ↓c-myc	(231)
Soyasaponin A1, A	*In vitro*	Abelson murine leukemia virus-induced tumor macrophage (RAW 264.7)	↓TLR4/MyD88 signaling	(232)
Oleanolic Acid	*In vitro*	Hepatocellular cancer cells (HepG2)	↓NF-κB; ↓Nrf-2/ARE	(233)
	In vitro and *in-silico*	Hepatocellular cancer cells (HepG2)	↓NF-κB; ↓Nrf-2	(234)
Lycopene	*In vitro*	Breast cancer cell (MDA-MB-231); Prostate cancer cell (PC3)	↓NF-κB; ↓IκB kinase; ↓IKKβ kinase	(235)
Geraniol	*In vivo*	Wistar albino rats	↓NF-κB	(236)
Andrographolide	*In vitro*	Abelson murine leukemia virus-induced tumor macrophage (RAW 264.7)	↓NF-κB; ↓STAT3; ↓iNOS; ↓COX-2	(237)
Celastrol	*In vitro*	Prostate carcinoma cell (PC-3)	↓NF-κB; ↓IL-6	(238)
	In vitro	Breast cancer cells (MDA-MB-468, MDA-MB-231)	↓NF-κB; ↓cell migration; ↓cell invasion; ↓IL-6	(239)
Actein	*In vitro*	Breast cancer cells (MDA-MB-453)	↓NF-κB; ↓MEK; ↑cytoplasmic calcium	(240)
Diosgenin	*In vitro*	Laryngocarcinoma cells (HEp-2); Human melanoma cells (M4Beu)	↑Apoptosis; ↑AIF; ↑Bax/Bcl-2 ratio; ↑ p53	(243)
	In vitro	Human colorectal cancer cells (HT-29, HCT-116)	↑Apoptosis; ↑COX-2; ↑DNA fragmentation; ↑caspase-3; ↑5-lipoxygenase	(244)
	In vitro	Human colorectal cancer cells (HT-29)	↑Apoptosis; ↑p38 MAPK; ↑DR5; ↓Akt	(245)

and invasion of gastric (MGC-803) and hepatocellular (Huh7and BEL7402) cancer cells *in vitro via* the TLR2/NF-κB and receptor-interacting protein 1 (RIP1)/NF-κB pathways (284, 285). In a similar study, phenethyl isothiocyanate (**Figure 7**) in combination with xanthohumol activated Nrf-2 and suppressed NF-κB in pancreatic cancer cells (286) and B-cell acute lymphocytic leukemia (287). Moreover, inhibition of NF-κB and MAPK signaling is the main anticancer mechanism of phenethyl isothiocyanate against AGS cell lines (288). The indolequinazoline alkaloid evodiamine is widely present in many medicinal plants belonging to the tetradium family. Evodiamine (**Figure 7**) and its derivatives targeted the c-Met, NF-κB, Smad2/3, and TGF-β/hepatocyte growth factor pathways in prostate, hepatocellular, lung, and melanoma carcinoma cells (289–292). It was reported that microsclerodermin A inhibited NF-κB, promoted apoptosis, and diminished cytokine release in pancreatic and breast cancer cells (293, 294). Additionally, treatment of prostate, lung, and pancreatic cancer cells (295–298) with matrine and oxymatrine inhibited angiogenesis, VEGF, NF-κB, and CXCR4. Nobiletin (**Figure 7**) is a citrus flavonoid with several pharmacological activities, including anticarcinogenic, antioxidative, neuroprotective, and anti-inflammatory effects. Nobiletin modulated the activity of the Cd36/STAT3/NF-κB pathway and inhibited the growth and migration of breast cancer cell lines MCF-7 and MDA-MB-231 (299). Similarly, it leads to the downregulation of Akt, HIF-1α, NF-κB, and VEGF in OVCAR-3 ovarian cancer cells and suppression of TRIF/receptor interacting serine/threonine kinase 1 (RIPK1)/Fas associated *via* death domain (FADD), TRIF protein, caspase-8, and TLR3/IRF-3 in LNCaP and PC-3 cell lines (300, 301). Additionally, nobiletin diminished the invasion and migration of AGS cells and downregulated FAK/PI3K/Akt, c-Raf, Rac-1, cell division control protein 42 homolog (Cdc42), as well as the NF-κB, MMP-2, and MMP-9 signaling pathways (302).

Ulmus davidiana Nakai glycoprotein (303), phenylpropenone derivatives (304), libanoridin (305), and alisol B 23-acetate (306)

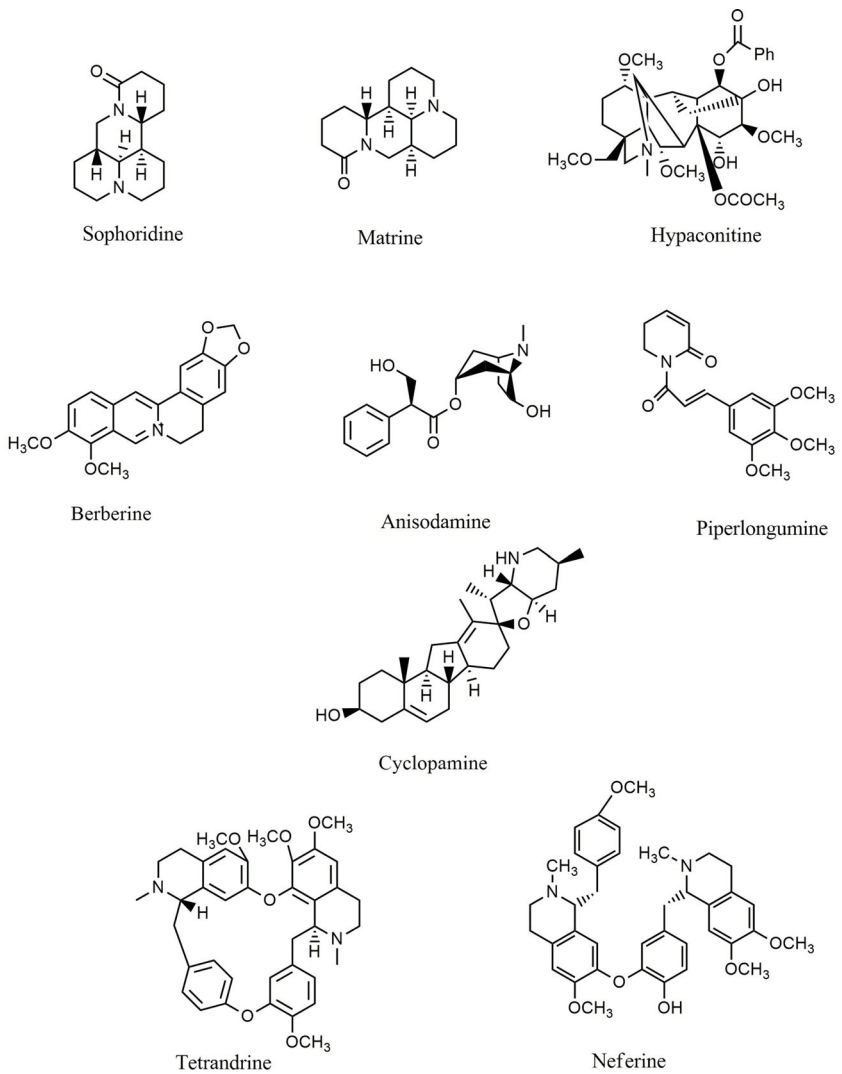

FIGURE 6 | Chemical structures of selected alkaloids that modulate the TLR/NF-κB/NLRP signaling in cancer.

decreased the proliferation and migration of colon carcinoma cells *via* inactivation of inflammatory and angiogenic pathways. Deguelin (**Figure 7**) downregulated EGFR, c-Myc, pAkt, p-ERK, p-STAT3, c-met, survivin, and NF-κB in xenograft athymic mice models of breast cancer cell lines MDA-MB-231, MDA-MB-468, BT-549, and BT-20 (307). Withaferin A, a steroidal lactone presents in *Withania somnifera*, exerts several pharmacological activities such as anti-inflammatory, anticancer, and cardioprotective effects. Withaferin A significantly downregulated the liver X receptor-a, NF-κB, and angiogenesis pathways in the hepatocellular carcinoma cell line QGY-7703 (308). Furthermore, withaferin A downregulated caspase-1 and AIM-2 in THP-1 cells (309). Similarly, Zingerone (vanillylacetone) (**Figure 7**) is another known agent with anticancer properties that inhibited NF-κB, p42/44, and MAPK/AP1signaling and attenuated the migration and invasion of human hepatocellular carcinoma cells (310). Moreover, osthole and ophiopogonin D (**Figure 7**) suppressed the PI3K/Akt, NF-κB, and AP-1 pathways in A549 and H1299 lung cancer cells (311–314). Embelin (315), plumbagin (316, 317), indole glucosinolates (318), thymoquinone (319, 320), decursinol angelate (321), polysaccharide agaricus blazei murill (322), and 19-a-hydroxyurs-12(13)-ene-28-oic acid-3-O-b-D-glucopyranoside (HEG) (323) are some of the other miscellaneous agents that have promising anticancer potential against MDAMB-231, pancreatic PANC1, Ehrlich ascites carcinoma, fibrosarcoma HT1080, and chronic myeloid leukemia (CML) KBM-5 cancer cell lines *in vitro* and *in vivo*.

Overall, sulfur-containing compounds demonstrate critical biological properties and therefore have meaningful potential for the prevention and treatment of cancers. These phytochemicals could target multiple signals affecting cancer progression, especially TLR/NF-κB/NLRP signaling and cross-talked pathways, to support cancer immunotherapy and chemotherapy. **Table 4** provides the various anticancer sulfur and miscellaneous

TABLE 3 | Anticancer alkaloids interfering with the TLR/NF-κB/NLRP pathway and interconnected mediators against chemoresistance.

Compound	Types of study	Cell line(s)/tumor model(s)	Mechanisms of action	References
Sophoridine	*In vitro*	Mouse gastric carcinoma cell (MFC)	↓TLR4/IRF-3 pathway; ↓IL-10; ↓CD206; ↓Arg-1; ↑IL-12α; ↑IFN-β; ↑iNOS	(246)
Matrine	*In vitro*	Mouse lung cancer cells	↑TLR7; ↑TLR8; ↑MyD88; ↑TRAF-6; ↑IKK; ↑IL-12; ↑IL-6; ↑TNF-α	(247)
	In vitro	Breast cancer cell (MDA-MB-231)	↓NF-κB; ↓ratios of Bcl-2/Bax; ↓p-Akt; ↓MMP-9; ↓MMP-2; ↓EGF; ↓VEGFR1	(248)
	In vitro and *in vivo*	Prostate cancer cells (DU145 and PC3); Xenograft Balb/c nude mice model	↓NF-κB; ↓MMP-9; ↓MMP-2; ↓p-p65	(249)
Hypaconitine	*In vitro*	Human lung carcinoma cell (A549)	↓Cell adhesion; ↓cell invasion; ↓Cell migration; ↓TGF-β1; ↓NF-κB	(250)
Alpinetin	*In vitro* and *in vivo*	Breast cancer cells (MCF-7,4T1, MDA-MB-231); BALB/C female mice	↓NF-κB; ↓HIF-1α transcription; ↓ROS/NF-κB/HIF-1α	(251)
Berberine	*In vitro*	Human lung carcinoma cell (A549)	↓JAK2/VEGF/NF-κB/AP-1; ↓cell proliferation; ↑apoptosis; ↓MMP-2; ↓Bcl-2/Bax	(253)
	In vitro	Human lung cells (H1299 and A549)	↓NF-κB/COX-2; ↓AP-2β/hTERT; ↓Akt/ERK; ↑caspase/cyt c signaling	(252)
	In vitro	Human lung cell (A549)	↑Apoptosis; ↓cyclins	(254)
	In vitro	Breast cancer cell (MDA-MB-231)	↓NLRP3; ↓IL-1β; ↓IL-1α; ↓P2X7; ↓IL-6; ↓TNF-α	(255)
	In vitro	Tongue SCC cells (SCC-4)	↓NF-κB; ↓cell migration; ↓invasion; ↓FAK; ↓ IKK; ↓ MMP-2; ↓ MMP-9; ↓ u-PA	(256)
	In vivo	Sprague Dawley rats	↓NF-κB; ↓PCNA; ↓malonaldehyde; ↓IL-1β; ↓IL-6; ↓TNF-α; ↓SOD; ↓CAT; ↓GSH	(257)
	In vitro	Breast cancer cell (MDA-MB-231)	↓NF-κB; ↓TNF-α; ↓IL-6	(258)
	In vitro	Human gastric cancer cell (SNU-1)	↓NF-κB; ↓p38/JNK pathway; ↑Apoptosis; ↑Caspase	(260)
	In vitro	Human non-small-cell lung cancer cell (NSCLC)	↓p50/p65 NF-κB; ↓AP-2α; ↓AP-2β; ↓pAkt; ↓pERK; ↑cyt c release; ↑cleavage of caspase; ↑cleavage PARP	(259)
Anisodamine	*In vitro* and *in vivo*	Hepatocellular carcinoma cells (HepG2); BALB/C nude mice	↓NLRP3; ↓IFN-γ; ↓IL-27; ↓IL-4; ↓TNF-α	(261)
Cyclopamine	*In vitro*	Human erythroleukemia cells (HEL and TF1a)	↓Cell proliferation; ↑apoptosis; ↑COX-2; ↑PKC; ↑ PARP cleavage; ↓MAPK; ↓Akt	(262)
Cepharanthine & Tetrandrine	*In vitro*	T cell leukemia (Jurkat)	↑Apoptosis; ↑p-JNK; ↑Phosphorylation of p38; ↑cyclin A2; ↑cyclin B1; ↓cylcin D1; ⊥S phase cell cycle	(263)
Piperlongumine	*In vitro*	Prostate cancer cells (PC-3, LNCaP, DU-145)	↓NF-κB; ↓IL-6; ↓IL-8; ↓MMP-9; ↓ICAM-1	(264)
	In vitro	Renal cell carcinoma (PNX0010, 786-O)	↓NF-κB; ↓C-Met; ↓Akt/mTOR; ↓Erk/MAPK; ↓STAT3	(266)
	In vivo	Mouse model of colon cancer	↓NF-κB; ↓COX-2; ↓JAK/STAT	(268)
	In vitro	Human lung cancer cell (A549)	↓NF-κB p65; ↓Akt; ↓Cyclin D1; ↓CDK4; ↓CDK6; ↓p-Rb; ↑pERK1/2	(267)
	In vitro	Multiple myeloma (U266); Breast cell cancer (MCF-7); T cell leukemia Jurkat; Lung adenocarcinoma cell (H1299); Squamous cell (SCC4); CML (KBM-5)	↓NF-κB; ↓cyclin D1; ↓Bcl-2; ↓VEGF; ↓Bcl-XL; ↓c-IAP-2; ↓ICAM-1; ↓survivin; ↓COX-2; ↓IL-6; ↓CXCR-4; ↓c-IAP-1; ↓c-Myc	(265)
Harmine	*In vitro* and *in vivo*	Melanoma cell (B16F-10); C57BL/6 mice	↓VEGF; ↓MMP; ↓TIMP; ↓iNOS; ↓COX-2	(269)
Fangchinoline	*In vitro*	Human CML cell (KBM5); Multiple myeloma cell (U266)	↓NF-κB; ↑apoptosis; ↓AP-1	(270)
Sinapine	*In vitro*	Breast cancer cell (MCF-7)	↓NF-κB; ↓FGFR4/FRS2α-ERK1/2	(271)
Gramine	*In vivo*	Male golden Syrian hamsters	↓NF-κB; ↓cell proliferation; ↓STAT3; ↓ EGFR/PI3K/Akt/mTOR; ↓JAK/STAT3	(272)
Cepharanthine	*In vitro* and *in vivo*	Human OSCC cells (B88 and HSC3); Athymic nude mice	↓NF-κB; ↓angiogenesis; ↓VEGF; ↓IL-8	(273)
Piperine	*In vivo*	Wistar rats' models of colon cancer	↓NF-κB/Nrf-2/Keap-1/HO-1	(275)
	In vitro and *in vivo*	Human cervical cancer cell (HeLa); Mice xenograft models	↓STAT3/NF-κB; ↓Bcl-2; ↓p-STAT3	(274)

(Continued)

TABLE 3 | Continued

Compound	Types of study	Cell line(s)/tumor model(s)	Mechanisms of action	References
Lamellarin D	*In vitro*	Human leukemia cell (K562)	↑Apoptosis; ⊥G0/G1 cell cycle arrest; ↓CDK1; ↓smad3-5; ↓TGF-β; ↓IL-1β; ↓IL-6; ↓IL-8; ↑p27; ↑p53; ↑STGC3	(276)
Ipobscurine	*In vitro*	Melanoma cell (B16F-10);	↓NF-κB; ↑Caspase-3; ↑p53; ↑Bax; ↓Bcl-2; ⊥G1 cell cycle arrest	(277)
Chelerythrine	*In vitro*	Prostate cancer cells (DU145, PC-3)	↓MMP-2; ↓MMP-9; ↓uPA; ↓NF-κB; ↓AP-1; ↓p-p65, c-Fos; ↓c-Jun protein	(278)
Dihydrochelerythrine	*In vitro*	Human glioblastoma cells (U251 and GL-15); Murine glioblastoma cell (C6)	↓NF-κB; ↓cell viability	(279)
Tryptanthrin	*In vitro* and *in vivo*	Murine breast cancer model (4T1) Breast cancer cell (MCF-7)	↓NF-κB; ↑E-cadherin; ↓MMP-2; ↓Snail; ↓NOS1; ↓COX-2; ↓IL-2; ↓IL-10; ↓TNF-α	(280)
Neferine	*In vivo*	Wistar rats	↓NF-κB; ↓PI3K/AKT/mTOR	(281)

compounds in interfering with the TLR/NF-κB/NLRP pathway against chemoresistance.

PHYTOCHEMICALS IN COMBINATION WITH ANTICANCER DRUGS POTENTIATE CHEMOTHERAPY AND IMMUNOTHERAPY

Despite the recent progress in designing, synthesizing, and introducing new pharmaceutical drugs, natural products and bioactive molecules isolated from plants exert undeniable roles in the treatment of various cancers. Currently, the most important treatment option for malignant tumors is chemotherapy, which may lead to numerous side effects and promote drug resistance in patients. The use of natural products for the treatment of cancer is not only economically efficient, but also exerts multiple prophylactic, protective, and therapeutic roles in the treatment process that may reduce the side effects of chemotherapy and radiotherapy and decrease drug resistance (6, 13, 324–326).

Numerous studies have investigated the *in vitro* and *in vivo* advantages of adding curcumin to various anticancer treatment regimens. Liposomal curcumin has sensitized mouse models of cervical cancer to paclitaxel treatment (327). Curcumin also facilitated the induction of cell death by paclitaxel in MCF7 and MDA-MB-234 cell lines (328, 329). It was reported that curcumin induced cell apoptosis and increased paclitaxel sensitivity in cervical cancer cells through interfering with NF-κB, p53, and caspase-3 signaling (330). In similar studies, curcumin significantly sensitized breast cancer cells to cyclophosphamide and paclitaxel through modulation of NF-κB, protein kinase C (PKC), histone deacetylase (HDAC), and telomerase (331). Combining curcumin with oxaliplatin reversed the acquired resistance in an *in vitro* model of colorectal cancer by interfering with the CXC-chemokine/NF-κB pathway (332). In addition, curcumin increased the chemosensitivity of several platinum-based drugs *via* arresting the cell cycle in the G2/M phase, inducing apoptosis, and downregulating NF-κB (333). Similarly, co-delivery of curcumin and dasatinib led to the enhanced antitumor activity of dasatinib against colon cancer cells *via* diminished insulin-like growth factor type 1 receptor, c-Src, and EGFR signaling (334). Moreover, curcumin worked synergistically with tamoxifen to suppress the growth of MCF-7/LCC9 and MCF-7/LCC2 cells in an *in vitro* model of breast cancer by facilitating cell cycle arrest and inactivating the Akt/mTOR, Src, and NF-κB pathways (335). Furthermore, curcumin sensitized MDA-MB-231 cells to retinoic acid (336) and enhanced the efficacy, as well as diminished the toxicity, of doxorubicin (337). The anticancer potential of sorafenib against Huh7 cells and an athymic mice model of hepatocellular carcinoma was enhanced when combined with curcumin as evident by decreased expression of MMP-9 and NF-κB/p65 (338). Another well-known polyphenolic compound, resveratrol, sensitized PC3 and DU145 prostate cancer cells *in vitro* to cisplatin-induced apoptosis *via* inhibition of COX-2 and NF-κB pathways (339). In a similar study, resveratrol significantly increased the efficacy of cisplatin in xenografted mice and MDA-MB-231 cancer cells *via* decreased activity of p-ERK, TGF-β1, Smad2, vimentin, p-Akt, NF-κB, p-PI3K, and p-JNK (340). Furthermore, resveratrol sensitized colorectal cancer cells to 5-fluorouracil (5-FU) by inducing apoptosis and downregulating NF-κB (341). Additionally, resveratrol improved the gemcitabine-induced apoptosis of PaCa cells *via* inhibition of NF-κB and diminished expression of cyclin D1, VEGF, intercellular adhesion molecule-1 (ICAM-1), COX-2, and MMP-9 (342). Apigenin is another polyphenolic substance that potentiated the antitumor activity of several antineoplastic agents, including paclitaxel (343), tamoxifen (344), gemcitabine (345, 346), doxorubicin (347), and cisplatin (348) against various *in vitro* and *in vivo* cancer models. Polyphenol quercetin is another anticancer compound that works synergistically with paclitaxel (349, 350), tamoxifen (351), cisplatin (352, 353), adriamycin (354), and gemcitabine (355) to suppress the growth of various models of cancer *via* enhanced ROS production, cell cycle arrest, ER stress, and apoptosis. Similarly, various studies have reported the advantages of adding EGCG to enhance the antitumor activity of sunitinib, irinotecan, doxorubicin, gemcitabine, and cisplatin against human lung (A549, H460, and H1975) (356, 357), colorectal (HCT116 and RKO) (358), bladder (SW780 and

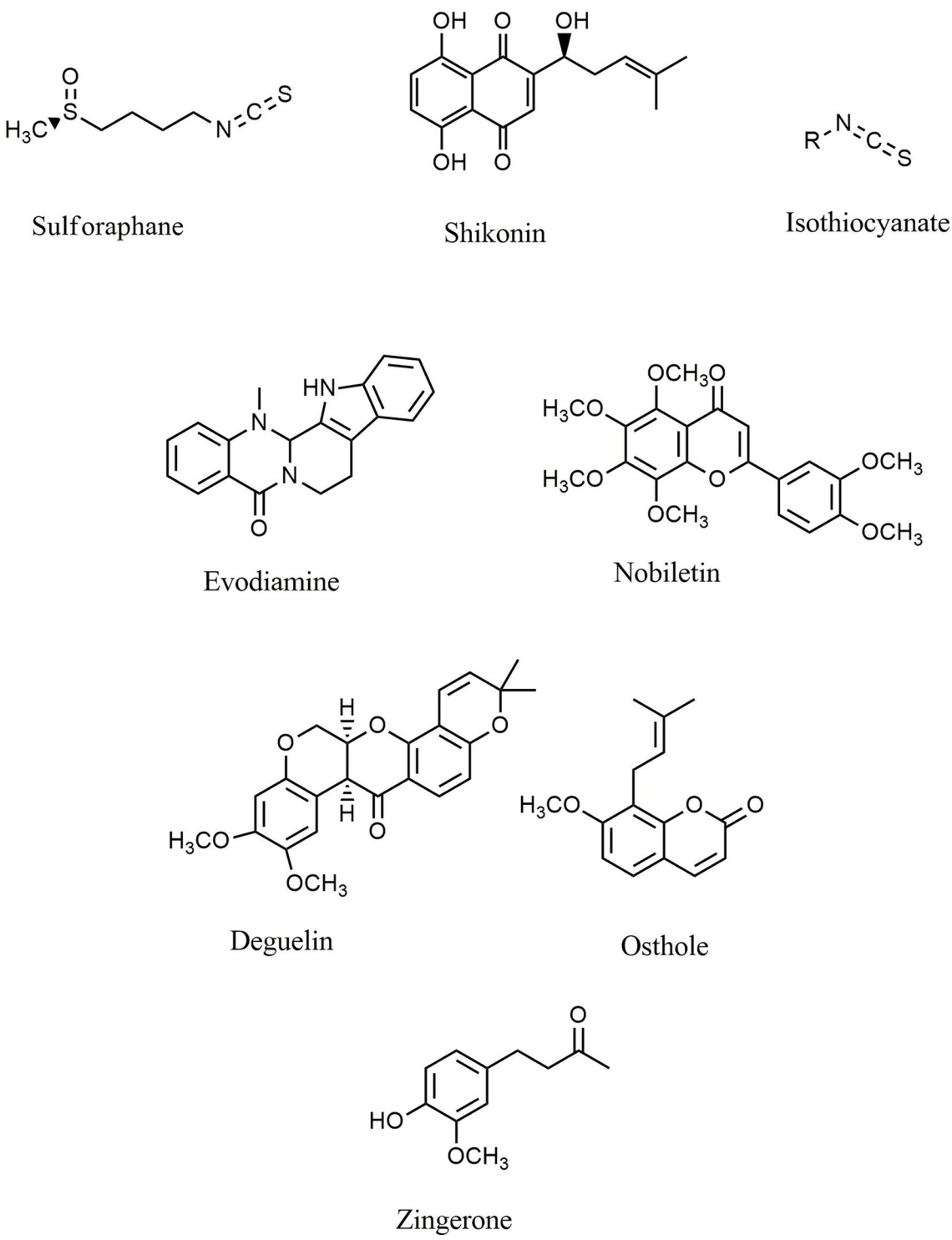

FIGURE 7 | Chemical structures of selected sulfur-containing compounds and miscellaneous agents with effect on TLR/NF-κB/NLRP signaling in cancer.

T24) (359), pancreatic (MIA PaCa-2 and Panc-1) (360), and ovarian (OVCAR3 and SKOV3) (361) cancer cells, respectively. The results emphasized that EGCG could potentate the antineoplastic activity of the aforementioned drugs by increasing the sensitivity of the cancer cells, thereby enhancing their antiproliferative activity, damaging DNA, interfering with the NF-κB/MDM2/p53 pathway, inhibiting Akt, and elevating copper transporter 1 (CTR1). Likewise, cotreatment of naringin

TABLE 4 | Anticancer sulfur compounds and miscellaneous agents interfering with the TLR/NF-κB/NLRP pathway and interconnected mediators against chemoresistance.

Compound	Types of study	Cell line(s)/tumor model(s)	Mechanisms of action	References
Sulforaphane	*In vitro*	Squamous cell carcinoma (PCI15A)	↓TLR3; ↓NF-κB	(282)
	In vitro	Breast cancer cell (MCF-7)	↓NF-κB; ↓MMP-9; ↓Phosphorylation of IκB;	(283)
Shikonin	*In vitro*	Human gastric cancer cell (MGC-803)	↓TLR2; ↓NF-κB; ↓Cell invasion; ↓MMP-2; ↓MMP-7; ↓p65 NF-κB	(285)
	In vitro and *in vivo*	Hepatocellular carcinoma (Huh7 and BEL7402); Xenograft mice	↓RIP1/NF-κB; ↓Akt	(284)
Xanthohumol & phenethyl isothiocyanate	*In vitro*	Pancreatic cancer cell (PANC-1)	↓NF-κB; ↑Nrf-2; ↑GSTP; ↑NQO1; ↑SOD; ↓MMP-2; ↓MMP-7; ↓MMP-9; ↓FAK	(286)
Xanthohumol	*In vitro* and *in vivo*	B-cell acute lymphocytic leukemia; Xenograft mouse model	↓NF-κB; ↓FAK; ↓Akt	(287)
Phenethyl isothiocyanate	*In vitro*	Gastric cancer cell (AGS)	↓Cell migration; ↓cell invasion; ↓MAPK; ↓NF-κB	(288)
Evodiamine	*In vitro*	Prostate cancer (DU145, PC-3)	↓Cellular growth; ↑apoptosis	(291)
	In vitro	Lung cancer cell line (A549)	↓Akt/NF–κB; ↑apoptosis; ↓GSH; ↓SHH/GLI1	(290)
	In vitro	Melanoma cell (A375-S2)	↓PI3K/Akt/caspase; ↓Fas-L/NF-κB	(289)
Evodiamine derivatives	*In vitro* and *in vivo*	Hepatocellular carcinoma cells (HepG2, Huh-7, MHCC-LM9); Nude male mice	↓Topo I; ⊥G2/M cell cycle arrest; ↑Apoptosis; ↓cell migration; ↓cell invasion; ↓tumor volume; ↓tumor weight	(292)
Marine	*In vitro*	Breast cancer cell (MDA-MB-231); Monocytic leukemia cell (THP-1)	↓NF-κB; ↓cytokine release; ↓phosphorylation of p65; ↓phosphorylation of IκB	(294)
	In vitro	Pancreatic cancer cells (PANC-1, AsPC-1, MIA PaCa-2, BxPC-3)	↓NF-κB; ↑Apoptosis	(293)
Matrine	*In vitro*	Human lung carcinoma cell (A549); Pancreatic cancer cells (MIA PaCa-2); Prostate cancer cells (DU145)	↓NF-κB; ↓CXCR4; ↓MMP-9, MMP-2	(298)
	In vitro	Prostate cancer cell (PC-3, DU145)	↓NF-κB	(296)
	In vitro	Prostate cancer cell (DU145)	↓NF-κB; ↓GADD45B; ↓MMP-2; ↓MMP-9	(297)
Oxymatrine	*In vitro* and *in vivo*	Pancreatic cancer cells (PANC-1); BALB/C male mice	↓NF-κB; ↓VEGF	(295)
Nobiletin	*In vitro*	Breast cancer cells (MDA-MB-231, MCF-7)	↓Cd36/Stat3/NF-κB; ↓angiogenesis; ↓migration; ↓invasion; ↓STAT3; ↓CD36;	(299)
	In vitro	Ovarian cancer cells (OVCAR-3, A2780/CP70)	↓NF-κB; ↓tumor growth; ↓angiogenesis; ↓Akt; ↓HIF-1α; ↓VEGF	(300)
	In vitro	Prostate cancer cell (PC-3, LNCaP)	↓TRIF protein; ↓caspase-8; ↓TRIF/RIPK1/FADD; ↓TLR3/IRF-3	(301)
	In vitro	Gastric adenocarcinoma (AGS)	↓NF-κB; ↓FAK/PI3K/Akt	(302)
UDN glycoprotein	*In vivo*	Male mice (ICR)	↓NF-κB	(303)
Phenylpropenone derivatives	*In vitro*	Human colon carcinoma cell (HT-29)	↓NF-κB; ↓PERK; ↓RTKs; ↓VEGF	(304)
Libanoridin	*In vitro*	Human colon carcinoma cell (HT-29)	↓iNOS; ↓COX-2; ↓TNF-α; ↓IL-1β	(305)
Alisol B 23-acetate	*In vivo*	Male C57BL/6J mice	↓TLR; ↓NF-κB; ↓MAPK; ↓phosphorylation of p38; ↓PERK; ↓PJNK	(306)
Deguelin	*In vitro* and *in vivo*	Xenograft athymic mice; MDA-MB-231, MDA-MB-468, BT-549 and BT-20 cells	↓NF-κB; ↓EGFR; ↓c-Myc	(307)
Withaferin A	*In vitro*	Hepatocellular carcinoma cell (QGY-7703)	↓NF-κB; ↓liver X receptor-a; ↓angiogenesis	(308)
	In vitro	Monocytic leukemia cell (THP-1)	↓Caspase-1; ↓AIM-2; ↓TGF-β	(309)
Zingerone	*In vitro*	Hepatocellular carcinoma cell (SNU182)	↓Cell migration; ↓cell invasion; ↓MMP-2; MMP-9; ↓Smad2/3; ↓NF-κB; ↓P42/44 MAPK/AP1	(310)
Ophiopogonin D	*In vitro*	Lung cancer cell (A549)	↓NF-κB; ↓cell proliferation; ↓PI3K/Akt; ↓AP-1	(314)
Osthole	*In vitro*	Lung cancer cell (A549)	↓NF-κB	(312)
	In vitro	Lung adenocarcinoma cells (H1299 and A549)	↓NF-κB; ↓MMP-9	(311)
	In vitro	Cervical cancer cells (HeLa, SiHa, C–33A and CaSki)	↓ATM/NF–κB; ↑E–cadherin; ↓vimentin; ↑DNA damage; ↓NF-κB	(313)
Embelin	*In vitro* and *in vivo*	Breast cancer cell (MDA-MB-231)	↓NF-κB; ↓Cell invasion; ↓Cell migration; ↓CXCR4; ↓MMP-9; MMP-2	(315)

(Continued)

TABLE 4 | Continued

Compound	Types of study	Cell line(s)/tumor model(s)	Mechanisms of action	References
Plumbagin	*In vitro* and *in vivo*	Pancreatic cancer cells (PANC1, BxPC3); Xenograft SCID male mice	↓NF-κB; ↓EGFR; ↓STAT3	(316)
	In vitro	Gastric cancer cells (SGC-7901, MKN-28, AGS)	↓NF-κB	(317)
Ondole glucosinolates	*In vitro* and *in vivo*	Ehrlich ascites carcinoma cells; Albino mice	↓NF-κB; ↓IL-6; ↓IL-1β; ↓TNF-α; ↓NO	(318)
Thymoquinone	*In vitro*	Human myeloid cells (KBM-5)	↓NF-κB; ↑Apoptosis; ↓VEGF	(319)
	In vitro	Metastatic human (A375) and mouse (B16F10) melanoma cells	↓NLRP3; ↓NF-κB	(320)
Decursinol angelate	*In vitro*	Fibrosarcoma cell (HT1080); Breast cancer cell (MDA-MB-231)	↓NF-κB; ↓PI3K; ↓ERK; ↓β1-integrin; ↓MMP-9	(321)
Polysaccharide agaricus blazei murill	*In vivo*	TLR2-/- mice	↓TLR2; ↑IL-12, ↓Arg-1; ↑iNOS	(322)
HEG	*In vivo*	Swiss albino Wistar	↓NF-κB; ↓COX-2; ↓PGE2	(323)

with doxorubicin (362) and paclitaxel (363) amplified their anticancer activity against human esophageal and prostate cancer cells, respectively. Moreover, baicalin improved the chemosensitivity to cisplatin (364) and doxorubicin (365) in lung and breast cancer cells, respectively, by inducing cell cycle arrest, apoptosis, and DNA damage. Furthermore, arctigenin sensitized various cancer cell lines, including SW620, HepG2, H460, HeLa, SW480, and K562, to cisplatin treatment (366–368). Morin (369), chrysin (370), and pterostilbene (371) are some of the other polyphenolic compounds that increased the cytotoxicity of antineoplastic agents in several *in vitro* models of cancer.

In addition to polyphenols, terpenes also showed a significant ability to increase the sensitivity of different cancer cell lines to various drugs, such as 5-FU, gefitinib, cisplatin, doxorubicin, and gemcitabine. Combination therapy of cisplatin and paclitaxel with zerumbone, a sesquiterpene agent, enhanced ROS production and p53 expression, as well as inhibited the JAK2/STAT3 pathway in prostate and lung cancer cells (372, 373). It was reported that andrographolide augmented the doxorubicin-mediated antitumor activity in different cancer cells through the blockade of JAK/STAT3 signaling (374, 375) and its coadministration with gemcitabine promoted apoptosis and inhibited STAT3 in pancreatic cancer cells (376). Furthermore, treatment with andrographolide increased cisplatin-induced antineoplastic activity against lung cancer cells (377). Carnosic acid is another triterpenoid compound that, in combination with cisplatin and tamoxifen, promoted apoptosis in lung (378) and breast (379) cancer cells. In addition to carnosic acid, triptolide showed significant anticancer properties and amplified the *in vitro* and *in vivo* anticancer activity of various chemotherapeutic agents, including cisplatin (380–382), paclitaxel (383), hydroxycamptothecin (384, 385), gemcitabine (386), and doxorubicin (387), in several cancer types, including bladder (EJ, UMUC3, and T24R2), breast (MDA-MB-231, BT549, and MCF7), lung (A549), and gastric (SC-M1) cancer cell lines. Another triterpenoid compound, ursolic acid, potentiated the therapeutic effects of gemcitabine, oxaliplatin, cisplatin, and paclitaxel in human pancreatic and colorectal cancer cells by promoting apoptosis and inhibiting the inflammatory microenvironment and NF-κB p65 signaling (388–391). Moreover, treatment with oridonin overcame antibiotic resistance and augmented the antineoplastic effects of doxorubicin, cisplatin, and gemcitabine *via* increased expression of Bax, induction of apoptosis, downregulation of Bcl−2, and inhibition of MMP in the *in vivo* and *in vitro* models of lung, breast, pancreatic, and ovarian cancers (392–395). In a similar study, ginsenoside Rg3 enhanced the cytotoxicity of paclitaxel in breast cancer cells by regulating the expression of Bax/Bcl-2 and suppressing NF-κB signaling (396). Additionally, ginsenoside Rg3 amplified cisplatin therapy in the lung cancer cell lines H1299, SPC-A1, and A549 by inhibiting the NF-κB pathway (397, 398). Another study found that co-administration of ginsenoside Rg3 and gefitinib increased the cytotoxicity of gefitinib against lung cancer *in vitro* (399). The results demonstrated that the main mechanisms by which ginsenoside Ro enhances the anti-malignant effects of 5-FU occurs by accumulating DNA damage, inhibiting DNA repair, downregulating DNA replication, and delaying the degradation of checkpoint kinase 1 (CHEK1) (400). The treatment combination of docetaxel and ginsenoside Rg3 increased activation of the apoptotic pathway in colon and prostate cancer cells *via* suppression of NF-κB (401, 402). Lycopene, a carotenoid agent, improved cisplatin-induced apoptosis in HeLa cancer cells *via* inhibition of NF-κB activation (403).

Alkaloids, like other secondary metabolites, enhance the *in vitro* and *in vivo* anticancer activities of various drugs by elevating their antiproliferative effects and promoting apoptosis and cell cycle arrest. The combined effects of doxorubicin and berberine on lung (404) and breast (405, 406) cancer cells inhibited the STAT3, high mobility group box 1 (HMGB1)-TLR4 axis and downregulated the expression of Nanog and miRNA-21. Cisplatin and berberine combined therapy also inhibited cell growth, promoted apoptosis, created DNA breaks, and interfered with miR-93/PTEN/Akt signaling in MCF-7 and A2780 cells (407, 408). Moreover, berberine increased the chemotherapy potential of irinotecan against *in vitro* models of colon cancer through the suppression of

NF-κB (409). Another alkaloid compound, piperlongumine, induced apoptosis and potentiated the anticarcinogenic activity of doxorubicin, paclitaxel, oxaliplatin, cisplatin, and gemcitabine *via* suppression of the JAK2/STAT3 pathway and induction of oxidative stress in breast, intestinal, gastric, HNSCC, colorectal, and pancreatic cancer cells (410–415). In a similar study, harmine, in combination with paclitaxel, suppressed the invasion and migration of SGC-7901 and MKN-45 gastric cancer cell lines *via* downregulation of MMP-9 and COX-2 (416, 417). In addition, harmine suppressed the proliferation of pancreatic cancer cells *in vitro* by enhancing the cytotoxicity of gemcitabine (418). Likewise, several studies have reported the advantages of combining matrine with irinotecan and cisplatin to augment their antitumor activity against human colorectal (HT29) (419), urothelial bladder (EJ and T24) (420), liver (HepG2) (421), and cervical (U14) (422) cancer cell lines. The results suggested that matrine significantly potentiated the antineoplastic effects of both irinotecan and cisplatin and increased the sensitivity of the aforementioned cancer cells to treatment through induction of apoptosis, facilitation of cell cycle arrest, and enhanced activity of topoisomerase I, ROS, β–catenin, Bax, caspase-3, caspase-7, and caspase-9. Treatment with sophoridine inhibited the growth of lung cancer cells by amplifying cisplatin sensitivity *via* activation of Hippo and p53 signaling (423).

Sulforaphane could significantly sensitize human breast, lung, colorectal, and bladder cancer cells to variant chemotherapeutic agents *via* downregulation of NF-κB, induction of cell cycle arrest, and reduction of cyclin A and p-Akt (424–427). Furthermore, sulforaphane increased the *in vitro* and *in vivo* antiproliferative activity of salinomycin in colorectal cancer cells *via* diminished signaling of the PI3K/Akt pathway (428). Moreover, shikonin reversed gemcitabine tolerance in a xenograft model of pancreatic cancer *via* modulation of the NF-κB signaling pathway (429). Treatment with shikonin potentiated the antitumor efficacy of gefitinib in lung cancer cells through suppression of the PKM2/STAT3/cyclin D1 pathway (430). Shikonin also increased the sensitization of paclitaxel against esophageal cancer cells by promoting apoptosis (431). Additionally, shikonin enhanced 4-hydroxytamoxifen-induced apoptosis in breast cancer cells by activating mechanisms involved in apoptosis and its related signaling pathways (432). It was reported that co-treatment of breast cancer cells with phenethyl isothiocyanate and paclitaxel induced apoptosis, arrested the cell cycle, and inhibited cell growth (433, 434). Garcinol induced the death of the breast cancer cell lines MCF7, MDAMB231, and SKBR3 *via* triggering p53-dependent upregulation of Bax and downregulation of Bcl-xL (435). It also potentiated cisplatin sensitivity in HNSCC (436) and ovarian (437) cancer cells, as well as enhanced paclitaxel sensitivity in breast cancer cells (438) *via* inhibition of survivin, NF-κB/Twist-related protein 1 (Twist1), VEGF, caspase-3/calcium-independent phospholipase A2 (iPLA2), cyclin D1, Bcl-2, and PI3K/Akt signaling.

Hispidin (439), genistein (440, 441), guggulsterone (442), ginkgolide B (443), icariin (444), and zyflamend (445) potentiated the antineoplastic activity of gemcitabine in several cancer types, including pancreatic, osteosarcoma, and gallbladder cancers. Cisplatin in combination with tangeretin (446), galangin (447), and cepharanthine (448) decreased the proliferation and invasion of esophageal, lung, and ovarian cancer cells. Cotreatment of paclitaxel with icariside II (449) and caffeic acid (450), as well as combined treatment of 5-FU with oxymatrine (451), troxerutin (452), and calebin (453) increased the sensitivity of colon, lung, and melanoma cancer cells. Parthenolide (454) elevated oxaliplatin toxicity in A549 cells. The anticancer activity of doxorubicin was enhanced when combined with forbesione and isomorellin (455). Dioscin potentiated the effects of adriamycin in the K562 leukemia cell line (456).

In summary, phytochemicals have the potential to increase the sensitivity of various cancer cells and animal tumor models to several anticancer drugs. Phytochemicals augment chemoresistance through interfering with many processes, such as cell cycle arrest, DNA damage, angiogenesis, and variant signaling pathways, especially TLR/NF-κB/NLRP (**Table 5**).

NANOFORMULATIONS OF PHYTOCHEMICALS AGAINST CHEMORESISTANCE AND IMMUNOTHERAPY RESISTANCE

Mutations and long-term chemotherapy lead to the development of chemoresistance, prompting the need for progressively increasing dosages of anticancer drugs. Consequently, these higher concentrations of chemotherapeutic agents are toxic to noncancerous cells (457). Nanoparticles are increasingly used due to their improved bioavailability, protection of drug molecules, high specificity for cancer cells, and decreased clearance. Combining the versatile capabilities of nanoparticles with the aforementioned benefits of phytochemicals created the concept of phytonanomedicine, which revolutionized cancer therapy (458). Phytonanomedicine utilizes the valuable properties of phytochemicals merged with the nano-size, high surface area, optical activity, and surface reactivity of nanoparticles to achieve active or passive tissue-specific drug delivery. The application of phytonanocompounds may reduce the toxicity and side effects of chemotherapeutic agents, while increasing their efficacy, thereby combating chemoresistance (459).

Flavones are the most prominent natural phytochemical that regulates the functions of Bax, Bid, and Bak proteins. Additional mechanisms by which phytochemicals combat chemoresistance are altering the expression of selected genes during mitosis or meiosis, regulating the expression of mutated genes like p21 and p53, and interfering with DNA repair mechanisms. Liposomes, polymeric nanoparticles, polymeric micelles, nanodispersion, and dendrimers, among others, are efficient nanocarriers that are often used (460).

Quercetin-loaded mesoporous silica decorated with chondroitin sulfate potentiated the delivery of paclitaxel,

TABLE 5 | Phytochemicals in combination with anticancer drugs potentiate chemotherapy and immunotherapy: focusing on TLR/NF-κB/NLRP pathway.

Compound	Antineoplastic Agent	Types of study	Cell line(s)/cancer model(s)	Mechanisms of action	References
Curcumin	Paclitaxel	*In vitro* and *in vivo*	Xenograft model of human cervical cancer; Human cervical cancer (HeLa)	↓NF-κB; ↓tumor incidence; ↓tumor volume; ↓survival signals; ↓Akt; ↓MAPKs; ↓cell proliferation; ↓angiogenesis	(327)
	Paclitaxel	*In vitro*	Breast cancer cells (MDA-MB-231, MCF-7)	↑apoptosis; ↑necrosis	(329)
	Paclitaxel	*In vitro*	Breast cancer cells (MDA-MB-231, MCF-7)	↓NF-κB; ↓c-Ha-Ras; ↓Rho-A; ↓p53; ↓Bcl-XL; ↓Bcl-2	(328)
	Paclitaxel	*In vitro*	Cervical cancer cells (HeLa, CaSki)	↑apoptosis; ↑p53; ↑cleavage of caspase–3; ↓cell growth; ↓NF–κB–p53–caspase–3	(330)
	Paclitaxel & Cyclophosphamide	*In vitro* and *in vivo*	Breast cancer cells (MDA-MB-231, MCF-7); Swiss albino mice	↓NF-κB; ↓PKC; ↓HDAC; ↓telomerase	(331)
	Oxaliplatin	*In vitro*	Colorectal adenocarcinoma (LoVo, HT29, and DLD1)	↓Akt/NF-κB; ↓CXC-Chemokine/NF-κB; ↓NF-κB	(332)
	Cisplatin; Carboplatin; Oxaliplatin	*In vitro*	Human colorectal cancer cell (HT-29)	↓NF-κB; G2/M arrest; ↑apoptosis	(333)
	Dasatinib	*In vitro* and *in vivo*	Human colon cancer cell (SW-620, HCT-116, HT-29); Female min mice	↓NF-κB activity; ↓IGF-1R; ↓C-Src; ↓EGFRs; ↓cell growth	(334)
	Tamoxifen	*In vitro*	Breast cancer cells (MCF-7/LCC9 and MCF-7/LCC2)	↓NF-κB; ↓Akt/mTOR; ↓Src; ⊥ G2/M cell cycle arrest	(335)
	Retinoic acid	*In vitro*	Breast cancer cell lines (MDA-MB-231 and MD-MB-468)	↓FABP5; ↓PPARβ/δ; ↓VEGF-A; ↓PDK1	(336)
	Doxorubicin	*In vivo*	Xenograft 4T1 tumor-bearing mice	↓NF-κB	(337)
	Sorafenib	*In vitro* and *in vivo*	Hepatocellular carcinoma (Huh7); Athymic BALB/c nu/nu mice	↓NF-κB/p65; ↓MMP-9	(338)
Resveratrol	Cisplatin	*In vitro* and *in vivo*	Breast cancer cells (MDA-MB-231); Xenografts BALB/c mice	↓tumor growth; ↓TGF-β1; ↓Fibronectin	(483)
	Cisplatin	*In vitro*	Prostate cancer cell (PC3 and DU145)	↑Apoptosis; ↓COX-2; ↓NF-κB; ↑DUSP1	(339)
	Cisplatin	*In vitro*	Non-small cell lung cancer cell (NCI-H460)	↓Cell invasion; ↓cell migration; ↑apoptosis; ↓NF-κB; ↓Bcl-2; ↑caspase-3; ↑p53; ↑Bax; ↑p21; ⊥G0/G1 phases cell cycle	(340)
	5-fluorouracil (5-FU)	*In vitro*	Colorectal cancer cells (SW480R, HCT116)	↓IκBα kinase; ↓IκBα phosphorylation; ↓NF-κB	(341)
Apigenin	Paclitaxel	*In vitro*	Cervical cancer cell (HeLa)	↑Apoptosis; ↑ROS; ↓SOD activity; ↑cleavage of caspase-2	(343)
	Tamoxifen	*In vitro*	Breast cancer cells (MCF-7)	↑Apoptosis; ⊥G2/M phase cell cycle; ↑p53; ↓Cyclin B1	(344)
	Gemcitabine	*In vitro*	Pancreatic cancer cells (CD18, AsPC-1)	↓Cell proliferation; ⊥ G2/M and S phases cell cycle; ↑apoptosis; ↓pAkt	(346)
	Gemcitabine	*In vitro* and *in vivo*	Pancreatic cancer cells (MiaPaca-2, AsPC-1); Xenograft BALB/c nude mice	↓NF-κB; ↓tumor growth; ↓Akt; ↑apoptosis	(345)
	Doxorubicin	*In vitro*	Human prostate cancer cell (PC3)	↑Caspases; ↑Bax; ↑cyt c; ↓Bcl-XL; ↑p21; ↑p27; ↓Snail; ↓Twist; ↓MMPs; ↓pERK; ↑PTEN; ↓pPI3K; ↓pAkt	(347)
	Cisplatin	*In vitro*	Human prostate cancer cell (PC3)	↑Apoptosis; ↑Caspase-8; ↑Apaf-1; ↑p53; ↓Bcl-2; ↑p21; ⊥G2/M and S phases cell cycle	(348)
	Cisplatin	*In vitro* and *in vivo*	Human bladder cancer cells (UMUC2, T24); Swiss albino inbred mice	↓Tumor growth; ↑Mice survival	(353)
	Cisplatin	*In vitro* and *in vivo*	Oral squamous cell carcinoma (cell lines Tca-8113 and SCC-15); Xenograft mice models	↓NF-κB; ↑apoptosis; ↑caspase-8 and caspase-9; ↓xIAP	(352)
	Adriamycin	*In vitro* and *in vivo*	P388 leukemia cells; Xenograft mice models	↑NF-κB; ⊥S phase cell cycle; ↑Caspase-3; ↓Bcl-2; ↑Bax	(354)
	Gemcitabine	*In vitro*	Pancreatic cancer cells (PANC-1, BxPC-3); Hepatocellular carcinoma cell (Huh-7, HepG2)	⊥S phase cell cycle; ↑p53; ↓cyclin D1	(355)

(Continued)

TABLE 5 | Continued

Compound	Antineoplastic Agent	Types of study	Cell line(s)/cancer model(s)	Mechanisms of action	References
EGCG	Sunitinib	*In vitro* and *in vivo*	Human lung carcinoma (H460 and H1975); Breast carcinoma cells (MCF-7); Xenograft mouse model	↓IRS/MAPK/p-S6K1; ↓PI3K/Akt; ↓MEK/ERK	(357)
	Cisplatin	*In vitro* and *in vivo*	Mice bearing Ehrlich ascites carcinoma; Cervical cancer cell (HeLa); Lung cancer cells (A549); Monocytic leukemia cell (THP-1)	↓NF-κB activation; ↓cyclin D1, ↓MMP-9, and VEGF	(356)
	Irinotecan	*In vitro*	Colorectal cancer cell (HCT116 and RKO)	↓Cell migration; ↓Cell invasion; ⊥S phase cell cycle; ⊥G2 phase cell cycle; ↓topoisomerase I; ↑DNA damage; ↑apoptosis; ↑autophagy	(358)
	Doxorubicin	*In vitro*	Bladder cancer cells (SW780 and T24)	↓NF-κB; ↓MDM2; ↑p53; ↑p21; ↑cleaved-PARP	(359)
	Gemcitabine	*In vitro* and *in vivo*	Pancreatic cancer cells (MIA PaCa-2 and Panc-1); C57BL/6J mice	↓Cell growth; ↓cell invasion; ↓cell migration; ↓Akt	(360)
	Cisplatin	*In vitro* and *in vivo*	Ovary cancer cell (OVCAR3, SKOV3); Xenograft mouse model	↑Cisplatin; ↑DNA-Pt adducts; ↑copper transporter 1	(361)
Naringin	Doxorubicin	*In vitro* and *in vivo*	Esophageal cancer stem cell (YM1); Xenograft mouse model	↓Tumor size; ↓systemic toxicity; ↓Cell viability; ↑apoptosis; ⊥S phase cell cycle	(362)
	Paclitaxel	*In vitro*	Prostate cancer cells (PC3, DU145, and LNCaP)	↓Cell survival; ↑apoptosis; ⊥ G1 phase cell cycle	(363)
Baicalin	Cisplatin	*In vitro*	Lung cancer cells (A549 and A549/DPP)	⊥S1 phase cell cycle; ↑apoptosis; ↑DNA damage; ↑Bax; ↓Bcl-2; ↓cyclin D1; ↓DNA repair	(364)
	Doxorubicin	*In vitro*	Breast cancer cells (MCF-7, MDA-MB-23)	↑ROS; ↑apoptosis	(365)
Arctigenin	Cisplatin	*In vitro*	Colorectal cancer cells (SW480 and SW620)	↑Autophagy; ↑apoptosis; ↑Cleaved caspase-3; ↑LC3-II; ↓LC3-I	(368)
	Cisplatin	*In vitro*	Non small lung cancer cell (H460)	↓Survivin; ⊥G1/G0 phase cell cycle; ↑apoptosis; ↑cleavage of caspase-3	(367)
	Cisplatin	*In vitro*	Hepatocellular cancer cells (HepG2); Human cervical cancer (HeLa)	↓STAT3; ↓pSTAT3; ↓Src; ↓JAK1; ↓JAK2; ↓ERK; ↓Akt	(366)
Morin		*In vitro*	Ovarian cancer cells (SK-OV-3, TOV-21G)	↓Cell viability; ↓cell proliferation; ↑apoptosis; ↑galectin-3	(369)
Chrysin	Doxorubicin	*In vitro*	Lung cancer cells (H157, H1975, A549, H460)	↓GSH; ↑cell death	(370)
Pterostilbene	Tamoxifen	*In vitro*	Breast cancer cells (ZR-751 and MCF7)	↓Cell viability; ↑apoptosis	(371)
Zerumbone	Cisplatin	*In vitro*	Human NSCLC cells (A549 and NCI-H460)	↑p53; ↑ROS	(372)
		In vitro	Prostate cancer cells (DU145 and PC3)	↓Cell growth; ↓JAK2; ⊥G0/G1 phase cell cycle; ↑apoptosis	(373)
Andrographolide	Doxorubicin	*In vitro*	Hepatocellular cancer cell (HepG2); Cervical cancer cell (HeLa); Breast cancer cell (MDA-MB-231); Colorectal cancer cell (HCT116)	↓JAK-STAT3 pathway; ↓pSTAT3; ↓JAK1/2; ↑Apoptosis	(374)
	Doxorubicin	*In vitro* and *in vivo*	Murine breast cancer cell (4T1); Xenograft BALB/c nude mice	↓Tumor growth; ↓HUVEC; ↓VEGFR2; ↓cell migration; ↓cell invasion	(375)
	Gemcitabine	*In vitro*	Pancreatic cancer cells (SW1990, Panc-1, AsPC-1, BxPC-3, and Capan-1)	↓STAT3; ↓Akt; ↑Apoptosis; ↑$p21^{Waf1}$; ↑Bax; ↓Cyclin D1; ↓cyclin E; ↓survivin; ↓X-IAP; ↓Bcl-2	(376)
	Cisplatin	*In vitro* and *in vivo*	Human NSCLC cell (A549, LLC); C57BL/6 mice	↑Apoptosis; ↓LC3B-I; ↓LC3B-II; ↓Atg5	(377)
Carnosic acid	Cisplatin	*In vitro* and *in vivo*	Mouse Lewis lung cancer cell (LLC); C57BL/6 mice	↑IFN-γ; ↑FasL; ↑granzyme B; ↓MDSC; ↓iNOS2; ↓Arg-1; ↓MMP-9	(378)
	Tamoxifen	*In vitro* and *in vivo*	Breast cancer cells (MCF-7 and T47D); Mouse xenograft model	↑Apoptosis; ↑caspase-3; ↓Bcl-2; ↓Bcl-XL; ↑DcR1; ↑DcR2; ↑TRAIL; ↑Bax; ↑Bad	(379)
Triptolide	Cisplatin	*In vitro* and *in vivo*	Human gastric adenocarcinoma (AGS, SC-M1); SCID mouse xenograft model	↑Apoptosis	(380)
	Cisplatin	*In vitro*	Breast cancer cells (BT549, MDA-MB-231)	↑DNA breaks; ⊥S phase cell cycle; ↑DNA damage; ↓PARP1; ↓XRCC1; ↓RAD51	(382)
	Cisplatin	*In vitro*	Human bladder cancer cells (T24R2)	↑Caspase-9; ↑PARP; ↑cyt c; ↓pAkt; ↓pERK	(381)
	Paclitaxel		Human lung adenocarcinoma cell (A549); Xenografts balb/c-nude mice	↓Tumor growth; ↓tumor volume; ↓tumor size	(383)

(Continued)

TABLE 5 | Continued

Compound	Antineoplastic Agent	Types of study	Cell line(s)/cancer model(s)	Mechanisms of action	References
		In vitro and *in vivo*			
	Hydroxycamptothecin	*In vitro*	Bladder cancer cell (EJ, UMUC3)	⊥G1 phase cell cycle; ↓CDK4; ↓CDK6; ↓Cyclin D1; ↓Akt	(385)
	Hydroxycamptothecin	*In vitro*	Pancreatic cancer cell (PANC-1)	↓NF-κB; ↑caspase-9, caspase-3	(384)
	Doxorubicin	*In vitro*	MDA-MB-231 and MCF7	↑Apoptosis; ↓ATM; ↑DDR; ↑DNA break	(387)
Ursolic acid	Gemcitabine	*In vitro* and *in vivo*	Human pancreatic cancer cells (Panc-28, MIA PaCa-2, AsPC-1); Orthotopic nude mouse model	↓NF-κB; ↓STAT3; ↓cell proliferation; ↑apoptosis; ↓angiogenic	(389)
	Oxaliplatin	*In vitro* and *in vivo*	Colorectal cancer cells (RKO, SW620, LoVo, SW480); Xenograft mouse model	↓NF-κB; ↓cell proliferation; ↑Apoptosis; ↓ERK1/2; ↓JNK; ↓Akt; ↓IKKα; ↓pMAPK; ↓PI3K/Akt;	(390)
	Cisplatin	*In vitro*	Human cervical cancer cells (C-33A, HeLa, ME-180, SiHa);	↓NF-κB p65; ↑apoptosis; ↓Cell growth; ↓Bcl-2	(391)
	Paclitaxel	*In vitro* and *in vivo*	Ovarian carcinoma cells (HEC-1A and OVCAR-3); Nude mouse xenograft model	↓PI3K/Akt/NF-κB; ↑apoptosis; ↑pJNK; ↓pAkt; ↑JNK	(388)
Oridonin	Cisplatin	*In vitro*	Human ovarian cancer cells (A2780, SKOV3)	↑Apoptosis; ↓MMP; ⊥G0/G1 phase cell cycle	(393)
	Gemcitabine	*In vitro*	Pancreatic cancer cell (PANC−1)	↓Bcl−2/Bax ratio; ↑Cyt c; ↑caspase−3; ↑caspase −9; ↑apoptosis; ⊥G1 phase cell cycle	(392)
	Doxorubicin	*In vitro*	Breast cancer cell (MDA-MB-231)	↑Apoptosis; ↓Bcl-2/Bax; ↓PARP; ↓caspase 3; ↓survivin; ↓blood vessel formation	(394)
	Cisplatin	*In vitro*	Lung cancer cell (A549/DDP); Xenograft BABL/c mice	↑Tumor inhibition	(395)
Ginsenoside Rg3	Paclitaxel	*In vitro* and *in vivo*	Breast cancer cell (BT-549, MDA-MB-231, MDA-MB-453); Xenograft BALB/c nu/nu mice	↓NF-κB	(396)
	Cisplatin	*In vitro* and *in vivo*	Human NSCLC cell lines (H1299, SPC-A1, and A549); Xenograft tumor mice model	↓NF-κB	(398)
	Cisplatin	*In vitro*	Human NSCLC cell line (A549)	↓NF-κB p65; ↓PD-L1; ↓Akt	(397)
	Gefitinib	*In vitro*	Human NSCLC cell line (H1299, A549)	↓Cell migration; ↑Bax; ↑cleaved-caspase-3; ↓Bcl-2	(399)
	5-FU	*In vitro*	Esophageal squamous cell carcinoma (TE-1, ECA-109); Lung cancer cells (H460)	↑DNA damage; ↓DNA repair; ↓DNA replication; ↓CHEK1 degradation; ↓autophagy	(400)
	Docetaxel	*In vitro*	Colon cancer cells (HCT116, SW620)	↓NF-κB; ↑Bax; ↑caspase-3; ↑Caspase-9	(401)
	Docetaxel	*In vitro*	Prostate cancer cells (DU145, LNCaP, PC-3)	↓NF-κB; ↑apoptosis; ⊥G0/G1 phase cell cycle	(402)
Lycopene	Cisplatin	*In vitro*	Cervical cancer cell (HeLa)	↓NF-κB; ↓cell viability; ↑Bax; ↓Bcl-2; ↑Nrf-2	(403)
Berberine	Doxorubicin	*In vitro*	Lung cancer cell (NCI-H1975, NCI-H460)	↓STAT3; ↓cell proliferation; ↑Apoptosis	(404)
	Doxorubicin	*In vitro*	Breast cancer cell (MCF-7)	↓Nanog; ↓miRNA-21	(405)
	Doxorubicin	*In vitro*	Breast cancer cell (4T1)	↓HMGB1-TLR4 axis	(406)
	Cisplatin	*In vitro*	Ovarian cancer cell (A2780)	↓miR-93/PTEN/Akt; ↑Apoptosis; ⊥G0/G1 phase cell cycle; ↓miR-93	(407)
	Cisplatin	*In vitro*	Breast cancer cell (MCF-7)	↓Cell growth; ↑DNA breaks; ↑Apoptosis; ↑Capase-3; ↑Cleaved capspase-3; ↑Caspase-9; ↓Bcl-2	(408)
	Irinotecan	*In vitro*	Colon cancer cells (HCT116)	↓NF-κB; ↓c-IAP1, c-IAP2, survivin and Bcl-XL	(409)
Piperlongumine	Oxaliplatin	*In vitro* and *in vivo*	Gastric cancer cell (BMS-582949, SP600125); Nude mice xenograft model	↑ROS; ↓TrxR1; ↑DNA damage; ↑p38; ↑JNK	(414)
	Oxaliplatin	*In vitro* and *in vivo*	Colon cancer cells (HCT-116, LoVo); Xenograft mouse model	↑Oxidative stress; ↑ROS; ↑Apoptosis	(413)
	Cisplatin	*In vitro* and *in vivo*	HNSCC (AMC-HN3 and AMC-HN9); BALB/c athymic nude mice	↑ROS; ↑JNK; ↑PARP; ⊥Sub-G1 phase cell cycle	(410)
	gemcitabine	*In vitro* and *in vivo*	Pancreatic cells (PCNA and Ki-67); Xenograft mouse model	↓NF-κB	(411)
	Doxorubicin		Breast cancer cells (MDA-MB-231, MDA-MB-453); Mice models	↑Apoptosis; ↓JAK2/STAT3; ↓cell growth; ↑apoptosis	(412)

(Continued)

TABLE 5 | Continued

Compound	Antineoplastic Agent	Types of study	Cell line(s)/cancer model(s)	Mechanisms of action	References
		In vitro and *in vivo*			
Harmine	Paclitaxel	*In vitro*	Gastric cancer cells (SGC-7901 and MKN-45)	↓Cell migration; ↓cell invasion; ↓MMP-9; ↓COX-2	(416)
	Paclitaxel	*In vitro*	Gastric cancer cell (SGC-7901)	↓Bcl-2; ↑Bax; ↓PCNA; ↓COX-2	(417)
	Gemcitabine	*In vitro*	Pancreatic cancer cells (BxPC-3, CFPAC-1, PANC-1, SW-1990)	↑Apoptosis; ↓cell proliferation; ↑cleavage of PARP; ↑caspase-3; ↓Akt/mTOR	(418)
Matrine	Irinotecan	*In vitro*	Colorectal cancer cell (HT29)	↑Apoptosis; ↑topoisomerase I; ↑Bax; ↑caspase-3	(419)
	Cisplatin	*In vitro* and *in vivo*	Mouse cervical cancer cell (U14); Kunming mice	↑TSLC1; ↓tumor growth	(422)
Sophoridine	Cisplatin	*In vitro* and *in vivo*	Lung cancer cells (NCIH446, NCI-H1299, NCI-H460, A549); Xenograft model in BALB/c mice	↑p53; ↑Hippo signaling	(423)
Sulforaphane	Everolimus	*In vitro*	Bladder cancer cells (TCCSUP, RT112, UMUC3)	↓Cell growth; ↓cell proliferation; ↑p19; ↑p27; ↓phosphorylation of CDK1; ↓CDK1; ↓cyclin B; ⊥S phase cell cycle	(427)
	Oxaliplatin	*In vitro*	Colorectal cancer cells (Caco-2)	↓Cell proliferation; ↓ATP; ↑DNA cleavage; ↑caspase-3	(424)
	Gefitinib	*In vitro*	Lung adenocarcinoma cell (PC9)	↓Cell proliferation; ↓SHH; ↓SMO; ↓GLI1	(426)
	Paclitaxel	*In vitro*	Breast cancer cell lines (MDA-MB-231 and MCF-7)	↓NF−κB	(425)
	Salinomycin	*In vitro* and *in vivo*	Colorectal cancer cells (Caco-2 and CX-1); Xenografted nude mice	↓PI3K/Akt; ↑p53; ↑apoptosis; ↓Bcl-2; ↑Bax; ↑Bax/Bcl-2 ratio; ↑PARP cleavage	(428)
Shikonin	Gemcitabine	*In vitro* and *in vivo*	Pancreatic cancer cell (BxPC-3, PANC-1, AsPC-1); Xenograft mouse model	↓NF-κB; ↓tumor growth; ↓Cell proliferation; ↓micro vessel density; ↑apoptosis;	(429)
	Gefitinib	*In vitro* and *in vivo*	Human NSCLC cells (HCC827, H1299, A549, H1975); Nude mice	↑PKM2; ↓cell proliferation; ⊥G0/G1 phase cell cycle; ↑apoptosis; ↓PKM2/STAT3/cyclin D1	(430)
	Paclitaxel	*In vitro*	Esophageal cancer cells (KYSE270, KYSE150)	↑Apoptosis; ↓cell growth; ↓cell mitotic; ↓Bcl-2; ↑p53	(431)
	4-hydroxytamoxifen	*In vitro* and *in vivo*	Breast cancer cell lines (MCF−7 and MDA−MB −435S); BALB/c mice model	↑Apoptosis; ↓mitochondrial membrane potential; ↑ROS; ↓PI3K/AKT/caspase 9	(432)
Phenethyl isothiocyanate	Paclitaxel	*In vitro*	Breast cancer cells (MCF7, MDA-MB-231)	↓Cell growth; ↑Apoptosis; ⊥G2/M phase cell cycle	(433)
	Paclitaxel	*In vitro*	Breast cancer cells (MCF7, MDA-MB-231)	↑Apoptosis; ↑acetylation of alpha-tubulin; ↓Cdk1; ↓Bcl-2; ↑Bax; ↑cleavage of PARP	(434)
Garcinol	Cisplatin	*In vitro*	Ovarian cancer cells OVCAR-3	↓NF-κB; ↓PI3K/Akt phosphorylation; ↑Bax; ↓p-PI3K; ↓pAkt proteins; ⊥S phase cell cycle; ↑apoptosis	(437)
	Paclitaxel	*In vitro* and *in vivo*	Breast cancer cell (4T1); Balb/c mice metastasis model	↓NF-κB/Twist1; ↓caspase-3/iPLA2; ⊥G2/M phase arrest	(438)
Hispidin	Gemcitabine	*In vitro*	Pancreatic cancer cells (BxPC-3 and AsPC-1)	↓NF-κB; ↓cell proliferation; ↓Bcl-2; ↑tumor suppressor p53; ↑cleaved caspase-3; ↑cleaved PARP	(439)
Genistein	Gemcitabine	*In vitro*	Osteosarcoma cells (MG-63 and U2OS)	↓Akt/NF-κB	(440)
Genistein	Gemcitabine	*In vitro* and *in vivo*	–	↓NF-κB; ↓Akt	(441)
Ginkgolide B	Gemcitabine	*In vitro*	Pancreatic cancer cell (BxPC-3 and CAPAN1)	↓PAFR/NF-κB	(443)
Icariin	Gemcitabine	*In vitro* and *in vivo*	Human gallbladder carcinoma cell (GBC-SD and SGC-996); BALB/c (nu/nu) mice	↓NF-κB; ⊥G0/G1 phase arrest; ↓Bcl-2; ↓Bcl-XL	(444)
Zyflamend	Gemcitabine	*In vitro* and *in vivo*	Pancreatic cancer cell (AsPC-1, BxPC-3, MIA PaCa-2, PANC-1); Orthotopic mouse model	↓NF-κB	(445)

(Continued)

TABLE 5 | Continued

Compound	Antineoplastic Agent	Types of study	Cell line(s)/cancer model(s)	Mechanisms of action	References
Tangeretin	Cisplatin	*In vitro*	Human lung cancer cell (A549, A2780)	↓NF-κB; ↓PI3K/Akt; ↓apoptosis; ↓p-Akt; ↓phospho-GSK-3β; ↓phospho-BAD; ⊥G2-M phase arrest	(446)
Galangin	Cisplatin	*In vitro* and *in vivo*	Mice xenograft model	↓NF-κB; ↓STAT3; ↓Bcl-2/Bax; ↓p-STAT3/p65; ↓Bcl-2	(447)
Cepharanthine	Cisplatin	*In vitro* and *in vivo*	Human ESCC cell line (Eca109); BALB/c nude mice	↑TNFR1-JNK; ↓Bcl-2	(448)
Icariside II	Paclitaxel	*In vitro*	Human melanoma cell (A375)	↑Apoptosis; ↑cleaved caspase-3; ↓IL-8; ↓VEGF; ↓TLR4	(449)
Caffeic acid	Paclitaxel	*In vitro*	Human lung cancer cell (A549 and H1299)	↓NF-κB	(450)
Oxymatrine	5-FU	*In vitro*	Colon cancer cell (HCT-8/5-FU)	↓NF-κB; ↓vimentin	(451)
Troxerutin	5-FU	*In vitro* and *in vivo*	Human gastric cancer (SGC7901); Mice xenograft model	↓STAT3/NF-κB; ↓Bcl-2	(452)
Calebin a	5-FU	*In vitro*	Colorectal cancer cell (HCT116)	↓p65-NF-κB	(453)
Parthenolide	Oxaliplatin	*In vitro*	Human lung cancer cell (A549)	↓NF-κB; ↑apoptosis; ↓COX-2; ↓PGE2	(454)
Forbesione and isomorellin	Doxorubicin	*In vitro*	Human cholangiocarcinoma cells (KKU-100, KKU-M139, KKU-M156)	↓NF-κB; ↑Bax/Bcl-2; ↑caspase-9; ↓survivin	(455)
Dioscin	Adriamycin	*In vitro*	Leukemia K562 cell	↓NF-κB ↓MDR1	(456)

overcoming MDR in breast cancer cells. Such co-administration successfully targeted CD44 receptor-mediated targeting with a low half-maximal inhibitory concentration (IC_{50}) value by increasing cell cycle arrest in the G2/M phase and destroying microtubules. Quercetin also decreased paclitaxel efflux by downregulating the expression of P-gp (349). In another study, Zafar et al. (461) used phosphorylated chitosan nanoparticles loaded with α-lipoic acid to overcome chemotherapy resistance. The nanodelivery system was able to cross the cell barrier and expose the MDA-MB-231 cells to a high load of the therapeutic agent. Similar nanoparticles were also used for loading quercetin and paclitaxel simultaneously (462). The efficacy of curcumin and temozolomide co-delivery to chemoresistant cells was highlighted by Bagherian et al. (458). In this study, the curcumin nanomicelles demonstrated high cytotoxic effects against U87 cells by attenuating apoptotic and autophagic mediators. Zafar et al. (461) also used a phytochemical, thymoquinone, to prevent chemoresistance to docetaxel (e.g., endosomes escape). The neoplastic agent was loaded in chitosan nanoparticles and exhibited cytotoxicity against MCF-7 and MDA-MAB-231 cancer cell lines. Recently, a functionalized dendrimer has also been employed to co-deliver siRNA and curcumin to target HeLa cancer cells. Such co-administration increased the cytotoxicity against cancer cells by reducing Bcl-2 and improving apoptosis (463). Baicalein nanoparticles targeted folate and hyaluronic acid to display anticancer effects on paclitaxel-resistant lung cancer cells by decreasing tumor growth and cell viability (464). The nanosuspension of another flavonoid, chrysin, showed anticancer effects against HepG2 cells by blocking cell growth (465). The phytosome of luteolin, another flavonoid, exhibited anticancer activity against MDA-MB-231 cells by reducing the expression of Nrf-2/HO-1 and decreasing cell viability (466). Poly-lactic acid (PLA)-polyethylene glycol (PEG) nanoformulation of luteolin also demonstrated anticancer effects against TU212 HNSCC cells, H292 lung cancer cells, and a xenograft mouse model of head and neck cancer (467).

Nanostructured lipid carriers were also used for dual drug loading of imatinib and curcumin to target the CD20 receptor of lymphoma cells. This co-delivery system displayed promising responses in resistant tumor cells (468). By regulating oxidative stress and apoptosis, phyto-nanocomposites diffuse into the organelles of cancer cells and overcome chemoresistance through multiple signaling pathways, including TLR/NF-κB/NLRP, ERK/MAPK/JNK, stress-activated protein kinase/JNK, TRAIL, PI3K/Akt, and p53/caspase mediated apoptotic pathways (469).

Poly(lactic-co-glycolic acid nanoparticles of 4-methyl-7-hydroxy coumarin (a synthetic coumarin) and dendrosomal nanoformulation of farnesiferol c (a coumarin) demonstrated anticancer effects by decreasing cell proliferation in gastric cancer cells and by modulating the Bax/Bcl-2 ratio (470). Other phytochemicals, such as flavonolignans PEG nanoliposomes, silibinin, and glycyrrhizic acid, demonstrated anticancer effects by decreasing cell viability in HepG2 cells (471).

A nanoformulation of honokiol, a lignan, showed anticancer effects in lung cancer cell lines by inducing cell cycle arrest in the G0/G1 phase (459). Silver nanoparticles of plumbagin, a naphthoquinone, induced apoptosis in the human skin cancer cells HaCaT and A431, producing free radicals and increasing pyruvate kinase activity (472). Liposomal phytochemicals may possess anticancer effects in intravenous usage. The liposomal carrier significantly increased plasma levels of curcumin in a dose-dependent manner in cancer patients. In one clinical study, liposomal curcumin showed acceptable plasma concentration

with a significant but temporary decrease in tumor markers such as prostate-specific antigen and carcinoembryonic antigen, in patients with metastatic tumors. Additionally, liposomal curcumin inhibited sphingosine kinase (473). Lipocurcumin is known to be a safe drug that significantly suppresses cancer markers *via* apoptosis and cell cycle arrest. The curcumin nanoparticle suppressed STAT3/NF-κB, thereby inducing apoptosis. Accordingly, the phase Ib/IIa clinical trial showed no drug-related severe toxicity while maintaining an inhibitory effect on cancer resistance. Such nanoparticles could target cancer-specific mediators in solid tumors (473).

The hyaluronic acid-modified PEGylated liposomes of doxorubicin-stigmasterol were used against chemoresistant breast cancer (474). Gold nanoparticles have shown promising potential in both cancer chemotherapy and immunotherapy (475). Resveratrol gold nanoparticles improved antitumor activity through mitochondrial accumulation and apoptosis both *in vitro* and *in vivo*. Gold nanoresveratrol also elevated the expression of caspase-8 and Bax, while reducing pro-caspase-3 and pro-caspase-9. Ginseng-derived nanoparticles are another phytonanocompound that induced M2 to M1 macrophage polarization through TLR4 and MyD88 signaling. It also produced ROS and increased apoptosis of melanoma cells (476).

Various nanoparticles may represent a novel class of nano-targeted systems in cancer immunotherapy and chemotherapy (**Table 6**).

CONCLUSION, CURRENT LIMITATIONS, AND FUTURE PERSPECTIVES

Agrowing number of reports have highlighted the difficulty of chemoresistance when administering chemotherapy and immunotherapy. Several complex pathophysiological mechanisms behind chemoresistance have been discovered. Of those mechanisms, TLR/NF-κB/NLRP has been identified as a crucial aspect in the development of chemoresistance. The TLR/NF-κB/NLRP pathway is interconnected with several inflammatory, oxidative stress, and apoptotic mediators. Thus, there is an urgent need to develop novel multi-targeted agents to overcome drug resistance and restore the sensitivity of current chemotherapeutic drugs. Plant secondary metabolites (e.g., polyphenols, alkaloids, terpenes/terpenoids, and sulfur compounds) are potential multi-targeted anticancer agents that may combat chemoresistant dysregulated mediators. We have also reviewed the potential of phytochemicals in the modulation of the tumor microenvironment (13, 33, 480). Despite the

TABLE 6 | Phytonanocompounds against chemoresistance, by targeting TLR/NF-κB/NLRP pathway and interconnected mediators.

Compound	Nanoparticle type	Type of study	Cell line(s) cancer model(s)	Mechanisms of action	References
Curcumin	NLCs; liposome	*In vitro*	Cervical cancer cell (HeLa); Glioblastoma cells (U87 MG); Prostate cancer cell lines (LNCaP & C4-2B)	↓Bcl-2; ↑apoptosis; ↓PSA, CEA, CA 19-9; ↑sphingosine kinase inhibitory activity	(463, 477)
Quercetin	Different nanoparticles	*In vitro* and *in vivo*	Brest cancer cell line; Human prostate cancer (PC-3); Nude male BALB/c mice	↑cd44 activity; ↑apoptosis; ↑G2M phase arrest; ↓P-gp expression	(349)
Coumarins	Dendrosome	*In vitro*	Gastric adenocarcinoma (AGS)	↑Apoptosis; ↑DNA fragmentation; ↑caspase-3	(470)
Silibinins	Nanoliposome	*In vitro*	Hepatocellular carcinoma cell (HepG2)	↓Cell viability	(471)
Resveratrol	Nanoparticles based on poly(epsilon-aprolactone) and poly(D,L-lactic-co-glycolic acid)-poly(ethylene glycol); Gold NPs	*In vitro* and *in vivo*	Prostate cancer cells (PC-3, LNCaP, DU-145)	↓Cell growth & proliferation; ↑ROS; ↑caspase-3; caspase-8; ↑Apoptosis; ↑Bax; ↓pro-caspase-3; pro-caspase-9	(478)
Honokiol	Nanomicellar	*In vitro* and *in vivo*	Lewis lung cancer LL/2 cell lines	↑Cell cycle arrest at G0/G1 phase	(459)
Plumbagin	Different nanoparticles	*In vitro*	Epidermoid carcinoma cell (HacaT, A431)	↑Free radicals; ↑pyruvate kinase activity	(472)
Biacalein	Different nanoparticles	*In vitro*	Human lung cancer cell (A549)	↓Cell viability	(465)
Luteolin	Different nanoparticles	*In vitro*	Breast cancer cells (MDA-MB-231); Human lung cancer cell (H292)	↓Nrf-2 expression; ↑Akt	(466)
Ginseng	Different nanoparticles	*In vivo* and *in vitro*	Melanoma cells	↑TLR4; ↑ROS; ↑M1 macrophages	(476).
Taxan alkaloids	Liposome & polymeric micelle formulation	*In vivo*	Gastric cancer; Prostate cancer cell lines (PC3, DU145, and LNCaP)	↓Cell survival; ↑apoptosis; ⊥G1 phase cell cycle	(479)
Taxan alkaloids	Liposome	*In vitro*	Colon cancer cells (HCT116, SW620); Prostate cancer cells (DU145, LNCaP, PC-3)	↓P-gp	(401)
Vinca alkaloids	Liposome	*In vitro*	Colorectal cancer cell (HCT116 and RKO)	↑DNA damage; ↑cell cycle arrest	(358)

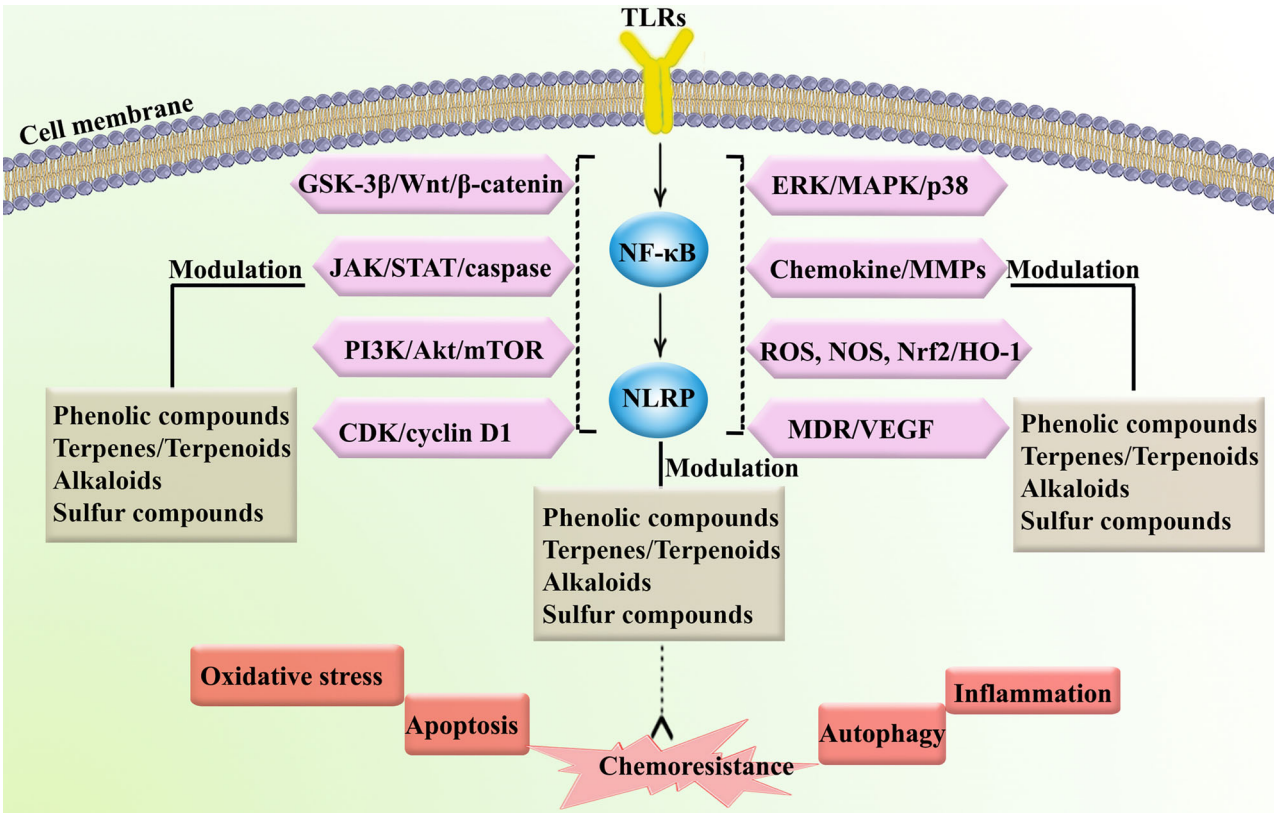

FIGURE 8 | Targeting chemoresistance-related signaling pathways and interconnected mediators by phytochemicals. CDK, cyclin-dependent kinase; ERK, extracellular-regulated kinase; GSK-3, glycogen synthase kinase-3; HO-1, heme oxygenase 1; JAK, Janus kinase; NOS, nitric oxide synthase; MAPK, mitogen-activated protein kinase; MDR, multidrug resistance; MMP; matrix-metalloproteinase; mTOR, mammalian target of rapamycin; NLRP, nod-like receptor pyrin domain-containing; NOS, nitric oxide synthase; Nrf-2, nuclear factor-erythroid factor 2-related factor 2; PI3K, phosphoinositide 3-kinases; ROS, reactive oxygen species; STAT, signal transducer and activator of transcription; VEGF, vascular endothelial growth factor.

effectiveness of plant secondary metabolites in regulating chemoresistance-associated pathways, their low solubility, poor bioavailability, instability, and low selectivity limit clinical efficacy and therapeutic uses in cancer treatment. The applicability of nanotechnology has greatly improved bioavailability, cellular uptake, efficacy, and specificity of anticancer phytochemicals, thereby overcome those pharmacokinetic limitations (6, 13, 457, 481). In line with this, liposomes, polymeric nanoparticles, micelles, nanodispersion, nanostructured lipid carriers, and dendrimers of plant secondary metabolites have played pivotal roles in reducing chemoresistance (482).

In this systematic and comprehensive review, the critical roles of phytochemicals have been highlighted in the modulation of TLR/NF-κB/NLRP to combat chemoresistance. The need to develop novel delivery systems of plant secondary metabolites and targeted therapy is also highlighted. Further research should be performed involving additional dysregulated mechanisms in chemoresistance which may reshape therapeutic approaches to utilize plant-derived secondary metabolites (**Figure 8**). Additional studies should consist of extensive *in vitro* and *in vivo* experimentation to further unveil emergent chemoresistance signaling pathways, as well as well-controlled clinical trials. Such reports may reform current therapeutic strategies, allowing treatment methods to obtain higher potency/efficacy with fewer side effects and less chemoresistance by using phytochemicals that target the TLR/NF-κB/NLRP signaling pathway.

DATA AVAILABILITY STATEMENT

The original contributions presented in this study are included in the article/supplementary material. Further inquiries can be directed to the corresponding author.

AUTHOR CONTRIBUTIONS

Conceptualization, AB and SF. Literature search and collection: SF, SM, AY, and FN. Writing-original draft: SF, SM, AY, and FN. Writing-review and editing, SF, CW, and AB. Supervision: AB. Project administration: AB. All authors contributed to the article and approved the submitted version.

REFERENCES

1. Zheng H-C. The Molecular Mechanisms of Chemoresistance in Cancers. *Oncotarget* (2017) 8(35):59950. doi: 10.18632/oncotarget.19048
2. Ji X, Lu Y, Tian H, Meng X, Wei M, Cho WC. Chemoresistance Mechanisms of Breast Cancer and Their Countermeasures. *Biomed Pharmacother* (2019) 114:108800. doi: 10.1016/j.biopha.2019.108800
3. Cooke SL, Brenton JD. Evolution of Platinum Resistance in High-Grade Serous Ovarian Cancer. *Lancet Oncol* (2011) 12(12):1169–74. doi: 10.1016/S1470-2045(11)70123-1
4. Ntoufa S, Vilia MG, Stamatopoulos K, Ghia P, Muzio M. Toll-Like Receptors Signaling: A Complex Network for NF-κb Activation in B-Cell Lymphoid Malignancies. *Semin Cancer Biol* (2016) 39:15–25. doi: 10.1016/j.semcancer.2016.07.001
5. Li Q, Yang G, Feng M, Zheng S, Cao Z, Qiu J, et al. NF-κb in Pancreatic Cancer: Its Key Role in Chemoresistance. *Cancer Lett* (2018) 421:127–34. doi: 10.1016/j.canlet.2018.02.011
6. Fakhri S, Moradi SZ, Ash-Rafzadeh A, Bishayee A. Targeting Cellular Senescence in Cancer by Plant Secondary Metabolites: A Systematic Review. *Pharmacol Res* (2021):105961. doi: 10.1016/j.phrs.2021.105961
7. Moloudizargari M, Asghari MH, Nabavi SF, Gulei D, Berindan-Neagoe I, Bishayee A, et al. Targeting Hippo Signaling Pathway by Phytochemicals in Cancer Therapy. *Semin Cancer Biol* (2020). doi: 10.1016/j.semcancer.2020.05.005
8. Tewari D, Bawari S, Sharma S, DeLiberto LK, Bishayee A. Targeting the Crosstalk Between Canonical Wnt/β-Catenin and Inflammatory Signaling Cascades: A Novel Strategy for Cancer Prevention and Therapy. *Pharmacol Ther* (2021) 227:107876. doi: 10.1016/j.pharmthera.2021.107876
9. Bose S, Banerjee S, Mondal A, Chakraborty U, Pumarol J, Croley CR, et al. Targeting the JAK/STAT Signaling Pathway Using Phytocompounds for Cancer Prevention and Therapy. *Cells* (2020) 9(6):1451. doi: 10.3390/cells9061451
10. Tewari D, Patni P, Bishayee A, Sah AN, Bishayee A. Natural Products Targeting the PI3K-Akt-mTOR Signaling Pathway in Cancer: A Novel Therapeutic Strategy. *Semin Cancer Biol* (2019). doi: 10.1016/j.semcancer.2019.12.008
11. Yun BD, Son SW, Choi SY, Kuh HJ, Oh T-J, Park JK. Anti-Cancer Activity of Phytochemicals Targeting Hypoxia-Inducible Factor-1 Alpha. *Int J Mol Sci* (2021) 22(18):9819. doi: 10.3390/ijms22189819
12. Tewari D, Nabavi SF, Nabavi SM, Sureda A, Farooqi AA, Atanasov AG, et al. Targeting Activator Protein 1 Signaling Pathway by Bioactive Natural Agents: Possible Therapeutic Strategy for Cancer Prevention and Intervention. *Pharmacol Res* (2018) 128:366–75. doi: 10.1016/j.phrs.2017.09.014
13. Fakhri S, Moradi SZ, Farzaei MH, Bishayee A. Modulation of Dysregulated Cancer Metabolism by Plant Secondary Metabolites: A Mechanistic Review. *Semin Cancer Biol* (2020). doi: 10.1016/j.semcancer.2020.02.007
14. Marin JJ, Lozano E, Herraez E, Asensio M, Di Giacomo S, Romero MR, et al. Chemoresistance and Chemosensitization in Cholangiocarcinoma. *Biochim Biophys Acta (BBA)-Mol Basis Dis* (2018) 1864(4):1444–53. doi: 10.1016/j.bbadis.2017.06.005
15. Qiu J, Zheng Q, Meng X. Hyperglycemia and Chemoresistance in Breast Cancer: From Cellular Mechanisms to Treatment Response. *Front Oncol* (2021) 11:51. doi: 10.3389/fonc.2021.628359
16. Chen C-Y, Kao C-L, Liu C-M. The Cancer Prevention, Anti-Inflammatory and Anti-Oxidation of Bioactive Phytochemicals Targeting the TLR4 Signaling Pathway. *Int J Mol Sci* (2018) 19(9):2729. doi: 10.3390/ijms19092729
17. Chauhan A, Islam A, Prakash H, Singh S. Phytochemicals Targeting NF-κb Signaling: Potential Anti-Cancer Interventions. *J Pharm Anal* (2021). doi: 10.1016/j.jpha.2021.07.002
18. Seok JK, Kang HC, Cho Y-Y, Lee HS, Lee JY. Regulation of the NLRP3 Inflammasome by Post-Translational Modifications and Small Molecules. *Front Immunol* (2021) 11:3877. doi: 10.3389/fimmu.2020.618231
19. Bukowski K, Kciuk M, Kontek R. Mechanisms of Multidrug Resistance in Cancer Chemotherapy. *Int J Mol Sci* (2020) 21(9). doi: 10.3390/ijms21093233
20. Hasan S, Taha R, El Omri H. Current Opinions on Chemoresistance: An Overview. *Bioinformation* (2018) 14(2):80. doi: 10.6026/97320630014080
21. Khatoon E, Banik K, Harsha C, Sailo BL, Thakur KK, Khwairakpam AD, et al. Phytochemicals in Cancer Cell Chemosensitization: Current Knowledge and Future Perspectives. *Semin Cancer Biol* (2020). doi: 10.1016/j.semcancer.2020.06.014
22. Pietroiusti A, Campagnolo L, Fadeel B. Interactions of Engineered Nanoparticles With Organs Protected by Internal Biological Barriers. *Small* (2013) 9(9-10):1557–72. doi: 10.1002/smll.201201463
23. Salama L, Pastor ER, Stone T, Mousa SA. Emerging Nanopharmaceuticals and Nanonutraceuticals in Cancer Management. *Biomedicines* (2020) 8(9). doi: 10.3390/biomedicines8090347
24. Lyall RM, Hwang JL, Cardarelli C, FitzGerald D, Akiyama S, Gottesman MM, et al. Isolation of Human KB Cell Lines Resistant to Epidermal Growth Factor-Pseudomonas Exotoxin Conjugates. *Cancer Res* (1987) 47(11):2961–6.
25. Akbari B, Farajnia S, Ahdi Khosroshahi S, Safari F, Yousefi M, Dariushnejad H, et al. Immunotoxins in Cancer Therapy: Review and Update. *Int Rev Immunol* (2017) 36(4):207–19. doi: 10.1080/08830185.2017.1284211
26. Li S, Gao M, Li Z, Song L, Gao X, Han J, et al. P53 and P-Glycoprotein Influence Chemoresistance in Hepatocellular Carcinoma. *Front Biosci (Elite Ed)* (2018) 10:461–8. doi: 10.2741/e833
27. Giddings EL, Champagne DP, Wu M-H, Laffin JM, Thornton TM, Valenca-Pereira F, et al. Mitochondrial ATP Fuels ABC Transporter-Mediated Drug Efflux in Cancer Chemoresistance. *Nat Commun* (2021) 12(1):1–19. doi: 10.1038/s41467-021-23071-6
28. Liu X. ABC Family Transporters. *Adv Exp Med Biol* (2019) 1141:13–100. doi: 10.1007/978-981-13-7647-4_2
29. Guo F, Zhang H, Jia Z, Cui M, Tian J. Chemoresistance and Targeting of Growth Factors/Cytokines Signalling Pathways: Towards the Development of Effective Therapeutic Strategy for Endometrial Cancer. *Am J Cancer Res* (2018) 8(7):1317.
30. Hombach-Klonisch S, Mehrpour M, Shojaei S, Harlos C, Pitz M, Hamai A, et al. Glioblastoma and Chemoresistance to Alkylating Agents: Involvement of Apoptosis, Autophagy, and Unfolded Protein Response. *Pharmacol Ther* (2018) 184:13–41. doi: 10.1016/j.pharmthera.2017.10.017
31. Abbaszadeh F, Fakhri S, Khan H. Targeting Apoptosis and Autophagy Following Spinal Cord Injury: Therapeutic Approaches to Polyphenols and Candidate Phytochemicals. *Pharmacol Res* (2020) 160:105069. doi: 10.1016/j.phrs.2020.105069
32. Fakhri S, Tomas M, Capanoglu E, Hussain Y, Abbaszadeh F, Lu B, et al. Antioxidant and Anticancer Potentials of Edible Flowers: Where do We Stand? *Crit Rev Food Sci Nutr* (2021), 1–57. doi: 10.1080/10408398.2021.1931022
33. Fakhri S, Khodamorady M, Naseri M, Farzaei MH, Khan H. The Ameliorating Effects of Anthocyanins on the Cross-Linked Signaling Pathways of Cancer Dysregulated Metabolism. *Pharmacol Res* (2020) 159:104895. doi: 10.1016/j.phrs.2020.104895
34. Rahman N, Khan H, Zia A, Khan A, Fakhri S, Aschner M, et al. Bcl-2 Modulation in P53 Signaling Pathway by Flavonoids: A Potential Strategy Towards the Treatment of Cancer. *Int J Mol Sci* (2021) 22(21):11315. doi: 10.3390/ijms222111315
35. Ahmad I, Fakhri S, Khan H, Jeandet P, Aschner M, Yu Z-L. Targeting Cell Cycle by β-Carboline Alkaloids *In Vitro*: Novel Therapeutic Prospects for the Treatment of Cancer. *Chem-Biol Interact* (2020) 330:109229. doi: 10.1016/j.cbi.2020.109229
36. Deng J, Bai X, Feng X, Ni J, Beretov J, Graham P, et al. Inhibition of PI3K/Akt/mTOR Signaling Pathway Allevia*t*es Ovarian Cancer Chemoresistance Through Reversing Epithelial-Mesenchymal Transition and Decreasing Cancer Stem Cell Marker Expression. *BMC Cancer* (2019) 19(1):1–12. doi: 10.1186/s12885-019-5824-9
37. Yang W, Liu Y, Xu QQ, Xian YF, Lin ZX. Sulforaphene Ameliorates Neuroinflammation and Hyperphosphorylated Tau Protein *via* Regulating the PI3K/Akt/GSK-3β Pathway in Experimental Models of Alzheimer's Disease. *Oxid Med Cell Longev* (2020):4754195. doi: 10.1155/2020/4754195
38. Colombo M, Platonova N, Giannandrea D, Palano MT, Basile A, Chiaramonte R. Re-Establishing Apoptosis Competence in Bone Associated Cancers *via* Communicative Reprogramming Induced

Through Notch Signaling Inhibition. *Front Pharmacol* (2019) 10:145. doi: 10.3389/fphar.2019.00145
39. Xi G, Hayes E, Lewis R, Ichi S, Mania-Farnell B, Shim K, et al. CD133 and DNA-PK Regulate MDR1 *via* the PI3K- or Akt-NF-κb Pathway in Multidrug-Resistant Glioblastoma Cells *In Vitro*. *Oncogene* (2016) 35 (2):241–50. doi: 10.1038/onc.2015.78
40. Vo TT, Letai A. BH3-Only Proteins and Their Effects on Cancer. *Adv Exp Med Biol* (2010) 687:49–63. doi: 10.1007/978-1-4419-6706-0_3
41. Campbell KJ, Tait SWG. Targeting BCL-2 Regulated Apoptosis in Cancer. *Open Biol* (2018) 8(5). doi: 10.1098/rsob.180002
42. Sharma P, Hu-Lieskovan S, Wargo JA, Ribas A. Primary, Adaptive, and Acquired Resistance to Cancer Immunotherapy. *Cell* (2017) 168(4):707–23. doi: 10.1016/j.cell.2017.01.017
43. Kim TY, Leem E, Lee JM, Kim SR. Control of Reactive Oxygen Species for the Prevention of Parkinson's Disease: The Possible Application of Flavonoids. *Antioxid (Basel)* (2020) 9(7). doi: 10.3390/antiox9070583
44. Gong J, Chehrazi-Raffle A, Reddi S, Salgia R. Development of PD-1 and PD-L1 Inhibitors as a Form of Cancer Immunotherapy: A Comprehensive Review of Registration Trials and Future Considerations. *J Immunother Cancer* (2018) 6(1):8. doi: 10.1186/s40425-018-0316-z
45. DuPage M, Mazumdar C, Schmidt LM, Cheung AF, Jacks T. Expression of Tumour-Specific Antigens Underlies Cancer Immunoediting. *Nature* (2012) 482(7385):405–9. doi: 10.1038/nature10803
46. Xu-Monette ZY, Zhang M, Li J, Young KH. PD-1/PD-L1 Blockade: Have We Found the Key to Unleash the Antitumor Immune Response? *Front Immunol* (2017) 8:1597:1597. doi: 10.3389/fimmu.2017.01597
47. Galluzzi L, Buqué A, Kepp O, Zitvogel L, Kroemer G. Immunological Effects of Conventional Chemotherapy and Targeted Anticancer Agents. *Cancer Cell* (2015) 28(6):690–714. doi: 10.1016/j.ccell.2015.10.012
48. Sokol L, Koelzer VH, Rau TT, Karamitopoulou E, Zlobec I, Lugli A. Loss of Tapasin Correlates With Diminished CD8(+) T-Cell Immunity and Prognosis in Colorectal Cancer. *J Transl Med* (2015) 13:279. doi: 10.1186/s12967-015-0647-1
49. Gao M, Gao L, Yang G, Tao Y, Hou J, Xu H, et al. Myeloma Cells Resistance to NK Cell Lysis Mainly Involves an HLA Class I-Dependent Mechanism. *Acta Biochim Biophys Sin (Shanghai)* (2014) 46(7):597–604. doi: 10.1093/abbs/gmu041
50. Rieth J, Subramanian S. Mechanisms of Intrinsic Tumor Resistance to Immunotherapy. *Int J Mol Sci* (2018) 19(5). doi: 10.3390/ijms19051340
51. Gao J, Shi LZ, Zhao H, Chen J, Xiong L, He Q, et al. Loss of IFN-γ Pathway Genes in Tumor Cells as a Mechanism of Resistance to Anti-CTLA-4 Therapy. *Cell* (2016) 167(2):397–404.e399. doi: 10.1016/j.cell.2016.08.069
52. Possick JD. Pulmonary Toxicities From Checkpoint Immunotherapy for Malignancy. *Clin Chest Med* (2017) 38(2):223–32. doi: 10.1016/j.ccm.2016.12.012
53. Pan D, Kobayashi A, Jiang P, Ferrari de Andrade L, Tay RE, Luoma AM, et al. A Major Chromatin Regulator Determines Resistance of Tumor Cells to T Cell-Mediated Killing. *Science* (2018) 359(6377):770–5. doi: 10.1126/science.aao1710
54. Spranger S, Bao R, Gajewski TF. Melanoma-Intrinsic β-Catenin Signalling Prevents Anti-Tumour Immunity. *Nature* (2015) 523(7559):231–5. doi: 10.1038/nature14404
55. Dhillon AS, Hagan S, Rath O, Kolch W. MAP Kinase Signalling Pathways in Cancer. *Oncogene* (2007) 26(22):3279–90. doi: 10.1038/sj.onc.1210421
56. Peng W, Chen JQ, Liu C, Malu S, Creasy C, Tetzlaff MT, et al. Loss of PTEN Promotes Resistance to T Cell-Mediated Immunotherapy. *Cancer Discov* (2016) 6(2):202–16. doi: 10.1158/2159-8290.cd-15-0283
57. Yoshida GJ. Metabolic Reprogramming: The Emerging Concept and Associated Therapeutic Strategies. *J Exp Clin Cancer Res* (2015) 34:111. doi: 10.1186/s13046-015-0221-y
58. Dietl K, Renner K, Dettmer K, Timischl B, Eberhart K, Dorn C, et al. Lactic Acid and Acidification Inhibit TNF Secretion and Glycolysis of Human Monocytes. *J Immunol* (2010) 184(3):1200–9. doi: 10.4049/jimmunol.0902584
59. Chang CH, Qiu J, O'Sullivan D, Buck MD, Noguchi T, Curtis JD, et al. Metabolic Competition in the Tumor Microenvironment Is a Driver of Cancer Progression. *Cell* (2015) 162(6):1229–41. doi: 10.1016/j.cell.2015.08.016
60. Kawasaki T, Kawai T. Toll-Like Receptor Signaling Pathways. *Front Immunol* (2014) 5:461. doi: 10.3389/fimmu.2014.00461
61. Webb JT, Behar M. Topology, Dynamics, and Heterogeneity in Immune Signaling. *Wiley Interdiscip Rev: Syst Biol Med* (2015) 7(5):285–300. doi: 10.1002/wsbm.1306
62. Dajon M, Iribarren K, Cremer I. Toll-Like Receptor Stimulation in Cancer: A Pro-and Anti-Tumor Double-Edged Sword. *Immunobiology* (2017) 222 (1):89–100. doi: 10.1016/j.imbio.2016.06.009
63. Yang H, Zhou H, Feng P, Zhou X, Wen H, Xie X, et al. Reduced Expression of Toll-Like Receptor 4 Inhibits Human Breast Cancer Cells Proliferation and Inflammatory Cytokines Secretion. *J Exp Clin Cancer Res* (2010) 29 (1):1–8. doi: 10.1186/1756-9966-29-92
64. Moradi-Marjaneh R, Hassanian SM, Fiuji H, Soleimanpour S, Ferns GA, Avan A, et al. Toll Like Receptor Signaling Pathway as a Potential Therapeutic Target in Colorectal Cancer. *J Cell Physiol* (2018) 233 (8):5613–22. doi: 10.1002/jcp.26273
65. Zhao S, Zhang Y, Zhang Q, Wang F, Zhang D. Toll-Like Receptors and Prostate Cancer. *Front Immunol* (2014) 5:352. doi: 10.3389/fimmu.2014.00352
66. Yusuf N, Nasti TH, Long JA, Naseemuddin M, Lucas AP, Xu H, et al. Protective Role of Toll-Like Receptor 4 During the Initiation Stage of Cutaneous Chemical Carcinogenesis. *Cancer Res* (2008) 68(2):615–22. doi: 10.1158/0008-5472.CAN-07-5219
67. Park GB, Jeong JY, Kim D. Modified TLR-Mediated Downregulation of miR-125b-5p Enhances CD248 (Endosialin)-Induced Metastasis and Drug Resistance in Colorectal Cancer Cells. *Mol Carcinog* (2020) 59(2):154–67. doi: 10.1002/mc.23137
68. Meng Q, Liang C, Hua J, Zhang B, Liu J, Zhang Y, et al. A miR-146a-5p/TRAF6/NF-kB P65 Axis Regulates Pancreatic Cancer Chemoresistance: Functional Validation and Clinical Significance. *Theranostics* (2020) 10 (9):3967. doi: 10.7150/thno.40566
69. Tan S-F, Dunton W, Liu X, Fox TE, Morad SA, Desai D, et al. Acid Ceramidase Promotes Drug Resistance in Acute Myeloid Leukemia Through NF-κb-Dependent P-Glycoprotein Upregulation. *J Lipid Res* (2019) 60 (6):1078–86. doi: 10.1194/jlr.M091876
70. Lee C, Do HTT, Her J, Kim Y, Seo D, Rhee I. Inflammasome as a Promising Therapeutic Target for Cancer. *Life Sci* (2019) 231:116593. doi: 10.1016/j.lfs.2019.116593
71. Terlizzi M, Casolaro V, Pinto A, Sorrentino R. Inflammasome: Cancer's Friend or Foe? *Pharmacol Ther* (2014) 143(1):24–33. doi: 10.1016/j.pharmthera.2014.02.002
72. Balistreri CR, Ruvolo G, Lio D, Madonna R. Toll-Like Receptor-4 Signaling Pathway in Aorta Aging and Diseases:"Its Double Nature". *J Mol Cell Cardiol* (2017) 110:38–53. doi: 10.1016/j.yjmcc.2017.06.011
73. Rahimifard M, Maqbool F, Moeini-Nodeh S, Niaz K, Abdollahi M, Braidy N, et al. Targeting the TLR4 Signaling Pathway by Polyphenols: A Novel Therapeutic Strategy for Neuroinflammation. *Ageing Res Rev* (2017) 36:11–9. doi: 10.1016/j.arr.2017.02.004
74. Cen X, Liu S, Cheng K. The Role of Toll-Like Receptor in Inflammation and Tumor Immunity. *Front Pharmacol* (2018) 9:878. doi: 10.3389/fphar.2018.00878
75. Nagai Y, Akashi S, Nagafuku M, Ogata M, Iwakura Y, Akira S, et al. Essential Role of MD-2 in LPS Responsiveness and TLR4 Distribution. *Nat Immunol* (2002) 3(7):667–72. doi: 10.1038/ni809
76. Huang L, Xu H, Peng G. TLR-Mediated Metabolic Reprogramming in the Tumor Microenvironment: Potential Novel Strategies for Cancer Immunotherapy. *Cell Mol Immunol* (2018) 15(5):428–37. doi: 10.1038/cmi.2018.4
77. Takeda K, Akira S. Microbial Recognition by Toll-Like Receptors. *J Dermatol Sci* (2004) 34(2):73–82. doi: 10.1016/j.jdermsci.2003.10.002
78. Koh Y-C, Yang G, Lai C-S, Weerawatanakorn M, Pan M-H. Chemopreventive Effects of Phytochemicals and Medicines on M1/M2 Polarized Macrophage Role in Inflammation-Related Diseases. *Int J Mol Sci* (2018) 19(8):2208. doi: 10.3390/ijms19082208
79. Prabhu DS, Selvam AP, Rajeswari VD. Effective Anti-Cancer Property of Pouteria Sapota Leaf on Breast Cancer Cell Lines. *Biochem Biophys Rep* (2018) 15:39–44. doi: 10.1016/j.bbrep.2018.06.004
80. Fakhri S, Pesce M, Patruno A, Moradi SZ, Iranpanah A, Farzaei MH, et al. Attenuation of Nrf2/Keap1/ARE in Alzheimer's Disease by Plant Secondary

Metabolites: A Mechanistic Review. *Molecules* (2020) 25(21):4926. doi: 10.3390/molecules25214926
81. Moradi SZ, Jalili F, Farhadian N, Joshi T, Wang M, Zou L, et al. Polyphenols and Neurodegenerative Diseases: Focus on Neuronal Regeneration. *Crit Rev Food Sci Nutr* (2020), 1–16. doi: 10.1080/10408398.2020.1865870
82. Moradi SZ, Momtaz S, Bayrami Z, Farzaei MH, Abdollahi M. Nanoformulations of Herbal Extracts in Treatment of Neurodegenerative Disorders. *Front Bioeng Biotechnol* (2020) 8:238. doi: 10.3389/fbioe.2020.00238
83. Fakhri S, Iranpanah A, Gravandi MM, Moradi SZ, Ranjbari M, Majnooni MB, et al. Natural Products Attenuate PI3K/Akt/mTOR Signaling Pathway: A Promising Strategy in Regulating Neurodegeneration. *Phytomedicine* (2021) 91:153664. doi: 10.1016/j.phymed.2021.153664
84. Fakhri S, Nouri Z, Moradi SZ, Akkol EK, Piri S, Sobarzo-Sánchez E, et al. Targeting Multiple Signal Transduction Pathways of SARS-CoV-2: Approaches to COVID-19 Therapeutic Candidates. *Molecules* (2021) 26 (10):2917. doi: 10.3390/molecules26102917
85. Fakhri S, Piri S, Moradi SZ, Khan H. Phytochemicals Targeting Oxidative Stress, Interconnected Neuroinflammatory and Neuroapoptotic Pathways Following Radiation. *Curr Neuropharmacol* (2021). doi: 10.2174/1570159X19666210809103346
86. Li P-M, Li Y-L, Liu B, Wang W-J, Wang Y-Z, Li Z. Curcumin Inhibits MHCC97H Liver Cancer Cells by Activating ROS/TLR-4/Caspase Signaling Pathway. *Asian Pac J Cancer Prev* (2014) 15(5):2329–34. doi: 10.7314/APJCP.2014.15.5.2329
87. Ren B, Luo S, Tian X, Jiang Z, Zou G, Xu F, et al. Curcumin Inhibits Liver Cancer by Inhibiting DAMP Molecule HSP70 and TLR4 Signaling. *Oncol Rep* (2018) 40(2):895–901. doi: 10.3892/or.2018.6485
88. Tian S, Liao L, Zhou Q, Huang X, Zheng P, Guo Y, et al. Curcumin Inhibits the Growth of Liver Cancer by Impairing Myeloid−Derived Suppressor Cells in Murine Tumor Tissues. *Oncol Lett* (2021) 21(4):1–1.
89. Zhang L, Tao X, Fu Q, Ge C, Li R, Li Z, et al. Curcumin Inhibits Cell Proliferation and Migration in NSCLC Through a Synergistic Effect on the TLR4/MyD88 and EGFR Pathways. *Oncol Rep* (2019) 42(5):1843–55. doi: 10.3892/or.2019.7278
90. Eskiler GG, Özkan AD, Kaleli S, Bilir C. Inhibition of TLR4/TRIF/IRF3 Signaling Pathway by Curcumin in Breast Cancer Cells. *J Pharm Pharm Sci* (2019) 22:281–91. doi: 10.18433/jpps30493
91. Meyer C, Pries R, Wollenberg B. Established and Novel NF-κb Inhibitors Lead to Downregulation of TLR3 and the Proliferation and Cytokine Secretion in HNSCC. *Oral Oncol* (2011) 47(9):818–26. doi: 10.1016/j.oraloncology.2011.06.010
92. Shishodia S, Amin HM, Lai R, Aggarwal BB. Curcumin (Diferuloylmethane) Inhibits Constitutive NF-κb Activation, Induces G1/S Arrest, Suppresses Proliferation, and Induces Apoptosis in Mantle Cell Lymphoma. *Biochem Pharmacol* (2005) 70(5):700–13. doi: 10.1016/j.bcp.2005.04.043
93. Wong TS, Chan WS, Li CH, Liu RW, Tang WW, Tsao SW, et al. Curcumin Alters the Migratory Phenotype of Nasopharyngeal Carcinoma Cells Through Up-Regulation of E-Cadherin. *Anticancer Res* (2010) 30(7):2851–6.
94. Deng Z, Xu X-Y, Yunita F, Zhou Q, Wu Y-R, Hu Y-X, et al. Synergistic Anti-Liver Cancer Effects of Curcumin and Total Ginsenosides. *World J Gastrointest Oncol* (2020) 12(10):1091. doi: 10.4251/wjgo.v12.i10.1091
95. Li X, Ma S, Yang P, Sun B, Zhang Y, Sun Y, et al. Anticancer Effects of Curcumin on Nude Mice Bearing Lung Cancer A549 Cell Subsets SP and NSP Cells. *Oncol Lett* (2018) 16(5):6756–62. doi: 10.3892/ol.2018.9488
96. Wu X, Koh GY, Huang Y, Crott JW, Bronson RT, Mason JB. The Combination of Curcumin and Salsalate is Superior to Either Agent Alone in Suppressing Pro-Cancerous Molecular Pathways and Colorectal Tumorigenesis in Obese Mice. *Mol Nutr Food Res* (2019) 63(8):1801097. doi: 10.1002/mnfr.201801097
97. Hao J, Dai X, Gao J, Li Y, Hou Z, Chang Z, et al. Curcumin Suppresses Colorectal Tumorigenesis *via* the Wnt/β–Catenin Signaling Pathway by Downregulating Axin2. *Oncol Lett* (2021) 21(3):1–1. doi: 10.3892/ol.2021.12447
98. Xiang L, He B, Liu Q, Hu D, Liao W, Li R, et al. Antitumor Effects of Curcumin on the Proliferation, Migration and Apoptosis of Human Colorectal Carcinoma HCT−116 Cells. *Oncol Rep* (2020) 44(5):1997–2008. doi: 10.3892/or.2020.7765
99. El-Mesallamy H, Salman TM, Ashmawey AM, Osama N. Evaluating the Role of Curcum Powder as a Protective Factor Against Bladder Cancer-An Experimental Study. *Asian Pac J Cancer Prev* (2012) 13(10):5287–90. doi: 10.7314/APJCP.2012.13.10.5287
100. Shrestha S, Zhu J, Wang Q, Du X, Liu F, Jiang J, et al. Melatonin Potentiates the Antitumor Effect of Curcumin by Inhibiting Ikkκ/NF-κb/COX-2 Signaling Pathway. *Int J Oncol* (2017) 51(4):1249–60. doi: 10.3892/ijo.2017.4097
101. Bisht S, Feldmann G, Soni S, Ravi R, Karikar C, Maitra A, et al. Polymeric Nanoparticle-Encapsulated Curcumin (" Nanocurcumin"): A Novel Strategy for Human Cancer Therapy. *J Nanobiotechnol* (2007) 5(1):1–18. doi: 10.1186/1477-3155-5-3
102. Dhillon N, Aggarwal BB, Newman RA, Wolff RA, Kunnumakkara AB, Abbruzzese JL, et al. Phase II Trial of Curcumin in Patients With Advanced Pancreatic Cancer. *Clin Cancer Res* (2008) 14(14):4491–9. doi: 10.1158/1078-0432.CCR-08-0024
103. Kim JM, Noh EM, Kwon KB, Kim JS, You YO, Hwang JK, et al. Curcumin Suppresses the TPA-Induced Invasion Through Inhibition of Pkcα-Dependent MMP-Expression in MCF-7 Human Breast Cancer Cells. *Phytomedicine* (2012) 19(12):1085–92. doi: 10.1016/j.phymed.2012.07.002
104. Cao F, Liu T, Xu Y, Xu D, Feng S. Curcumin Inhibits Cell Proliferation and Promotes Apoptosis in Human Osteoclastoma Cell Through MMP-9, NF-κb and JNK Signaling Pathways. *Int J Clin Exp Pathol* (2015) 8(6):6037–45.
105. Hu A, Huang JJ, Li RL, Lu ZY, Duan JL, Xu WH, et al. Curcumin as Therapeutics for the Treatment of Head and Neck Squamous Cell Carcinoma by Activating SIRT1. *Sci Rep* (2015) 5:13429. doi: 10.1038/srep13429
106. Zhu GH, Dai HP, Shen Q, Ji O, Zhang Q, Zhai YL. Curcumin Induces Apoptosis and Suppresses Invasion Through MAPK and MMP Signaling in Human Monocytic Leukemia SHI-1 Cells. *Pharm Biol* (2016) 54(8):1303–11. doi: 10.3109/13880209.2015.1060508
107. Zhu G, Shen Q, Jiang H, Ji O, Zhu L, Zhang L. Curcumin Inhibited the Growth and Invasion of Human Monocytic Leukaemia SHI-1 Cells *In Vivo* by Altering MAPK and MMP Signalling. *Pharm Biol* (2020) 58(1):25–34. doi: 10.1080/13880209.2019.1701042
108. Yang L, Hu Z, Zhu J, Liang Q, Zhou H, Li J, et al. Systematic Elucidation of the Mechanism of Quercetin Against Gastric Cancer *via* Network Pharmacology Approach. *BioMed Res Int* (2020) 2020:3860213. doi: 10.1155/2020/3860213
109. Masuelli L, Di Stefano E, Fantini M, Mattera R, Benvenuto M, Marzocchella L, et al. Resveratrol Potentiates the *In Vitro* and *In Vivo* Anti-Tumoral Effects of Curcumin in Head and Neck Carcinomas. *Oncotarget* (2014) 5 (21):10745–62. doi: 10.18632/oncotarget.2534
110. Srivastava NS, Srivastava RAK. Curcumin and Quercetin Synergistically Inhibit Cancer Cell Proliferation in Multiple Cancer Cells and Modulate Wnt/β-Catenin Signaling and Apoptotic Pathways in A375 Cells. *Phytomedicine* (2019) 52:117–28. doi: 10.1016/j.phymed.2018.09.224
111. Mutlu Altundağ E, Yılmaz AM, Serdar BS, Jannuzzi AT, Koçtürk S, Yalçın AS. Synergistic Induction of Apoptosis by Quercetin and Curcumin in Chronic Myeloid Leukemia (K562) Cells: II. Signal Transduction Pathways Involved. *Nutr Cancer* (2021) 73(4):703–12. doi: 10.1080/01635581.2020.1767167
112. Yusuf N, Nasti TH, Meleth S, Elmets CA. Resveratrol Enhances Cell-Mediated Immune Response to DMBA Through TLR4 and Prevents DMBA Induced Cutaneous Carcinogenesis. *Mol Carcinog* (2009) 48 (8):713–23. doi: 10.1002/mc.20517
113. Panaro MA, Carofiglio V, Acquafredda A, Cavallo P. And Cianciulli, AAnti-Inflammatory Effects of Resveratrol Occur *via* Inhibition of Lipopolysaccharide-Induced NF-κb Activation in Caco-2 and SW480 Human Colon Cancer Cells. *Br J Nutr* (2012) 108(9):1623–32. doi: 10.1017/S0007114511007227
114. Estrov Z, Shishodia S, Faderl S, Harris D, Van Q, Kantarjian HM, et al. Resveratrol Blocks Interleukin-1β–Induced Activation of the Nuclear Transcription Factor NF-κb, Inhibits Proliferation, Causes S-Phase Arrest, and Induces Apoptosis of Acute Myeloid Leukemia Cells. *Blood* (2003) 102 (3):987–95. doi: 10.1182/blood-2002-11-3550
115. Li W, Ma J, Ma Q, Li B, Han L, Liu J, et al. Resveratrol Inhibits the Epithelial-Mesenchymal Transition of Pancreatic Cancer Cells *via* Suppression of the

PI-3k/Akt/NF-κb Pathway. *Curr Med Chem* (2013) 20(33):4185–94. doi: 10.2174/09298673113209990251
116. Salla M, Pandya V, Bhullar KS, Kerek E, Wong YF, Losch R, et al. Resveratrol and Resveratrol-Aspirin Hybrid Compounds as Potent Intestinal Anti-Inflammatory and Anti-Tumor Drugs. *Molecules* (2020) 25(17):3849. doi: 10.3390/molecules25173849
117. Ivanov VN, Partridge MA, Johnson GE, Huang SX, Zhou H, Hei TK. Resveratrol Sensitizes Melanomas to TRAIL Through Modulation of Antiapoptotic Gene Expression. *Exp Cell Res* (2008) 314(5):1163–76. doi: 10.1016/j.yexcr.2007.12.012
118. Kim YA, Lee WH, Choi TH, Rhee SH, Park KY, Choi YH. Involvement of P21waf1/CIP1, pRB, Bax and NF-kappaB in Induction of Growth Arrest and Apoptosis by Resveratrol in Human Lung Carcinoma A549 Cells. *Int J Oncol* (2003) 23(4):1143–9.
119. Rasheduzzaman M, Jeong JK, Park SY. Resveratrol Sensitizes Lung Cancer Cell to TRAIL by P53 Independent and Suppression of Akt/NF-κb Signaling. *Life Sci* (2018) 208:208–20. doi: 10.1016/j.lfs.2018.07.035
120. Huang H, Lin H, Zhang X, Li J. Resveratrol Reverses Temozolomide Resistance by Downregulation of MGMT in T98G Glioblastoma Cells by the NF-κb-Dependent Pathway. *Oncol Rep* (2012) 27(6):2050–6. doi: 10.3892/or.2012.1715
121. Yu HB, Zhang HF, Zhang X, Li DY, Xue HZ, Pan CE, et al. Resveratrol Inhibits VEGF Expression of Human Hepatocellular Carcinoma Cells Through a NF-Kappa B-Mediated Mechanism. *Hepatogastroenterology* (2010) 57(102-103):1241–6.
122. Wang Z, Zhang L, Ni Z, Sun J, Gao H, Cheng Z, et al. Resveratrol Induces AMPK-Dependent MDR1 Inhibition in Colorectal Cancer HCT116/L-OHP Cells by Preventing Activation of NF-κb Signaling and Suppressing cAMP-Responsive Element Transcriptional Activity. *Tumour Biol* (2015) 36 (12):9499–510. doi: 10.1007/s13277-015-3636-3
123. Gao J, Ma F, Wang X, Li G. Combination of Dihydroartemisinin and Resveratrol Effectively Inhibits Cancer Cell Migration *via* Regulation of the DLC1/TCTP/Cdc42 Pathway. *Food Funct* (2020) 11(11):9573–84. doi: 10.1039/d0fo00996b
124. Fan S-H, Wang Y-Y, Lu J, Zheng Y-L, Wu D-M, Li M-Q, et al. Luteoloside Suppresses Proliferation and Metastasis of Hepatocellular Carcinoma Cells by Inhibition of NLRP3 Inflammasome. *PloS One* (2014) 9(2):e89961. doi: 10.1371/journal.pone.0089961
125. Ho HH, Chang CS, Ho WC, Liao SY, Wu CH, Wang CJ. Anti-Metastasis Effects of Gallic Acid on Gastric Cancer Cells Involves Inhibition of NF-kappaB Activity and Downregulation of PI3K/AKT/small GTPase Signals. *Food Chem Toxicol* (2010) 48(8-9):2508–16. doi: 10.1016/j.fct.2010.06.024
126. Zeng M, Su Y, Li K, Jin D, Li Q, Li Y, et al. Gallic Acid Inhibits Bladder Cancer T24 Cell Progression Through Mitochondrial Dysfunction and PI3K/Akt/NF-κb Signaling Suppression. *Front Pharmacol* (2020) 11:1222. doi: 10.3389/fphar.2020.01222
127. Han M, Song Y, Zhang X. Quercetin Suppresses the Migration and Invasion in Human Colon Cancer Caco-2 Cells Through Regulating Toll-Like Receptor 4/Nuclear Factor-Kappa B Pathway. *Pharmacogn Mag* (2016) 12 (Suppl 2):S237. doi: 10.4103/0973-1296.182154
128. Priyadarsini RV, Murugan RS, Maitreyi S, Ramalingam K, Karunagaran D, Nagini S. The Flavonoid Quercetin Induces Cell Cycle Arrest and Mitochondria-Mediated Apoptosis in Human Cervical Cancer (HeLa) Cells Through P53 Induction and NF-κb Inhibition. *Eur J Pharmacol* (2010) 649(1-3):84–91. doi: 10.1016/j.ejphar.2010.09.020
129. Youn H, Jeong J-C, Jeong YS, Kim E-J, Um S-J. Quercetin Potentiates Apoptosis by Inhibiting Nuclear Factor-kappaB Signaling in H460 Lung Cancer Cells. *Biol Pharm Bull* (2013) 36(6):944–51. doi: 10.1248/bpb.b12-01004
130. Mukherjee A, Khuda-Bukhsh AR. Quercetin Down-Regulates IL-6/STAT-3 Signals to Induce Mitochondrial-Mediated Apoptosis in a Nonsmall-Cell Lung-Cancer Cell Line, A549. *J Pharmacopuncture* (2015) 18(1):19. doi: 10.3831/KPI.2015.18.002
131. Erdogan S, Turkekul K, Dibirdik I, Doganlar O, Doganlar ZB, Bilir A, et al. Midkine Downregulation Increases the Efficacy of Quercetin on Prostate Cancer Stem Cell Survival and Migration Through PI3K/AKT and MAPK/ERK Pathway. *Biomed Pharmacother* (2018) 107:793–805. doi: 10.1016/j.biopha.2018.08.061
132. Kıyga E, Şengelen A, Adıgüzel Z, Önay Uçar E. Investigation of the Role of Quercetin as a Heat Shock Protein Inhibitor on Apoptosis in Human Breast Cancer Cells. *Mol Biol Rep* (2020) 47(7):4957–67. doi: 10.1007/s11033-020-05641-x
133. Zhang W, Yin G, Dai J, Sun YU, Hoffman RM, Yang Z, et al. Chemoprevention by Quercetin of Oral Squamous Cell Carcinoma by Suppression of the NF-κb Signaling Pathway in DMBA-Treated Hamsters. *Anticancer Res* (2017) 37(8):4041–9. doi: 10.21873/anticanres.11789
134. Wu T-C, Chan S-T, Chang C-N, Yu P-S, Chuang C-H, Yeh S-L. Quercetin and Chrysin Inhibit Nickel-Induced Invasion and Migration by Downregulation of TLR4/NF-κb Signaling in A549 Cells. *Chem-Biol Interact* (2018) 292:101–9. doi: 10.1016/j.cbi.2018.07.010
135. Chua KV, Fan C-S, Chen C-C, Chen L-L, Hsieh S-C, Huang T-S. Octyl Gallate Induces Pancreatic Ductal Adenocarcinoma Cell Apoptosis and Suppresses Endothelial-Mesenchymal Transition-Promoted M2-Macrophages, Hsp90α Secretion, and Tumor Growth. *Cells* (2020) 9(1):91. doi: 10.3390/cells9010091
136. Ellis LZ, Liu W, Luo Y, Okamoto M, Qu D, Dunn JH, et al. Green Tea Polyphenol Epigallocatechin-3-Gallate Suppresses Melanoma Growth by Inhibiting Inflammasome and IL-1β Secretion. *Biochem Biophys Res Commun* (2011) 414(3):551–6. doi: 10.1016/j.bbrc.2011.09.115
137. Wang T, Zhou H, Xie H, Mu Y, Xu Y, Liu J, et al. Epigallocatechin-3-Gallate Inhibits TF and TNF-α Expression Induced by the Anti-β2gpi/β2gpi Complex in Human THP-1 Cells. *Int J Mol Med* (2014) 33(4):994–1002. doi: 10.3892/ijmm.2014.1635
138. Belguise K, Guo S, Sonenshein GE. Activation of FOXO3a by the Green Tea Polyphenol Epigallocatechin-3-Gallate Induces Estrogen Receptor α Expression Reversing Invasive Phenotype of Breast Cancer Cells. *Cancer Res* (2007) 67(12):5763–70. doi: 10.1158/0008-5472.CAN-06-4327
139. Pianetti S, Guo S, Kavanagh KT, Sonenshein GE. Green Tea Polyphenol Epigallocatechin-3 Gallate Inhibits Her-2/Neu Signaling, Proliferation, and Transformed Phenotype of Breast Cancer Cells. *Cancer Res* (2002) 62(3):652–5.
140. Hoffmann J, Junker H, Schmieder A, Venz S, Brandt R, Multhoff G, et al. EGCG Downregulates IL-1RI Expression and Suppresses IL-1-Induced Tumorigenic Factors in Human Pancreatic Adenocarcinoma Cells. *Biochem Pharmacol* (2011) 82(9):1153–62. doi: 10.1016/j.bcp.2011.07.063
141. Sen T, Moulik S, Dutta A, Choudhury PR, Banerji A, Das S, et al. Multifunctional Effect of Epigallocatechin-3-Gallate (EGCG) in Downregulation of Gelatinase-A (MMP-2) in Human Breast Cancer Cell Line MCF-7. *Life Sci* (2009) 84(7-8):194–204. doi: 10.1016/j.lfs.2008.11.018
142. Fang CY, Wu CC, Hsu HY, Chuang HY, Huang SY, Tsai CH, et al. EGCG Inhibits Proliferation, Invasiveness and Tumor Growth by Up-Regulation of Adhesion Molecules, Suppression of Gelatinases Activity, and Induction of Apoptosis in Nasopharyngeal Carcinoma Cells. *Int J Mol Sci* (2015) 16 (2):2530–58. doi: 10.3390/ijms16022530
143. Luo KW, Wei C, Lung WY, Wei XY, Cheng BH, Cai ZM, et al. EGCG Inhibited Bladder Cancer SW780 Cell Proliferation and Migration Both *In Vitro* and *In Vivo via* Down-Regulation of NF-κb and MMP-9. *J Nutr Biochem* (2017) 41:56–64. doi: 10.1016/j.jnutbio.2016.12.004
144. Nishikawa T, Nakajima T, Moriguchi M, Jo M, Sekoguchi S, Ishii M, et al. A Green Tea Polyphenol, Epigalocatechin-3-Gallate, Induces Apoptosis of Human Hepatocellular Carcinoma, Possibly Through Inhibition of Bcl-2 Family Proteins. *J Hepatol* (2006) 44(6):1074–82. doi: 10.1016/j.jhep.2005.11.045
145. Xu P, Yan F, Zhao Y, Chen X, Sun S, Wang Y, et al. Green Tea Polyphenol EGCG Attenuates MDSCs-Mediated Immunosuppression Through Canonical and Non-Canonical Pathways in a 4T1 Murine Breast Cancer Model. *Nutrients* (2020) 12(4). doi: 10.3390/nu12041042
146. Saldanha SN, Kala R, Tollefsbol TO. Molecular Mechanisms for Inhibition of Colon Cancer Cells by Combined Epigenetic-Modulating Epigallocatechin Gallate and Sodium Butyrate. *Exp Cell Res* (2014) 324(1):40–53. doi: 10.1016/j.yexcr.2014.01.024
147. Johnson JL, De Mejia EG. Flavonoid Apigenin Modified Gene Expression Associated With Inflammation and Cancer and Induced Apoptosis in Human Pancreatic Cancer Cells Through Inhibition of GSK-3β/NF-κ B Signaling Cascade. *Mol Nutr Food Res* (2013) 57(12):2112–27. doi: 10.1002/mnfr.201300307

148. Shukla S, Gupta S. Suppression of Constitutive and Tumor Necrosis Factor α-Induced Nuclear Factor (NF)-κb Activation and Induction of Apoptosis by Apigenin in Human Prostate Carcinoma PC-3 Cells: Correlation With Down-Regulation of NF-κb-Responsive Genes. *Clin Cancer Res* (2004) 10 (9):3169–78. doi: 10.1158/1078-0432.CCR-03-0586
149. Erdogan S, Doganlar O, Doganlar ZB, Serttas R, Turkekul K, Dibirdik I, et al. The Flavonoid Apigenin Reduces Prostate Cancer CD44+ Stem Cell Survival and Migration Through PI3K/Akt/NF-κb Signaling. *Life Sci* (2016) 162:77–86. doi: 10.1016/j.lfs.2016.08.019
150. Bauer D, Mazzio E, Soliman KF. Whole Transcriptomic Analysis of Apigenin on Tnfα Immuno-Activated MDA-MB-231 Breast Cancer Cells. *Cancer Genom-Proteom* (2019) 16(6):421–31. doi: 10.21873/cgp.20146
151. Mafuvadze B, Liang Y, Besch-Williford C, Zhang X, Hyder SM. Apigenin Induces Apoptosis and Blocks Growth of Medroxyprogesterone Acetate-Dependent BT-474 Xenograft Tumors. *Hormones Cancer* (2012) 3(4):160–71. doi: 10.1007/s12672-012-0114-x
152. Shukla S, Shankar E, Fu P, MacLennan GT, Gupta S. Suppression of NF-κb and NF-κb-Regulated Gene Expression by Apigenin Through Iκbα and IKK Pathway in TRAMP Mice. *PloS One* (2015) 10(9):e0138710. doi: 10.1371/journal.pone.0138710
153. Chen K-C, Chen C-Y, Lin C-J, Yang T-Y, Chen T-H, Wu L-C, et al. Luteolin Attenuates TGF-β1-Induced Epithelial–Mesenchymal Transition of Lung Cancer Cells by Interfering in the PI3K/Akt–NF-κb–Snail Pathway. *Life Sci* (2013) 93(24):924–33. doi: 10.1016/j.lfs.2013.10.004
154. Huang W-C, Liou C-J, Shen S-C, Hu S, Hsiao C-Y, Wu S-J. Luteolin Attenuates IL-1β-Induced THP-1 Adhesion to ARPE-19 Cells *via* Suppression of NF-κb and MAPK Pathways. *Mediators Inflammation* (2020). doi: 10.1155/2020/9421340
155. Radziejewska I, Borzym-Kluczyk M, Leszczyńska K. Luteolin Alters MUC1 Extracellular Domain, sT Antigen, ADAM–17, IL–8, IL–10 and NF–κb Expression in Helicobacter Pylori–Infected Gastric Cancer CRL–1739 Cells: A Preliminary Study. *Biomed Rep* (2021) 14(2):1–1. doi: 10.3892/br.2020.1395
156. Park S-H, Kim J-H, Lee D-H, Kang J-W, Song H-H, Oh S-R, et al. Luteolin 8-C-β-Fucopyranoside Inhibits Invasion and Suppresses TPA-Induced MMP-9 and IL-8 *via* ERK/AP-1 and ERK/NF-κb Signaling in MCF-7 Breast Cancer Cells. *Biochimie* (2013) 95(11):2082–90. doi: 10.1016/j.biochi.2013.07.021
157. Maruthanila V, Elancheran R, Roy NK, Bhattacharya A, Kunnumakkara AB, Kabilan S, et al. In Silico Molecular Modelling of Selected Natural Ligands and Their Binding Features With Estrogen Receptor Alpha. *Curr Comput-Aided Drug Des* (2019) 15(1):89–96. doi: 10.2174/1573409914666181008165356
158. Du Y, Jia C, Liu Y, Wang J, Sun K. Isorhamnetin Enhances the Radiosensitivity of A549 Cells Through Interleukin-13 and the NF-κ B Signaling Pathway. *Front Pharmacol* (2020) 11:2324. doi: 10.3389/fphar.2020.610772
159. Hu S, Huang L, Meng L, Sun H, Zhang W, Xu Y. Isorhamnetin Inhibits Cell Proliferation and Induces Apoptosis in Breast Cancer *via* Akt and Mitogen –Activated Protein Kinase Kinase Signaling Pathways. *Mol Med Rep* (2015) 12(5):6745–51. doi: 10.3892/mmr.2015.4269
160. Liu X, Tian S, Liu M, Jian L, Zhao L. Wogonin Inhibits the Proliferation and Invasion, and Induces the Apoptosis of HepG2 and Bel7402 HCC Cells Through NF–κb/Bcl-2, EGFR and EGFR Downstream ERK/AKT Signaling. *Int J Mol Med* (2016) 38(4):1250–6. doi: 10.3892/ijmm.2016.2700
161. Dürr C, Hanna BS, Schulz A, Lucas F, Zucknick M, Benner A, et al. Tumor Necrosis Factor Receptor Signaling is a Driver of Chronic Lymphocytic Leukemia That can be Therapeutically Targeted by the Flavonoid Wogonin. *haematologica* (2018) 103(4):688. doi: 10.3324/haematol.2017.177808
162. Monteiro R, Calhau C, Silva AOE, Pinheiro-Silva S, Guerreiro S, Gärtner F, et al. Xanthohumol Inhibits Inflammatory Factor Production and Angiogenesis in Breast Cancer Xenografts. *J Cell Biochem* (2008) 104 (5):1699–707. doi: 10.1002/jcb.21738
163. Wang Y, Chen Y, Wang J, Chen J, Aggarwal B, Pang X, et al. Xanthohumol, a Prenylated Chalcone Derived From Hops, Suppresses Cancer Cell Invasion Through Inhibiting the Expression of CXCR4 Chemokine Receptor. *Curr Mol Med* (2012) 12(2):153–62. doi: 10.2174/156652412798889072
164. Yamaguchi M, Murata T, Shoji M, Weitzmann MN. The Flavonoid P-Hydroxycinnamic Acid Mediates Anticancer Effects on MDA-MB-231 Human Breast Cancer Cells *In Vitro*: Implications for Suppression of Bone Metastases. *Int J Oncol* (2015) 47(4):1563–71. doi: 10.3892/ijo.2015.3106
165. Yao Y, Zhao K, Yu Z, Ren H, Zhao L, Li Z, et al. Wogonoside Inhibits Invasion and Migration Through Suppressing TRAF2/4 Expression in Breast Cancer. *J Exp Clin Cancer Res* (2017) 36(1):1–14. doi: 10.1186/s13046-017-0574-5
166. Cheng CY, Hu CC, Yang HJ, Lee MC, Kao ES. Inhibitory Effects of Scutellarein on Proliferation of Human Lung Cancer A549 Cells Through ERK and Nfκb Mediated by the EGFR Pathway. *Chin J Physiol* (2014) 57 (4):182–7. doi: 10.4077/cjp.2014.Bac200
167. Yang F, Li J, Zhu J, Wang D, Chen S, Bai X. Hydroxysafflor Yellow A Inhibits Angiogenesis of Hepatocellular Carcinoma *via* Blocking ERK/MAPK and NF-κb Signaling Pathway in H22 Tumor-Bearing Mice. *Eur J Pharmacol* (2015) 754:105–14. doi: 10.1016/j.ejphar.2015.02.015
168. Moon DO, Kim MO, Lee JD, Choi YH, Kim GY. Rosmarinic Acid Sensitizes Cell Death Through Suppression of TNF-α-Induced NF-κb Activation and ROS Generation in Human Leukemia U937 Cells. *Cancer Lett* (2010) 288 (2):183–91. doi: 10.1016/j.canlet.2009.06.033
169. Cao W, Mo K, Wei S, Lan X, Zhang W, Jiang W. Effects of Rosmarinic Acid on Immunoregulatory Activity and Hepatocellular Carcinoma Cell Apoptosis in H22 Tumor-Bearing Mice. *Kor J Physiol Pharmacol* (2019) 23(6):501–8. doi: 10.4196/kjpp.2019.23.6.501
170. Tsai JJ, Chen JH, Chen CH, Chung JG, Hsu FT. Apoptosis Induction and ERK/NF-κb Inactivation are Associated With Magnolol-Inhibited Tumor Progression in Hepatocellular Carcinoma *In Vivo*. *Environ Toxicol* (2020) 35 (2):167–75. doi: 10.1002/tox.22853
171. Shi Q, Jiang Z, Yang J, Cheng Y, Pang Y, Zheng N, et al. A Flavonoid Glycoside Compound From Murraya Paniculata (L.) Interrupts Metastatic Characteristics of A549 Cells by Regulating STAT3/NF-κb/COX-2 and EGFR Signaling Pathways. *AAPS J* (2017) 19(6):1779–90. doi: 10.1208/s12248-017-0134-0
172. Bodduluru LN, Kasala ER, Barua CC, Karnam KC, Dahiya V, Ellutla M. Antiproliferative and Antioxidant Potential of Hesperetin Against Benzo (a) Pyrene-Induced Lung Carcinogenesis in Swiss Albino Mice. *Chem-Biol Interact* (2015) 242:345–52. doi: 10.1016/j.cbi.2015.10.020
173. Averett C, Bhardwaj A, Arora S, Srivastava SK, Khan MA, Ahmad A, et al. Honokiol Suppresses Pancreatic Tumor Growth, Metastasis and Desmoplasia by Interfering With Tumor-Stromal Cross-Talk. *Carcinogenesis* (2016) 37(11):1052–61. doi: 10.1093/carcin/bgw096
174. Lv X-Q, Qiao X-R, Su L, Chen S-Z. Honokiol Inhibits EMT-Mediated Motility and Migration of Human Non-Small Cell Lung Cancer Cells *In Vitro* by Targeting C-FLIP. *Acta Pharmacol Sin* (2016) 37(12):1574–86. doi: 10.1038/aps.2016.81
175. Park BB, sun Yoon J, shil Kim E, Choi J, woong Won Y, hye Choi J, et al. Inhibitory Effects of Eupatilin on Tumor Invasion of Human Gastric Cancer MKN-1 Cells. *Tumor Biol* (2013) 34(2):875–85. doi: 10.1007/s13277-012-0621-y
176. Serttas R, Koroglu C, Erdogan S. Eupatilin Inhibits the Proliferation and Migration of Prostate Cancer Cells Through Modulation of PTEN and NF-κb Signaling. *Anticancer Agents Med Chem* (2021) 21(3):372–82. doi: 10.2174/1871520620666200811113549
177. Lu H, Yang Y, Gad E, Wenner CA, Chang A, Larson ER, et al. Polysaccharide Krestin is a Novel TLR2 Agonist That Mediates Inhibition of Tumor Growth *via* Stimulation of CD8 T Cells and NK Cells. *Clin Cancer Res* (2011) 17 (1):67–76. doi: 10.1158/1078-0432.CCR-10-1763
178. Jiang H, Zeng L, Dong X, Guo S, Xing J, Li Z, et al. Tilianin Extracted From Dracocephalum Moldavica L. Induces Intrinsic Apoptosis and Drives Inflammatory Microenvironment Response on Pharyngeal Squamous Carcinoma Cells *via* Regulating TLR4 Signaling Pathways. *Front Pharmacol* (2020) 11:205. doi: 10.3389/fphar.2020.00205
179. Dhanalakshmi S, Singh RP, Agarwal C, Agarwal R. Silibinin Inhibits Constitutive and TNF Alpha-Induced Activation of NF-Alpha B and Sensitizes Human Prostate Carcinoma DU145 Cells to TNF Alpha-Induced Apoptosis. *Oncogene* (2002) 21(11):1759–67. doi: 10.1038/sj.onc.1205240
180. Hagelgans A, Nacke B, Zamaraeva M, Siegert G, Menschikowski M. Silibinin Down-Regulates Expression of Secreted Phospholipase A2 Enzymes in Cancer Cells. *Anticancer Res* (2014) 34(4):1723–9.
181. Ting H, Deep G, Kumar S, Jain AK, Agarwal C, Agarwal R. Beneficial Effects of the Naturally Occurring Flavonoid Silibinin on the Prostate Cancer Microenvironment: Role of Monocyte Chemotactic Protein-1 and Immune

Cell Recruitment. *Carcinogenesis* (2016) 37(6):589–99. doi: 10.1093/carcin/bgw039
182. Rehman MU, Tahir M, Ali F, Khan AQ, Khan R, Lateef A, et al. Chrysin Suppresses Renal Carcinogenesis *via* Amelioration of Hyperproliferation, Oxidative Stress and Inflammation: Plausible Role of NF-? B. *Free Radical Biol Med* (2012) 53):S50. doi: 10.1016/j.freeradbiomed.2012.10.133
183. Lirdprapamongkol K, Sakurai H, Abdelhamed S, Yokoyama S, Athikomkulchai S, Viriyaroj A, et al. Chrysin Overcomes TRAIL Resistance of Cancer Cells Through Mcl-1 Downregulation by Inhibiting STAT3 Phosphorylation. *Int J Oncol* (2013) 43(1):329–37. doi: 10.3892/ijo.2013.1926
184. Rehman MU, Tahir M, Khan AQ, Khan R, Lateef A, Oday OH, et al. Chrysin Suppresses Renal Carcinogenesis *via* Amelioration of Hyperproliferation, Oxidative Stress and Inflammation: Plausible Role of NF-κb. *Toxicol Lett* (2013) 216(2-3):146–58. doi: 10.1016/j.toxlet.2012.11.013
185. Kasala ER, Bodduluru LN, Barua CC, Madhana RM, Dahiya V, Budhani MK, et al. Chemopreventive Effect of Chrysin, a Dietary Flavone Against Benzo(a) Pyrene Induced Lung Carcinogenesis in Swiss Albino Mice. *Pharmacol Rep* (2016) 68(2):310–8. doi: 10.1016/j.pharep.2015.08.014
186. Dong W, Chen A, Chao X, Li X, Cui Y, Xu C, et al. Chrysin Inhibits Proinflammatory Factor-Induced EMT Phenotype and Cancer Stem Cell-Like Features in HeLa Cells by Blocking the NF-κb/Twist Axis. *Cell Physiol Biochem* (2019) 52(5):1236–50. doi: 10.33594/000000084
187. Rastogi N, Gara RK, Trivedi R, Singh A, Dixit P, Maurya R, et al. (6)-Gingerolinduced Myeloid Leukemia Cell Death Is Initiated by Reactive Oxygen Species and Activation of miR-27b Expression. *Free Radical Biol Med* (2014) 68:288–301. doi: 10.1016/j.freeradbiomed.2013.12.016
188. Ishikawa C, Senba M, Mori N. Butein Inhibits NF-κb, AP-1 and Akt Activation in Adult T-Cell Leukemia/Lymphoma. *Int J Oncol* (2017) 51 (2):633–43. doi: 10.3892/ijo.2017.4026
189. Murtaza I, Adhami VM, Hafeez BB, Saleem M, Mukhtar H. Fisetin, a Natural Flavonoid, Targets Chemoresistant Human Pancreatic Cancer AsPC-1 Cells Through DR3-Mediated Inhibition of NF-κb. *Int J Cancer* (2009) 125 (10):2465–73. doi: 10.1002/ijc.24628
190. Suh Y, Afaq F, Johnson JJ, Mukhtar H. A Plant Flavonoid Fisetin Induces Apoptosis in Colon Cancer Cells by Inhibition of COX2 and Wnt/EGFR/NF-κb-Signaling Pathways. *Carcinogenesis* (2009) 30(2):300–7. doi: 10.1093/carcin/bgn269
191. Chien CS, Shen KH, Huang JS, Ko SC, Shih YW. Antimetastatic Potential of Fisetin Involves Inactivation of the PI3K/Akt and JNK Signaling Pathways With Downregulation of MMP-2/9 Expressions in Prostate Cancer PC-3 Cells. *Mol Cell Biochem* (2010) 333(1-2):169–80. doi: 10.1007/s11010-009-0217-z
192. Li J, Qu W, Cheng Y, Sun Y, Jiang Y, Zou T, et al. The Inhibitory Effect of Intravesical Fisetin Against Bladder Cancer by Induction of P53 and Down-Regulation of NF-Kappa B Pathways in a Rat Bladder Carcinogenesis Model. *Basic Clin Pharmacol Toxicol* (2014) 115(4):321–9. doi: 10.1111/bcpt.12229
193. Yi C, Zhang Y, Yu Z, Xiao Y, Wang J, Qiu H, et al. Melatonin Enhances the Anti-Tumor Effect of Fisetin by Inhibiting COX-2/iNOS and NF-κb/P300 Signaling Pathways. *PloS One* (2014) 9(7):e99943. doi: 10.1371/journal.pone.0099943
194. Zhang XJ, Jia SS. Fisetin Inhibits Laryngeal Carcinoma Through Regulation of AKT/NF-κb/mTOR and ERK1/2 Signaling Pathways. *BioMed Pharmacother* (2016) 83:1164–74. doi: 10.1016/j.biopha.2016.08.035
195. Al-Halabi R, Bou Chedid M, Abou Merhi R, El-Hajj H, Zahr H, Schneider-Stock R, et al. Gallotannin Inhibits NFκB Signaling and Growth of Human Colon Cancer Xenografts. *Cancer Biol Ther* (2011) 12(1):59–68. doi: 10.4161/cbt.12.1.15715
196. Tian Y, Li X, Li H, Lu Q, Sun G, Chen H. Astragalus Mongholicus Regulate the Toll-Like-Receptor 4 Meditated Signal Transduction of Dendritic Cells to Restrain Stomach Cancer Cells. *Afr J Tradit Complement Altern* (2014) 11 (3):92–6. doi: 10.4314/ajtcam.v11i3.13
197. Chen M, Cai F, Zha D, Wang X, Zhang W, He Y, et al. Astragalin-Induced Cell Death is Caspase-Dependent and Enhances the Susceptibility of Lung Cancer Cells to Tumor Necrosis Factor by Inhibiting the NF-κb Pathway. *Oncotarget* (2017) 8(16):26941–58. doi: 10.18632/oncotarget.15264
198. Yang M, Li W-Y, Xie J, Wang Z-L, Wen Y-L, Zhao C-C, et al. Astragalin Inhibits the Proliferation and Migration of Human Colon Cancer HCT116 Cells by Regulating the NF-κb Signaling Pathway. *Front Pharmacol* (2021) 12. doi: 10.3389/fphar.2021.639256
199. Umesalma S, Sudhandiran G. Differential Inhibitory Effects of the Polyphenol Ellagic Acid on Inflammatory Mediators NF-κb, iNOS, COX-2, TNF-α, and IL-6 in 1, 2-Dimethylhydrazine-Induced Rat Colon Carcinogenesis. *Basic Clin Pharmacol Toxicol* (2010) 107(2):650–5. doi: 10.1111/j.1742-7843.2010.00565.x
200. Anitha P, Priyadarsini RV, Kavitha K, Thiyagarajan P, Nagini S. Ellagic Acid Coordinately Attenuates Wnt/β-Catenin and NF-κb Signaling Pathways to Induce Intrinsic Apoptosis in an Animal Model of Oral Oncogenesis. *Eur J Nutr* (2013) 52(1):75–84. doi: 10.1007/s00394-011-0288-y
201. Cheng H, Lu C, Tang R, Pan Y, Bao S, Qiu Y, et al. Ellagic Acid Inhibits the Proliferation of Human Pancreatic Carcinoma PANC-1 Cells *In Vitro* and *In Vivo*. *Oncotarget* (2017) 8(7):12301–10. doi: 10.18632/oncotarget.14811
202. Manna SK, Aggarwal RS, Sethi G, Aggarwal BB, Ramesh GT. Morin (3,5,7,2',4'-Pentahydroxyflavone) Abolishes Nuclear factor-kappaB Activation Induced by Various Carcinogens and Inflammatory Stimuli, Leading to Suppression of Nuclear factor-kappaB-Regulated Gene Expression and Up-Regulation of Apoptosis. *Clin Cancer Res* (2007) 13 (7):2290–7. doi: 10.1158/1078-0432.ccr-06-2394
203. Sharma SH, Kumar JS, Chellappan DR, Nagarajan S. Molecular Chemoprevention by Morin–A Plant Flavonoid That Targets Nuclear Factor Kappa B in Experimental Colon Cancer. *Biomed Pharmacother* (2018) 100:367–73. doi: 10.1016/j.biopha.2018.02.035
204. Kim DM, Koo SY, Jeon K, Kim MH, Lee J, Hong CY, et al. Rapid Induction of Apoptosis by Combination of Flavopiridol and Tumor Necrosis Factor (TNF)-α or TNF-Related Apoptosis-Inducing Ligand in Human Cancer Cell Lines. *Cancer Res* (2003) 63(3):621–6.
205. Liu XY, Li SG, Li YY, Cheng B, Tan B, Wang G. Puerarin Inhibits Proliferation and Induces Apoptosis by Upregulation of miR-16 in Bladder Cancer Cell Line T24. *Oncol Res* (2018) 26(8):1227–34. doi: 10.3727/096504018x15178736525106
206. Jung YY, Lee JH, Nam D, Narula AS, Namjoshi OA, Blough BE, et al. Anti-Myeloma Effects of Icariin Are Mediated Through the Attenuation of JAK/STAT3-Dependent Signaling Cascade. *Front Pharmacol* (2018) 9:531. doi: 10.3389/fphar.2018.00531
207. Peerzada KJ, Faridi AH, Sharma L, Bhardwaj SC, Satti NK, Shashi B, et al. Acteoside-Mediates Chemoprevention of Experimental Liver Carcinogenesis Through STAT-3 Regulated Oxidative Stress and Apoptosis. *Environ Toxicol* (2016) 31(7):782–98. doi: 10.1002/tox.22089
208. Shen KH, Hung SH, Yin LT, Huang CS, Chao CH, Liu CL, et al. Acacetin, a Flavonoid, Inhibits the Invasion and Migration of Human Prostate Cancer DU145 Cells *via* Inactivation of the P38 MAPK Signaling Pathway. *Mol Cell Biochem* (2010) 333(1-2):279–91. doi: 10.1007/s11010-009-0229-8
209. Kim HR, Park CG, Jung JY. Acacetin (5,7-Dihydroxy-4'-Methoxyflavone) Exhibits *In Vitro* and *In Vivo* Anticancer Activity Through the Suppression of NF-κb/Akt Signaling in Prostate Cancer Cells. *Int J Mol Med* (2014) 33 (2):317–24. doi: 10.3892/ijmm.2013.1571
210. Li W, Du Q, Li X, Zheng X, Lv F, Xi X, et al. Eriodictyol Inhibits Proliferation, Metastasis and Induces Apoptosis of Glioma Cells *via* PI3K/Akt/NF-κb Signaling Pathway. *Front Pharmacol* (2020) 11:114. doi: 10.3389/fphar.2020.00114
211. Lv F, Du Q, Li L, Xi X, Liu Q, Li W, et al. Eriodictyol Inhibits Glioblastoma Migration and Invasion by Reversing EMT *via* Downregulation of the P38 MAPK/GSK-3β/ZEB1 Pathway. *Eur J Pharmacol* (2021) 900:174069. doi: 10.1016/j.ejphar.2021.174069
212. Liu Y, Piao XJ, Xu WT, Zhang Y, Zhang T, Xue H, et al. Calycosin Induces Mitochondrial-Dependent Apoptosis and Cell Cycle Arrest, and Inhibits Cell Migration Through a ROS-Mediated Signaling Pathway in HepG2 Hepatocellular Carcinoma Cells. *Toxicol* In Vitro (2021) 70:105052. doi: 10.1016/j.tiv.2020.105052
213. Lee HJ, Auh QS, Lee YM, Kang SK, Chang SW, Lee DS, et al. Growth Inhibition and Apoptosis-Inducing Effects of Cudraflavone B in Human Oral Cancer Cells *via* MAPK, NF-κb, and SIRT1 Signaling Pathway. *Planta Med* (2013) 79(14):1298–306. doi: 10.1055/s-0033-1350619
214. Choi J, Jiang X, Jeong JB, Lee SH. Anticancer Activity of Protocatechualdehyde in Human Breast Cancer Cells. *J Med Food* (2014) 17(8):842–8. doi: 10.1089/jmf.2013.0159
215. Zhu H, Zou X, Wan J, Wang L, Qian K-J, Cai L-P, et al. Reversal of Cisplatin Resistance in Ovarian Cancer Cells Mediated by Naringin-Induced COX-2

Expression Through the NF-κb Signaling Pathway. *Int J Clin Exp Med* (2017) 10:7590–6.
216. Kim M, Miyamoto S, Yasui Y, Oyama T, Murakami A, Tanaka T. Zerumbone, a Tropical Ginger Sesquiterpene, Inhibits Colon and Lung Carcinogenesis in Mice. *Int J Cancer* (2009) 124(2):264–71. doi: 10.1002/ijc.23923
217. Zhang Q-Q, Zhou D-L, Ding Y, Liu H-Y, Lei Y, Fang H-Y, et al. Andrographolide Inhibits Melanoma Tumor Growth by Inactivating the TLR4/NF-κb Signaling Pathway. *Melanoma Res* (2014) 24(6):545–55. doi: 10.1097/CMR.0000000000000117
218. Zhang Q-Q, Ding Y, Lei Y, Qi C-L, He X-D, Lan T, et al. Andrographolide Suppress Tumor Growth by Inhibiting TLR4/NF-κb Signaling Activation in Insulinoma. *Int J Biol Sci* (2014) 10(4):404. doi: 10.7150/ijbs.7723
219. Zhang R, Zhao J, Xu J, Jiao DX, Wang J, Gong ZQ, et al. Andrographolide Suppresses Proliferation of Human Colon Cancer SW620 Cells Through the TLR4/NF−κb/MMP−9 Signaling Pathway. *Oncol Lett* (2017) 14(4):4305–10. doi: 10.3892/ol.2017.6669
220. Tang B, Tang F, Wang Z, Qi G, Liang X, Li B, et al. Upregulation of Akt/NF-κb-Regulated Inflammation and Akt/Bad-Related Apoptosis Signaling Pathway Involved in Hepatic Carcinoma Process: Suppression by Carnosic Acid Nanoparticle. *Int J Nanomed* (2016) 11:6401. doi: 10.2147/IJN.S101285
221. Zheng L, Jia J, Dai H, Wan L, Liu J, Hu L, et al. Triptolide-Assisted Phosphorylation of P53 Suppresses Inflammation-Induced NF-κb Survival Pathways in Cancer Cells. *Mol Cell Biol* (2017) 37(15):e00149–00117. doi: 10.1128/MCB.00149-17
222. Hong O-Y, Jang H-Y, Park K-H, Jeong Y-J, Kim J-S, Chae HS. Triptolide Inhibits Matrix Metalloproteinase-9 Expression and Invasion of Breast Cancer Cells Through the Inhibition of NF-κb and AP-1 Signaling Pathways. *Oncol Lett* (2021) 22(1):1–9. doi: 10.3892/ol.2021.12823
223. Chang HJ, Kim MH, Baek MK, Park JS, Chung IJ, Shin BA, et al. Triptolide Inhibits Tumor Promoter-Induced uPAR Expression *via* Blocking NF-kappaB Signaling in Human Gastric AGS Cells. *Anticancer Res* (2007) 27 (5a):3411–7.
224. Zhu W, Ou Y, Li Y, Xiao R, Shu M, Zhou Y, et al. A Small-Molecule Triptolide Suppresses Angiogenesis and Invasion of Human Anaplastic Thyroid Carcinoma Cells *via* Down-Regulation of the Nuclear Factor-κb Pathway. *Mol Pharmacol* (2009) 75(4):812–9. doi: 10.1124/mol.108.052605
225. Wang H, Ma D, Wang C, Zhao S, Liu C. Triptolide Inhibits Invasion and Tumorigenesis of Hepatocellular Carcinoma MHCC-97h Cells Through NF-κb Signaling. *Med Sci Monit* (2016) 22:1827–36. doi: 10.12659/msm.898801
226. Xiang S, Zhao Z, Zhang T, Zhang B, Meng M, Cao Z, et al. Triptonide Effectively Suppresses Gastric Tumor Growth and Metastasis Through Inhibition of the Oncogenic Notch1 and NF-κb Signaling Pathways. *Toxicol Appl Pharmacol* (2020) 388:114870. doi: 10.1016/j.taap.2019.114870
227. Zhao J, Zheng H, Sui Z, Jing F, Quan X, Zhao W, et al. Ursolic Acid Exhibits Anti-Inflammatory Effects Through Blocking TLR4-MyD88 Pathway Mediated by Autophagy. *Cytokine* (2019) 123:154726. doi: 10.1016/j.cyto.2019.05.013
228. Shanmugam MK, Manu KA, Ong TH, Ramachandran L, Surana R, Bist P, et al. Inhibition of CXCR4/CXCL12 Signaling Axis by Ursolic Acid Leads to Suppression of Metastasis in Transgenic Adenocarcinoma of Mouse Prostate Model. *Int J Cancer* (2011) 129(7):1552–63. doi: 10.1002/ijc.26120
229. Wang J, Guo W, Chen W, Yu W, Tian Y, Fu L, et al. Melatonin Potentiates the Antiproliferative and Pro-Apoptotic Effects of Ursolic Acid in Colon Cancer Cells by Modulating Multiple Signaling Pathways. *J Pineal Res* (2013) 54(4):406–16. doi: 10.1111/jpi.12035
230. Luo J, Hu YL, Wang H. Ursolic Acid Inhibits Breast Cancer Growth by Inhibiting Proliferation, Inducing Autophagy and Apoptosis, and Suppressing Inflammatory Responses *via* the PI3K/AKT and NF-κb Signaling Pathways *In Vitro*. *Exp Ther Med* (2017) 14(4):3623–31. doi: 10.3892/etm.2017.4965
231. Saikia M, Retnakumari AP, Anwar S, Anto NP, Mittal R, Shah S, et al. Heteronemin, a Marine Natural Product, Sensitizes Acute Myeloid Leukemia Cells Towards Cytarabine Chemotherapy by Regulating Farnesylation of Ras. *Oncotarget* (2018) 9(26):18115–27. doi: 10.18632/oncotarget.24771
232. Chen J, Ullah H, Zheng Z, Gu X, Su C, Xiao L, et al. Soyasaponins Reduce Inflammation by Downregulating MyD88 Expression and Suppressing the Recruitments of TLR4 and MyD88 Into Lipid Rafts. *BMC Complement Med Ther* (2020) 20:1–16. doi: 10.1186/s12906-020-2864-2
233. Narożna M, Krajka-Kuźniak V, Bednarczyk-Cwynar B, Kleszcz R, Baer-Dubowska W. The Effect of Novel Oleanolic Acid Oximes Conjugated With Indomethacin on the Nrf2-ARE And NF-κb Signaling Pathways in Normal Hepatocytes and Human Hepatocellular Cancer Cells. *Pharmaceuticals* (2021) 14(1):32. doi: 10.3390/ph14010032
234. Narożna M, Krajka-Kuźniak V, Bednarczyk-Cwynar B, Kucińska M, Kleszcz R, Kujawski J, et al. Conjugation of Diclofenac With Novel Oleanolic Acid Derivatives Modulate Nrf2 and NF-κb Activity in Hepatic Cancer Cells and Normal Hepatocytes Leading to Enhancement of Its Therapeutic and Chemopreventive Potential. *Pharmaceuticals* (2021) 14(7):688. doi: 10.3390/ph14070688
235. Assar EA, Vidalle MC, Chopra M, Hafizi S. Lycopene Acts Through Inhibition of Iκb Kinase to Suppress NF-κb Signaling in Human Prostate and Breast Cancer Cells. *Tumor Biol* (2016) 37(7):9375–85. doi: 10.1007/s13277-016-4798-3
236. Madankumar A, Tamilarasi S, Premkumar T, Gopikrishnan M, Nagabhishek N, Devaki T. Geraniol Attenuates 4NQO-Induced Tongue Carcinogenesis Through Downregulating the Activation of NF-κb in Rats. *Mol Cell Biochem* (2017) 434(1):7–15. doi: 10.1007/s11010-017-3030-0
237. Lee K-C, Chang H-H, Chung Y-H, Lee T-Y. Andrographolide Acts as an Anti-Inflammatory Agent in LPS-Stimulated RAW264. 7 Macrophages by Inhibiting STAT3-Mediated Suppression of the NF-κb Pathway. *J Ethnopharmacol* (2011) 135(3):678–84. doi: 10.1016/j.jep.2011.03.068
238. Chiang K-C, Tsui K-H, Chung L-C, Yeh C-N, Chen W-T, Chang P-L, et al. Celastrol Blocks Interleukin-6 Gene Expression *via* Downregulation of NF-κb in Prostate Carcinoma Cells. *PloS One* (2014) 9(3):e93151. doi: 10.1371/journal.pone.0093151
239. Su D, Wang WB, Wu XY, Li MY, Yan XL, Hua ZH, et al. Meriolin1 Induces Cell Cycle Arrest, Apoptosis, Autophagy and Targeting the Akt/MAPKs Pathways in Human Neuroblastoma SH-SY5Y Cells. *J Pharm Pharmacol* (2020) 72(4):561–74. doi: 10.1111/jphp.13224
240. Einbond LS, Mighty J, Redenti S, Wu H-A. Actein Induces Calcium Release in Human Breast Cancer Cells. *Fitoterapia* (2013) 91:28–38. doi: 10.1016/j.fitote.2013.07.025
241. Sung B, Prasad S, Yadav VR, Aggarwal BB. Cancer Cell Signaling Pathways Targeted by Spice-Derived Nutraceuticals. *Nutr Cancer* (2012) 64(2):173–97. doi: 10.1080/01635581.2012.630551
242. Yadav VR, Prasad S, Sung B, Kannappan R, Aggarwal BB. Targeting Inflammatory Pathways by Triterpenoids for Prevention and Treatment of Cancer. *Toxins* (2010) 2(10):2428–66. doi: 10.3390/toxins2102428
243. Corbiere C, Liagre B, Terro F, Beneytout J-L. Induction of Antiproliferative Effect by Diosgenin Through Activation of P53, Release of Apoptosis-Inducing Factor (AIF) and Modulation of Caspase-3 Activity in Different Human Cancer Cells. *Cell Res* (2004) 14(3):188–96. doi: 10.1038/sj.cr.7290219
244. Lepage C, Liagre B, Cook-Moreau J, Pinon A, Beneytout J-L. Cyclooxygenase-2 and 5-Lipoxygenase Pathways in Diosgenin-Induced Apoptosis in HT-29 and HCT-116 Colon Cancer Cells. *Int J Oncol* (2010) 36(5):1183–91. doi: 10.3892/ijo_00000601
245. Lepage C, Léger DY, Bertrand J, Martin F, Beneytout JL, Liagre B. Diosgenin Induces Death Receptor-5 Through Activation of P38 Pathway and Promotes TRAIL-Induced Apoptosis in Colon Cancer Cells. *Cancer Lett* (2011) 301(2):193–202. doi: 10.1016/j.canlet.2010.12.003
246. Zhuang H, Dai X, Zhang X, Mao Z, Huang H. Sophoridine Suppresses Macrophage-Mediated Immunosuppression Through TLR4/IRF3 Pathway and Subsequently Upregulates CD8+ T Cytotoxic Function Against Gastric Cancer. *Biomed Pharmacother* (2020) 121:109636. doi: 10.1016/j.biopha.2019.109636
247. Wang J-k, Zhao B-S, Wang M, Liu C-Y, Li Y-Q, Ma Q-T, et al. Anti-Tumor and Phenotypic Regulation Effect of Matrine on Dendritic Cells Through Regulating TLRs Pathway. *Chin J Integr Med* (2021) 27(7):520–6. doi: 10.1007/s11655-020-3433-8
248. Yu P, Liu Q, Liu K, Yagasaki K, Wu E, Zhang G. Matrine Suppresses Breast Cancer Cell Proliferation and Invasion *via* VEGF-Akt-NF-κ B Signaling. *Cytotechnology* (2009) 59(3):219–29. doi: 10.1007/s10616-009-9225-9
249. Huang H, Du T, Xu G, Lai Y, Fan X, Chen X, et al. Matrine Suppresses Invasion of Castration-Resistant Prostate Cancer Cells by Downregulating MMP-2/9 *via* NF-κb Signaling Pathway. *Int J Oncol* (2017) 50(2):640–8. doi: 10.3892/ijo.2016.3805

250. Hai-Tao F, Wen-Wen Z, Jin-Jian L, Yi-Tao W, Xiu-Ping C. Hypaconitine Inhibits TGF-β1-Induced Epithelial–Mesenchymal Transition and Suppresses Adhesion, Migration, and Invasion of Lung Cancer A549 Cells. *Chin J Natural Medicines* (2017) 15(6):427–35.
251. Zhang T, Guo S, Zhu X, Qiu J, Deng G, Qiu C. Alpinetin Inhibits Breast Cancer Growth by ROS/NF-κb/HIF-1α Axis. *J Cell Mol Med* (2020) 24 (15):8430–40. doi: 10.1111/jcmm.15371
252. Lu JJ, Fu L, Tang Z, Zhang C, Qin L, Wang J, et al. Melatonin Inhibits AP-2β/hTERT, NF-κb/COX-2 and Akt/ERK and Activates Caspase/Cyto C Signaling to Enhance the Antitumor Activity of Berberine in Lung Cancer Cells. *Oncotarget* (2016) 7(3):2985–3001. doi: 10.18632/oncotarget.6407
253. Li J, Liu F, Jiang S, Liu J, Chen X, Zhang S, et al. Berberine Hydrochloride Inhibits Cell Proliferation and Promotes Apoptosis of Non-Small Cell Lung Cancer *via* the Suppression of the MMP2 and Bcl-2/Bax Signaling Pathways. *Oncol Lett* (2018) 15(5):7409–14. doi: 10.3892/ol.2018.8249
254. Kumar R, Awasthi M, Sharma A, Padwad Y, Sharma R. Berberine Induces Dose-Dependent Quiescence and Apoptosis in A549 Cancer Cells by Modulating Cell Cyclins and Inflammation Independent of mTOR Pathway. *Life Sci* (2020) 244:117346. doi: 10.1016/j.lfs.2020.117346
255. Yao M, Fan X, Yuan B, Takagi N, Liu S, Han X, et al. Berberine Inhibits NLRP3 Inflammasome Pathway in Human Triple-Negative Breast Cancer MDA-MB-231 Cell. *BMC Complement Altern Med* (2019) 19(1):1–11. doi: 10.1186/s12906-019-2615-4
256. Ho Y-T, Yang J-S, Li T-C, Lin J-J, Lin J-G, Lai K-C, et al. Berberine Suppresses *In Vitro* Migration and Invasion of Human SCC-4 Tongue Squamous Cancer Cells Through the Inhibitions of FAK, IKK, NF-κb, U-PA and MMP-2 and -9. *Cancer Lett* (2009) 279(2):155–62. doi: 10.1016/j.canlet.2009.01.033
257. Karnam KC, Ellutla M, Bodduluru LN, Kasala ER, Uppulapu SK, Kalyankumarraju M, et al. Preventive Effect of Berberine Against DMBA-Induced Breast Cancer in Female Sprague Dawley Rats. *Biomed Pharmacother* (2017) 92:207–14. doi: 10.1016/j.biopha.2017.05.069
258. Zhao L, Zhang C. Berberine Inhibits MDA-MB-231 Cells by Attenuating Their Inflammatory Responses. *BioMed Res Int* (2020). doi: 10.1155/2020/3617514
259. Fu L, Chen W, Guo W, Wang J, Tian Y, Shi D, et al. Berberine Targets AP-2/hTERT, NF-κb/COX-2, HIF-1α/VEGF and Cytochrome-C/Caspase Signaling to Suppress Human Cancer Cell Growth. *PloS One* (2013) 8(7): e69240. doi: 10.1371/journal.pone.0069240
260. Wang Y, Zhou M, Shang D. Berberine Inhibits Human Gastric Cancer Cell Growth *via* Deactivation of P38/JNK Pathway, Induction of Mitochondrial-Mediated Apoptosis, Caspase Activation and NF-κb Inhibition. *J BUON* (2020) 25(1):314–8.
261. Li P, Liu Y, He Q. Anisodamine Suppressed the Growth of Hepatocellular Carcinoma Cells, Induced Apoptosis and Regulated the Levels of Inflammatory Factors by Inhibiting NLRP3 Inflammasome Activation. *Drug Des Dev Ther* (2020) 14:1609. doi: 10.2147/DDDT.S243383
262. Ghezali L, Leger DY, Limami Y, Cook-Moreau J, Beneytout J-L. Cyclopamine and Jervine Induce COX-2 Overexpression in Human Erythroleukemia Cells But Only Cyclopamine has a Pro-Apoptotic Effect. *Exp Cell Res* (2013) 319(7):1043–53. doi: 10.1016/j.yexcr.2013.01.014
263. Xu W, Wang X, Tu Y, Masaki H, Tanaka S, Onda K, et al. Tetrandrine and Cepharanthine Induce Apoptosis Through Caspase Cascade Regulation, Cell Cycle Arrest, MAPK Activation and PI3K/Akt/mTOR Signal Modification in Glucocorticoid Resistant Human Leukemia Jurkat T Cells. *Chem-Biol Interact* (2019) 310. doi: 10.1016/j.cbi.2019.108726
264. Ginzburg S, Golovine KV, Makhov PB, Uzzo RG, Kutikov A, Kolenko VM. Piperlongumine Inhibits NF-κb Activity and Attenuates Aggressive Growth Characteristics of Prostate Cancer Cells. *Prostate* (2014) 74(2):177–86. doi: 10.1002/pros.22739
265. Han JG, Gupta SC, Prasad S, Aggarwal BB. Piperlongumine Chemosensitizes Tumor Cells Through Interaction With Cysteine 179 of Iκbα Kinase, Leading to Suppression of NF-κb-Regulated Gene Products. *Mol Cancer Ther* (2014) 13(10):2422–35. doi: 10.1158/1535-7163.mct-14-0171
266. Golovine K, Makhov P, Naito S, Raiyani H, Tomaszewski J, Mehrazin R, et al. Piperlongumine and its Analogs Down-Regulate Expression of C-Met in Renal Cell Carcinoma. *Cancer Biol Ther* (2015) 16(5):743–9. doi: 10.1080/15384047.2015.1026511
267. Seok JS, Jeong CH, Petriello MC, Seo HG, Yoo H, Hong K, et al. Piperlongumine Decreases Cell Proliferation and the Expression of Cell Cycle-Associated Proteins by Inhibiting Akt Pathway in Human Lung Cancer Cells. *Food Chem Toxicol* (2018) 111:9–18. doi: 10.1016/j.fct.2017.10.058
268. Kumar S, Agnihotri N. Piperlongumine Targets NF-κb and its Downstream Signaling Pathways to Suppress Tumor Growth and Metastatic Potential in Experimental Colon Cancer. *Mol Cell Biochem* (2021) 476(4):1765–81. doi: 10.1007/s11010-020-04044-7
269. Hamsa T, Kuttan G. Harmine Inhibits Tumour Specific Neo-Vessel Formation by Regulating VEGF, MMP, TIMP and Pro-Inflammatory Mediators Both *In Vivo* and *In Vitro*. *Eur J Pharmacol* (2010) 649(1-3):64–73. doi: 10.1016/j.ejphar.2010.09.010
270. Jung YY, Shanmugam MK, Chinnathambi A, Alharbi SA, Shair OH, Um J-Y, et al. Fangchinoline, a Bisbenzylisoquinoline Alkaloid can Modulate Cytokine-Impelled Apoptosis *via* the Dual Regulation of NF-κb and AP-1 Pathways. *Molecules* (2019) 24(17):3127. doi: 10.3390/molecules24173127
271. Guo Y, Ding Y, Zhang T, An H. Sinapine Reverses Multi-Drug Resistance in MCF-7/Dox Cancer Cells by Downregulating FGFR4/FRS2α-ERK1/2 Pathway-Mediated NF-κb Activation. *Phytomedicine* (2016) 23(3):267–73. doi: 10.1016/j.phymed.2015.12.017
272. Ramu A, Kathiresan S, Ramadoss H, Nallu A, Kaliyan R, Azamuthu T. Gramine Attenuates EGFR-Mediated Inflammation and Cell Proliferation in Oral Carcinogenesis *via* Regulation of NF-κb and STAT3 Signaling. *Biomed Pharmacother* (2018) 98:523–30. doi: 10.1016/j.biopha.2017.12.049
273. Harada K, Ferdous T, Itashiki Y, Takii M, Mano T, Mori Y, et al. Cepharanthine Inhibits Angiogenesis and Tumorigenicity of Human Oral Squamous Cell Carcinoma Cells by Suppressing Expression of Vascular Endothelial Growth Factor and Interleukin-8. *Int J Oncol* (2009) 35(5):1025–35. doi: 10.3892/ijo_00000417
274. Han SZ, Liu HX, Yang LQ, Cui LD, Xu Y. Piperine (PP) Enhanced Mitomycin-C (MMC) Therapy of Human Cervical Cancer Through Suppressing Bcl-2 Signaling Pathway *via* Inactivating STAT3/NF-κb. *BioMed Pharmacother* (2017) 96:1403–10. doi: 10.1016/j.biopha.2017.11.022
275. Rehman MU, Rashid S, Arafah A, Qamar W, Alsaffar RM, Ahmad A, et al. Piperine Regulates Nrf-2/Keap-1 Signalling and Exhibits Anticancer Effect in Experimental Colon Carcinogenesis in Wistar Rats. *Biology* (2020) 9(9):302. doi: 10.3390/biology9090302
276. Zhang N, Wang D, Zhu Y, Wang J, Lin H. Inhibition Effects of Lamellarin D on Human Leukemia K562 Cell Proliferation and Underlying Mechanisms. *Asian Pac J Cancer Prev* (2014) 15(22):9915–9. doi: 10.7314/APJCP.2014.15.22.9915
277. Hamsa T, Kuttan G. Ipobscurine, an Indole Alkaloid From Ipomoea Obscura, Inhibits Tumor Cell Invasion and Experimental Metastasis by Inducing Apoptosis. *J Environ Pathol Toxicol Oncol* (2011) 30(2):163–78. doi: 10.1615/JEnvironPatholToxicolOncol.v30.i2.70
278. Yang B, Zhang D, Qian J, Cheng Y. Chelerythrine Suppresses Proliferation and Metastasis of Human Prostate Cancer Cells *via* Modulating MMP/TIMP/NF-κb System. *Mol Cell Biochem* (2020) 474(1-2):199–208. doi: 10.1007/s11010-020-03845-0
279. Silva TCC, de Faria Lopes GP, de J.M.-F.N., de Oliveira DM, Pereira E, Pitanga BPS, et al. Specific Cytostatic and Cytotoxic Effect of Dihydrochelerythrine in Glioblastoma Cells: Role of NF-κb/β-Catenin and STAT3/IL-6 Pathways. *Anticancer Agents Med Chem* (2018) 18(10):1386–93. doi: 10.2174/1871520618666180412122101
280. Zeng Q, Luo C, Cho J, Lai D, Shen X, Zhang X, et al. Tryptanthrin Exerts Anti-Breast Cancer Effects Both *In Vitro* and *In Vivo* Through Modulating the Inflammatory Tumor Microenvironment. *Acta Pharm* (2021) 71(2):245–66. doi: 10.2478/acph-2021-0020
281. Sivalingam K, Amirthalingam V, Ganasan K, Huang CY, Viswanadha VP. Neferine Suppresses Diethylnitrosamine-Induced Lung Carcinogenesis in Wistar Rats. *Food Chem Toxicol* (2019) 123:385–98. doi: 10.1016/j.fct.2018.11.014
282. Zhu J, Ghosh A, Coyle EM, Lee J, Hahm E-R, Singh SV, et al. Differential Effects of Phenethyl Isothiocyanate and D, L-Sulforaphane on TLR3 Signaling. *J Immunol* (2013) 190(8):4400–7. doi: 10.4049/jimmunol.1202093
283. Lee Y-R, Noh E-M, Han J-H, Kim J-M, Hwang B-M, Kim B-S, et al. Sulforaphane Controls TPA-Induced MMP-9 Expression Through the NF-κb Signaling Pathway, But Not AP-1, in MCF-7 Breast Cancer Cells. *BMB Rep* (2013) 46(4):201. doi: 10.5483/bmbrep.2013.46.4.160
284. Gong K, Li W. Shikonin, a Chinese Plant-Derived Naphthoquinone, Induces Apoptosis in Hepatocellular Carcinoma Cells Through Reactive Oxygen Species:

A Potential New Treatment for Hepatocellular Carcinoma. *Free Radic Biol Med* (2011) 51(12):2259–71. doi: 10.1016/j.freeradbiomed.2011.09.018

285. Liu JP, Liu D, Gu JF, Zhu MM, Cui L. Shikonin Inhibits the Cell *via*bility, Adhesion, Invasion and Migration of the Human Gastric Cancer Cell Line MGC-803 *via* the Toll-Like Receptor 2/Nuclear Factor-Kappa B Pathway. *J Pharm Pharmacol* (2015) 67(8):1143–55. doi: 10.1111/jphp.12402
286. Krajka-Kuźniak V, Cykowiak M, Szaefer H, Kleszcz R, Baer-Dubowska W. Combination of Xanthohumol and Phenethyl Isothiocyanate Inhibits NF-κb and Activates Nrf2 in Pancreatic Cancer Cells. *Toxicol Vitro* (2020) 65:104799. doi: 10.1016/j.tiv.2020.104799
287. Benelli R, Ven R, Ciarlo M, Carlone S, Barbieri O, Ferrari N. The AKT/NF-κb Inhibitor Xanthohumol is a Potent Anti-Lymphocytic Leukemia Drug Overcoming Chemoresistance and Cell Infiltration. *Biochem Pharmacol* (2012) 83(12):1634–42. doi: 10.1016/j.bcp.2012.03.006
288. Yang MD, Lai KC, Lai TY, Hsu SC, Kuo CL, Yu CS, et al. Phenethyl Isothiocyanate Inhibits Migration and Invasion of Human Gastric Cancer AGS Cells Through Suppressing MAPK and NF-κb Signal Pathways. *Anticancer Res* (2010) 30(6):2135–43.
289. Wang C, Li S, Wang MW. Evodiamine-Induced Human Melanoma A375-S2 Cell Death was Mediated by PI3K/Akt/caspase and Fas-L/NF-kappaB Signaling Pathways and Augmented by Ubiquitin-Proteasome Inhibition. *Toxicol* In Vitro (2010) 24(3):898–904. doi: 10.1016/j.tiv.2009.11.019
290. Lin L, Ren L, Wen L, Wang Y, Qi J. Effect of Evodiamine on the Proliferation and Apoptosis of A549 Human Lung Cancer Cells. *Mol Med Rep* (2016) 14 (3):2832–8. doi: 10.3892/mmr.2016.5575
291. Hwang Y, Kim HC, Shin EJ. Enhanced Neurogenesis Is Involved in Neuroprotection Provided by Rottlerin Against Trimethyltin-Induced Delayed Apoptotic Neuronal Damage. *Life Sci* (2020) 262:118494. doi: 10.1016/j.lfs.2020.118494
292. Fan X, Deng J, Shi T, Wen H, Li J, Liang Z, et al. Design, Synthesis and Bioactivity Study of Evodiamine Derivatives as Multifunctional Agents for the Treatment of Hepatocellular Carcinoma. *Bioorg Chem* (2021) 114:105154. doi: 10.1016/j.bioorg.2021.105154
293. Guzmán EA, Maers K, Roberts J, Kemami-Wangun HV, Harmody D, Wright AE. The Marine Natural Product Microsclerodermin A Is a Novel Inhibitor of the Nuclear Factor Kappa B and Induces Apoptosis in Pancreatic Cancer Cells. *Investigat N Drugs* (2015) 33(1):86–94. doi: 10.1007/s10637-014-0185-3
294. Sperlich J, Kerr R, Teusch N. The Marine Natural Product Pseudopterosin Blocks Cytokine Release of Triple-Negative Breast Cancer and Monocytic Leukemia Cells by Inhibiting NF-κb Signaling. *Mar Drugs* (2017) 15(9):262. doi: 10.3390/md15090262
295. Chen H, Zhang J, Luo J, Lai F, Wang Z, Tong H, et al. Antiangiogenic Effects of Oxymatrine on Pancreatic Cancer by Inhibition of the NF-κb-Mediated VEGF Signaling Pathway. *Oncol Rep* (2013) 30(2):589–95. doi: 10.3892/or.2013.2529
296. Li Q, Lai Y, Wang C, Xu G, He Z, Shang X, et al. Matrine Inhibits the Proliferation, Invasion and Migration of Castration-Resistant Prostate Cancer Cells Through Regulation of the NF-κb Signaling Pathway. *Oncol Rep* (2016) 35(1):375–81. doi: 10.3892/or.2015.4341
297. Huang H, Wang Q, Du T, Lin C, Lai Y, Zhu D, et al. Matrine Inhibits the Progression of Prostate Cancer by Promoting Expression of GADD45B. *Prostate* (2018) 78(5):327–35. doi: 10.1002/pros.23469
298. Jung YY, Um J-Y, Narula AS, Namjoshi OA, Blough BE, Kumar AP, et al. Identification of Matrine as a Novel Regulator of the Cxcr4 Signaling Axis in Tumor Cells. *Int J Mol Sci* (2020) 21(13):4731. doi: 10.3390/ijms21134731
299. Sp N, Kang DY, Kim DH, Park JH, Lee HG, Kim HJ, et al. Nobiletin Inhibits CD36-Dependent Tumor Angiogenesis, Migration, Invasion, and Sphere Formation Through the Cd36/Stat3/Nf-Kb Signaling Axis. *Nutrients* (2018) 10(6):772. doi: 10.3390/nu10060772
300. Chen J, Chen AY, Huang H, Ye X, Rollyson WD, Perry HE, et al. The Flavonoid Nobiletin Inhibits Tumor Growth and Angiogenesis of Ovarian Cancers *via* the Akt Pathway. *Int J Oncol* (2015) 46(6):2629–38. doi: 10.3892/ijo.2015.2946
301. Ozkan AD, Sarihan M, Kaleli S. Evaluation of the Effects of Nobiletin on Toll-Like Receptor 3 Signaling Pathways in Prostate Cancer *In Vitro*. *Nutr Cancer* (2021) 73(7):1138–44. doi: 10.1080/01635581.2020.1841247
302. Lee YC, Cheng TH, Lee JS, Chen JH, Liao YC, Fong Y, et al. Nobiletin, a Citrus Flavonoid, Suppresses Invasion and Migration Involving FAK/PI3K/Akt and Small GTPase Signals in Human Gastric Adenocarcinoma AGS Cells. *Mol Cell Biochem* (2011) 347(1-2):103–15. doi: 10.1007/s11010-010-0618-z
303. Lee S-J, Lim K-T. Inhibitory Effect of Phytoglycoprotein on Tumor Necrosis Factor-α and Interleukin-6 at Initiation Stage of Colon Cancer in 1, 2-Dimethylhydrazine-Treated ICR Mice. *Toxicol Appl Pharmacol* (2007) 225 (2):198–205. doi: 10.1016/j.taap.2007.07.010
304. Lee J-S, Kang Y, Kim JT, Thapa D, Lee E-S, Kim J-A. The Anti-Angiogenic and Anti-Tumor Activity of Synthetic Phenylpropenone Derivatives Is Mediated Through the Inhibition of Receptor Tyrosine Kinases. *Eur J Pharmacol* (2012) 677(1-3):22–30. doi: 10.1016/j.ejphar.2011.12.012
305. Kang K-H, Kong C-S, Seo Y, Kim M-M, Kim S-K. Anti-Inflammatory Effect of Coumarins Isolated From Corydalis Heterocarpa in HT-29 Human Colon Carcinoma Cells. *Food Chem Toxicol* (2009) 47(8):2129–34. doi: 10.1016/j.fct.2009.05.036
306. Zhu H-C, Jia X-K, Fan Y, Xu S-H, Li X-Y, Huang M-Q, et al. Alisol B 23-Acetate Ameliorates Azoxymethane/Dextran Sodium Sulfate-Induced Male Murine Colitis-Associated Colorectal Cancer *via* Modulating the Composition of Gut Microbiota and Improving Intestinal Barrier. *Front Cell Infect Microbiol* (2021) 11. doi: 10.3389/fcimb.2021.640225
307. Mehta R, Katta H, Alimirah F, Patel R, Murillo G, Peng X, et al. Deguelin Action Involves C-Met and EGFR Signaling Pathways in Triple Negative Breast Cancer Cells. *PloS One* (2013) 8(6):e65113. doi: 10.1371/journal.pone.0065113
308. Shiragannavar VD, Gowda NGS, Kumar DP, Mirshahi F, Santhekadur PK. Withaferin A Acts as a Novel Regulator of Liver X Receptor-α in HCC. *Front Oncol* (2021) 10:3124. doi: 10.3389/fonc.2020.628506
309. Ngoungoure FP, Owona BA. Withaferin A Modulates AIM2 Inflammasome and Caspase-1 Expression in THP-1 Polarized Macrophages. *Exp Cell Res* (2019) 383(2):111564. doi: 10.1016/j.yexcr.2019.111564
310. Kim Y-J, Jeon Y, Kim T, Lim W-C, Ham J, Park YN, et al. Combined Treatment With Zingerone and its Novel Derivative Synergistically Inhibits TGF-β1 Induced Epithelial-Mesenchymal Transition, Migration and Invasion of Human Hepatocellular Carcinoma Cells. *Bioorg Med Chem Lett* (2017) 27(4):1081–8. doi: 10.1016/j.bmcl.2016.12.042
311. Kao SJ, Su JL, Chen CK, Yu MC, Bai KJ, Chang JH, et al. Osthole Inhibits the Invasive Ability of Human Lung Adenocarcinoma Cells *via* Suppression of NF-κb-Mediated Matrix Metalloproteinase-9 Expression. *Toxicol Appl Pharmacol* (2012) 261(1):105–15. doi: 10.1016/j.taap.2012.03.020
312. Feng H, Lu J-J, Wang Y, Pei L, Chen X. Osthole Inhibited TGF β-Induced Epithelial–Mesenchymal Transition (EMT) by Suppressing NF-κb Mediated Snail Activation in Lung Cancer A549 Cells. *Cell Adhes Migr* (2017) 11(5-6):464–75. doi: 10.1080/19336918.2016.1259058
313. Che Y, Li J, Li Z, Li J, Wang S, Yan Y, et al. Osthole Enhances Antitumor Activity and Irradiation Sensitivity of Cervical Cancer Cells by Suppressing ATM/Nf–κb Signaling. *Oncol Rep* (2018) 40(2):737–47. doi: 10.3892/or.2018.6514
314. Lee JH, Kim C, Lee S-G, Yang WM, Um J-Y, Sethi G, et al. Ophiopogonin D Modulates Multiple Oncogenic Signaling Pathways, Leading to Suppression of Proliferation and Chemosensitization of Human Lung Cancer Cells. *Phytomedicine* (2018) 40:165–75. doi: 10.1016/j.phymed.2018.01.002
315. Lee H, Ko JH, Baek SH, Nam D, Lee SG, Lee J, et al. Embelin Inhibits Invasion and Migration of MDA-MB-231 Breast Cancer Cells by Suppression of CXC Chemokine Receptor 4, Matrix Metalloproteinases-9/2, and Epithelial–Mesenchymal Transition. *Phytother Res* (2016) 30 (6):1021–32. doi: 10.1002/ptr.5612
316. Hafeez BB, Jamal MS, Fischer JW, Mustafa A, Verma AK. Plumbagin, a Plant Derived Natural Agent Inhibits the Growth of Pancreatic Cancer Cells in *In Vitro* and *In Vivo via* Targeting EGFR, Stat3 and NF-κb Signaling Pathways. *Int J Cancer* (2012) 131(9):2175–86. doi: 10.1002/ijc.27478
317. Li J, Shen L, Lu FR, Qin Y, Chen R, Li J, et al. Plumbagin Inhibits Cell Growth and Potentiates Apoptosis in Human Gastric Cancer Cells *In Vitro* Through the NF-κb Signaling Pathway. *Acta Pharmacol Sin* (2012) 33(2):242–9. doi: 10.1038/aps.2011.152
318. Salem AZ, Medhat D, Fathy SA, Mohamed MR, El-Khayat Z, El-Daly SM. Indole Glucosinolates Exhibit Anti-Inflammatory Effects on Ehrlich Ascites Carcinoma Cells Through Modulation of Inflammatory Markers and miRNAs. *Mol Biol Rep* (2021) 48(10):6845–55. doi: 10.1007/s11033-021-06683-5

319. Sethi G, Ahn KS, Aggarwal BB. Targeting Nuclear Factor-κb Activation Pathway by Thymoquinone: Role in Suppression of Antiapoptotic Gene Products and Enhancement of Apoptosis. *Mol Cancer Res* (2008) 6(6):1059–70. doi: 10.1158/1541-7786.MCR-07-2088
320. Ahmad I, Muneer KM, Tamimi IA, Chang ME, Ata MO, Yusuf N. Thymoquinone Suppresses Metastasis of Melanoma Cells by Inhibition of NLRP3 Inflammasome. *Toxicol Appl Pharmacol* (2013) 270(1):70–6. doi: 10.1016/j.taap.2013.03.027
321. Kim W-J, Lee M-Y, Kim J-H, Suk K, Lee W-H. Decursinol Angelate Blocks Transmigration and Inflammatory Activation of Cancer Cells Through Inhibition of PI3K, ERK and NF-κb Activation. *Cancer Lett* (2010) 296 (1):35–42. doi: 10.1016/j.canlet.2010.03.012
322. Liu Y, Zhang L, Zhu X, Wang Y, Liu W, Gong W. Polysaccharide Agaricus Blazei Murill Stimulates Myeloid Derived Suppressor Cell Differentiation From M2 to M1 Type, Which Mediates Inhibition of Tumour Immune-Evasion *via* the Toll-Like Receptor 2 Pathway. *Immunology* (2015) 146 (3):379–91. doi: 10.1111/imm.12508
323. Verma A, Ahmed B, Anwar F, Rahman M, Patel DK, Kaithwas G, et al. Novel Glycoside From Wedelia Calendulacea Inhibits Diethyl Nitrosamine-Induced Renal Cancer *via* Downregulating the COX-2 and PEG 2 Through Nuclear Factor-κb Pathway. *Inflammopharmacology* (2017) 25 (1):159–75. doi: 10.1007/s10787-017-0310-y
324. Choudhari AS, Mandave PC, Deshpande M, Ranjekar P, Prakash O. Phytochemicals in Cancer Treatment: From Preclinical Studies to Clinical Practice. *Front Pharmacol* (2020) 10:1614. doi: 10.3389/fphar.2019.01614
325. Rizeq B, Gupta I, Ilesanmi J, AlSafran M, Rahman MM, Ouhtit A. The Power of Phytochemicals Combination in Cancer Chemoprevention. *J Cancer* (2020) 11(15):4521. doi: 10.7150/jca.34374
326. Dehelean CA, Marcovici I, Soica C, Mioc M, Coricovac D, Iurciuc S, et al. Plant-Derived Anticancer Compounds as New Perspectives in Drug Discovery and Alternative Therapy. *Molecules* (2021) 26(4):1109. doi: 10.3390/molecules26041109
327. Sreekanth C, Bava S, Sreekumar E, Anto R. Molecular Evidences for the Chemosensitizing Efficacy of Liposomal Curcumin in Paclitaxel Chemotherapy in Mouse Models of Cervical Cancer. *Oncogene* (2011) 30 (28):3139–52. doi: 10.1038/onc.2011.23
328. Quispe-Soto ET, Calaf GM. Effect of Curcumin and Paclitaxel on Breast Carcinogenesis. *Int J Oncol* (2016) 49(6):2569–77. doi: 10.3892/ijo.2016.3741
329. Calaf GM, Ponce-Cusi R, Carrión F. Curcumin and Paclitaxel Induce Cell Death in Breast Cancer Cell Lines. *Oncol Rep* (2018) 40(4):2381–8. doi: 10.3892/or.2018.6603
330. Dang Y-P, Yuan X-Y, Tian R, Li D-G, Liu W. Curcumin Improves the Paclitaxel–Induced Apoptosis of HPV–positive Human Cervical Cancer Cells *via* the NF–κb–P53–Caspase–3 Pathway. *Exp Ther Med* (2015) 9 (4):1470–6. doi: 10.3892/etm.2015.2240
331. Roy M, Mukherjee S, Sarkar R, Biswas J. Curcumin Sensitizes Chemotherapeutic Drugs *via* Modulation of PKC, Telomerase, NF-κb and HDAC in Breast Cancer. *Ther Deliv* (2011) 2(10):1275–93. doi: 10.4155/tde.11.97
332. de Porras VR, Bystrup S, Martínez-Cardús A, Pluvinet R, Sumoy L, Howells L, et al. Curcumin Mediates Oxaliplatin-Acquired Resistance Reversion in Colorectal Cancer Cell Lines Through Modulation of CXC-Chemokine/NF-κb Signalling Pathway. *Sci Rep* (2016) 6(1):1–17. doi: 10.1038/srep24675
333. Wang YT, Liu HS, Su CL. Curcumin-Enhanced Chemosensitivity of FDA-Approved Platinum (II)-Based Anti-Cancer Drugs Involves Downregulation of Nuclear Endonuclease G and NF-κb as Well as Induction of Apoptosis and G2/M Arrest. *Int J Food Sci Nutr* (2014) 65(3):368–74. doi: 10.3109/09637486.2013.871694
334. Nautiyal J, Banerjee S, Kanwar SS, Yu Y, Patel BB, Sarkar FH, et al. Curcumin Enhances Dasatinib-Induced Inhibition of Growth and Transformation of Colon Cancer Cells. *Int J Cancer* (2011) 128(4):951–61. doi: 10.1002/ijc.25410
335. Jiang M, Huang O, Zhang X, Xie Z, Shen A, Liu H, et al. Curcumin Induces Cell Death and Restores Tamoxifen Sensitivity in the Antiestrogen-Resistant Breast Cancer Cell Lines MCF-7/LCC2 and MCF-7/Lcc9. *Molecules* (2013) 18(1):701–20. doi: 10.3390/molecules18010701
336. Thulasiraman P, McAndrews DJ, Mohiudddin IQ. Curcumin Restores Sensitivity to Retinoic Acid in Triple Negative Breast Cancer Cells. *BMC Cancer* (2014) 14:724. doi: 10.1186/1471-2407-14-724
337. Wang WJ, Wang SZ, Liu TL, Ma Y, Huang SJ, Lei L, et al. Resveratrol: Multi-Targets Mechanism on Neurodegenerative Diseases Based on Network Pharmacology. *Front Pharmacol* (2020) 11:694. doi: 10.3389/fphar.2020.00694
338. Hu XL, Guo LP, Song Q, Zhang Q, Chen Y, Wang J, et al. Kukoamine B, an Amide Alkaloid, Protects Against NMDA-Induced Neurotoxicity and Potential Mechanisms *In Vitro*. *Neurochem Int* (2015) 87:66–76. doi: 10.1016/j.neuint.2015.06.001
339. Martínez-Martínez D, Soto A, Gil-Araujo B, Gallego B, Chiloeches A, Lasa M. Resveratrol Promotes Apoptosis Through the Induction of Dual Specificity Phosphatase 1 and Sensitizes Prostate Cancer Cells to Cisplatin. *Food Chem Toxicol* (2019) 124:273–9. doi: 10.1016/j.fct.2018.12.014
340. Karthikeyan S, Hoti SL, Prasad NR. Resveratrol Loaded Gelatin Nanoparticles Synergistically Inhibits Cell Cycle Progression and Constitutive NF-kappaB Activation, and Induces Apoptosis in Non-Small Cell Lung Cancer Cells. *Biomed Pharmacother* (2015) 70:274–82. doi: 10.1016/j.biopha.2015.02.006
341. Buhrmann C, Shayan P, Kraehe P, Popper B, Goel A, Shakibaei M. Resveratrol Induces Chemosensitization to 5-Fluorouracil Through Up-Regulation of Intercellular Junctions, Epithelial-To-Mesenchymal Transition and Apoptosis in Colorectal Cancer. *Biochem Pharmacol* (2015) 98(1):51–68. doi: 10.1016/j.bcp.2015.08.105
342. Harikumar KB, Kunnumakkara AB, Sethi G, Diagaradjane P, Anand P, Pandey MK, et al. Resveratrol, a Multitargeted Agent, can Enhance Antitumor Activity of Gemcitabine *In Vitro* and in Orthotopic Mouse Model of Human Pancreatic Cancer. *Int J Cancer* (2010) 127(2):257–68. doi: 10.1002/ijc.25041
343. Xu Y, Xin Y, Diao Y, Lu C, Fu J, Luo L, et al. Synergistic Effects of Apigenin and Paclitaxel on Apoptosis of Cancer Cells. *PloS One* (2011) 6(12):e29169. doi: 10.1371/journal.pone.0029169
344. Hasani NAH, Amin IM, Kamaludin R, Rosdyd N.M.M.N.M., Ibahim MJ, Kadir SHSA. P53 and Cyclin B1 Mediate Apoptotic Effects of Apigenin AND Rutin in ERï¡+-Breast Cancer MCF-7 Cells. *J Teknologi* (2018) 80(1). doi: 10.11113/jt.v80.10704
345. Lee SH, Ryu JK, Lee K-Y, Woo SM, Park JK, Yoo JW, et al. Enhanced Anti-Tumor Effect of Combination Therapy With Gemcitabine and Apigenin in Pancreatic Cancer. *Cancer Lett* (2008) 259(1):39–49. doi: 10.1016/j.canlet.2007.09.015
346. Strouch MJ, Milam BM, Melstrom LG, McGill JJ, Salabat MR, Ujiki MB, et al. The Flavonoid Apigenin Potentiates the Growth Inhibitory Effects of Gemcitabine and Abrogates Gemcitabine Resistance in Human Pancreatic Cancer Cells. *Pancreas* (2009) 38(4):409–15. doi: 10.1097/MPA.0b013e318193a074
347. Ayyildiz A, Koc H, Turkekul K, Erdogan S. Co-Administration of Apigenin With Doxorubicin Enhances Anti-Migration and Antiproliferative Effects *via* PI3K/PTEN/AKT Pathway in Prostate Cancer Cells. *Exp Oncol* (2021) 43 (2):125–34. doi: 10.32471/exp-oncology.2312-8852
348. Erdogan S, Turkekul K, Serttas R, Erdogan Z. The Natural Flavonoid Apigenin Sensitizes Human CD44+ Prostate Cancer Stem Cells to Cisplatin Therapy. *Biomed Pharmacother* (2017) 88:210–7. doi: 10.1016/j.biopha.2017.01.056
349. Liu M, Fu M, Yang X, Jia G, Shi X, Ji J, et al. Paclitaxel and Quercetin Co-Loaded Functional Mesoporous Silica Nanoparticles Overcoming Multidrug Resistance in Breast Cancer. *Colloids Surf B Biointerf* (2020) 196:111284. doi: 10.1016/j.colsurfb.2020.111284
350. Zhang X, Huang J, Yu C, Xiang L, Li L, Shi D, et al. Quercetin Enhanced Paclitaxel Therapeutic Effects Towards PC-3 Prostate Cancer Through ER Stress Induction and ROS Production. *OncoTargets Ther* (2020) 13:513. doi: 10.2147/OTT.S228453
351. Tan XH, Zhang KK, Xu JT, Qu D, Chen LJ, Li JH, et al. Luteolin Alle*via*tes Methamphetamine-Induced Neurotoxicity by Suppressing PI3K/Akt Pathway-Modulated Apoptosis and Autophagy in Rats. *Food Chem Toxicol* (2020) 137. doi: 10.1016/j.fct.2020.111179
352. Li X, Guo S, Xiong XK, Peng BY, Huang JM, Chen MF, et al. Combination of Quercetin and Cisplatin Enhances Apoptosis in OSCC Cells by Downregulating xIAP Through the NF-κb Pathway. *J Cancer* (2019) 10 (19):4509–21. doi: 10.7150/jca.31045

353. Oršolić N, Odeh D, Jembrek MJ, Knežević J, Kučan D. Interactions Between Cisplatin and Quercetin at Physiological and Hyperthermic Conditions on Cancer Cells *In Vitro* and *In Vivo*. *Molecules* (2020) 25(14):3271. doi: 10.3390/molecules25143271
354. Han Y, Yu H, Wang J, Ren Y, Su X, Shi Y. Quercetin Alle*via*tes Myocyte Toxic and Sensitizes Anti-Leukemic Effect of Adriamycin. *Hematol (Amsterdam Netherlands)* (2015) 20(5):276–83. doi: 10.1179/1607845414Y.0000000198
355. Liu Z-j, Xu W, Han J, Liu Q-Y, Gao L-F, Wang X-H, et al. Quercetin Induces Apoptosis and Enhances Gemcitabine Therapeutic Efficacy Against Gemcitabine-Resistant Cancer Cells. *Anti-Cancer Drugs* (2020) 31(7):684–92. doi: 10.1097/CAD.0000000000000933
356. Singh M, Bhatnagar P, Mishra S, Kumar P, Shukla Y, Gupta KC. PLGA-Encapsulated Tea Polyphenols Enhance the Chemotherapeutic Efficacy of Cisplatin Against Human Cancer Cells and Mice Bearing Ehrlich Ascites Carcinoma. *Int J Nanomed* (2015) 10:6789–809. doi: 10.2147/ijn.s79489
357. Zhou Y, Tang J, Du Y, Ding J, Liu J-Y. The Green Tea Polyphenol EGCG Potentiates the Antiproliferative Activity of Sunitinib in Human Cancer Cells. *Tumor Biol* (2016) 37(7):8555–66. doi: 10.1007/s13277-015-4719-x
358. Wu W, Dong J, Gou H, Geng R, Yang X, Chen D, et al. EGCG Synergizes the Therapeutic Effect of Irinotecan Through Enhanced DNA Damage in Human Colorectal Cancer Cells. *J Cell Mol Med* (2021). doi: 10.1111/jcmm.16718
359. Luo K-W, Zhu X-H, Zhao T, Zhong J, Gao H-C, Luo X-L, et al. EGCG Enhanced the Anti-Tumor Effect of Doxorubicine in Bladder Cancer *via* NF-κb/MDM2/p53 Pathway. *Front Cell Dev Biol* (2020) 8. doi: 10.3389/fcell.2020.606123
360. Wei R, Cortez Penso NE, Hackman RM, Wang Y, Mackenzie GG. Epigallocatechin-3-Gallate (EGCG) Suppresses Pancreatic Cancer Cell Growth, Invasion, and Migration Partly Through the Inhibition of Akt Pathway and Epithelial–Mesenchymal Transition: Enhanced Efficacy When Combined With Gemcitabine. *Nutrients* (2019) 11(8):1856. doi: 10.3390/nu11081856
361. Wang X, Jiang P, Wang P, Yang CS, Wang X, Feng Q. EGCG Enhances Cisplatin Sensitivity by Regulating Expression of the Copper and Cisplatin Influx Transporter CTR1 in Ovary Cancer. *PloS One* (2015) 10(4):e0125402. doi: 10.1371/journal.pone.0125402
362. Tajaldini M, Samadi F, Khosravi A, Ghasemnejad A, Asadi J. Protective and Anticancer Effects of Orange Peel Extract and Naringin in Doxorubicin Treated Esophageal Cancer Stem Cell Xenograft Tumor Mouse Model. *Biomed Pharmacother* (2020) 121:109594. doi: 10.1016/j.biopha.2019.109594
363. Erdogan S, Doganlar O, Doganlar ZB, Turkekul K. Naringin Sensitizes Human Prostate Cancer Cells to Paclitaxel Therapy. *Prostate Int* (2018) 6(4):126–35. doi: 10.1016/j.prnil.2017.11.001
364. Yin Z, Chen E, Cai X, Gong E, Li Y, Xu C, et al. Baicalin Attenuates XRCC1-Mediated DNA Repair to Enhance the Sensitivity of Lung Cancer Cells to Cisplatin. *J Recept Signal Transduct* (2021), 1–10. doi: 10.1080/10799893.2021.1892132
365. Lin M-Y, Cheng W-T, Cheng H-C, Chou W-C, Chen H-I, Ou H-C, et al. Baicalin Enhances Chemosensitivity to Doxorubicin in Breast Cancer Cells *via* Upregulation of Oxidative Stress-Mediated Mitochondria-Dependent Apoptosis. *Antioxidants* (2021) 10(10):1506. doi: 10.3390/antiox10101506
366. Yao X, Zhu F, Zhao Z, Liu C, Luo L, Yin Z. Arctigenin Enhances Chemosensitivity of Cancer Cells to Cisplatin Through Inhibition of the STAT3 Signaling Pathway. *J Cell Biochem* (2011) 112(10):2837–49. doi: 10.1002/jcb.23198
367. Wang HQ, Jin JJ, Wang J. Arctigenin Enhances Chemosensitivity to Cisplatin in Human Nonsmall Lung Cancer H460 Cells Through Downregulation of Survivin Expression. *J Biochem Mol Toxicol* (2014) 28(1):39–45. doi: 10.1002/jbt.21533
368. Wang Y, Lina L, Xu L, Yang Z, Qian Z, Zhou J, et al. Arctigenin Enhances the Sensitivity of Cisplatin Resistant Colorectal Cancer Cell by Activating Autophagy. *Biochem Biophys Res Commun* (2019) 520(1):20–6. doi: 10.1016/j.bbrc.2019.09.086
369. Brechbuhl HM, Kachadourian R, Min E, Chan D, Day BJ. Chrysin Enhances Doxorubicin-Induced Cytotoxicity in Human Lung Epithelial Cancer Cell Lines: The Role of Glutathione. *Toxicol Appl Pharmacol* (2012) 258(1):1–9. doi: 10.1016/j.taap.2011.08.004
370. Bieg D, Sypniewski D, Nowak E, Bednarek I. Morin Decreases Galectin-3 Expression and Sensitizes Ovarian Cancer Cells to Cisplatin. *Arch Gynecol Obstetr* (2018) 298(6):1181–94. doi: 10.1007/s00404-018-4912-4
371. Mannal P, McDonald D, McFadden D. Pterostilbene and Tamoxifen Show an Additive Effect Against Breast Cancer *In Vitro*. *Am J Surg* (2010) 200(5):577–80. doi: 10.1016/j.amjsurg.2010.07.022
372. Hu Z, Zeng Q, Zhang B, Liu H, Wang W. Promotion of P53 Expression and Reactive Oxidative Stress Production is Involved in Zerumbone-Induced Cisplatin Sensitization of Non-Small Cell Lung Cancer Cells. *Biochimie* (2014) 107:257–62. doi: 10.1016/j.biochi.2014.09.001
373. Jorvig JE, Chakraborty A. Zerumbone Inhibits Growth of Hormone Refractory Prostate Cancer Cells by Inhibiting JAK2/STAT3 Pathway and Increases Paclitaxel Sensitivity. *Anti-Cancer Drugs* (2015) 26(2):160–6. doi: 10.1097/CAD.0000000000000171
374. Zhou J, Ong C-N, Hur G-M, Shen H-M. Inhibition of the JAK-STAT3 Pathway by Andrographolide Enhances Chemosensitivity of Cancer Cells to Doxorubicin. *Biochem Pharmacol* (2010) 79(9):1242–50. doi: 10.1016/j.bcp.2009.12.014
375. Kang X, Zheng Z, Liu Z, Wang H, Zhao Y, Zhang W, et al. Liposomal Codelivery of Doxorubicin and Andrographolide Inhibits Breast Cancer Growth and Metastasis. *Mol Pharm* (2018) 15(4):1618–26. doi: 10.1021/acs.molpharmaceut.7b01164
376. Bao G-Q, Shen B-Y, Pan C-P, Zhang Y-J, Shi M-M, Peng C-H. Andrographolide Causes Apoptosis *via* Inactivation of STAT3 and Akt and Potentiates Antitumor Activity of Gemcitabine in Pancreatic Cancer. *Toxicol Lett* (2013) 222(1):23–35. doi: 10.1016/j.toxlet.2013.06.241
377. Yuwen D, Mi S, Ma Y, Guo W, Xu Q, Shen Y, et al. Andrographolide Enhances Cisplatin-Mediated Anticancer Effects in Lung Cancer Cells Through Blockade of Autophagy. *Anti-Cancer Drugs* (2017) 28(9):967–76. doi: 10.1097/CAD.0000000000000537
378. Wen L, Tian-Cong W, Dong-Mei H, Yue H, Ting F, Wen-Jie G, et al. Carnosic Acid Enhances the Anti-Lung Cancer Effect of Cisplatin by Inhibiting Myeloid-Derived Suppressor Cells. *Chin J Natural Medicines* (2018) 16(12):907–15. doi: 10.1016/S1875-5364(18)30132-8
379. Han N-n, Zhou Q, Huang Q, Liu K-J. Carnosic Acid Cooperates With Tamoxifen to Induce Apoptosis Associated With Caspase-3 Activation in Breast Cancer Cells *In Vitro* and *In Vivo*. *Biomed Pharmacother* (2017) 89:827–37. doi: 10.1016/j.biopha.2017.01.084
380. Li C-J, Chu C-Y, Huang L-H, Wang M-H, Sheu L-F, Yeh J-I, et al. Synergistic Anticancer Activity of Triptolide Combined With Cisplatin Enhances Apoptosis in Gastric Cancer *In Vitro* and *In Vivo*. *Cancer Lett* (2012) 319(2):203–13. doi: 10.1016/j.canlet.2012.01.006
381. Ho J-N, Byun S-S, Lee S, Oh JJ, Hong SK, Lee SE, et al. Synergistic Antitumor Effect of Triptolide and Cisplatin in Cisplatin Resistant Human Bladder Cancer Cells. *J Urol* (2015) 193(3):1016–22. doi: 10.1016/j.juro.2014.09.007
382. Zhang Z, Sun C, Zhang L, Chi X, Ji J, Gao X, et al. Triptolide Interferes With XRCC1/PARP1-Mediated DNA Repair and Confers Sensitization of Triple-Negative Breast Cancer Cells to Cisplatin. *Biomed Pharmacother* (2019) 109:1541–6. doi: 10.1016/j.biopha.2018.11.008
383. Liu J, Cheng H, Le Han ZQ, Zhang X, Gao W, Zhao K, et al. Synergistic Combination Therapy of Lung Cancer Using Paclitaxel-and Triptolide-Coloaded Lipid–Polymer Hybrid Nanoparticles. *Drug Des Dev Ther* (2018) 12:3199. doi: 10.2147/DDDT.S172199
384. Yang SW, Wang W, Xie XY, Zhu WP, Li FQ. *In Vitro* Synergistic Cytotoxic Effect of Triptolide Combined With Hydroxycamptothecin on Pancreatic Cancer Cells. *Am J Chin Med* (2011) 39(1):121–34. doi: 10.1142/S0192415X11008695
385. Cheng W, Xiang W, Wang S, Xu K. Tanshinone IIA Ameliorates Oxaliplatin-Induced Neurotoxicity *via* Mitochondrial Protection and Autophagy Promotion. *Am J Transl Res* (2019) 11(5):3140–9.
386. Yang Y, Zhang L-J, Bai X-G, Xu H-J, Jin Z-L, Ding M. Synergistic Antitumour Effects of Triptolide Plus Gemcitabine in Bladder Cancer. *Biomed Pharmacother* (2018) 106:1307–16. doi: 10.1016/j.biopha.2018.07.083
387. Deng Y, Li F, He P, Yang Y, Yang J, Zhang Y, et al. Triptolide Sensitizes Breast Cancer Cells to Doxorubicin Through the DNA Damage Response Inhibition. *Mol Carcinog* (2018) 57(6):807–14. doi: 10.1002/mc.22795
388. Li J, Liang X, Yang X. Ursolic Acid Inhibits Growth and Induces Apoptosis in Gemcitabine-Resistant Human Pancreatic Cancer *via* the JNK and PI3K/

Akt/NF-κb Pathways. *Oncol Rep* (2012) 28(2):501–10. doi: 10.3892/or.2012.1827

389. Prasad S, Yadav VR, Sung B, Gupta SC, Tyagi AK, Aggarwal BB. Ursolic Acid Inhibits the Growth of Human Pancreatic Cancer and Enhances the Antitumor Potential of Gemcitabine in an Orthotopic Mouse Model Through Suppression of the Inflammatory Microenvironment. *Oncotarget* (2016) 7(11):13182. doi: 10.18632/oncotarget.7537
390. Shan J, Xuan Y, Zhang Q, Zhu C, Liu Z, Zhang S. Ursolic Acid Synergistically Enhances the Therapeutic Effects of Oxaliplatin in Colorectal Cancer. *Protein Cell* (2016) 7(8):571–85. doi: 10.1007/s13238-016-0295-0
391. Li L, Hou Y, Yu J, Lu Y, Chang L, Jiang M, et al. Synergism of Ursolic Acid and Cisplatin Promotes Apoptosis and Enhances Growth Inhibition of Cervical Cancer Cells *via* Suppressing NF-κb P65. *Oncotarget* (2017) 8 (57):97416. doi: 10.18632/oncotarget.22133
392. Liu D-L, Bu H-Q, Jin H-M, Zhao J-F, Li Y, Huang H. Enhancement of the Effects of Gemcitabine Against Pancreatic Cancer by Oridonin *via* the Mitochondrial Caspase-Dependent Signaling Pathway. *Mol Med Rep* (2014) 10(6):3027–34. doi: 10.3892/mmr.2014.2584
393. Ma S, Tan W, Du B, Liu W, Li W, Che D, et al. Oridonin Effectively Reverses Cisplatin Drug Resistance in Human Ovarian Cancer Cells *via* Induction of Cell Apoptosis and Inhibition of Matrix Metalloproteinase Expression. *Mol Med Rep* (2016) 13(4):3342–8. doi: 10.3892/mmr.2016.4897
394. Li J, Wu Y, Wang D, Zou L, Fu C, Zhang J, et al. Oridonin Synergistically Enhances the Anti-Tumor Efficacy of Doxorubicin Against Aggressive Breast Cancer *via* Pro-Apoptotic and Anti-Angiogenic Effects. *Pharmacol Res* (2019) 146:104313. doi: 10.1016/j.phrs.2019.104313
395. Fan X, Wang T, Ji Z, Li Q, Shen H, Wang J. Synergistic Combination Therapy of Lung Cancer Using Lipid-Layered Cisplatin and Oridonin Co-Encapsulated Nanoparticles. *Biomed Pharmacother* (2021) 141:111830. doi: 10.1016/j.biopha.2021.111830
396. Yuan Z, Jiang H, Zhu X, Liu X, Li J. Ginsenoside Rg3 Promotes Cytotoxicity of Paclitaxel Through Inhibiting NF-κb Signaling and Regulating Bax/Bcl-2 Expression on Triple-Negative Breast Cancer. *Biomed Pharmacother* (2017) 89:227–32. doi: 10.1016/j.biopha.2017.02.038
397. Jiang Z, Yang Y, Yang Y, Zhang Y, Yue Z, Pan Z, et al. Ginsenoside Rg3 Attenuates Cisplatin Resistance in Lung Cancer by Downregulating PD-L1 and Resuming Immune. *Biomed Pharmacother* (2017) 96:378–83. doi: 10.1016/j.biopha.2017.09.129
398. Wang J, Tian L, Khan MN, Zhang L, Chen Q, Zhao Y, et al. Ginsenoside Rg3 Sensitizes Hypoxic Lung Cancer Cells to Cisplatin *via* Blocking of NF-κb Mediated Epithelial–Mesenchymal Transition and Stemness. *Cancer Lett* (2018) 415:73–85. doi: 10.1016/j.canlet.2017.11.037
399. Dai Y, Wang W, Sun Q, Tuohayi J. Ginsenoside Rg3 Promotes the Antitumor Activity of Gefitinib in Lung Cancer Cell Lines. *Exp Ther Med* (2019) 17(1):953–9. doi: 10.3892/etm.2018.7001
400. Zheng K, Li Y, Wang S, Wang X, Liao C, Hu X, et al. Inhibition of Autophagosome-Lysosome Fusion by Ginsenoside Ro *via* the ESR2-NCF1-ROS Pathway Sensitizes Esophageal Cancer Cells to 5-Fluorouracil-Induced Cell Death *via* the CHEK1-Mediated DNA Damage Checkpoint. *Autophagy* (2016) 12(9):1593–613. doi: 10.1080/15548627.2016.1192751
401. Kim SM, Lee SY, Yuk DY, Moon DC, Choi SS, Kim Y, et al. Inhibition of NF-κb by Ginsenoside Rg3 Enhances the Susceptibility of Colon Cancer Cells to Docetaxel. *Arch Pharm Res* (2009) 32(5):755–65. doi: 10.1007/s12272-009-1515-4
402. Kim SM, Lee SY, Cho JS, Son SM, Choi SS, Yun YP, et al. Combination of Ginsenoside Rg3 With Docetaxel Enhances the Susceptibility of Prostate Cancer Cells *via* Inhibition of NF-κb. *Eur J Pharmacol* (2010) 631(1-3):1–9. doi: 10.1016/j.ejphar.2009.12.018
403. Aktepe OH, Şahin TK, Güner G, Arik Z, Yalçin Ş. Lycopene Sensitizes the Cervical Cancer Cells to Cisplatin *via* Targeting Nuclear Factorkappa B (NF-?B) Pathway. *Turk J Med Sci* (2021) 51(1):368–74. doi: 10.3906/sag-2005-413
404. Zhu T, Li L-L, Xiao G-F, Luo Q-Z, Liu Q-Z, Yao K-T, et al. Berberine Increases Doxorubicin Sensitivity by Suppressing STAT3 in Lung Cancer. *Am J Chin Med* (2015) 43(07):1487–502. doi: 10.1142/S0192415X15500846
405. Ebeid SA, Abd El Moneim NA, Ghoneim H.E.-D.M., El-Benhawy SA, Ismail SE. Combination of Doxorubicin and Berberine Generated Synergistic Anticancer Effect on Breast Cancer Cells Through Down-Regulation of Nanog and miRNA-21 Gene Expression. *Middle East J Cancer* (2020) 11 (3):273–85.
406. Zheng X, Zhao Y, Jia Y, Shao D, Zhang F, Sun M, et al. Biomimetic Co-Assembled Nanodrug of Doxorubicin and Berberine Suppresses Chemotherapy-Exacerbated Breast Cancer Metastasis. *Biomaterials* (2021) 271. doi: 10.1016/j.biomaterials.2021.120716
407. Chen Q, Qin R, Fang Y, Li H. Berberine Sensitizes Human Ovarian Cancer Cells to Cisplatin Through miR-93/PTEN/Akt Signaling Pathway. *Cell Physiol Biochem* (2015) 36(3):956–65. doi: 10.1159/000430270
408. Zhao Y, Jing Z, Li Y, Mao W. Berberine in Combination With Cisplatin Suppresses Breast Cancer Cell Growth Through Induction of DNA Breaks and Caspase-3-Dependent Apoptosis. *Oncol Rep* (2016) 36(1):567–72. doi: 10.3892/or.2016.4785
409. Yu M, Tong X, Qi B, Qu H, Dong S, Yu B, et al. Berberine Enhances Chemosensitivity to Irinotecan in Colon Cancer *via* Inhibition of NF-κb. *Mol Med Rep* (2014) 9(1):249–54. doi: 10.3892/mmr.2013.1762
410. Roh J-L, Kim EH, Park JY, Kim JW, Kwon M, Lee B-H. Piperlongumine Selectively Kills Cancer Cells and Increases Cisplatin Antitumor Activity in Head and Neck Cancer. *Oncotarget* (2014) 5(19):9227. doi: 10.18632/oncotarget.2402
411. Wang Y, Wu X, Zhou Y, Jiang H, Pan S, Sun B. Piperlongumine Suppresses Growth and Sensitizes Pancreatic Tumors to Gemcitabine in a Xenograft Mouse Model by Modulating the NF-Kappa B Pathway. *Cancer Prev Res* (2016) 9(3):234–44. doi: 10.1158/1940-6207.CAPR-15-0306
412. Chen D, Ma Y, Li P, Liu M, Fang Y, Zhang J, et al. Piperlongumine Induces Apoptosis and Synergizes With Doxorubicin by Inhibiting the JAK2-STAT3 Pathway in Triple-Negative Breast Cancer. *Molecules* (2019) 24(12):2338. doi: 10.3390/molecules24122338
413. Chen W, Lian W, Yuan Y, Li M. The Synergistic Effects of Oxaliplatin and Piperlongumine on Colorectal Cancer are Mediated by Oxidative Stress. *Cell Death Dis* (2019) 10(8):1–12. doi: 10.1038/s41419-019-1824-6
414. Zhang P, Shi L, Zhang T, Hong L, He W, Cao P, et al. Piperlongumine Potentiates the Antitumor Efficacy of Oxaliplatin Through ROS Induction in Gastric Cancer Cells. *Cell Oncol* (2019) 42(6):847–60. doi: 10.1007/s13402-019-00471-x
415. Rawat L, Hegde H, Hoti SL, Nayak V. Piperlongumine Induces ROS Mediated Cell Death and Synergizes Paclitaxel in Human Intestinal Cancer Cells. *Biomed Pharmacother* (2020) 128:110243. doi: 10.1016/j.biopha.2020.110243
416. Sun K, Tang XH, Xie YK. Paclitaxel Combined With Harmine Inhibits the Migration and Invasion of Gastric Cancer Cells Through Downregulation of Cyclooxygenase−2 Expression. *Oncol Lett* (2015) 10(3):1649–54. doi: 10.3892/ol.2015.3425
417. Yu XJ, Sun K, Tang XH, Zhou CJ, Sun H, Yan Z, et al. Harmine Combined With Paclitaxel Inhibits Tumor Proliferation and Induces Apoptosis Through Down-Regulation of Cyclooxygenase-2 Expression in Gastric Cancer. *Oncol Lett* (2016) 12(2):983–8. doi: 10.3892/ol.2016.4696
418. Wu L-W, Zhang J-K, Rao M, Zhang Z-Y, Zhu H-J, Zhang C. Harmine Suppresses the Proliferation of Pancreatic Cancer Cells and Sensitizes Pancreatic Cancer to Gemcitabine Treatment. *OncoTargets Ther* (2019) 12:4585. doi: 10.2147/OTT.S205097
419. Duan L, Deng L, Wang D, Ma S, Li C, Zhao D. Treatment Mechanism of Matrine in Combination With Irinotecan for Colon Cancer. *Oncol Lett* (2017) 14(2):2300–4. doi: 10.3892/ol.2017.6407
420. Liao X-Z, Tao L-T, Liu J-H, Gu Y-Y, Xie J, Chen Y, et al. Matrine Combined With Cisplatin Synergistically Inhibited Urothelial Bladder Cancer Cells *via* Down-Regulating VEGF/PI3K/Akt Signaling Pathway. *Cancer Cell Int* (2017) 17(1):1–14. doi: 10.1186/s12935-017-0495-6
421. Hu G, Cao C, Deng Z, Li J, Zhou X, Huang Z, et al. Effects of Matrine in Combination With Cisplatin on Liver Cancer. *Oncol Lett* (2021) 21(1):1–1. doi: 10.3892/ol.2020.12327
422. Yang A, Zhu J, Xu F, Yang J, Wang Y, Wei M, et al. Anticancer Effect of a Combination of Cisplatin and Matrine on Cervical Cancer U14 Cells and U14 Tumor-Bearing Mice, and Possible Mechanism of Action Involved. *Trop J Pharm Res* (2021) 20(8):1631–8.
423. Zhu L, Huang S, Li J, Chen J, Yao Y, Li L, et al. Sophoridine Inhibits Lung Cancer Cell Growth and Enhances Cisplatin Sensitivity Through Activation

of the P53 and Hippo Signaling Pathways. *Gene* (2020) 742:144556. doi: 10.1016/j.gene.2020.144556
424. Kaminski BM, Weigert A, Brüne B, Schumacher M, Wenzel U, Steinhilber D, et al. Sulforaphane Potentiates Oxaliplatin-Induced Cell Growth Inhibition in Colorectal Cancer Cells *via* Induction of Different Modes of Cell Death. *Cancer Chemother Pharmacol* (2011) 67(5):1167–78. doi: 10.1007/s00280-010-1413-y
425. Kim SH, Park HJ, Moon DO. Sulforaphane Sensitizes Human Breast Cancer Cells to Paclitaxel–Induced Apoptosis by Downregulating the NF–κb Signaling Pathway. *Oncol Lett* (2017) 13(6):4427–32. doi: 10.3892/ol.2017.5950
426. Wang F, Wang W, Li J, Zhang J, Wang X, Wang M. Sulforaphane Reverses Gefitinib Tolerance in Human Lung Cancer Cells *via* Modulation of Sonic Hedgehog Signaling. *Oncol Lett* (2018) 15(1):109–14. doi: 10.3892/ol.2017.7293
427. Justin S, Rutz J, Maxeiner S, Chun FK-H, Juengel E, Blaheta RA. Chronic Sulforaphane Administration Inhibits Resistance to the mTOR-Inhibitor Everolimus in Bladder Cancer Cells. *Int J Mol Sci* (2020) 21(11):4026. doi: 10.3390/ijms21114026
428. Liu F, Lv R-B, Liu Y, Hao Q, Liu S-J, Zheng Y-Y, et al. Salinomycin and Sulforaphane Exerted Synergistic Antiproliferative and Proapoptotic Effects on Colorectal Cancer Cells by Inhibiting the PI3K/Akt Signaling Pathway *In Vitro* and *In Vivo*. *OncoTargets Ther* (2020) 13:4957. doi: 10.2147/OTT.S246706
429. Wang Y, Zhou Y, Jia G, Han B, Liu J, Teng Y, et al. Shikonin Suppresses Tumor Growth and Synergizes With Gemcitabine in a Pancreatic Cancer Xenograft Model: Involvement of NF-κb Signaling Pathway. *Biochem Pharmacol* (2014) 88(3):322–33. doi: 10.1016/j.bcp.2014.01.041
430. Tang J-c, Ren Y-G, Zhao J, Long F, Chen J-Y, Jiang Z. Shikonin Enhances Sensitization of Gefitinib Against Wild-Type EGFR Non-Small Cell Lung Cancer *via* Inhibition PKM2/stat3/cyclinD1 Signal Pathway. *Life Sci* (2018) 204:71–7. doi: 10.1016/j.lfs.2018.05.012
431. Du W, Hao X, Yuan Z, Wang Y, Zhang X, Liu J. Shikonin Potentiates Paclitaxel Antitumor Efficacy in Esophageal Cancer Cells *via* the Apoptotic Pathway. *Oncol Lett* (2019) 18(3):3195–201. doi: 10.3892/ol.2019.10662
432. Lin H-Y, Han H-W, Wang Y-S, He D-L, Sun W-X, Feng L, et al. Shikonin and 4-Hydroxytamoxifen Synergistically Inhibit the Proliferation of Breast Cancer Cells Through Activating Apoptosis Signaling Pathway *In Vitro* and *In Vivo*. *Chin Med* (2020) 15(1):1–14. doi: 10.1186/s13020-020-00305-1
433. Liu K, Cang S, Ma Y, Chiao JW. Synergistic Effect of Paclitaxel and Epigenetic Agent Phenethyl Isothiocyanate on Growth Inhibition, Cell Cycle Arrest and Apoptosis in Breast Cancer Cells. *Cancer Cell Int* (2013) 13(1):1–8. doi: 10.1186/1475-2867-13-10
434. Cang S, Ma Y, Chiao J-W, Liu D. Phenethyl Isothiocyanate and Paclitaxel Synergistically Enhanced Apoptosis and Alpha-Tubulin Hyperacetylation in Breast Cancer Cells. *Exp Hematol Oncol* (2014) 3(1):1–6. doi: 10.1186/2162-3619-3-5
435. Choudhury B, Kandimalla R, Elancheran R, Bharali R, Kotoky J. Garcinia Morella Fruit, a Promising Source of Antioxidant and Anti-Inflammatory Agents Induces Breast Cancer Cell Death *via* Triggering Apoptotic Pathway. *Biomed Pharmacother* (2018) 103:562–73. doi: 10.1016/j.biopha.2018.04.068
436. Li F, Shanmugam MK, Siveen KS, Wang F, Ong TH, Loo SY, et al. Garcinol Sensitizes Human Head and Neck Carcinoma to Cisplatin in a Xenograft Mouse Model Despite Downregulation of Proliferative Biomarkers. *Oncotarget* (2015) 6(7):5147–63. doi: 10.18632/oncotarget.2881
437. Zhang J, Fang H, Zhang J, Guan W, Xu G. Garcinol Alone and in Combination With Cisplatin Affect Cellular Behavior and PI3K/AKT Protein Phosphorylation in Human Ovarian Cancer Cells. *Dose-Response* (2020) 18(2). doi: 10.1177/1559325820926732
438. Tu SH, Chiou YS, Kalyanam N, Ho CT, Chen LC, Pan MH. Garcinol Sensitizes Breast Cancer Cells to Taxol Through the Suppression of Caspase-3/Ipla2 and NF-κb/Twist1 Signaling Pathways in a Mouse 4T1 Breast Tumor Model. *Food Funct* (2017) 8(3):1067–79. doi: 10.1039/c6fo01588c
439. Chandimali N, Huynh DL, Jin WY, Kwon T. Combination Effects of Hispidin and Gemcitabine *via* Inhibition of Stemness in Pancreatic Cancer Stem Cells. *Anticancer Res* (2018) 38(7):3967–75. doi: 10.21873/anticanres.12683
440. Zhang B, Shi ZL, Liu B, Yan XB, Feng J, Tao HM. Enhanced Anticancer Effect of Gemcitabine by Genistein in Osteosarcoma: The Role of Akt and Nuclear Factor-κb. *Anti-Cancer Drugs* (2010) 21(3):288–96. doi: 10.1097/CAD.0b013e328334da17
441. Liang C, Li H, Shen C, Lai J, Shi Z, Liu B, et al. Genistein Potentiates the Anti-Cancer Effects of Gemcitabine in Human Osteosarcoma *via* the Downregulation of Akt and Nuclear Factor-κb Pathway. *Anticancer Agents Med Chem* (2012) 12(5):554–63. doi: 10.2174/187152012800617867
442. Ahn DW, Seo JK, Lee SH, Hwang JH, Lee JK, Ryu JK, et al. Enhanced Antitumor Effect of Combination Therapy With Gemcitabine and Guggulsterone in Pancreatic Cancer. *Pancreas* (2012) 41(7):1048–57. doi: 10.1097/MPA.0b013e318249d62e
443. Lou C, Lu H, Ma Z, Liu C, Zhang Y. Ginkgolide B Enhances Gemcitabine Sensitivity in Pancreatic Cancer Cell Lines *via* Inhibiting PAFR/NF-Kb Pathway. *Biomed Pharmacother* (2019) 109:563–72. doi: 10.1016/j.biopha.2018.10.084
444. Zhang DC, Liu JL, Ding YB, Xia JG, Chen GY. Icariin Potentiates the Antitumor Activity of Gemcitabine in Gallbladder Cancer by Suppressing NF-κb. *Acta Pharmacol Sin* (2013) 34(2):301–8. doi: 10.1038/aps.2012.162
445. Kunnumakkara AB, Sung B, Ravindran J, Diagaradjane P, Deorukhkar A, Dey S, et al. Zyflamend Suppresses Growth and Sensitizes Human Pancreatic Tumors to Gemcitabine in an Orthotopic Mouse Model Through Modulation of Multiple Targets. *Int J Cancer* (2012) 131(3):E292–303. doi: 10.1002/ijc.26442
446. Arafa ESA, Zhu Q, Barakat BM, Wani G, Zhao Q, El-Mahdy MA, et al. Tangeretin Sensitizes Cisplatin-Resistant Human Ovarian Cancer Cells Through Downregulation of Phosphoinositide 3-Kinase/Akt Signaling Pathway. *Cancer Res* (2009) 69(23):8910–7. doi: 10.1158/0008-5472.CAN-09-1543
447. Yu S, Gong LS, Li NF, Pan YF, Zhang L. Galangin (GG) Combined With Cisplatin (DDP) to Suppress Human Lung Cancer by Inhibition of STAT3-Regulated NF-κb and Bcl-2/Bax Signaling Pathways. *Biomed Pharmacother* (2018) 97:213–24. doi: 10.1016/j.biopha.2017.10.059
448. Zhou P, Li Z, Xu D, Wang Y, Bai Q, Feng Y, et al. Cepharanthine Hydrochloride Improves Cisplatin Chemotherapy and Enhances Immunity by Regulating Intestinal Microbes in Mice. *Front Cell Infect Microbiol* (2019) 9:225(JUN). doi: 10.3389/fcimb.2019.00225
449. Wu J, Guan M, Wong PF, Yu H, Dong J, Xu J. Icariside II Potentiates Paclitaxel-Induced Apoptosis in Human Melanoma A375 Cells by Inhibiting TLR4 Signaling Pathway. *Food Chem Toxicol* (2012) 50(9):3019–24. doi: 10.1016/j.fct.2012.06.027
450. Lin CL, Chen RF, Chen JYF, Chu YC, Wang HM, Chou HL, et al. Protective Effect of Caffeic Acid on Paclitaxel Induced Anti-Proliferation and Apoptosis of Lung Cancer Cells Involves NF-κb Pathway. *Int J Mol Sci* (2012) 13(5):6236–45. doi: 10.3390/ijms13056236
451. Liang L, Wu J, Luo J, Wang L, Chen ZX, Han CL, et al. Oxymatrine Reverses 5-Fluorouracil Resistance by Inhibition of Colon Cancer Cell Epithelial-Mesenchymal Transition and NF-κb Signaling *In Vitro*. *Oncol Lett* (2020) 19(1):519–26. doi: 10.3892/ol.2019.11090
452. Xu GY, Tang XJ. Troxerutin (TXN) Potentiated 5-Fluorouracil (5-Fu) Treatment of Human Gastric Cancer Through Suppressing STAT3/NF-κb and Bcl-2 Signaling Pathways. *Biomed Pharmacother* (2017) 92:95–107. doi: 10.1016/j.biopha.2017.04.059
453. Buhrmann C, Kunnumakkara AB, Popper B, Majeed M, Aggarwal BB, Shakibaei M. Calebin a Potentiates the Effect of 5-Fu and Tnf-ß (Lymphotoxin a) Against Human Colorectal Cancer Cells: Potential Role of NF-KB +. *Int J Mol Sci* (2020) 21(7). doi: 10.3390/ijms21072393
454. Fang LJ, Shao XT, Wang S, Lu GH, Xu T, Zhou JY. Sesquiterpene Lactone Parthenolide Markedly Enhances Sensitivity of Human A549 Cells to Low-Dose Oxaliplatin *via* Inhibition of NF-κb Activation and Induction of Apoptosis. *Planta Med* (2010) 76(3):258–64. doi: 10.1055/s-0029-1186083
455. Hahnvajanawong C, Wattanawongdon W, Chomvarin C, Anantachoke N, Kanthawong S, Sripa B, et al. Synergistic Effects of Isomorellin and Forbesione With Doxorubicin on Apoptosis Induction in Human Cholangiocarcinoma Cell Lines. *Cancer Cell Int* (2014) 14(1). doi: 10.1186/1475-2867-14-68
456. Wang LJ, Meng Q, Wang CY, Liu Q, Peng JY, Huo XK, et al. Dioscin Restores the Activity of the Anticancer Agent Adriamycin in Multidrug-Resistant Human Leukemia K562/Adriamycin Cells by Down-Regulating MDR1 *via* a Mechanism Involving NF-Kappa B Signaling Inhibition. *J Natural Prod* (2013) 76(5):909–14. doi: 10.1021/np400071c

457. Lagoa R, Silva J, Rodrigues JR, Bishayee A. Advances in Phytochemical Delivery Systems for Improved Anticancer Activity. *Biotechnol Adv* (2020) 38:107382. doi: 10.1016/j.biotechadv.2019.04.004
458. Bagherian A, Mardani R, Roudi B, Taghizadeh M, Banfshe HR, Ghaderi A, et al. Combination Therapy With Nanomicellar-Curcumin and Temozolomide for *In Vitro* Therapy of Glioblastoma Multiforme *via* Wnt Signaling Pathways. *J Mol Neurosci* (2020) 70(10):1471–83. doi: 10.1007/s12031-020-01639-z
459. Qiu N, Cai LL, Xie D, Wang G, Wu W, Zhang Y, et al. Synthesis, Structural and *In Vitro* Studies of Well-Dispersed Monomethoxy-Poly(Ethylene Glycol)-Honokiol Conjugate Micelles. *BioMed Mater* (2010) 5(6):065006. doi: 10.1088/1748-6041/5/6/065006
460. More MP, Deshmukh PK. Development of Amine-Functionalized Superparamagnetic Iron Oxide Nanoparticles Anchored Graphene Nanosheets as a Possible Theranostic Agent in Cancer Metastasis. *Drug Delivery Transl Res* (2020) 10(4):862–77. doi: 10.1007/s13346-020-00729-0
461. Zafar S, Akhter S, Ahmad I, Hafeez Z, Alam Rizvi MM, Jain GK, et al. Improved Chemotherapeutic Efficacy Against Resistant Human Breast Cancer Cells With Co-Delivery of Docetaxel and Thymoquinone by Chitosan Grafted Lipid Nanocapsules: Formulation Optimization, *In Vitro* and *In Vivo* Studies. *Colloids Surf B Biointerf* (2020) 186:110603. doi: 10.1016/j.colsurfb.2019.110603
462. Wang Y, Yu H, Wang S, Gai C, Cui X, Xu Z, et al. Targeted Delivery of Quercetin by Nanoparticles Based on Chitosan Sensitizing Paclitaxel-Resistant Lung Cancer Cells to Paclitaxel. *Mater Sci Eng C Mater Biol Appl* (2021) 119:111442. doi: 10.1016/j.msec.2020.111442
463. Ghaffari M, Dehghan G, Baradaran B, Zarebkohan A, Mansoori B, Soleymani J, et al. Co-Delivery of Curcumin and Bcl-2 siRNA by PAMAM Dendrimers for Enhancement of the Therapeutic Efficacy in HeLa Cancer Cells. *Colloids Surf B Biointerf* (2020) 188:110762. doi: 10.1016/j.colsurfb.2019.110762
464. Liu A, Wang W, Fang H, Yang Y, Jiang X, Liu S, et al. Baicalein Protects Against Polymicrobial Sepsis-Induced Liver Injury *via* Inhibition of Inflammation and Apoptosis in Mice. *Eur J Pharmacol* (2015) 748:45–53. doi: 10.1016/j.ejphar.2014.12.014
465. Li X, Huang JM, Wang JN, Xiong XK, Yang XF, Zou F. Combination of Chrysin and Cisplatin Promotes the Apoptosis of Hep G2 Cells by Up-Regulating P53. *Chem Biol Interact* (2015) 232:12–20. doi: 10.1016/j.cbi.2015.03.003
466. Meng G, Chai K, Li X, Zhu Y, Huang W. Luteolin Exerts Pro-Apoptotic Effect and Anti-Migration Effects on A549 Lung Adenocarcinoma Cells Through the Activation of MEK/ERK Signaling Pathway. *Chem Biol Interact* (2016) 257:26–34. doi: 10.1016/j.cbi.2016.07.028
467. Majumdar D, Jung KH, Zhang H, Nannapaneni S, Wang X, Amin AR, et al. Luteolin Nanoparticle in Chemoprevention: *In Vitro* and *In Vivo* Anticancer Activity. *Cancer Prev Res (Phila)* (2014) 7(1):65–73. doi: 10.1158/1940-6207.capr-13-0230
468. Varshosaz J, Jandaghian S, Mirian M, Sajjadi SE. Co-Delivery of Rituximab Targeted Curcumin and Imatinib Nanostructured Lipid Carriers in Non-Hodgkin Lymphoma Cells. *J Liposome Res* (2021) 31(1):64–78. doi: 10.1080/08982104.2020.1720718
469. Dhupal M, Oh JM, Tripathy DR, Kim SK, Koh SB, Park KS. Immunotoxicity of Titanium Dioxide Nanoparticles *via* Simultaneous Induction of Apoptosis and Multiple Toll-Like Receptors Signaling Through ROS-Dependent SAPK/JNK and P38 MAPK Activation. *Int J Nanomed* (2018) 13:6735–50. doi: 10.2147/ijn.s176087
470. Aas Z, Babaei E, Hosseinpour Feizi MA, Dehghan G. Anti-Proliferative and Apoptotic Effects of Dendrosomal Farnesiferol C on Gastric Cancer Cells. *Asian Pac J Cancer Prev* (2015) 16(13):5325–9. doi: 10.7314/apjcp.2015.16.13.5325
471. Ochi MM, Amoabediny G, Rezayat SM, Akbarzadeh A, Ebrahimi B. *In Vitro* Co-Delivery Evaluation of Novel Pegylated Nano-Liposomal Herbal Drugs of Silibinin and Glycyrrhizic Acid (Nano-Phytosome) to Hepatocellular Carcinoma Cells. *Cell J* (2016) 18(2):135–48. doi: 10.22074/cellj.2016.4308
472. Israelsen WJ, Vander Heiden MG. Pyruvate Kinase: Function, Regulation and Role in Cancer. *Semin Cell Dev Biol* (2015) 43:43–51. doi: 10.1016/j.semcdb.2015.08.004
473. Bolger GT, Licollari A, Tan A, Greil R, Vcelar B, Greil-Ressler S, et al. Pharmacokinetics of Liposomal Curcumin (Lipocurc™) Infusion: Effect of Co-Medication in Cancer Patients and Comparison With Healthy Individuals. *Cancer Chemother Pharmacol* (2019) 83(2):265–75. doi: 10.1007/s00280-018-3730-5
474. Gautam M, Thapa RK, Gupta B, Soe ZC, Ou W, Poudel K, et al. Phytosterol-Loaded CD44 Receptor-Targeted PEGylated Nano-Hybrid Phyto-Liposomes for Synergistic Chemotherapy. *Expert Opin Drug Delivery* (2020) 17(3):423–34. doi: 10.1080/17425247.2020.1727442
475. Ahn S, Lee IH, Kang S, Kim D, Choi M, Saw PE, et al. Gold Nanoparticles Displaying Tumor-Associated Self-Antigens as a Potential Vaccine for Cancer Immunotherapy. *Adv Healthc Mater* (2014) 3(8):1194–9. doi: 10.1002/adhm.201300597
476. Cao M, Yan H, Han X, Weng L, Wei Q, Sun X, et al. Ginseng-Derived Nanoparticles Alter Macrophage Polarization to Inhibit Melanoma Growth. *J Immunother Cancer* (2019) 7(1):326. doi: 10.1186/s40425-019-0817-4
477. Thangapazham RL, Puri A, Tele S, Blumenthal R, Maheshwari RK. Evaluation of a Nanotechnology-Based Carrier for Delivery of Curcumin in Prostate Cancer Cells. *Int J Oncol* (2008) 32(5):1119–23. doi: 10.3892/ijo.32.5.1119
478. Ashrafizadeh M, Javanmardi S, Moradi-Ozarlou M, Mohammadinejad R, Farkhondeh T, Samarghandian S, et al. .
479. Lee SW, Kim YM, Cho CH, Kim YT, Kim SM, Hur SY, et al. An Open-Label, Randomized, Parallel, Phase II Trial to Evaluate the Efficacy and Safety of a Cremophor-Free Polymeric Micelle Formulation of Paclitaxel as First-Line Treatment for Ovarian Cancer: A Korean Gynecologic Oncology Group Study (KGOG-3021). *Cancer Res Treat* (2018) 50(1):195–203. doi: 10.4143/crt.2016.376
480. Kooshki L, Mahdavi P, Fakhri S, Akkol EK, Khan H. Targeting Lactate Metabolism and Glycolytic Pathways in the Tumor Microenvironment by Natural Products: A Promising Strategy in Combating Cancer. *BioFactors* (2021). doi: 10.1002/biof.1799
481. Kashyap D, Tuli HS, Yerer MB, Sharma A, Sak K, Srivastava S, et al. Natural Product-Based Nanoformulations for Cancer Therapy: Opportunities and Challenges. *Semin Cancer Biol* (2021) 69:5–23. doi: 10.1016/j.semcancer.2019.08.014
482. Colone M, Calcabrini A, Stringaro A. Drug Delivery Systems of Natural Products in Oncology. *Molecules* (2020) 25(19):4560. doi: 10.3390/molecules25194560
483. Yang M-D, Sun Y, Zhou W-J, Xie X-Z, Zhou Q-M, Lu Y-Y, et al. Resveratrol Enhances Inhibition Effects of Cisplatin on Cell Migration and Invasion and Tumor Growth in Breast Cancer MDA-MB-231 Cell Models *In Vivo* and *In Vitro*. *Molecules* (2021) 26(8):2204. doi: 10.3390/molecules27010220

Conflict of Interest: The authors declare that the research was conducted in the absence of any commercial or financial relationships that could be construed as a potential conflict of interest.

Publisher's Note: All claims expressed in this article are solely those of the authors and do not necessarily represent those of their affiliated organizations, or those of the publisher, the editors and the reviewers. Any product that may be evaluated in this article, or claim that may be made by its manufacturer, is not guaranteed or endorsed by the publisher.

frontiers in Oncology

ORIGINAL RESEARCH
published: 03 March 2022
doi: 10.3389/fonc.2022.839603

α-Hederin Inhibits the Proliferation of Hepatocellular Carcinoma Cells *via* Hippo-Yes-Associated Protein Signaling Pathway

Tongqing Chen†, Dongdong Sun†, Qijuan Wang, Tingting Zhou, Jiani Tan, Changliang Xu, Haibo Cheng and Weixing Shen**

Jiangsu Collaborative Innovation Center of Traditional Chinese Medicine Prevention and Treatment of Tumor, The First Clinical Medical College of Nanjing University of Chinese Medicine, Jiangsu, China

OPEN ACCESS

Edited by:
Nand K. Roy, Case Western Reserve University, United States

Reviewed by:
Qing Ji, Shanghai University of Traditional Chinese Medicine, China
Wenxue Li, Guangzhou Center for Disease Control and Prevention, China

***Correspondence:**
Weixing Shen
weixingshen@njucm.edu.cn
Haibo Cheng
haibocheng@njucm.edu.cn

†These authors have contributed equally to this work

Specialty section:
This article was submitted to Pharmacology of Anti-Cancer Drugs, a section of the journal Frontiers in Oncology

Received: *20 December 2021*
Accepted: *10 February 2022*
Published: *03 March 2022*

Citation:
Chen T, Sun D, Wang Q, Zhou T, Tan J, Xu C, Cheng H and Shen W (2022) α-Hederin Inhibits the Proliferation of Hepatocellular Carcinoma Cells via Hippo-Yes-Associated Protein Signaling Pathway. Front. Oncol. 12:839603. doi: 10.3389/fonc.2022.839603

Aims: Yes-associated protein (YAP), a downstream protein in the Hippo signaling pathway, plays an important role in tumor proliferation, including in hepatocellular carcinoma (HCC). α-hederin, a monodesmosidic triterpenoid saponin isolated from *Fructus akebiae*, displayed anti-cancer effects on several cancer cell lines but the precise mechanism has not been ascertained. In the present study, we explored the effects of α-hederin on cell proliferation and apoptosis in human HCC cell lines and the underlying mechanisms.

Main Method: Cell proliferation and apoptosis were assessed using 5-ethynyl-2'-deoxyuridine staining, colony formation, flow cytometry. The expression patterns of components of Hippo signaling pathway and apoptotic genes were further examined *via* RT-qPCR and immunoblotting. A xenograft tumor model in nude mice was used to evaluate the anti-HCC effects of α-hederin *in vivo*.

Results: α-hederin promoted the apoptosis and inhibited the proliferation of SMMC-7721 and HepG2 cells *in vitro*, and remarkably inhibited the tumor size and weight in the xenograft mouse model. Additionally, α-hederin increased the expression of pro-apoptosis proteins and suppressed the expression of anti-apoptosis proteins. Moreover, α-hederin treatment upregulated the expression of Hippo signaling pathway-related proteins and genes, while, effectively reduced the level of nuclear YAP, which resulted in the inhibition of proliferation and the induction of apoptosis of HCC cells. Finally, the effects of α-hederin on HCC cell proliferation and apoptosis were alleviated by XMU-MP-1, a Mst1/2 inhibitor *in vitro*.

Significance: We identified α-hederin is a novel agonist of Hippo signaling pathway and possesses an anti-HCC efficacy through inhibiting YAP activity.

Keywords: α-hederin, hepatocellular carcinoma (HCC), Hippo signaling pathway, YAP protein, nuclear translocation

INTRODUCTION

Liver cancer is one of the most malignant cancers with poor prognosis which already be the third leading cause of cancer-related death worldwide. Hepatocellular carcinoma (HCC) is the most common type of primary liver cancer, and its incidence and mortality keeps increasing (1). The higher recurrence and metastasis are responsible for the poor outcome (2). Although significant progress achieved from current basic and clinical investigations, our understanding of the tumorigenesis mechanisms in HCC is remained elusive. The complex pathology of HCC has limited the development of effective therapeutic intervention, prompting people to devote understanding of the tumorigenesis mechanisms and the therapeutic strategy discovery, including the search for effective substances in natural small molecule compounds for the treatment of HCC.

Recent studies have revealed that several developmental pathways, such as Hippo/Yes-associated protein (YAP) signaling, contribute to hepatic carcinogenesis (3). The Hippo signaling pathway was originally identified in Drosophila melanogaster and later in mammals (4, 5). It is an evolutionarily-conserved signaling pathway that plays an important role in organ size control, tissue regeneration, as well as tumor suppression (6). The core molecules of Hippo signaling pathway are serine/threonine kinases, mammalian sterile 20-like kinase 1/2 (Mst1/2), and large tumor suppressor 1/2 (Lats1/2), Mst1/2 kinases phosphorylate and activate Lats1/2, which in turn phosphorylates two transcriptional co-activators, YAP and WW domain-containing transcription regulator 1 (TAZ), contributing to their cytoplasmic sequestration and functional suppression (7–10). Moreover, accumulating evidence shows that dysregulation of the Hippo pathway is associated with a broad spectrum of cancers, such as liver cancer (11), breast cancer (12), non-small cell lung cancer (13), colon cancer (14).

α-hederin, an oleanane-type saponin is present in many plants. Several studies have proposed that α-hederin had an anti-cancer activity. For example, it inhibited interleukin 6–induced epithelial–mesenchymal transition in colon cancer cells and induced apoptosis in non-small cell lung cancer by increasing the killing effect of Tax (15, 16). Recently, researchers reported that α-hederin could induce apoptosis of HCC cells *via* the mitochondrial pathway mediated by increased intracellular ROS (17). However, the molecular mechanisms of α-hederin in anti-HCC progression are not fully understood. Based on the pretesting research, we found α-hederin could induce cell death in several hepatoma cells, so we speculate that Hippo signaling pathway might be involved in this mechanism. In the present study, we evaluated the effect of α-hederin on HCC proliferation in vivo and in vitro and explored the underlying molecular mechanism through investigating Hippo-YAP signaling pathway.

MATERIALS AND METHODS

All methods were performed in accordance with the relevant guidelines and regulations of our institution.

Cell Culture and Reagents

The human SMMC-7721, HepG2, and Huh-7 HCC cell lines were purchased from ATCC. The cells were cultured in Dulbecco's Minimum Essential Medium (DMEM) (Gibco, USA) with 10% FBS (Foetal Bovine Serum, BI), 100 U/mL penicillin, and 100 U/mL streptomycin at 37°C in a humidified atmosphere with 5% CO_2. α-hederin was purchased from Chengdu Herbpurify CO., LTD (purity>98%). Dimethyl sulfoxide (DMSO) was used as solvent.

Cell Viability Assay

Cells were seeded at a density of 8×10^3 cells per well in 96-well plate and treated with 0, 2.5, 5, 10, 20, 40, 80 uM of α-hederin for 12 h, 24 h or 48 h followed by incubating with MTT solution for 4 h. The absorbance of each well was measured at 490 nm using the plate reader (TECAN SPARK 10M). Cell proliferation was assessed using MTT according to the manufacturer's protocol (Beyotime, China).

Western Blot

Antibodies: YAP (ab56701, abcam, 1:5000), Lats1 (ab70561, abcam,1:5000), p-YAP (ab62751, abcam,1:1000), Bax (ab32503, abcam,1:5000), Bcl-2 (ab196495, abcam,1:1000), TAZ (ab224239, abcam,1:5000), Caspase-3 (ab13847, abcam,1:500), GAPDH (ImmunoWay, YM3029,1:5000), Mst1 (CST,3682s,1:1000), TEAD1 (ab133533, abcam,1:5000), Cleaved-caspase3 (CST,9664s,1:1000), Phospho-Lats1/Lats2 (PA5-64591, Invitrogen,1:1000), Histone H3 (ImmunoWay, YM3038,1:5000).

Briefly, protein concentrations of tissues or cells were quantified by BCA protein assay kit (Thermo Scientific, Waltham, MA, USA). Sample of proteins (25 μg) were separated by 10% sodium dodecyl sulfate-polyacrylamide gel and transferred to PVDF membrane, then blocked by 5% non-fat milk in PBST buffer (PBS buffer containing 0.05% Triton-100) for 1 h at room temperature. The membranes were incubated overnight with primary antibodies at 4°C, after 3 times washing in PBST buffer, the membranes were incubated with the secondary antibodies for 1 h at room temperature. Signals were detected by using an ECL substrate (Thermo Scientific) and exposure with the Tanon 5500 imaging system. The intensity of the bands was quantified by densitometry.

Immunofluorescence Assays

After drug treatment, cells were gently washed by PBS for three times and fixed with 4% fresh paraformaldehyde-phosphate (BL539A, Biosharp) for 15 min, then permeabilized with 0.5% Triton X-100 in PBS for 10 min at room temperature. After blocking in 10% goat serum and 5% BSA in PBS-T for 30 min, cells were incubated with primary antibody against YAP (1: 100) in 5% BSA overnight at 4°C. After washing three times with PBS-T, cells were incubated with secondary antibodies (1:200 dilution) for 1 h at room temperature. The coverslips were treated with DAPI for 5 min for nuclear staining. An inverted fluorescence microscope (Nikon Eclipse Ti, Nikon, Japan) was used for imaging.

Flow Cytometry Analysis for Cell Cycle and Apoptosis

Apoptosis assay was monitored by flow cytometry. Cells were seeded at a density of 3 $\times 10^{5}$/ml in six-well plates. After attachment, cells were treated with α-hederin at different concentrations for 24 h. Supernatants of the cultures were collected and the attached cells were collected by digestion with pancreatin (S330JV, BasalMedia) followed by centrifugation (2000 rpm, 2min) after washing twice with PBS. Cells were re-suspended in 500 ul of 1×Binding Buffer and incubated with 5 ul of Annexin V-FITC and 5 ul of PI Staining Solution for 15 min. The next steps were followed according to the manufacturer's instructions (Key GEN BioTECH).

For cell cycle analysis, cells were synchronized at the G0/G1 phase by serum starvation for 24 h and then released into cell cycle by re-addition of 10% FBS. After α-hederin treatment at different concentrations for 24 h, cells were collected and fixed in 75% ethanol at −20°C overnight, then re-suspended in precooled PBS for 3 times. Cell cycles were detected by the flow cytometer (Beckman Coulter) at 488 nm excitation wavelength and the data were analyzed with FlowJo/Modfit 5 software.

5-ethynyl-2'-Deoxyuridine Staining

To assess *in vitro* proliferation, the cells were supplemented with fresh medium containing 10 μM EdU and incubated for 2 h at room temperature after α-hederin treatment at different concentrations. Cell nuclei were counterstained with DAPI at room temperature for 10 min. EdU-positive cells were quantified using fluorescence microscopy (Nikon Eclipse Ti, Nikon, Japan).

Colony Formation Assay

Cells were seeded in six-well plates and treated with different concentrations of α-hederin for 24 h. Then, the medium was replaced with α-hederin free medium and continued to incubate for about 14 days. The cells were fixed with 4% paraformaldehyde and stained with Giemsa stain at room temperature. After a final series of rinses and air dry, photographs were taken for colony quantification.

RT- qPCR Analysis

Total RNA was extracted using the Trizol reagent (Invitrogen, Carlsbad, CA) according to the manufacturer instructions. 1 μg of total RNA was reversed transcription to cDNA by using the *Evo M-MLV* RT Mix Kit with gDNA Clean for qPCR (AG11728, ACCURATE BIOTECHNOLOGY, HUNAN, Co.,Ltd). The qPCR was performed using the SYBR Green Premix *Pro Taq* HS qPCR Kit (AG11701, ACCURATE BIOTECHNOLOGY, HUNAN, Co., Ltd). The expression level of individual genes was analyzed by the comparative Ct method ($2^{-\Delta\Delta Ct}$ method) and normalized according to the expression of the housekeeping gene.

Animal Experiments

All animal experiments were approved by our Animal Ethics Committee of Nanjing University of Chinese Medicine (Nanjing, China), and all experiments were performed in accordance with relevant guidelines and regulations. For each mouse, 0.2 ml (2.5×10^{7}/ml) HepG2 cell suspension was injected subcutaneously into the right axillary region of female BALB/c nude mice (6 weeks). All animals were maintained in a pathogen-free and temperature-controlled environment with 12 h light/dark cycle and standard laboratory diet. The animals were randomized into three groups (n=8 per group): control group, α-hederin group (5 mg/kg), and positive group DDP (Cisplatin, 5 mg/kg). Tumor growth was calculated with calipers every three days, and the volume was calculated according to the formula: volume = $(\text{width})^2 \times \text{length}/2$. The body weight of the mice was recorded every three days. At the end of experiments, xenotransplant tumors (three mice per group were chosen randomly to be identified by western blot), livers, mouse blood and kidney were harvested for additional analysis.

Live Animal Imaging

For fluorescence imaging *in vivo*, mice were imaged using an IVIS Spectrum *In Vivo* Imaging System (Caliper Life Sciences). HepG2 cells were transfected with a green fluorescent protein (GFP) vector [Zhongqiao Xinzhou Science and Technology Co. (Shanghai, China)]. Prior to *in-vivo* imaging, the mice were anesthetized with isoflurane. Excitation of fluorophore were performed at 488 nm for GFP. The signals were analyzed with Living Image Software (PerkinElmer).

Hematoxylin-Eosin Staining

The xenograft tumor tissues from different groups of mice were fixed in 4% paraformaldehyde for over 12 h and were embedded in paraffin. Then, the tissues were cut into 4 μm thick sections and stained with hematoxylin and eosin (HE).

Immunohistochemistry Staining

For Immunohistochemistry, paraffin sections were incubated with a blocking solution and then incubated with anti-YAP antibody (Abcam, ab52771) at 4°C overnight. After washing, sections were incubated with biotinylated secondary antibodies at room temperature for 30 min. Sections were visualized with 3, 3'-diaminobenzidine and then counterstained and dehydrated for microscopic observation (×100, ×200, Nikon, Japan).

TUNEL Staining Assay

The One Step TUNEL Apoptosis Assay Kit (Beyotime) was used for TUNEL assay. The 4um-thick paraffin-embedded tissue sections were dewaxed with xylene and rehydrated in an ethanol gradient. Then, the slices were treated with 20 ug/ml proteinase K for 30min at 37°C. After washed three times with PBS for 5min, the slices were incubated with TUNEL reaction mixture for 1 h at 37°C away from light, washed three times in PBS, then incubated with DAPI-containing anti-fluorescence quenching tablets and observed under a fluorescence microscope.

Statistical Analysis

All data are presented as the mean ± standard deviation (SD) of at least three independent experiments. Student's t-test determined statistical differences between samples and the Bonferroni *post hoc* procedure was performed for a one-way analysis of variance (ANOVA) of statistical comparisons

between more than two samples. GraphPad Prism 7.0 (GraphPad, La Jolla, CA, USA) was used to create the resulting data charts. Statistical significance was considered to be $p < 0.05$ or $p < 0.01$.

RESULTS

α-Hederin Inhibited the Proliferation of HCC Cell Lines

To investigate the effects of α-hederin on HCC cells proliferation, we treated HCC cell lines with indicated concentrations of α-hederin for 12 h, 24 h, and 48 h. Notably, α-hederin inhibited the growth of HCC cell lines in a time and dose-dependent manner (**Figure 1A**). The IC50 values of HepG2, SMMC-7721, Huh-7 cells at 24 h were 18.5 μM, 17.72 μM, 21.89 μM, respectively. Accordingly, the treatment of α-hederin at 10 μM (low concentration) and 20 μM (high concentration)for 24 h was selected for subsequent experiments. By Flow cytometry, we found thatα-hederin significantly promoted the accumulation of the G2/M phase compared with the control group (**Figure 1B**). In addition, the EdU assay revealed a marked reduction of the proliferative ability of HepG2 and SMMC-7721 cells after being treated with low and high concentrations of α-hederin (**Figure 1C**).

To further confirm the inhibitory effect of α-hederin on hepatoma cell proliferation, cell clone formation experiment was performed (**Figure 1D**). Our results clearly displayed that α-hederin inhibited the colony-formation at the indicated concentration. The results described above indicate that α-hederin exerted an inhibitory effect on the proliferation of HCC cells.

α-Hederin Promoted Apoptosis of HCC Cell Lines *In Vitro*

Apoptosis of HCC cells induced by α-hederin was analyzed by flow cytometry and morphological observation. We found that α-hederin increased the proportion of apoptotic cells (**Figure 2A**). Compared with that of control cells, the proportion of apoptosis in HepG2 cells treated with 10 μM or 20 μM α-hederin increased from 3.95% to 26.13% and 69.58% respectively. Similar results were found in SMMC-7721 cells, the proportion of apoptotic cells increased from 4.85% to 18.78% and 54.7% respectively by 10 μM or 20 μM α-hederin treatment. The effect of apoptosis induced by α-hederin was verified at the level of protein expression. The apoptosis-related proteins were determined by Western blot. The results revealed that the expression of Bax and cleaved-caspase3 were obviously increased by α-hederin treatment, while the expression of Bcl-2 and caspase-3 in HepG2 and SMMC-7721 cells were significantly decreased in a dose-dependent manner (**Figure 2B**). Furthermore, the expression of genes associated with apoptosis and proliferation were measured. As shown in **Figure 2C**, the proliferation-associated genes including CTGF, BIRC2, AREG, and Cyclin D1 in HCC cells were significantly decreased by α-hederin treatment compared with the control cells.

α-Hederin Inhibited YAP Activation *via* Upregulating Hippo- Signaling Pathway

YAP is a downstream protein of Hippo signaling pathway, and plays a key role in hepatic carcinogenesis. We firstly investigated the native expression of YAP at gene and protein level in Huh-7, HepG2, and SMMC-7721 cells. As shown in **Figure 3A**, both YAP gene and protein highly expressed in HepG2 and SMMC-7721 cells compared with Huh-7 cells. Therefore, in the present study, HepG2 cells and SMMC-7721 cells were used. Crucial molecules of Hippo signaling pathway in HepG2 and SMMC-7721 cells were further examined. We found that α-hederin treatment suppressed YAP/TAZ protein expression, but elevated the expression of Mst1, Lats1, P-Lats, P-YAP in a dose dependent manner. Accordingly, the level of TEAD1 transcription factor was downregulated (**Figure 3B**). RT-qPCR results revealed that α-hederin treatment effectively enhanced Mst1 and Lats1 gene expression while downregulated YAP gene expression in HepG2 and SMMC-7721 cells (**Figure 3C**).

YAP is inactivated by phosphorylation followed by degradation in the cytoplasm (7, 18, 19). To verify whether α-hederin could inhibit YAP signaling activity, fluorescence staining followed by confocal microscopy was used. Our results showed that in both HepG2 and SMMC-7721 cells, α-hederin treatment cells revealed a significantly decreased distribution of green fluorescence in the nucleus and an increased cytoplasmic staining in comparing with that in control cells (**Figure 3D**), and the reduced level of nuclear YAP was confirmed by immunoblotting (**Figure 3E**). These results suggested that the inhibitory effect of α-hederin on HCC cell proliferation may be due to the suppression of YAP activation caused by the upregulated Mst1 activation.

Inhibition of Mst1/2 Activation Reversed the Inhibitory Effect of α-Hederin on Hepatoma Cell Proliferation

To further verify the role of Mst1/2 in the suppression of hepatoma cell proliferation caused by α-hederin, HepG2 and SMMC-7721 cells were treated with Mst1/2 inhibitor XMU-MP-1 (3 μmol) for 3 h or 6 h before exposure to α-hederin. Immunoblot results revealed that XMU-MP-1 effectively inhibited the expression of Mst1 and downstream kinase Lats1 (**Figure 4A**). Additionally, XMU-MP-1 suppressed the α-hederin-induced reductions in cell density and the irregular morphology of HepG2 and SMMC-7721 cells. Moreover, the results of flow cytometric analysis showed XMU-MP-1 treatment not only ameliorated apoptosis, but also prevented cell cycle arrest induced by α-hederin (**Figures 4B, C**). Data from the EdU assay showed that XMU-MP-1 treatment reversed the inhibition of proliferation caused by α-hederin in HepG2 and SMMC-7721 cells (**Figure 4D**).

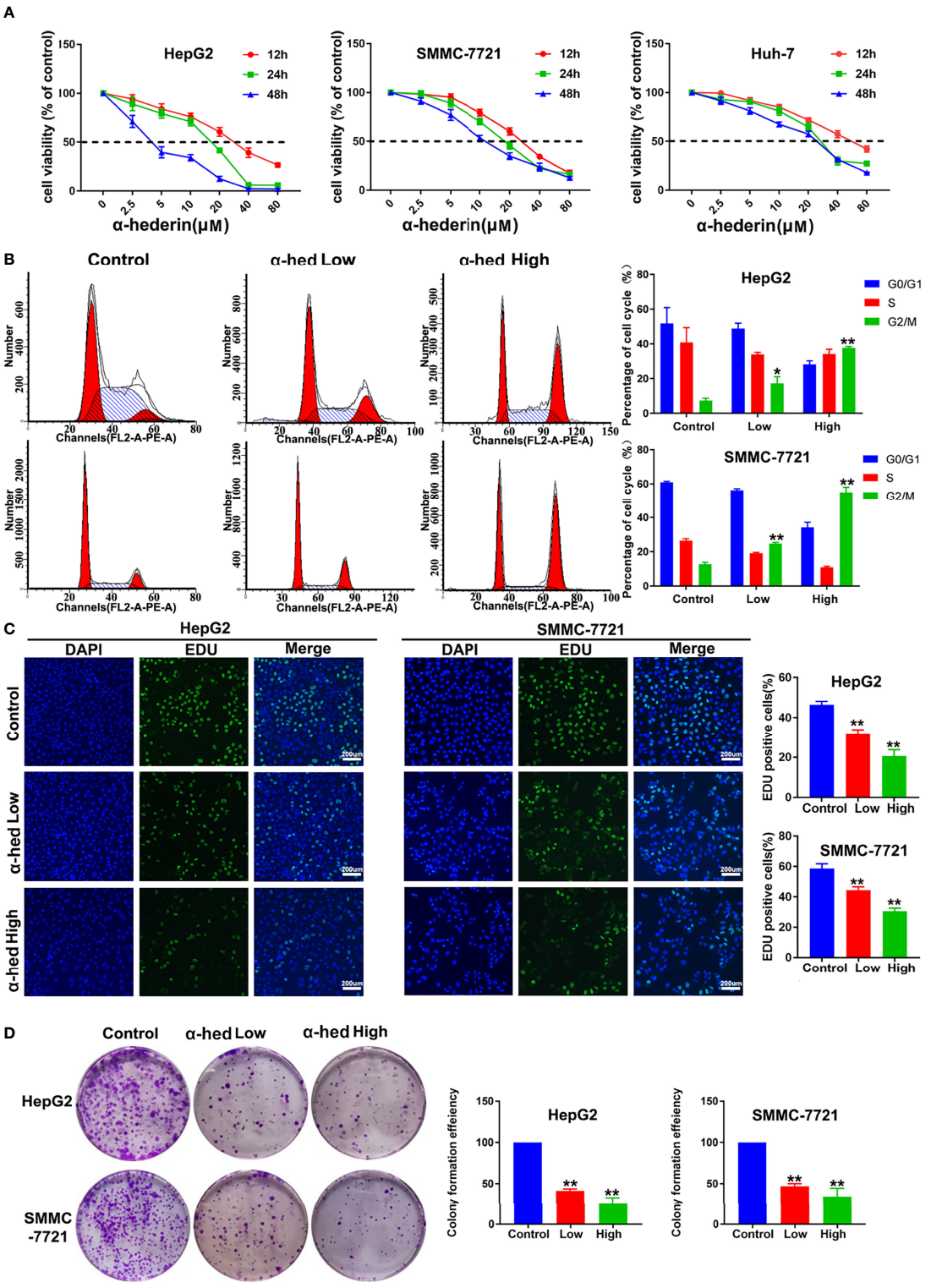

FIGURE 1 | α-hederin inhibited the proliferation of HCC cell lines. **(A)** HepG2, SMMC-7721 or Huh-7 cells were treated with the indicated concentrations of α-hederin for 12, 24 or 48 hours, followed by MTT cell viability assay. **(B)** Cell cycle analysis of HepG2 and SMMC-7721 cells treated with α-hederin at low (10 μM) or high (20 μM) concentration for 24 hours. **(C)** Representative images and analysis of EdU staining in HepG2 and SMMC-7721 cells treated with α-hederin at low (10 μM) or high (20 μM) concentration for 24 hours. **(D)** Representative images and quantitative analysis of colony numbers of HepG2 and SMMC-7721 cells treated with α-hederin at low (10 μM) or high (20 μM) concentration for 24 hours. Significance: $^{*}p < 0.05$ versus control, $^{**}p < 0.01$ versus control.

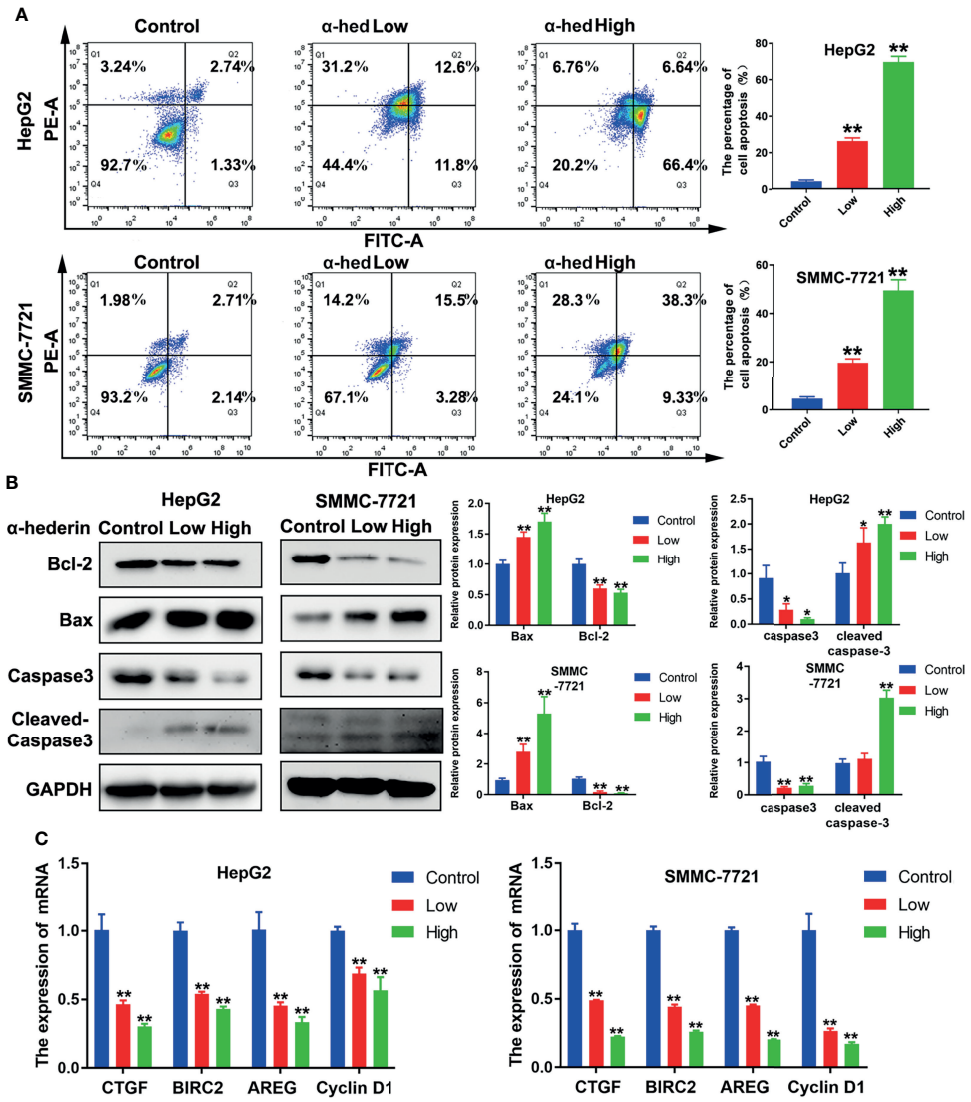

FIGURE 2 | α-hederin promoted apoptosis of HCC cell lines *in vitro*. **(A)** Analysis of apoptosis in HepG2 and SMMC-7721 cells treated with α-hederin for 24 hours by flow cytometry. **(B)** The protein levels of Bax, Bcl-2, caspase 3, and cleaved caspase 3 were detected by Western blot in HepG2 and SMMC-7721 cells treated with the indicated concentrations of α-hederin for 24 hours. **(C)** Analysis of genes associated with cell proliferation and apoptosis in HepG2 and SMMC-7721 cells treated with α-hederin for 24 hours. Significance: $^{*}p < 0.05$; $^{**}p < 0.01$ versus control.

α-Hederin-Induced Mst1 Upregulation Was Responsible for the Inhibition of YAP Signaling Pathway

To further validate whether the decreased YAP activation induced by α-hederin was due to the increased Mst 1/2 activity. HepG2 and SMMC-7721 cells were treated with α-hederin or a combination of α-hederin/XMU-MP-1 for 24 h. Immunoblot revealed that XMU-MP-1 treatment reversed the α-hederin-induced expression changes of Mst1, Lats1, P-Lats1/2, YAP, P-YAP, TAZ in HCC cells (**Figure 5A**). These results were also supported by RT-qPCR analysis (**Figure 5B**). Moreover, XMU-MP-1 could partially reverse the α-hederin-induced decrease of the mRNA expression of YAP target genes involved in proliferation and apoptosis (**Figure 5C**). Furthermore, the immunofluorescence analysis results showed that XMU-MP-1 treatment prevented the reduction of nuclear YAP induced by α-hederin (**Figure 5D**). Our results demonstrated that the Hippo signaling pathway played a critical role in α-hederin-medicated inhibition of cell proliferation and promotion of apoptosis in HCC cell lines.

α-Hederin Attenuated Xenograft Tumor Growth of Human HCC *In Vivo*

Although we have been already verified that α-hederin could inhibit the proliferation of human HCC cells and induce its

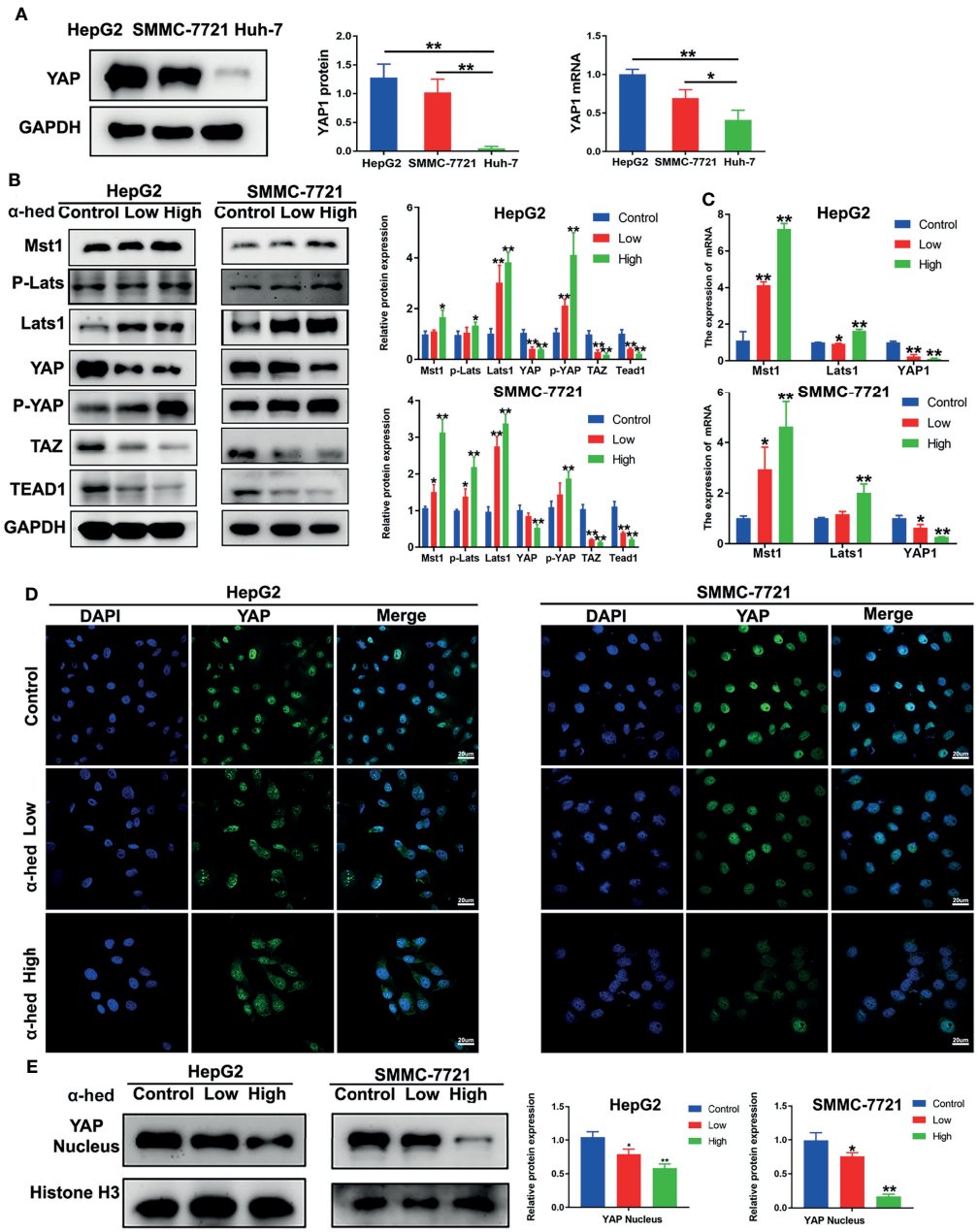

FIGURE 3 | α-hederin inhibited YAP activation *via* upregulating the activation of Hippo signaling pathway. **(A)** The protein and mRNA and levels of YAP in HepG2, SMMC-7721, Huh-7 cells. **(B)** HepG2 and SMMC-7721 cells were treated with α-hederin at low (10 μM) or high (20 μM) concentration for 24 h, and then the proteins involved in Hippo-YAP signaling pathway were analyzed by Western blot, followed by densitometric quantification. **(C)** The mRNA levels of Mst1, Lats1, YAP in HepG2 and SMMC-7721 cells treated with α-hederin for 24 hours were measured by RT-qPCR. **(D)** Immunofluorescence analysis of YAP in HepG2 and SMMC-7721 cells. **(E)** The nuclear levels of YAP in HepG2 and SMMC-7721 cells treated with α-hederin at low (10 μM) or high (20 μM) were analyzed by Western blot. Significance: $^{*}p < 0.05$ versus control, $^{**}p < 0.01$ versus control.

apoptosis *in vitro*, but whether α-hederin could display the same effects *in vivo* should be investigated. HepG2 cells which are stably transformed with green fluorescent protein were injected into BALB/c nude mice, then treated with α-hederin or DDP as a positive control. *In-vivo* fluorescence imaging confirmed that the fluorescence intensity of HepG2 cells was significantly attenuated and the areas of fluorescence were restricted by α-hederin treatment (**Figure 6A**). Compared with the control mice, the α-hederin-treated mice exhibited a smaller tumor size and lower tumor weight (**Figures 6B, C, E**). Besides, the kidney index and bodyweight of mice in the α-hederin group were higher than in the DDP group, this means α-hederin has low side effects

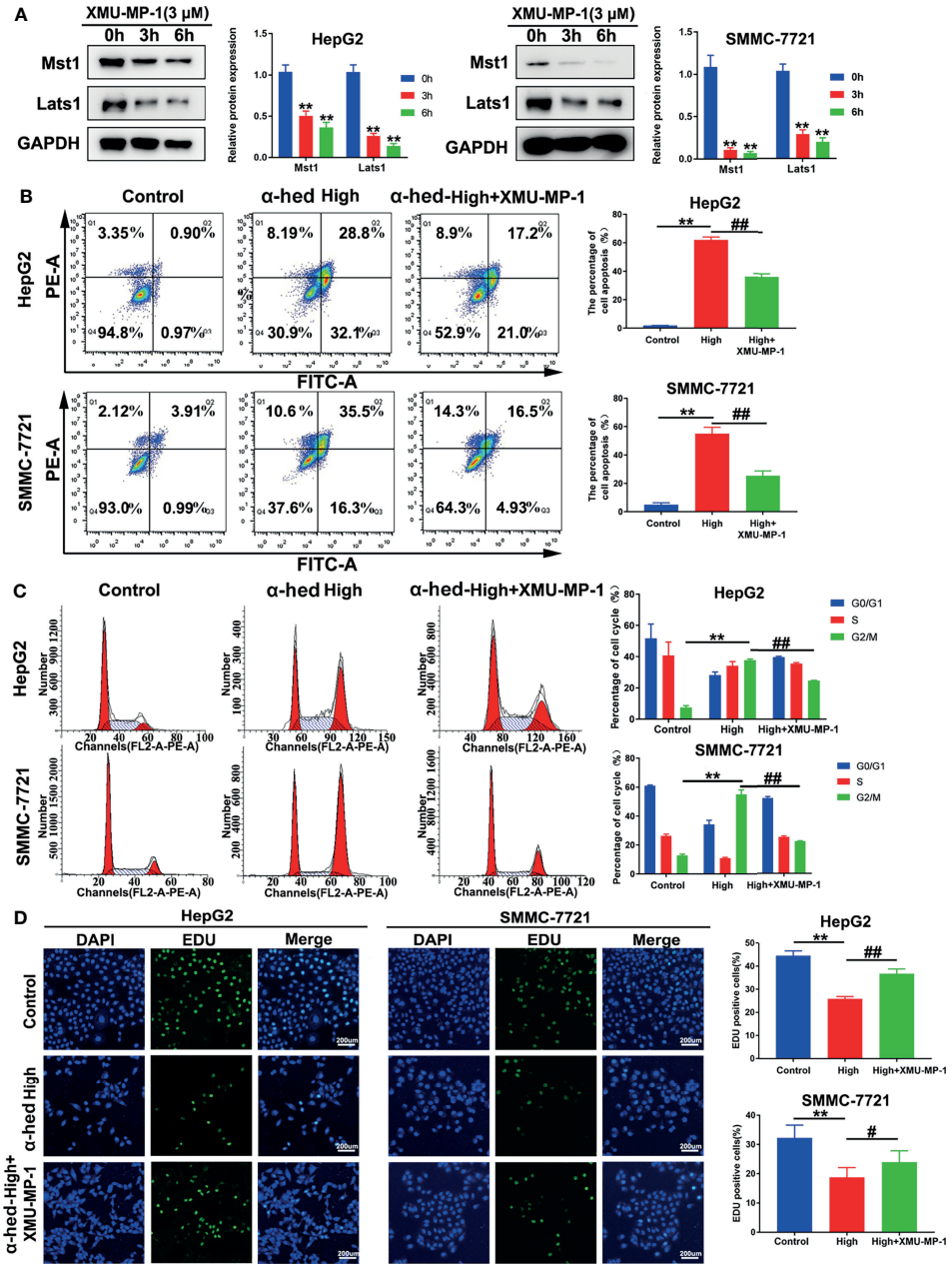

FIGURE 4 | Inhibition of Mst1 activation reversed the effect of α-hederin on hepatoma cell proliferation. **(A)** Western blot analysis of Mst1 and Lats1 expression in HepG2 and SMMC-7721 cells treated with XMU-MP-1 for 3 h or 6 h. **(B)** Flow cytometric analysis of apoptotic HepG2 and SMMC-7721 cells after α-hederin or α-hederin/XMU-MP-1 treatment. **(C)** Flow cytometric analysis of G1- and G2/M-phase subpopulations in HepG2 and SMMC-7721 cells treated with α-hederin or α-hederin/XMU-MP-1. **(D)** Cell proliferation assay using EDU labeling in HepG2 and SMMC-7721 cells treated with α-hederin or α-hederin/XMU-MP-1. Significance: $^{**}p < 0.01$ versus control, #p<0.05 versus High concentration, $\#\#p < 0.01$ versus High concentration.

(**Figures 6D, F, G**). The sections of the HepG2 xenograft tumor were analyzed by HE staining (**Figure 6H**). Compared with the control group, neoplastic cells in α-hederin or DDP treatment group underwent cell death as evidenced by nuclear pyknosis and loss disintegration of cellular architecture, this result was consistent with restricted xenograft tumor size (**Figures 6B, C**) and induced apoptosis in **Figure 2**. The expression of YAP was analyzed in tumor sections (**Figure 6I**) and total proteins were extracted from tumor tissue (**Figure 6J**). After treatment with α-hederin and DDP, the expression of the apoptosis-promoting protein (Bax) was upregulated, whereas the apoptosis-inhibiting protein (Bcl-2) was downregulated. Besides, the main upstream Hippo pathway kinases (MST1, LATS1) were upregulated. More importantly, the expression of P-YAP was increased, whereas

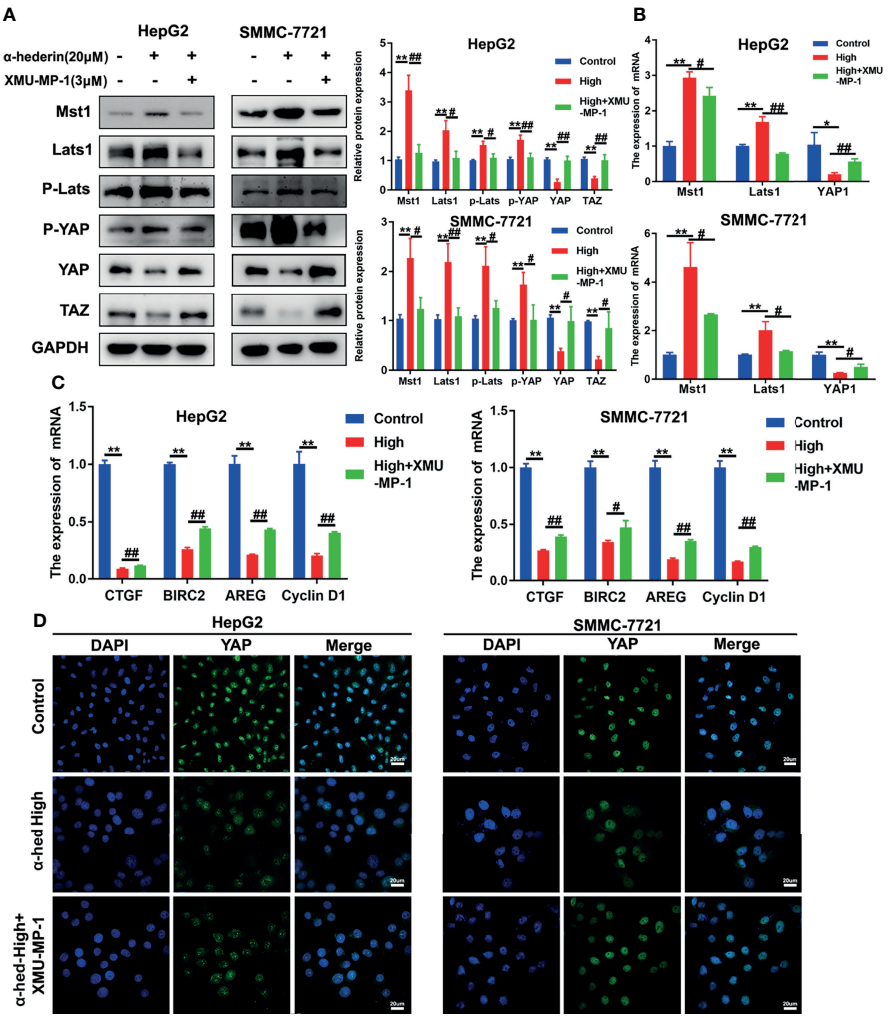

FIGURE 5 | α-hederin-induced Mst1 upregulation was responsible to the inhibition of YAP signaling pathway. **(A)** The expression of proteins involved in Hippo-YAP signaling pathway in HepG2 and SMMC-7721 cells that treated with α-hederin or α-hederin/XMU-MP-1 was analyzed by Western blot. **(B)** The expression of Hippo-YAP signaling target genes in HepG2 and SMMC-7721 cells that treated with α-hederin or α-hederin/XMU-MP-1 was analyzed by RT-qPCR. **(C)** Analysis of genes associated with cell proliferation and apoptosis in HepG2 and SMMC-7721 cells treated with α-hederin or α-hederin/XMU-MP-1. **(D)** Representative immunofluorescence images of YAP in HepG2 and SMMC-7721 cells with the indicated treatment. Significance: $^{*}p < 0.05$ versus control, $^{**}p < 0.01$ versus control, $\#p < 0.05$ versus High concentration, $\#\#p < 0.01$ versus High concentration.

that of YAP was decreased after treatment with α-hederin and DDP. Besides, TUNEL staining assay showed more apoptosis cells in α-hederin and DDP group (**Figure 6K**).

DISCUSSION

In this study, we have identified that α-hederin as a potential suppressor in hepatocellular carcinoma *via* inhibiting YAP activity. Taking advantage of live animal imaging, we clearly showed that α-hederin exhibited a strong inhibitory effect on liver cancer growth and progression. Besides, our data showed that α-hederin increased the expression of Hippo signaling pathway proteins MST1, LATS1, P-LATS, and P-YAP in HCC. Moreover, the effects of above proteins expression could be reversed by XMU-MP-1, a reversible Mst1/2 inhibitor. Thus, our data provided a novel mechanism of α-hederin in inhibiting hepatocellular carcinoma through the Mst1/2-mediated activation of Hippo signaling pathway.

HCC is one of the most common types of liver cancer, with a global cancer mortality rate of 8.2% (20). Considerable progress in the understanding of HCC pathogenesis in recent years entails substantial advances in the diagnosis and therapy of that disease (21–23). Chinese herbs, such as evodiamine and limonin (24, 25), were reported to have alleviatory effects on HCC progression. Fruit of Fiverleaf Akebia, a traditional Chinese medicine, is widely used in the clinic. The active ingredient, α-

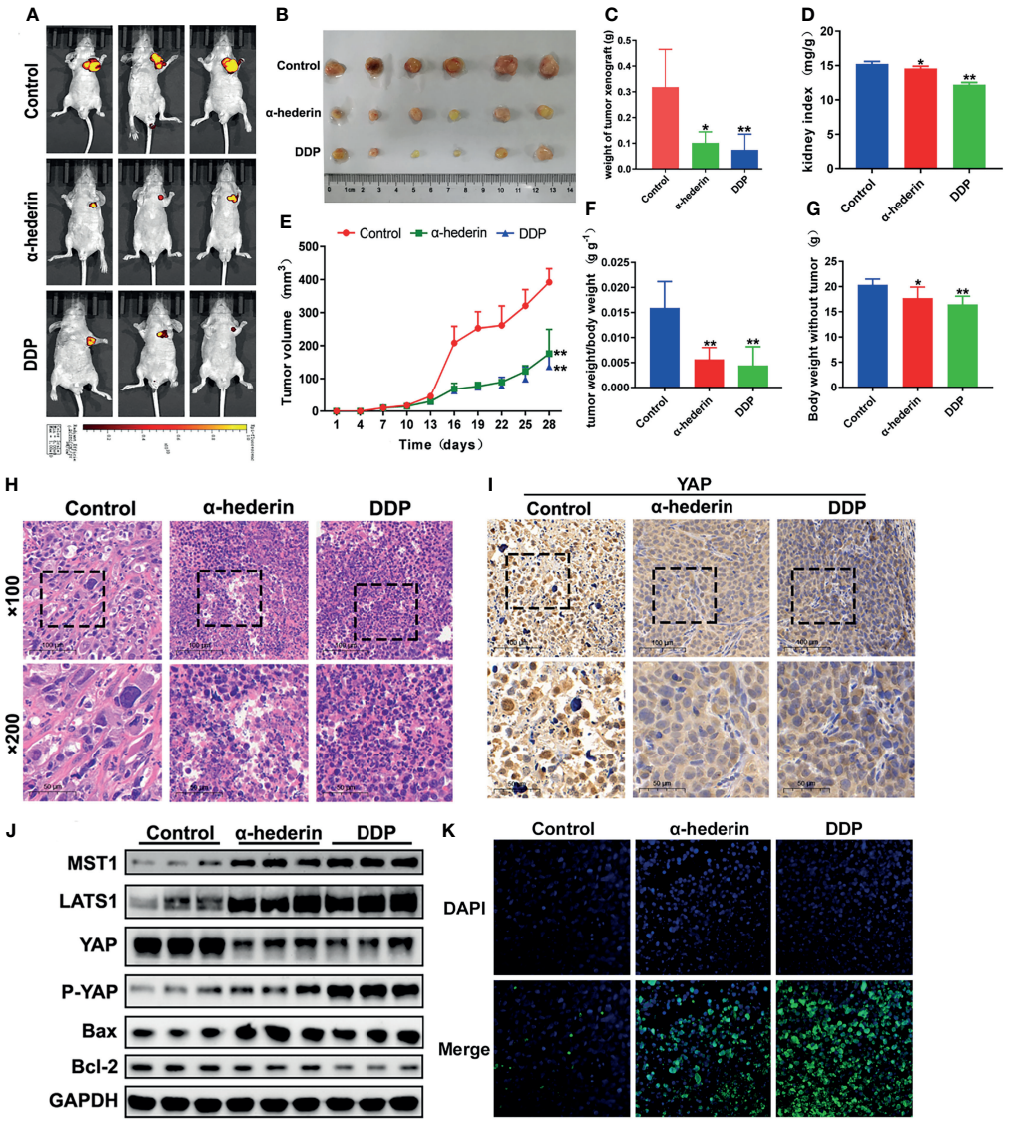

FIGURE 6 | α-hederin attenuated xenograft HCC tumor growth *in vivo* through inhibiting YAP signaling pathway. **(A)** *In vivo* imaging of the HepG2 cell xenograft model mice. **(B)** Representative images of tumors collected from HepG2 cell xenograft model mice treated with PBS, α-hederin and DDP. **(C)** Weight of xenograft tumors harvested from mice. **(D)** Kidney index (kidney weight/bodyweight). **(E)** Tumor volumes were measured at different time points. **(F)** The ratio of tumor weight/body weight. **(G)** Mice body weight subtracted tumor at the end point. **(H)** HE staining of representative tumor tissues from different groups. **(I)** Immunohistochemistry analysis of YAP in mouse tumor tissues. **(J)** Immunoblot analysis of Hippo-YAP signaling pathway-related proteins and apoptosis-related proteins in the tumor tissues. **(K)** TUNEL staining of tumor tissues. Significance: $^{*}p < 0.05$ versus control, $^{**}p < 0.01$ versus control.

hederin, has been confirmed to induce apoptosis in various human cancer cell lines.

The Hippo signaling pathway is the master regulator of organ development and also plays a critical role in live size control (26, 27). Besides, the Hippo signaling pathway has been implicated in cancer development. Both YAP and TAZ are key downstream effectors of the Hippo pathway and have been confirmed upregulated in a wide range of human cancer (28, 29). Upon activation, YAP and TAZ accumulate in the nucleus and then bind to the transcription factors such as TEAD, thereby regulate the expression of target genes that promote cell proliferation and cell survival. An earlier clinical study has confirmed that YAP expression was up-regulated in HCC patients (30). In our experiment, YAP overexpression was clearly observed in HepG2, SMMC-7721 cells, but not Huh-7 cells.

To our knowledge, there are no studies have identified the potential role of α-hederin in the Hippo signaling pathway in HCC cell lines. In the current study, we explored whether α-hederin exerted its anti-tumor activity by mediating Hippo signaling pathway both *in vivo* and vitro. The real-time PCR

results revealed dramatic alterations in main components of Hippo signaling pathway. In HCC cell line, α-hederin treatment led to the significant inhibition of YAP expression through the upregulation of Mst and Lats phosphorylation, leading to phosphorylation and decreased nuclear translocation of YAP. The majority kinases of Hippo signaling pathway play a critical role in tumor suppression, and thus, present optimal small molecular targets. Therefore, inhibiting YAP/TAZ-TEAD by upregulating Hippo signaling pathway activity is an attractive and viable option for cancer therapy (31). Furthermore, development a small molecular agonist that could effectively restore the function of Mst1/2 or Lats1/2 kinases is a major challenge (32). XMU-MP-1 is a reversible and selective Mst1/2 inhibitor, could effectively inhibit Hippo signaling pathway (33). The function of XMU-MP-1 partially reversed phenotypes through suppressing the upregulation of Mst1/Lats1 and YAP phosphorylation induced by α-hederin. As we all know, Mst1 is an upstream kinase of YAP and also have other important cellular targets. Limited relevant research showed that Lats1/2 is still active and suppressed YAP activity in the absence of Mst1/2 (34). In that case, a future interest is to assess whether knockout Lats1/2 can directly reverse the effects of α-hederin treatment in HCC cell lines. Furthermore, relevant research found that YAP and TAZ in normal hepatocytes and tumor cells act through a competitive mechanism to eliminate tumor cells (35). Therefore, the specific mechanisms of Hippo signaling pathway remain to be elucidated. In summary, our study suggests that α-hederin exerted an anti-HCC effect through upregulating Hippo signaling pathway activation, which resulted in the inhibition of YAP activity. However, the further research is warranted to establish the precise mechanisms underlying the action of α-hederin along with validation in various animal models and clinical studies.

CONCLUSION

Our results revealed that α-hederin acted as a new agonist of the Mst1-mediated Hippo signaling pathway and played an inhibitory role in hepatocellular carcinoma (HCC) growth through inhibiting YAP activity. The data obtained in this study provide an important base for further research into the utility of α-hederin as a potential therapeutic or preventive candidate agent for hepatocellular carcinoma (HCC) therapy.

DATA AVAILABILITY STATEMENT

The original contributions presented in the study are included in the article/**Supplementary Material**. Further inquiries can be directed to the corresponding authors.

ETHICS STATEMENT

The animal study was reviewed and approved by the Animal Ethics Committee of Nanjing University of Chinese Medicine.

AUTHOR CONTRIBUTIONS

WS supported and supervised the study. TC, QW, and TZ performed the animal experimental assays. TC, JT, and CX analyzed data. TC, HC, and QW, conducted the study. TC wrote the manuscript. All authors contributed to the article and approved the submitted version.

FUNDING

This work was supported by the National Natural Science Foundation of China (81973523, 81930117), A Project Funded by the Priority Academic Program Development of Jiangsu Higher Education Institutions.

SUPPLEMENTARY MATERIAL

The Supplementary Material for this article can be found online at: https://www.frontiersin.org/articles/10.3389/fonc.2022.839603/full#supplementary-material

REFERENCES

1. Sung H, Ferlay J, Siegel RL, Laversanne M, Soerjomataram I, Jemal A, et al. Global Cancer Statistics 2020: GLOBOCAN Estimates of Incidence and Mortality Worldwide for 36 Cancers in 185 Countries. *CA Cancer J Clin* (2021) 71(3):209–49. doi: 10.3322/caac.21660
2. Ikeda M, Morizane C, Ueno M, Okusaka T, Ishii H, Furuse J, et al. Chemotherapy for Hepatocellular Carcinoma: Current Status and Future Perspectives. *Jpn J Clin Oncol* (2018) 48(2):103–14. doi: 10.1093/jjco/hyx180
3. Kolluri A, Ho M. The Role of Glypican-3 in Regulating Wnt, YAP, and Hedgehog in Liver Cancer. *Front Oncol* (2019) 9:708. doi: 10.3389/fonc.2019.00708
4. Justice RW, Zilian O, Woods DF, Noll M, Bryant PJ. The Drosophila Tumor Suppressor Gene Warts Encodes a Homolog of Human Myotonic Dystrophy Kinase and Is Required for the Control of Cell Shape and Proliferation. *Genes Dev* (1995) 9(5):534–46. doi: 10.1101/gad.9.5.534
5. Xu T, Wang W, Zhang S, Stewart RA, Yu W. Identifying Tumor Suppressors in Genetic Mosaics: The Drosophila Lats Gene Encodes a Putative Protein Kinase. *Dev (Cambridge England)* (1995) 121(4):1053–63. doi: 10.1242/dev.121.4.1053
6. Zeng Q, Hong W. The Emerging Role of the Hippo Pathway in Cell Contact Inhibition, Organ Size Control, and Cancer Development in Mammals. *Cancer Cell* (2008) 13(3):188–92. doi: 10.1016/j.ccr.2008.02.011
7. Zhao B, Li L, Lei Q, Guan K-L. The Hippo-YAP Pathway in Organ Size Control and Tumorigenesis: An Updated Version. *Genes Dev* (2010) 24(9):862–74. doi: 10.1101/gad.1909210
8. Chan EHY, Nousiainen M, Chalamalasetty RB, Schäfer A, Nigg EA, Silljé HHW, et al. The Ste20-Like Kinase Mst2 Activates the Human Large Tumor Suppressor Kinase Lats1. *Oncogene* (2005) 24(12):2076–86. doi: 10.1038/sj.onc.1208445
9. Dong J, Feldmann G, Huang J, Wu S, Zhang N, Comerford SA, et al. Elucidation of a Universal Size-Control Mechanism in Drosophila and Mammals. *Cell* (2007) 130(6):1120–33. doi: 10.1016/j.cell.2007.07.019

10. Hao Y, Chun A, Cheung K, Rashidi B, Yang X. Tumor Suppressor LATS1 Is a Negative Regulator of Oncogene YAP. *J Biol Chem* (2008) 283(9):5496–509. doi: 10.1074/jbc.M709037200
11. Zhang S, Zhou D. Role of the Transcriptional Coactivators YAP/TAZ in Liver Cancer. *Curr Opin Cell Biol* (2019) 61:64–71. doi: 10.1016/j.ceb.2019.07.006
12. Feng X, Zhang M, Wang B, Zhou C, Mu Y, Li J, et al. CRABP2 Regulates Invasion and Metastasis of Breast Cancer Through Hippo Pathway Dependent on ER Status. *J Exp Clin Cancer Res: CR* (2019) 38(1):361. doi: 10.1186/s13046-019-1345-2
13. Dhanasekaran SM, Alejandro Balbin O, Chen G, Nadal E, Kalyana-Sundaram S, Pan J, et al. Transcriptome Meta-Analysis of Lung Cancer Reveals Recurrent Aberrations in NRG1 and Hippo Pathway Genes. *Nat Commun* (2014) 5:5893. doi: 10.1038/ncomms6893
14. Sebio A, Matsusaka S, Zhang W, Yang D, Ning Y, Stremitzer S, et al. Germline Polymorphisms in Genes Involved in the Hippo Pathway as Recurrence Biomarkers in Stages II/III Colon Cancer. *Pharmacogenomics J* (2016) 16 (4):312–9. doi: 10.1038/tpj.2015.64
15. Sun D, Shen W, Zhang F, Fan H, Xu C, Li L, et al. α-Hederin Inhibits Interleukin 6-Induced Epithelial-to-Mesenchymal Transition Associated With Disruption of JAK2/STAT3 Signaling in Colon Cancer Cells. *Biomed Pharmacother = Biomed Pharmacother* (2018) 101:107–14. doi: 10.1016/j.biopha.2018.02.062
16. Zhan YJ, Wang K, Li Q, et al. The Novel Autophagy Inhibitor Alpha-Hederin Promoted Paclitaxel Cytotoxicity by Increasing Reactive Oxygen Species Accumulation in Non-Small Cell Lung Cancer Cells. *Int J Mol Sci* (2018) 19 (10):1–15. doi: 10.3390/ijms19103221
17. Li J, Wu D-D, Zhang J-X, Wang J, Ma J-J, Hu X, et al. Mitochondrial Pathway Mediated by Reactive Oxygen Species Involvement in α-Hederin-Induced Apoptosis in Hepatocellular Carcinoma Cells. *World J Gastroenterol* (2018) 24 (17):1901–10. doi: 10.3748/wjg.v24.i17.1901
18. Yu F, Zhao B, Panupinthu N, Jewell JL, Lian I, Wang LH, et al. Regulation of the Hippo-YAP Pathway by G-Protein-Coupled Receptor Signaling. *Cell* (2012) 150(4):780–91. doi: 10.1016/j.cell.2012.06.037
19. Zhao B, Wei X, Li W, Udan RS, Yang Q, Kim J, et al. Inactivation of YAP Oncoprotein by the Hippo Pathway Is Involved in Cell Contact Inhibition and Tissue Growth Control. *Genes Dev* (2007) 21(21):2747–61. doi: 10.1101/gad.1602907
20. Bray F, Ferlay J, Soerjomataram I, Siegel RL, Torre LA, Jemal A. Global Cancer Statistics 2018: GLOBOCAN Estimates of Incidence and Mortality Worldwide for 36 Cancers in 185 Countries. *Ca-A Cancer J Clin* (2018) 68(6):394–424. doi: 10.3322/caac.21492
21. Luo Y, Fang L, Yu HQ, Zhang J, Lin XT, Liu XY, et al. P53 Haploinsufficiency and Increased Mtor Signaling Define a Subset of Aggressive Hepatocellular Carcinoma. *J Hepatol* (2020) 74(1):96–108. doi: 10.1016/j.jhep.2020.07.036
22. Komoll R, Hu Q, Olarewaju O, von Döhlen L, Yuan Q, Xie Y, et al. Microrna-342-3p Is a Potent Tumour Suppressor in Hepatocellular Carcinoma. *J Hepatol* (2020) 74(1):122–34. doi: 10.1016/j.jhep.2020.07.039
23. Dong P, Wang X, Liu L, Tang W, Ma L, Zeng W, et al. Dampened VEPH1 Activates Mtorc1 Signaling by Weakening the TSC1/TSC2 Association in Hepatocellular Carcinoma. *J Hepatol* (2020) 73(6):1446–59. doi: 10.1016/j.jhep.2020.06.027
24. Tang Z, Tang Y, Li L, Liu T, Yang J. Limonin Provokes Hepatocellular Carcinoma Cells With Stemness Entry Into Cycle *via* Activating PI3K/Akt Signaling. *Biomed Pharmacother = Biomed Pharmacother* (2019) 117:109051. doi: 10.1016/j.biopha.2019.109051
25. Zhao S, Xu K, Jiang R, Li DY, Guo XX, Zhou P, et al. Evodiamine Inhibits Proliferation and Promotes Apoptosis of Hepatocellular Carcinoma Cells *via* the Hippo-Yes-Associated Protein Signaling Pathway. *Life Sci* (2020) 251:117424. doi: 10.1016/j.lfs.2020.117424
26. Johnson R, Halder G. The Two Faces of Hippo: Targeting the Hippo Pathway for Regenerative Medicine and Cancer Treatment. *Nat Rev Drug Discov* (2014) 13(1):63–79. doi: 10.1038/nrd4161
27. Hong L, Cai Y, Jiang M, Zhou D, Chen L. The Hippo Signaling Pathway in Liver Regeneration and Tumorigenesis. *Acta Biochim Biophys Sin* (2015) 47 (1):46–52. doi: 10.1093/abbs/gmu106
28. Harvey K, Zhang X, Thomas D. The Hippo Pathway and Human Cancer. *Nat Rev Cancer* (2013) 13(4):246–57. doi: 10.1038/nrc3458
29. Moroishi T, Hansen C, Guan K. The Emerging Roles of YAP and TAZ in Cancer. *Nat Rev Cancer* (2015) 15(2):73–9. doi: 10.1038/nrc3876
30. Shu B, Zhai M, Miao X, He C, Deng C, Fang Y, et al. Serotonin and YAP/VGLL4 Balance Correlated With Progression and Poor Prognosis of Hepatocellular Carcinoma. *Sci Rep* (2018) 8(1):9739. doi: 10.1038/s41598-018-28075-9
31. Pobbati A, Hong W. A Combat With the YAP/TAZ-TEAD Oncoproteins for Cancer Therapy. *Theranostics* (2020) 10(8):3622–35. doi: 10.7150/thno.40889
32. Guo L, Teng L. YAP/TAZ for Cancer Therapy: Opportunities and Challenges (Review). *Int J Oncol* (2015) 46(4):1444–52. doi: 10.3892/ijo.2015.2877
33. Fan F, He Z, Kong L, Chen Q, Yuan Q, Zhang S, et al. Pharmacological Targeting of Kinases MST1 and MST2 Augments Tissue Repair and Regeneration. *Sci Trans Med* (2016) 8(352):352ra108. doi: 10.1126/scitranslmed.aaf2304
34. Moroishi T, Park H, Qin B, Chen Q, Meng Z, Plouffe SW, et al. A YAP/TAZ-Induced Feedback Mechanism Regulates Hippo Pathway Homeostasis. *Genes Dev* (2015) 29(12):1271–84. doi: 10.1101/gad.262816.115
35. Moya I, Castaldo S, Van den Mooter L, Soheily S, Sansores-Garcia L, Jacobs J, et al. Peritumoral Activation of the Hippo Pathway Effectors YAP and TAZ Suppresses Liver Cancer in Mice. *Sci (New York NY.)* (2019) 366(6468):1029–34. doi: 10.1126/science.aaw9886

Conflict of Interest: The authors declare that the research was conducted in the absence of any commercial or financial relationships that could be construed as a potential conflict of interest.

Publisher's Note: All claims expressed in this article are solely those of the authors and do not necessarily represent those of their affiliated organizations, or those of the publisher, the editors and the reviewers. Any product that may be evaluated in this article, or claim that may be made by its manufacturer, is not guaranteed or endorsed by the publisher.

frontiers in Pharmacology

ORIGINAL RESEARCH
published: 10 March 2022
doi: 10.3389/fphar.2022.837055

Comparative Proteomics Analysis Reveals the Reversal Effect of Cryptotanshinone on Gefitinib-Resistant Cells in Epidermal Growth Factor Receptor-Mutant Lung Cancer

Peiheng Cai[1†], *Gaofan Sheng*[1†], *Shiqin Jiang*[1], *Daifei Wang*[1], *Zhongxiang Zhao*[2], *Min Huang*[1] *and Jing Jin*[1*]

[1]School of Pharmaceutical Sciences, Sun Yat-sen University, Guangzhou, China, [2]School of Chinese Materia Medica, Guangzhou University of Chinese Medicine, Guangzhou, China

OPEN ACCESS

Edited by:
Nand K. Roy,
Case Western Reserve University,
United States

Reviewed by:
Quan Xia,
First Affiliated Hospital of Anhui Medical University, China
Weiqiang Lu,
East China Normal University, China

***Correspondence:**
Jing Jin
jinjing@mail.sysu.edu.cn

†These authors have contributed equally to this work and share first authorship

Specialty section:
This article was submitted to Pharmacology of Anti-Cancer Drugs, a section of the journal Frontiers in Pharmacology

Received: 16 December 2021
Accepted: 18 January 2022
Published: 10 March 2022

Citation:
Cai P, Sheng G, Jiang S, Wang D, Zhao Z, Huang M and Jin J (2022) Comparative Proteomics Analysis Reveals the Reversal Effect of Cryptotanshinone on Gefitinib-Resistant Cells in Epidermal Growth Factor Receptor-Mutant Lung Cancer. Front. Pharmacol. 13:837055. doi: 10.3389/fphar.2022.837055

Cryptotanshinone (CTS) is a lipophilic constituent of *Salvia miltiorrhiza*, with a broad-spectrum anticancer activity. We have observed that CTS enhances the efficacy of gefitinib in human lung cancer H1975 cells, yet little is known about its molecular mechanism. To explore how CTS enhances H1975 cell sensitivity to gefitinib, we figured out differential proteins of H1975 cells treated by gefitinib alone or in combination with CTS using label-free liquid chromatography-tandem mass spectrometry (LC-MS/MS). Gene Ontology (GO), Kyoto Encyclopedia of Genes and Genomes (KEGG), and protein–protein interaction (PPI) bioinformatic analyses of the differential proteins were performed. CTS enhanced H1975 cell sensitivity to gefitinib *in vitro* and *in vivo*, with 115 and 128 differential proteins identified, respectively. GO enrichment, KEGG analysis, and PPI network comprehensively demonstrated that CTS mainly impacted the redox process and fatty acid metabolism in H1975 cells. Moreover, three differential proteins, namely, catalase (CAT), heme oxygenase 1 (HMOX1), and stearoyl-CoA desaturase (SCD) were validated by RT-qPCR and Western blot. In conclusion, we used a proteomic method to study the mechanism of CTS enhancing gefitinib sensitivity in H1975 cells. Our finding reveals the potential protein targets of CTS in overcoming gefitinib resistance, which may be therapeutical targets in lung cancer.

Keywords: cryptotanshinone, gefitinib, resistance, proteomics, nonsmall cell lung cancer

INTRODUCTION

Lung cancer is one of the most malignant tumors, with high morbidity and mortality over the world. About 80% of lung cancers are non-small cell lung cancers (NSCLCs), and epidermal growth factor receptor (EGFR) gene mutations are considered to prompt NSCLC development (Sharma et al., 2007). Although EGFR-tyrosine kinase inhibitors (TKIs) have shown good clinical efficacy, therapy resistance inevitably occurs. With long-term use of first-line EGFR-TKIs, most patients would develop acquired resistance after a median of 12 months (Nagano et al., 2018). Mechanisms of

resistance to EGFR-TKIs are complicated, including T790M secondary mutation, activation of alternative or downstream pathways, histological transformation, etc., (Yu et al., 2014). Hence overcoming the resistance to EGFR-TKIs has become a hotspot of research.

Cryptotanshinone (CTS), a lipid-soluble compound extracted from the roots of traditional Chinese medicine *Salvia miltiorrhiza*, is mainly used to treat cardiovascular and inflammatory diseases (Li et al., 2021). Recent studies show that CTS also has antitumor properties, mainly by inducing apoptosis, inhibiting cancer cell proliferation, metastasis and invasion, inhibiting angiogenesis, and drug efflux (Ashrafizadeh et al., 2021). Although CTS has been found to reverse chemoresistance by multiple mechanisms, however, the mechanism of CTS in enhancing gefitinib sensitivity is still unclear.

Differential proteomics, also known as comparative proteomics, studies the changes in proteome in different physiological or pathological states between samples in order to find key differential proteins as markers for qualitative and functional analysis (Yang et al., 2019). Over the years, many techniques have been developed for protein separation, digestion, enrichment, identification, as well as absolute and relative quantification (Megger et al., 2013). One quantitative method is labeling-based quantification, represented by stable isotope labeling by amino acids in cell culture (SILAC) and isobaric tags for relative and absolute quantification (iTRAQ). The other is label-free quantification utilizing LC-MS/MS for relative quantification, which has a large dynamic range and high proteome coverage (Li et al., 2012). Differential proteomics has been widely used in the mechanism study of traditional Chinese medicines at the protein level (Yang et al., 2019). Comparative proteomic studies of anticancer phytochemicals have found plentiful targets, such as cyclins, cytoskeleton proteins, and metabolic enzymes (Wong et al., 2016), either confirming known cancer biomarkers or uncovering new ones. For example, a study employing two-dimensional difference gel electrophoresis with mass spectrometry to investigate the effect of honokiol in human thyroid cancer cells showed that honokiol regulates proteins involving cytoskeleton, protein folding, transcription control, and glycolysis (Chou et al., 2018). Another study using the iTRAQ method to study the mechanism of triptolide in A549 cells found candidate proteins involved in the PARP1/AIF pathway, nuclear Akt signaling, and metastasis processes (Li et al., 2018).

This article reports that CTS increases the sensitivity of gefitinib-resistant H1975 cells to gefitinib, a first-line EGFR-TKI. To explore its mechanism, label-free proteomics is used to identify the differential proteins under gefitinib treatment alone or in combination with CTS. The expression levels of three selected differential proteins, CAT, HMOX1, and SCD were verified. This study reveals the potential targets of CTS in H1975 cells, providing evidence of CTS as a gefitinib sensitizer to overcome resistance in clinical cancer therapy.

MATERIALS AND METHODS

Chemicals and reagents

Ammonium bicarbonate (NH_4HCO_3), ethanol, formic acid (FA), chloroform ($CHCl_3$), and isopropanol with analytical purity were purchased from Tianjin ZhiYuan Reagent Co., Ltd., (Tianjin, China). Acetone, acetonitrile (ACN), urea, dithiothreitol (DTT), and trifluoroacetic acid (TFA), with purity higher than 99.0%, were purchased from Shanghai Aladdin Biochemical Technology Co., Ltd., (Shanghai, China). DMSO and iodoacetamide (IAM) with purity higher than 99% was purchased from Sigma-Aldrich Trading Co. Ltd., (MO, United States). Gefitinib was purchased from Yuanye Bio-Technology Co., Ltd., (Shanghai, China), and CTS was purchased from Winherb (Shanghai, China).

Cell culture and viability assay

Human lung cancer H1975 cells were obtained from the National Collection of Authenticated Cell Cultures (Shanghai, China). H1975 cells were maintained in RPMI-1640 medium (Corning, United States) containing 10% FBS (Gibco, United States) and 1% penicillin/streptomycin (Cellgro, United States) at 37°C and 5% CO_2. Gefitinib (4.47 mg) and CTS (2.96 mg) were dissolved, respectively, in 100 μl of DMSO as the stock solutions, stored at −20°C, and diluted with culture medium before use. Before treatment, cells were seeded in 96-well plates (Corning, United States) at a density of 5×10^3 cells per well and allowed to attach overnight. Cells were exposed to gefitinib (10, 20, and 40 μM), CTS (2.5 and 5 μM), and combinations of them, respectively, for 72 h. Cell viability was tested by CCK-8 (Dojindo, Japan) according to the manufacturer's instructions. Absorbance was measured at 450 nm by a microplate reader (THERMO Electron, United States). Cell survival rate was calculated. Each group has four replicates.

Animal model and treatment

Animal experiments were performed with the approval of the Animal Ethical and Welfare Committee of Sun Yat-sen University. SPF male BALB/c mice weighing 18–22 g at 3–4 months were purchased from the Beijing Vital River Laboratory Animal Technology Co. Ltd. All mice were kept in a specific pathogen-free animal room at 20°C–25°C and 40–70% humidity with a 12 h light–dark cycle, provided with water and feed *ad libitum*. H1975 cells were suspended in PBS and injected subcutaneously to the left armpit of the mice (5×10^6 cells/0.1 ml per mouse). The formula $width^2 \times length2$ was used to measure tumor size. Once the tumor size reached 50–100 mm^3 (within 5–7 days), the mice were randomly assigned into four groups (n = 10 mice/group) for daily drug administration: 1) vehicle control group (1% Tween-80 ig. and corn oil ip.); 2) Gef group (50 mg/kg Gef ig. and corn oil ip.); 3) CTS group (1% Tween-80 ig. and 20 mg/kg CTS ip.); and 4) Gef + CTS group (50 mg/kg Gef ig. and 20 mg/kg CTS ip.). After 17 days of administration, mice were sacrificed. Tumor tissues were weighed and stored at −80°C.

Sample preparation for proteome

Protein extraction

Treated cells were washed with PBS (Gibco, USA) and lysed with RIPA containing 1% PMSF (both from Beyotime, China) on ice for 30 min. Cell lysate was scraped, collected, and sonicated with 35% amplitude on ice for 10–15 s. After centrifugation at 12,000 × *g*, 4°C for 20 min in a centrifuge (Eppendorf, Germany), the supernatant was obtained as cellular protein solution. For tissue sample, 100 mg of tissue in 1 ml of RIPA containing 1% PMSF was homogenated four times under 5,000 rpm for 8 s with a 10 s interval by a homogenator (Birtin, France). After centrifugation at 12,000 × *g*, 4°C for 20 min, the supernatant was obtained as tissue protein solution. Protein concentrations were measured with a BCA Protein Assay Kit (Thermo, United States).

Acetone Precipitation and Enzymatic Hydrolysis

The protein solution (300 μg of protein diluted with 50 mM NH_4HCO_3 to 100 μl) was added with 400 μl of cold acetone, mixed, and precipitated overnight at 4°C. After centrifugation at 15,000 × *g*, 4°C for 30 min, the supernatant was discarded, and the precipitate was washed with cold acetone, 70% ethanol, and acetone in sequence, 500 μl for each. The sample was centrifuged at 15,000 × *g*, 4°C for 30 min after each wash, and the supernatant was discarded. After evaporated to dry in a fume hood, the final precipitate was resuspended with 50 μl of 8 M UA buffer (in 0.1 M Tris/HCl, pH 8.5), shaken at room temperature for 2 h until the precipitate was completely dissolved. A 2 μl diluted DTT solution was added (DTT final concentration = 2 mM), mixed, and the sample was placed in a 30°C water bath for 1.5 h. Then 13 μl of diluted IAM solution was added (IAM final concentration = 10 mM), mixed, and the sample was placed in darkness for 40 min. Then it was diluted with 50 mM NH_4HCO_3 to 600 μl (urea final concentration= 0.7 mol/L), added with 20 μl of 0.25 μg/μl Trypsin (Promega, United States) with trypsin/protein ratio 1:60 (w/w), mixed, and hydrolyzed overnight at 37°C. Then 10% TFA was used to stop the reaction by acidifying the solution to a final concentration of 0.4%.

C18 Stage Tip Peptide Desalting

To activate C18 stage tip, 200 μl of methanol was added, centrifuged at 1,200 × *g* for 10 min, and the effluent was discarded, and repeated three times. To equilibrate tip, 200 μl of 80% ACN/0.1% FA was added, centrifuged at 4,000 × *g* for 4 min, and the effluent was discarded, and repeated three times. Then 200 μl of 0.1% TFA was added to tip, centrifuged at 6,000 × *g* for 4 min, the effluent was discarded, and repeated three times. A 5 μg digested protein sample was dissolved in 200 μl of 0.1% TFA, and the sample was loaded twice, centrifuged at 2,000 × *g* for 12 min, and the effluent was discarded. For salt elution, 200 μl of 0.1% TFA was added to tip, centrifuged at 6,000 × *g* for 4 min, and the effluent was discarded. For TFA elution, 200 μl of 0.1% FA was added to tip, centrifuged at 6,000 × *g* for 4 min, and the effluent was discarded, and repeated twice. Then 180 μl of 80% ACN/0.1% FA was added to tip, centrifuged at 2,000 × *g* for 4 min, and repeated twice. The effluent was collected and vacuum dried overnight. The dried sample was redissolved with 10 μl of 0.1% FA and centrifuged at 16,000 × *g* for 10 min. The supernatant was transferred to the sample bottle.

Label-free liquid chromatography-tandem mass spectrometry analysis

A C18 column (75 μm × 150 mm, NanoViper C18, 2 μm, 100 Å; Thermo, PA, United States) was used to separate peptide samples in 0.1% formic acid in the Nano LC-Q Exactive Plus mass spectrometer (Thermo, United States). Eluent A was 0.1% formic acid aqueous solution, and eluent B was 0.1% formic acid 80% acetonitrile solution. The elution gradient is set as follows: 0–95 min, 3%→32% (B); 95–105 min, 32%→100% (B); 105–120 min, 100% (B), the total running time is 120 min at a flow rate of 300 nl/min. All MS and MS2 spectra were collected, where the 10 strongest ions were fragmented by collision-induced dissociation. A full mass scan in the range of 355–1,700 m/z was obtained, with a mass resolution of 70,000. The LC-MS/MS data were analyzed by searching the UniProt Human database (https://www.uniprot.org/proteomes/UP000005640) downloaded on December 7, 2017 using Thermo Proteome Discoverer 2.2. Parameters were set, and some modifications were made as described: Fixed modification: ureido modification; dynamic modification: oxidation modification; enzyme: trypsin; precursor mass tolerance: 20 ppm, maximum; missing cut sites: 2; fragment quality tolerance: 0.02 Da; target false discovery rate (FDR) (strict): 0.01; and target FDR (loose): 0.05. Verification was based on the Q value. Result was exported from Thermo Proteome Discoverer 2.2 to Excel for analysis. Proteins meeting all the criteria ($p < 0.05$, high protein FDR confidence, and abundance ratio > 1.5 or <0.67) were recognized as differential proteins.

Bioinformatics analysis

GO enrichment analysis of differential proteins was performed using DAVID 6.8 (https://david.ncifcrf.gov/). Pathway analysis was performed on KEGG platform (http://kobas.cbi.pku.edu.cn/index.php). PPI analysis was performed using STRING 11.0 (https://string-db.org/cgi/input.pl).

Western blot analysis

Protein samples were prepared as described in protein extraction and denatured by loading buffer. Protein, 25 μg per sample, was electrophoresed on SDS-PAGE gels (10%–12%) and blotted onto PVDF membranes (Amersham Hybond, United States). After blocking with 5% milk, the membranes were incubated at 4°C overnight with the following primary antibodies: β-actin (Cell Signaling, United States), catalase (CAT, Sangon, China), heme oxygenase 1 (HMOX1, Santa Cruz, United States), and stearoyl-CoA desaturase (SCD, Sangon, China). Anti-rabbit secondary antibodies (Cell Signaling, United States) were used. Target protein expressions were detected by chemiluminescence and quantified using ImageJ.

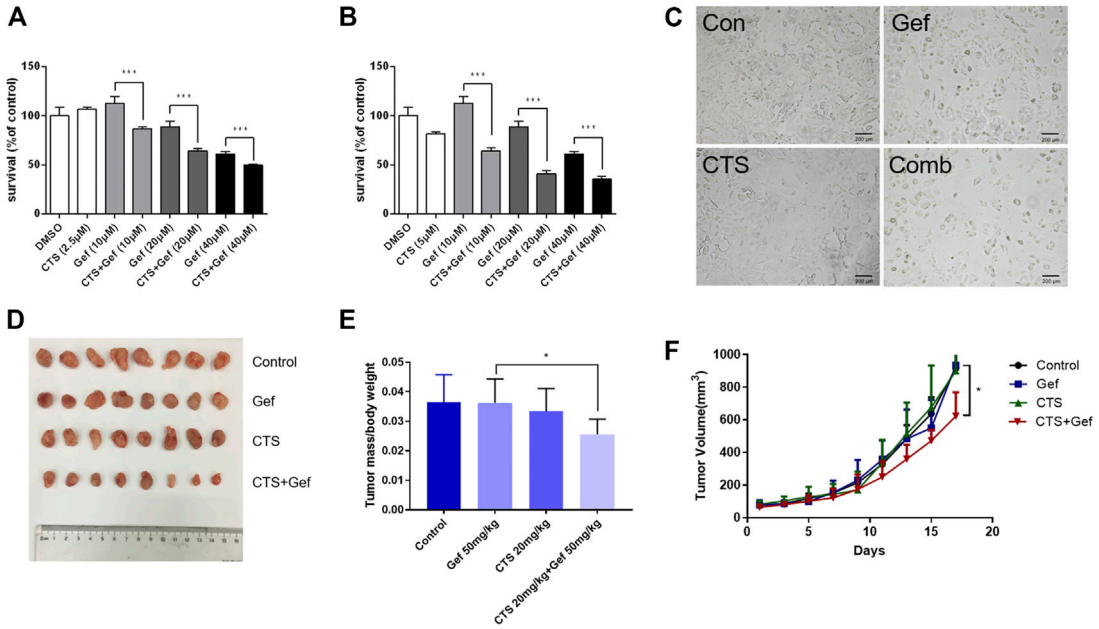

FIGURE 1 | CTS increases the sensitivity to gefitinib in H1975 cells and xenografts in nude mice. **(A,B)** H1975 cells were treated with different concentrations of gefitinib (0, 10, 20, and 40 μM) alone or in combination with 2.5 μM **(A)** or 5 μM **(B)** CTS for 72 h. The cell viability was determined by CCK-8 ($n = 5$). Data are represented as the means ± SD, and significant differences are indicated as $^{*}p < 0.05$, $^{**}p < 0.01$, and $^{***}p < 0.001$. **(C)** H1975 cells were treated with 0.1% DMSO, 20 μM Gef, 5 μM CTS, and 20 μM Gef with 5 μM CTS, respectively, and cell morphology was imaged. **(D–F)** Tumor-bearing BALB/c nude mice were assigned into four groups ($n = 8$ per group) and treated with vehicle, Gef (50 mg/kg), CTS (20 mg/kg), and a combination of CTS and Gef for 17 days. Tumors in each treatment group were photographed **(D),** and tumor weights were measured **(E)**. Tumor volumes were measured every 2 days **(F)**.

Quantitative RT-PCR

Treated cells in 12-well plates were washed with PBS, added with 500 μl of Trizol (Takara, Japan). After 15 min of incubation at 4°C with shaking, cell lysate was obtained and added with 500 μl of $CHCl_3$. For tissue sample, 50 mg of tissue in 500 μl of Trizol was homogenated four times under 5,000 rpm for 8 s with a 10 s interval in a homogenator. A 400 μl supernatant was transferred and added with 80 μl of $CHCl_3$. Cell lysate or tissue supernatant added with $CHCl_3$ was vortexed for 15 min, let stay for 3 min, and then centrifuged at 12,000 × *g*, 4°C for 15 min; 100 μl of supernatant was transferred and added with 200 μl of isopropanol, and gently shaken upside down 15 times. After staying for 10 min, the sample was centrifuged at 4°C and 12,000 × *g* for 10 min, and the supernatant was discarded as much as possible. Precipitate was upside down washed with 400 μl of 75% ethanol in diethyl pyrocarbonate (DEPC) water solution. The sample was centrifuged at 12,000 × *g*, 4°C for 8 min. The supernatant was removed as much as possible, and the precipitate was dried in a fume hood. Dried precipitate was dissolved in 20 μl of DEPC water, and the RNA concentration was measured by Nanodrop 2000 (Thermo Fisher, United States). Genome DNA was removed, and reverse transcription was performed using Prime Script RT reagent kit (Takara, Japan), and RT-qPCR was performed using Takara SYBR ® Premix Ex Taq™ II (Takara, Japan) in a 7500 Real Time PCR System (Applied Biosystems, United States). Sequences of primers (Sangon, China) were as follows: β-actin (forward: CATGTA CGTTGCTATCCAGGC, reverse: CTCCTTAATGTCACGCAC GAT), CAT (forward: TGGAGCTGGTAACCCAGTAGG, reverse: CCTTTGCCTTGGAGTATTTGGTA), HMOX1 (forward: AAGACTGCGTTCCTGCTCAAC, reverse: AAA GCCCTACAGCAACTGTCG), and SCD (forward: TCTAGC TCCTATACCACCACCA, reverse: TCGTCTCCAACTTAT CTCCTCC).

Statistical analysis

All experiments were repeated three times. All data were in mean ± SD. GraphPad Prism 7 was used for data analysis and drawing. Results were considered statistically significant when $p < 0.05$.

RESULTS

Cryptotanshinone inhibits H1975 cell proliferation and sensitizes H1975 cell to gefitinib

To investigate the effect of cryptotanshinone (CTS) on chemosensitivity of human lung cancer, the gefitinib-resistant H1975 cells were treated with different concentrations of gefitinib alone or together with CTS. After 72 h of treatment, cell viability reduced significantly under combinatorial treatment of CTS and gefitinib (CTS + Gef) than gefitinib (Gef) alone (**Figures 1A, B**). In addition, cell number reduction was confirmed by microscopic

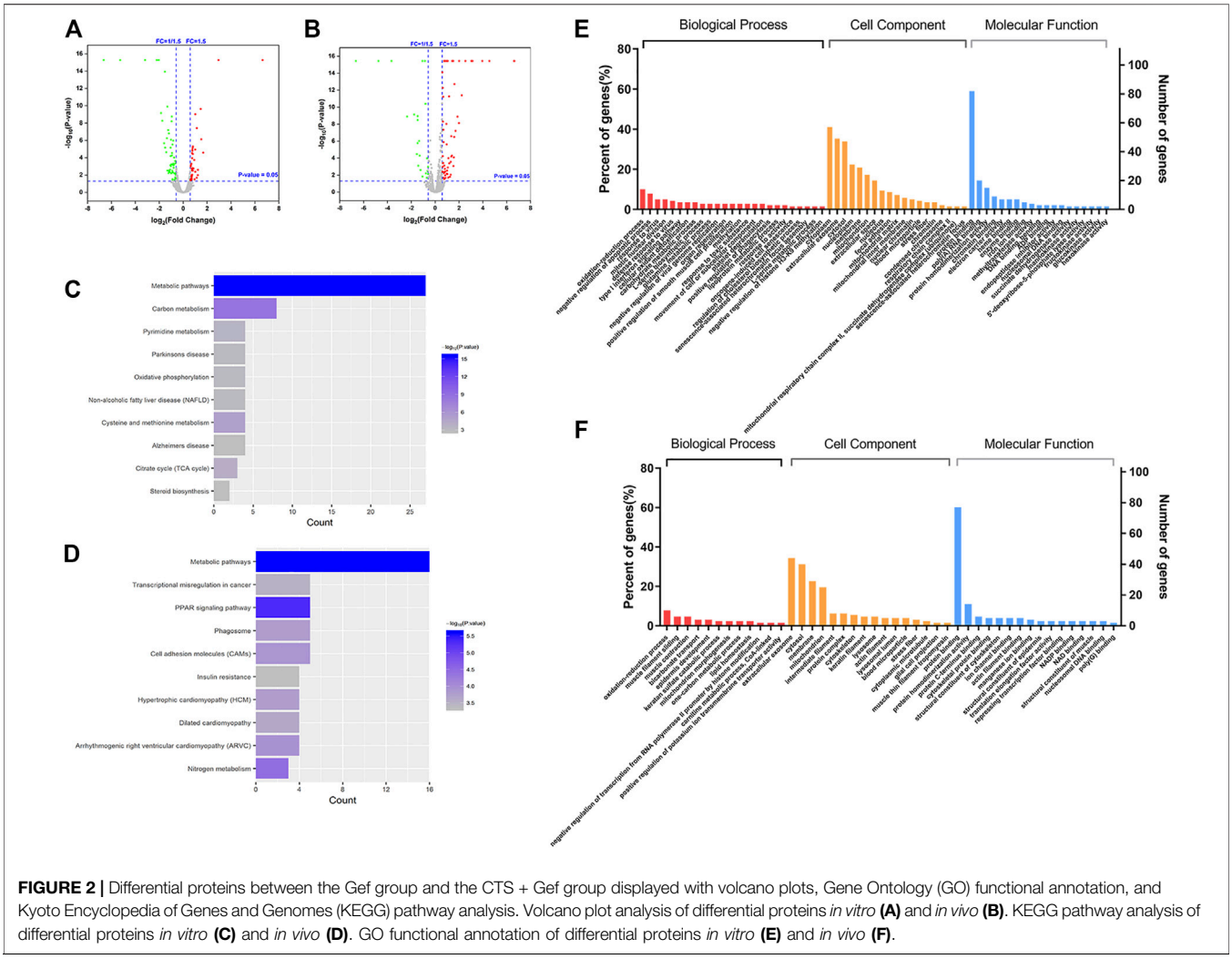

FIGURE 2 | Differential proteins between the Gef group and the CTS + Gef group displayed with volcano plots, Gene Ontology (GO) functional annotation, and Kyoto Encyclopedia of Genes and Genomes (KEGG) pathway analysis. Volcano plot analysis of differential proteins *in vitro* **(A)** and *in vivo* **(B)**. KEGG pathway analysis of differential proteins *in vitro* **(C)** and *in vivo* **(D)**. GO functional annotation of differential proteins *in vitro* **(E)** and *in vivo* **(F)**.

observation (**Figure 1C**). The drug interaction coefficients (CDI) were below 0.8 (<1), indicating that CTS enhanced the sensitivity of H1975 cells to Gef.

To examine the sensitizing effect of CTS *in vivo*, BALB/c mice with H1975 subcutaneous xenograft were established. Although no significant tumor-inhibitory effect could be observed under CTS or Gef treatment, combination of CTS and Gef markedly inhibited tumor growth (**Figures 1D–F**), with 34.59% inhibitory efficiency compared with the Gef group. The Q value is 5.32 (>1.15), indicating a synergistic effect of CTS plus Gef.

Identification of differential proteins under gefitinib and cryptotanshinone combination treatment versus gefitinib monotherapy

In order to identify the differential proteins, cell and tissue samples from the Gef group and the CTS + Gef group were quantitatively analyzed with Nano LC-Q Exactive Plus. Under the criteria of fold change >1.5 or <0.67, totally 115 and 128 differential proteins were detected in cell and tissue samples, respectively (**Figures 2A, B**). There were 58 proteins downregulated and 57 upregulated in cell samples; there were 43 proteins downregulated and 85 upregulated in tissue samples, as listed in the **Supplementary Material**.

Gene Ontology analysis

The differential proteins were annotated with Gene Ontology (GO) functions, with their *p*-value scores. The differential proteins in cell samples between the Gef group and the CTS + Gef group were located primarily in the cytoplasm and extracellular matrix. The main biological activities these proteins were involved in were redox process, blood coagulation process, protein binding, protein homodimerization, and RNA binding (**Figure 2E**). Differential proteins in tissue samples were located primarily in the extracellular matrix and cytoplasm. They were mainly involved in the redox process, muscle contraction, protein binding, and protein homodimerization (**Figure 2F**). Therefore, the differential proteins between the Gef group and the combination group had the most enriched GO terms in redox process and protein binding.

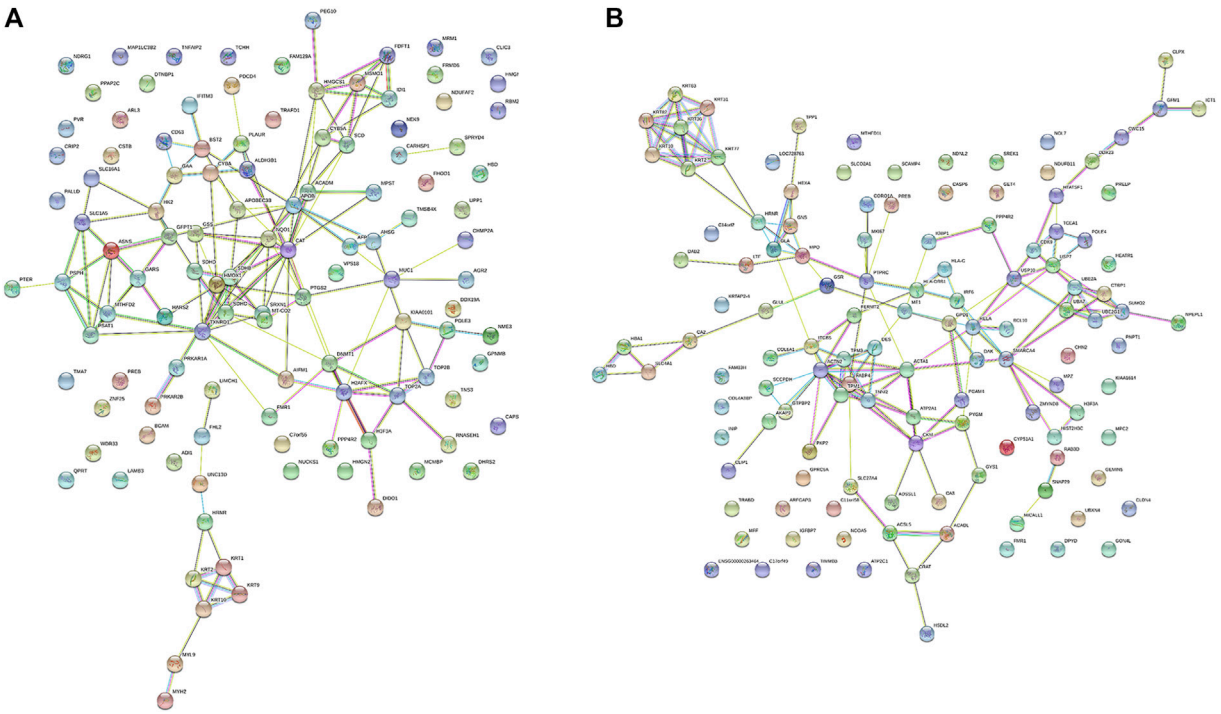

FIGURE 3 | The protein–protein interaction (PPI) network of differential proteins between the Gef group and the CTS + Gef group. The PPI network of differential proteins in H1975 cells **(A)** and tumor tissues **(B)**.

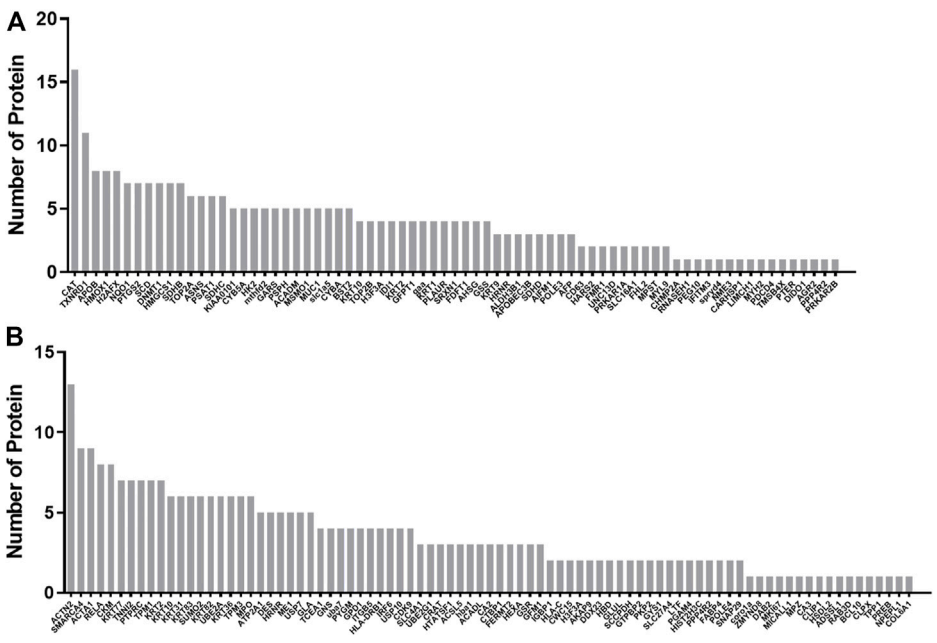

FIGURE 4 | Statistics of interactions with differential proteins from the PPI network. Statistics of interactions with differential proteins in H1975 cells **(A)** and tumor tissues **(B)** from the PPI network.

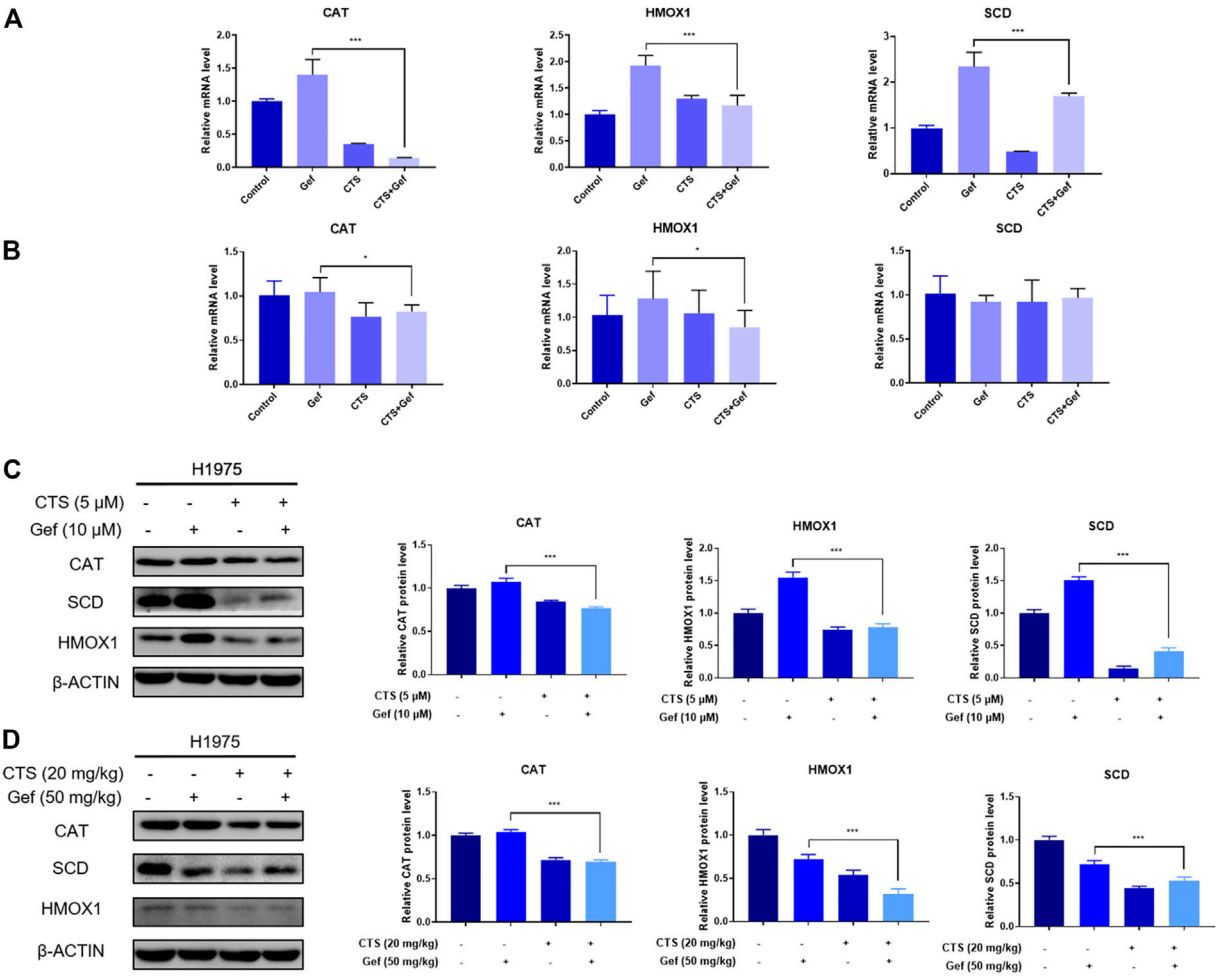

FIGURE 5 | CTS or/and Gef treatment regulated the transcription and expression levels of the differential proteins. **(A,C)** The mRNA **(A)** and protein **(C)** levels of CAT, HMOX1, and SCD in H1975 cells under combination of CTS (5 μM) and Gef (10 μM) compared with Gef (10 μM) for 72 h. **(B,D)** The mRNA **(B)** and protein **(D)** levels of CAT, HMOX1, and SCD in tumor tissues under combination of CTS (20 mg/kg, ip) and Gef (50 mg/kg, ig) compared with Gef (50 mg/kg, ig) for 17 days. Data are represented as the means ± SD (n = 3), and significant differences are indicated as $^{*}p < 0.05$, $^{**}p < 0.01$, and $^{***}p < 0.001$.

Kyoto Encyclopedia of Genes and Genomes pathway analysis

The pathways related to differential proteins were revealed by KEGG pathway analysis. In cell samples, the differential proteins were closely related to metabolic pathways, carbon metabolism, pyrimidine metabolism, oxidative phosphorylation, cysteine and methionine metabolism, and TCA cycle (**Figure 2C**). The differential proteins in tissue samples were closely associated with metabolic pathways, transcriptional misregulation in cancer, PPAR signaling pathways, phagosome, cell adhesion molecules, and nitrogen metabolism (**Figure 2D**). It was deduced that CTS exerts its effect through metabolic pathway change.

Protein–protein interaction network analysis

The protein–protein interaction network among the differential proteins are shown (**Figures 3A,B**), with the number of interacting proteins counted (**Figures 4A,B**). In cell samples, 115 differential proteins constituted a PPI network, which displayed a central cluster with CAT as the core, surrounded by TXNRD1 (thioredoxin reductase 1), HMOX1, NQO1 NAD(P)H (quinone oxidoreductase 1), SCD, and other proteins related to oxidative stress and fatty acid metabolism (**Figure 3A**). In tissue samples, 128 differential proteins also constituted a PPI network, at the core of which was FABP4 (fatty acid-binding protein 4) linked with other proteins related to carbohydrate metabolism and fatty acid metabolism (**Figure 3B**). This comprehensive analysis implied that CTS may enhance Gef sensitivity by impacting the oxidative stress pathway and fatty acid metabolism in cancer cells.

RT-qPCR and Western blot validation of differential proteins

The mRNA levels of differential proteins were examined by RT-qPCR. The *in vitro* mRNA levels of CAT, HMOX1, and SCD were

markedly increased in the Gef group than those in the control, but reduced after combination treatment compared to the Gef group (**Figure 5A**). The *in vivo* mRNA levels of CAT and HMOX1 were significantly reduced with combination treatment than those with Gef, but no significant difference was found in the mRNA level of SCD (**Figure 5B**). Expressions of the differential proteins were verified by Western blot. As expected, the levels of CAT, HMOX1, and SCD in the combination group were significantly lower than those in the Gef group, both *in vitro* and *in vivo* (**Figures 5C, D**). Therefore, combination treatment of CTS and Gef significantly suppressed the expression of CAT, HMOX1, and SCD compared with Gef treatment.

DISCUSSION

The use of traditional herbal medicines in anticancer therapy is a promising strategy to overcome resistance. The active constituent from traditional Chinese medicine *Salvia miltiorrhiza*, CTS, is found with antineoplastic activity and promotes the efficacy of many anticancer drugs (Fu et al., 2020). In this study, we discovered that CTS enhances the sensitivity of H1975 cells to gefitinib. To identify the molecular targets of CTS in H1975, we employed label-free proteomics and found the differential proteins in H1975 cells under gefitinib monotherapy or gefitinib in combination with CTS. Differential proteins *in vitro* and *in vivo* were further grouped into different GO terms and KEGG pathways. Results showed that redox process and protein binding are the most enriched GO terms, and metabolic pathway is the most relevant pathway. In addition, PPI analysis further revealed the interaction network of these differential proteins. Collectively, our study provides a landscape of proteins and their related pathways regulated by CTS in H1975 cells treated with gefitinib.

Core proteins in the PPI network, namely, CAT, HMOX1, and SCD, were chosen and validated by RT-qPCR and Western blot. These proteins exhibit an increase under gefitinib treatment, but show a decrease after a combination of CTS with gefitinib. Thus, we inferred that these proteins may have a causal role in gefitinib resistance and could be the targets in gefitinib-sensitizing effect. Furthermore, since all three validated proteins are enzymes, their activities could be evaluated in future study.

Some differential proteins, such as CAT, TXNRD1, HMOX1, and NQO1, are involved in oxidative stress, while some others, such as SCD and FABP4, are important in fatty acid metabolism. Therefore, we speculated that oxidative stress and fatty acid metabolism are the most affected processes in the sensitizing effect of CTS.

Tumor cells establish an altered redox balance with both increased levels of ROS (reactive oxygen species) and elevated levels of antioxidant proteins than its normal counterparts, making them particularly sensitive to oxidative insults (Moloney and Cotter, 2018). This suggests manipulation of ROS levels to be a promising anticancer strategy. Many studies have confirmed that increasing ROS levels drive oxidative stress-induced cancer cell death. Notably, CTS has been found to induce ROS-dependent cell death in gastric and colon cancer cells (Liu et al., 2017; Xu et al., 2017). These provide evidence that CTS performs its antitumor effect partly by affecting redox homeostasis.

CAT, a heme protein mainly in the peroxisomes of most cells, converts H_2O_2 into H_2O and O_2 in the absence of any cofactors (Reczek and Chandel, 2017). Cancer tissues are reported to have an altered expression level of CAT. Interestingly, CAT was found downregulated in human lung cancer (Ho et al., 2001; Yoo et al., 2008), suggesting that lung cancer cells are sensitive to oxidative stress. Treatment downregulating CAT has been shown efficacious to sensitize breast cancer cells to pro-oxidant therapy (Glorieux and Calderon, 2018). Therefore, CTS may sensitize lung cancer cells to gefitinib by inhibiting CAT.

HMOX1, an enzyme that degrades heme to carbon monoxide, ferrous iron, and biliverdin (Dunn et al., 2014), is highly inducible by stresses and plays a major role in protection against oxidative injuries. Elevated HMOX1 expression is found in a variety of tumors, supporting tumor cell survival, promoting proliferation and angiogenesis, as well as resisting apoptosis (Was et al., 2010). HMOX1 inhibitor suppresses thyroid tumor growth (Yang et al., 2018) and potentiates metformin efficacy in prostate cancer cells (Raffaele et al., 2019). Furthermore, inhibition of HMOX1 can also enhance cancer immunotherapy (Schillingmann et al., 2019). Collectively, inhibition of HMOX1 is a feasible anticancer approach, which could account for the activity of CTS in lung cancer.

Fatty acid metabolic reprogramming in cancer has received increasing notice for their crucial roles as structural membrane components, energy sources, and secondary messengers (Koundouros and Poulogiannis, 2020).

SCD is the enzyme that converts saturated fatty acids to Δ9-monounsaturated fatty acids, implicated in a variety of cancers. Increased expression of SCD is correlated with cancer aggressiveness and poor outcomes in patients (Tracz-Gaszewska and Dobrzyn, 2019). Many SCD inhibitors have been developed and tested preclinically. Blockade of SCD leads to reduced content of unsaturated fatty acids and suppression of NF-κB signaling, thereby restraining ovarian cancer stem cells (Li et al., 2017). Combinatory use of SCD inhibitor reverts resistance of lung cancer stem cells to cisplatin and enhances sensitivity of hepatic cancer cells to sorafenib (Ma et al., 2017; Pisanu et al., 2017).

Fatty acid-binding proteins (FABPs) are a family of highly conserved lipid chaperone molecules with varied functions. One of its members, FABP4, is reported to be overexpressed in cancers, such as prostate and ovarian cancers (Uehara et al., 2014 ; Gharpure et al., 2018), but it is found to suppress cell proliferation in hepatocellular carcinomas and endometrial cancers (Zhong et al., 2018; Wu et al., 2021). The role of FABP4 in cancer is still unclear. FABP4 has been found upregulated by CTS in the tissue sample of our study, and whether CTS enhances gefitinib efficacy through FABP4 remains to be explored.

Many studies have shown that CTS affects redox homeostasis. CTS is reported to induce ROS production, which entails autophagic cell death in A549 lung cancer cells (Hao et al., 2016). It is consistent with our observation that CTS sensitizes H1975 cells to oxidative insults by downregulating the detoxifying enzymes CAT and HMOX1. In our previous study, CTS was found

to reverse cisplatin resistance in human lung carcinoma A549 cells through downregulating the Nrf2 pathway (Xia et al., 2015). Since *HMOX1* is a target gene of Nrf2, a transcription factor responsive to oxidative stress (Bai et al., 2016), it is possible that CTS suppresses HMOX1 expression by downregulating Nrf2. Interestingly, CTS is also found to ameliorate inflammation and oxidative stress by activating the Nrf2-HMOX1 pathway in nontumorous contexts (Wang et al., 2018; Zhou et al., 2019), implying a dual role of CTS in oxidative stress response. However, the dependency of resistant lung cancer on the Nrf2-HMOX1 pathway and CTS effect on this pathway remain to be explored.

CTS is found with a regulatory role in lipid metabolism. Several studies identified that CTS counters diabetes and obesity (Kim et al., 2007), and also attenuates hepatic steatosis (Nagappan et al., 2019) by activation of AMP-activated protein kinase (AMPK), a suppressor of lipogenesis (Kikuchi and Tsukamoto, 2020). We have found that CTS inhibits SCD, involving fatty acid metabolism. Concerning the relationship between SCD and AMPK, a study showed that inhibition of SCD1 in cancer cells promoted the activation of AMPK and the subsequent reduction of glucose-mediated lipogenesis (Scaglia et al., 2009). In addition, an integrated proteomic and metabolomic research on CTS in treating acne showed that CTS remedies abnormalities in unsaturated fatty acid synthetic enzymes and metabolites (Zhu et al., 2021). Therefore, it is possible that CTS modulates lipid and fatty acid metabolism in resistant cancer cells by regulating the SCD and AMPK pathways.

There are some limitations in our study. First, we studied the combination effect of CTS and gefitinib only in H1975 cell line, and whether CTS has a similar effect in other lung cancer cells remains to be further determined. Second, the underlying mechanisms of drug combination were not very clear in this study, and further in-depth research will be carried out to make the result more convincing.

In conclusion, our study offers an insight into the mechanism of CTS in enhancing the sensitivity of H1975 lung cancer cell to gefitinib. Potential target proteins have been identified by proteomics with the expression of three selected proteins validated. Bioinformatics analysis revealed the sensitizing effect of CTS on Gef therapy is associated with oxidative stress and fatty acid metabolism. These findings have clinical implications that combinatory use of CTS may be useful to treat gefitinib- resistant lung cancer.

DATA AVAILABILITY STATEMENT

The data presented in the study are deposited in the PRIDE repository, accession number PXD031533.

ETHICS STATEMENT

The animal study was reviewed and approved by the Animal Ethical and Welfare Committee of Sun Yat-sen University.

AUTHOR CONTRIBUTIONS

PC and JJ conceived the study. PC performed the experiments. PC, DW, GS, and SJ analyzed the data. MH and ZZ contributed the reagents, materials, and analysis tools. PC and GS wrote the manuscript. All authors approved the final submitted version of the manuscript.

FUNDING

This work was supported by the National Natural Science Foundations of China (81973561, 81573658), the Guangdong Provincial Key Laboratory of Construction Foundation (2017B030314030, 2020B1212060034), and the Guangdong Basic and Applied Basic Research Foundation (2019A1515011365).

SUPPLEMENTARY MATERIAL

The Supplementary Material for this article can be found online at: https://www.frontiersin.org/articles/10.3389/fphar.2022.837055/full#supplementary-material

REFERENCES

Ashrafizadeh, M., Zarrabi, A., Orouei, S., Saberifar, S., Salami, S., Hushmandi, K., et al. (2021). Recent Advances and Future Directions in Anti-tumor Activity of Cryptotanshinone: A Mechanistic Review. *Phytother Res.* 35 (1), 155–179. doi:10.1002/ptr.6815

Bai, X., Chen, Y., Hou, X., Huang, M., and Jin, J. (2016). Emerging Role of NRF2 in Chemoresistance by Regulating Drug-Metabolizing Enzymes and Efflux Transporters. *Drug Metab. Rev.* 48 (4), 541–567. doi:10.1080/03602532.2016.1197239

Chou, H. C., Lu, C. H., Su, Y. C., Lin, L. H., Yu, H. I., Chuang, H. H., et al. (2018). Proteomic Analysis of Honokiol-Induced Cytotoxicity in Thyroid Cancer Cells. *Life Sci.* 207, 184–204. doi:10.1016/j.lfs.2018.06.002

Chung-man Ho, J., Zheng, S., Comhair, S. A., Farver, C., and Erzurum, S. C. (2001). Differential Expression of Manganese Superoxide Dismutase and Catalase in Lung Cancer. *Cancer Res.* 61 (23), 8578–8585.

Dunn, L. L., Midwinter, R. G., Ni, J., Hamid, H. A., Parish, C. R., and Stocker, R. (2014). New Insights into Intracellular Locations and Functions of Heme Oxygenase-1. *Antioxid. Redox Signal.* 20 (11), 1723–1742. doi:10.1089/ars.2013.5675

Fu, L., Han, B., Zhou, Y., Ren, J., Cao, W., Patel, G., et al. (2020). The Anticancer Properties of Tanshinones and the Pharmacological Effects of Their Active Ingredients. *Front. Pharmacol.* 11, 193. doi:10.3389/fphar.2020.00193

Gharpure, K. M., Pradeep, S., Sans, M., Rupaimoole, R., Ivan, C., Wu, S. Y., et al. (2018). FABP4 as a Key Determinant of Metastatic Potential of Ovarian Cancer. *Nat. Commun.* 9, 2923. doi:10.1038/s41467-018-04987-y

Glorieux, C., and Calderon, P. B. (2018). Catalase Down-Regulation in Cancer Cells Exposed to Arsenic Trioxide Is Involved in Their Increased Sensitivity to a Pro-oxidant Treatment. *Cancer Cel Int* 18, 24. doi:10.1186/s12935-018-0524-0

Hao, W., Zhang, X., Zhao, W., Zhu, H., Liu, Z. Y., Lu, J., et al. (2016). Cryptotanshinone Induces Pro-death Autophagy through JNK Signaling Mediated by Reactive Oxygen Species Generation in Lung Cancer Cells. *Anticancer Agents Med. Chem.* 16 (5), 593–600. doi:10.2174/1871520615666150907093036

Kikuchi, K., and Tsukamoto, H. (2020). Stearoyl-CoA Desaturase and Tumorigenesis. *Chem. Biol. Interact* 316, 108917. doi:10.1016/j.cbi.2019.108917

Kim, E. J., Jung, S. N., Son, K. H., Kim, S. R., Ha, T. Y., Park, M. G., et al. (2007). Antidiabetes and Antiobesity Effect of Cryptotanshinone via Activation of AMP-Activated Protein Kinase. *Mol. Pharmacol.* 72 (1), 62–72. doi:10.1124/mol.107.034447

Koundouros, N., and Poulogiannis, G. (2020). Reprogramming of Fatty Acid Metabolism in Cancer. *Br. J. Cancer* 122 (1), 4–22. doi:10.1038/s41416-019-0650-z

Li, F., Zhao, D., Yang, S., Wang, J., Liu, Q., Jin, X., et al. (2018). ITRAQ-based Proteomics Analysis of Triptolide on Human A549 Lung Adenocarcinoma Cells. *Cell Physiol Biochem* 45 (3), 917–934. doi:10.1159/000487286

Li, H., Gao, C., Liu, C., Liu, L., Zhuang, J., Yang, J., et al. (2021). A Review of the Biological Activity and Pharmacology of Cryptotanshinone, an Important Active Constituent in Danshen. *Biomed. Pharmacother.* 137, 111332. doi:10.1016/j.biopha.2021.111332

Li, J., Condello, S., Thomes-Pepin, J., Ma, X., Xia, Y., Hurley, T. D., et al. (2017). Lipid Desaturation Is a Metabolic Marker and Therapeutic Target of Ovarian Cancer Stem Cells. *Cell Stem Cell* 20 (3), 303–e5. doi:10.1016/j.stem.2016.11.004

Li, Z., Adams, R. M., Chourey, K., Hurst, G. B., Hettich, R. L., and Pan, C. (2012). Systematic Comparison of Label-free, Metabolic Labeling, and Isobaric Chemical Labeling for Quantitative Proteomics on LTQ Orbitrap Velos. *J. Proteome Res.* 11 (3), 1582–1590. doi:10.1021/pr200748h

Liu, C., Sun, H. N., Luo, Y. H., Piao, X. J., Wu, D. D., Meng, L. Q., et al. (2017). Cryptotanshinone Induces ROS-Mediated Apoptosis in Human Gastric Cancer Cells. *ONCOTARGET* 8 (70), 115398–115412. doi:10.18632/oncotarget.23267

Ma, M. K. F., Lau, E. Y. T., Leung, D. H. W., Lo, J., Ho, N. P. Y., Cheng, L. K. W., et al. (2017). Stearoyl-CoA Desaturase Regulates Sorafenib Resistance via Modulation of ER Stress-Induced Differentiation. *J. Hepatol.* 67 (5), 979–990. doi:10.1016/j.jhep.2017.06.015

Megger, D. A., Bracht, T., Meyer, H. E., and Sitek, B. (2013). Label-free Quantification in Clinical Proteomics. *Biochim. Biophys. Acta* 1834 (8), 1581–1590. doi:10.1016/j.bbapap.2013.04.001

Moloney, J. N., and Cotter, T. G. (2018). ROS Signalling in the Biology of Cancer. *Semin. Cel Dev Biol* 80, 50–64. doi:10.1016/j.semcdb.2017.05.023

Nagano, T., Tachihara, M., and Nishimura, Y. (2018). Mechanism of Resistance to Epidermal Growth Factor Receptor-Tyrosine Kinase Inhibitors and a Potential Treatment Strategy. *Cells* 7 (11). doi:10.3390/cells7110212

Nagappan, A., Kim, J. H., Jung, D. Y., and Jung, M. H. (2019). Cryptotanshinone from the Salvia Miltiorrhiza Bunge Attenuates Ethanol-Induced Liver Injury by Activation of AMPK/SIRT1 and Nrf2 Signaling Pathways. *Int. J. Mol. Sci.* 21 (1). doi:10.3390/ijms21010265

Pisanu, M. E., Noto, A., De Vitis, C., Morrone, S., Scognamiglio, G., Botti, G., et al. (2017). Blockade of Stearoyl-CoA-Desaturase 1 Activity Reverts Resistance to Cisplatin in Lung Cancer Stem Cells. *Cancer Lett.* 406, 93–104. doi:10.1016/j.canlet.2017.07.027

Raffaele, M., Pittalà, V., Zingales, V., Barbagallo, I., Salerno, L., Li Volti, G., et al. (2019). Heme Oxygenase-1 Inhibition Sensitizes Human Prostate Cancer Cells towards Glucose Deprivation and Metformin-Mediated Cell Death. *Int. J. Mol. Sci.* 20 (10). doi:10.3390/ijms20102593

Reczek, C. R., and Chandel, N. S. (2017). The Two Faces of Reactive Oxygen Species in Cancer. *Annu. Rev. Cancer Biol.* 1 (1), 79–98. doi:10.1146/annurev-cancerbio-041916-065808

Scaglia, N., Chisholm, J. W., and Igal, R. A. (2009). Inhibition of stearoylCoA Desaturase-1 Inactivates Acetyl-CoA Carboxylase and Impairs Proliferation in Cancer Cells: Role of AMPK. *PloS one* 4 (8), e6812. doi:10.1371/journal.pone.0006812

Schillingmann, D. A., Riese, S. B., Vijayan, V., Tischer-Zimmermann, S., Schmetzer, H., Maecker-Kolhoff, B., et al. (2019). Inhibition of Heme Oxygenase-1 Activity Enhances Wilms Tumor-1-specific T-Cell Responses in Cancer Immunotherapy. *Int. J. Mol. Sci.* 20 (3). doi:10.3390/ijms20030482

Sharma, S. V., Bell, D. W., Settleman, J., and Haber, D. A. (2007). Epidermal Growth Factor Receptor Mutations in Lung Cancer. *Nat. Rev. Cancer* 7 (3), 169–181. doi:10.1038/nrc2088

Tracz-Gaszewska, Z., and Dobrzyn, P. (2019). Stearoyl-CoA Desaturase 1 as a Therapeutic Target for the Treatment of Cancer. *Cancers (Basel)* 11 (7). doi:10.3390/cancers11070948

Uehara, H., Takahashi, T., Oha, M., Ogawa, H., and Izumi, K. (2014). Exogenous Fatty Acid Binding Protein 4 Promotes Human Prostate Cancer Cell Progression. *Int. J. Cancer* 135 (11), 2558–2568. doi:10.1002/ijc.28903

Wang, W., Wang, X., Zhang, X. S., and Liang, C. Z. (2018). Cryptotanshinone Attenuates Oxidative Stress and Inflammation through the Regulation of Nrf-2 and NF-Kb in Mice with Unilateral Ureteral Obstruction. *Basic Clin. Pharmacol. Toxicol.* 123 (6), 714–720. doi:10.1111/bcpt.13091

Was, H., Dulak, J., and Jozkowicz, A. (2010). Heme Oxygenase-1 in Tumor Biology and Therapy. *Curr. Drug Targets* 11 (12), 1551–1570. doi:10.2174/1389450111009011551

Wong, F. C., Tan, S. T., and Chai, T. T. (2016). Phytochemical-mediated Protein Expression Profiling and the Potential Applications in Therapeutic Drug Target Identifications. *Crit. Rev. Food Sci. Nutr.* 56(Suppl. 1), S162–S170. doi:10.1080/10408398.2015.1045967

Wu, Z., Jeong, J.-H., Ren, C., Yang, L., Ding, L., Li, F., et al. (2021). Fatty Acid-Binding Protein 4 (FABP4) Suppresses Proliferation and Migration of Endometrial Cancer Cells via PI3K/Akt Pathway. *Ott* 14, 3929–3942. doi:10.2147/OTT.S311792

Xia, C., Bai, X., Hou, X., Gou, X., Wang, Y., Zeng, H., et al. (2015). Cryptotanshinone Reverses Cisplatin Resistance of Human Lung Carcinoma A549 Cells through Down-Regulating Nrf2 Pathway. *Cel Physiol Biochem* 37 (2), 816–824. doi:10.1159/000430398

Xu, Z., Jiang, H., Zhu, Y., Wang, H., Jiang, J., Chen, L., et al. (2017). Cryptotanshinone Induces ROS-dependent Autophagy in Multidrug-Resistant colon Cancer Cells. *Chem. Biol. Interact* 273, 48–55. doi:10.1016/j.cbi.2017.06.003

Yang, P. S., Hsu, Y. C., Lee, J. J., Chen, M. J., Huang, S. Y., and Cheng, S. P. (2018). Heme Oxygenase-1 Inhibitors Induce Cell Cycle Arrest and Suppress Tumor Growth in Thyroid Cancer Cells. *Int. J. Mol. Sci.* 19 (9). doi:10.3390/ijms19092502

Yang, Y. Y., Yang, F. Q., and Gao, J. L. (2019). Differential Proteomics for Studying Action Mechanisms of Traditional Chinese Medicines. *Chin. Med.* 14, 1. doi:10.1186/s13020-018-0223-8

Yoo, D. G., Song, Y. J., Cho, E. J., Lee, S. K., Park, J. B., Yu, J. H., et al. (2008). Alteration of APE1/ref-1 Expression in Non-small Cell Lung Cancer: the Implications of Impaired Extracellular Superoxide Dismutase and Catalase Antioxidant Systems. *Lung Cancer* 60 (2), 277–284. doi:10.1016/j.lungcan.2007.10.015

Yu, H. A., Riely, G. J., and Lovly, C. M. (2014). Therapeutic Strategies Utilized in the Setting of Acquired Resistance to EGFR Tyrosine Kinase Inhibitors. *Clin. Cancer Res.* 20 (23), 5898–5907. doi:10.1158/1078-0432.CCR-13-2437

Zhong, C. Q., Zhang, X. P., Ma, N., Zhang, E. B., Li, J. J., Jiang, Y. B., et al. (2018). FABP4 Suppresses Proliferation and Invasion of Hepatocellular Carcinoma Cells and Predicts a Poor Prognosis for Hepatocellular Carcinoma. *Cancer Med.* 7 (6), 2629–2640. doi:10.1002/cam4.1511

Zhou, Y., Wang, X., Ying, W., Wu, D., and Zhong, P. (2019). Cryptotanshinone Attenuates Inflammatory Response of Microglial Cells via the Nrf2/HO-1 Pathway. *Front. Neurosci.* 13, 852. doi:10.3389/fnins.2019.00852

Zhu, Z., Chen, T., Wang, Z., Xue, Y., Wu, W., Wang, Y., et al. (2021). Integrated Proteomics and Metabolomics Link Acne to the Action Mechanisms of Cryptotanshinone Intervention. *Front. Pharmacol.* 12, 700696. doi:10.3389/fphar.2021.700696

Conflict of Interest: The authors declare that the research was conducted in the absence of any commercial or financial relationships that could be construed as a potential conflict of interest.

Publisher's Note: All claims expressed in this article are solely those of the authors and do not necessarily represent those of their affiliated organizations, or those of the publisher, the editors, and the reviewers. Any product that may be evaluated in this article, or claim that may be made by its manufacturer, is not guaranteed or endorsed by the publisher.

frontiers in Oncology

ORIGINAL RESEARCH
published: 11 March 2022
doi: 10.3389/fonc.2022.823491

Knockdown of AKR1C3 Promoted Sorafenib Sensitivity Through Inhibiting the Phosphorylation of AKT in Hepatocellular Carcinoma

Jia Zheng[1†], Zhihong Yang[2†], Yanlei Li[3†], Li Yang[4] and Ruili Yao[2]*

[1] Department of Clinical Medicine, Tangshan Vocational and Technical College, Tangshan, China, [2] Department of Basic Medicine, Tangshan Vocational and Technical College, Tangshan, China, [3] Department of Pathology, Tianjin Medical University, Tianjin, China, [4] Department of Obstetrics and Gynecology, Tangshan Workers' Hospital, Tangshan, China

OPEN ACCESS

Edited by:
Nand K. Roy,
Case Western Reserve University, United States

Reviewed by:
Esra Erdal,
Dokuz Eylul University, Turkey
Zhuo-Xun Wu,
St. John's University, United States

****Correspondence:***
Zhihong Yang
tsyangzhihong@126.com

[†]These authors have contributed equally to this work

Specialty section:
This article was submitted to Pharmacology of Anti-Cancer Drugs, a section of the journal Frontiers in Oncology

Received: *27 November 2021*
Accepted: *31 January 2022*
Published: *11 March 2022*

Citation:
Zheng J, Yang Z, Li Y, Yang L and Yao R (2022) Knockdown of AKR1C3 Promoted Sorafenib Sensitivity Through Inhibiting the Phosphorylation of AKT in Hepatocellular Carcinoma. Front. Oncol. 12:823491. doi: 10.3389/fonc.2022.823491

Background: Sorafenib, which can induce ferroptosis, is a multikinase inhibitor for enhancing survival in advanced hepatocellular carcinoma (HCC). However, a considerable challenge for the treatment of HCC is sorafenib resistance. Therefore, targeting the relationship between sorafenib resistance and ferroptosis genes may provide a novel approach for the treatment of HCC.

Materials and Methods: We analyzed the gene expression and clinicopathological factors from The Cancer Genome Atlas Liver Hepatocellular Carcinoma (TCGA-LIHC), International Cancer Genome Consortium (ICGC), and Gene Expression Omnibus (GEO) databases (GSE109211/GSE62813). The statistical analysis was conducted in R. Cell proliferation was assayed by MTT, cell colony-forming assay, and wound healing assay. Immunofluorescence assay and Western blot were used to evaluate the expression of AKT.

Results: Many ferroptosis-related genes were upregulated in the sorafenib-resistant group. Aldo-keto reductase 1C3 (AKR1C3) was highly expressed in sorafenib-resistant patients, and the high expression of AKR1C3 was associated with the poor prognosis of patients from the TCGA and ICGC databases. MTT and colony-forming assays showing AKR1C3 overexpression enhanced the proliferation of HCC cells and acute sorafenib resistance. Knockdown of AKR1C3 inhibited the proliferation of HCC cells and increased the drug sensitivity of sorafenib. Immunofluorescence assay and Western blot proved that AKR1C3 promoted the phosphorylation of AKT.

Conclusion: AKR1C3 can induce sorafenib resistance through promoting the phosphorylation of AKT in HCC. AKR1C3 inhibitors may be used in conjunction with sorafenib to become a better therapeutic target for HCC.

Keywords: sorafenib, hepatocellular carcinoma, AKR1C3, Akt, drug resistance

INTRODUCTION

According to statistics from the International Cancer Research Center, hepatocellular carcinoma (HCC) is one of the most common malignant tumors and has a high death rate around the world (1). It progresses rapidly and has a poor prognosis. Chemotherapy is still the first treatment option for advanced HCC (2, 3). However, drug resistance often leads to failure of chemotherapy in HCC patients. Further exploration of the molecular mechanism is essential for the discovery of new chemotherapy drugs.

Ferroptosis is a kind of programmed necrosis, which is mainly caused by lipid peroxidation outside the mitochondria and the increase of ferroptosis-dependent ROS. Abnormal iron metabolism and the imbalance of the two main redox systems (lipid peroxidation and thiols) are the main stimulus factors for the production of ROS. Ferroptosis is one of the basic mechanisms of sorafenib in the treatment of HCC. Many factors related to ferroptosis have been shown to be related to liver cancer (4). Retinoblastoma (RB) protein-deficient HCC cells have a two to three times higher mortality rate than cells with normal levels of RB protein. The susceptibility of RB protein-inactivated HCC to ferroptosis is due to the increase in the concentration of reactive oxygen species in the mitochondria, which increases the cells' oxidative stress response (5). Metallothionein-1g (MT-1G) is a new type of negative regulator of ferroptosis in hepatocellular carcinoma. MT-1G gene knockdown increases sorafenib-induced ferroptosis (6).

Aldo-keto reductase 1C3 (AKR1C3) is also known as a member of the human aldo-keto reductase family (7). The human AKR1C family is composed of four enzymes, AKR1C1–4, and AKR1C3, a monomeric, cytosolic, NAD(P) (H)-dependent oxidoreductase, is expressed in the prostate, adrenals, breast, and uterus (8, 9). Many studies have demonstrated that AKR1C3 promoted the metastasis of castration-resistant prostate cancer (10) and colorectal cancer (11). Besides, the role of AKR1C3 in many types of treatment resistance was discovered. Pharmacologic inhibition of AKR1C3 increased cellular doxorubicin content and restored drug DNA binding, cytotoxicity, and subcellular localization (12). AKR1C3 is highly expressed in metastatic and recurrent prostate cancer and in enzalutamide-resistant prostate xenograft tumors. Inhibition of AKR1C3 enzymatic activity resulted in significant inhibition of enzalutamide-resistant tumor growth (13). AKR1C3 inhibitors can overcome abiraterone resistance by reducing endocrine androgen levels and reducing AR transcription activity (14). AKR1C3 mediated doxorubicin resistance through activation of the anti-apoptosis PTEN/Akt pathway *via* PTEN loss (15). AKR1C3 is overexpressed in acute myeloid leukemia and T-cell acute lymphoblastic leukemia (16). The main mechanism of action of AKR1C3 is related to ROS production and oxidative stress signaling pathway Nrf2/antioxidant response element genes (17). Increasing evidence indicates that AKR1C3 expression is a prognostic factor for tumor progression and drug resistance in a variety of malignancies. AKR1C3 inducing sorafenib resistance in hepatocellular carcinoma remains unclear.

Through bioinformatics analysis, our study found the relationship between AKR1C3 and sorafenib resistance and further proved that AKR1C3 downregulation can significantly increase the sensitivity of liver cancer cells to sorafenib. This regulatory effect is likely to be achieved through the phosphorylation of AKT.

METHODS

Bioinformatic Analysis

The microarray datasets GSE109211 (18) and GSE62813 (19) were downloaded from the Gene Expression Omnibus (GEO) database. GSE109211 contains the gene expression data of patients who were sensitive and resistant to sorafenib (21 sorafenib treatment responders and 46 non-responders). The raw data were standardized and analyzed by the R package "limma" from the Bioconductor project. RNA with |log2 fold change (FC)| >1.5 and *P*-value <0.05 is considered a differentially expressed gene (DEG). The online website DAVID (http://david-d.ncifcrf.gov/) was used for gene ontology annotation and KEGG pathway enrichment analysis of DEG. One hundred and twenty-one ferroptosis-related genes are from the website FerrDb. FerrDb-DEG was selected with |log2 multiple change (FC)| >1.5 and *P*-value <0.05. The data were all visualized by the R package "ggplot2." The expression of AKR1C3 in a variety of tumor tissues was validated using the Human Protein Atlas (HPA) database.

Plasmid Construction

Overexpression plasmids for AKR1C3 were obtained by cloning the amplified cDNA into pcDNA3.1 vectors (V79020, Invitrogen, San Diego, USA) and were verified by DNA sequencing (Tsingke, Beijing, China). Short interference RNAs (shRNAs) for AKR1C3 and the corresponding negative controls were purchased from GeneCopoeia (GeneCopoeia, China).

Cell Culture and Transduction

Human hepatoma cell lines Huh7 and HepG2 were obtained from the Chinese Academy of Sciences, Shanghai Institutes for Biological Sciences (Shanghai, China) and cultured in Dulbecco's modified Eagle's medium (DMEM, HyClone, USA). Cells (1×10^5) in six-well plates were incubated for 24 h in a serum-free medium and then underwent transduction with plasmids using Lipofectamine 2000 (Invitrogen, San Diego, USA). After transduction, puromycin (1 μg/ml) was added for the selection.

MTT

Cell proliferation was analyzed by the 3-(4,5-dimethylthiazoleyl)-2,5-diphenyltetrazolium bromide (MTT) assay and performed according to the manufacturer's protocol. HCC cells with different groups were seeded into 96-well plates at 3,000 cells/well and incubated for 48 h. In brief, the medium was removed and 100 μl fresh medium with 10% MTT solution inside was added to each well and incubated at 37°C for 2 h. The absorbance of the samples was measured at 450 nm.

Colony-Forming Assay

Cells (2×10^4) were seeded in six-well plates and incubated for 48 h. The medium was replaced by RPMI-1640 containing 10% serum for 5 days. After washing with cold PBS, the colonies were fixed using 4% polymethanol for 15 min and stained using 0.3% crystal violet solution for 30 min at room temperature.

Wound Healing Assay

Cells (6 × 105/well) were inoculated into six-well plates. After the cells reached 60% confluence, wounds were created. Then, the cells were washed three times in PBS and cultured in complete medium. Phase-contrast microscopy was employed to photograph the wounded area for 0 and 48 h. The percentage of wound closure was calculated by using ImageJ software.

Quantitative Real-Time PCR

TRIzol® reagent (Invitrogen, USA) was used to extract total RNA from cancer cells. RNAs were reversely transcribed into cDNAs by PrimeScript RT reagent kit (TaKaRa, Japan). qRT-PCR was performed using SYBR Prime Script RT-PCR kit (TaKaRa, Japan), and the primer sequences were listed as follows: GAPDH forward, 5′-GGAGCGAGATCCCTCCAAAAT-3′; GAPDH reverse, 5′-GGCTGTTGTCATACTTCTCATGG-3′, AKR1C3 forward, 5′-GGGATCTCAACGAGACAAACG-3′; AKR1C3 reverse, 5′-AAAGGACTGGGTCCTCCAAGA.

Western Blot Analysis

Cells were washed with ice-cold PBS and split with RIPA buffer. Then, cell lysis was quantified by BCA Protein Assay kit (Beijing Solarbio Science & Technology Co., Ltd., China). Twenty-microgram protein samples were subjected to 10% SDS-PAGE and transferred onto PVDF membranes. The membranes were then blocked with 5% non-fat milk for 1.5 h at room temperature. Subsequently, the membranes were incubated with primary antibodies (AKR1C3, ab209899, Abcam, USA, 1:1,000 dilution; p-AKT, #4060, Cell Signaling Technology, USA, 1:500 dilution; AKT, #9272, Cell Signaling Technology, USA, 1:1,000 dilution) overnight at 4°C. β-Actin (AC026, ABclonal, China, 1:1,000 dilution) was used as the loading control. The membranes were washed with TBST and incubated with secondary antibodies conjugated with horseradish peroxidase (HRP) at room temperature for 1 h. Bands were scanned by the enhanced chemiluminescence (ECL) detection system (Thermo Fisher Scientific Inc., Waltham, MA, USA).

Immunofluorescence Assay

HCC cells were washed with PBS, fixed with 5% paraformaldehyde (PFA), and permeabilized in 0.1% Triton X-100. Then, the cells were blocked with 5% BSA for half an hour and incubated overnight at 4°C with p-AKT (1:50 dilution, #4060, Cell Signaling Technology, USA). On the second day, the cells were rewarmed for 30 min and washed with PBS three times. The section with the secondary antibody (Santa Cruz Biotechnology, Santa Cruz, USA) was incubated for 2 h. The nuclei were counterstained with DAPI. Laser confocal scanning microscopy was used to capture the experimental results (Leica TCS-SP5, Germany).

Statistical Analysis

Student's *t*-test was used to compare gene expression between sensitivity and resistance to sorafenib. Proportion differences were compared by chi-square test. The OS between different groups was compared by Kaplan–Meier analysis and log-rank test. All statistical analyses were performed using R software (version 3.5.3) or SPSS (version 23.0). If not specified above, a *P*-value of less than 0.05 is considered statistically significant.

RESULTS

AKR1C3 Was Overexpressed in Sorafenib-Resistant HCCs

To investigate the molecular mechanism of sorafenib resistance in HCC, we explored the GEO database (GSE109211). We identified 1,773 genes with significant upregulation and 1,845 genes with significant downregulation in the sorafenib-sensitive group compared with the sorafenib-resistant group [|log2 fold change (FC)| > 1 and *P*-value < 0.05] (**Figure 1A**). Then, we next analyzed a series of ferroptosis regulators from the FerrDb database (http://www.zhounan.org/ferrdb/). Many ferroptosis-related genes were upregulated in the sorafenib-resistant group compared with those in the sorafenib-sensitive group in the GSE109211 database (**Figure 1B**). We identified 859 genes with significant overexpression and 844 genes reduced significantly in sorafenib-resistant cells of the GSE62813 database [|log2 fold change (FC)| > 1 and *P*-value<0.05] (**Figure 1C**). We made the intersection of the two groups and found 131 genes overexpressed and 52 genes reduced significantly (**Figure 1D**). Through gene enrichment analyzed by KEGG and GO, the results revealed that the pathway associated with ferroptosis was enriched in the sorafenib-resistant group (**Figures 1E, F**).

We found that the mRNA level of AKR1C3 was increased obviously in the resistant HCC (**Figure 1B**). TCGA contains 370 HCC samples that included AKR1C3 expression data and various clinical characteristics. The distribution of AKR1C3 expression and the survival status of HCC patients in TCGA were shown in **Figure 2A**. The K-M survival plots showed that the group with high AKR1C3 expression had poor overall survival rates (*P*-value = 0.0139, **Figure 2B**). The expression of AKR1C3 in HCC samples was higher than that in normal liver tissue (**Figure 2C**). However, increased expression of AKR1C3 was not significantly correlated with tumor histologic grade (**Figure 2D**). Using logistic regression, univariate analysis uncovered a correlation between AKR1C3 and clinical information and pathological stage (**Figure 2E**). The distribution of AKR1C3 expression and the survival status of HCC patients from the International Cancer Genome Consortium (ICGC) database are shown in **Figure 1F**. The survival analyses of AKR1C3 in the ICGC cohort confirmed

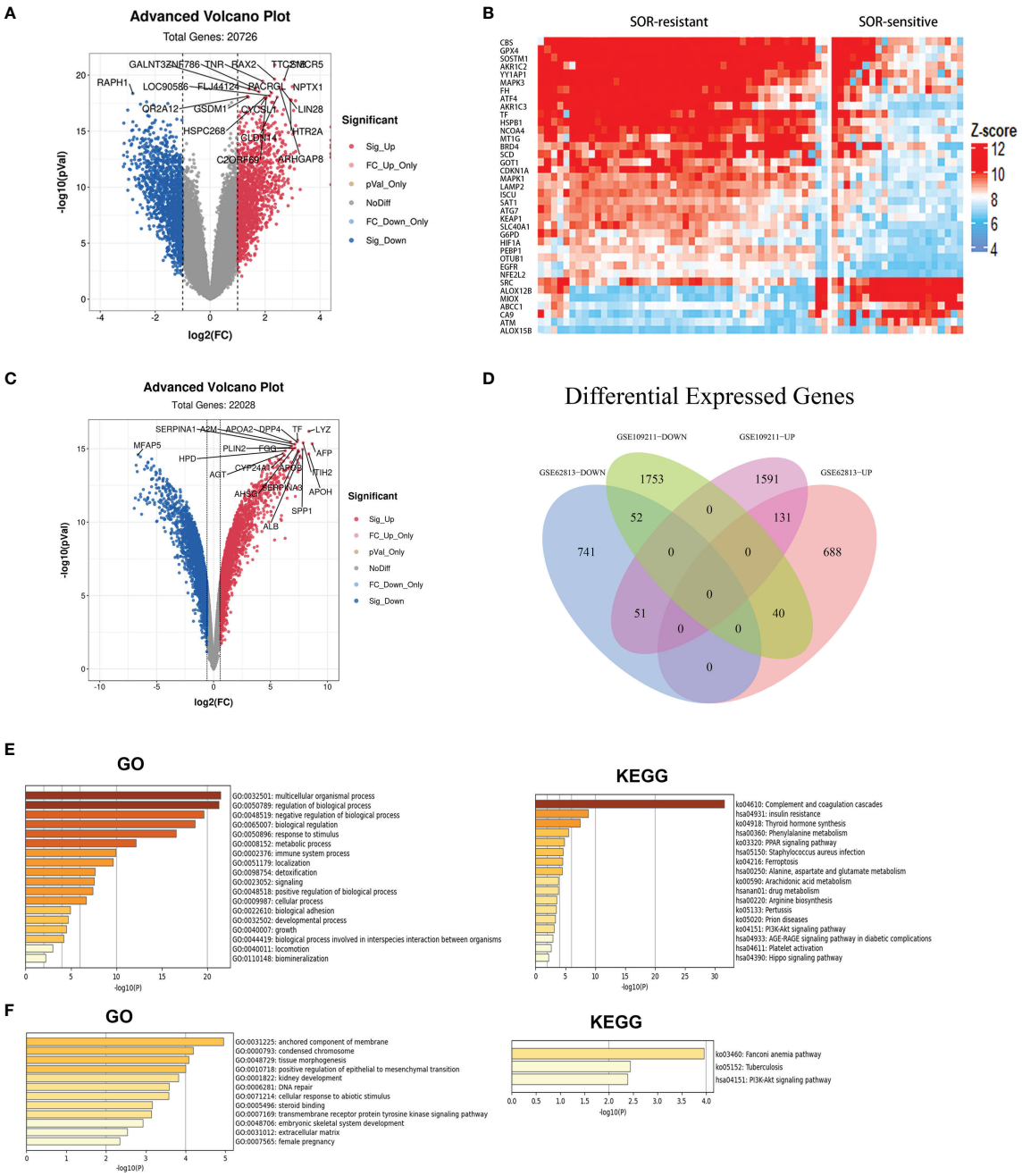

FIGURE 1 | The expression of ferroptosis-related genes between sorafenib-resistant and sorafenib-sensitive patients. **(A)** Different genes in the sorafenib-resistant group and sorafenib-sensitive group from the GEO datasets (GSE109211) were presented in the volcano map. Red dots represent significant overexpression genes and blue dots represent significantly reduced genes. **(B)** Heat maps showing 30 ferroptosis-related genes were overexpressed and 7 ferroptosis-related genes were reduced in sorafenib-resistant patients. **(C)** Different genes in the sorafenib-resistant group and sorafenib-sensitive group from the GSE62813 dataset. **(D)** The Venn diagram of different genes in the GSE109211/GSE62813 datasets. **(E)** KEGG and GO pathway enrichment of overexpression genes. **(F)** KEGG and GO pathway enrichment of genes reduced.

that AKR1C3 was correlated with poor OS in HCC (all adjusted $P < 0.00135$, **Figure 2G**). These results indicated that upregulation of AKR1C3 may be associated with sorafenib resistance in HCC patients and the development of HCC.

AKR1C3 Promotes HCC Cell Proliferation

Several investigations have found that AKR1C3 in cancer cells plays an important role on a more aggressive phenotype. The expression of AKR1C3 in a variety of tumor tissues is shown in

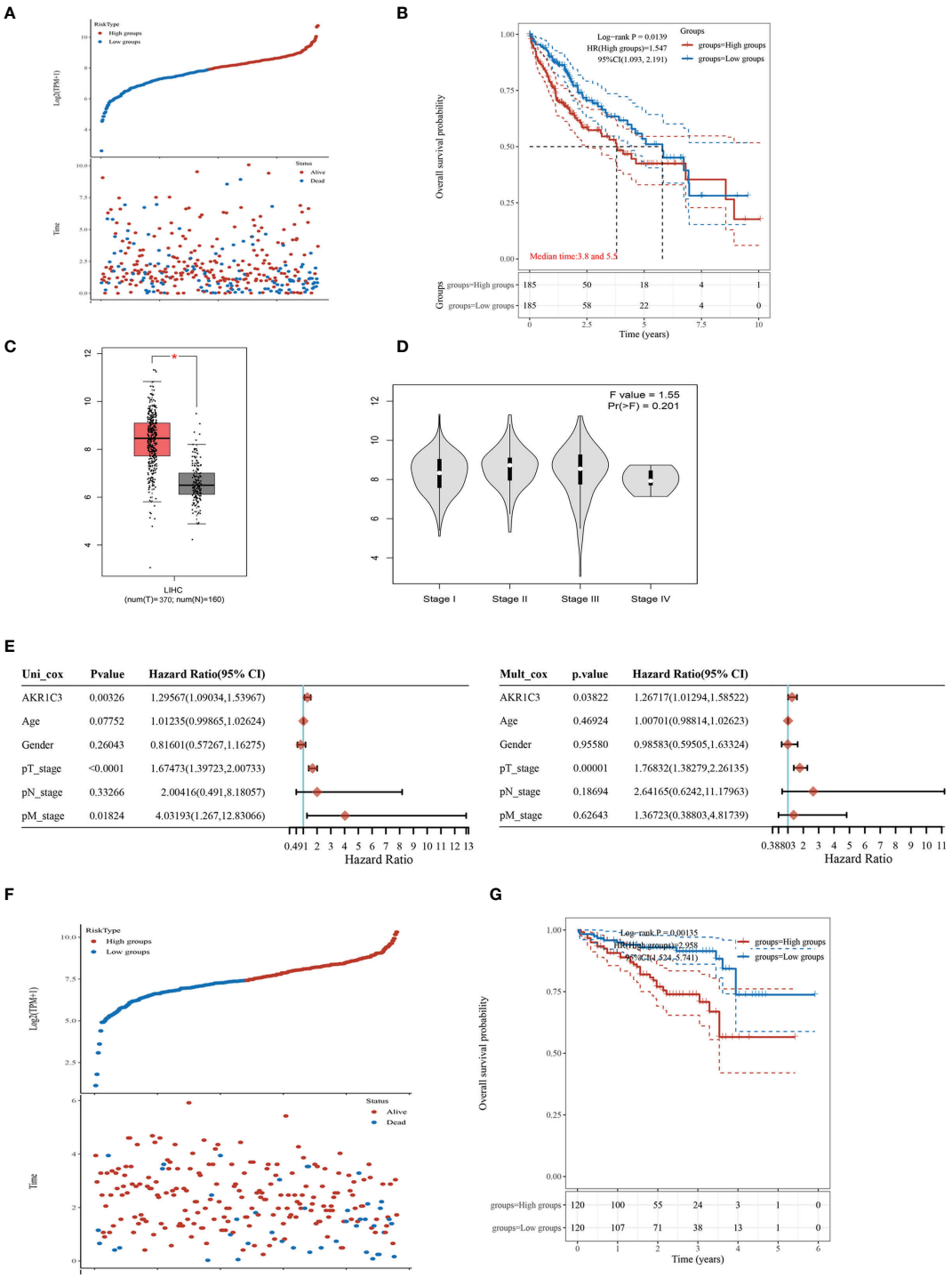

FIGURE 2 | The expression of aldo-keto reductase 1C3 (AKR1C3) in liver hepatocellular carcinoma (LIHC). **(A)** AKR1C3 expression distribution and survival status based on The Cancer Genome Atlas (TCGA). **(B)** Survival analysis of AKR1C3 in LIHC based on the TCGA data. **(C)** The mRNA expression of AKR1C3 between normal and tumor tissues in TCGA. **(D)** Expression of AKR1C3 correlated with clinical stage. **(E)** Correlation between overall survival and multivariable characteristics in TCGA patients *via* Cox regression and multivariate survival model. **(F)** AKR1C3 expression distribution and survival status in the ICGC. **(G)** Survival analysis of AKR1C3 in LIHC based on the ICGC data. Data are presented as mean ± SD and are representative of three independent experiments. *$P < 0.05$.

Figure 3A. From the HPA database, we also observed that AKR1C3 was mainly expressed in the cytoplasm and nucleus in HCC tissues (**Figure 3B**). HepG2 and Huh7 cells were transfected with AKR1C3 overexpressed plasmids, and transfection efficiency was detected by qPCR and Western blot (**Figures 3C, F**). It was found that compared with control, the overexpression of AKR1C3 increased liver cancer cell proliferation using the MTT assay (**Figure 3I**). We knockdown the AKR1C3 gene in HepG2 and Huh7 cells with three candidate lentivirus-harboring shRNAs (shRNA-1, shRNA-2, and shRNA-3). qPCR and Western blot were also used to confirm the effects of AKR1C3 knockdown on liver cancer cells, and the highest knockdown effectiveness was chosen for the subsequent experiments (**Figures 3D, E, G, H**). We noticed that, compared with the control group, the knockdown of AKR1C3 decreased the proliferation ability of HepG2 and Huh7 cells in MTT (**Figure 3J**). In the cell colony-forming assays and wound healing assays (**Figures 4A–D**), AKR1C3 overexpression in HCC cells increased the numbers of colony-forming cells and the cells' migration ability. AKR1C3 knockdown in HCC cells suppressed the colony-forming and the migration ability of the cells. Together, these findings suggested that AKR1C3 might be mechanistically important for cell growth and migration.

Knockdown of AKR1C3 Enhances Sorafenib Sensitivity in HCC Cells

To evaluate whether AKR1C3 is related to sorafenib sensitivity in HCC cells, we generated a series of expression about cell proliferation. To determine this, we treated HepG2 and Huh7 cells with 0, 5, 10, 15, and 20 μM sorafenib for 48 h, and these cells included AKR1C3 overexpressed or AKR1C3 knockdown cells and the corresponding control groups. We observed that AKR1C3 overexpression significantly increased cell viability to resist sorafenib in the MTT and cell colony-forming assays (**Figures 5A, B**) and enhanced cell migration in the wound healing assays (**Figure 5C**). Meanwhile, the MTT and cell colony-forming assays showed that AKR1C3 knockdown can significantly suppress the proliferation of liver cancer cells treated with 10 μM sorafenib for 48 h (**Figures 5D, E**). In the sorafenib treatment group, downregulation of AKR1C3 significantly reduced cell migration in the wound healing assays (**Figure 5F**). Together, these findings demonstrate that knockdown of AKR1C3 in liver cancer cells induced sensitivity toward sorafenib treatment.

AKR1C3 Influences Sorafenib Sensitivity Through AKT Phosphorylation in Liver Cancer Cells

Previous studies have shown that AKR1C3 promoted tumor proliferation and may be correlated with the phosphorylation of AKT (20, 21). We found that the mRNA level of AKT was upregulated obviously in sorafenib-resistant patients compared with sorafenib-sensitive patients (**Figure 6A**). To confirm the protein expression of AKT and p-AKT in liver cancer cells, we first performed a Western blot. The results indicated that there was no significant change in the expression of total AKT, when AKR1C3 was overexpressed in liver cancer cells (**Figure 6B**), while that of p-AKT was upregulated significantly in overexpressed AKR1C3 cells and in AKR1C3 overexpression cells with 10 μM sorafenib (**Figure 6B**). Immunofluorescence staining further showed that the fluorescence intensity of p-AKT was increased in overexpressed AKR1C3 cells in the nucleus and cytoplasm (**Figure 6C**). Moreover, AKR1C3 in HepG2 cells with 10 μM sorafenib can promote the expression of p-AKT (**Figure 6C**). To further explore the role of p-AKT in AKR1C3 resistance to sorafenib, we performed MTT experiments with a p-AKT inhibitor (AZD5363). The efficiency of the p-AKT inhibitor was detected by Western blot (**Figure 6D**). We treated HepG2 cells (control, overexpressing AKR1C3) with or without 5 nM AZD5363 for 72 h. All cells were treated with 10 μM sorafenib and then the MTT assay was performed. It was found that AZD5363 can significantly reduce cell proliferation caused by AKR1C3 overexpression in HepG2 cells (**Figure 6E**). Based on these findings, we concluded that AKR1C3 enhanced the resistance of sorafenib by increasing the expression of p-AKT in HCC cells.

DISCUSSION

Most patients with liver cancer are diagnosed when the progress is already at advanced stages or when cancer has already metastasized. During this time, surgery is difficult to achieve sufficient curative effect, and the prognosis is very poor. Sorafenib is the only drug approved by the FDA for advanced liver cancer, but due to its frequent drug resistance, it can only extend the survival period by 2.8 months, which is far from meeting the needs of the patients (22). Therefore, it is urgent to find the resistance mechanism of sorafenib to better extend the survival period of patients.

Sorafenib can induce ferroptosis and exert antitumor effects. Some studies have found that some pathways can resist ferroptosis induced by sorafenib. For example, the p62/Keap1/NRF2 pathway can directly regulate the expression of ferroptosis genes to inhibit ferroptosis caused by sorafenib in HCC (23). The oxidative stress molecules MTIG, TXNRD1, MTHFD1L, and NADPH have all been shown to be related to ferroptosis (24, 25). It is reported that FGF19/FGFR4 inhibits sorafenib-induced ROS production and apoptosis (26), and FGF19/FGFR4 is the upstream of NRF2 (27). In our experiment, a dataset of patients with sorafenib treatment was used. Based on the DEGs between different response groups, we performed GO and KEGG analyses. We discovered that oxidative stress, energy metabolism, and ferroptosis pathways were enriched in the sorafenib-resistant group (**Figures 1E, F**). Many ferroptosis-related genes were upregulated in the sorafenib-resistant group, which may be related to the high metabolic level of tumors. Tumors with high malignancy and poor prognosis tend to have higher metabolic levels.

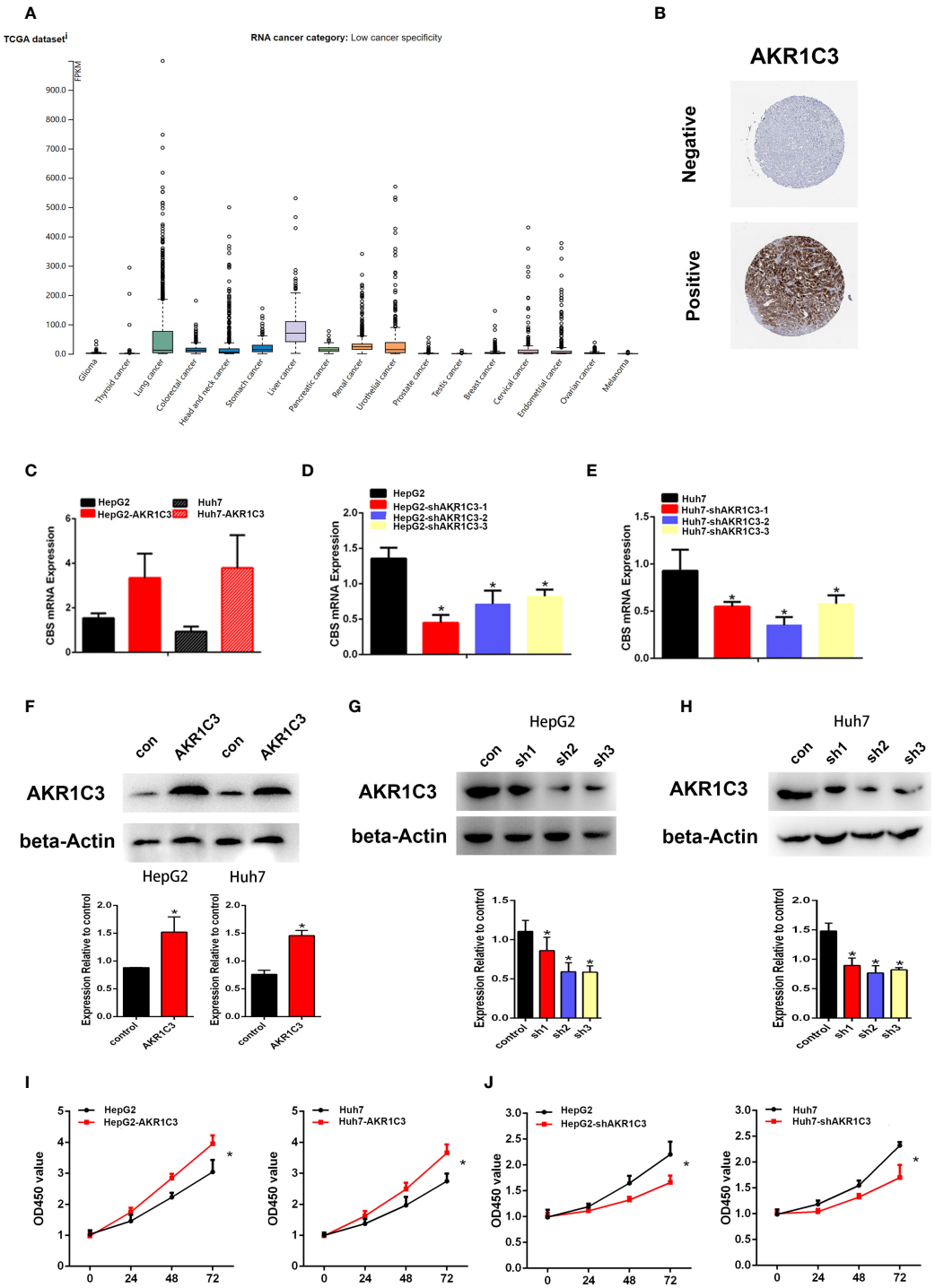

FIGURE 3 | The expression of AKR1C3 in different types of tumor tissues. **(A)** The protein level of AKR1C3 in different types of tumor tissues from the HPA database. **(B)** The expression of AKR1C3 in LIHC was presented by immunohistochemistry from the HPA. **(C)** The overexpression effects of AKR1C3 in HepG2 and Huh7 cells were measured by qRT-PCR. **(D, E)** The knockdown effects of AKR1C3 in HepG2 and Huh7 cells were measured by qRT-PCR. **(F)** The overexpression effects of AKR1C3 in HepG2 and Huh7 cells were measured by Western blot. **(G, H)** The knockdown effects of AKR1C3 in HepG2 and Huh7 cells were measured by Western blot. **(I, J)** The viability of HepG2 and Huh7 cells was measured by the MTT assay. Data are presented as mean ± SD and are representative of three independent experiments. *$P < 0.05$.

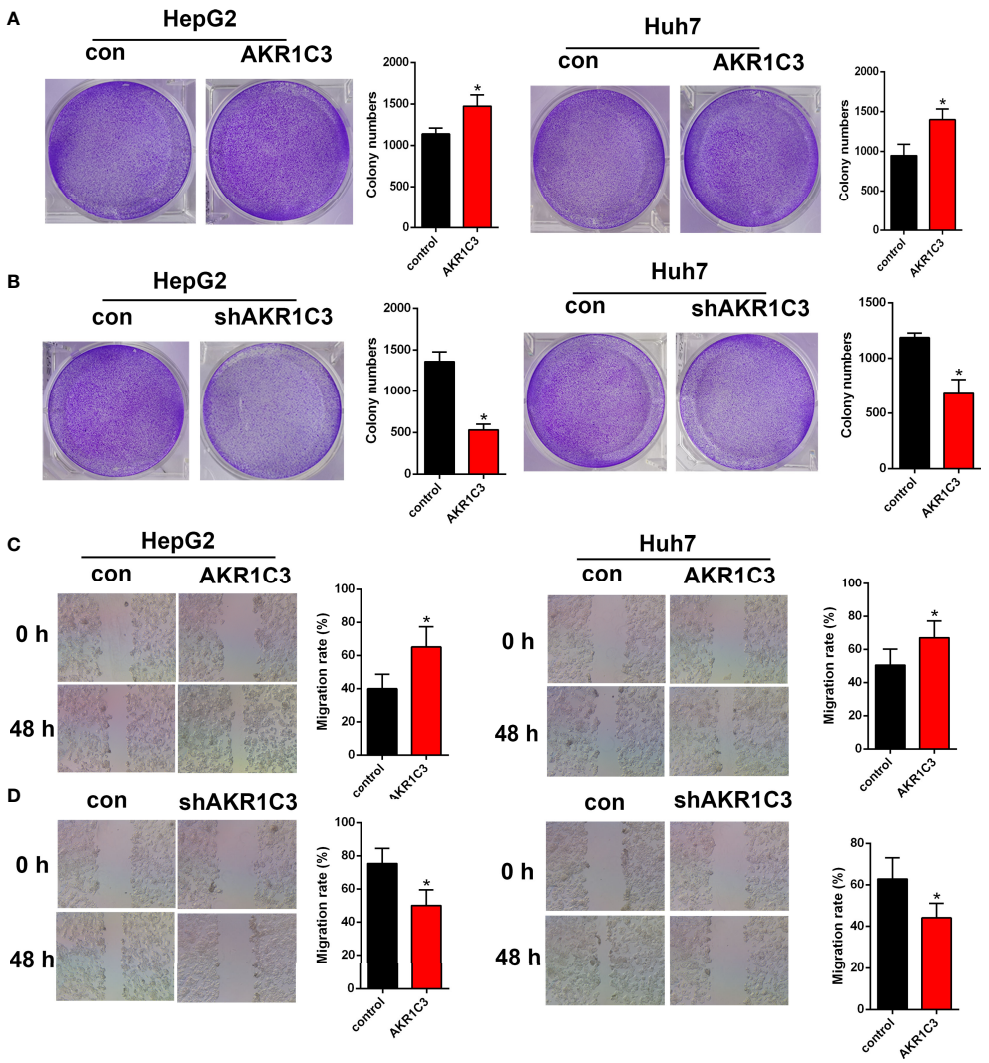

FIGURE 4 | The effect of AKR1C3 on cell proliferative activity. **(A, B)** Colony formation assays in HepG2 and Huh7 cells transfected with AKR1C3 overexpression plasmids and AKR1C3 knockdown plasmids. **(C, D)** The migration of HepG2 and Huh7 cells transfected with AKR1C3 overexpression plasmids and AKR1C3 knockdown plasmids was detected by wound healing assays. Data are presented as mean ± SD and are representative of three independent experiments. *$P < 0.05$.

Current studies have proven that the AKR1C family is used as NADPH-dependent 3-, 17-, and 20-ketosteroid reductases, and different types have strong substrate specificity. AKR1C3 is mainly involved in cell proliferation and differentiation in a hormone-independent manner (28). The expression of AKR1C3, as a radioresistance-associated gene, is associated with various diseases, such as breast cancer (29), PC (30), esophageal cancer (31), and non-small cell lung cancer (NSCLC) (32). In our experiments, downregulation of AKR1C3 restrained cell proliferation and increased the sensitivity of liver cancer cells to sorafenib, and upregulation of AKR1C3 increased cell proliferation in HCC cells. Hepatocellular carcinoma displays a high degree of hypoxia (33) and expresses high levels of AKR1C3 (34). PR-104 is activated by reductases under hypoxia or by AKR1C3 to form cytotoxic nitrogen mustards. A previous study evaluated the safety and efficacy of PR-104 plus sorafenib in HCC. However, because of the compromised clearance of PR-104A and the clinically significant toxicities (thrombocytopenia mainly and neutropenia), the study was discontinued (35). Our results demonstrated that the PI3K–AKT signaling pathway was enriched in sorafenib resistance groups and overexpression of AKR1C3 in HCC cells can activate AKT. The activation of the AKT signal was often shown to be related to the treatment outcome, and it has been observed that it leads to resistance to chemotherapy and radiation therapy (36, 37). AKT phosphorylation was regulated by AKR1C3 and might be responsible for eliminating over-produced ROS in esophageal adenocarcinoma (EAC) cells (20). The intracellular ROS levels were induced by cadmium treatment. In addition, cadmium elicited the AKR1C3 expression which partially passed through

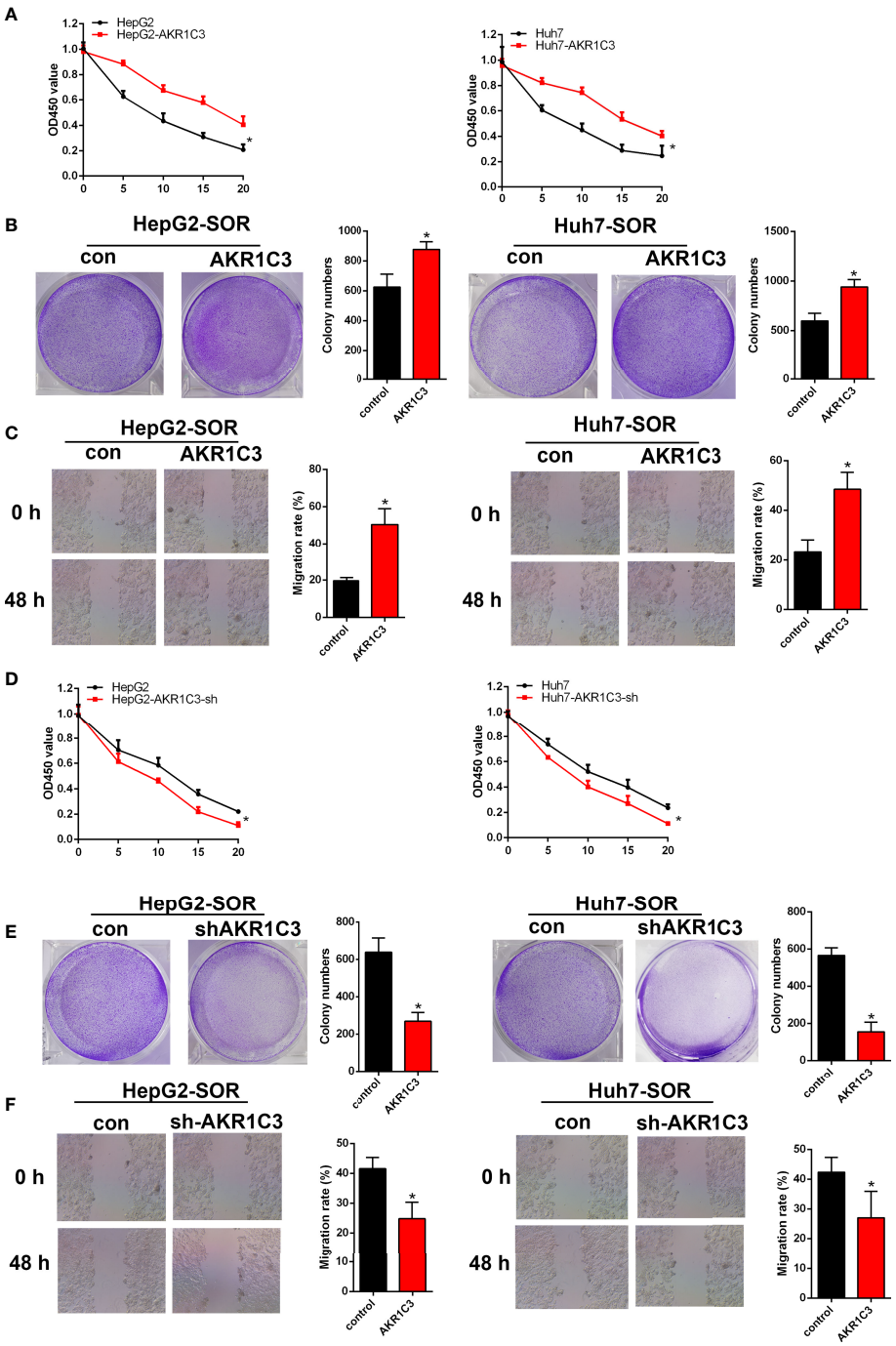

FIGURE 5 | AKR1C3 enhances sorafenib resistance in HCC cells. **(A)** The viability of AKR1C3 overexpression cells after being treated with sorafenib (0, 5, 10, 15, and 20 μM) was measured by the MTT assay. **(B)** Colony formation assays in AKR1C3 overexpression cells treated with sorafenib (10 μM). **(C)** Wound healing assays in AKR1C3 overexpression cells treated with sorafenib (10 μM). **(D)** The viability of AKR1C3 knockdown cells after being treated with sorafenib (0, 5, 10, 15, and 20 μM) was measured by the MTT assay. **(E)** Colony formation assays in AKR1C3 knockdown cells treated with sorafenib (10 μM). **(F)** Wound healing assays in AKR1C3 knockdown cells treated with sorafenib (10 μM). Data are presented as mean ± SD and are representative of three independent experiments. *$P < 0.05$.

the activation of PI3K (21). AKR1C3-mediated DOX resistance might result from the activation of anti-apoptosis PTEN/Akt pathway *via* PTEN loss in breast cancer (15). Overexpression of AKR1C3 to eliminate reactive oxygen species (ROS) allows the continuous activation of the AKT pathway in tumor cells upregulated by AKR1C3, thereby reducing cell apoptosis. Whether AKT is a direct target of AKR1C3 in HCC, we will further design experiments to confirm this speculation.

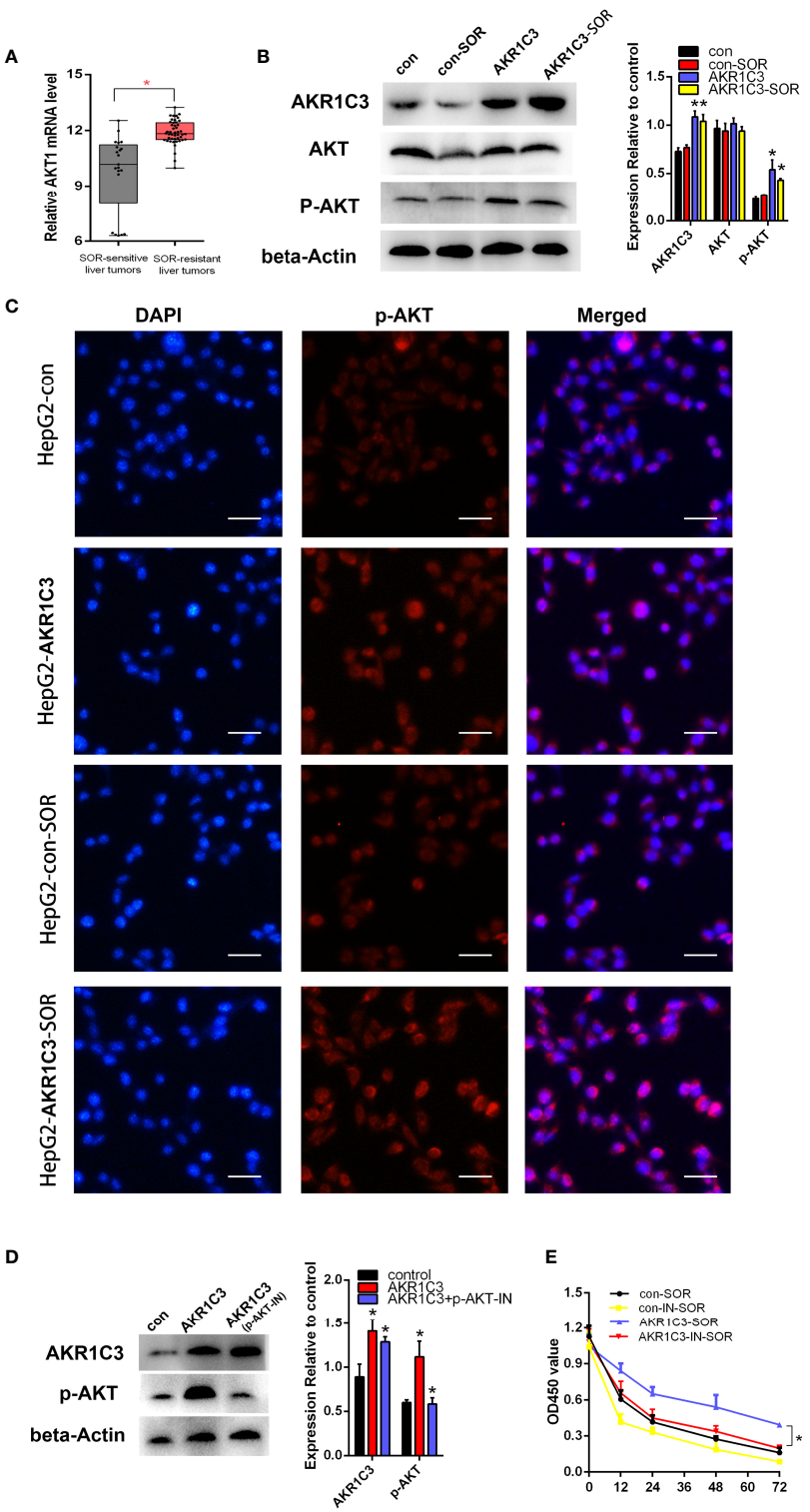

FIGURE 6 | AKR1C3 promoted sorafenib resistance through AKT phosphorylation in liver cancer cells. **(A)** The mRNA expression level of AKT in sorafenib-sensitive (n = 21) and sorafenib-resistant (n = 46) patients. **(B)** The protein levels of AKR1C3, AKT, and p-AKT in HepG2 cells (control group and AKR1C3 overexpression group) treated with or without sorafenib (10 μM). **(C)** Immunostaining images of p-AKT in HepG2 cells (AKR1C3 overexpression group and control group) treated with sorafenib (10 μM) or without sorafenib; scale bars, 50 μm. **(D)** The efficiency of the p-AKT inhibitor was detected by Western blot. **(E)** The MTT assay of HepG2 cells (control, overexpressing AKR1C3) with or without 5 nM AZD5363 for 72 h. Data are presented as mean ± SD and are representative of three independent experiments. *P < 0.05.

In summary, we found that AKR1C3 expression was induced obviously in the sorafenib-resistant group and knockdown of AKR1C3 suppressed p-Akt protein levels, ultimately leading to the decrease of HCC cell proliferation. In this respect, elucidating AKR1C3 might be a promising strategy for improving responses to sorafenib and overcoming drug resistance.

DATA AVAILABILITY STATEMENT

The datasets presented in this study can be found in online repositories. The names of the repository/repositories and accession number(s) can be found in the article/**Supplementary Material**.

AUTHOR CONTRIBUTIONS

ZY and JZ designed the research studies. ZY, JZ, LY, and RY contributed to the methodology. YL acquired the data. JZ, LY, and RY were responsible for the formal analysis. ZY wrote the original draft of the manuscript. ZY acquired funding. All authors contributed to the article and approved the submitted version.

FUNDING

This work was financially sponsored by grants from the Tangshan Talent Funding Project A202010008.

REFERENCES

1. Jemal A, Bray F, Center MM, Ferlay J, Ward E, Forman D. Global Cancer Statistics. *CA: Cancer J Clin* (2011) 61:69–90. doi: 10.3322/caac.20107
2. Beste LA, Leipertz SL, Green PK, Dominitz JA, Ross D, Ioannou GN. Trends in Burden of Cirrhosis and Hepatocellular Carcinoma by Underlying Liver Disease in US Veterans, 2001-2013. *Gastroenterology* (2015) 149:1471–82.e1475; quiz e1417–78. doi: 10.1053/j.gastro.2015.07.056
3. Walker M, El-Serag HB, Sada Y, Mittal S, Ying J, Duan Z, et al. Cirrhosis Is Under-Recognised in Patients Subsequently Diagnosed With Hepatocellular Cancer. *Aliment Pharmacol Ther* (2016) 43:621–30. doi: 10.1111/apt.13505
4. Mou Y, Wang J, Wu J, He D, Zhang C, Duan C, et al. Ferroptosis, a New Form of Cell Death: Opportunities and Challenges in Cancer. *J Hematol Oncol* (2019) 12:34. doi: 10.1186/s13045-019-0720-y
5. Louandre C, Marcq I, Bouhlal H, Lachaier E, Godin C, Saidak Z, et al. The Retinoblastoma (Rb) Protein Regulates Ferroptosis Induced by Sorafenib in Human Hepatocellular Carcinoma Cells. *Cancer Lett* (2015) 356:971–7. doi: 10.1016/j.canlet.2014.11.014
6. Nie J, Lin B, Zhou M, Wu L, Zheng T. Role of Ferroptosis in Hepatocellular Carcinoma. *J Cancer Res Clin Oncol* (2018) 144:2329–37. doi: 10.1007/s00432-018-2740-3
7. Endo S, Oguri H, Segawa J, Kawai M, Hu D, Xia S, et al. Development of Novel AKR1C3 Inhibitors as New Potential Treatment for Castration-Resistant Prostate Cancer. *J Med Chem* (2020) 63:10396–411. doi: 10.1021/acs.jmedchem.0c00939
8. Lin HK, Jez JM, Schlegel BP, Peehl DM, Pachter JA, Penning TM. Expression and Characterization of Recombinant Type 2 3 Alpha-Hydroxysteroid Dehydrogenase (HSD) From Human Prostate: Demonstration of Bifunctional 3 Alpha/17 Beta-HSD Activity and Cellular Distribution. *Mol Endocrinol* (1997) 11:1971–84. doi: 10.1210/mend.11.13.0026
9. Yepuru M, Wu Z, Kulkarni A, Yin F, Barrett CM, Kim J, et al. Steroidogenic Enzyme AKR1C3 Is a Novel Androgen Receptor-Selective Coactivator That Promotes Prostate Cancer Growth. *Clin Cancer Res* (2013) 19:5613–25. doi: 10.1158/1078-0432.CCR-13-1151
10. Zhao J, Zhang M, Liu J, Liu Z, Shen P, Nie L, et al. AKR1C3 Expression in Primary Lesion Rebiopsy at the Time of Metastatic Castration-Resistant Prostate Cancer Is Strongly Associated With Poor Efficacy of Abiraterone as a First-Line Therapy. *Prostate* (2019) 79:1553–62. doi: 10.1002/pros.23875
11. Nakarai C, Osawa K, Akiyama M, Matsubara N, Ikeuchi H, Yamano T, et al. Expression of AKR1C3 and CNN3 as Markers for Detection of Lymph Node Metastases in Colorectal Cancer. *Clin Exp Med* (2015) 15:333–41. doi: 10.1007/s10238-014-0298-1
12. Heibein AD, Guo B, Sprowl JA, Maclean DA, Parissenti AM. Role of Aldo-Keto Reductases and Other Doxorubicin Pharmacokinetic Genes in Doxorubicin Resistance, DNA Binding, and Subcellular Localization. *BMC Cancer* (2012) 12:381. doi: 10.1186/1471-2407-12-381
13. Liu C, Lou W, Zhu Y, Yang JC, Nadiminty N, Gaikwad NW, et al. Intracrine Androgens and AKR1C3 Activation Confer Resistance to Enzalutamide in Prostate Cancer. *Cancer Res* (2015) 75:1413–22. doi: 10.1158/0008-5472.CAN-14-3080
14. Liu C, Armstrong CM, Lou W, Lombard A, Evans CP, Gao AC. Inhibition of AKR1C3 Activation Overcomes Resistance to Abiraterone in Advanced Prostate Cancer. *Mol Cancer Ther* (2017) 16:35–44. doi: 10.1158/1535-7163.MCT-16-0186
15. Zhong T, Xu F, Xu J, Liu L, Chen Y. Aldo-Keto Reductase 1C3 (AKR1C3) Is Associated With the Doxorubicin Resistance in Human Breast Cancer *via* PTEN Loss. *Biomed Pharmacother = Biomed Pharmacother* (2015) 69:317–25. doi: 10.1016/j.biopha.2014.12.022
16. Verma K, Zang T, Penning TM, Trippier PC. Potent and Highly Selective Aldo-Keto Reductase 1C3 (AKR1C3) Inhibitors Act as Chemotherapeutic Potentiators in Acute Myeloid Leukemia and T-Cell Acute Lymphoblastic Leukemia. *J Med Chem* (2019) 62:3590–616. doi: 10.1021/acs.jmedchem.9b00090
17. Liu Y, He PC, Chen PC, Liu PC, Feng PC, Liu PC, et al. Overview of AKR1C3: Inhibitor Achievements and Disease Insights. *J Med Chem* (2020) 63:11305–29. doi: 10.1021/acs.jmedchem.9b02138
18. Pinyol R, Montal R, Bassaganyas L, Sia D, Takayama T, Chau GY, et al. Molecular Predictors of Prevention of Recurrence in HCC With Sorafenib as Adjuvant Treatment and Prognostic Factors in the Phase 3 STORM Trial. *Gut* (2019) 68:1065–75. doi: 10.1136/gutjnl-2018-316408
19. van Malenstein H, Dekervel J, Verslype C, Van Cutsem E, Windmolders P, Nevens F, et al. Long-Term Exposure to Sorafenib of Liver Cancer Cells Induces Resistance With Epithelial-to-Mesenchymal Transition, Increased Invasion and Risk of Rebound Growth. *Cancer Lett* (2013) 329:74–83. doi: 10.1016/j.canlet.2012.10.021
20. Zhou C, Wang Z, Li J, Wu X, Fan N, Li D, et al. Aldo-Keto Reductase 1C3 Mediates Chemotherapy Resistance in Esophageal Adenocarcinoma *via* ROS Detoxification. *Cancers* (2021) 13 (10):2403. doi: 10.3390/cancers13102403
21. Lee YJ, Lee GJ, Baek BJ, Heo SH, Won SY, Im JH, et al. Cadmium-Induced Up-Regulation of Aldo-Keto Reductase 1C3 Expression in Human Nasal Septum Carcinoma RPMI-2650 Cells: Involvement of Reactive Oxygen Species and Phosphatidylinositol 3-Kinase/Akt. *Environ Toxicol Pharmacol* (2011) 31:469–78. doi: 10.1016/j.etap.2011.03.006
22. Llovet JM, Ricci S, Mazzaferro V, Hilgard P, Gane E, Blanc JF, et al. Sorafenib in Advanced Hepatocellular Carcinoma. *N Engl J Med* (2008) 359:378–90. doi: 10.1056/NEJMoa0708857
23. Sun X, Ou Z, Chen R, Niu X, Chen D, Kang R, et al. Activation of the P62-Keap1-NRF2 Pathway Protects Against Ferroptosis in Hepatocellular Carcinoma Cells. *Hepatology* (2016) 63:173–84. doi: 10.1002/hep.28251
24. Lee D, Xu IM, Chiu DK, Lai RK, Tse AP, Lan , Li L, et al. Folate Cycle Enzyme MTHFD1L Confers Metabolic Advantages in Hepatocellular Carcinoma. *J Clin Invest* (2017) 127:1856–72. doi: 10.1172/JCI90253
25. Lee D, Xu IM, Chiu DK, Leibold J, Tse AP, Bao MH, et al. Induction of Oxidative Stress Through Inhibition of Thioredoxin Reductase 1 Is an Effective Therapeutic Approach for Hepatocellular Carcinoma. *Hepatology* (2019) 69:1768–86. doi: 10.1002/hep.30467

26. Gao L, Wang X, Tang Y, Huang S, Hu CA, Teng Y. FGF19/FGFR4 Signaling Contributes to the Resistance of Hepatocellular Carcinoma to Sorafenib. *J Exp Clin Cancer Res* (2017) 36:8. doi: 10.1186/s13046-016-0478-9
27. Teng Y, Zhao H, Gao L, Zhang W, Shull AY, Shay C. FGF19 Protects Hepatocellular Carcinoma Cells Against Endoplasmic Reticulum Stress *via* Activation of FGFR4-GSK3beta-Nrf2 Signaling. *Cancer Res* (2017) 77:6215–25. doi: 10.1158/0008-5472.CAN-17-2039
28. Penning TM. Aldo-Keto Reductase (AKR) 1C3 Inhibitors: A Patent Review. *Expert Opin Ther Pat* (2017) 27:1329–40. doi: 10.1080/13543776.2017.1379503
29. Xu D, Aka JA, Wang R, Lin SX. 17beta-Hydroxysteroid Dehydrogenase Type 5 Is Negatively Correlated to Apoptosis Inhibitor GRP78 and Tumor-Secreted Protein PGK1, and Modulates Breast Cancer Cell Viability and Proliferation. *J Steroid Biochem Mol Biol* (2017) 171:270–80. doi: 10.1016/j.jsbmb.2017.04.009
30. Sun SQ, Gu X, Gao XS, Li Y, Yu H, Xiong W, et al. Overexpression of AKR1C3 Significantly Enhances Human Prostate Cancer Cells Resistance to Radiation. *Oncotarget* (2016) 7:48050–8. doi: 10.18632/oncotarget.10347
31. Li X, Hong X, Gao X, Gu X, Xiong W, Zhao J, et al. Methyl Jasmonate Enhances the Radiation Sensitivity of Esophageal Carcinoma Cells by Inhibiting the 11-Ketoprostaglandin Reductase Activity of AKR1C3. *Cancer Manag Res* (2018) 10:3149–58. doi: 10.2147/CMAR.S166942
32. Xie L, Yu J, Guo W, Wei L, Liu Y, Wang X, et al. Aldo-Keto Reductase 1C3 may be a New Radioresistance Marker in Non-Small-Cell Lung Cancer. *Cancer Gene Ther* (2013) 20:260–6. doi: 10.1038/cgt.2013.15
33. Wu XZ, Xie GR, Chen D. Hypoxia and Hepatocellular Carcinoma: The Therapeutic Target for Hepatocellular Carcinoma. *J Gastroenterol Hepatol* (2007) 22:1178–82. doi: 10.1111/j.1440-1746.2007.04997.x
34. Guise CP, Abbattista MR, Singleton RS, Holford SD, Connolly J, Dachs GU, et al. The Bioreductive Prodrug PR-104A Is Activated Under Aerobic Conditions by Human Aldo-Keto Reductase 1C3. *Cancer Res* (2010) 70:1573–84. doi: 10.1158/0008-5472.CAN-09-3237
35. Abou-Alfa GK, Chan SL, Lin CC, Chiorean EG, Holcombe RF, Mulcahy MF, et al. PR-104 Plus Sorafenib in Patients With Advanced Hepatocellular Carcinoma. *Cancer Chemother Pharmacol* (2011) 68:539–45. doi: 10.1007/s00280-011-1671-3
36. Manning BD, Toker A. AKT/PKB Signaling: Navigating the Network. *Cell* (2017) 169:381–405. doi: 10.1016/j.cell.2017.04.001
37. Revathidevi S, Munirajan AK. Akt in Cancer: Mediator and More. *Semin Cancer Biol* (2019) 59:80–91. doi: 10.1016/j.semcancer.2019.06.002

Conflict of Interest: The authors declare that the research was conducted in the absence of any commercial or financial relationships that could be construed as a potential conflict of interest.

Publisher's Note: All claims expressed in this article are solely those of the authors and do not necessarily represent those of their affiliated organizations, or those of the publisher, the editors and the reviewers. Any product that may be evaluated in this article, or claim that may be made by its manufacturer, is not guaranteed or endorsed by the publisher.

frontiers in Oncology

ORIGINAL RESEARCH
published: 22 March 2022
doi: 10.3389/fonc.2022.851300

Gracillin Shows Potential Efficacy Against Non-Small Cell Lung Cancer Through Inhibiting the mTOR Pathway

Yamei Li[1,2†], Hai Liu[3†], Xiaoxuan Liu[1,2], Bang Xiao[1,4], Minhong Zhang[1], Yaoling Luo[1], Mingchun Li[5] and Jianqiong Yang[1]*

[1] The Clinical Medicine Research Center of the First Clinical Medical College, Gannan Medical University, Ganzhou, China, [2] College of Pharmacy, Gannan Medical University, Ganzhou, China, [3] National Engineering Research Center for Modernization of Traditional Chinese Medicine-Hakka Medical Resources Branch, Gannan Medical University, Ganzhou, China, [4] School of Rehabilitation Medicine, Gannan Medical University, Ganzhou, China, [5] Department of Oncology of the First Clinical Medical College, Gannan Medical University, Ganzhou, China

OPEN ACCESS

Edited by:
Devesh Tewari,
Lovely Professional University, India

Reviewed by:
Qingbin Cui,
University of Toledo, United States
Sonam Mittal,
Medical College of Wisconsin, United States

***Correspondence:**
Jianqiong Yang
yangjianqiong2010@163.com

[†]These authors have contributed equally to this work

Specialty section:
This article was submitted to Pharmacology of Anti-Cancer Drugs, a section of the journal Frontiers in Oncology

Received: 09 January 2022
Accepted: 28 February 2022
Published: 22 March 2022

Citation:
Li Y, Liu H, Liu X, Xiao B, Zhang M, Luo Y, Li M and Yang J (2022) Gracillin Shows Potential Efficacy Against Non-Small Cell Lung Cancer Through Inhibiting the mTOR Pathway. Front. Oncol. 12:851300. doi: 10.3389/fonc.2022.851300

The leading cause of cancer deaths is lung cancer, non-small cell lung cancer (NSCLC), the most common type of lung cancers, remains a difficult cancer to treat and cure. It is urgent to develop new products to treat NSCLS. Gracillin, extracted from *Reineckia carnea*, *Dioscorea villosa*, and other medicinal plants, has anti-tumor potential with toxic effect on a variety of tumor cells such as NSCLC. However, the anti-NSCLC mechanism of gracillin is not completely clear. In this study, A549 cells and athymic nude mice were used as models to evaluate the anti-NSCLC effects of gracillin. The antiproliferative activity of gracillin on A549 cells was conducted by CCK-8, and obvious autophagy was observed in gracillin-treated A549 through transmission electron microscopy. Furthermore, the expressions of Beclin-1, LC3-II, and WIPI1 were upregulated, while the expression of p62 was downregulated in gracillin-treated A549. The further mechanism study found that the mTOR signaling pathway was significantly inhibited by gracillin. Accordingly, the PI3K/Akt pathway positively regulating mTOR was inhibited, and AMPK negatively regulating mTOR was activated. Meanwhile, LC3-II transformation was found to be significantly reduced after WIPI1 was silenced in A549 cells but increased after gracillin treatment. It also proves that WIPI is involved in the process of gracillin regulating A549 autophagy. At last, the anti-tumor growth activity of gracillin *in vivo* was validated in A549-bearing athymic nude mice. In conclusion, gracillin has anti-NSCLC activity by inducing autophagy. The mechanism maybe that gracillin inhibited the mTOR signaling pathway. Gracillin has the potential to be a candidate product for the treatment of NSCLC in the future.

Keywords: gracillin, non-small cell lung cancer, autophagy, mTOR signaling pathway, anti-tumor

INTRODUCTION

Lung cancer is still one of the most common malignant tumors so far and the leading cause of cancers-related deaths in the world (1–3). According to data released in 2018, 1.8 million patients worldwide have died from lung cancer and the number of lung cancer patients increases sharply each year (4). NSCLC accounts for about 85% of lung cancers, and more than half of patients with lung cancer are diagnosed as NSCLC at the advanced stage of the disease (5). The current treatment methods for NSCLC mainly include surgery, radiotherapy, chemotherapy, immunotherapy, targeted therapy, etc. (6).However, the cumulative survival rate of patients with NSCLC within 5 years is still very low, only 16.8% (4). With the advent of precision medicine, great breakthroughs have been made in immunotherapy and targeted therapy for NSCLC, such as programmed death receptor 1/programmed death receptor ligand 1 inhibitors (PD-1/PD-L1 inhibitors) (7) and epidermal growth factor-tyrosine kinase inhibitors (EGFR-TKI) (8). Although these have contributed greatly to the treatment of lung cancer, they are not applicable to all patients. In addition, drug resistance and adverse reactions exist in the clinical treatment process, so that it is difficult to achieve the expected curative effect (9, 10). Therefore, it is necessary to find safe and effective new drugs for the treatment of NSCLC.

Traditional Chinese medicine (TCM) has a long history, and it has been reported that many compounds in TCM have strong antitumor activity, such as paclitaxel (11), triptolide (12), etc. It may be an efficient and fast way to find effective drugs against NSCLC from TCM. Gracillin is a steroidal saponin compound and is found in a variety of plants including *Rhizoma paridis* (13), *Pairs polyphylla* (14), *Dioscorea villosa* (15), *Acontum carmichaeli* (16), *Solanum incanum*, and *Solanum xanthocarpum* (17). According to reports, gracillin has anti-tumor, anti-inflammatory (18), pro-apoptotic (19), anti-bacterial (20) and other pharmacological effects. In particular, its potent antitumor effects *in vivo* and *in vitro* have attracted widespread attention. Chen found that gracillin induces human leukemia HL60 cell apoptosis and cell cycle G1 block *via* oxidative stress pathway (21); Min found that gracillin disrupts complex II-mediated mitochondrial function by inactivating succinate dehydrogenase, which resulted in decreased mitochondrial membrane potential, oxidative phosphorylation, and ATP production, at the same time, increased mitochondrial ROS production (22). And then they found that gracillin exerts a powerful anti-tumor effect mainly by inhibiting the production of bioenergy mediated by glycolysis and oxidative phosphorylation in tumor cells (23).Yang found that Gracillin exhibits a powerful anti-colorectal cancer effect by inhibiting the STAT3 pathway (24). The anti-tumor potential of gracillin is obvious, but there are relatively few studies on anti-tumor mechanisms, mainly involving apoptosis and energy metabolism. Our previous study found that gracillin can induce apoptosis of A549 cells by up-regulating Bax, casepase3, cytochrome C and down-regulating Bcl-2, which is related to the regulation of mitochondrial pathway (25). The Bcl-2 protein family plays a key role in regulating apoptosis and autophagy. It has been demonstrated that the autophagy-related protein Beclin-1 with BH3 domain can directly regulate autophagy by binding to Bcl-2 (26). In this context, we performed high-throughput screening of gracillin-treated A549 cells and found that many differentially expressed genes were enriched on autophagy-related regulatory networks. Therefore, we wondered whether gracillin affects A549 cell proliferation by regulating autophagy.

Autophagy, known as type 2 programmed cell death (27), functions to degrade damaged and redundant organelles and misfolded proteins, providing the molecular building and energy source to keep cells alive (28, 29). However, excessive autophagy can lead to autophagic cell death (30). mTOR is a very important regulator in the regulation of autophagy. mTOR inhibition has significant activity against a broad range of human cancers *in vitro* and in human tumor xenograft models (31). In this study, based on high-throughput screening, we found that WD repeat domain phosphoinositide-interacting protein 1 (WIPI1) was significantly highly expressed. And WIPI1 was reported as an autophagy-related gene (32). The prerequisite for the formation of autophagosomes is phosphatidyl alcohol-3-phosphate (PtdIn3p), which requires the participation of WIPI protein to function on the autophagosome membrane. WIPI represent the human proteome in the PROPPIN protein family, which fold into seven-bladed β-propeller proteins that bind PtdIn3P (33). Therefore, we first determined the antiproliferative effect of gracillin on A549 cells, and then confirmed that it could induce autophagy in A549 cells. Then, we studied the molecular mechanism of gracillin-activated autophagy and explored the role of WIPI1. Finally, the antitumor effect of gracillin was determined in athymic mice bearing A549 cells. Gracillin may be one of the drug candidates for the treatment of non-small cell lung cancer in the future.

MATERIALS AND METHODS

Antibodies and Regents

Gracillin (HPLC > 98%) was isolated from *Reineckia carnea* and confirmed to be a steroidal saponin compound through structural identification, with the molecular formula $C_{45}H_{72}O_7$ (**Figure 1A**). The compound was dissolved in dimethyl sulfoxide (DMSO) for experiments. The antibodies against SQSTM/P62, Beclin-1, LC3B, Atg12, PI3K kinase, phospho-PI3K kinase, Akt, phospho-Akt, AMPK and phospho-AMPKα were purchased from Cell Signaling Technology. The antibody against GAPDH was purchased from Beijing Apply Gene Technology Co., Ltd. The antibody against WIPI1 was purchased from Abcam Co. The horseradish peroxidase (HRP)-conjugated goat anti-mouse IgG, HRP-conjugated goat anti-rabbit IgG, the mTOR antibody, phospho-mTOR antibody, and the ultra-wide molecular weight marker (10 - 310 KDa) were purchased from Proteintech. The protein marker (10 - 180 KDa), Matrigel and Lipofectamine 2000 Reagent were purchased from Thermo Fisher Scientific Co. The WIPI1 forward primer (5'-TGCCATCACCTTCAATGCCTCAG-3')

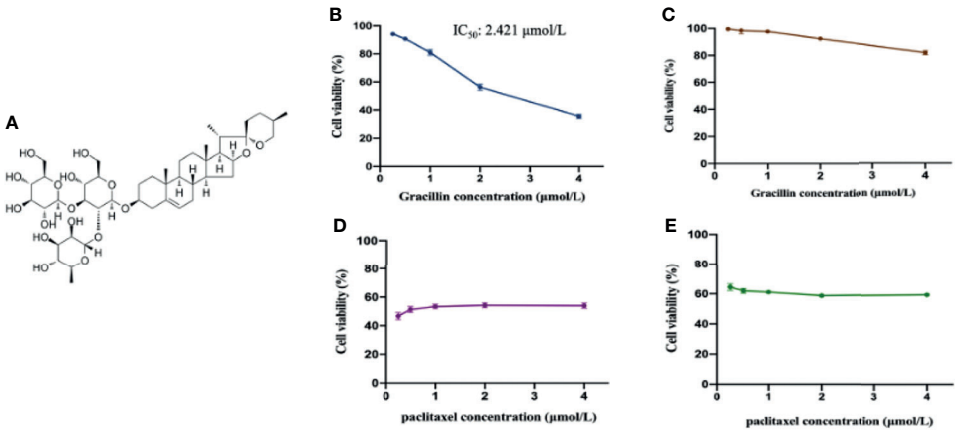

FIGURE 1 | The anti-proliferative effect of gracillin on A549 cells and BEAS-2B cells. **(A)** The chemical structure of gracillin (PubChem CID: 159861). **(B)** The cytotoxicity of gracillin on A549 cells treated for 24 hours. **(C)** The cytotoxicity of gracillin on BEAS-2B cells for 24 hours. **(D)** The cytotoxicity of paclitaxel on A549 cells for 24 hours. **(E)** The cytotoxicity of paclitaxel on BEAS-2B cells for 24 hours.

and the reverse primer (5'-GCCATCCAGCGAAACCCAGAC-3') were synthesized from Shanghai Sangon Biological Engineering Co., Ltd. The Trizol lysate was purchased from Ambion Co. The q-PCR kit and cDNA reverse transcription kit were purchased from Beijing Transgen Biotechnology Co., Ltd. The RIPA strong lysate, blasticidin and rapamycin were purchased from Beijing Solarbio Technology Co., Ltd. The PEGFP-LC3B plasmid was purchased from Wuhan Miaoling Biotechnology Co., Ltd. The cell counting kit-8 (CCK-8) was purchased from Glpbio Co. Human WIPI1 small interfering RNA (siRNA) lentivirus was constructed from Shanghai Novo Biotechnology. 3-Methyladenine(3-MA) was purchased from Med Chem Express Co.

Cell Culture

A549 cells and BEAS-2B cells were purchased from the cell bank of the Type Culture Collection Committee of the Chinese Academy of Sciences (Shanghai, China). The cells were cultured in F12K medium supplemented with 10% FBS, 100 U/mL penicillin and 100 μg/mL streptomycin. All cells were grown in a humidified atmosphere at 37°C and 5% CO_2.

Cell Proliferation Assay

Exponentially growing A549 cells were obtained and seeded in a 96-well plate with 3×10^3 cells per well. When the cell growth density reaches more than 70%, four groups were set up, namely the control group, the experimental group, the positive control group (paclitaxel), and the blank group. The cells of the experimental group are treated by gracillin (0.25, 0.5, 1, 2, 4 μmol/L). After 24 hours, the old medium was discarded, and 100 μL of fresh F12K complete medium and 10 μL of CCK-8 reaction solution were added. Then, the 96-well plate was placed in a 37°C constant temperature incubator and incubated for 2 hours. Finally, varioskan™ flash multimode reader (Thermo Fisher Scientific, Waltham, MA, USA) was used to determine the absorbance at 450nm. In addition, gracillin was further evaluated for its cytotoxic effect on human normal lung bronchial epithelial cells (BEAS-2B). The IC_{50} value of gracillin for 24 hours is calculated by the Logit method. The cell survival rate is calculated as follows:

$$\text{cell survival rate}\,(\%) = \frac{(\text{the average OD value of the experimental group} - \text{the average OD value of the blank group})}{(\text{the average OD value of the control group} - \text{the average OD value of the blank group})}$$

Experiment of Inhibiting or Promoting Autophagy on the Proliferation of A549 Cells

First, the logarithmic growth A549 cells were seeded in a 96-well plate with 3×10^3 cells per well. Secondly, when the cell confluence reaches more than 70%, the cells were treated by gracillin together with the 3-MA or Rapamycin. 3-MA is an inhibitor of phosphatidylinositol 3-kinase, and specifically blocks autophagosome formation in Autophagy. Rapamycin is an inhibitor of mTOR, which can switch the autophagy-specific protein phosphorylase mode to promote autophagy. The CCK-8 method was used to detect cell proliferation. All experiments were repeated at least 3 times.

Morphological Observation Experiment of Autophagosome

Detecting autophagy-related structures in the cytoplasm by transmission electron microscopy (TEM) is the gold standard for determining autophagy. 2% glutaraldehyde fixation was used to fix the sample overnight, then the sample was post-fixed, filmed, TEM filming and image collection in the electron microscope room. The changes in organelles such as Golgi complex, endoplasmic reticulum, lysosome, and mitochondria in the cytoplasm were observed to determine whether

autophagosomes with independent double-layer membrane structures were formed.

pEGFP-LC3 Plasmid Transfection

Exponentially growing A549 cells were obtained and seeded in a laser confocal dish with 1×10^5 cells When the cell confluence reached about 70%, pEGFP-LC3 plasmid was transfected into A549 cells using Lipofectamine 2000 (Invitrogen, Carlsbad, CA, USA) following the manufacturer's instructions. After 6 - 8 hours of transfection, it was replaced with a new medium and placed in a 37°C, 5% CO2, saturated humidity incubator for 24 hours. The transfected cells were treated by autophagy inhibitor (3-MA) and gracillin for 24 hours, and then stained with DAPI for 10 minutes. The fluorescent spots were observed under a Zeiss carlzeis lsm880 confocal laser microscope.

Western Blot Analysis

Cells and tumor tissues are lysed on ice for 30 minutes with RIPA lysis buffer containing protease inhibitors (PMSF) and phosphatase inhibitors. Equal amounts of the total protein (20 μg for cells, 50 μg for tissues) were separated by 8% - 15% SDS-PAGE gel. After electrophoresis, the proteins on the SDS-PAGE gel were transferred to the polyvinylidene fluoride membrane (PVDF). Then, the membrane was blocked for 1 hour in a TBST solution containing 5% skimmed milk powder or Bovine Serum Albumin (BSA) at room temperature. Furthermore, the membrane was incubated overnight with the different primary antibodies at 4°C. Next, the membrane will be further incubated for 1 hour with horseradish peroxidase (HRP) conjugated secondary antibody at room temperature. Finally, the protein bands on the membrane were visualized by Super Enhanced chemiluminescence detection reagents (Applygen Technologies Inc., Beijing, China) and detected by Chemi Dox XRS chemiluminescence imaging system (Bio-Rad, California, USA). The protein bands were quantified by Image J (NIH, USA) and the relative expression of the target protein was calculated by using GAPDH as an internal control. All data comes from three independent experiments.

Quantitative Real-time PCR (qRT-PCR)

qRT-PCR is usually used to quantify the expression changes of gene at the mRNA level. A549 cells were seeded in 6-well plate with 2×10^5 cells per well and placed in 37°C, 5% CO_2 incubator. When growth density is greater than 70%, the cells were treated by gracillin (0.25, 0.5, 1, 2 μmol/L) for 24 hours. Trizol was used to extract the total RNA of the cells according to the instructions, and the concentration was measured by ultra-micro-UV spectrophotometer (Thermo Scientific, Massachusetts, USA). Then, the total RNA was reverse transcribed into cDNA with Easy Script ® one-step gDNA removal and cDNA synthesis supermix kit (TransGen Biotech, Beijing, Chain). Subsequently, the cDNA was amplified and monitored in real time with the Perfect StartTM Green qPCR SuperMix kit (TransGen Biotech, Beijing, Chain) and CFX ConnectTM fluorescent quantitative PCR detection system (Bio-Rad, California, USA). The PCR primers of WIPI 1 are shown in "2.1". The thermal cycling conditions are 94°C for 30 seconds; 94°C for 5 seconds; 60°C for 15 seconds; 72°C for 10 seconds; 40 cycles. The relative quantification of genes was analyzed according to the 2-ΔΔCt method [ΔΔCt = ΔCt (treatment)-ΔCt (control)]. GAPDH was used as an endogenous control. Each sample was analyzed three times.

Transfecting A549 Cells With WIPI1 Knockout Lentivirus

The shRNA sequence targeting the human WIPI1 gene was inserted into the PDS126 vector to generate the WIPI1-si plasmid. The sequence that silences WIPI1 expression is 5'-GCTCTCTAGTGTTCAGTATGG-3'. First, logarithmic growth A549 cells were seeded in a 6-well plate with 2×10^5 cells/well. When cell confluence reached 80%, the lentiviral particles targeting WIPI1 were transfected into cells with the optimal multiplicity of infection (MOI=10) for transfection. 6 - 8 hours after transfection, the transfection efficiency was observed by fluorescence microscope. Then, the blasticidin medium containing 16μg/mL was cultured continuously for 3 weeks, and the medium was changed every 3 days. Finally, a stably transfected cell line was screened out. The total RNA and total protein of the stable cell line were extracted, and the interference efficiency of the lentivirus was detected by q-PCR and Western blot. Then, the medium containing 4 μg/mL blasticidin was used to maintain a stable environment, and the selected cells were re-seeded in a 6-well plate at 2×10^5 cells/well. Simultaneously one control group (empty vector-containing lentivirus-infected group) and five experimental groups with different concentrations gracillin (0, 0.25, 0.5, 1, 2 μmol/L) were set up. When the cell growth density reached 70% or more, the cells were treated by gracillin for 24 hours. Finally, the total cell protein was collected.

Animal Experiment

The animal experiments were conducted under the guidance of the Animal Protection and Ethics Committee of Gannan Medical University. Forty BALB/c mice (4-6 weeks, 18-20 g), male and female, were purchased from Hunan Slack Jingda Experimental Animal Co., Ltd. (SCXK (Xiang) 2019-0004), 4 mice per cage. Mice are raised under standard animal feeding conditions (12 hours light/dark cycle) and controlled ambient temperature (25 ± 2°C) with free access to standard mouse food and water. All mice were acclimatized to the above-mentioned environment for one week before the start of the experiment. For the cell line xenotransplantation experiment, each mouse was inoculated with 5×10^6 A549 cells in the right armpit of the mouse. Starting from the observable tumor tissue, the tumor volume was measured with a vernier caliper every day. the tumor volume was calculated by using the following formula: tumor volume (mm^3) = (short diameter)^2 × (long diameter) × 0.5. When the tumor volume reached 100mm^3, the optimized mice were randomly divided into 5 groups (n=8), including a negative control group, three gracillin treatment groups and a positive

control group. The three gracillin treatment groups were treated by different concentrations of gracillin (high dose 20 mg/Kg, medium dose 10 mg/Kg, low dose 5 mg/Kg) for 6 days a week for two consecutive weeks. In the negative control group, the mice were treated by solvent (corn oil and 5% DMSO) in the same way. The positive control group was treated by paclitaxel, three times a week for two weeks. During the treatment, the body weight and tumor volume of the mice were measured daily. Last, all mice were sacrificed, tumor tissues were collected, weighed, and photographed. Also, the tumor tissue was frozen in liquid nitrogen or immediately fixed in formalin for further study.

Hematoxylin and Eosin (H&E) Staining

The heart, liver, kidney, and lungs of the mice were fixed with 4% paraformaldehyde and embedded in paraffin and sectioned. The slides were first deparaffinized and hydrated, then stained with hematoxylin solution and eosin solution, respectively, followed by dehydration, and finally, mounted. Representative images were obtained by the digital slice scanning analysis system Tissue FAXS plus (Tissue Gnostics, Austria).

Ki67 Immunohistochemical Staining

Harvested tumors were paraffin-embedded and analyzed by immunohistochemistry. Tumor cell proliferation was analyzed using an antibody against Ki-67. That is, the slides were first deparaffinized and hydrated, then subjected to antigen retrieval, followed by blocked with BSA blocking solution, incubated with an anti-mouse polyclonal antibody against Ki67 at 4°C, the next day, sequentially incubated with secondary antibodies and performed DAB staining. Finally, the slides were permanently mounted with neutral resin and the images were recorded by the digital slice scanning analysis system Tissue FAXS plus.

Statistical Analysis

All data were expressed as mean ± SD. The data was analyzed by GraphPad Prism 8.0 (San Diego, California, USA). The difference between the two groups was analyzed using independent sample *t* test, and the difference between multiple groups was analyzed using one-way analysis of variance (ANOVA) test. All the data provided have been verified by at least three independent experiments. When $P \leq 0.05$, the difference was considered to have statistically significant.

RESULTS

Gracillin Inhibits the Proliferation of A549 Cells

In this study, CCK-8 was used to study the anti-proliferative effects of gracillin in A549 cells and BEAS-2B cells. After treatment of gracillin for 24 hours, the results showed that gracillin significantly inhibited the cell viability of A549 in concentration-dependent manner (**Figure 1B**) with half maximal inhibitory concentration (IC_{50}) value of 2.421 μmol/L. Meanwhile, gracillin had almost no effect on the proliferation of BEAS-2B cells (**Figure 1C**). Although paclitaxel showed a strong antiproliferative effect on the proliferation of A549 cells (**Figure 1D**), it also showed the same effect on the proliferation of BEAS-2B cells (**Figure 1E**). In general, gracillin had strong proliferation inhibitory effect on human NSCLC cells and had little effect on the proliferation of normal lung epithelial cells.

Gracillin-Induced Autophagic Cell Death in A549 Cells

In this study, CCK-8 was used to examine the effect of gracillin-induced autophagic death in the presence of autophagy inhibitors and agonists. The results show that the number of dead cells in the rapamycin and gracillin together treatment group was greater than the gracillin (2 μmol/L) treatment group. At the same time, the number of dead cells in the gracillin treatment group was greater than the 3-MA and gracillin together treatment group. The number of dead cells in the 3-MA or rapamycin treatment group was relatively small, but the number of dead cells in the former was smaller than that in the

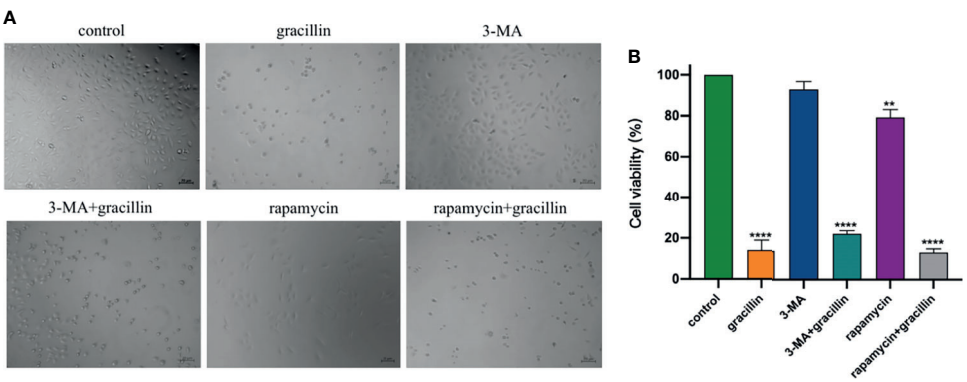

FIGURE 2 | Anti-proliferation effect of gracillin in combination with 3-MA or rapamycin on A549 cells. **(A)** The growth of cells in 6 different treatment groups observed under the microscope. **(B)** The statistical results of the inhibition rate of the 6 groups on A549 cells, compared with the control group, $^{**}P \leq 0.01$, $^{****}P \leq 0.0001$.

latter (**Figure 2**). In summary, gracillin can induce autophagy in A549 cells and cause cells death.

Observation of Autophagosomes by Transmission Electron Microscope and Laser Scanning Confocal Microscope

A549 cells were treated by 2μmol/L gracillin for 6 h, 12 h, and 24 h, respectively. The autophagosomes were observed by transmission electron microscopy. It was found that the autophagosomes were observed in the gracillin-treated group compared with the control group (**Figure 3A**). Observing the LC3 punctate aggregation is also one of the indicators to judge the occurrence of autophagy. LC3 protein is widely present in cells, when autophagy occurs, LC3 protein aggregates on the surface of autophagosomes and transforms into a punctate distribution. Because pEGFP-LC3 carries green fluorescent label, it can be judged whether the cells have autophagy by observing the degree of punctate aggregation of green fluorescent by Laser Scanning Confocal Microscope. After the pEGFP-LC3 plasmid was transfected into the cells, the LC3 punctate aggregation of the gracillin-treated cells could be observed, while the control group cells rarely had LC3 punctate aggregation (**Figure 3B**).

Gracillin Affects the Expression of Autophagy-Related Proteins

After treated by gracillin for 24 hours, the expression changes of Beclin-1, P62 and LC3 in A549 cells were detected by Western blot. The results showed that the expression of Beclin-1 was significantly up-regulated, the expression of P62 was significantly down-regulated. The transformation from LC3-I to LC3-II was significantly increased. In general, gracillin could change the expression of autophagy-related proteins in A549 cells (**Figure 4**).

The Expression of WIPI1 at Gene and Protein Levels

The bioinformatics analysis of gracillin-treated A549 cells showed that the gene WIPI1 is significantly differently expressed (**Figure 5A**) and can bind to phosphatidyl alcohol-3-phosphate, which is necessary for the formation of autophagosomes, through differential expression of genes Cluster analysis (**Figure 5B**), GO function enrichment analysis (**Figure 5C**) and KEGG pathway enrichment analysis (**Figure 5D**). Then we verified the results of bioinformatics analysis by q-PCR (**Figure 5E**) and Western blot (**Figure 5F**), and the results showed that the gracillin-treated A549 cells were up-regulated at both protein and gene levels. When 3-MA inhibited autophagy, the expression of WIPI1 was down-regulated, but the cells treated by 3-MA and gracillin (2μmol/L) together, the expression of WIPI1 was up-regulated (**Figure 5G**).

Gracillin Reverses the Autophagy Inhibitory Effect of 3-MA

3-MA blocks the formation of autophagosomes by inhibiting the class III phosphatidylinositol 3-kinases (PI3K). Under the Laser Scanning Confocal Microscope, it can be observed that the degree of punctate aggregation with green fluorescent (pEGFP-LC3) was significantly reduced in A549 cells of 3-MA treatment group. But it was significantly increased in cells treated with 3-MA and gracillin together (**Figure 6A**). The extent to which autophagy is inhibited by 3-MA can be reversed by gracillin, which is achieved by up-regulating Beclin-1(**Figure 6B**), promoting the transformation of LC3 to LC3-II (**Figure 6D**), and down-regulating P62 (**Figure 6C**).

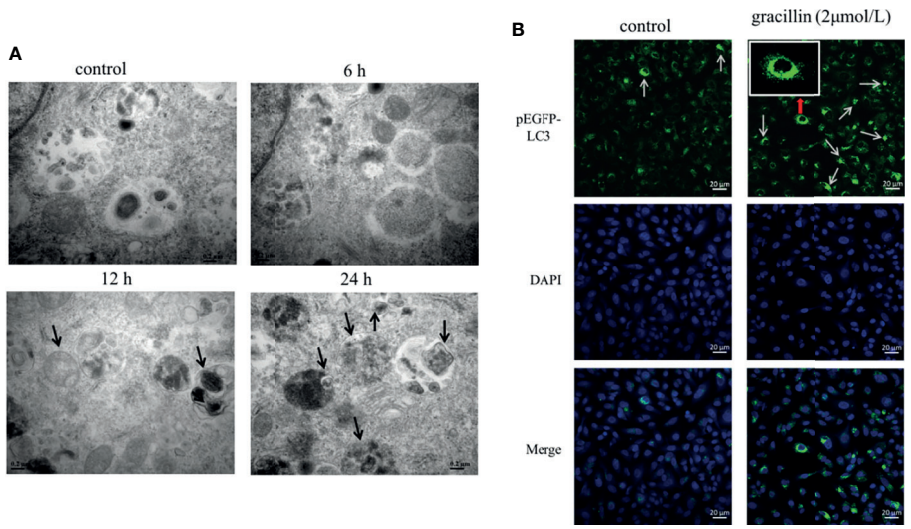

FIGURE 3 | The effect of gracillin on autophagosome production. **(A)** Transmission electron microscope image of A549 cells treated with gracillin. The arrow indicates the autophagosome or autolysosome. **(B)** Confocal laser image of A549 cells transfected with pEGFP-LC3 plasmid and treated with gracillin. The nucleus was stained with DAPI. The arrow in the figure indicates the punctate aggregation of LC3 on the autophagosome membrane.

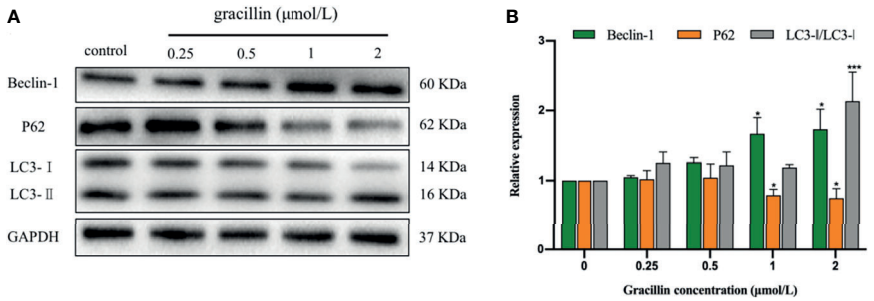

FIGURE 4 | The effect of gracillin on autophagy-related proteins in A549 cells. **(A)** Western blot analysis of Beclin-1, P62, LC3-Ianld LC3-II and A549 cells treated with gracillin (0, 0.25, 0.5, 1, 2 μmol/L) for 24 hours. The full picture is in **Supplementary Figure 1**. **(B)** The relative protein expression levels of Beclin-1, P62, LC3-I, and LC3-II were quantified by normalization to GAPDH, compared with the control group, $^{*}P \leq 0.05$, $^{***}P \leq 0.001$.

Gracillin Inhibits mTOR Signaling Pathway

The kinase mTOR plays a key role in the progress of autophagy and activates autophagy by inhibiting phospho-mTOR (p-mTOR). mTOR is a downstream target for PI3K/AKT, and AMPK, the activation of which suppresses autophagy. Inhibit phospho-PI3K (p-PI3K) and phospho-Akt (p-Akt) or activate phospho-AMPK (p-AMPK) can cause p-mTOR to be inhibited to activate autophagy. In this study, after A549 cells were treated with gracillin for 24 hours, the total protein levels of PI3K, Akt, AMPK, and mTOR were not significantly changed. p-PI3K, p-Akt and p-mTOR were significantly down-regulated, and p-AMPK was significantly up-regulated (**Figure 7**). In general, gracillin could activate autophagy by inhibiting mTOR signaling pathway.

WIPI1 Participates in Gracillin-Induced Autophagy

After transfecting A549 with a lentivirus targeting WIPI1, the cells can be observed with green fluorescence under a fluorescence microscope, and the stable cells can be screened by blasticidin (**Figure 8A**). At the same time, the expression of WIPI1 in stable cells was detected and found that the expression

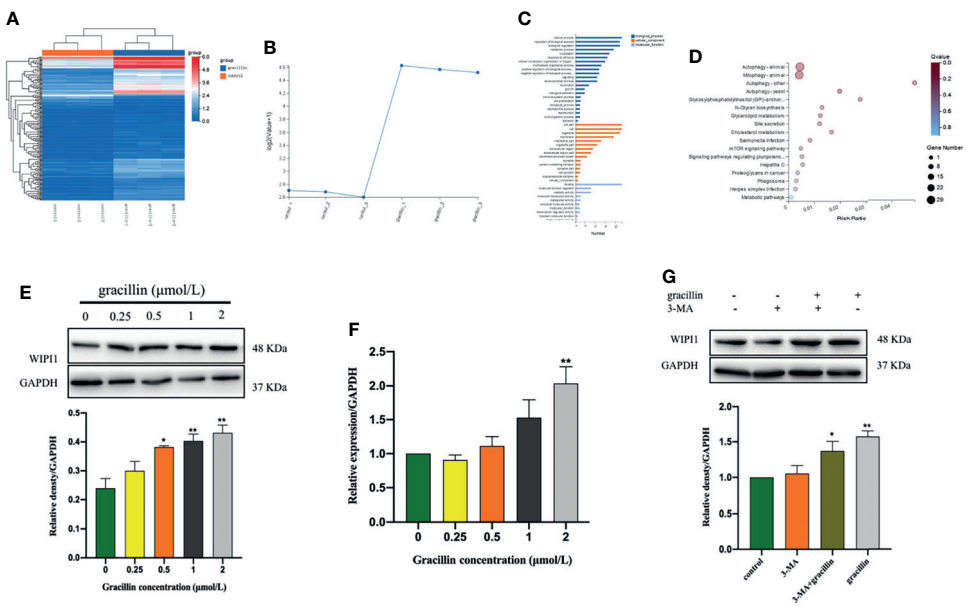

FIGURE 5 | Gracillin caused changes in the expression of WIPI1 in A549 cells. **(A)** Cluster analysis of all differential gene expression in A549 cells treated with gracillin 2 μmol/L for 24 hours. **(B)** Differentially high expression of WIPI1. **(C)** GO function enrichment analysis, WIPI1 is enriched to the biological functions involved in the formation of autophagosome membranes. **(D)** KEGG Pathway enrichment analysis, WIPI1 is enriched into the signal pathway related to animal autophagy. **(E, F)** The differential expression of WIPI1 was verified by q-PCR and Western blotting. **(G)** The effect of combined use of gracillin and 3-MA on the expression of WIPI1. The full picture is in **Supplementary Figure 2**. Compared with the control group, $^{*}P \leq 0.05$, $^{**}P \leq 0.01$.

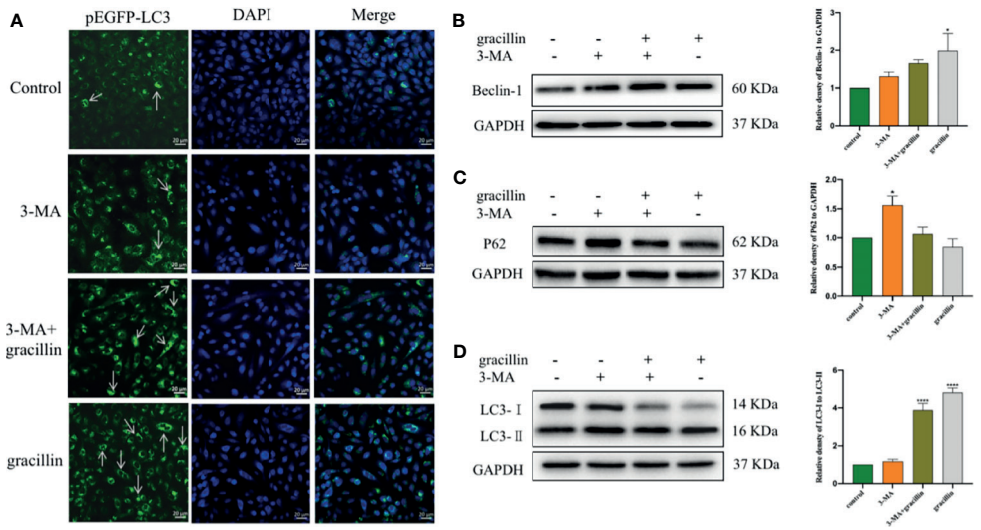

FIGURE 6 | After 3-MA inhibits autophagy, the effect of gracillin on the degree of autophagy in A549 cells and the protein expression of Beclin-1, P62, LC3-land LC3-. **(A)** Confocal laser image of gracillin-treated A549 cells. The nucleus was stained with DAPI. The arrow in the figure indicates the punctate aggregation of LC3 on the autophagosome membrane. One of the fluorescent punctation represents an autophagosome. **(B)** Western blot analysis of Beclin-1 and relative protein expression levels were quantified by normalization to GAPDH. **(C)** Western blot analysis of P62 and relative protein expression levels were quantified by normalization to GAPDH. **(D)** Western blot analysis of LC3 and relative protein expression levels are expressed as LC3-II/LC3-I. The full picture is in **Supplementary Figure 3**. Compared with the control group, $^{*}P \leq 0.05$, $^{****}P \leq 0.0001$.

of si-RNA-WIPI1 group was significantly interfered compared with the control group (**Figure 8B**). In addition, we found that the protein expression of Beclin-1 and P62 were not affected by WIPI1 (**Figure 8C**), while the protein expression of LC3 was significantly affected (**Figure 8E**). To verify whether WIPI1 is involved in gracillin-induced autophagy, we treated the stable cells with gracillin, and then collected proteins for Western blot experiment. The results showed that although gracillin showed an up-regulation trend for LC3-II, the up-regulation trend was not obvious compared with the control group (**Figure 8D**). In other words, silencing WIPI1 influences gracillin-induced autophagy.

Gracillin Inhibits NSCLC Tumor Growth in Xenograft Model

We further verified the anti-tumor effect of gracillin by establishing tumor xenograft model. When the tumor growth

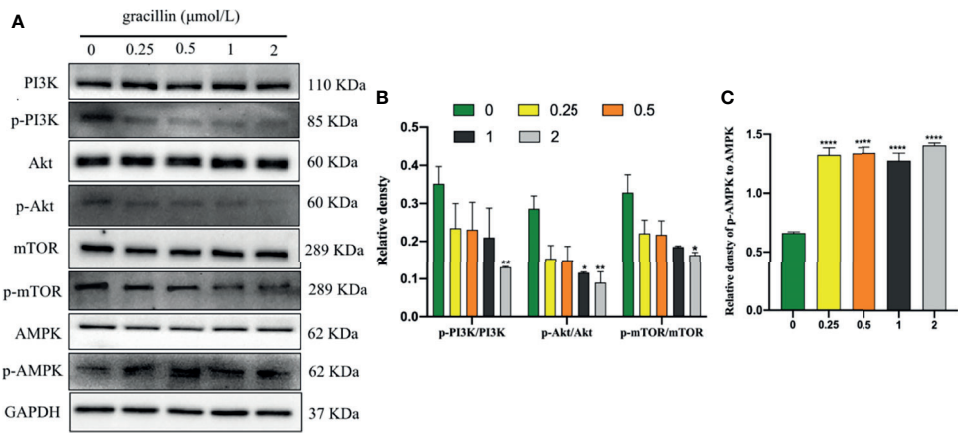

FIGURE 7 | Gracillin induces autophagy in A549 cells through the mTOR signaling pathway. **(A)** Western blot analysis of PI3K, p-PI3K, Akt, p-Akt, AMPK, p-AMPK, mTOR, p-mTOR and GAPDH in A549 cells treated with gracillin (0, 0.25, 0.5, 1, 2 μmol/L) for 24 hours. **(B)** The relative protein expression levels of p-PI3K, p-Akt, and p-mTOR are quantified using PI3K, Akt, and mTOR as standards. **(C)** The relative protein expression level of p-AMPK is quantified with AMPK as standard. The full picture is in **Supplementary Figure 4**. Compared with the control group, $^{*}P \leq 0.05$, $^{**}P \leq 0.01$, $^{****}P \leq 0.0001$.

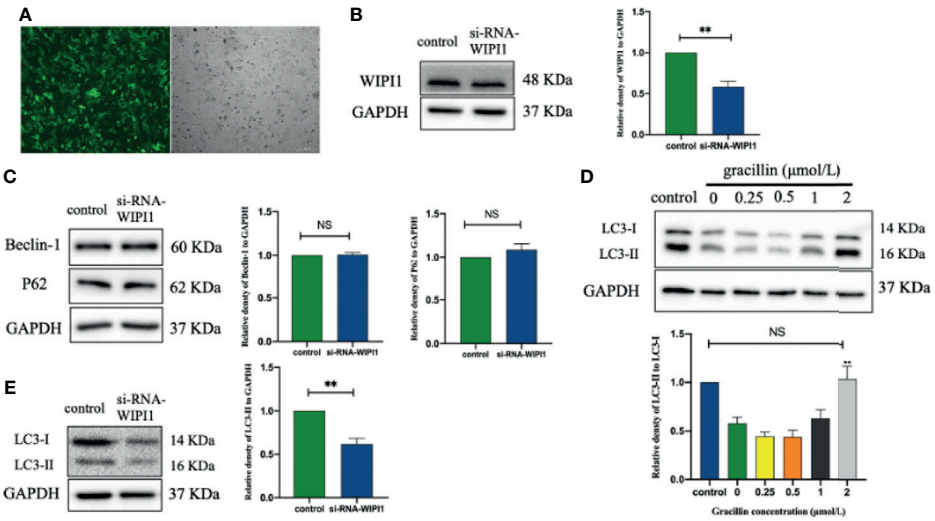

FIGURE 8 | The effect of gracillin on autophagy in A549 cells with WIPI1 gene silenced. **(A)** Fluorescence microscope image of A549 cells with WIPI1 silenced (MOI = 10). **(B)** Western blot verified the effect of WIPI1 being silenced and the relative protein expression level of WIPI1 was quantified by normalization to GAPDH. **(C)** Western blot and relative protein expression levels of Beclin-1 and P62 were quantified by normalization to GAPDH. **(E)** Western blot and relative protein expression level of LC3 are expressed as LC3-II/LC3-I. **(D)** The effect of gracillin on LC3-Iand LC3-II in A549 cells with WIPI1 gene silenced. The full picture is in **Supplementary Figure 5**. Compared with the control group, $^{**}P \leq 0.01$, NS $P > 0.05$.

reached approximately 100mm^3, the mice were treated with gracillin (20 mg/kg, 10 mg/kg, or 5 mg/kg) six days a week for two consecutive weeks. The results clearly showed that the tumor volume growth rate of gracillin-treated mice was significantly lower than that of the control group with dose-dependence (**Figures 9A, D**). At the same time, the tumor weight of the mice in the gracillin-treated groups were also significantly reduced (**Figure 9C**). Meanwhile, Ki67 immunohistochemical staining showed that the proliferation of tumor cells was significantly inhibited by gracillin (**Figure 9B**).

In addition, we also extracted the liver, lung, heart, and kidney of the mice and performed H&E staining. The results showed that gracillin had no obvious toxicity to the liver, lung, heart, and kidney of the mice (**Figure 9E**). The specific manifestations are

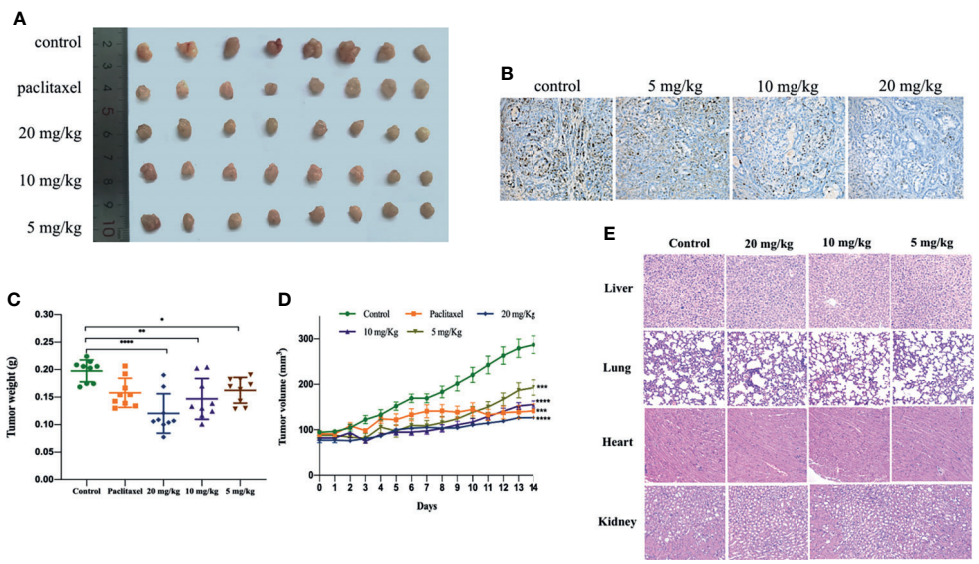

FIGURE 9 | Gracillin inhibits tumor growth in nude mouse models induced by A549. After tumor formation, mice were treated by intraperitoneal injection of gracillin (5, 10, 20 mg/kg) for 2 weeks (n = 8, female and male). **(A)** The mice tumor picture; **(B)** Ki67 immunohistochemical staining; **(C)** tumor volume; **(D)** tumor weight; **(E)** H&E stained image of liver, lung, heart and kidney of gracillin-treated mice. *P ≤ 0.05, **P ≤ 0.01, ***P ≤ 0.001, ****P ≤ 0.0001.

as follows: hepatic cords are arranged regularly, and cells are clearly stained; alveoli are evenly distributed and structured, with a small amount of connective tissue between adjacent alveoli; myocardial tissue is stained uniformly and clearly, cells are arranged neatly and densely, and muscle fibers are aligned and arranged regularly; the structure of the glomerulus is clear, and the shape of the renal tubules is regular.

In conclusion, gracillin has been shown to have an effective inhibitory effect on tumor growth in athymic nude mice carrying A549. In summary, gracillin has shown potential inhibitory effect on tumor of A549 bearing athymic nude mice.

DISCUSSION

According to the latest research report, lung cancer has the highest mortality rate among all cancers (34). As the most classic subtype of lung cancer, NSCLC has malignant metastasis potential and low cure rate (35). Curing NSCLC remains a huge challenge so far. Therefore, it is necessary to find effective and safety drugs. In this experiment, A549 cells, which have been extensively used in the study of NSCLC were employed, were selected as study subjects. Now many compounds derived from TCM displayed potent anti-tumor effect in many cancers. Based on our previous study, we found that a steroidal saponin, gracillin, has significant anti-proliferation activity in A549 cells. Gracillin has been validated to inhibit the proliferation of various tumor cells (19, 21). However, there are relatively few studies on its anti-tumor mechanism. In this study, gracillin was used as a drug candidate against NSCLC, and its anti-tumor effect and mechanism were explored through cell models and animal models.

In this study, the proliferation of A549 cells was significantly inhibited by gracillin, but the proliferation of BEAS-2B cells was inhibited to a lesser extent. In addition, when A549 cells were treated by 3-MA or rapamycin together with gracillin, it was found that the anti-proliferative effect of gracillin in combination with rapamycin was stronger than that in combination with 3-MA, indicating that gracillin Positive induction of autophagy in A549 cells. Autophagy plays a vital role in cancer and has become a potential target for cancer treatment (36). In this study, we found that there are obvious double-layer membranes or multilayer membrane structures in gracillin-treated A549 cells, which indicates that gracillin activates autophagy. The same result can be obtained by observing the pEGFP-LC3 punctate aggregation. At the same time, gracillin induces autophagy by up-regulating Beclin-1, promoting LC3-II transitions, and down-regulating P62. We also found that when 3-MA inhibited autophagy in A549 cells, it could be reversed gracillin-treated A549 cells. Beclin-1 is the mammalian homolog of yeast Atg6 and plays a key role in controlling Vps34-mediated vesicle transport and autophagy induction (37). P62 is an important selective autophagy adaptor protein, which participates in the process of removing ubiquitinated protein as a receptor and transport ubiquitinated protein to the proteasome for degradation (38). LC3 is a marker of the autophagy process. After the synthesis of LC3 protein, the C-terminal 5 peptides are cleaved by Atg4, the glycine residues are exposed, and cytoplasmic localized LC3-I is produced. When autophagy occurs, LC3-I will be modified and processed by ubiquitin-like systems including Atg7 and Atg3 and coupled with phosphatidylethanolamine (PE) to form LC3-II and localize on the inner and outer membranes of autophagy (39). Therefore, the degree of autophagy could be judged by observing the pEGFP-LC3 punctate aggregation on the autophagosome membrane by laser confocal microscope.

Based on the results of high-throughput screening, Further research found that WIPI1 was significantly overexpressed at the mRNA level in gracillin-treated A549 cells. WIPI1 is a new gene that has the potential to become an autophagy marker. It is a homolog of Atg18, located in autophagosomes and early endosomes, and plays an important role in the migration of macrophages (40, 41). The formation of autophagosomes in mammals is related to endosomes, and WIPI1 specifically acts in the formation and fission of tubulo-vesicular endosomal transport carriers (42). In addition, when 3-MA inhibited autophagy, the expression of WIPI1 protein was down-regulated, but this phenomenon could be reversed by gracillin, indicating that WIPI1 is closely related to autophagy in A549 cells. Because WIPI1 has a typical seven-bladed β-propeller structure that can bind to PI3P produced downstream of mTOR (33), the difference in the expression of WIPI1 caused by gracillin may be related to mTOR-related signaling pathways. In this research, it was proved that gracillin inhibits mTOR signaling pathway through down-regulate the expression of p-PI3K and p-Akt and up-regulate the expression of p-AMPK. In addition, found that silencing WIPI1 would reduce the expression of LC3-II, thereby reducing autophagy. But this phenomenon can be alleviated by gracillin, which may be caused by the inability of WIPI1 to be completely silenced. But this phenomenon can be alleviated by gracillin, which may be because WIPI1 cannot be completely silenced.

To study the anti-tumor effect of gracillin in NSCLC, we established a tumor model of athymic nude mice carrying A549. It was found that the tumor growth rate of mice with gracillin treatment was slower than the control group, and the high dose of gracillin (20 mg/kg) has a better anti-tumor effect compared with the paclitaxel treatment group. At the same time, we found that the paclitaxel-treated mice died or became emaciated in the late treatment period, whereas the gracillin-treated mice did not. From the H&E staining results of liver, lung, heart, and kidney of mice, it can be found that gracillin is basically non-toxic to mice, and literature reports can also prove this result (24). Study on the anti-tumor mechanism, absorption, and metabolism of gracillin *in vivo* will become the direction of our future research.

CONCLUSION

In conclusion, this study found that gracillin has anti-tumor effects on NSCLC, and its anti-tumor mechanism is the regulation of autophagy through the mTOR signaling pathways

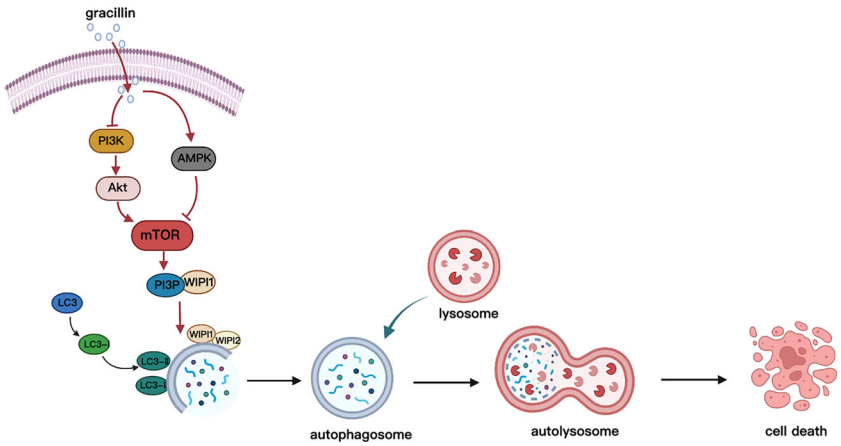

FIGURE 10 | Schematic diagram of gracillin inducing autophagic death of A549 cells. Gracillin regulates the mTOR signaling pathway in A549 cells to induce autophagy death. Gracillin inhibits p-mTOR by inhibiting p-PI3K and p-Akt and activating p-AMPK. WIPI1 is involved in the downstream regulation of autophagy by mTOR.

(**Figure 10**). We cautiously proposed that gracillin has great potential in the treatment of NSCLC.

DATA AVAILABILITY STATEMENT

The original contributions presented in the study are included in the article/**Supplementary Material**. Further inquiries can be directed to the corresponding author.

ETHICS STATEMENT

The animal study was reviewed and approved by the Animal Protection and Ethics Committee of Gannan Medical University.

AUTHOR CONTRIBUTIONS

JY and HL conceived and designed the experiments, contributed new reagents and analysis tools, and supervised all the research. YLL, XL, and BX performed the experiments. YML wrote the original manuscript. YML, MZ, ML, and YLL analyzed the data. JY and HL revised the manuscript. All authors contributed to the article and approved the submitted version.

FUNDING

This work was supported by the National Natural Science Foundation of China (No. 31460082), Key Projects of Traditional Chinese Medicine Science and Technology Plan of Jiangxi Province (2021Z016), Science and Technology Project of Jiangxi Provincial Health Commission (202210946), Key R&D Project of Ganzhou Science and Technology Plan (202101124809).

SUPPLEMENTARY MATERIAL

The Supplementary Material for this article can be found online at: https://www.frontiersin.org/articles/10.3389/fonc.2022.851300/full#supplementary-material

REFERENCES

1. Torre LA, Siegel RL, Jemal A. Lung Cancer Statistics. *Adv Exp Med Biol* (2016) 893:1–19. doi: 10.1007/978-3-319-24223-1_1
2. Ferlay J, Colombet M, Soerjomataram I, Mathers C, Parkin DM, Pineros M, et al. Estimating the Global Cancer Incidence and Mortality in 2018: GLOBOCAN Sources and Methods. *Int J Cancer* (2019) 144(8):1941–53. doi: 10.1002/ijc.31937
3. Siegel RL, Miller KD, Jemal A. Cancer Statistic. *CA Cancer J Clin* (2019) 69 (1):7–34. doi: 10.3322/caac.21551
4. Bray F, Ferlay J, Soerjomataram I, Siegel RL, Torre LA, Jemal A. Global Cancer Statistics 2018: GLOBOCAN Estimates of Incidence and Mortality Worldwide for 36 Cancers in 185 Countries. *CA Cancer J Clin* (2018) 68 (6):394–424. doi: 10.3322/caac.21492
5. Torre LA, Bray F, Siegel RL, Ferlay J, Lortet-Tieulent J, Jemal A. Global Cancer Statistic. *CA Cancer J Clin* (2015) 65(2):87–108. doi: 10.3322/caac.21262
6. Chen RL, Zhao J, Zhang XC, Lou NN, Chen HJ, Yang X, et al. Crizotinib in Advanced non-Small-Cell Lung Cancer With Concomitant ALK Rearrangement and C-Met Overexpression. *BMC Cancer* (2018) 18(1):1171. doi: 10.1186/s12885-018-5078-y
7. Villaruz LC, Socinski MA. The Clinical Utility of PD-L1 Testing in Selecting non-Small Cell Lung Cancer Patients for PD1/PD-L1-Directed Therapy. *Clin Pharmacol Ther* (2016) 100(3):212–4. doi: 10.1002/cpt.385
8. Ettinger DS, Wood DE, Aisner DL, Akerley W, Bauman JR, Bharat A, et al. NCCN Guidelines Insights: Non-Small Cell Lung Cancer, Version 2.2021. *J Natl Compr Canc Netw* (2021) 19(3):254–66. doi: 10.6004/jnccn.2021.0013
9. Garassino MC, Martelli O, Broggini M, Farina G, Veronese S, Rulli E, et al. Erlotinib Versus Docetaxel as Second-Line Treatment of Patients With Advanced non-Small-Cell Lung Cancer and Wild-Type EGFR Tumours (TAILOR): A Randomised Controlled Trial. *Lancet Oncol* (2013) 14 (10):981–8. doi: 10.1016/S1470-2045(13)70310-3

10. Zhou B, Tang C, Li J. K-RAS Mutation and Resistance to Epidermal Growth Factor Receptor-Tyrosine Kinase Inhibitor Treatment in Patients With Nonsmall Cell Lung Cancer. *J Cancer Res Ther* (2017) 13(4):699–701. doi: 10.4103/jcrt.JCRT_468_17
11. Meng Z, Lv Q, Lu J, Yao H, Lv X, Jiang F, et al. Prodrug Strategies for Paclitaxel. *Int J Mol Sci* (2016) 17(5):796. doi: 10.3390/ijms17050796
12. Liaw K, Sharma R, Sharma A, Salazar S, Appiani La Rosa S, Kannan RM. Systemic Dendrimer Delivery of Triptolide to Tumor-Associated Macrophages Improves Anti-Tumor Efficacy and Reduces Systemic Toxicity in Glioblastoma. *J Control Release* (2021) 329:434–44. doi: 10.1016/j.jconrel.2020.12.003
13. Wang Q, Xu G, Jiang Y. [Analgesic and Sedative Effects of the Chinese Drug Rhizoma Paridis]. *Zhongguo Zhong Yao Za Zhi* (1990) 15(2):109–111, 128.
14. Nguyen VT, Darbour N, Bayet C, Doreau A, Raad I, Phung BH, et al. Selective Modulation of P-Glycoprotein Activity by Steroidal Saponines From Paris Polyphylla. *Fitoterapia* (2009) 80(1):39–42. doi: 10.1016/j.fitote.2008.09.010
15. Yang DJ, Lu TJ, Hwang LS. Isolation and Identification of Steroidal Saponins in Taiwanese Yam Cultivar (Dioscorea Pseudojaponica Yamamoto). *J Agric Food Chem* (2003) 51(22):6438–44. doi: 10.1021/jf030390j
16. Shim SH, Lee SY, Kim JS, Son KH, Kang SS. Norditerpenoid Alkaloids and Other Components From the Processed Tubers of Aconitum Carmichaeli. *Arch Pharm Res* (2005) 28(11):1239–43. doi: 10.1007/BF02978206
17. Raju J, Mehta R. Cancer Chemopreventive and Therapeutic Effects of Diosgenin, a Food Saponin. *Nutr Cancer* (2009) 61(1):27–35. doi: 10.1080/01635580802357352
18. Song YX, Ou YM, Zhou JY. Gracillin Inhibits Apoptosis and Inflammation Induced by Lipopolysaccharide (LPS) to Alleviate Cardiac Injury in Mice *via* Improving miR-29a. *Biochem Biophys Res Commun* (2020) 523(3):580–7. doi: 10.1016/j.bbrc.2019.11.129
19. Liu W, Wang Y, Chen J, Lin Z, Lin M, Lin X, et al. Beneficial Effects of Gracillin From Rhizoma Paridis Against Gastric Carcinoma *via* the Potential TIPE2-Mediated Induction of Endogenous Apoptosis and Inhibition of Migration in BGC823 Cells. *Front Pharmacol* (2021) 12:669199. doi: 10.3389/fphar.2021.669199
20. Zheng W, Yan CM, Zhang YB, Li ZH, Li Z, Li XY, et al. Antiparasitic Efficacy of Gracillin and Zingibernsis Newsaponin From Costus Speciosus (Koen Ex. Retz) Sm. Against Ichthyophthirius Multifiliis. *Parasitology* (2015) 142(3):473–9. doi: 10.1017/S0031182014001358
21. Chen CR, Zhang J, Wu KW, Liu PY, Wang SJ, Chen DY, et al. Gracillin Induces Apoptosis in HL60 Human Leukemic Cell Line *via* Oxidative Stress and Cell Cycle Arrest of G1. *Pharmazie* (2015) 70(3):199–204.
22. Min HY, Jang HJ, Park KH, Hyun SY, Park SJ, Kim JH, et al. The Natural Compound Gracillin Exerts Potent Antitumor Activity by Targeting Mitochondrial Complex II. *Cell Death Dis* (2019) 10(11):810. doi: 10.1038/s41419-019-2041-z
23. Min HY, Pei H, Hyun SY, Boo HJ, Jang HJ, Cho J, et al. Potent Anticancer Effect of the Natural Steroidal Saponin Gracillin Is Produced by Inhibiting Glycolysis and Oxidative Phosphorylation-Mediated Bioenergetics. *Cancers (Basel)* (2020) 12(4):913. doi: 10.3390/cancers12040913
24. Yang L, Zhu T, Ye H, Shen Y, Li Z, Chen L, et al. Gracillin Shows Potent Efficacy Against Colorectal Cancer Through Inhibiting the STAT3 Pathway. *J Cell Mol Med* (2021) 25(2):801–12. doi: 10.1111/jcmm.16134
25. Yang J, Cao L, Li Y, Liu H, Zhang M, Ma H, et al. Gracillin Isolated From Reineckia Carnea Induces Apoptosis of A549 Cells *via* the Mitochondrial Pathway. *Drug Des Devel Ther* (2021) 15:233–43. doi: 10.2147/DDDT.S278975
26. Xu HD, Qin ZH. Beclin 1, Bcl-2 and Autophagy. *Adv Exp Med Biol* (2019) 1206:109–26. doi: 10.1007/978-981-15-0602-4_5
27. Mizushima N. Autophagy: Process and Function. *Genes Dev* (2007) 21(22):2861–73. doi: 10.1101/gad.1599207
28. Klionsky DJ. Autophagy Revisited: A Conversation With Christian De Duve. *Autophagy* (2008) 4(6):740–3. doi: 10.4161/auto.6398
29. Feng Y, He D, Yao Z, Klionsky DJ. The Machinery of Macroautophagy. *Cell Res* (2014) 24(1):24–41. doi: 10.1038/cr.2013.168
30. Levy JMM, Towers CG, Thorburn A. Targeting Autophagy in Cancer. *Nat Rev Cancer* (2017) 17(9):528–42. doi: 10.1038/nrc.2017.53
31. Zhang Q, Wang X, Cao S, Sun Y, He X, Jiang B, et al. Berberine Represses Human Gastric Cancer Cell Growth *In Vitro* and *In Vivo* by Inducing Cytostatic Autophagy *via* Inhibition of MAPK/mTOR/p70S6K and Akt Signaling Pathways. *BioMed Pharmacother* (2020) 128:110245. doi: 10.1016/j.biopha.2020.110245
32. Tsuyuki S, Takabayashi M, Kawazu M, Kudo K, Watanabe A, Nagata Y, et al. Detection of WIPI1 mRNA as an Indicator of Autophagosome Formation. *Autophagy* (2014) 10(3):497–513. doi: 10.4161/auto.27419
33. Bakula D, Muller AJ, Zuleger T, Takacs Z, Franz-Wachtel M, Thost AK, et al. WIPI3 and WIPI4 Beta-Propellers are Scaffolds for LKB1-AMPK-TSC Signalling Circuits in the Control of Autophagy. *Nat Commun* (2017) 8:15637. doi: 10.1038/ncomms15637
34. Tabnak P, HajiEsmailPoor Z, Soraneh S. Ferroptosis in Lung Cancer: From Molecular Mechanisms to Prognostic and Therapeutic Opportunities. *Front Oncol* (2021) 11:792827. doi: 10.3389/fonc.2021.792827
35. Chen X, Wu Q, Chen Y, Zhang J, Li H, Yang Z, et al. Diosmetin Induces Apoptosis and Enhances the Chemotherapeutic Efficacy of Paclitaxel in non-Small Cell Lung Cancer Cells *via* Nrf2 Inhibition. *Br J Pharmacol* (2019) 176(12):2079–94. doi: 10.1111/bph.14652
36. Kocaturk NM, Akkoc Y, Kig C, Bayraktar O, Gozuacik D, Kutlu O. Autophagy as a Molecular Target for Cancer Treatment. *Eur J Pharm Sci* (2019) 134:116–37. doi: 10.1016/j.ejps.2019.04.011
37. Russell RC, Tian Y, Yuan H, Park HW, Chang YY, Kim J, et al. ULK1 Induces Autophagy by Phosphorylating Beclin-1 and Activating VPS34 Lipid Kinase. *Nat Cell Biol* (2013) 15(7):741–50. doi: 10.1038/ncb2757
38. Lamark T, Svenning S, Johansen T. Regulation of Selective Autophagy: The P62/SQSTM1 Paradigm. *Essays Biochem* (2017) 61(6):609–24. doi: 10.1042/EBC20170035
39. Tanida I, Ueno T, Kominami E. LC3 and Autophagy. *Methods Mol Biol* (2008) 445:77–88. doi: 10.1007/978-1-59745-157-4_4
40. Bakula D, Takacs Z, Proikas-Cezanne T. WIPI Beta-Propellers in Autophagy-Related Diseases and Longevity. *Biochem Soc Trans* (2013) 41(4):962–7. doi: 10.1042/BST20130039
41. Liao CC, Ho MY, Liang SM, Liang CM. Recombinant Protein Rvp1 Upregulates BECN1-Independent Autophagy, MAPK1/3 Phosphorylation and MMP9 Activity *via* WIPI1/WIPI2 to Promote Macrophage Migration. *Autophagy* (2013) 9(1):5–19. doi: 10.4161/auto.22379
42. De Leo MG, Berger P, Mayer A. WIPI1 Promotes Fission of Endosomal Transport Carriers and Formation of Autophagosomes Through Distinct Mechanisms. *Autophagy* (2021) 17(11):3644–70. doi: 10.1080/15548627.2021.1886830

Conflict of Interest: The authors declare that the research was conducted in the absence of any commercial or financial relationships that could be construed as a potential conflict of interest.

Publisher's Note: All claims expressed in this article are solely those of the authors and do not necessarily represent those of their affiliated organizations, or those of the publisher, the editors and the reviewers. Any product that may be evaluated in this article, or claim that may be made by its manufacturer, is not guaranteed or endorsed by the publisher.

frontiers | Frontiers in Oncology

ORIGINAL RESEARCH
published: 08 April 2022
doi: 10.3389/fonc.2022.855603

Bruceine H Mediates EGFR-TKI Drug Persistence in NSCLC by Notch3-Dependent β-Catenin Activating FOXO3a Signaling

Jiahui Wu[1], *Xiao He*[2], *Ziwei Xiong*[1], *Lingyu Shi*[1], *Daofeng Chen*[3], *Yulin Feng*[2*] *and Quan Wen*[1*]

[1] Pharmacy, Jiangxi University of Chinese Medicine, Jiangxi, China, [2] National Pharmaceutical Engineering Center for Solid Preparation in Chinese Herbal Medicine, Jiangxi, China, [3] Pharmacy, Fudan University of Pharmacy, Shanghai, China

Tyrosine kinase inhibitors (TKIs) targeting epidermal growth factor receptor (EGFR) protein serve as a critical pillar in the treatment of non-small cell lung cancer (NSCLC), but resistance is universal. Identifying the potential key factors of drug resistance to EGFR-TKIs is essential to treat patients with EGFR mutant lung cancer. Our research here shows that bruceine H suppressed the proliferation, migration, and invasion of lung cancer cells; inhibited the growth of human NSCLC cell xenografts; and enhanced the therapeutic effects of gefitinib in the PC-9/GR xenograft models, possibly by inhibiting Notch3. In order to analyze the potential targets of the combination of Notch3 and EGFR-TKIs on resistance to EGFR, we analyzed the differences of gene expression between NSCLC tissues and EGFR-driven gefitinib-resistant tumoral groups and then identify through the WGCNA key genes that may provide therapeutic targets for TKI-resistant lung cancer xenograft models. We confirmed that EGFR-TKI in combination with Notch3 inhibitor can inhibit the expression of β-catenin and enhance the level of FOXO3a, leading to improved recurrence-free survival and overall survival of the xenotransplantation model. These results support that the combination of gefitinib and bruceine H may provide a promising alternative strategy for treating acquired EGFR-TKI resistance in patients with NSCLC.

Keywords: bruceine H, Notch3 inhibitor, EGFR-TKI, acquired resistance, non-small cell lung cancer

OPEN ACCESS

Edited by:
Maria Teresa Esposito, University of Roehampton London, United Kingdom

Reviewed by:
Giuliana Papoff, National Research Council (CNR), Italy
Manoj Garg, Amity University, India

***Correspondence:**
Yulin Feng
fengyulin2003@126.com
Quan Wen
qwen12@fudan.edu.cn

Specialty section:
This article was submitted to Pharmacology of Anti-Cancer Drugs, a section of the journal Frontiers in Oncology

Received: *15 January 2022*
Accepted: *08 March 2022*
Published: *08 April 2022*

Citation:
Wu J, He X, Xiong Z, Shi L, Chen D, Feng Y and Wen Q (2022) Bruceine H Mediates EGFR-TKI Drug Persistence in NSCLC by Notch3-Dependent β-Catenin Activating FOXO3a Signaling. Front. Oncol. 12:855603. doi: 10.3389/fonc.2022.855603

INTRODUCTION

Lung cancer leads to more cancer deaths than breast, prostate, colorectal, and brain cancers grouped together (1). About a quarter of cancer deaths are caused by lung cancer. Lung cancer is classified into small cell lung cancer (SCLC) and non-small cell lung cancer, among which NSCLC cases account for about 83% of lung cancer, including squamous cell carcinoma, adenocarcinoma, and large cell lung cancer (2). Since there are no symptoms or no obvious symptoms in the early stage of NSCLC, most patients are diagnosed at stage IIIB or even stage IV at their first diagnosis, at which time the surgical treatment is not effective and the risk of recurrence is high, so medical treatment is mainly applied (3). The low survival rate of NSCLC patients reflects that most of them (57%) are diagnosed with drug resistance and metastatic diseases, and their 5-year relative survival rate is 23% (1, 4).

In recent years, with the renewal of treatment methods, the improvement of chemotherapeutic agents, and the diversification of therapeutic strategies, the clinical therapeutic effect of lung cancer is obvious to all, but the drug resistance, metastasis, and low long-term survival rates are still critical challenges.

Brucea javanica (L.) Merr. is known to contain a large number of quassinoids, some of which possess a wide spectrum of biological activities, including anticancer (5), cancer chemopreventive (6), and cytotoxic activities (7). Previous studies showed that bruceine D (BD), a Notch inhibitor that can be derived from *B. javanica* seeds, exerts remarkable anticancer efficacy against human malignancies by Wnt/β-catenin (8) and MAPK pathways (9). Moreover, BD or brusatol can significantly increase the sensitivity of sorafenib or gefitinib to TKI-resistant tumors (8, 10). Although many studies have reported the antitumor activity of BD, it also showed certain cytotoxic activity to a normal human cell line (**Figure S1**). Bruceine H (BH) had only one more hydroxyl substitution at C-13 in its structure compared with bruceine D, improving its aqueous solubility and reducing its toxicity to normal cells.

Gefitinib is the first EGFR tyrosine kinase selective inhibitor (EGFR-TKI), which shows a fine curative effect on recurrent or advanced NSCLC (11). Lung cancer patients, who have undergone treatment for a few months, have been apparently resistant to gefitinib. Somatic activating mutations of EGFR, including the L858R mutation, G719X mutation, and deletion of exon 19 (12), are related to the sensitivity to EGFR-TKIs. In addition to EGFR mutations accounting for acquired resistance mechanisms, T790M site mutation (13); MET amplification and HER2 hyperactivation (14); fibroblast growth factor receptor (FGFR) (15), KRAS (16), PIK3CA, and B-Raf proto-oncogene (BRAF) V600E mutations (17); overexpression of EGF (18); and activation of MAPK (19) may also contribute to the EGFR-TKI acquired resistance. Increasing studies have reported that Notch inhibitor mediates EGFR-TKI drug persistence in the EGFR mutant NSCLC (20, 21).

The Notch signaling pathway is associated with the regulation of cellular proliferation, differentiation, and apoptosis during embryonic development and whole adulthood (22). Although the normal Notch signaling plays an important role in lung development and formation, especially in the transformation of lung plasticity and repair, its abnormal activity has been demonstrated to be related to the occurrence and progression of lung cancer, including NSCLC (23, 24). Twenty years ago, the discovery that Notch could be first implicated as a catalyst for NSCLC pathogenesis was made when a translocation of a somatic chromosome t (15, 19), resulting in overexpression of the Notch3 gene, was found in poorly differentiated and invasive lung adenocarcinoma (25). Recent findings indicate that Notch3 overexpression not only is responsible for the initiation of non-small cell lung cancer (26, 27), but also can reduce the expression of E-cadherin, upregulate fibronectin, and promote EMT (28) and tumor invasion (29). Therefore, inhibiting Notch3 could potentially make EGFR-TKI-resistant NSCLC more susceptible. Furthermore, the Notch3-dependent β-catenin signal has been shown to contribute to drug resistance associated with the second mutation of EGFR (20), while β-catenin binding to FOXO3a regulates the inhibitory effect of FOXO3a on EMT (30), which we speculate that Notch3-dependent β-catenin and FOXO3a signaling pathways possibly have a hand in resistance to EGFR-TKIs.

In this study, bruceine D and H, characterized by the core structure of tetracyclic triterpene, were extracted from *B. javanica*. We found that both of them are bound to Notch3 protein with a high affinity in computational modeling. Our *in-vitro* and *in-vivo* model system of gefitinib-induced drug-persistent cells (DPCs) has demonstrated Notch3 as a critical mediator of this effect, but the precise mechanisms by which Notch3 maintains specific targeting of this pathway are not understood. For this reason, we sought to identify differentially expressed genes (DEGs) and study the interactions among them in gefitinib-resistant lung cancer to identify drug-resistant core genes and drug targets. The experimental results show that Notch3 inhibition might be a potent strategy to treat patients with drug resistance and tumor recurrence of NSCLC.

MATERIALS AND METHODS

Compounds and Reagents

Brucea javanica seeds were purchased from Guangxi Zhuang Autonomous Region, People's Republic of China, and authenticated by Prof. Guo-Yue Zhong (Jiangxi University of Chinese Medicine). BD and BH were extracted from the seeds of *B. javanica* and identified on the basis of nuclear magnetic resonance (NMR) data (the separation method is described in detail in the **Supplementary Material**); their purity was ≥95% based on high-performance liquid chromatography (HPLC) analysis. Gefitinib was provided by Meilun (ZD1839, Dalian, China). The primary antibodies NOTCH3 (mouse), β-catenin (mouse), EGFR, phospho-EGFR (Tyr1068), FOXO3a (mouse), CBP (Lys1535)/p300 (Lys1499), and β-actin were from Cell Signaling Technology (CST, Danvers, MA, USA). Bax, Bcl-2, caspase-3, and cleaved caspase-3 were provided by Santa Cruz Biotechnology (SCBT, Dallas, TX, USA). The secondary antibodies were HRP-conjugated anti-rabbit IgG and anti-mouse IgG (Abcam, Cambridge, UK).

Cell Lines and Cell Culture

The human NSCLC cell lines (A549, PC-9, and PC-9/GR) and other cell lines (16HBE and LO2) were purchased from the American Type Culture Collection (ATCC, Manassas, VA, USA). A549 and LO2 cells were cultured in RPMI-1640 (Solarbio, Beijing, China) containing 10% fetal bovine serum (FBS, Gibco, Carlsbad, CA, USA), and PC-9 and 16HBE cells were cultured in DMEM (Solarbio) with 10% FBS. The PC-9/GR cells, a gefitinib-resistant strain of human lung adenocarcinoma cell, were grown in DMEM with 10% FBS and gefitinib (800 ng/ml). All cell lines were cultivated at 37°C under 5% CO_2.

Cell Viability Assay

The Cell Counting Kit-8 assays (Beyotime, Shanghai, China) were performed to assess cell viability. A549 (5×10^3/100 µl/well), PC-9 (6×10^3/100 µl/well), or PC-9/GR cells (6×10^3/100 µl/well) were cultured overnight in 96-well plates (NEST, Wuxi, China) and were then treated with several concentrations of BD, BH, and/or gefitinib at the indicated concentration for 24 or 48 h. Then, the cells were incubated for an additional 2 h with 100 µl of RPMI-1640/DMEM and 10 µl of CCK-8 solution at 37°C. Microplate readers (Infinite F500, Tecan, Mannedorf, Switzerland) were used to measure the absorbance (*A*) at 450 nm. All samples were assessed in triplicate.

Wound Healing Assay for Migration

A549 cells (3×10^5/ml/well) were seeded into a six-well plate. After overnight culture, when the fusion rate reached 95%–100%, the sterile pipette tip was perpendicular to the plate plane, and a straight wound was drawn on the cell monolayer. Following treatment with BD or BH, the migration of the cells was examined under a microscope (×4, Nikon, Tokyo, Japan), and pictures were obtained at 0 and 48 h. The computation of the cell migration formula is as follows: relative migration area (%) = (0 h wound area – 48 h wound area)/0 h wound area × 100%.

Transwell Migration and Matrigel Invasion Assays

The Transwell insert in a 24-well plate (8 µm, Corning, NY, USA) was taken out, and a 600-µl medium containing 10% FBS was added to the bottom chamber. The A549 cells were resuspended with 10% FBS culture medium, and the diluted cell suspension (3×10^5/300 µl) was cultured in the top chamber and then incubated with or without Matrigel (BD BioCoat). After 12 h, the medium in the top chamber was changed to RPMI-1640 without FBS, and BD or BH with different concentrations was added (31). After an additional 12 h, the cells that migrated or invaded the bottom side of the polycarbonate film were fixed with methanol for 30 min and then stained for 15 min with 0.1% crystal violet (Solarbio), after which their number was assessed under a microscope (×4, Nikon).

Apoptosis Analysis by Flow Cytometry

Cells (4×10^5) were seeded in six-well plates, incubated overnight, and treated for 48 h with BH or gefitinib alone or combined before staining before examining with an Annexin V-FITC Apoptosis Detection Kit (Yeasen, Shanghai, China). After being digested with trypsin without EDTA, the cells were washed gently with culture medium and twice with cold PBS. The pellet was resuspended in 400 µl of 1× binding buffer, the resuspended cells were transferred to flow tubes, then Annexin V-FITC (5 µl) and propidium iodide (10 µl) were added, and the mixture was incubated for 15 min at room temperature in the dark. The percentage of apoptotic cells was determined by flow cytometry (Backman, CA, USA) and FlowJo V10 software.

Docking Analysis

The ligand molecule was downloaded from the PubChem database (https://pubchem.ncbi.nlm.nih.gov/) and it was further converted to a PDB file using Open Babel GUI. The crystal structures of EGFR and Notch3 corresponding to PDB ID (3G5Z, 4ZLP) were obtained from the PDB database (https://www.rcsb.org/). The crystal water and other small molecules were removed from the protein structure by PyMOL (https://pymol.org), then hydrogens and charges were added using the AutoDock tool (http://autodock.scripps.edu/). Discovery Studio (http://dstudio19.csc.fi:9944) was used to predict the hydrophobic interaction between BD, BH, and gefitinib with the active site of the residue, along with the force of binding.

Identification of Potential Resistance Targets in NSCLC Based on Weighted Gene Co-Expression Network Analysis and Differential Gene Correlation Analysis

The Gene Expression Omnibus (GEO) database (https://www.ncbi.nlm.nih.gov/geoprofiles/) was searched to download two microarray datasets (GSE115864 and GSE33532), and then their gene expression level and differential expression were analyzed. The detailed clinical information and complete mRNA expression profile data of 552 lung adenocarcinoma (LUAD) samples and 504 lung squamous cell carcinoma (LUSC) samples were obtained from The Cancer Genome Atlas database (TCGA, https://tcga-data.nci.nih.gov/tcga/) (accessed on May 12, 2021). We used the limma (linear models for microarray data) tool (32) to screen DEGs between PC-9 cells resistant to gefitinib and PC-9/GR treated with Notch3 inhibition and gefitinib, overlapped with the most significant module identified by weighted gene co-expression network analysis (WGCNA) (33) to obtain the hub genes, and then we subsequently carried out Gene Ontology (GO) functional annotation analysis and Kyoto Encyclopedia of Genes and Genomes (KEGG) pathway enrichment analysis. Then, the key genes were predicted by Cytoscape plugin cytoHubba, and six key genes were selected according to the expression patterns in GEO and TCGA databases. Finally, the diagnostic value of the top six key genes was further verified by survival analysis and expression level in mutant lung cancer.

Western Blotting

The total proteins of cells and tissues were extracted with RIPA cleavage buffer containing a protease inhibitor cocktail, phenylmethylsulfonyl fluoride (PMSF, Solarbio). The cell lysates (20 µg) were run on SDS-polyacrylamide gel (6%–10%) and transferred to the polyvinylidene fluoride membrane (PVDF, Millipore, MA, USA) by electrophoresis. The membrane was blocked with 5% skim milk in TBST for 2 h, incubated overnight with the corresponding primary antibody at 4°C, and then incubated with the corresponding secondary antibody at room temperature for 2 h. The reaction products were detected by chemiluminescence by ECL Western Blotting Detection System. Finally, quantitative analysis was carried out with ImageJ software.

H&E and TUNEL Staining

The heart, liver, spleen, lung, kidney, and tumor tissues were embedded in paraffin, and the sections (4 μm) were stained with hematoxylin–eosin (H&E, Solarbio) and then examined and analyzed under a Leica DM6B microscope (Leica Microsystems, Wetzlar, Germany).

A TUNEL Assay Kit (Yeasen) was used to detect apoptosis. Briefly, the tumor section was dewaxed and incubated with proteinase K at 37°C for 20 min, followed by incubation with labeling buffer containing terminal deoxynucleotidyl transferase (TdT) and digoxigenin-labeled deoxyuridine triphosphate (dUTP). Then, the tissues were stained with 4′,6-diamidino-2-phenylindole (DAPI) to stain the cell nucleus. TUNEL-positive cells were quantified by counting positively stained cells.

Immunocytochemistry and Immunohistochemistry

The PC-9/GR cells were added to glass slides in six-well plates and treated with BH and gefitinib in different concentrations, and DMSO served as an untreated control. The primary FOXO3a antibody (CST) was diluted at 1:100 and incubated at 4°C overnight. Afterward, the goat anti-rabbit IgG secondary antibody (dilution ratio: 1:400; Abcam) was added to the fixed PC-9/GR cells in a dark condition for 1 h and the nuclei were stained with DAPI (CST) for 5 min. Finally, fluorescence images were captured using the LAS AF Lite software and Leica DM6B microscope (Leica Microsystems).

The tumor section was dewaxed and repaired with antigen, 3% H_2O_2 was added, and then the section was sealed with 10% goat serum at room temperature for 30 min. The first antibody against Ki-67 and Notch3 (CST) was incubated overnight at 4°C, and the second antibody was incubated at room temperature for 30 min. After DAB staining, the sections were counterstained with hematoxylin for 2 min and then observed and analyzed under a Leica microscope.

Tumor Xenografts

The animal procedures were approved by the Ethics Committee of the Experimental Animal Center of Jiangxi University of Chinese Medicine (Nanchang, China, SCXK 2016-0006) and conducted following the Guide for the Care and Use of Laboratory Animals. Four-week-old male BALB/c nude mice (weighing 16–17 g, SPF grade) were obtained from Shanghai Shrek Experimental Animal Co., Ltd. (Shanghai, China). The xenotransplantation model was established by subcutaneous injection of A549 or PC-9/GR cells in nude mice, which were collected with PBS and mixed with an equal volume of Matrigel at a final concentration of 1×10^7/ml. Approximately 100 mm^3 of tumor volume was reached, and mice were randomly divided into four groups: vehicle control, gefitinib alone, BH alone, or a combination of gefitinib and BH. Gefitinib (25, 50 mg/kg) and BH (2.5, 5 mg/kg) were dissolved in 0.5% CMC-Na containing 5% DMSO and administered every day by oral gavage. Measurements of tumor size and body weight were conducted every 2 days with a vernier caliper and an electronic balance. Nodule growth was quantified by using the following formula: tumor volume (mm^3) = (short-diameter)^2 × large-diameter × π/6.

Toxicity and Pharmacokinetic Study

At the end of the experiment, blood samples were taken and analyzed by blood routine. The remaining blood samples were precipitated, followed by a 15-min centrifugation (3,000 rpm) at 4°C, and the serum was taken for biochemical analysis. The lungs and spleen were weighed and recorded. H&E staining of the heart, liver, spleen, lungs, and kidneys was performed to evaluate the cytotoxic effects of BH.

We administered BH by gavage and intravenous administration to SD rats (male, 200–220 g, $n = 6$) after they had fasted for 12 h. For oral gavage, the BH was dissolved in DMSO/0.5% CMC-Na (5/95, v/v/), and for intravenous administration, it was dissolved in DMSO/0.9% NaCl (5/95, v/v/), and then the blood samples were collected at intervals to determine the pharmacokinetic (PK) profiles of SD rats.

Statistical Analysis

All the experimental data were analyzed by GraphPad Prism 8.0 software (USA). The results were expressed as the average ± SEM of at least three independent experiments. Double-tailed *t*-test and ANOVA were used; when $^*P < 0.05$, $^{**}P < 0.01$, or $^{***}P < 0.001$, it was considered to be statistically significant.

RESULTS

The Structure of the Notch Inhibitors BH and BD

The structures of BH and BD are presented in **Figure 1A**, which were identified by ^1H and ^{13}C nuclear magnetic resonance (NMR) (**Figures S6–S9**). HPLC analysis was performed in our study to confirm that the purity of BH and BD was ≥95% (**Figure 1B**). Bruceine H and gefitinib showed very good binding affinity (−31.9, −20.0 kcal/mol) with the amino acid residues PHE98, TRP48 and GLU123, ARG216 of the target protein EGFR (3G5Z), respectively. Furthermore, the Notch inhibitors BH and BD were also docked to find the interaction and binding affinity (LibDockScore:169.0, 165.2 >120) with the target protein Notch3 (4ZLP). BH and BD bind to the same sites on the Notch3 HD domain in modeling, despite the different chemical formula (**Figure 1C**). This shows that both of these compounds have similar affinity to Notch3 protein, and in the subsequent study of the cell model, BH and BD have also been proven to have similar antitumor activity.

BH Significantly Suppressed Migration and Invasion and Induced Apoptosis in NSCLC Cells

The NSCLC cell lines A549 (EGFR wild-type KRAS mutation) and PC-9 (EGFR exon 19 deletion) were treated with BH and BD at different concentrations for 24 and 48 h, respectively. The results showed that gefitinib, BH, and BD could inhibit the proliferation of A549 and PC-9 cells in a dose-dependent manner.

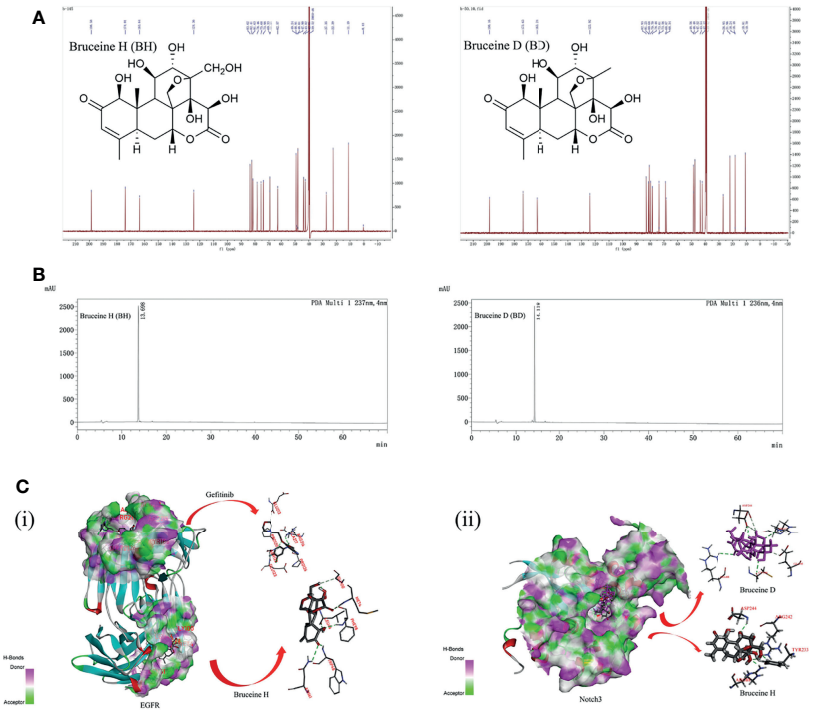

FIGURE 1 | The interaction of bruceine H (BH) with Notch3 and epidermal growth factor receptor (EGFR) proteins. **(A)** Chemical structure of BH and bruceine D (BD) by ^{13}C NMR spectrum. **(B)** The purity of BH and BD by HPLC chromatogram. **(C)** Computational modeling of BH binding to Notch3 and EGFR. (i) 3D interaction of BH and gefitinib with the EGFR protein. (ii) 3D interaction of BH and BD with the Notch3 protein.

The IC_{50} (48 h) values of gefitinib, BH, and BD against A549 cells were 23.60, 25.54, and 26.80 μM, and the IC_{50} values against PC-9 cells were 11.44, 12.57, and 21.84 μM, respectively (**Figure 2A**). The inhibitory effect of BH on cell proliferation was similar to that of BD, especially on A549 cells.

Given the role that migration and invasion of cancer cells play in cancer metastasis and patient mortality, further investigation of BH and BD for their effect on migration and invasion was conducted. Wound healing assay showed that the migration of A549 cells was impaired by 4 μM BH (**Figure 2B**). Transwell cell invasion assay results demonstrated that BH and BD can exert significant anti-invasive and antimigratory actions toward A549 in a dose-dependent manner (**Figures 2C, D**). In an attempt to determine whether the proliferative inhibition by BH was related to apoptosis, cells from A549 and PC-9 were treated with BH for 48 h to determine the percentage of apoptotic cells. **Figure 2E** shows that the proportion of apoptotic cells increased after treatment with various concentrations of BH, as well as the early apoptosis rate in A549 cells, while the late apoptotic rate of PC-9 cells increased, relative to the control conditions. It is noteworthy that BD shows higher sensitivity in 16HBE and LO2 cell lines than BH (**Figure S1**). Taken together, BH exhibited not only potent antitumor activities but also no apparent toxicity to normal human cell lines and was selected for further studies. Then, we further determined whether BH would synergize with gefitinib to decrease the PC-9/GR cell viability.

BH Combined With Gefitinib Inhibited Gefitinib-Resistant Cell Lines PC-9/GR and Notch3 Signaling

Lung cancer with EGFR exon 19 deletion is known to have the greatest prevalence, which is present in 1.57% of AACR GENIE cases (34). As compared with PC-9 cells, gefitinib-resistant PC-9 cells (PC-9/GR) contain the same exon 19 deletions of the EGFR gene but show low sensitivity to gefitinib and lower expression of FOXO3a (**Figure 3A**). PC-9 cells harboring EGFR activation mutation were sensitive to gefitinib, IC_{50} at 11.44 μM, while PC-9/GR was resistant to gefitinib under long-term low concentration of gefitinib, IC_{50} at 51.30 μμ (**Figure 3B**). **Figures 3C, D** show that drug synergism in PC-9/GR was calculated using CalcuSyn 2.0 software when BH and gefitinib are combined according to their IC_{50} concentrations. It was discovered that drug synergy increased as drug concentration was increased, and the drug synergy was the strongest at an inhibition rate of 80%. As a result of gefitinib treatment alone, PC-9/GR is no longer sensitive to gefitinib, and BH and gefitinib combined improved the inhibitory effect compared with a single treatment. To explore the effects of BH and gefitinib on the apoptosis of PC-9/GR cells, the results of flow cytometry showed that low-dose BH or gefitinib alone had little effects, while a combination of BH and gefitinib obviously induced apoptosis in PC-9/GR cells compared with gefitinib monotherapy (**Figures 3E, F**).

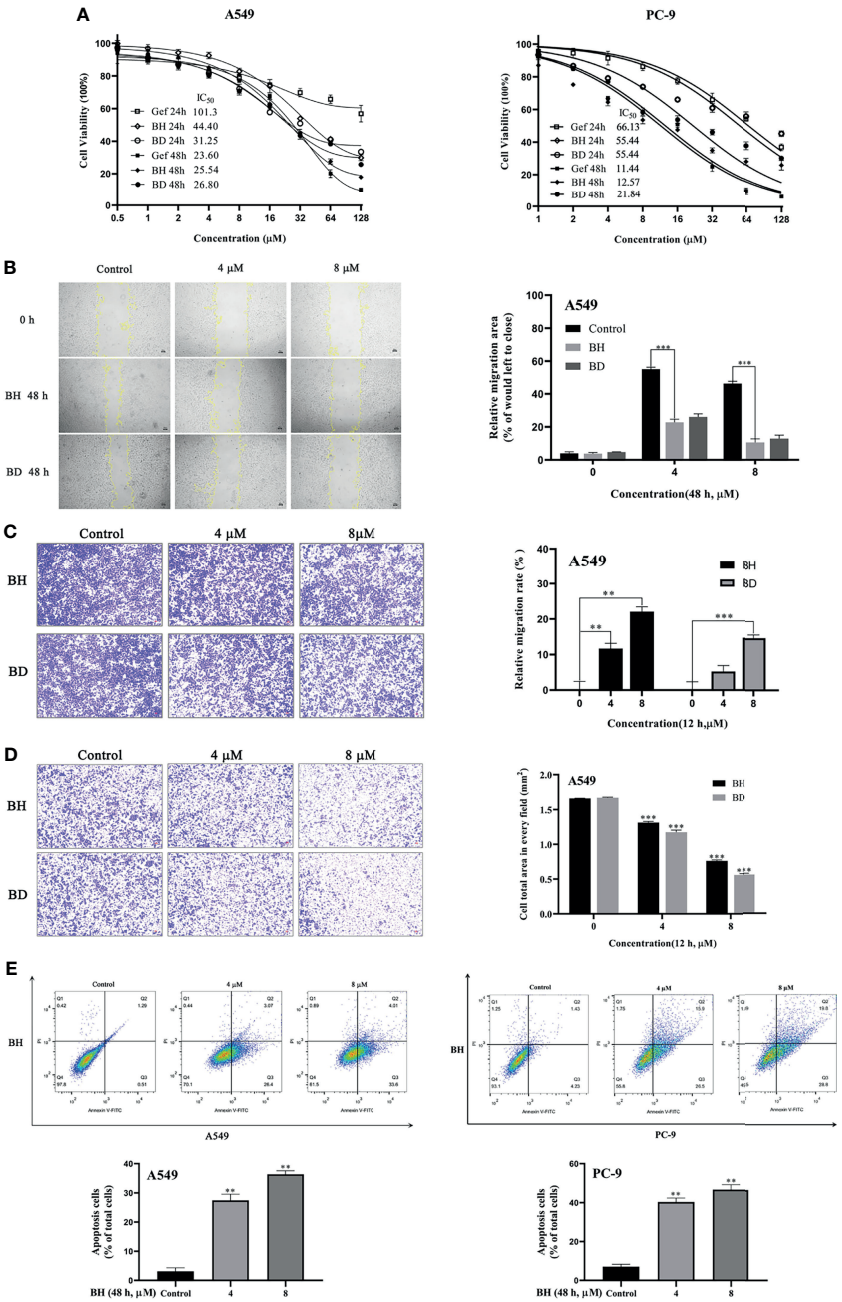

FIGURE 2 | Antitumor effects of BH and BD against non-small cell lung cancer (NSCLC) cell lines *in vitro*. **(A)** The proliferation of cells as well as the IC_{50} was determined in A549 and PC-9 cells after 24 and 48 h. **(B)** Cell migration of A549 cells was detected by wound healing assay. **(C, D)** Transwell migration and Matrigel invasion assays of A549 cells were measured. **(E)** The apoptosis of A549 and PC-9 cells was measured using flow cytometry 48 h after treatment with BH. All experiments were independently conducted at least three times and showed representative data. "**" represents BH group vs. the Control group (**$p < 0.01$, ***$p < 0.001$).

Subsequently, the extracts of PC-9/GR cells treated with BH and/or gefitinib for 48 h were prepared for immunoblotting. The Western blot analysis showed that BH combined with gefitinib treatment deregulated the anti-apoptotic protein (Bcl-2) and significantly increased the expression of Bax. Additionally, compared with the vehicle and gefitinib or BH alone, the expression of cleaved caspase-3 was remarkably increased and caspase-3 was inhibited (**Figure 4A**). Together, these results indicate that bruceine H in combination with gefitinib results in a significant induction of PC-9/GR apoptosis. Additionally, the level of FOXO3a was activated and β-catenin levels were suppressed by a combination of gefitinib and BH (**Figure 4B**). We found that, through inhibiting the activity of β-catenin and activating FOXO3a in drug-resistant cells, BH enhanced the

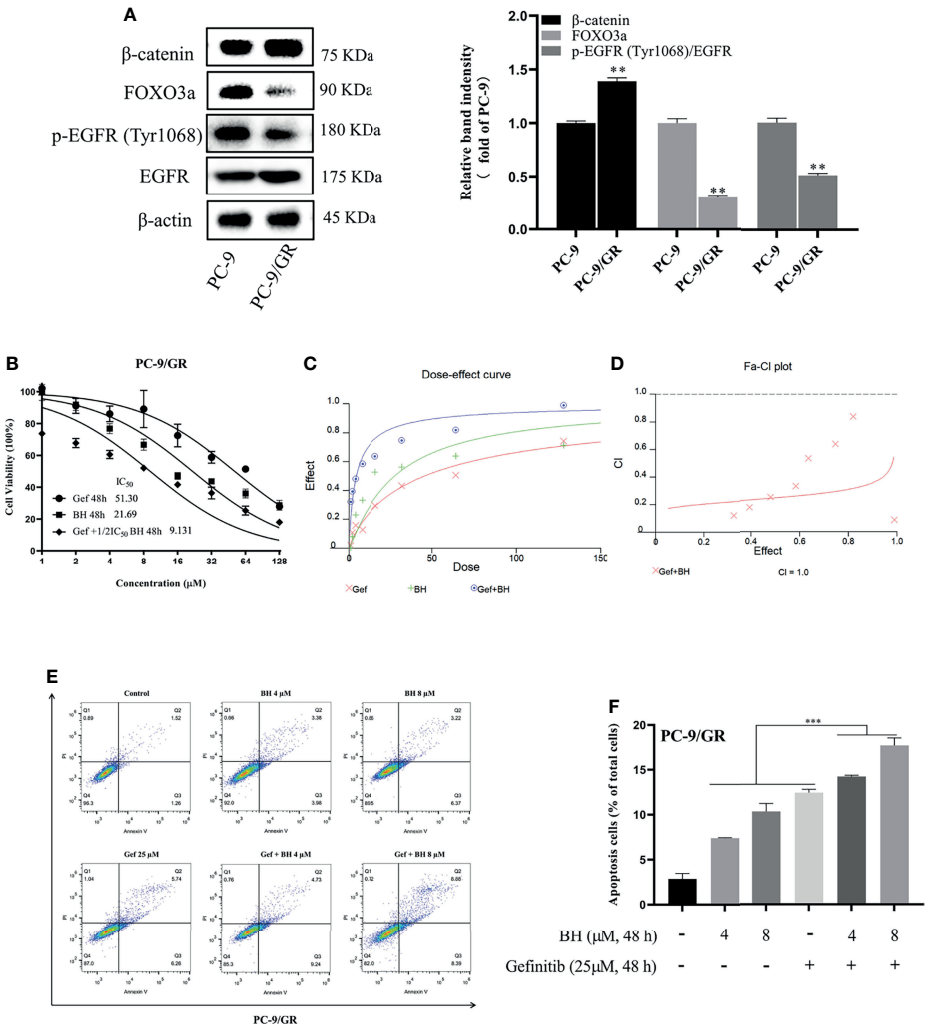

FIGURE 3 | BH significantly enhanced gefitinib sensitivity *in vitro*. **(A)** The different expressions of β-catenin, FOXO3a, p-EGFR (Tyr1068), and EGFR in PC-9 and PC-9/GR cells were measured by Western blot. **(B)** PC-9/GR cells were incubated with BH, gefitinib, and combination at the indicated concentrations for 48 h. **(C, D)** The combined action curve of gefitinib and BH and the synergistic effect index of drug combination in PC-9/GR cells (CI = 1 when the two drugs were superimposed, CI < 1 when the combination of drugs appeared synergistic effect, CI > 1 when antagonistic effect appeared). **(E, F)** Representative flow cytometry of PC-9/GR cells treated with gefitinib alone or combined with BH for 24 h. "***" represents BH group vs. the Control group (**p < 0.01, ***p < 0.001).

sensitivity of PC-9/GR cells to gefitinib. To clarify the role of FOXO3a, we confirmed the increase of FOXO3a protein accumulation in PC-9/GR cells by immunofluorescence staining (**Figures 4C, D**). These results indicated that BH significantly enhanced gefitinib sensitivity in PC-9/GR cells by β-catenin activating the FOXO3a signaling pathway.

Identifying Hub Genes of EGFR-TKI Drug Persistence in EGFR Mutant by DEGs and WGCNA

Based on the analysis of the differentially expressed genes between EGFR inhibition and combined EGFR and Notch inhibition in EGFR mutant of NSCLC, a total of 936 DEGs were identified, consisting of 366 upregulated and 570 downregulated DEGs (**Figure 5A**). On the other hand, the difference of gene expression between 80 non-small cell lung cancer samples and 20 marginal samples yielded 2,817 DEGs, consisting of 1,097 high-expression genes and 1,720 low-expression genes (**Figure 5B**). **Figures 5C, D** represent the heatmap of the expression levels of these DEGs. The 259 NSCLC samples from the TCGA database (**Table S1**), with a clear record of a canonical mutation in KRAS, were used to establish a co-expression module for WGCNA to evaluate the correlation between potential genes and EGFR mutations in patients with non-small cell lung cancer. Cluster analysis demonstrated that the mutation in the sample has a certain relationship with smoking history, and the longer the smoking period, the more likely it is that the mutation of lung cancer would occur (**Figure S2A**). Besides, the power value of

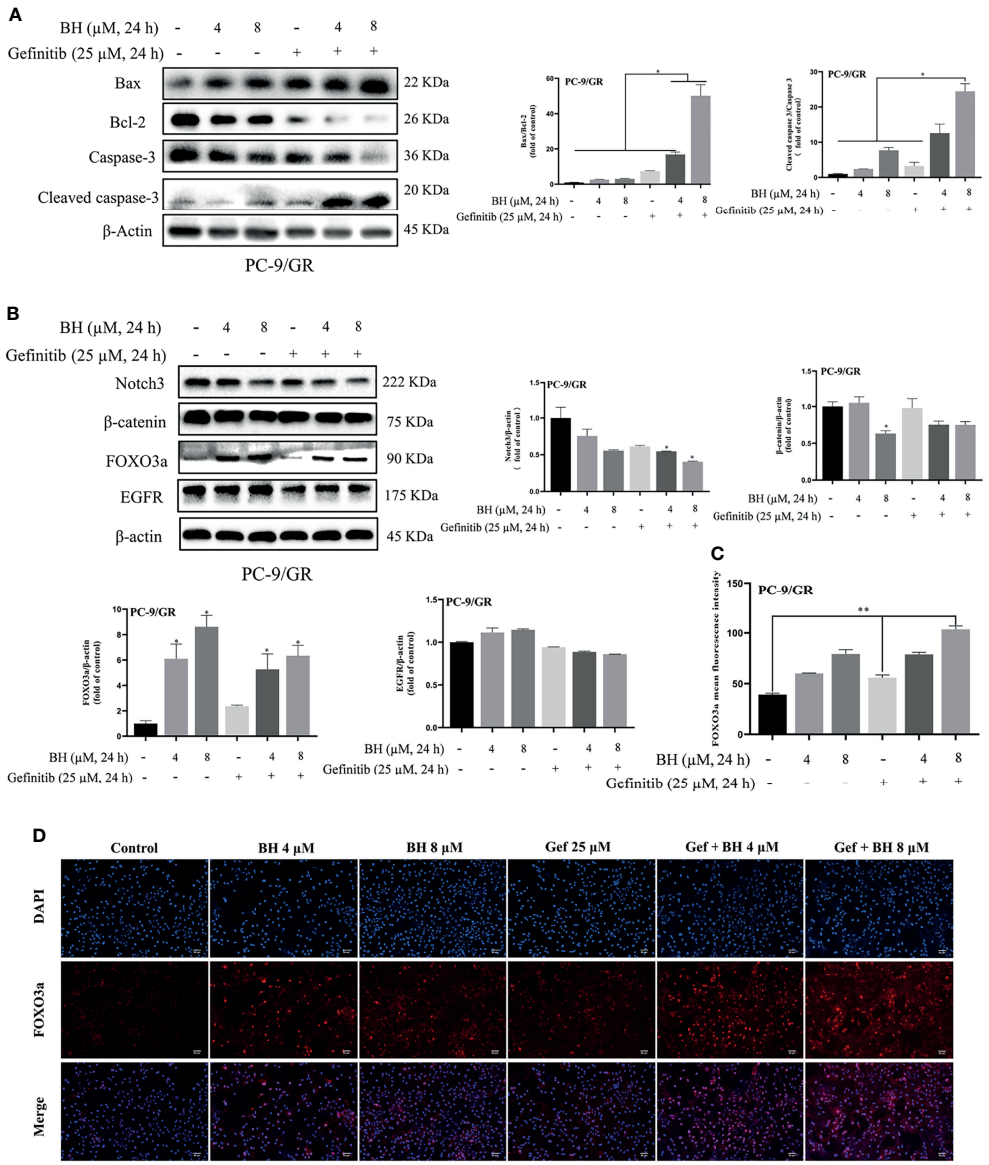

FIGURE 4 | BH modulates the expression of multiple proteins. **(A)** Western bolt was used to detect the expression of cleaved caspase-3, caspase-3, Bcl-2, and Bax protein. **(B)** The protein levels of Notch3, β-catenin, FOXO3a, and EGFR in PC-9/GR cells treated with BH (4, 8 μM) and/or gefitinib (25 μM) for 24 h. **(C, D)** Immunofluorescent images of PC-9/GR cells represented the accumulation of FOXO3a. Scale bars, 50 μm. "*" represents Gef +BH group, BH group, Gef group vs. the Control group (*$p < 0.05$, **$p < 0.01$).

β = 4 (scale-free R^2 = 0.91) was set to ensure low mean connectivity and high-scale independence (**Figures S2B, C**). A total of nine modules (**Figures S2D, E**) were identified through the average linkage hierarchical clustering and segmented the clustering results under the set criteria (dissimilarity = 0.25). The correlation of the modules with clinical traits, including tumor-normal and EGFR-TKI mutant, is shown in **Figures 5E–G**. Finally, the 742 gene sequences in the blue module were intersected with mutant-specific DEGs to identify 89 genes that regulated drug persistence in patients with NSCLC with EGFR mutations (**Figure 5H**).

GO Function and KEGG Pathway Annotation of Module Hub Genes

GO function and KEGG pathway enrichment analyses were performed to assess the function of 89 genes, which intersected the blue module genes and the two differential overlapping genes. The top 10 results of GO that include terms of biological process (BP), cellular component (CC), and molecular function (MF) are shown in **Figure 6A**. The most significant enrichment terms of BP, CC, and MF for EGFR-TKI drug persistence were "sterol biosynthetic process", "clathrin-coated endocytic vesicle membrane", and "nuclear receptor binding", respectively.

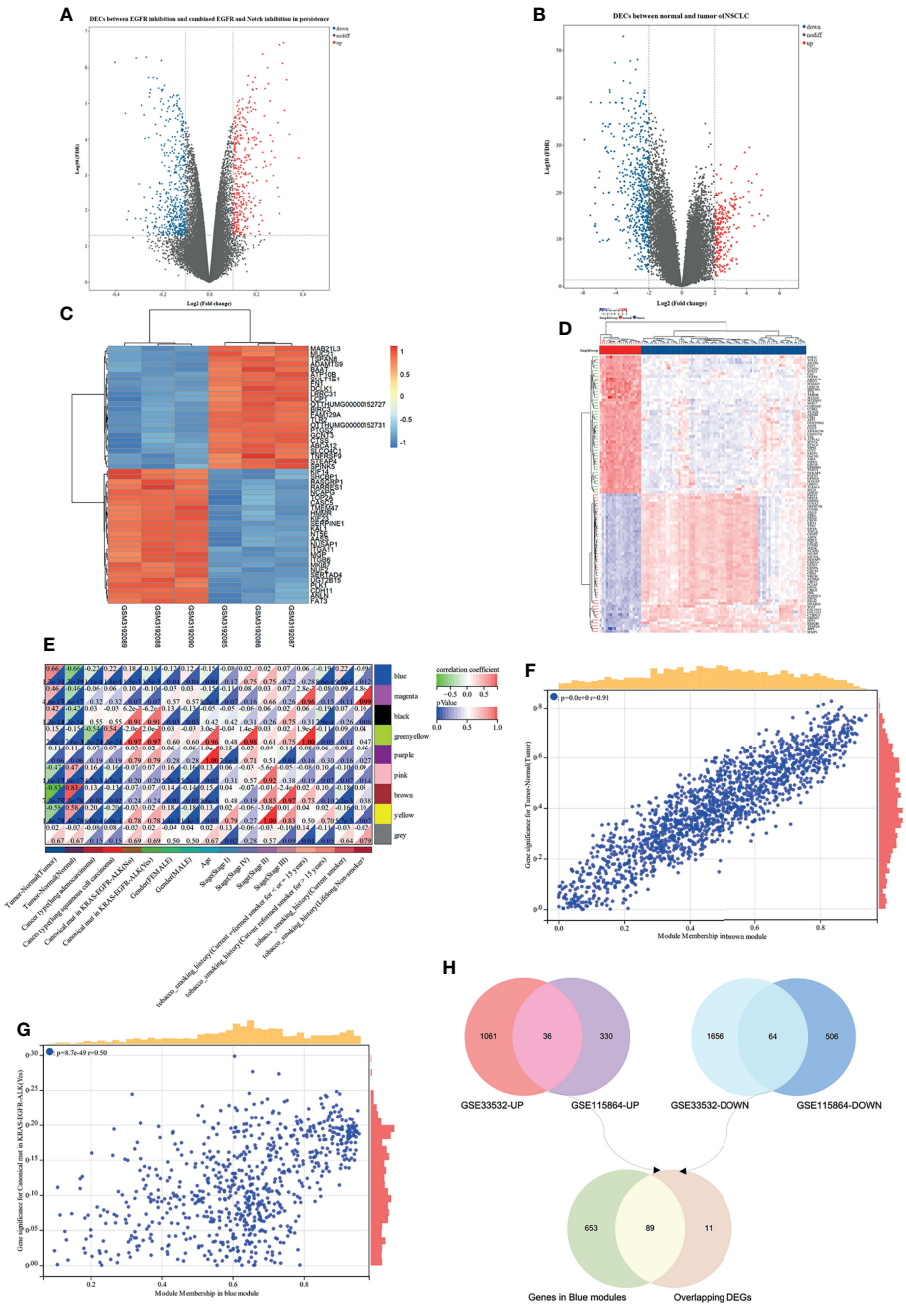

FIGURE 5 | WGCNA and differentially expressed genes (DEGs) of EGFR-TKI drug persistence in EGFR mutant NSCLC. **(A)** Volcano maps of DEGs between two groups: EGFR inhibition and combined EGFR and Notch inhibition in EGFR mutant of NSCLC. **(B)** Volcano maps of DEGs between normal and tumor. Upregulated genes are shown in red and downregulated genes are shown in green dots. **(C, D)** Heatmap showing the expression level of the top 50 DEGs. **(E)** Each column represents a clinical feature and each row represents a module eigengene; red represents a positive correlation and green represents a negative correlation; the darker the hue, the higher the correlation. **(F, G)** Scatter plot of eigengene modules. **(H)** Venn diagram showed the intersection of overlapping DEGs of N-T DEGs and E-N DEGs and genes in blue modules.

Twenty significantly enriched KEGG pathways were identified in these overlapping genes (**Figure 6B**). The most significant KEGG pathways, including the FOXO and Notch signaling pathways, might be related to the EGFR resistance response of NSCLC patients.

The survival analysis of the genes in the above network was conducted to determine the prognostic value of the six hub genes in NSCLC. In the relapse-free survival (RFS) analyses based on sequencing data of 1,925 NSCLC patients, high NOTCH3 and NCBP2 expression levels were associated with shorter NSCLC

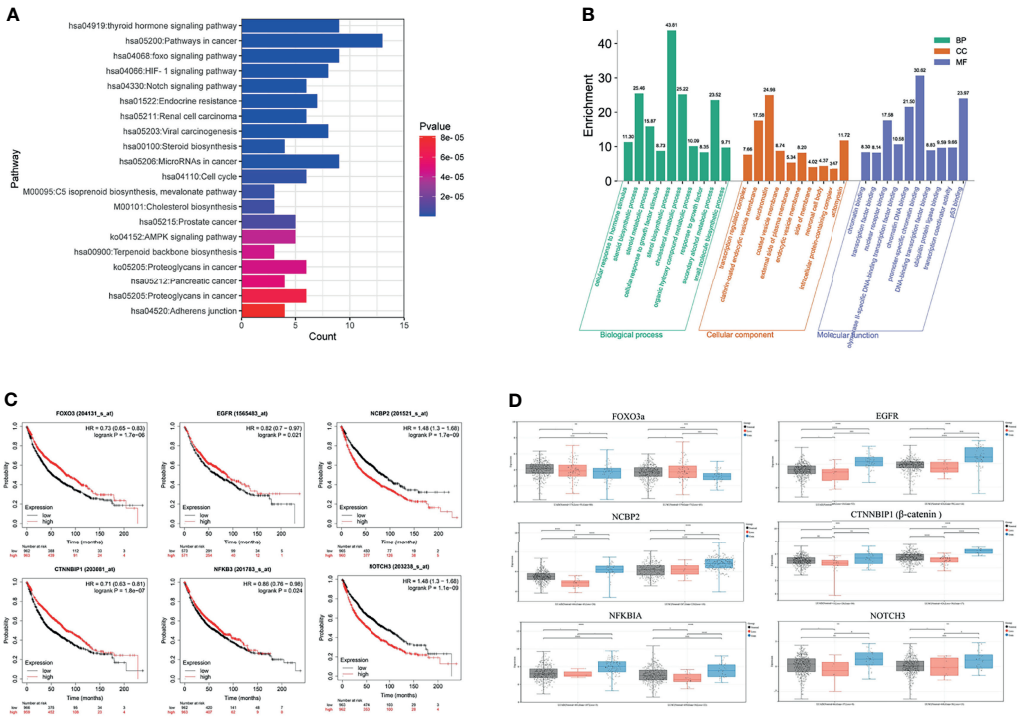

FIGURE 6 | Function and pathway enrichment analysis and key gene cluster. **(A)** KEGG enrichment analysis. **(B)** GO enrichment analysis. **(C)** Kaplan–Meier survival curves of six prognostic biomarkers screened from the hub gene. **(D)** Contrast of the expression of the six hub genes in the EGFR mutant LUAD and LUSC dataset.

survival times (**Figure 6C**, $P < 0.01$). Furthermore, individuals expressing high levels of FOXO3a had a more favorable prognosis than those expressing low levels of the gene. We analyzed the expression levels of FOXO3a, EGFR, NCBP2, CTNNBIP1, NFKBIA, and NOTCH3 at different resistance statuses in LUAD and LUSC in the TCGA database (**Figure 6D**). The result indicated that the Notch3 and β-catenin genes were overexpressed in EGFR resistance processes in NSCLC.

BH Inhibited the Growth of Human Lung Cancer Cell Xenografts

Subcutaneous mouse xenografts of the NSCLC cell line A549 were further used to evaluate BH's antitumor effect. BH significantly inhibited the growth of human lung cancer (A549) xenografts after 16 days of treatment with 2.5 or 5 mg/kg dose given *via* intragastric administration, and the inhibitory effect of 2.5 mg/kg brucine H was similar to that of the effective drug gefitinib (**Figures 7A, B**). For A549 xenograft tumors, tumor volumes and tumor weights decreased dose-dependently in the 2.5- and 5-mg/kg treatment groups (**Figure S3A**) without significant changes in body weight. Meanwhile, there were no significant changes in organ indexes of the heart, kidney, liver, lung, and spleen tissues (**Figure S3B**), indicating that BH treatment did not cause harmful side effects in tumor-bearing mice. Moreover, tumor cell apoptosis was evaluated by HE staining, and the mitotic index (Ki-67) and Notch3 signal were detected through immunohistochemistry (IHC) and Western blotting. In contrast to the vehicle group, BH caused significant cancer cell apoptosis, and the number of Ki-67-positive cells in cancer tissues was decreased (**Figures 7C, D, F**). Notch3 expression in tumor xenografts decreased in a dose-dependent manner in the BH treatment group compared with that in the model group, according to the IHC analysis (**Figure 7E**). Additionally, in the BH treatment group, the expression of FOXO3a increased in the tumor tissues, whereas Notch3, β-catenin, and Bcl-2 protein levels decreased (**Figure 7F**). The results showed that BH significantly suppressed excessive Notch3 signaling and displayed potent antitumor activity against human lung cancer cell xenograft models.

BH Enhanced the Antitumor Effects of Gefitinib in TKI-Resistant Lung Cancer Xenografts

To further determine the therapeutic effect of BH combined with gefitinib, we established a nude mouse xenograft model of PC-9/GR cells. The results revealed that treatment with BH at 2.5 mg/kg alone or a low dose of gefitinib (25 mg/kg) alone showed a slight inhibitory effect on tumor growth of PC-9/GR by intragastric administration, respectively (**Figure 8A**), while co-administration of BH (2.5 mg/kg) and gefitinib (25 mg/kg) significantly suppressed xenograft tumor growth (**Figures 8B, C**). There were no significant changes in body weights and HE staining of the heart, kidney, liver, lung, and spleen tissues

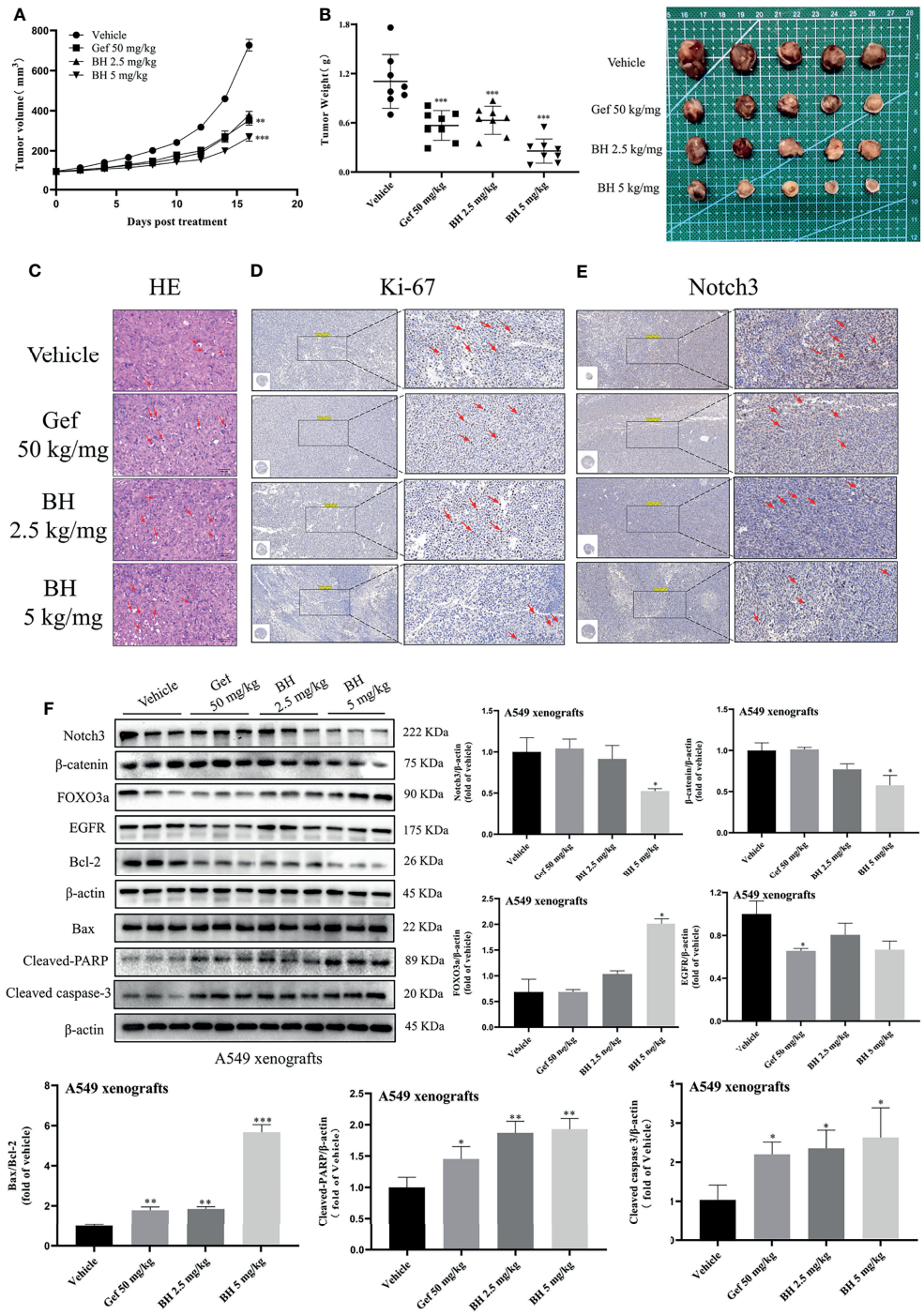

FIGURE 7 | BH inhibits the growth of lung cancer xenografts in BALB/c athymic nude mice. **(A, B)** Tumor volume and tumor weight. **(C)** H&E staining of tumor tissues, and the scale bar was 100 μm. **(D, E)** IHC was used to detect the protein levels of Ki-67 and Notch3 of A549 xenografts, and the scale bar was 200 μm. **(F)** Protein levels of Notch3, β-catenin, FOXO3a, EGFR, Bcl-2, Bax, cleaved caspase-3, and cleaved-PARP in tumor samples were determined by Western blot. "*" represents Gef +BH group, BH group, Gef group vs. the group (*p < 0.05, **p < 0.01, ***p< 0.001).

(**Figures S4A, B**). In addition, BH and gefitinib combination treatment caused significant cancer cell apoptosis compared with a single treatment, increased significantly the number of TUNEL-positive cells in cancer tissues, and reduced the number of Ki-67-positive cells in cancer tissues (**Figures 8D–F**). Also, IHC staining demonstrated that the level of Notch3 was inhibited by BH and gefitinib combination (**Figure 8G**). Western blotting further proved that the

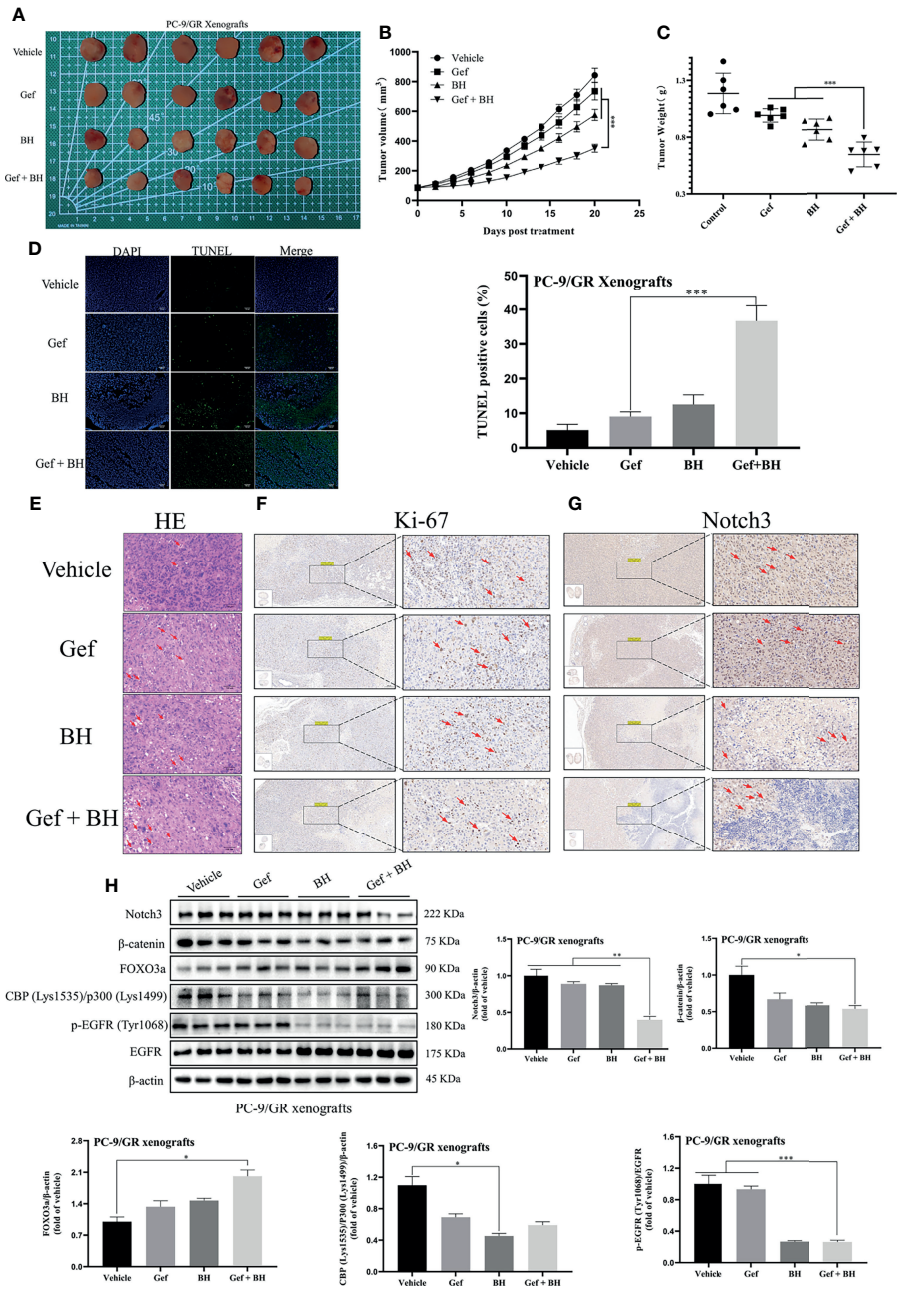

FIGURE 8 | Combination of BH and gefitinib suppressed the growth of PC-9/GR xenografts tumor. **(A)** Representative pictures of tumors. $n = 6$ per group. **(B)** Tumor volume of PC-9/GR xenografts. **(C)** Tumor weights and size of PC-9/GR xenografts. **(D, E)** TUNEL assay and H&E staining were performed to examine histological morphology and apoptosis of tumor tissues, and the scale bar was 100 μm. **(F, G)** The protein levels of Ki-67 and Notch3 of PC-9/GR xenografts were detected by IHC, and the scale bar was 200 μm. **(H)** The expressions of Notch3, β-catenin, FOXO3a, p-EGFR (Tyr1068), EGFR, and BPC (Lys1535)/P300 (Lys1499) of PC-9/GR xenografts were measured by Western blot. "*" represents Gef +BH group, BH group, Gef group vs. the group (*$p < 0.05$, **$p < 0.01$, ***$p < 0.001$).

expression of Notch3, as well as β-catenin downstream genes CBP (Lys1535)/p300 (Lys1499) and p-EGFR (Tyr1068) in the tumor tissues, was reduced (**Figure 8H**). Taken together, combining a Notch3 inhibitor with gefitinib inhibits the growth of TKI-resistant lung cancer xenografts more effectively than either treatment separately.

To prove that BH had no significant toxicity *in vivo*, the organ (**Table S2**), blood routine (**Table S3**), and biochemical indexes (**Table S4**) of nude mice were determined. Compared with the model group or positive drug group, we did observe no significant changes in the coefficients of lung and spleen and in the levels of white blood cells, lymphocytes, and neutrophils in

TABLE 1 | Preliminary pharmacokinetic parameters for BH[a].

Parameter	2 mg/kg iv	10 mg/kg po
Clearance (CL, L h^{-1} kg^{-1})	1.911	
Volume of distribution (V_{ss}, L/kg)	26.52	
Half-life ($T_{1/2}$, h)	9.694	3.353
Time of maximum concentration (T_{max}, h)		1
Maximum concentration (C_{max}, ng/ml)	477.4	146.6
AUC_{0-last} (ng h/ml)	943.5	961.2
AUC_{0-inf} (ng h/ml)	1,051.6	976.2
Oral bioavailability (*F*, %)		20.38

[a]*Values are the average of three runs.*

the whole blood and in the levels of total cholesterol, triglycerides, low-density lipoprotein, and high-density lipoprotein in the serum. As a result, we examined the preliminary pharmacokinetic parameters (**Table 1 and Tables S5–S7** in the **Supplementary Material**) of BH after intravenous and oral administration in SD rats. The preliminary pharmacokinetic parameters for a single dose of the compound BH after intravenous (2 mg/kg) and oral administration (10 mg/kg) were as follows: the half-life ($T_{1/2}$) was 9.694 and 3.353 h, maximum concentration (C_{max}) was 477.4 and 146.6 ng/ml, and the area under the plasma concentration–time curve (AUC_{0-last}) was 943.5 and 961.2 ng h/ml, respectively. The results showed that oral bioavailability (*F*) was 20.38%.

DISCUSSION

So far, lung cancer patients, with EGFR-TKI resistance, are difficult to be treated by targeted therapy (35), and the combination regimen will also be affected by adverse reactions and the patients' physical conditions (36). Therefore, it is urgent to seek new targeted therapies to abate drug resistance in patients with NSCLC. **Figure 8** shows that we and others have reported that inhibiting EGFR potently induces β-catenin through a non-canonical Notch3-dependent mechanism (20), which induces the combination of β-catenin and FOXO3a gene, thus promoting the expression of alternative target genes (37). For example, FOXO3a acts as a transcriptional coactivator of β-catenin and enhances the expression of EGFR target genes (38). FOXO3a, a transcription factor of the forkhead family, is a key regulator of crucial proteins associated with cell cycle progression, apoptosis, proliferation, metabolism, and tumorigenesis (39, 40). Many studies showed that FOXO3a expression is identified as a potential biomarker for the diagnosis, prognosis, and treatment of multiple malignant tumors (41, 42). Interestingly, an integrated genomic approach revealed that low expression of FOXO3a is associated with drug resistance in lung cancer cells (43). These findings indicate that FOXO3a could be a potential target of chemotherapeutic drugs, and its activity may increase the chemosensitivity of cancer cells to agents such as gefitinib.

To this end, we screened a series of small molecules with antitumor activity from *B. javanica* and docked them with Notch3 and EGFR proteins. BH and BD were predicted to bind with the same sites on Notch3 HD domain and showed similar affinity in molecular docking analysis, while they also demonstrated similar antitumor effects in previous cell model studies. BH and BD strongly inhibit the survival, migration, and invasion of NSCLC cell lines and induce cell apoptosis. However, the sensitivity of BD to 16HBE and LO2 cell lines is significantly higher than that of BH. In this study, the hub gene of EGFR-TKI drug persistence in EGFR mutants was screened on the basis of differentially expressed genes and WGCNA, in order to explore potential drug resistance targets. Through the comprehensive analysis of co-expression network construction, functional enrichment, and hub gene screening, six EGFR and Notch inhibition-related key genes related to EGFR-TKI drug persistence were screened. We further demonstrated that BH inhibited the proliferation of NSCLC subcutaneous mouse xenografts, and verified the expression of four proteins (NOTCH3, CTNNBIP1, EGFR, and FOXO3a) from the hub targets of the WGCNA and GEO co-expression network. In Western blotting and IHC analysis, BH significantly induced the expression of FOXO3a in tumor tissue, whereas BH downregulated the expression of FOXO3a upstream regulators (NOTCH3, β-catenin) and Bcl-2 downstream genes in tumor tissue. These results are consistent with the expression patterns analyzed in GEO and TCGA databases, showing that patients with high levels of FOXO3a are better able to overcome EGFR-TKI resistance and survive longer. Therefore, we further investigated the effect of brucine H on EGFR-TKI drug persistence of NSCLC through the Notch3/β-catenin signal pathway. We used the gefitinib-resistant NSCLC cell line PC-9/GR obtained from continuous exposure to gefitinib to examine the role of FOXO3a and the effect of BH. The protein level of β-catenin in PC-9/GR was higher than that in PC-9, but the reverse was found in FOXO3a. Furthermore, BH and gefitinib synergistically induced cell apoptosis in PC-9/GR and inhibited the protein levels of β-catenin, thus activating FOXO3a, but gefitinib alone could not. It suggested that BH may enhance the sensitivity of resistant cells to gefitinib through inhibition of β-catenin and FOXO3a activation. We then explored the therapeutic benefit of BH–gefitinib combination using a xenograft model of PC-9/GR cells. Gefitinib showed a slight inhibition of tumor growth, but BH–gefitinib together showed an important reduction in xenograft tumor growth. Further immunohistochemical staining and Western blotting showed that the combined therapy could increase the expression of FOXO3a and inhibit the expression of Notch3, β-catenin, and pY1068-EGFR. We speculated that inhibition of EGFR and activation of FOXO3a potently induce β-catenin *via* a Notch3-dependent mechanism, which promotes the sustained development of drugs in animal models and the early development of clinical drug resistance. Dual targeting of EGFR and Notch3 may have a greater impact on inhibiting TKI-resistant lung cancer cell xenograft growth than focusing on either pathway alone, and the transcription factor p300/CBP contains an acetyltransferase domain that directly interacts with Notch3 *via* modulation of acetylation to promote degradation of Notch3 (44), so P300/CBP levels may be a useful mechanism-related marker of Notch3 activity in these patients.

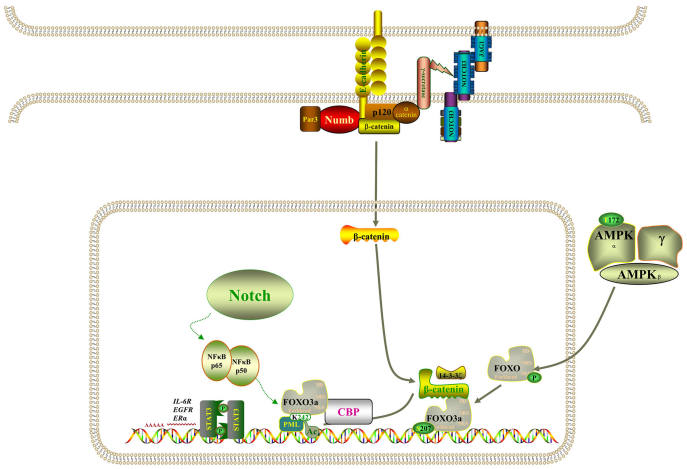

FIGURE 9 | Model of the regulatory signaling networks of Notch3/β-catenin/FOXO3a in EGFR-TIK resistance and CSC properties of lung cancer.

However, the molecular mechanism of acquired drug resistance involves the combined action of multiple pathways and multiple targets, which is much more complicated than we expected. There is increasing evidence that Notch3 and other carcinogenic driving mechanisms will have synergistic effects, in which the irregular expression and/or mutation of Notch3, in combination with other mutations, likely results in a more serious phenotype and more resistance to treatment (45). It has been demonstrated that activation of β-catenin activity leads to tumor proliferation and reduced mouse survival in xenograft models, that EGFR tyrosine kinase inhibitor can activate β-catenin and Notch3 by inhibiting EGFR signal, and that knocking out Notch3 reduces β-catenin activity and resistance to targeted drugs (20, 46, 47). In addition, β-catenin correlates negatively with FOXO3a expression, and FOXO3a knockdown resulted in significantly higher expression levels of β-catenin (48). Based on evidence that the Wnt–β-catenin and Notch3 pathways play a part in tumorigenesis and that there is an interaction between FOXO3a and β-catenin, we speculate that Notch3 controls the expression of FOXO3a through non-classical dependence on β-catenin in lung cancer cell resistance, thereby regulating EGFR signal. The study also found that the activity of Notch3 is also necessary in the evolution of the refractory treatment of EGFR mutant NSCLC, which has been identified as the substrate of EGFR-mediated tyrosine phosphorylation, and inhibiting EGFR activity will reduce tyrosine phosphorylation, thus enhancing Notch3 activity (21). Remarkably, Notch3 overexpression was also observed in KRAS-mutated lung adenocarcinoma cells and correlated positively with aldehyde dehydrogenase (ALDH) expression, resulting in enhanced CSC phenotype (49, 50). Furthermore, activation of NF-κB through miR-155 has been reported to downregulate FOXO3a, which brought about the acquisition of gefitinib resistance in patients with NSCLC that carried EGFR mutations (43). On the other hand, when the signal dynamics model of leukemia T cells was set up, it was observed that Notch3 could activate NF-κB by associating with the pTα chain of the pre-T-cell receptor (51). As shown in **Figure 9**, Notch signaling may also act through nuclear NF-κB on FOXO3a. It is clear from all the evidence that not only Notch3 contributes to the occurrence and development of non-small cell lung cancer but also related proteins within its pathway are involved in drug resistance and recurrence.

CONCLUSIONS

Based on our study results, we concluded that BH substantially suppressed Notch3 signaling in human lung cancer, resulting in powerful antitumor activity in human lung cancer both *in vitro* and *in vivo*, and that it can improve the sensitivity of resistant NSCLC to gefitinib. In the meantime, these data establish new insights into the functional interaction among EGFR, Notch3, β-catenin, and FOXO3a: Notch3 is activated when EGFR-TIK inhibits EGFR and then stimulates β-catenin in a non-classical way, and β-catenin acts on EGFR in combination with FOXO3a; therefore, inhibition of Notch3 provides a potential combined treatment strategy for EGFR-TIK-resistant lung cancer.

DATA AVAILABILITY STATEMENT

The original contributions presented in the study are included in the article/**Supplementary Material**. Further inquiries can be directed to the corresponding authors.

ETHICS STATEMENT

The animal study was reviewed and approved by Jiangxi University of Chinese Medicine Animal Care Committee (SCXK 2016-0006).

AUTHOR CONTRIBUTIONS

All authors contributed to the concept and design of the study. All authors contributed to the article and approved the submitted version.

FUNDING

This work was supported by the National Natural Science Foundation of China (81860684), Jiangxi Natural Science Foundation (GJJ190689, 20212ACB206007), National Key R&D Program of China (2019YFC1712302), and Construction of First-Class Discipline of TCM Pharmacy in Jiangxi Province (JXSYLXKZHYAO016).

SUPPLEMENTARY MATERIAL

The Supplementary Material for this article can be found online at: https://www.frontiersin.org/articles/10.3389/fonc.2022.855603/full#supplementary-material

REFERENCES

1. National Cancer Institute. *SEER Cancer Statistics Review* (1975-2018). Available at: https://seer.cancer.gov/csr/1975_2018/ (Accessed May 12, 2021).
2. Miller KD, Nogueira L, Mariotto AB, Rowland JH, Yabroff KR, Alfano CM, et al. Cancer Treatment and Survivorship Statistics, 2019. *CA Cancer J Clin* (2019) 69(5):363–85. doi: 10.3322/caac.21565
3. Ettinger DS, Wood DE, Aisner DL, Akerley W, Bauman J, Chirieac LR, et al. Non-Small Cell Lung Cancer, Version 5.2017, NCCN Clinical Practice Guidelines in Oncology. *J Natl Compr Canc Netw* (2017) 15(4):504–35. doi: 10.6004/jnccn.2017.0050
4. Siegel RL, Miller KD, Fuchs HE, Jemal A. Cancer Statistics, 2021. *CA Cancer J Clin* (2021) 71(1):7–33. doi: 10.3322/caac.21654
5. Zhang P, Tao W, Lu C, Fan L, Jiang Q, Yang C, et al. Bruceine A Induces Cell Growth Inhibition and Apoptosis Through PFKFB4/GSK3β Signaling in Pancreatic Cancer. *Pharmacol Res* (2021) 169:105658. doi: 10.1016/j.phrs.2021.105658
6. Meiyanto E, Larasati YA. The Chemopreventive Activity of Indonesia Medicinal Plants Targeting on Hallmarks of Cancer. *Adv Pharm Bull* (2019) 9(2):219–30. doi: 10.15171/apb.2019.025
7. Zhao M, Lau ST, Leung PS, Che CT, Lin ZX. Seven Quassinoids From Fructus Bruceae With Cytotoxic Effects on Pancreatic Adenocarcinoma Cell Lines. *Phytother Res* (2011) 25(12):1796–800. doi: 10.1002/ptr.3477
8. Cheng Z, Yuan X, Qu Y, Li X, Wu G, Li C, et al. Bruceine D Inhibits Hepatocellular Carcinoma Growth by Targeting β-Catenin/Jagged1 Pathways. *Cancer Lett* (2017) 403:195–205. doi: 10.1016/j.canlet.2017.06.014
9. Fan J, Ren D, Wang J, Liu X, Zhang H, Wu M, et al. Bruceine D Induces Lung Cancer Cell Apoptosis and Autophagy *via* the ROS/MAPK Signaling Pathway *In Vitro* and In Vivo. *Cell Death Dis* (2020) 11(2):126. doi: 10.1038/s41419-020-2317-3
10. Park SH, Kim JH, Ko E, Kim JY, Park MJ, Kim MJ, et al. Resistance to Gefitinib and Cross-Resistance to Irreversible EGFR-TKIs Mediated by Disruption of the Keap1-Nrf2 Pathway in Human Lung Cancer Cells. *FASEB J* (2018) 32(11):fj201800011R. doi: 10.1096/fj.201800011R
11. Maemondo M, Inoue A, Kobayashi K, Sugawara S, Oizumi S, Isobe H, et al. Gefitinib or Chemotherapy for Non-Small-Cell Lung Cancer With Mutated EGFR. *N Engl J Med* (2010) 362(25):2380–8. doi: 10.1056/NEJMoa0909530
12. Sari M, Aydiner A. Rare Mutations of Epidermal Growth Factor Receptor in Epidermal Growth Factor Receptor-Tyrosine Kinase Inhibitor-Naive Non-Small Cell Lung Carcinoma and the Response to Erlotinib Therapy. *J Cancer Res Ther* (2020) 16(1):132–8. doi: 10.4103/jcrt.JCRT_757_19
13. Zhou J, Hu Q, Zhang X, Zheng J, Xie B, Xu Z, et al. Sensitivity to Chemotherapeutics of NSCLC Cells With Acquired Resistance to EGFR-TKIs is Mediated by T790M Mutation or Epithelial-Mesenchymal Transition. *Oncol Rep* (2018) 39(4):1783–92. doi: 10.3892/or.2018.6242
14. Takezawa K, Pirazzoli V, Arcila ME, Nebhan CA, Song X, de Stanchina E, et al. HER2 Amplification: A Potential Mechanism of Acquired Resistance to EGFR Inhibition in EGFR-Mutant Lung Cancers That Lack the Second-Site EGFRT790M Mutation. *Cancer Discov* (2012) 2(10):922–33. doi: 10.1158/2159-8290.Cd-12-0108
15. Biello F, Burrafato G, Rijavec E, Genova C, Barletta G, Truini A, et al. Fibroblast Growth Factor Receptor (FGFR): A New Target for Non-Small Cell Lung Cancer Therapy. *Anticancer Agents Med Chem* (2016) 16(9):1142–54. doi: 10.2174/1871520616666160204112347
16. Sankar K, Gadgeel SM, Qin A. Molecular Therapeutic Targets in Non-Small Cell Lung Cancer. *Expert Rev Anticancer Ther* (2020) 20(8):647–61. doi: 10.1080/14737140.2020.1787156
17. Chen CH, Wang BW, Hsiao YC, Wu CY, Cheng FJ, Hsia TC, et al. Pkcδ-Mediated SGLT1 Upregulation Confers the Acquired Resistance of NSCLC to EGFR TKIs. *Oncogene* (2021) 40(29):4796–808. doi: 10.1038/s41388-021-01889-0
18. Nakata A, Gotoh N. Recent Understanding of the Molecular Mechanisms for the Efficacy and Resistance of EGF Receptor-Specific Tyrosine Kinase Inhibitors in Non-Small Cell Lung Cancer. *Expert Opin Ther Targets* (2012) 16(8):771–81. doi: 10.1517/14728222.2012.697155
19. Dhillon AS, Hagan S, Rath O, Kolch W. MAP Kinase Signalling Pathways in Cancer. *Oncogene* (2007) 26(22):3279–90. doi: 10.1038/sj.onc.1210421
20. Arasada RR, Shilo K, Yamada T, Zhang J, Yano S, Ghanem R, et al. Notch3-Dependent β-Catenin Signaling Mediates EGFR TKI Drug Persistence in EGFR Mutant NSCLC. *Nat Commun* (2018) 9(1):3198. doi: 10.1038/s41467-018-05626-2
21. Arasada RR, Amann JM, Rahman MA, Huppert SS, Carbone DP. EGFR Blockade Enriches for Lung Cancer Stem-Like Cells Through Notch3-Dependent Signaling. *Cancer Res* (2014) 74(19):5572–84. doi: 10.1158/0008-5472.Can-13-3724
22. Sharif A, Shaji A, Chammaa M, Pawlik E, Fernandez-Valdivia R. Notch Transduction in Non-Small Cell Lung Cancer. *Int J Mol Sci* (2020) 21(16):5691. doi: 10.3390/ijms21165691
23. Kong Y, Glickman J, Subramaniam M, Shahsafaei A, Allamneni KP, Aster JC, et al. Functional Diversity of Notch Family Genes in Fetal Lung Development. *Am J Physiol Lung Cell Mol Physiol* (2004) 286(5):L1075–83. doi: 10.1152/ajplung.00438.2002
24. Rock JR, Gao X, Xue Y, Randell SH, Kong YY, Hogan BL. Notch-Dependent Differentiation of Adult Airway Basal Stem Cells. *Cell Stem Cell* (2011) 8(6):639–48. doi: 10.1016/j.stem.2011.04.003
25. Dang TP, Gazdar AF, Virmani AK, Sepetavec T, Hande KR, Minna JD, et al. Chromosome 19 Translocation, Overexpression of Notch3, and Human Lung Cancer. *J Natl Cancer Inst* (2000) 92(16):1355–7. doi: 10.1093/jnci/92.16.1355
26. Oser MG, Sabet AH, Gao W, Chakraborty AA, Schinzel AC, Jennings RB, et al. The KDM5A/RBP2 Histone Demethylase Represses NOTCH Signaling to Sustain Neuroendocrine Differentiation and Promote Small Cell Lung Cancer Tumorigenesis. *Genes Dev* (2019) 33(23-24):1718–38. doi: 10.1101/gad.328336.119
27. Chen CY, Chen YY, Hsieh MS, Ho CC, Chen KY, Shih JY, et al. Expression of Notch Gene and Its Impact on Survival of Patients With Resectable Non-Small Cell Lung Cancer. *J Cancer* (2017) 8(7):1292–300. doi: 10.7150/jca.17741
28. Liu L, Chen X, Wang Y, Qu Z, Lu Q, Zhao J, et al. Notch3 is Important for TGF-β-Induced Epithelial-Mesenchymal Transition in Non-Small Cell Lung Cancer Bone Metastasis by Regulating ZEB-1. *Cancer Gene Ther* (2014) 21(9):364–72. doi: 10.1038/cgt.2014.39
29. Shi C, Qian J, Ma M, Zhang Y, Han B. Notch 3 Protein, Not its Gene Polymorphism, is Associated With the Chemotherapy Response and Prognosis of Advanced NSCLC Patients. *Cell Physiol Biochem* (2014) 34(3):743–52. doi: 10.1159/000363039

30. Liu H, Yin J, Wang H, Jiang G, Deng M, Zhang G, et al. FOXO3a Modulates WNT/β-Catenin Signaling and Suppresses Epithelial-to-Mesenchymal Transition in Prostate Cancer Cells. *Cell Signal* (2015) 27(3):510–8. doi: 10.1016/j.cellsig.2015.01.001
31. Zhang X, Yue P, Page BD, Li T, Zhao W, Namanja AT, et al. Orally Bioavailable Small-Molecule Inhibitor of Transcription Factor Stat3 Regresses Human Breast and Lung Cancer Xenografts. *Proc Natl Acad Sci USA* (2012) 109(24):9623–8. doi: 10.1073/pnas.1121606109
32. Ritchie ME, Phipson B, Wu D, Hu Y, Law CW, Shi W, et al. Limma Powers Differential Expression Analyses for RNA-Sequencing and Microarray Studies. *Nucleic Acids Res* (2015) 43(7):e47. doi: 10.1093/nar/gkv007
33. Győrffy B, Surowiak P, Budczies J, Lánczky A. Online Survival Analysis Software to Assess the Prognostic Value of Biomarkers Using Transcriptomic Data in Non-Small-Cell Lung Cancer. *PloS One* (2013) 8(12):e82241. doi: 10.1371/journal.pone.0082241
34. AACR Project GENIE. Powering Precision Medicine Through an International Consortium. *Cancer Discov* (2017) 7(8):818–31. doi: 10.1158/2159-8290.Cd-17-0151
35. Rosell R, Carcereny E, Gervais R, Vergnenegre A, Massuti B, Felip E, et al. Erlotinib Versus Standard Chemotherapy as First-Line Treatment for European Patients With Advanced EGFR Mutation-Positive Non-Small-Cell Lung Cancer (EURTAC): A Multicentre, Open-Label, Randomised Phase 3 Trial. *Lancet Oncol* (2012) 13(3):239–46. doi: 10.1016/s1470-2045(11)70393-x
36. Mitsudomi T, Morita S, Yatabe Y, Negoro S, Okamoto I, Tsurutani J, et al. Gefitinib Versus Cisplatin Plus Docetaxel in Patients With Non-Small-Cell Lung Cancer Harbouring Mutations of the Epidermal Growth Factor Receptor (WJTOG3405): An Open Label, Randomised Phase 3 Trial. *Lancet Oncol* (2010) 11(2):121–8. doi: 10.1016/s1470-2045(09)70364-x
37. Sumida T, Lincoln MR, Ukeje CM, Rodriguez DM, Akazawa H, Noda T, et al. Activated β-Catenin in Foxp3(+) Regulatory T Cells Links Inflammatory Environments to Autoimmunity. *Nat Immunol* (2018) 19(12):1391–402. doi: 10.1038/s41590-018-0236-6
38. Carbajo-Pescador S, Mauriz JL, García-Palomo A, González-Gallego J. FoxO Proteins: Regulation and Molecular Targets in Liver Cancer. *Curr Med Chem* (2014) 21(10):1231–46. doi: 10.2174/09298673216613122820570 3
39. Liu Y, Ao X, Ding W, Ponnusamy M, Wu W, Hao X, et al. Critical Role of FOXO3a in Carcinogenesis. *Mol Cancer* (2018) 17(1):104. doi: 10.1186/s12943-018-0856-3
40. Yadav RK, Chauhan AS, Zhuang L, Gan B. FoxO Transcription Factors in Cancer Metabolism. *Semin Cancer Biol* (2018) 50:65–76. doi: 10.1016/j.semcancer.2018.01.004
41. Qian Z, Ren L, Wu D, Yang X, Zhou Z, Nie Q, et al. Overexpression of FoxO3a is Associated With Glioblastoma Progression and Predicts Poor Patient Prognosis. *Int J Cancer* (2017) 140(12):2792–804. doi: 10.1002/ijc.30690
42. Liu HB, Gao XX, Zhang Q, Liu J, Cui Y, Zhu Y, et al. Expression and Prognostic Implications of FOXO3a and Ki67 in Lung Adenocarcinomas. *Asian Pac J Cancer Prev* (2015) 16(4):1443–8. doi: 10.7314/apjcp.2015.16.4.1443
43. Chiu CF, Chang YW, Kuo KT, Shen YS, Liu CY, Yu YH, et al. NF-κb-Driven Suppression of FOXO3a Contributes to EGFR Mutation-Independent Gefitinib Resistance. *Proc Natl Acad Sci USA* (2016) 113(18):E2526–35. doi: 10.1073/pnas.1522612113
44. Palermo R, Checquolo S, Giovenco A, Grazioli P, Kumar V, Campese AF, et al. Acetylation Controls Notch3 Stability and Function in T-Cell Leukemia. *Oncogene* (2012) 31(33):3807–17. doi: 10.1038/onc.2011.533
45. Sosa Iglesias V, Giuranno L, Dubois LJ, Theys J, Vooijs M. Drug Resistance in Non-Small Cell Lung Cancer: A Potential for NOTCH Targeting? *Front Oncol* (2018) 8:267. doi: 10.3389/fonc.2018.00267
46. Li Y, Chen F, Shen W, Li B, Xiang R, Qu L, et al. WDR74 Induces Nuclear β-Catenin Accumulation and Activates Wnt-Responsive Genes to Promote Lung Cancer Growth and Metastasis. *Cancer Lett* (2020) 471:103–15. doi: 10.1016/j.canlet.2019.12.011
47. Diluvio G, Del Gaudio F, Giuli MV, Franciosa G, Giuliani E, Palermo R, et al. NOTCH3 Inactivation Increases Triple Negative Breast Cancer Sensitivity to Gefitinib by Promoting EGFR Tyrosine Dephosphorylation and its Intracellular Arrest. *Oncogenesis* (2018) 7(5):42. doi: 10.1038/s41389-018-0051-9
48. Tian Y, Qi P, Hu X. Downregulated FOXO3a Associates With Poor Prognosis and Promotes Cell Invasion and Migration *via* WNT/β-Catenin Signaling in Cervical Carcinoma. *Front Oncol* (2020) 10:903. doi: 10.3389/fonc.2020.00903
49. Ali SA, Justilien V, Jamieson L, Murray NR, Fields AP. Protein Kinase Cι Drives a NOTCH3-Dependent Stem-Like Phenotype in Mutant KRAS Lung Adenocarcinoma. *Cancer Cell* (2016) 29(3):367–78. doi: 10.1016/j.ccell.2016.02.012
50. Aguirre A, Rubio ME, Gallo V. Notch and EGFR Pathway Interaction Regulates Neural Stem Cell Number and Self-Renewal. *Nature* (2010) 467(7313):323–7. doi: 10.1038/nature09347
51. Ruan ZB, Fu XL, Li W, Ye J, Wang RZ, Yin YG, et al. Effect of Notch1, 2, 3 Genes Silencing on Notch and Nuclear Factor-κb Signaling Pathway of Macrophages Derived From Patients With Coronary Artery Disease. *Zhonghua Xin Xue Guan Bing Za Zhi* (2016) 44(9):786–92. doi: 10.3760/cma.j.issn.0253-3758.2016.09.011

Conflict of Interest: The authors declare that the research was conducted in the absence of any commercial or financial relationships that could be construed as a potential conflict of interest.

Publisher's Note: All claims expressed in this article are solely those of the authors and do not necessarily represent those of their affiliated organizations, or those of the publisher, the editors and the reviewers. Any product that may be evaluated in this article, or claim that may be made by its manufacturer, is not guaranteed or endorsed by the publisher.

frontiers | Frontiers in Oncology

ORIGINAL RESEARCH
published: 20 May 2022
doi: 10.3389/fonc.2022.859275

Lumiflavin Reduces Cisplatin Resistance in Cancer Stem-Like Cells of OVCAR-3 Cell Line by Inducing Differentiation

Ruhui Yang[1,2], *Bingjin Liu*[1], *Mingyue Yang*[3], *Feng Xu*[1], *Songquan Wu*[4] *and Shufang Zhao*[5*]

[1] School of Medicine and Pharmaceutical Engineering, Taizhou Vocational and Technical College, Taizhou, China, [2] Department of Pharmacology, Lishui University School of Medicine, Lishui, China, [3] Clinical Department, China Medical University, Shenyang, China, [4] Department of Immunology, Lishui University School of Medicine, Lishui, China, [5] Molecular Biology Laboratory, Lishui University School of Medicine, Lishui, China

OPEN ACCESS

Edited by:
Nand K. Roy,
Case Western Reserve University, United States

Reviewed by:
Yong Li,
Guangdong Provincial Hospital of Chinese Medicine, China
Harika Atmaca,
Celal Bayar University, Turkey

***Correspondence:**
Shufang Zhao
zsf20140108@sohu.com

Specialty section:
This article was submitted to Pharmacology of Anti-Cancer Drugs, a section of the journal Frontiers in Oncology

Received: *21 January 2022*
Accepted: *18 April 2022*
Published: *20 May 2022*

Citation:
Yang R, Liu B, Yang M, Xu F, Wu S and Zhao S (2022) Lumiflavin Reduces Cisplatin Resistance in Cancer Stem-Like Cells of OVCAR-3 Cell Line by Inducing Differentiation. Front. Oncol. 12:859275. doi: 10.3389/fonc.2022.859275

Ovarian cancer stem-like cells (CSCs) play a vital role in drug resistance and recurrence of ovarian cancer. Inducing phenotypic differentiation is an important strategy to enhance the effects of chemotherapy and reduce the drug resistance of CSCs. This study found that lumiflavin, a riboflavin decomposition product, reduced the development of CSC resistance and enhanced the chemotherapy effect of cisplatin (DDP) on CSCs in DDP-resistant ovarian cancer OVCAR-3 cell line (CSCs/DDP) and was related to the induction of CSC phenotypic differentiation. Results showed that the development of DDP-resistant OVCAR-3 cells was related to the increase in the proportion of CSCs/DDP, and the treatment with lumiflavin reduced the DDP-resistance levels of OVCAR-3 cells and proportion of CSCs/DDP. Further investigation found that lumiflavin synergistic with DDP increased apoptosis, decreased mitochondrial membrane potential, and inhibited the clonal formation of CSCs/DDP. Meanwhile, *in vivo* experiments showed that lumiflavin dose-dependently enhanced the chemotherapy effect of DDP on tumor-bearing nude mice inoculated by CSCs/DDP. Lumiflavin treatment also reduced the ratio of CD133+/CD177+ to CD44+/CD24 cells, which is the identification of CSCs, in CSCs/DDP. In addition, transcriptome sequencing results suggested that the role of lumiflavin was related to the notch and stem cell pathway, and Western blot analysis showed that lumiflavin inhibited the protein expression of notch signaling pathway in CSCs/DDP. In conclusion, lumiflavin reduces the development of the drug resistance of OVCAR-3 cell and increases the sensitivity of CSCs/DDP to DDP by inducing phenotypic differentiation, which may have a potential role in the chemotherapy treatment of ovarian cancer.

Keywords: lumiflavin, ovarian cancer, cancer stem-like cells, drug resistance, phenotypic differentiation

INTRODUCTION

Although most patients with advanced ovarian cancer respond well to paclitaxel and platinum to the initial chemotherapy, 70% – 85% of patients, including those who have a significant effect on the treatment, still relapse within a few years after receiving systemic chemotherapy or cytoreductive surgery (1). Ovarian cancer stem-like cells (CSCs), a subgroup of tumor cells that exhibit the ability of stem cells (i.e., self-renewal, multidirectional differentiation, and the ability to cause tumorigenesis and metastasis) in tumor tissues, are considered responsible for the generation and recurrence of drug resistance in ovarian cancer cells (2, 3).

Currently, the failure to kill CSCs effectively is an important reason for ovarian cancer relapse after chemotherapy (4). CSCs are generally in the G0 cell phase, with high telomerase activity and DNA repair ability, as well as anti-apoptotic genes to evade chemotherapy damage; CSCs that have not been killed by chemotherapy in ovarian cancer become the "seeds" of recurrence and metastasis (5–8). The CSC hypothesis explains the mechanism of tumor recurrence and drug resistance. Therefore, therapies that target CSCs selectively may offer a greater promise for treating ovarian cancer.

Previous studies in our laboratory have shown that riboflavin is an important factor in maintaining the characteristics of CSCs (9, 10). Lumiflavin, a flavin analogue (**Figure 1**), is a competitive inhibitor of riboflavin. Our previous studies have proved that lumiflavin reduced the enrichment of ovarian cancer CSCs to riboflavin, lessened the tolerance of CSCs to DDP, improved the damage effect of chemotherapy drugs, and enhanced the radiotherapy effect on CSCs (11). However, the effect of lumiflavin on the development of drug resistance in ovarian cancer, especially on drug-resistant CSCs, is still vague. In this study, the CSCs of OVCAR-3 cell line was used to verify the effect of lumiflavin on the formation of drug resistance in ovarian cancer.

Inducing differentiation is an important strategy to kill CSCs effectively and reduce the formation of drug resistance (12, 13), such as morphogen-driven signaling cascade (14), and epigenetic differentiation therapy (15). Clinically common differentiation-inducing agents, such as all-trans retinoic acid (ATRA), a metabolic intermediate of vitamin A, reduce the invasiveness and tumorigenicity of CSCs by blocking angiogenic cytokines in glioblastoma (16). It can also induce the differentiation of breast cancer CSCs, reduce the invasion and migration of cells, and improve the sensitivity to tumor treatment (17). Previous studies showed that the effect of lumiflavin was related to its reduction in the CSC proportion (11, 18). Therefore, we speculated that lumiflavin may affect the differentiation of ovarian cancer CSCs. To assess this hypothesis, the present study investigated the effects of lumiflavin on DDP resistance of ovarian cancer CSCs and the relationship between these effects and phenotypic differentiation of CSCs. Results suggest that lumiflavin has therapeutic value in alleviating the development of drug resistance in ovarian cancer.

MATERIALS AND METHODS

Cell Lines, Drugs, Animals, Reagents, and Equipment

Human ovarian cancer cell lines OVCAR-3 (Shanghai Cell Bank of Chinese Academy of Sciences), Lumiflavin (98%, TRC, Canada), DDP (National Institutes for Food and Drug Control of China), Accuri C6 flow cytometry (BD Biosciences, U.S.A) and Western blot system (Bio-Rad, USA), Specific pathogen-free BALB/c nude female mice with an age of approximately 6 weeks and weight of 18–22 g were provided by Shanghai Slack Laboratory Animal Co., Ltd. (Shanghai, China). The mice were housed in a temperature-controlled room under a 12 h dark/light cycle and were allowed access to food and water ad libitum. This study was conducted in strict accordance with the

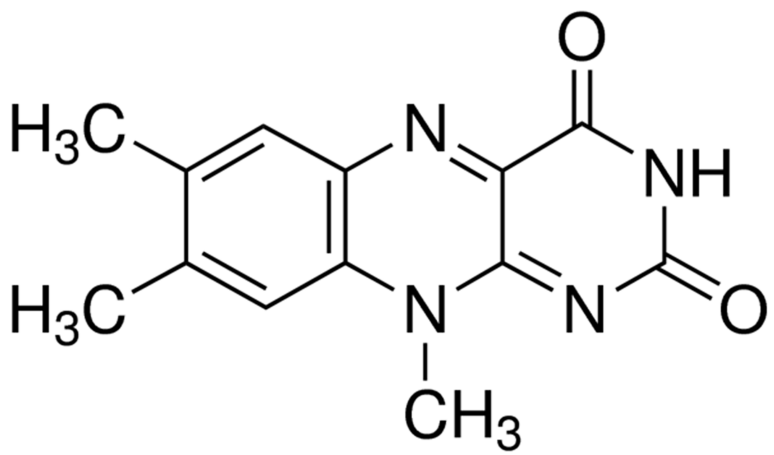

FIGURE 1 | Chemical structure of lumiflavin.

recommendations of the Guide for the Care and Use of Laboratory Animals of the National Institutes of Health, and its protocol was approved by the Animal Research Ethics Board of the Lishui University (Lishui, Zhejiang Province, China. Permit Number: 0803-2019).

Cell Culture and Induction of DDP-Resistance in OVCAR-3 Cell Line (OVCAR-3/DDP)

To induce the establishment of OVCAR-3/DDP, cells were maintained in DDP that were cultured in Dulbecco's modified Eagle Medium (DMEM) that contained 10% bovine serum supplemented with 1×10^5 IU/L each of penicillin and streptomycin at 37°C in 5% CO_2 atmosphere. The OVCAR-3/DDP cells were induced by medium dose of DDP and short-time treatment (19, 20). Briefly, drug concentration was increased by approximately twofold in the initial steps. OVCAR-3 cells in logarithmic growth phase were treated with DDP 5μM for 4 h, then the cells were washed with DDP free medium and continued culture. When the cells returned to the growth stage, the DDP concentration was increased, and the process was repeated. Liquid change and passage were repeated for 36 times, which lasts for 6 months, and these sublines were exposed to 640μM DDP in the end. The IC50 of OVCAR-3/DDP was 502.1μM, compared with parent cell, which was 20.93μM. OVCAR-3/DDP continued to grow in DDP free medium for 2 months and still maintained their drug resistance. Additionally, vehicle-treated parental cell line was kept in culture during this period as a normal cell line.

Isolation of Ovarian Cancer Stem-Like Cells (CSCs) and Analysis of Cell Surface Marker Expression by Flow Cytometry

As reported in previous studies, CSCs were isolated through magnetic bead sorting by using a magnetic cell sorting system (MACS) (11, 18). Briefly, the cells were harvested from each of the OVCAR-3 cell lines and OVCAR-3/DDP. According to the manufacturer's instructions, the cells were labeled with CD133 antibodies conjugated to magnetic beads. Subsequently, antibody positive and negative cells were separated using MACS–LS separation columns (Miltenyi Biotec). CD133+ cells were maintained in ultralow attachment plates (Corning Costar Corporation, USA) in knockout DMEM/F12 medium supplemented with 20% knockout serum replacement (Life Technologies), 10 ng/mL basic fibroblast growth factor with 10 ng/mL leukemia inhibitory factor, and 20 ng/mL epidermal growth factor.

To detect the purity and cell surface marker expression of CSCs (CD133+) of OVCAR-3/DDP or OVCAR-3, briefly (11, 18), the CD44 (antibodies, BD Biosciences), CD24 (antibodies, BD Biosciences), CD117 antibodies (Boster Biological Technology, China), and CD133 antibodies (Miltenyi Biotec) were tested by flow cytometry (BD Biosciences, San Jose, CA) according to the manufacturer's instructions. Cells from each group were collected and centrifuged at 1,500 g for 5 min and suspended with PBS twice. Cells were incubated with antibodies on ice for 40 min in the dark. After washing with cold PBS, the cells were resuspended in 200 μL PBS and subjected to analyses on a flow cytometer. CD24-FITC and CD117-FITC were detected by the FL1A channel, whereas CD44-PE and CD133-PE were detected by FL2A channel. The data were analyzed using the BD FACSDiva™ software to calculate the percentage of double positive.

Drug Inhibition Rate and IC_{50} Values

CSCs of OVCAR-3 and OVCAR-3/DDP (CSCs/DDP) were treated with 0, 10, 20, 40, and 80 μM of lumiflavin and 0, 40, 80, 160, 320 and 640 μM of DDP for 72 h. Surviving CSCs/DDP were compared with the CSCs combining cell viability/proliferation assays using the CCK-8 assay kit (Dojindo Laboratories, Japan) according to the manufacturer's instruction. The sensitivity of these paired cell lines is usually determined by exposing them to a range of drug concentrations and then assessing cell viability. The IC_{50} (drug concentration causing 50% growth inhibition) for these paired cell lines can be used to determine the increase in resistance known as the resistance index by the following equation (21):

$$\text{Resistance index} = \text{IC50 of Resistant Cell} \,/\, \text{IC50 of Normal Cell Line}$$

Mouse Xenograft Model

All animal studies adhered to the protocols approved by the Animal Research Ethics Board of the Lishui University (Lishui, Zhejiang Province, China. Permit Number: 0803-2019). The CSCs/DDP (1×10^5 cells) were resuspended in 50 μl Matrigel solution (1:1 dilution with DMEM) and injected subcutaneously under the outer skin of 6- to 8-week-old nude female mice (11). When the tumors reached a palpable size (100 mm^3), the mice were randomly divided into four groups, six mice/each group. Mice were intraperitoneal injected with DDP (CSCs/DDP group, DDP 5 mg/kg, once a week), CSCs/DDP + lumiflavin (4 mg/kg) (DDP 5 mg/kg, once a week; lumiflavin 4 mg/kg, once a day), CSCs/DDP + lumiflavin (8 mg/kg) (DDP 5 mg/kg, once a week; lumiflavin 8 mg/kg, once a day) and CSCs/DDP + lumiflavin (16 mg/kg) (DDP 5 mg/kg, once a week; lumiflavin 16 mg/kg, once a day). All groups of mice were treated for 25 days. The measurement of the length (mm), width (mm) and height (mm) of the tumor masses were performed twice weekly using electronic vernier calipers, and the tumor volumes (mm^3) were calculated using the following formula: $V = L \times W \times D \times \pi/6$, where V is the volume, L is the length, W is the width, and D is the depth.

Flow Cytometry Analysis for Cell Apoptosis

CSCs were treated with 0, 80 μM lumiflavin, and CSCs/DDP were treated with 80 μM DDP and 0, 20, 40, and 80 μM lumiflavin for 72h. For FCM analysis, 1×10^6 cells were harvested, collected by centrifugation (10 min, 2000×g) and washed three times with phosphate-buffered saline (PBS)

at 4°C. Prior to analysis, cells were resuspended in binding buffer (10 mM Hepes/NaOH, pH 7.4, 140 mM NaCl, 2.5 mM CaCl). Then, Cells were incubated with 5 μl Annexin V-FITC for 3 min and with 20 ng/mL propidium iodide (Multi Sciences Biotech Co., Ltd., Zhejiang, China) in the dark for 5 min. The apoptosis rate was detected by flow cytometry (BD Biosciences, San Jose, CA). The experiments were repeated three times independently and the results were presented as the mean ± standard deviation.

Colony Formation Assay

The colony formation capabilities of CSCs and CSCs/DDP were investigated. Briefly, 200 single-cell suspension were resuspended in culture medium into a six-hole plate. CSCs treated with 0 and 80 μM lumiflavin and CSCs/DDP treated with 80 μM DDP and 0, 20, 40, and 80 μM lumiflavin for 14 -15 days until colonies were formed. Colony cells with more than 50 cells were then counted as one positive colony according to laboratory reports (9, 11).

Cell Mitochondrial Membrane Potential Detected by Flow Cytometry

CSCs were treated with 0 and 80 μM lumiflavin, and CSCs/DDP treated with 80 μM DDP and 0, 20, 40, and 80 μM lumiflavin for 72 h in a 6-well plate. For mitochondrial membrane potential analysis, cells were collected, centrifuged and suspended, and the mitochondrial membrane potential (JC-1) probe (Beyotime Institute of Biotechnology, Jiangsu, China) was mixed. The mitochondrial membrane potential was detected by flow cytometry, according to the JC-1 probe instruction method. The Accuri C6 flow cytometry and the flow cytometry equipped with CellQuest software were used for data analysis.

RNA Sequencing Analysis

RNA-Seq by Switching Mechanism at 5' end of RNA Template (SMART) technology was used to study the transcriptome. After CSCs, CSCs/DDP were treated with 80 μm DDP, and CSCs/DDP were treated with 80 μm DDP and 80 μM lumiflavin for 72 h. Next, the cells were collected in TRIzol reagent (Shanghai Jierui Biotech Co., Ltd, Shanghai, China) and then lysed in reaction buffer. Single-cell SMART cDNA was generated by following the SMART-seq protocol (Hangzhou Lianchuan Biotechnology Co., Ltd). The raw data and cluster analysis was performed, and heatmap was generated using the tools in the Lianchuan BioCloud Platform (https://www.lc-bio.cn/overview). The gene ontology (GO) analysis was performed using GOseq packages, and KEGG Orthology (KO) analysis was performed on https://david.ncifcrf.gov/home.jsp (22, 23).

Western Blot Analysis

Western immunoblotting analysis was carried out for CSCs, CSCs/DDP treated with 80 μM DDP and CSCs/DDP treatment with 80 μM DDP and lumiflavin 80 μM for 72 h, as described previously (24, 25). Cellular proteins were extracted with RIPA buffer [150 mM NaCl, 50 mM Tris (pH 8.0), 10% glycerol, 2% Triton X-100, 1 mM ethylene diamine tetra acetic acid disodium, and a protein inhibitor mixture (Beyotime Biotechnology)]. For immunoblotting, solubilized proteins were loaded on a gel and resolved by 8% – 15% SDS-PAGE. The proteins were then transferred to PVDF membranes and incubated at 4°C overnight with primary antibodies Jagged1 (Jag1,Abcam,1:1000), Jagged2 (Jag2, Abcam,1:1000), Delta-like canonical notch ligand 1 (Dll1, Abcam,1:500), Delta-like canonical notch ligand 3 (Dll3, Cell Signaling Technology,1:1000), Delta-like canonical notch ligand 4 (Dll4, Cell Signaling Technology,1:1000), Notch1 (Abcam,1:1000), Notch2 (Abcam,1:5000), Notch3(Santa Cruz, 1:500), Notch4 (Santa Cruz, 1:500) or NICD (Cell Signaling Technology, 1:1000). Membranes were washed and incubated with anti-rabbit/anti-mouse antibodies (MultiSciences Biotech, 1:5000) for 1 h at room temperature. Chemiluminescent images of the blots were finally captured using a ChemiDoc System (Bio-Rad, USA). ImageJ software was used to calculate relative protein expression.

Data Analysis

All experiments were repeated at least three times and the data are presented as the mean ± S.D. Differences among data groups were evaluated for significance using the Student's *t* test of unpaired data (two-tailed). For animal studies, the data are presented as the mean ± S.E.M. The *F* test for the homogeneity of variance was conducted. The tumor volume was analyzed with one-way ANOVA using the software SPSS 11.5 for Windows (Chicago, IL, USA). Significant and highly significant differences were considered at $P < 0.05$ and $P < 0.01$, respectively.

RESULTS

Lumiflavin Treatment Reduces the Formation of Drug Resistance and Proportion of CSCs in OVCAR-3

In this study, we further investigated the effect of lumiflavin on the development of resistance in ovarian cancer cells. The drug resistance of ovarian cancer cell line OVCAR 3 (OVCAR 3/DDP) was induced by gradient concentration increase method (26), while treating with 0, 10, 20, 40, and 80 μm lumiflavin intervention. At the end, OVCAR-3 and OVCAR-3/DDP intervened with different concentrations of lumiflavin were treated with 0, 40, 80, 160, 320 and 640 μM DDP for 72 h, respectively. Cell viability was detected with CCK-8 assay kit. The results showed that the cell viability rate of the OVCAR-3 cells decreased in a dose-dependent manner with the increase in DDP concentration. Compared with normal OVCAR-3, the cell viability rate of the OVCAR-3 cells at 20 μM DDP and 160 μM DDP was 44% and 7%, respectively. In contrast, the cell viability rate of OVCAR-3/DDP at 160 μM DDP and 640 μM DDP was 85% and 38%, respectively, thereby indicating the significant resistance to DDP. The treatment of lumiflavin could reduce the drug resistance of OVCAR-3/DDP cells significantly, showing that after treatment with lumiflavin at

10, 20, 40, and 80 μM, the cell survival rate was 66%, 60%, 26% and 17% under 160 μM DDP, and 27%, 24%, 11% and 2% under 640 μM DDP, respectively, compared with OVCAR-3/DDP. The resistance index of the OVCAR-3/DDP cells after 0, 10, 20, 40, and 80 μM lumiflavin intervention groups was 18.9, 13.5, 9.5, 4.1, and 3.0, respectively, compared with OVCAR-3/DDP (**Figures 2A, B**).

The proportion of CSCs (CD133+CD177+ double positive cells) in OVCAR-3 and OVCAR-3/DDP was determined by flow cytometry. The results showed that compared with OVCAR-3 cells, the proportion of CSCs/DDP in OVCAR-3/DDP cells increased (P<0.01) (**Figures 2C, D**).

Lumiflavin Enhances the Chemotherapy Effect of DDP on CSCs/DDP

CSCs/DDP were separated from OVCAR-3/DDP to further study whether the effect of lumiflavin on OVCAR-3/DDP cells is associated with CSCs. CSCs, CSCs/DDP were treated with 80 μM DDP, and CSCs/DDP were treated with 80 μM DDP and 20, 40, 80 μM lumiflavin for 72 h. The apoptosis and clone formation ability were detected. The flow cytometry results of flow cytometry showed that the apoptosis rate of the OVCAR-3/DDP cells was 3.6% after 80 μM DDP treatment for 72 h, while whereas combined with 20, 40, and 80 μM lumiflavin, the apoptosis rate was 20%, 30.4%, and 43%, respectively (compared with the OVCAR-3/DDP cells, P < 0.01). The results of clone formation experiment showed that after 80 μM DDP intervention, the number of clones was 113.7/well in OVCAR-3/DDP cells, and 63.0/well, 54.3/well and 35.0/well after the combined treatment with 20, 40, and 80 μM lumiflavin, respectively (compared with the OVCAR-3/DDP cells, P < 0.01). These results showed that lumiflavin increased CSCs/DDP apoptosis rate and reduced cell clone formation ability in a dose-dependent manner (**Figures 3A–D**).

JC-1 is a cationic dye used for the detection of mitochondrial membrane potential, which can enter the negatively charged mitochondria and accumulate to form aggregates (27). Excited by fluorescence at 488 nm wavelength, JC-1 emits a red spectrum. The decrease in mitochondrial membrane potential will lead to the dissociation of JC-1 into monomer, and the green light will be emitted. Flow cytometry shows that the FL1-A signal is enhanced and the FL2-A signal is significantly decreased (28). The flow cytometry results showed that the proportion of JC-1 in OVCAR-3/DDP cells was 16.1% after 80 μM DDP treatment for 72 h, whereas combined with 20, 40, and 80 μM lumiflavin, proportions of JC-1 were 18.4%, 27.0%, and 47.1%, respectively (compared with the OVCAR-3/DDP cells, P < 0.01). This study showed that lumiflavin treatment increased the proportion of JC-1 in CSCs/DDP, thereby suggesting that mitochondrial membrane potential ($\Delta\psi m$) is decreased and induced CSC apoptosis (**Figures 3E, F**).

To further explore the effect of lumiflavin on CSCs/DDP *in vivo*, CSCs/DDP were subcutaneously inoculated in nude mice and treated with DDP (5 mg/kg) combined with lumiflavin (4, 8 and 16 mg/kg) for 25 d. The results showed that lumiflavin combined with DDP reduced tumor weight and inhibited tumor growth curve in a dose-dependent manner, compared with DDP alone (**Figures 3G–I**).

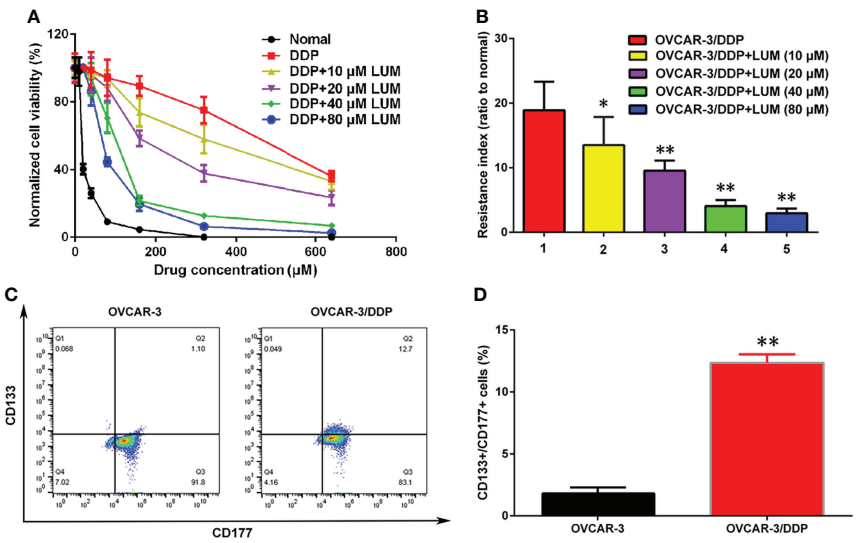

FIGURE 2 | Lumiflavin treatment reduces the development of DDP resistance of ovarian cancer OVCAR-3 cells line that is associated with cancer stem cells (CSCs). DDP resistance of ovarian cancer OVCAR-3 cell lines were induced by gradient concentration increment method (26), and treated with 10, 20, 40, and 80 μm lumiflavin intervention simultaneously. The cell inhibition rate and resistance index of OVCAR-3cells to DDP were detected by CCK-8 assay kit. The proportion of CSCs (CD133+/CD177+ double positive cells) in OVCAR-3 cells was detected by flow cytometry. **(A)** Inhibitory curves of lumiflavin and DDP on OVCAR-3 and OVCAR-3/DDP cells. **(B)** Resistance index of OVCAR-3/DDP cells compared with OVCAR-3 cells. **(C)** Flow detection results of CD133+/CD117+ cells ratio of OVCAR-3 and OVCAR-3/DDP cells. **(D)** Statistical analysis graph of **(C)**. Mean ± SD (n = 3). **P < 0.01 difference between groups; *P < 0.05 difference between groups. DDP, cisplatin; OVCAR-3/DDP, DDP resistant OVCAR-3 cell lines; LUM, lumiflavin.

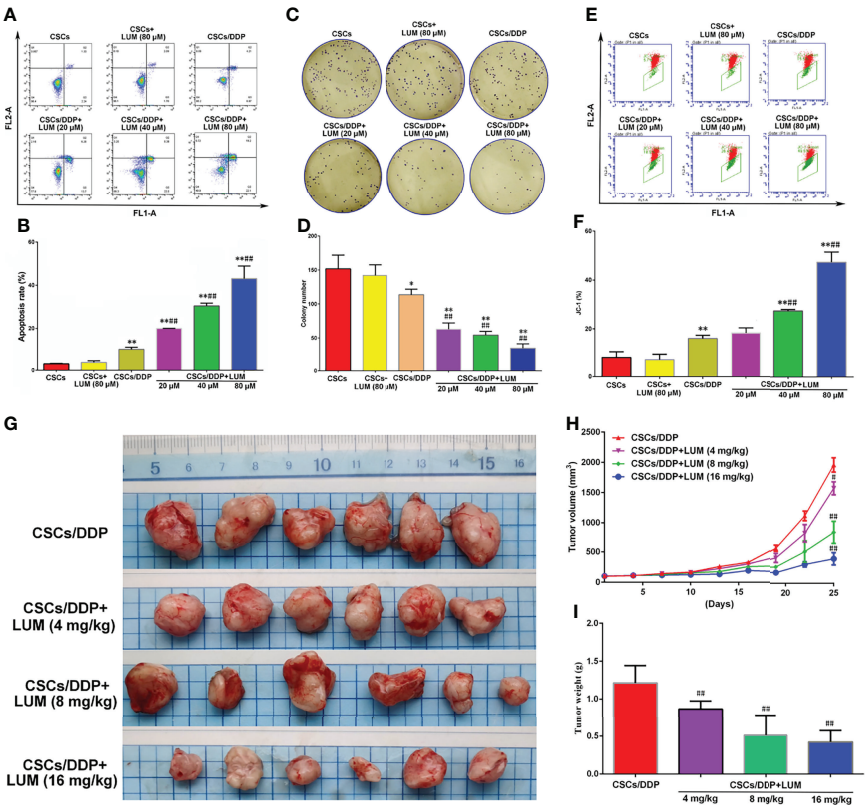

FIGURE 3 | Lumiflavin enhances the chemotherapy effect of DDP on DDP-resistant cancer stem cells (CSCs/DDP). CSCs, CSCs/DDP were treated with 80 μM DDP, and CSCs/DDP were treated with 80 μM DDP and 20, 40, 80 μM lumiflavin for 72 h. Apoptosis and clone formation ability were detected. Moreover cell mitochondrial membrane potential were tested by JC-1 prob (27, 28). CSCs/DDP were subcutaneously inoculated in nude mice and treated with DDP (DDP 5 mg/kg, once a week) combined with lumiflavin for 25 d. Tumor weight and inhibited tumor growth curve were measured. **(A)** Flow cytometry of cell apoptosis as detected using Annexin V-FITC. **(B)** Statistical analysis graph of **(A, C)** Images of colony formation assay. **(D)** Statistical analysis graph of **(C, E)** Flow cytometry scatter plot of the potential of the mitochondrial membrane (Δψm) of cells as detected through flow cytometry by using a JC-1 probe. **(F)** Statistical analysis graph of **(E)**. **(G)** Photograph of tumors. **(H)** Tumor growth curve of nude mice. **(I)** Statistical graph of tumor weight. Mean ± SD (n = 3, cells; n = 6, mice). $^{*}P < 0.05$ compared with the CSC group; $^{**}P < 0.01$ compared with the CSC group; $^{\#\#}P < 0.01$ compared with CSC/DDP group. CSCs, CSCs from OVCAR-3 cell lines; CSCs/DDP, CSCs from DDP resistant OVCAR-3 cell lines; LUM, lumiflavin.

Lumiflavin Treatment Affects the Phenotypic Differentiation of CSCs/DDP

CD133 and CD177 are highly expressed in CSCs and are required for the maintenance of CSCs (29). As illustrated in **Figure 4**, after 80 μM DDP treatment, the proportion of CD133 +/CD177+ cells in CSCs/DDP cells was 89.7%, whereas after combined treatment with 20, 40, and 80 μM lumiflavin, the proportion became 74.6%, 59.8%, and 31.6%, respectively. In addition, we also investigated the proportion of CD44+/CD24- cells, an important characteristic of CSCs (30), after 20, 40, and 80 μM lumiflavin treatment, the proportion was 63.4%, 49.0% and 18.2%, respectively, compared with 80.5% for CSCs/DDP cells. The results showed that after 72 h treatment with lumiflavin, the proportions of both types of cells decreased and showed dose dependence (compared with CSCs/DDP group, $P < 0.01$). These results suggested that lumiflavin combined with DDP could induce cell differentiation and inhibit the phenotypic maintenance ability of CSCs/DDP, as shown in **Figures 4A, B**.

Bioinformatics Analysis of the RNA-Seq Assay

To further explore the molecular mechanism of the combined effect of lumiflavin and DDP on CSCs/DDP, RNA-Seq was used to detect the transcriptome changes of CSCs/DDP treated with 80 μM lumiflavin and 80 μM DDP for 72 h. An example heat map showing the Log10 FC expression values of differentially expressed mRNA were plotted by heat map. We analyzed the statistical enrichment of differentially expressed genes in KEGG pathway. Based on the results of significantly differentially expressed analysis, six pathways were significantly enriched ($P < 0.05$). The most enriched pathways included stem cell signaling pathway, Notch signaling pathway, cell cycle, oxidative phosphorylation, and AMPK signaling pathway. Next, we performed GO analysis on all the differential mRNA, and the results showed that the differential gene functions focused on cell differentiation, oxidation–reduction process, population proliferation, as well as DNA-binding

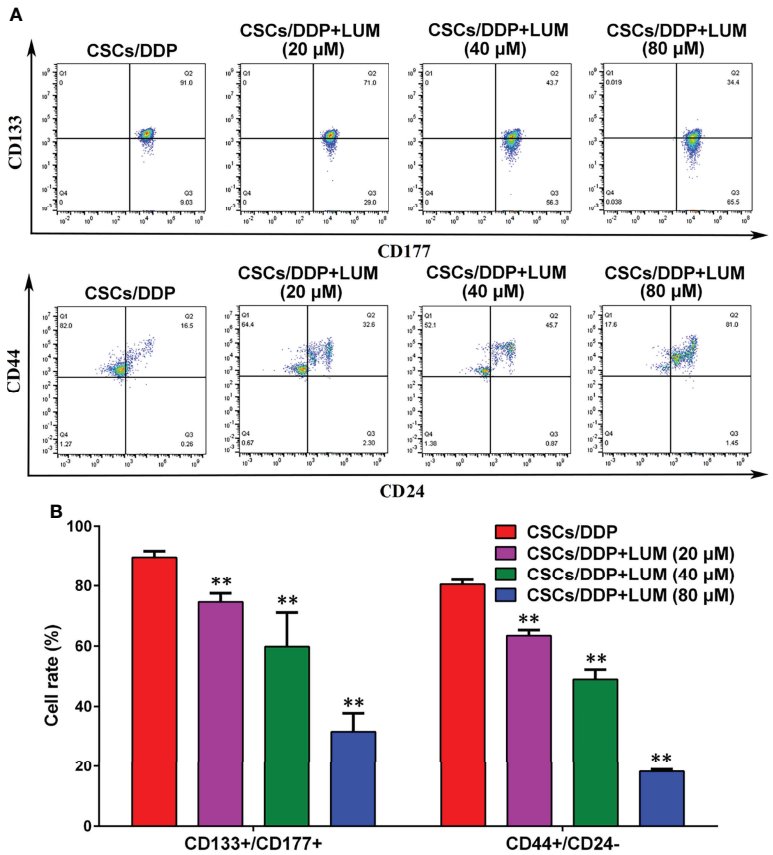

FIGURE 4 | Effects of lumiflavin treatment on phenotypic differentiation of DDP-resistant cancer stem cells (CSCs/DDP). CSCs, CSCs/DDP were treated with 80 μM DDP, and CSCs/DDP were treated with 80 μM DDP and 20, 40, 80 μM lumiflavin for 72 h. Co-expression of CD133+/CD117+, CD44+/CD177, and CD44+/CD24– of CSCs/DDP were detected through flow cytometry. **(A)** Flow detection results of CD133+/CD117+, CD44+/CD177, and CD44+/CD24- cells of CSCs/DDP. **(B)** Statistical analysis graph of **(A)**. $^{**}P < 0.01$ between groups. Mean ± SD ($n = 3$). CSCs/DDP, CSCs from DDP resistant OVCAR-3 cell lines; LUM, lumiflavin.

transcription factor activity, RNA polymerase II-specific. Among the cell components, it affects the nucleus, membrane, and cytoplasm (**Figures 5A–C**).

Lumiflavin Downregulated the Protein Expression of Notch Signaling Pathway in CSCs/DDP

Previous RNA-Seq assay revealed that the effect of lumiflavin on CSCs is related to the Notch signaling pathway, stem cell signaling pathway, cell cycle, oxidative phosphorylation, and AMPK signaling pathway. Moreover, Notch has important interactions with stem cell and AMPK signaling pathway and stem cell signaling pathway (31, 32). Next, CSCs, CSCs/DDP were treated with 80 μM DDP, and CSCs/DDP were treated with 80 μM DDP and 80 μM lumiflavin for 72 h. Western blotting was used to study the effects of lumiflavin on Notch signaling related proteins in ovarian cancer cell line CSCs/DDP. Moreover, the results show that Notch-1, Notch-2, Notch-3, and Notch ligands, just as Jag1, 2 and Dll 1, 3, 4 were increased in CSCs/DDP, compared with CSCs, whereas the expressions of Notch-1, Notch-2, Notch-3 and Jag1, 2 and Dll 3 were downregulated following lumiflavin treatment. Further confirmation showed that NICD expression was increased in CSCs/DDP, compared with CSCs, and reduced expression in CSCs/DDP treatment with lumiflavin (**Figures 6A, B**).

DISCUSSION

Cell line models have proven to be an effective tool for ovarian cancer research, and the study of the mechanism of drug-resistant cell lines will contribute to the development of anti-cancer drugs. Furthermore, cell lines taken from cancer patients before and after chemotherapy, are ideal models for drug resistance development (33, 34). In this study, drug-resistant ovarian cancer cell lines, such as OVCAR-3/DDP were established through induction, and the drug resistance index showed that the IC50 concentration of OVCAR-3/DDP was more than 18 times that of OVCAR-3cells. Simultaneous intervention with four concentrations of lumiflavin was found to dose-dependently shift the resistance curve of OVCAR-3/DDP and reduce the resistance index. The results of

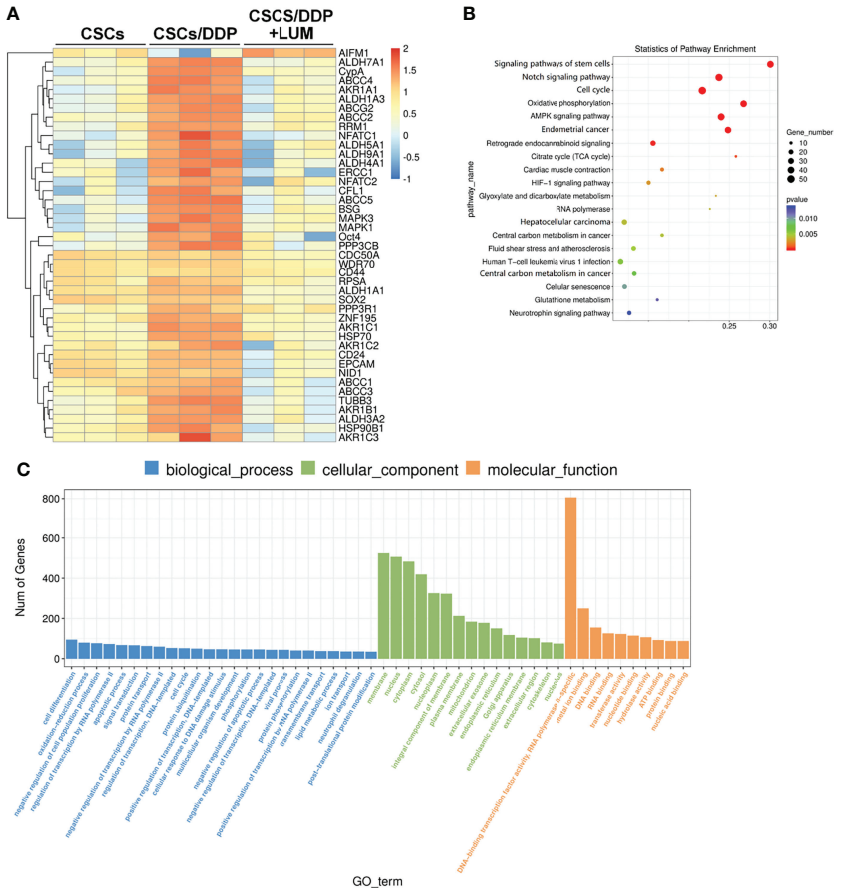

FIGURE 5 | RNA-seq analysis of transcriptome changes in lumiflavin on DDP-resistant cancer stem cells (CSCs/DDP). CSCs, CSCs/DDP were treated with 80 μM DDP, and CSCs/DDP were treated with 80 μM DDP and 80 μM lumiflavin for 72 h. The transcriptome changes were detected by RNA-Seq assay. **(A)** Enrichment analysis of RNA-Seq assay. **(B)** Scatter diagram of KEGG enrichment analysis results of RNA-Seq assay. **(C)** Gene ontology analysis was utilized to evaluate the canonical pathways in the RNA-Seq assay results. Mean ± SD (n = 3). CSCs, CSCs were separated from OVCAR-3 cells line; CSCs/DDP, CSCs were separated from OVCAR-3/DDP cells line; LUM, lumiflavin.

experiments *in vitro* have shown that the development of drug resistance can be weakened by simultaneous treatment with lumiflavin.

The hypothesized properties of CSCs subpopulations have been used to help explain the phenomena observed in cancer biology, and various approaches to CSCs in the search for these "cancers" have been applied to hematologic diseases and solid malignancies (35, 36). CSCs can be studied in two main methods. One is to isolate cells, such as CD133+, CD177+, or CD44+/CD24-, that have stem-like characteristics (37–40). Another approach is to take advantage of the CSCs' ability to excrete fluorescent dyes and obtain so-called "Side population (SP) cell" as study cells by flow cytometry sorting, and recent reports suggested that SP cells may represent different types of CSCs malignancies (41, 42). In this study, the proportion of CSCs (CD133+/CD177+) in OVCAR-3/DDP was significantly increased (13.1%) compared with that of OVCAR-3 (1.75%), which was similar to that in related studies (43, 44). These results suggest that CSCs acquire drug-resistance character more easily than normal non-cancer stem cells; and in the process of DDP chemotherapy, non-cancer stem cells are easier to be killed than CSCs. CSCs play a significant role in the induction of drug-resistant cells.

Apoptosis rate is an important indicator to reflect the killing effect of chemotherapy drugs, and the colony-forming capacity is an important characteristic of CSCs (45).In this study, lumiflavin increased the apoptosis rate and reduced the colony-forming capacity of CSCs/DDP. These results suggested that the effect of lumiflavin on OVCAR-3/DDP was related to CSCs/DDP.

The ability of CSCs to resist chemotherapy damage is stronger than that of ordinary cancer cells, and previous studies have found that it is related to the ability of CSCs to resist oxidative damage. Moreover, lumiflavin can attenuate the antioxidant damage ability of CSCs (11). This study confirmed that lumiflavin has the same role in oxidative damage in CSCs/DDP. Decreased mitochondrial capacity to resist oxidative damage leads to the accumulation of ROS, which is a key event

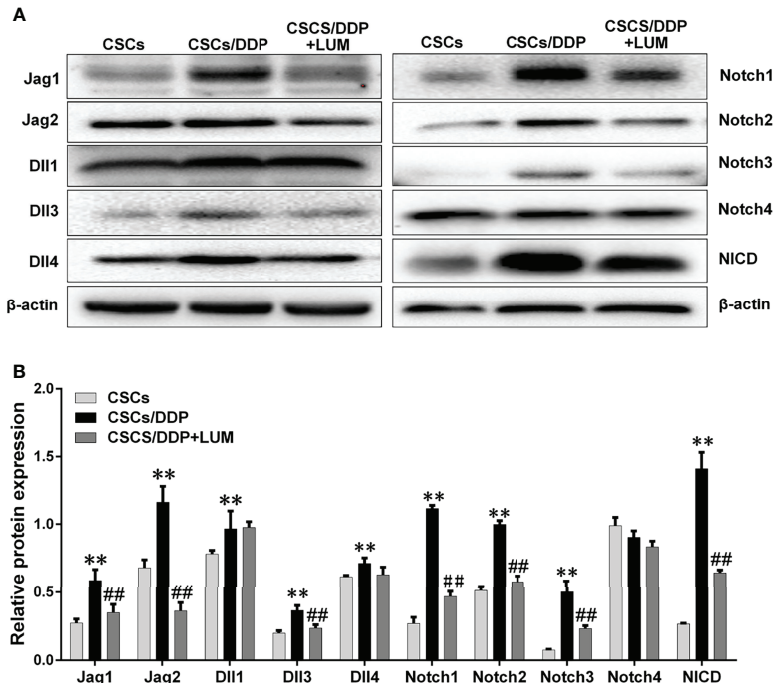

FIGURE 6 | Lumiflavin downregulated the protein expression of Notch signaling pathway in DDP-resistant cancer stem cells (CSCs/DDP). CSCs, CSCs/DDP were treated with 80 μM DDP, and CSCs/DDP were treated with 80 μM DDP and 80 μM lumiflavin for 72 h. The expression levels of Jag1, Jag2, Dll1, Dll3, Dll4, Notch1, Notch2, Notch3, Notch4, NICD, and β-actin were analyzed *via* Western blot by using specific antibodies. **(A)** Electrophoretograms of proteins. **(B)** Graph of relative protein expression as determined by Western blot analysis. $^{**}P < 0.01$ compared with CSC group; $^{\#\#}P < 0.01$ compared with CSCs/DDP group. Mean ± SD ($n = 5$). CSCs, CSCs were separated from OVCAR-3 cells line; CSCs/DDP, CSCs were separated from OVCAR-3/DDP cells line; LUM, lumiflavin.

in inducing apoptosis (46). The change in mitochondrial permeability and the decrease in transmembrane potential after mitochondrial damage are the initial events of the cascade of apoptosis, and mitochondrial dissipation leads to irreversible apoptosis (47, 48). In this study, lumiflavin-assisted DDP reduced mitochondrial transmembrane potential of CSCs/DDP, suggesting that the synergic effect of lumiflavin and DDP was related to increased mitochondrial damage. This point is consistent with our previous researches (11, 18).

The anti-injury characteristics of CSCs make it difficult for ordinary chemotherapy to kill CSCs effectively, so the differentiation of CSCs into normal cancer cells is a good strategy to kill CSCs effectively (12, 49). The flow cytometry results showed that the proportion of CD133+/CD177+ and CD44+/CD24- in CSCs/DDP decreased after lumiflavin intervention, suggesting that the synergistic effect of lumiflavin and DDP may be related to its differentiation. Thus, transcriptome sequencing analysis was performed on CSCs/DDP treated with lumiflavin, we found that the differences in mRNA expression were mainly concentrated in the Notch signaling pathway, which is the key pathway of CSCs characteristics (50, 51). Moreover, the biological function analysis of gene differences revealed that these genes concentrated in cell cycle and oxidative phosphorylation pathway. Together, they show that the effects of lumiflavin on CSCs/DDP are concentrated on the cell differentiation.

RNA-seq analysis showed significant changes in Notch signaling pathway, stem cell signaling pathway, cell cycle, oxidative phosphorylation and AMPK signaling pathway. Previous studies have confirmed that the effect of lumiflavin is related to oxidative phosphorylation and oxidative stress (11). Moreover, Notch is closely related to stem cell signaling pathway, AMPK signaling pathway and cell cycle (31, 52, 53). Notch pathway is also critical for CSC differentiation and drug resistance in cancer (54, 55). Therefore, we speculate the key role of the Notch pathway and further investigate its changes. As shown in **Figure 5**, compared with normal CSCs, the expression of ligands (e.g., Jag1, Jag2, Dll1, Dll3 and Dll14) of four Notch receptors (e.g., Notches 1 to 4) and NICD were up regulated in CSCs/DDP, compared with CSCs. It is suggested that Notch signaling pathway is enhanced and related to drug resistance of CSCs. However, these protein expressions were decreased, except DII 4 and Notch4, in lumiflavin treatment group, suggesting that the role of lumiflavin may be related to Notch pathway in CSCs/DDP phenotypic transformation.

In this study, the effect of lumiflavin on the development of drug resistance in CSCs of OVCAR-3 cell was studied, suggesting that lumiflavin can slow down the progress of CSCs/DDP and increase the killing effect of DDP on CSCs/DDP. It was preliminarily shown to be related to the differentiation of CSCs/DDP, but this study still had the following deficiencies: 1) Sequencing results showed that other important signaling

pathways, such as oxidative phosphorylation and AMPK signaling pathway, were significantly altered, and the roles of these pathways in this study have not been explored yet; and 2) CSCs will be subject to many influencing factors *in vivo*, which will affect the differentiation and drug resistance of CSCs. These problems will be elaborated in the future research.

DATA AVAILABILITY STATEMENT

The original contributions presented in the study are publicly available. This data can be found here: https://www.ncbi.nlm.nih.gov/bioproject/PRJNA810781.

ETHICS STATEMENT

The animal study was reviewed and approved by the Animal Research Ethics Board of the Lishui University.

AUTHOR CONTRIBUTIONS

RY conducted animal experiments and most of cell experiments and drafted the manuscript. BL conducted immunoassay and cell assay, participated in the animal experiments. FX participated in the design of the study and performed the statistical analysis. MY and SW participated in the writing of the manuscript. SW participated in the design of the study and proofread the manuscript. SZ participated in its design and the sequence alignment and drafted the manuscript. All authors read and approved the final manuscript.

FUNDING

This work was supported by grants from the Fund of Natural Science Foundation of Zhejiang Province, China [NO: LY20H310007], Department of Education of Zhejiang Province [NO: Y201839774], and Key project of Taizhou Vocational and Technical College [NO: 2022ZD02].

REFERENCES

1. Gupta S, Nag S, Aggarwal S, Rauthan A, Warrier N. Maintenance Therapy for Recurrent Epithelial Ovarian Cancer: Current Therapies and Future Perspectives–A Review. *J Ovarian Res* (2019) 12(1):1–15. doi: 10.1186/s13048-019-0579-0
2. Ottevanger PB. Ovarian Cancer Stem Cells More Questions Than Answers. In: *Seminars in Cancer Biology*. Elsevier: Academic Press (2017). 44:67–71
3. Pieterse Z, Amaya-Padilla MA, Singomat T, Binju M, Madjid BD, Yu Y, et al. Ovarian Cancer Stem Cells and Their Role in Drug Resistance. *Int J Biochem Cell Biol* (2019) 106:117–26. doi: 10.1016/j.biocel.2018.11.012
4. Keyvani V, Farshchian M, Esmaeili S-A, Yari H, Moghbeli M, Nezhad S-RK, et al. Ovarian Cancer Stem Cells and Targeted Therapy. *J Ovarian Res* (2019) 12(1):1–11. doi: 10.1186/s13048-019-0588-z
5. Najafzadeh N, Mazani M, Abbasi A, Farassati F, Amani M. Low-Dose All-Trans Retinoic Acid Enhances Cytotoxicity of Cisplatin and 5-Fluorouracil on CD44+ Cancer Stem Cells. *Biomed Pharmacot* (2015) 74:243–51. doi: 10.1016/j.biopha.2015.08.019
6. Liang DH, Choi DS, Ensor JE, Kaipparettu BA, Bass BL, Chang JC. The Autophagy Inhibitor Chloroquine Targets Cancer Stem Cells in Triple Negative Breast Cancer by Inducing Mitochondrial Damage and Impairing DNA Break Repair. *Cancer Lett* (2016) 376(2):249–58. doi: 10.1016/j.canlet.2016.04.002
7. Yamamoto M, Suzuki S, Togashi K, Sanomachi T, Seino S, Kitanaka C, et al. AS602801 Sensitizes Ovarian Cancer Stem Cells to Paclitaxel by Down-Regulating MDR1. *Anticancer Res* (2019) 39(2):609–17. doi: 10.21873/anticanres.13154
8. Koren E, Fuchs Y. The Bad Seed: Cancer Stem Cells in Tumor Development and Resistance. *Drug Resist Update* (2016) 28:1–12. doi: 10.1016/j.drup.2016.06.006
9. Yang RH, Song Y, Song-Quan WU, Shen XC. Intervention of Riboflavin Metabolism Improves Sensitivity of Ovarian Cancer HO8910 Cells to Cisplatin *In Vitro*. *Chin J Pharmacol Toxicol* (2016) 30(8):823–32. doi: 10.3867/j.issn.1000-3002.2016.08.005
10. Yang RH, Song ZX, Luo X. Effects of Riboflavin Metabolic Pathways Combination With Cisplatin on Adhesion and Migration of Ovarian Cancer Cells. *Chin Pharm J* (2017). 52(17):1510–4. doi: 10.11669/cpj.2017.17.007
11. Yang R, Wei Z, Wu S. Lumiflavin Increases the Sensitivity of Ovarian Cancer Stem-Like Cells to Cisplatin by Interfering With Riboflavin. *J Cell Mol Med* (2019) 23(8):5329–39. doi: 10.1111/jcmm.14409
12. Jin X, Jin X, Kim H. Cancer Stem Cells and Differentiation Therapy. *Tumor Biol* (2017) 39(10):1010428317729933. doi: 10.1177/1010428317729933
13. Frank NY, Schatton T, Frank MH. The Therapeutic Promise of the Cancer Stem Cell Concept. *J Clin Invest* (2010) 120(1):41–50. doi: 10.1172/JCI41004
14. Piccirillo S, Reynolds BA, Zanetti N, Lamorte G, Binda E, Broggi G, et al. Bone Morphogenetic Proteins Inhibit the Tumorigenic Potential of Human Brain Tumour-Initiating Cells. *Nature* (2006) 444(7120):761–5. doi: 10.1038/nature05349
15. Lotem J, Sachs L. Epigenetics and the Plasticity of Differentiation in Normal and Cancer Stem Cells. *Oncogene* (2006) 25(59):7663–72. doi: 10.1038/sj.onc.1209816
16. Campos B, Wan F, Farhadi M, Ernst A, Zeppernick F, Tagscherer KE, et al. Differentiation Therapy Exerts Antitumor Effects on Stem-Like Glioma Cells. *Clin Cancer Res* (2010) 16(10):2715–28. doi: 10.1158/1078-0432.CCR-09-1800
17. Yan Y, Li Z, Xu X, Chen C, Wei W, Fan M, et al. All-Trans Retinoic Acids Induce Differentiation and Sensitize a Radioresistant Breast Cancer Cells to Chemotherapy. *BMC Complement Altern Med* (2016) 16(1):1–11. doi: 10.1186/s12906-016-1088-y
18. Wu M, Huang Y, Song Z, Yang R. Lumiflavin Enhances the Effects of Ionising Radiation on Ovarian Cancer Stem-Like Cells by Inhibiting Autophagy. *Anticancer Agents Med Chem* (2021) 21(15):2004–11. doi: 10.2174/1871520621999210104201907
19. Nikounezhad N, Nakhjavani M, Shirazi FH. Generation of Cisplatin-Resistant Ovarian Cancer Cell Lines. *Iran Pharm J Sci* (2016) 12(1):11–20. doi: 10.22034/ijps.2017.31154
20. Kikuchi Y, Miyauchi M, Kizawa I, Oomori K, Kato K. Establishment of a Cisplatin-Resistant Human Ovarian Cancer Cell Line. *J Natl Cancer Instit* (1986) 77(6):1181–5. doi: 10.1093/jnci/77.6.1181
21. McDermott M, Eustace A, Busschots S, Breen L, Clynes M, O'Donovan N, et al. *In Vitro* Development of Chemotherapy and Targeted Therapy Drug-Resistant Cancer Cell Lines: A Practical Guide With Case Studies. *Front Oncol* (2014) 4:40. doi :10.3389/fonc.2014.00040
22. Wei L, Peng Y, Shao N, Zhou P. Downregulation of Tim-1 Inhibits the Proliferation, Migration and Invasion of Glioblastoma Cells *via* the miR-133a/TGFBR1 Axis and the Restriction of Wnt/β-Catenin Pathway. *Cancer Cell Int* (2021) 21(1):1–14. doi :10.1186/s12935-021-02036-1
23. Pan D, Zhang W, Zhang N, Xu Y, Chen Y, Peng J, et al. Oxymatrine Synergistically Enhances Doxorubicin Anticancer Effects in Colorectal Cancer. *Front Pharmacol* (2021) 12. doi :10.3389/fphar.2021.673432
24. Yang R, Hu Z, Zhang P, Wu S, Song Z, Shen X, et al. Probucol Ameliorates Hepatic Stellate Cell Activation and Autophagy is Associated With Farnesoid

X Receptor. *J Pharmacol Sci* (2019) 139(2):120–8. doi: 10.1016/j.jphs.2018.12.005
25. Ruhui Y, Guangli W, Lingyun L, Hanjiang H, Mingzhu Z, Linrong L, et al. Tespa1 Plays a Role in the Modulation of Airway Hyperreactivity Through the IL-4/STAT6 Pathway. *J Trans Med* (2021) 18(1):444. 2020
26. Xu J, Wu J, Fu C, Teng F, Liu S, Dai C, et al. Multidrug Resistant lncRNA Profile in Chemotherapeutic Sensitive and Resistant Ovarian Cancer Cells. *J Cell Physiol* (2018) 233(6):5034–43. doi: 10.1002/jcp.26369
27. Sivandzade F, Bhalerao A, Cucullo L. Analysis of the Mitochondrial Membrane Potential Using the Cationic JC-1 Dye as a Sensitive Fluorescent Probe. *Bio Protoc* (2019) 9(1):1–13. doi: 10.21769/BioProtoc.3128
28. Yong WK, Nurestri A. Xanthohumol Induces Growth Inhibition and Apoptosis in Ca Ski Human Cervical Cancer Cells. *Evid Base Complement Alternat Med* (2015) 2015:921306. doi: 10.1155/2015/921306
29. Bellio C, DiGloria C, Foster R, James K, Konstantinopoulos PA, Growdon WB, et al. PARP Inhibition Induces Enrichment of DNA Repair–Proficient CD133 and CD117 Positive Ovarian Cancer Stem Cells. *Mol Cancer Res* (2019) 17(2):431–45. doi: 10.1158/1541-7786.MCR-18-0594
30. Meng E, Long B, Sullivan P, McClellan S, Finan MA, Reed E, et al. CD44+/CD24− Ovarian Cancer Cells Demonstrate Cancer Stem Cell Properties and Correlate to Survival. *Clin Exp Metast* (2012) 29(8):939–48. doi: 10.1007/s10585-012-9482-4
31. Chiba S. Concise Review:Notch Signaling in Stem Cell Systems. *Stem Cells* (2006) 24(11):2437–47. doi: 10.1634/stemcells.2005-0661
32. Wang R, Li Y, Tsung A, Huang H, Du Q, Yang M, et al. iNOS Promotes CD24+ CD133+ Liver Cancer Stem Cell Phenotype Through a TACE/ADAM17-Dependent Notch Signaling Pathway. *Proc Natl Acad Sci* (2018) 115(43): E10127–36. doi: 10.1073/pnas.1722100115
33. Januchowski R, Sterzyńska K, Zaorska K, Sosińska P, Klejewski A, Brązert M, et al. Analysis of MDR Genes Expression and Cross-Resistance in Eight Drug Resistant Ovarian Cancer Cell Lines. *J Ovarian Res* (2016) 9(1):1–11. doi:10.1186/s13048-016-0278-z
34. Kazmierczak D, Jopek K, Sterzynska K, Ginter-Matuszewska B, Nowicki M, M. Rucinski and R. Januchowski: The Significance of MicroRNAs Expression in Regulation of Extracellular Matrix and Other Drug Resistant Genes in Drug Resistant Ovarian Cancer Cell Lines. *Int J Mol Sci* (2020) 21(7):2619. doi: 10.3390/ijms21072619
35. Novak D, Hüser L, Elton JJ, Umansky V, Altevogt P, Utikal J. SOX2 in Development and Cancer Biology. In: *Seminars in Cancer Biology*. Elsevier: Academic Press (2020) 67:74–82.
36. Bocci F, Gearhart-Serna L, Boareto M, Ribeiro M, Ben-Jacob E, Devi GR, et al. Toward Understanding Cancer Stem Cell Heterogeneity in the Tumor Microenvironment. *Proc Natl Acad Sci* (2019) 116(1):148–57. doi: 10.1073/pnas.1815345116
37. Bellio C, Foster R, Growdon WB, Rueda BR. Assessing the Efficacy of the Anti Metabolic Drug, CPI-613, for Targeting of Ovarian Cancer Stem Cells. In: *Cancer Res* (2016) 76(14 Supplement):2504.
38. Xiang T, Long H, He L, Han X, Lin K, Liang Z, et al. Interleukin-17 Produced by Tumor Microenvironment Promotes Self-Renewal of CD133+ Cancer Stem-Like Cells in Ovarian Cancer. *Oncogene* (2015) 34(2):165–76. doi: 10.1038/onc.2013.537
39. Yang B, Yan X, Liu L, Jiang C, Hou S. Overexpression of the Cancer Stem Cell Marker CD117 Predicts Poor Prognosis in Epithelial Ovarian Cancer Patients: Evidence From Meta-Analysis. *OncoTarget Ther* (2017) 10:2951. doi: 10.2147/OTT.S136549
40. Li X, Zhou N, Wang J, Liu Z, Wang X, Zhang Q, et al. Quercetin Suppresses Breast Cancer Stem Cells (CD44+/CD24−) by Inhibiting the PI3K/Akt/mTOR-Signaling Pathway. *Life Sci* (2018) 196:56–62. doi: 10.1016/j.lfs.2018.01.014
41. Shimoda M, Ota M, Okada Y. Isolation of Cancer Stem Cells by Side Population Method. In:*Cancer Stem Cells*. Springer: Humana Press, NY, New York (2018). p. 49–59.
42. Zhan Q, Wang C, Ngai S. Ovarian Cancer Stem Cells: A New Target for Cancer Therapy. *BioMed Res Int* (2013) 2013:1–10. doi: 10.1155/2013/916819
43. Wang X, Li X, Fu X, Bai M, Li X, Mei Q, et al. Eliminating Ovarian Cancer Stem Cells:A Potential Therapeutic Target for Ovarian Cancer Chemoresistance. *Curr Protein Pept Sci* (2015) 16(4):270–8. doi: 10.2174/1389203716041504291514 57
44. Niess H, Camaj P, Renner A, Ischenko I, Zhao Y, Krebs S, et al. Side Population Cells of Pancreatic Cancer Show Characteristics of Cancer Stem Cells Responsible for Resistance and Metastasis. *Target Oncol* (2015) 10 (2):215–27. doi: 10.1007/s11523-014-0323-z
45. Rajendran V, Jain MV. *In Vitro* Tumorigenic Assay:Colony Forming Assay for Cancer Stem Cells. *Methods Mol Biol* (2018) 89–95. doi: 10.1007/978-1-4939-7401-6_8
46. Kleih M, Böpple K, Dong M, Gaißler A, Heine S, Olayioye MA, et al. Direct Impact of Cisplatin on Mitochondria Induces ROS Production That Dictates Cell Fate of Ovarian Cancer Cells. *Cell Death Dis* (2019) 10(11):1–12. doi: 10.1038/s41419-019-2081-4
47. Zorova LD, Popkov VA, Plotnikov EY, Silachev DN, Pevzner IB, Jankauskas SS, et al. Mitochondrial Membrane Potential. *Anal Biochem* (2018) 552:50–9. doi: 10.1016/j.ab.2017.07.009
48. Luis-García ER, Becerril C, Salgado-Aguayo A, Aparicio-Trejo OE, Romero Y, Flores-Soto E, et al. Mitochondrial Dysfunction and Alterations in Mitochondrial Permeability Transition Pore (mPTP) Contribute to Apoptosis Resistance in Idiopathic Pulmonary Fibrosis Fibroblasts. *Int J Mol Sci* (2021) 22(15):7870. doi: 10.3390/ijms22157870
49. Zieker D, Bühler S, Üstündag Z, Königsrainer I, Manncke S, Bajaeifer K, et al. Induction of Tumor Stem Cell Differentiation—Novel Strategy to Overcome Therapy Resistance in Gastric Cancer. *Langenbeck's Arch Surg* (2013) 398 (4):603–8. doi: 10.1007/s00423-013-1058-5
50. Wang J, Sullenger BA, Rich JN. Notch Signaling in Cancer Stem Cells. *Notch Signal Embryol Cancer* (2012) 727:174–85. doi: 10.1007/978-1-4614-0899-4_13
51. Meisel CT, Porcheri C, Mitsiadis TA. Cancer Stem Cells, Quo Vadis? The Notch Signaling Pathway in Tumor Initiation and Progression. *Cells* (2020) 9 (8):1879. doi: 10.3390/cells9081879
52. Lahiry M, Kumar S, Hari K, Chedere A, Jolly M, Rangarajan A. AMPK-Fyn Signaling Promotes Notch1 Stability to Potentiate Hypoxia-Induced BreastCancer Stemness and Drug Resistance. *Sos Sci* (2020) 21:1–50. doi: 10.2139/ssrn.3586992
53. Sriuranpong V, Borges MW, Ravi RK, Arnold DR, Nelkin BD, Baylin SB, et al. Notch Signaling Induces Cell Cycle Arrest in Small Cell Lung Cancer Cells. *Cancer Res* (2001) 61(7):3200–5. doi: 10.1097/00002820-200104000-00012
54. Akbarzadeh M, Akbarzadeh S, Majidinia M. Targeting Notch Signaling Pathway as an Effective Strategy in Overcoming Drug Resistance in Ovarian Cancer. *Patholog-Res Pract* (2020) 216(11):153158. doi: 10.1016/j.prp.2020.153158
55. Venkatesh V, Nataraj R, Thangaraj GS, Karthikeyan M, Gnanasekaran A, Kaginelli SB, et al. Targeting Notch Signalling Pathway of Cancer Stem Cells. *Stem Cell Invest* (2018) 5:1–12. doi: 10.21037/sci.2018.02.02

Conflict of Interest: The authors declare that the research was conducted in the absence of any commercial or financial relationships that could be construed as a potential conflict of interest.

Publisher's Note: All claims expressed in this article are solely those of the authors and do not necessarily represent those of their affiliated organizations, or those of the publisher, the editors and the reviewers. Any product that may be evaluated in this article, or claim that may be made by its manufacturer, is not guaranteed or endorsed by the publisher.

Advantages of publishing in Frontiers

OPEN ACCESS
Articles are free to read for greatest visibility and readership

FAST PUBLICATION
Around 90 days from submission to decision

HIGH QUALITY PEER-REVIEW
Rigorous, collaborative, and constructive peer-review

TRANSPARENT PEER-REVIEW
Editors and reviewers acknowledged by name on published articles

Frontiers
Avenue du Tribunal-Fédéral 34
1005 Lausanne | Switzerland

Visit us: www.frontiersin.org
Contact us: frontiersin.org/about/contact

REPRODUCIBILITY OF RESEARCH
Support open data and methods to enhance research reproducibility

DIGITAL PUBLISHING
Articles designed for optimal readership across devices

FOLLOW US
@frontiersin

IMPACT METRICS
Advanced article metrics track visibility across digital media

EXTENSIVE PROMOTION
Marketing and promotion of impactful research

LOOP RESEARCH NETWORK
Our network increases your article's readership